Toxins and Ion transfers

Julien Barbier, Evelyne Benoit, Nicolas Gilles, Daniel Ladant, Marie-France Martin-Eauclaire, César Mattei, Jordi Molgó, Michel R. Popoff, Denis Servent

Collection
Rencontres en Toxinologie
Collection
Meetings on Toxinology

Toxines et Transferts ioniques

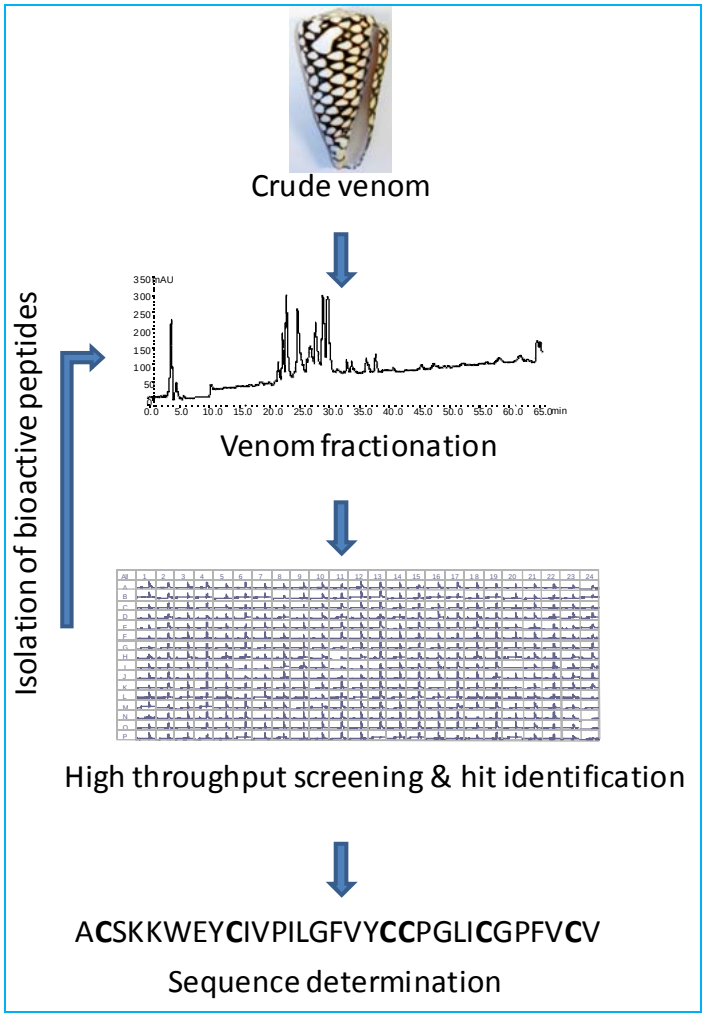

Toxins and Ion transfers

Comité d'édition – *Editorial committee :*
Julien BARBIER, Evelyne BENOIT, Nicolas GILLES, Daniel LADANT, Marie-France MARTIN-EAUCLAIRE, César MATTEI, Jordi MOLGÓ, Michel R. POPOFF, Denis SERVENT

Société Française pour l'Etude des Toxines
French Society of Toxinology

Illustration de couverture – *Cover picture* :

Application d'une analyse à haut débit pour $Na_v1.7$, basée sur la méthode FLIPR, pour la découverte d'inhibiteurs de canaux Na^+. L'identification et la séquence obtenue pour MrVIB du venin brut de *Conus marmoreus* sont illustrées ici. De Richard LEWIS, Ching-I Anderson WANG, Sébastien DUTERTRE et Irina VETTER (ce volume).

Application of a FLIPR-based high throughput assay for $Na_v1.7$ for the discovery of Na^+channel inhibitors. Illustrated is the identification and sequence obtained for MrVIB identified in the crude venom of Conus marmoreus*. From Richard LEWIS, Ching-I Anderson WANG, Sébastien DUTERTRE and Irina VETTER (this volume).*

Collection
Rencontres en Toxinologie
Collection
Meetings on Toxinology

La collection « Rencontres en Toxinologie » est publiée à l'occasion des colloques annuels « Rencontres en Toxinologie » organisés par la Société Française pour l'Etude des Toxines (SFET). Les ouvrages imprimés parus de 2001 à 2007 ont été édités par Elsevier (Paris, France) puis la Librairie Lavoisier (Cachan, France). Depuis 2008, ils sont édités par la SFET et diffusés sur le site http://www.sfet.asso.fr, en libre accès pour les auteurs et les lecteurs.

The series « Rencontres en Toxinologie » is published on the occasion of the annual Meetings on Toxinology organized by the French Society of Toxinology (SFET). The printed books of the series, from 2001 to 2007, were edited by Elsevier (Paris, France) and then the Librairie Lavoisier *(Cachan, France). Since 2008, they are edited by the SFET and are available on-line on the site http://www.sfet.asso.fr, with free access for authors and readers.*

Titres parus – *Previous titles*

Explorer, exploiter les toxines et maîtriser les organismes producteurs
Cassian Bon, Françoise Goudey-Perrière, Bernard Poulain, Simone Puiseux-Dao
Elsevier, Paris, 2001
ISBN : 2-84299-359-4

Toxines et recherches biomédicales
Françoise Goudey-Perrière, Cassian Bon, Simone Puiseux-Dao, Martin-Pierre Sauviat
Elsevier, Paris, 2002
ISBN : 2-84299-445-0

Toxinogenèse – Biosynthèse, ingénierie, polymorphisme et neutralisation des toxines
Françoise Goudey-Perrière, Cassian Bon, André Ménez, Simone Puiseux-Dao
Elsevier, Paris, 2003
ISBN : 2-84299-481-7

Envenimations, intoxinations
Françoise Goudey-Perrière, Evelyne Benoit, *Simone Puiseux-Dao*, *Cassian Bon*
Librairie Lavoisier, Cachan, 2004
ISBN : 2-7430-0749-4

Toxines et douleur
Cassian Bon, Françoise Goudey-Perrière, Max Goyffon, Martin-Pierre Sauviat
Librairie Lavoisier, Cachan, 2005
ISBN : 2-7430-0849-0

Toxines et cancer
Françoise Goudey-Perrière, Evelyne Benoit, Max Goyffon, Pascale Marchot
Librairie Lavoisier, Cachan, 2006
ISBN : 2-7430-0958-6

Toxines émergentes : nouveaux risques
Françoise Goudey-Perrière, Evelyne Benoit, Pascale Marchot, Michel R. Popoff
Librairie Lavoisier, Cachan, 2007
ISBN : 978-2-7430-1037-9

Toxines et fonctions cholinergiques neuronales et non neuronales
Evelyne Benoit, Françoise Goudey-Perrière, Pascale Marchot, Denis Servent
Publications de la SFET, Châtenay-Malabry, France, 2008
Epub on http://www.sfet.asso.fr - ISSN 1760-6004

Toxines et Signalisation - *Toxins and Signalling*
Evelyne Benoit, Françoise Goudey-Perrière, Pascale Marchot, Denis Servent
Publications de la SFET – *SFET Editions*, Châtenay-Malabry, France, 2009
Epub on http://www.sfet.asso.fr - ISSN 1760-6004

Avancées et nouvelles technologies en Toxinologie - *Advances and new technologies in Toxinology*
Julien Barbier, Evelyne Benoit, Pascale Marchot, César Mattéi, Denis Servent
Publications de la SFET – *SFET Editions*, Gif-sur-Yvette, France, 2010
Epub on http://www.sfet.asso.fr - ISSN 1760-6004

Cet ouvrage est publié à l'occasion du colloque « 19èmes Rencontres en Toxinologie », organisé par la Société Française pour l'Etude des Toxines (SFET) les 28 et 29 novembre 2011 à Paris.

This book is published on the occasion of the 19th Meeting on Toxinology, organized by the French Society of Toxinology (SFET) on November 28th and 29th, 2011, in Paris.

Sommaire - *Content*

Pages

Toxines comme outils et thérapeutiques – *Toxins as tools and therapeutics*

Divers – *Miscellaneous*

Toxines et Transferts ioniques – Toxins and Ion transfers
Rencontres en Toxinologie – Meeting on Toxinology, 2011
Editions de la SFET – SFET Editions
Accès libre en ligne sur le site – Free access on line on the site : http://www.sfet.asso.fr

Animal toxins targeting voltage-activated sodium ($Na_V1.9$) channels

Frank BOSMANS

Molecular Physiology and Biophysics Section, Porter Neuroscience Research Center, National Institute of Neurological Disorders and Stroke, National Institutes of Health, Bethesda, MD 20892, USA

Tel : +1-301-594-6760 ; E-mail : frank.bosmans@nih.gov

Abstract

Voltage-activated sodium (Na_V) channels are crucial for initiating and transmitting action potentials, an ability that places them amongst the most widely targeted ion channels by drugs and animal venoms. An increasing number of toxins isolated from animal venom have been shown to interfere with the voltage-driven activation process of Na_V channels, possibly by interacting with one or more of their voltage-sensors. This mini-review summarizes our recent work on identifying novel animal toxin receptor sites within Na_V channel voltage-sensors and illustrates how chimeric approaches can be used to uncover molecules that interact with $Na_V1.9$, an enigmatic Na_V channel involved in nociception.

Les toxines animales ciblant les canaux sodium ($Na_V1.9$) activés par le potentiel

Les canaux sodium dépendants du potentiel (ou canaux Na_V) sont cruciaux pour initier et transmettre des potentiels d'action, une capacité qui les place parmi les canaux les plus ciblés par les médicaments et les venins animaux. Il a été démontré qu'un nombre croissant de toxines isolées de venins animaux interfèrent avec le processus d'activation des canaux Na_V, peut-être en interagissant avec un ou plusieurs de leurs senseurs de potentiel. Cette mini-revue résume notre travail récent sur l'identification des sites de nouvelles toxines animales se fixant sur les senseurs de potentiel des canaux Na_V et démontre comment des approches chimériques peuvent être utilisées pour découvrir des molécules qui influent sur $Na_V1.9$, un canal Na_V énigmatique impliqué dans la sensation de douleur.

Keywords : *Animal toxin, pain, sodium channel, voltage-sensor.*

Na_V channel S3b-S4 paddle motifs

The Na_V channel (Goldin et al., 2000) pore-forming subunit consists of four connected domains (I-IV) (Catterall, 2000), each having six transmembrane segments (S1-S6) (*Figure 1a*). These similar entities consist of a voltage-sensor (S1-S4) and a portion of the structure that forms the sodium ion selective pore in the membrane (S5-S6). The pore can open or close when all four voltage-sensors move in response to changes in membrane voltage. It is thought that each of the four voltage-sensors activates in response to changes in membrane voltage, however, those in domains I-III are most important for channel opening, whereas the one in domain IV plays a distinctive role in inactivating the channel (Cha *et al.*, 1999; Sheets *et al.*, 1999; Horn *et al.*, 2000; Sheets *et al.*, 2000; Chanda and Bezanilla, 2002; Bosmans *et al.*, 2008; Campos *et al.*, 2008).

Despite their physiological significance, structural information on Na_V channels lags when compared to the structurally similar voltage-activated K^+ (Kv) channels, where recent data has revealed structural features important for channel function. More specifically, studies on Kv channel voltage-sensors have identified an S3b-S4 helix-turn-helix motif, the voltage-sensor paddle, which moves at the protein-lipid interface and drives activation of the voltage-sensors which, in turn, opens the pore (*Figure 1b*) (Jiang *et al.*, 2003; Alabi *et al.*, 2007; Long *et al.*, 2007; Chakrapani *et al.*, 2008; Swartz, 2008). Besides its vital role in channel gating, the paddle motif is also an important pharmacological target in Kv channels, as spider toxins that partition into membranes interact with this region to inhibit channel opening (Swartz and MacKinnon, 1997b, a; Li-Smerin and Swartz, 1998, 2000; Lee *et al.*, 2003; Phillips *et al.*, 2005; Alabi *et al.*, 2007; Swartz, 2007). Recently, we have shown that distinct paddle motifs also exist in each of the four voltage-sensors of Na_V channels and that they can be transplanted into the four-fold symmetric Kv channel to study them in isolation (Bosmans *et al.*, 2008; Milescu *et al.*, 2009). Furthermore, we demonstrated that each of the four paddle motifs is capable of interacting with toxins from tarantulas and scorpions and that multiple paddle motifs are often targeted by a single toxin. For example, it was shown that the tarantula toxin ProTx-II (Middleton *et al.*, 2002) can interact with the voltage-sensor in domain I, II and IV, whereas a related tarantula toxin, PaurTx3, only interacts with domain II (Bosmans *et al.*, 2008). It is also interesting that the profiles of toxin-paddle interactions vary for

different subtypes of Na_V channels. This chimeric approach was recently applied to $Na_V1.9$, a relatively unknown Na_V channel isoform involved in pain perception.

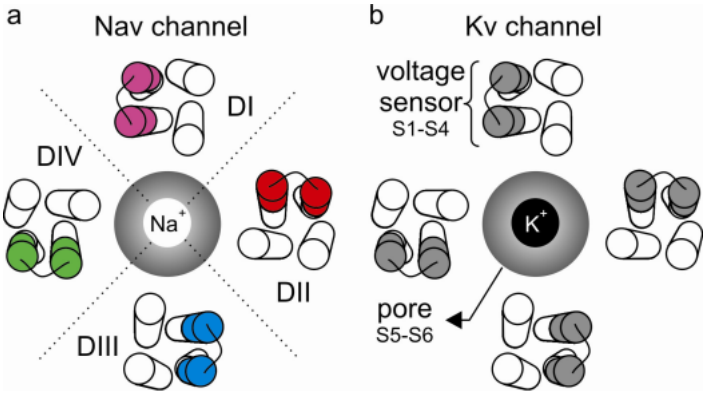

Figure 1. Cartoon representing top views of a Na_V channel (**a**) and a K_V channel (**b**). The central Na^+ or K^+ selective pore is surrounded by the four voltage-sensors in the four domains (delineated by dotted line). In the Na_V channel, the paddles (*color*) are not identical whereas in the K_V channel, the paddles (*grey*) are identical.

Figure 1. *Figure représentant des vues de dessus d'un canal Na_V (**a**) et un canal potassium (K_V) (**b**). Le pore central sélectif pour Na^+ ou K^+ est entouré par les quatre senseurs de potentiel dans les quatre domaines (délimités par la ligne en pointillés). Dans le canal Na_V, les palettes (*couleur*) ne sont pas identiques alors que dans le canal K_V, les palettes (*en gris*) sont identiques.*

Animal toxin pharmacology of $Na_V1.9$

Na_V channel expression is tissue-specific across different species. $Na_V1.7$ is mainly expressed in sensory and sympathetic neurons in the peripheral nervous system. $Na_V1.8$ and $Na_V1.9$ are sensory neuron-specific channels that are normally found within small-diameter dorsal root (DRG) and trigeminal ganglia but not in the central nervous system neurons (Momin and Wood, 2008). Selective knockout of $Na_V1.7$ expression in mouse nociceptors leads to a loss of acute mechanosensory and inflammatory pain (Nassar *et al.*, 2004). Also, various human heritable pain disorders such as erythermalgia and paroxysmal extreme pain disorder map to mutations in *SCN9A*, the gene encoding $Na_V1.7$ (Dib-Hajj *et al.*, 2008). Studies of $Na_V1.8$ in mice have revealed a role for this channel in inflammatory pain, neuropathic pain and noxious stimuli response (Joshi *et al.*, 2006; Dong *et al.*, 2007). $Na_V1.9$ knockout mice have a largely absent inflammatory hyperalgesia in response to inflammatory mediators (Priest *et al.*, 2005; Amaya *et al.*, 2006). Although knockout mice are an extremely valuable tool to reveal the physiological role of Na_V channels, the occurrence of genetic compensatory mechanisms might mask vital functional information. Therefore, the discovery of pharmacological tools that evoke a specific response from these channels is essential for elucidating their physiological function. To achieve this goal, heterologous expression and characterization of $Na_V1.7$, $Na_V1.8$, and $Na_V1.9$ in oocytes or mammalian cells is of great importance.

Although $Na_V1.9$ plays a key role in nociception, fundamental questions about its function and pharmacology remain unanswered because previous attempts to express this channel in heterologous systems have been unsuccessful (Blum *et al.*, 2002; Dib-Hajj *et al.*, 2002). In addition, studying $Na_V1.9$-mediated currents in native DRG neurons is technically challenging because only a fraction of isolated neurons produces a measurable amount of these currents and other Na_V channels activate over a similar voltage range. We circumvented heterologous expression obstacles by identifying and transplanting paddle motifs from the putative voltage-sensors of $Na_V1.9$ into four-fold symmetric Kv channels and investigated the function of $Na_V1.9$ voltage-sensors in channel gating and in forming toxin receptors (Bosmans *et al.*, 2011).

By taking advantage of the portable nature of paddle motifs within voltage-sensing domains (Alabi *et al.*, 2007; Bosmans *et al.*, 2008; Milescu *et al.*, 2009), we showed that these structural motifs also exist in each of the four $Na_V1.9$ voltage-sensors, and that they can be transplanted into Kv channels to be studied in isolation. Our results revealed that each of the $Na_V1.9$ paddle motifs can sense changes in membrane voltage and drive Kv channel voltage-sensor activation, similar to what was found for canonical Na_V channels (Bosmans *et al.*, 2008). Since the pharmacological sensitivities of $Na_V1.9$ remain unexplored, we exploited these paddle constructs to search for toxins that might interact with $Na_V1.9$ channels. To this end, we screened eighteen toxins from tarantula, scorpion and sea anemone venom against four $Na_V1.9$ paddle constructs and observed six toxins that potently inhibit one or more of the chimeras (AaHII, ProTx-I, TsVII, GrTx-SIA, HaTx, BomIV). In addition, we discovered that the $Na_V1.9$ paddle motifs from all four domains can interact with toxins from animal venom.

The two most interesting toxins that emerged from our screens were the scorpion toxin TsVII and the tarantula toxin ProTx-I, both of which interact strongly with $Na_V1.9$ paddle motifs and potently facilitate the

slowly activating and inactivating $Na_V1.9$-mediated current in rat DRG neurons (Cummins *et al.*, 1999; Maruyama *et al.*, 2004; Priest *et al.*, 2005; Coste *et al.*, 2007; Ostman *et al.*, 2008). In addition to targeting $Na_V1.9$, TsVII and ProTx-I have very different actions on $Na_V1.8$, the other TTX-resistant Na_V channel present in these sensory neurons. For example, TsVII produces a dramatic facilitation of $Na_V1.9$-mediated currents while only modestly inhibiting $Na_V1.8$, showing that the scorpion toxin can discriminate between these two TTX-resistant Na_V channels. Conversely, ProTx-I causes both a pronounced potentiation of $Na_V1.9$-mediated currents and a robust inhibition of $Na_V1.8$ (*Figure 2*), making this toxin a formidable tool to discriminate the currents generated by these two channel isoforms in DRG neurons. Taken together, our results suggest that $Na_V1.9$ channels possess functional voltage-sensors that interact with scorpion and tarantula toxins, features that are shared with canonical Na_V channel isoforms. Furthermore, our screening with a wide range of toxins demonstrate that $Na_V1.9$ has different pharmacological sensitivities than other Na_V channel isoforms, a property that may be exploited for drug design.

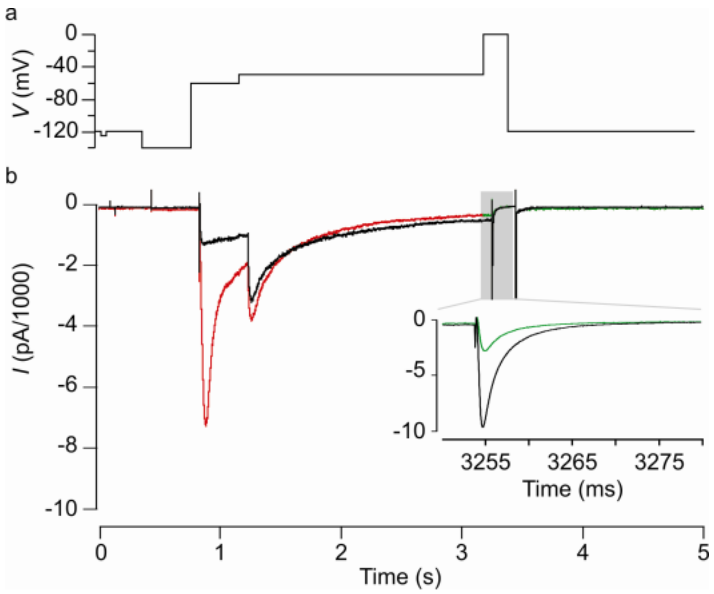

Figure 2. Effect of ProTx-I on native $Na_V1.9$- and $Na_V1.8$-mediated currents in rat DRG neurons. (**a**) Voltage protocol used to elicit both $Na_V1.9$ (first depolarization to -55 mV) and $Na_V1.8$-mediated currents (second depolarization to 0 mV) in a rat DRG neuron. (**b**) Evoked currents under control conditions (*black*) and after addition of 100 nM ProTx-I (*red* for $Na_V1.9$, *green* for $Na_V1.8$). $Na_V1.9$-mediated currents are potentiated whereas $Na_V1.8$-mediated currents are inhibited. Time scales for both currents are indicated in the X-axis. Experiment by Michelino Puopolo, Harvard Medical School (Bosmans *et al.*, 2011).

Figure 2. *Effet de ProTx-I sur les courants natifs* via *$Na_V1.9$ et $Na_V1.8$ dans les neurones DRG de rat. (**a**) Protocole de potentiel utilisé pour activer des courants* via *$Na_V1.9$ (première dépolarisation à -55 mV) et $Na_V1.8$ (deuxième dépolarisation à 0 mV) dans un neurone de DRG. (**b**) Courants évoqués dans des conditions de contrôle (*noir*) et après addition de 100 nM de ProTx-I (*rouge *pour $Na_V1.9$,* vert *pour $Na_V1.8$). Les courants* via *$Na_V1.9$ sont potentialisés mais ceux* via *$Na_V1.8$ sont inhibés. Les échelles de temps pour les deux courants sont indiquées dans l'axe des abscisses. Expérience menée par Michelino Puopolo, Harvard Medical School (Bosmans* et al.*, 2011).*

Acknowledgements. *The work summarized here was carried out by Frank Bosmans in the lab of Dr Kenton J Swartz (NINDS-NIH, USA) and by Michelino Puopulo in the lab of Dr Bruce P Bean (Harvard Medical School, USA) with support from Dr Marie-France Martin-Eauclaire (CRN2M-Marseille, France).*

References

Alabi AA, Bahamonde MI, Jung HJ, Kim JI, Swartz KJ (2007) Portability of paddle motif function and pharmacology in voltage sensors. *Nature* **450**: 370-375

Amaya F, Wang H, Costigan M, Allchorne AJ, Hatcher JP, Egerton J, Stean T, Morisset V, Grose D, Gunthorpe MJ, Chessell IP, Tate S, Green PJ, Woolf CJ (2006) The voltage-gated sodium channel Na(v)1.9 is an effector of peripheral inflammatory pain hypersensitivity. *J Neurosci* **26**: 12852-12860

Blum R, Kafitz KW, Konnerth A (2002) Neurotrophin-evoked depolarization requires the sodium channel Na(V)1.9. *Nature* **419**: 687-693

Bosmans F, Martin-Eauclaire MF, Swartz KJ (2008) Deconstructing voltage sensor function and pharmacology in sodium channels. *Nature* **456**: 202-208

Bosmans F, Puopolo M, Martin-Eauclaire MF, Bean BP, Swartz KJ (2011) Functional properties and toxin pharmacology of a dorsal root ganglion sodium channel viewed through its voltage sensors. *J Gen Physiol* **138**: 59-72

Campos FV, Chanda B, Beirao PS, Bezanilla F (2008) Alpha-scorpion toxin impairs a conformational change that leads to fast inactivation of muscle sodium channels. *J Gen Physiol* **132**: 251-263

Catterall WA (2000) From ionic currents to molecular mechanisms: the structure and function of voltage-gated sodium channels. *Neuron* **26**: 13-25

Cha A, Ruben PC, George AL, Jr., Fujimoto E, Bezanilla F (1999) Voltage sensors in domains III and IV, but not I and II, are immobilized by Na+ channel fast inactivation. *Neuron* **22**: 73-87

Chakrapani S, Cuello LG, Cortes DM, Perozo E (2008) Structural dynamics of an isolated voltage-sensor domain in a lipid bilayer. *Structure* **16**: 398-409

Chanda B, Bezanilla F (2002) Tracking voltage-dependent conformational changes in skeletal muscle sodium channel during activation. *J Gen Physiol* **120**: 629-645

Coste B, Crest M, Delmas P (2007) Pharmacological dissection and distribution of NaN/Nav1.9, T-type Ca^{2+} currents, and mechanically activated cation currents in different populations of DRG neurons. *J Gen Physiol* **129**: 57-77

Cummins TR, Dib-Hajj SD, Black JA, Akopian AN, Wood JN, Waxman SG (1999) A novel persistent tetrodotoxin-resistant sodium current in SNS-null and wild-type small primary sensory neurons. *J Neurosci* **19**: RC43

Dib-Hajj S, Black JA, Cummins TR, Waxman SG (2002) NaN/Nav1.9: a sodium channel with unique properties. *Trends Neurosci* **25**: 253-259

Dib-Hajj SD, Yang Y, Waxman SG (2008) Genetics and molecular pathophysiology of Na(v)1.7-related pain syndromes. *Adv Genet* **63**: 85-110

Dong XW, Goregoaker S, Engler H, Zhou X, Mark L, Crona J, Terry R, Hunter J, Priestley T (2007) Small interfering RNA-mediated selective knockdown of Na(V)1.8 tetrodotoxin-resistant sodium channel reverses mechanical allodynia in neuropathic rats. *Neuroscience* **146**: 812-821

Goldin AL, Barchi RL, Caldwell JH, Hofmann F, Howe JR, Hunter JC, Kallen RG, Mandel G, Meisler MH, Netter YB, Noda M, Tamkun MM, Waxman SG, Wood JN, Catterall WA (2000) Nomenclature of voltage-gated sodium channels. *Neuron* **28**: 365-368

Horn R, Ding S, Gruber HJ (2000) Immobilizing the moving parts of voltage-gated ion channels. *J Gen Physiol* **116**: 461-476

Jiang Y, Lee A, Chen J, Ruta V, Cadene M, Chait BT, MacKinnon R (2003) X-ray structure of a voltage-dependent K^+ channel. *Nature* **423**: 33-41

Joshi SK, Mikusa JP, Hernandez G, Baker S, Shieh CC, Neelands T, Zhang XF, Niforatos W, Kage K, Han P, Krafte D, Faltynek C, Sullivan JP, Jarvis MF, Honore P (2006) Involvement of the TTX-resistant sodium channel Nav1.8 in inflammatory and neuropathic, but not post-operative, pain states. *Pain* **123**: 75-82

Lee HC, Wang JM, Swartz KJ (2003) Interaction between extracellular Hanatoxin and the resting conformation of the voltage-sensor paddle in Kv channels. *Neuron* **40**: 527-536

Li-Smerin Y, Swartz KJ (1998) Gating modifier toxins reveal a conserved structural motif in voltage-gated Ca^{2+} and K^+ channels. *Proc Natl Acad Sci U S A* **95**: 8585-8589

Li-Smerin Y, Swartz KJ (2000) Localization and molecular determinants of the Hanatoxin receptors on the voltage-sensing domains of a K(+) channel. *J Gen Physiol* **115**: 673-684

Long SB, Tao X, Campbell EB, MacKinnon R (2007) Atomic structure of a voltage-dependent K^+ channel in a lipid membrane-like environment. *Nature* **450**: 376-382

Maruyama H, Yamamoto M, Matsutomi T, Zheng T, Nakata Y, Wood JN, Ogata N (2004) Electrophysiological characterization of the tetrodotoxin-resistant Na^+ channel, Na(v)1.9, in mouse dorsal root ganglion neurons. *Pflugers Arch* **449**: 76-87

Middleton RE, Warren VA, Kraus RL, Hwang JC, Liu CJ, Dai G, Brochu RM, Kohler MG, Gao YD, Garsky VM, Bogusky MJ, Mehl JT, Cohen CJ, Smith MM (2002) Two tarantula peptides inhibit activation of multiple sodium channels. *Biochemistry* **41**: 14734-14747

Milescu M, Bosmans F, Lee S, Alabi AA, Kim JI, Swartz KJ (2009) Interactions between lipids and voltage sensor paddles detected with tarantula toxins. *Nat Struct Mol Biol* **16**: 1080-1085

Momin A, Wood JN (2008) Sensory neuron voltage-gated sodium channels as analgesic drug targets. *Curr Opin Neurobiol* **18**: 383-388

Nassar MA, Stirling LC, Forlani G, Baker MD, Matthews EA, Dickenson AH, Wood JN (2004) Nociceptor-specific gene deletion reveals a major role for Nav1.7 (PN1) in acute and inflammatory pain. *Proc Natl Acad Sci U S A* **101**: 12706-12711

Ostman JA, Nassar MA, Wood JN, Baker MD (2008) GTP up-regulated persistent Na^+ current and enhanced nociceptor excitability require NaV1.9. *J Physiol* **586**: 1077-1087

Phillips LR, Milescu M, Li-Smerin Y, Mindell JA, Kim JI, Swartz KJ (2005) Voltage-sensor activation with a tarantula toxin as cargo. *Nature* **436**: 857-860

Priest BT, Murphy BA, Lindia JA, Diaz C, Abbadie C, Ritter AM, Liberator P, Iyer LM, Kash SF, Kohler MG, Kaczorowski GJ, MacIntyre DE, Martin WJ (2005) Contribution of the tetrodotoxin-resistant voltage-gated sodium channel NaV1.9 to sensory transmission and nociceptive behavior. *Proc Natl Acad Sci USA* **102**: 9382-9387

Sheets MF, Kyle JW, Hanck DA (2000) The role of the putative inactivation lid in sodium channel gating current immobilization. *J Gen Physiol* **115**: 609-620

Sheets MF, Kyle JW, Kallen RG, Hanck DA (1999) The Na channel voltage sensor associated with inactivation is localized to the external charged residues of domain IV, S4. *Biophys J* **77**: 747-757

Swartz KJ (2007) Tarantula toxins interacting with voltage sensors in potassium channels. *Toxicon* **49**: 213-230

Swartz KJ (2008) Sensing voltage across lipid membranes. *Nature* **456**: 891-897

Swartz KJ, MacKinnon R (1997a) Hanatoxin modifies the gating of a voltage-dependent K^+ channel through multiple binding sites. *Neuron* **18**: 665-673

Swartz KJ, MacKinnon R (1997b) Mapping the receptor site for hanatoxin, a gating modifier of voltage-dependent K^+ channels. *Neuron* **18**: 675-682

Toxines et Transferts ioniques – Toxins and Ion transfers
Rencontres en Toxinologie – Meeting on Toxinology, 2011
Editions de la SFET – SFET Editions
Accès libre en ligne sur le site – Free access on line on the site : http://www.sfet.asso.fr

Overview of the small voltage-gated K^+ channels blockers from Androctonus *venoms*

Marie-France MARTIN-EAUCLAIRE*, Pierre E. BOUGIS

CNRS UMR6231, CRN2M, IFR11 Institut Jean Roche, Université de la Méditerranée, Faculté de Médecine secteur Nord, CS80011, Bd Pierre Dramard, F-13344 Marseille cedex 15, France

** Corresponding author ; Tel : +33 (0) 491698914 ; Fax : +33 (0) 491698839 ; E-mail : marie-france.eauclaire@univmed.fr*

Abstract

Scorpion toxins have been used extensively to study the pharmacology of K^+ channels, as well as to decipher their pore topology, and an increasing amount of molecular data is still being published on this subject. During the last two decades, Androctonus *venoms have provided several structurally distinct families of peptides exhibiting different K^+-channel-blocking function. We have largely participated to their purification, chemical, pharmacological and immunological characterization. In this article, we summarize our contribution to the current knowledge on these toxin/channel interactions.*

Vue d'ensemble des petits peptides des venins d'Androctonus capables de bloquer des canaux K^+ activés par le potentiel

*Les toxines de scorpion ont été considérablement utilisées pour étudier la pharmacologie des canaux K^+ ainsi que pour décrypter la topologie du pore et une quantité croissante de résultats moléculaires continue d'être publiée sur ce sujet. Au cours des deux dernières décades, les venins d'*Androctonus *ont fourni plusieurs familles de peptides distincts structurellement et capables de bloquer la fonction de différent types de canaux K^+. Nous avons largement contribué à leur purification et à leur caractérisation chimique, pharmacologique et immunologique. Dans cet article, nous résumons notre contribution aux connaissances actuelles des interactions toxine/canal K^+.*

Keywords : *Potassium channels, scorpion toxins.*

Introduction

K^+ channel blockers' toxins (KTx) from scorpion venoms are short peptides, which typically contain between 30-40 amino-acid residues cross-linked by 3-4 disulphide bridges forming compact and resistant molecules. They block K^+ channels from the extracellular side by binding to the outer vestibule of K^+ channels and in most cases insert a Lys side chain into the channel pore (Park and Miller, 1992). They are often present at low concentrations in the venoms (from 0.01 to 1% by weight). Usually, they have almost no toxic effects in mice by subcutaneous (*s.c.*) injection. However, they could be very toxic when injected intracerebroventricularly (*i.c.v.*) into the brain. Based on sequence identity and cysteine pairing, they have been classified into four families, the α–, β–, γ– and κ-KTx (Tytgat *et al.*, 1999) and today more than 120 KTx ranging from 23 up to 64 amino acids are sequenced. Most of their structures exhibit the characteristic fold called Cystein-Stabilized-Helix (CSH) motif, constituted by one α-helix and two or three β-strands, in which two disulfide bridges covalently link a segment of the α-helix with one strand of the β–sheet structure, except for κ-KTxs which are formed by two parallel α-helices linked by two disulfide bridges. The α-KTx family is constituted of the shortest peptides having diverse specific blocking activities against voltage-gated (K_V) and calcium activated (K_{Ca}) channels. Longest peptides, with 45-68 amino acid residues reticulated by three disulfide bridges, have been later characterized and classified as the β-KTx family. They have two structural and functional domains: an α-helix in the N-terminal with cytolytic and antimicrobial activity, as well as a tightly folded C-terminal region with the CSH motif and K^+ channel-blocking activities (Diego-García *et al.*, 2008). At last, the α-KTx family was described as specific for hERG channel (Corona *et al.*, 2002).

This overview will summarize our main original contributions to the subject, in particular those obtained by the *Androctonus mauretanicus* venom analysis.

The smallest toxins in *Androctonus mauretanicus* venom: P01 (α-KTx8) and P05 (α-KTx5)

PO5 (α-KTx 5.2, 3415 Da) from *Androctonus mauretanicus* display high affinity (8 pM) and high specificity for

the so-called apamin-sensitive SK_{Ca} channel, as well as PO1 (α-KTx 8.1, 3177 Da) which is much less active on the SK_{Ca} (300pM). They belong to the α-KTx5.x's family (as Leiurotoxin1 or Scyllatoxin from the venom of the scorpion *Leiurus quinquestriatus Hebraeus*). Structure-function studies have shown that a highly positively charged region (in particular two Arg residues) of the α-helix exposed to the solvent is involved in binding to the receptor, as it is for the bee venom apamin (Sabatier *et al.*, 1993).

The Kaliotoxin subfamily (α-KTx3 subfamily)

The KTX structure-function relationship studies were first performed using synthetic analogs such as $KTX_{(1-37)}$, $KTX_{(1-37)\text{-amide}}$ and shortened peptides including $KTX_{(27-37)}$, $KTX_{(25-32)}$ and $KTX_{(1-11)}$ (Romi *et al.*, 1993). $KTX_{(27-37)}$ and $KTX_{(25-32)}$ but not $KTX_{(1-11)}$ competed with ^{125}I-KTX for its receptor on rat brain synaptosomes and act as antagonists of KTX. This demonstrated for the first time that the C-terminal region, particularly the β-sheet of the toxin, was involved in the interaction with the receptor and the channel blockade. KTX was further widely used by different international groups for probing the vestibule topology from the lymphocyte $K_V1.3$ channel. Synthetic KTX analogs have been used in combination with site-directed mutagenesis of the $K_V1.3$ channel to identify pairs of residues in the toxin and channel which interact specifically. It was found that the side chain of the Lys 27 residue enters deeply into the pore and interacts with the Asp 402 residue of each channel subunit (Aiyar *et al.*, 1995). Then, the KTX binding to a chimeric K^+ channel (KcsA-$K_V1.3$) was investigated using solid-state nuclear magnetic resonance (ssNMR) (Lange *et al.*, 2006). Significant chemical shift changes were observed for the KTX residues found in interaction with the channel, reflecting conformational changes involving β-sheet contacts between the first and third β-strand. For the channel, chemical-shift changes were seen also for channel residues in the KTX-binding region in both the pore helix and the selectivity filter. The ssNMR data directly show that Asp 64 in the KcsA-$K_V1.3$ vestibule represents an important interaction site for KTX. Large chemical-shift changes were seen for Gly 77, Tyr 78 and Gly 79 in the selectivity filter. Also, chemical-shift changes were observed for the side chains of Glu 71 and Asp 80 that form carboxyl-carboxylate pairs on the backside of the filter (Lange *et al.*, 2006).

The α-KTx_{15} subfamily : K_v4.x and hERG blockers

The first member of the α-KTx_{15} subfamily characterized from *Androctonus australis* was Aa1 (3869 Da) (Pisciotta *et al.*, 2000). At the primary sequence level, the toxin has an unusual N-terminal pyroglutamic acid. Aa1 totally blocked a fast I_A-type K^+ current from cerebellum granular cells. Shortly after, we have isolated a novel toxin from the venom of *Androctonus mauretanicus*, AmmTX3 (3827 Da), able to block a fast I_A-type K^+ current from striatal neurons in culture (Vacher *et al.*, 2002). Then, several cDNAs encoding two Aa1 isoforms, AaTX1 (3867 Da) and AaTX2 (3853 Da) were identified by PCR amplification from a venom gland cDNA library of *Androctonus australis* (Legros *et al.*, 2003) as well as in *Androctonus amoreuxi* (3769 Da). These toxins constitute the first members of the α-KTx_{15} family (*Figure 1*). From a pharmacological point of view, the molecules shared the same target in rat brain. Autoradiograms demonstrated a heterogeneous distribution of ^{125}I-toxin binding sites throughout the adult rat brain. High density of receptors was found in the striatum, hippocampus, superior colliculus and cerebellum (Vacher *et al.*, 2001). The nature of the K^+ channels blocked by the toxins was assessed by performing whole cell patch recording of the K^+ currents of striatal neurons and of cerebellum granular cells in primary culture. In all cases, the AmmTX3 inactivates the transient A-current, but the sustained K^+ current remains fully activated. Finally, analysis by electrophysiological recording of transient K^+ currents in mammalian cells transfected with diverse cloned K^+ channels showed that only the rapidly activating and inactivating $K_V4.1$-mediated current was inhibited by AmmTX3 [with a 50% blocking concentration (IC_{50}) of 105 nM]. The inhibition was less effective on $K_V4.2$ and $K_V4.3$ channels and the toxin did not affect other transient currents such as $K_V1.4$ and $K_V3.4$ (Vacher *et al.*, 2006).

Further, we have reported that the α-KTx_{15} peptides also show a significant hERG-blocking activity, like γ-KTx peptides. From a structural point of view, we have proposed that two separate functional surfaces, A and B, coexist on the molecule, and are responsible for two different K^+-current-blocking functions (Huys *et al.*, 2004). While α-KTxs interact with channels through their β-sheets, γ-KTxs modulate hERG through their α-helix. A common "hot spot" with 2 basic residues (Arg18 and Lys19 in the α-helix) confers hERG blockade activity to α-KTx_{15} peptides (Abdel-Mottaleb *et al.*, 2008).

		(Average mass in Da)
Aa1	ZNETNKK**C**QGGS**C**ASV**C**RRVIGVAAGK**C**INGR**C**V**C**YP	3851
AaTX1*	ZIETNKK**C**QGGS**C**ASV**C**RRVIGVAAGK**C**INGR**C**V**C**YP	3850
AaTX2*	ZVETNKK**C**QGGS**C**ASV**C**RRVIGVAAGK**C**INGR**C**V**C**YP	3839
AmmTX3	ZIETNKK**C**QGGS**C**ASV**C**RKVIGVAAGK**C**INGR**C**V**C**YP	3823
AamTX*	ZVQTNKK**C**KGGS**C**ASV**C**AKVIGVAAGK**C**INGR**C**V**C**YP	3722

Figure 1. Amino acid sequences of the *Androctonus* toxins from the α-KTx_{15} family. *depicted from cDNAs clones; Aa, *Androctonus australis*; Amm, *Androctonus mauretanicus*; Aam, *Androctonus amoreuxi*. Amino acids in red in the α-helix are crucial for hERG channel blockade and those in blue in the β-sheet for K_V channel blockade.

Figure 1. *Séquences d'acide aminés des toxines d'*Androctonus *de la famille α-KTx_{15}. *décrypté à partir d'ADNcs; Aa,* Androctonus australis*; Amm*, Androctonus mauretanicus*; Aam*, Androctonus amoreuxi*. Les acides aminés en rouge dans l'hélice-α sont cruciaux pour le blocage des canaux hERG et ceux en bleu dans le feuillet-β pour le blocage des canaux K_V.*

Conclusion

Scorpion venom remains a proven resource for novel compound discovery, especially for the pharmacologists. A total of 209 α-KTx amino acid sequences are now referenced in the UniProtKB data bank, but only some of these α-KTx peptides have really been shown able to block K^+ currents. For the other reported peptides there is often no direct evidence described for their function. While some of them represent new analogs of well-known families displaying unique selectivity or targeting, others exhibit novel structural features or activities. The majority of their action has been determined on the $K_V1.x$ subfamily or on the Ca^{2+}-activated K^+ channels (on SK_{Ca}-sensitive to the bee venom Apamin or on BK_{Ca}). The results that we obtained during the last two decades provide new insight into the possible targets of some α-KTxs purified from different North African *Androctonus* venoms. In particular, we have greatly contributed to the α-KTx_{15} family definition and pharmacological characterization. Moreover, KTX (α-KTx_{3-1}) was finally proved to be a wonderful tool, which helped us to depict the molecular mechanisms of interaction between K^+ channels and peptide inhibitors and to demonstrate that the binding of K^+ channel specific scorpion toxins does not take place only on the outer vestibule of the channel pore but also deeper into the selectivity filter. The binding involves a combination of hydrophobic, hydrogen bonding and electrostatic interactions, which induced significant structural rearrangements in both molecules. It was then proposed that structural flexibility of the K^+ channel and the toxin represents an important determinant for the high specificity of toxin/K^+ channel interactions (Lange *et al.*, 2006).

Acknowledgements. *We wish to thank Drs Abbas N., Bosmans F., Céard B., Legros C., Tytgat J. and Vacher H. for their contribution in the purification, pharmacological or electrophysiological characterization and cloning and mutagenesis of the* Androctonus *toxins blocking K_V channels.*

References

Abdel-Mottaleb Y, Corzo G, Martin-Eauclaire MF, Satake H, Céard B, Peigneur S, Nambaru P, Bougis PE, Possani LD, Tytgat J (2008) A common "hot spot" confers hERG blockade activity to alpha-scorpion toxins affecting K^+ channels. *Biochem Pharmacol* **76**: 805-815

Aiyar J, Withka JM, Rizzi JP, Singleton H, Andrews GC, Lin W, Boyd J, Hanson DC, Simon M, Dethlefs B (1995) Topology of the pore-region of a K^+ channel revealed by the NMR-derived structures of scorpion toxins. *Neuron* **15**: 1169–1181

Corona M, Gurrola GB, Merino E, Restano-Cassulini R, Valdez-Cruz NA, Garcia B, Ramïrez-Dominguez ME, Coronas FV, Zamudio FZ, Wanke E, Possani LD (2002) A large number of novel Ergtoxin-like genes and ERG K^+ channels blocking peptides from scorpions of the genus *Centruroides*. *FEBS Lett* **532**: 121–126

Crest M, Jacquet G, Gola M, Zerrouk H, Benslimane A, Rochat H, Mansuelle P, Martin-Eauclaire MF (1992) Kaliotoxin, a novel peptidyl inhibitor of neuronal BK-type Ca(2+)-activated K(+) channels characterized from *Androctonus mauretanicus mauretanicus* venom. *J Biol Chem* **267**: 1640-1647

Diego-García E, Abdel-Mottaleb Y., Schwartz EF, de la Vega RC, Tytgat J, Possani LD (2008) Cytolytic and K^+ channel blocking activities of beta-KTx and scorpine-like peptides purified from scorpion venoms. *Cell Mol Life Sci* **65**: 187-200

Huys I, Xu CQ, Wang CZ, Vacher H, Martin-Eauclaire MF, Chi CW, Tytgat J (2004) BmTx3, a scorpion toxin with two putative functional faces separately active on A-type K^+ and HERG currents. *Biochem J* **378**: 745-752

Lange A, Giller K, Hornig S, Martin-Eauclaire MF, Pongs O, Becker S, Baldus M (2006) Toxin-induced conformational changes in a potassium channel revealed by solid-state nmr. *Nature* **440**: 959–962

Legros C, Bougis PE, Martin-Eauclaire MF (2003) Characterisation of the genes encoding Aa1 isoforms from the scorpion *Androctonus australis. Toxicon* **41**: 115-119

Park CS, Miller C (1992) Interaction of charybdotoxin with permeant ions inside the pore of a K^+ channel. *Neuron* **9**: 307-313

Pisciotta M, Coronas FI, Bloch C, Prestipino G, Possani LD (2000) Fast K(+) currents from cerebellum granular cells are completely blocked by a peptide purified from *Androctonus australis* Garzoni scorpion venom. *Biochim Biophys Acta* **1468**: 203-212

Sabatier JM, Zerrouk H, Darbon H, Mabrouk K, Benslimane A, Rochat H, Martin-Eauclaire MF, Van Rietschoten J (1993) P05, a new leiurotoxin I-like scorpion toxin: synthesis and structure-activity relationships of the alpha-amidated analog, a ligand of Ca(2+)-activated K(+) channels with increased affinity *Biochemistry* **32**: 2763-2770

Tytgat J, Chandy KG, Garcia LM, Gutman GA, Martin-Eauclaire MF, Walt JJ, Possani LD (1999) A unified nomenclature for short chain peptides isolated from scorpion venoms: alpha-KTx molecular subfamilies. *Trends Pharmacol* Sci **20**: 445–447

Vacher H, Romi-Lebrun R, Mourre C, Lebrun B, Kourrich S, Masméjean F, Nakajima T, Legros C, Crest M, Bougis PE, Martin-Eauclaire MF (2001) A new class of scorpion toxin binding sites related to an A-type K^+ channel: pharmacological characterization and localization in rat brain. *FEBS Lett* **501**: 31-36

Vacher H, Alami M, Crest M, Possani LD, Bougis PE, Martin-Eauclaire MF (2002) Expanding the scorpion toxin alpha-KTX 15 family with AmmTX3 from *Androctonus mauretanicus*. *Eur J Biochem* **269**:6037-6041

Vacher H, Diochot S, Bougis PE, Martin-Eauclaire MF, Mourre C (2006) K_V4 channels sensitive to BmTX3 in rat nervous system: autoradiographic analysis of their distribution during brain ontogenesis. *Eur J Neurosci* **24**: 1325-1340

Toxines et Transferts ioniques – Toxins and Ion transfers
Rencontres en Toxinologie – Meeting on Toxinology, 2011
Editions de la SFET – SFET Editions
Accès libre en ligne sur le site – Free access on line on the site : http://www.sfet.asso.fr

Toxicity of sea anemone toxins related to their pharmacological activities on ion channels

Sylvie DIOCHOT[1,2*], Emmanuel DEVAL[1,2], Jacques NOEL[1,2], Laszlo BERESS[3], Michel LAZDUNSKI[1,2], Eric LINGUEGLIA[1,2]

[1] CNRS, Institut de Pharmacologie Moléculaire et Cellulaire, UMR 6097, 06560 Valbonne, France ; [2] Université de Nice-Sophia Antipolis, UMR 6097, 06560 Valbonne, France ; [3] IPF Pharmaceuticals, Feodor Lynen Strasse 31, Hanover 30625, Allemagne

** Corresponding author ; Tel : +33(0)4 9395 3422 ; Fax : +33(0)4 9395 7728 ; E-mail : spider@ipmc.cnrs.fr*

Abstract

Sea anemone peptides have been isolated since more than 30 years, the majority being highly toxic for their natural preys, crustaceans, but also for mammals. These neurotoxins which may have also cardiotonic properties are activators of voltage-dependent Na^+ channels. They represent a structural group of four β-fold peptides. Some of their basic and hydrophobic aminoacids are crucial determinants for their tissue and species selectivities. More recently, several groups of sea anemone peptides with different structures have been characterized with moderate toxicities on crustacean or mammals. They allowed the characterization of several subtypes of voltage-dependent K^+ channels involved in autoimmune diseases, and of acid-sensing ion channels (ASIC3) involved in pain processing. These last toxins could be promising tools for the design of new therapeutic molecules.

Toxicité des toxines d'anémones de mer en relation avec leur activité pharmacologique sur les canaux ioniques

De nombreuses toxines peptidiques de venins d'anémones de mer ont été isolées depuis plus de 30 ans du fait de leur activité hautement toxique chez leurs proies naturelles, les crustacés, mais aussi chez les mammifères. Il s'agit de toxines neuro-excitatrices parfois cardio-stimulantes activant les canaux Na^+ dépendants du potentiel. Elles forment un groupe structural homogène de toxines ayant 4 feuillets β dont la sélectivité inter-espèce et tissulaire semble dépendre de la présence de certains résidus d'acides aminés chargés ou hydrophobes. D'autres toxines, découvertes plus récemment, présentent des structures plus variables, avec des degrés de toxicité moindre chez les crustacés et mammifères. Ces dernières ont permis la caractérisation de sous-types de canaux K^+ dépendants du potentiel dont certains sont impliqués dans les maladies auto-immunes, et de certains canaux ASIC (canaux ioniques sensibles à l'acidité extracellulaire) impliqués dans la douleur. Ces dernières toxines sont des outils prometteurs pour la conception de nouvelles molécules thérapeutiques.

Keywords : *Acid-sensing ion channels, K_V channels, Na_V channels, sea anemone, toxicity.*

Introduction

Animal venom components are usually called toxins, a term which evokes danger for living animals and humans, and are considered as bioharzardous material. But what is the definition of a toxin? Generally an animal toxin is defined as a natural component of the venom, able to disturb nerve, muscle or cardiac function, resulting in an effect which contributes to immobilize preys or to kill predators. A toxin acts at a very low concentration, with a highly specific activity on a cell membrane receptor. Very interestingly, evidences have been accumulated showing that some toxins can also be of a great utility as pharmacological tools, having low or no toxicity, and usable for therapeutic purposes (Koh and Kini, 2011; Miljanich, 2004; Mouhat *et al.*, 2008).

Since more than 40 years, animal toxins have been isolated and characterized, first, due to a public health concern, to understand and treat the severe poisonings they are able to induce and which can be fatal in humans. Diverse degrees of toxicity are described such as cardiac arrhythmias, leading to cardiac arrest, neurological hyperexcitability, convulsions, hypertension, paralysis, blood perturbations (coagulation, hemolysis). Toxins (from spiders and scorpions) are also studied in agronomy, to discover new insecticides,

Abbreviations*: Acid Sensing Ion Channel (ASIC), Central Nervous System (CNS), Complete Freund's Adjuvant (CFA), Intra-CcerebroVentricular (i.c.v.), Intra-Cisternal (i.c.), Intra-Muscular (i.m.), Intra-Venous (i.v.), Molecular Weight (M. W.), Peripheral Nervous System (PNS), Sea Anemone (SA), TetrodoToXin (TTX), Voltage-gated Na^+ (Na_V) and K^+ (K_V) channels.*

because some for instance from spider and scorpions are very selective tools that provoke insect paralysis. Toxins can act on diverse specific targets including ion channels, cell receptors, and less specifically on membrane phospholipids. However, it has been also shown that venoms contain "non-toxic" toxins, which are not able to induce neither visible symptoms of toxicity nor lethality, when injected to mammals, insects or crustaceans. These "non-toxic" toxins are therefore particularly interesting tools to study the implication of the targeted receptors in diverse physiological functions and can sometimes lead to therapeutic applications.

Sea anemones belong to the phylum of *Cnidaria*, subdivided in three classes, *Hydrozoa*, *Scyphozoa* and *Anthozoa*. The last one includes around 6000 known species of sea anemones. The venom is present in specialized stinging organelles called nematocysts or cnidocysts, included in specialized cells, the cnidocytes. Nematocysts are distributed over the entire surface of the sea anemone body, which makes the venom difficult to extract. Usually, active components are extracted from the whole animal by using methanol/chloroform to obtain an aqueous extract which can be further separated by several steps of liquid chromatography (Beress *et al.*, 1975b).

The best characterized toxins in sea anemones are: (i) a group of peptides (or small proteins; M. W. from 3,000 to 6,000 Da) acting on ion channels of excitable membranes and (ii) cytolysins (M. W. 15,000-20,000 Da) which are proteins that have been characterized by their hemolytic activity. Most of the sea anemone peptides have a preference for crustaceans, their natural prey, but due to a closed evolutionary context, they also act on insects (Bosmans and Tytgat, 2007). To a lesser extent, and often due to their high affinity for specific ionic channels, they are also toxic for mammals. This review focuses on the sea anemone toxins effective on crustaceans and mammals, and describes their different degree of toxicity in relation with their specific molecular targets among different families of ion channels.

Diversity of neurotoxic and/or cardiotoxic sea anemone peptides affecting voltage-dependent Na^+ channels

The most studied sea anemone (SA) toxins have been isolated more than 40 years ago based on their ability to induce severe neurotoxic and/or cardiotoxic effects on a variety of crustacean, insect or mammal nerve and muscle preparations (Beress and Beress, 1975a; Norton, 1991; Romey *et al.*, 1976). These neurotoxins affect voltage-gated Na^+ channels (Na_V) which are supporting action potential initiation. Na_V channels are the molecular targets for toxins that can bind at six identified receptor sites, either by blocking the channel pore, either by modifying the gating properties of the channel (Catterall *et al.*, 2007). SA toxins bind to the receptor site 3, located on the domain IVS5-S6 of the α subunit of Na_V channels which is also targeted by scorpion and funnel web spider toxins. They have allowed identification of subtypes of channels because they act with high affinities on different neuronal, muscular, or cardiac Na_V. They slow-down the channel inactivation, allowing more Na^+ entry into the cells and prolong action potential duration. Generally, the sea anemone toxins acting on Na_V channels (SA-Na_V toxins) have voltage-dependent effects because they bind with more affinity at polarized membrane potentials.

The SA-Na_V toxins are polypeptides with molecular weights ranging between 3,000 and 5,000 Da that are cross-linked by 3 (or even more) disulfide bridges. Two different types have been described with distinct sequences and immunological properties. Type 1 toxins are isolated from Actiniidae (*Anemonia sp*, *Anthopleura sp*, *Bunodosoma sp*, *Condylactis sp*, see *Table 1*) and types 2 are isolated from Stichodactylidae families [*Radianthus* (*Heteractis*) *sp*, *Stichodactyla sp*; see *Table 1*; Bosmans and Tytgat, 2007]. The two types are also distinguished by their immunoreactivity, *i.e.* there is no antigenic cross-reactivity between them (Norton, 1991; Schweitz *et al.*, 1985). Structurally, the two types of SA-Na_V toxins contain four stranded anti-parallel β-sheets connected by two loops. One toxin, halcurin, possesses structural properties common to both type 1 and 2 toxins indicating that all these toxins have probably evolved from the same ancestral gene (Ishida *et al.*, 1997). The type 1 toxins display higher affinity for cardiac and skeletal muscle tetrodotoxin (TTX)-resistant Na_V channels. In brief, resistance of Na_V to TTX action is correlated to a high sensitivity to sea anemone toxins and *vice versa*.

Species selectivity can be observed for some toxins: AsI, AsIII, RpII, and ShI are inactive on Na_V channels of mammalian system whereas others, such as AsV, AP-A and AP-B, are both active on crustacean and also very active on mammalian Na_V channels (Kem *et al.*, 1989; Lazdunski *et al.*, 1986; Schweitz *et al.*, 1981).

Activity of highly neurotoxic SA toxins (characterized by trembling of tail, fasciculations, salivation, difficulty in breathing and paralysis) is related to an effect on TTX-resistant and TTX-sensitive Na_V channels (Norton *et al.*, 1981; Romey *et al.*, 1976; Schweitz *et al.*, 1981). The most neurotoxic SA toxins active on mammals are found in the two structural groups: AsII, AsV, AP-B, BgII, BgIII (type 1), and RPI –V (type 2) (*Table 1*). The most potent toxins for crustaceans are ShI, AETXII, and AETXIII (Norton, 1991; Shiomi *et al.*, 1997).

Neurotoxicity is sometime associated with cardiotoxicity resulting in paralysis after i.v. (mice), or i.m. (crustacean) administration, and can lead to death (convulsions, arrhythmia and ventricular fibrillation) using concentration as low as 2 µg/kg (i.c. in mammals, *Table 1*). The well known and characterized AsI, AsII and AsIII isolated from *Anemonia sulcata* are both active on crustacean inducing neurotoxic symptoms like tetanic contractions and paralysis in the crab after i.m. injections (Alsen, 1983). In mammal, cardiotoxic effects predominate after i.v. injection of AsI or AsII, compared to neurotoxic symptoms (Alsen, 1983). AsI and AsII (the most active) induce a significant cardiotonic (positive inotropic) effect (Alsen *et al.*, 1978; Renaud *et al.*, 1986) in different mammalian heart preparations. This effect is linked to the increased Na entry into cardiac cells coupled to a subsequent entry of Ca^{2+} through the Na/Ca exchanger. Cardiac effects are often characterized by a potent positive inotropic effect (case of AP-A at 0.1-1 µg/kg, i.v.) without any significant effect on heart or blood pressure, but at higher concentrations (>10 µg/kg, i.v.) they induce arrhythmia and

Table 1. Comparison of some sea anemone peptides structure, toxicities and targets.
Tableau 1. *Comparaison des structures, propriétés toxiques et cibles de peptides d'anémones de mer.*

Toxin (origin: ***Genus species***)	M. W. (AA)	Structure (PDB) classification	Specie / tissue selectivity	Toxicity: DL_{50} (µg/kg)	Target	References
AeK *Actinia equina*	3807(36)	2α, 6C SAK-I	?	?	K_V1	(Minagawa *et al.*, 1998)
AETXI *Anemonia erythrea*	4963(47)	4β, 6C Type 1	Crust	2 (crab) NL (i.v./mice)	Na_V?	(Shiomi *et al.*, 1997)
AETXII	6502(59)	New struct, 10C	Crust	0.5 (crab) NL (i.v./mice)	?	(Shiomi *et al.*, 1997)
AETXIII	6562(59)	New Struct, 10C	Crust	0.3 (crab) NL (iv/mice)	?	(Shiomi *et al.*, 1997)
AmI *Anthopleura maculata*	2803(27)	New	?	830 (crab)	?	(Honma *et al.*, 2005; Honma and Shiomi, 2006)
AmII	5128(45)	4β,6C SAKIII	?	NL (crab) paralytic	K_V?	(Honma *et al.*, 2005; Honma and Shiomi, 2006)
AmIII	5134(47)	4β, 6C Type 1	Crust	70 (crab)	Na_V?	(Honma *et al.*, 2005)
AsI (ATXI) *Anemonia sulcata*	4834(46)	4β, 6C (1ATX) Type 1	Crust Cardiac, neuron	4 (crab) 236 (i.c./mice)	Na_V?	(Alsen *et al.*, 1978; Beress and Beress, 1975a; Schweitz, 1984; Schweitz *et al.*, 1981)
AsII (ATXII)	4949(47)	4β, 6C Type 1	Crust& mammals Cardiac, neuron	4 (crab) 2.5 (i.c./mice)	Na_V	(Alsen *et al.*, 1978; Beress and Beress, 1975a; Schweitz, 1984)
AsIII	2932(27)		Crust Neuron	7 (crab) 300 (i.c./mice)	Na_V	(Beress and Beress, 1975a; Schweitz *et al.*, 1981)
AsV		4β, 6C Type 1	Crust, mammals Cardiac, neuron	<10 (crab) 2 (i.c./mice)	Na_V	(Schweitz *et al.*, 1981)
AsKC2	6772(58)	2β, 1α, 6C SAKII			$K_V1.2$	(Schweitz *et al.*, 1995)
AsKS	3834(36)	2α, 6C SAK-I			$K_V1.2$	(Diochot *et al.*, 1998; Schweitz *et al.*, 1995; Yeung *et al.*, 2005)
BDS-I	4715(43)	4β,6C (1BDS) SAKIII			K_V3	(Diochot *et al.*, 1998; Yeung *et al.*, 2005)
AP-A (AxI) *Anthopleura xanthogrammica*	5132(49)	4β, 6C (1AHL) Type 1	Crust, mammals Cardiac	22 (crab) 5 (i.c./mice) 66-400 (i.p./mice)	Na_V TTXr	(Schweitz, 1984; Shibata *et al.*, 1976)
AP-B (AxII)	5268(49)	4β, 6C (1APF) Type 1	Crust, mammals Neuron	78 (crab) 0.2 (i.c./mice)	Na_V	(Norton, 1978; Norton *et al.*, 1981)
AXPI-I	(58)	2β, 1α, 6C SAKII				(Minagawa *et al.*, 1997)
AP-C (APE2-1) *Anthopl. elegantissima*	4877(47)	4β, 6C Type 1	Crust, mammals Cardiac	1 (crab)	Na_V TTXr	(Bruhn *et al.*, 2001; Norton, 1978)
APETx1	4552(42)	4β,6C (1WQK) SAKIII	Cardiac		HERG	(Diochot *et al.*, 2003)
APETx2	4558(42)	4β,6C (1WXN) SAKIII	Neuron		ASIC3 $Na_V1.8$	(Blanchard *et al.*, 2011; Diochot *et al.*, 2004)
BgII *Bunodosoma granulifera*	5072(48)	4β, 6C Type 1	Insects, mammals Cardiac, neuron	0.4 (i.c./mice)	Na_V	(Bosmans *et al.*, 2002; Goudet *et al.*, 2001; Loret *et al.*, 1994)
BgK	4275(37)	2α, 6C SAK-I	Crust, mammals	4.5 (i.c./mice)	K_V1	(Aneiros *et al.*, 1993; Cotton *et al.*, 1997)
BcIV *Bunodosoma caissarum*	4669(41)	4β,6C SAKIII		NL >2000 (crab) paralytic	?	(Oliveira *et al.*, 2006)
CgII *Condylactis gigantea*		4β, 6C Type 1	Crust	0,2 (crab)		(Salgado and Kem, 1992)
SGI	5395(50)	4β, 6C Type 1	Crust	14 (crab) NL (i.v./mice)		(Schweitz *et al.*, 1981)
GiganTxI	(48)	4β, 6C Type 2	?	NL >1000(crab) paralytic NL>1000 (i.c./mice)	EGF activity	(Shiomi *et al.*, 2003)
Halcurin *Halcurias sp*	5080(47)	4β, 6C Type 1 & 2	Crust	6 (crab) NL >1000(mice)		(Ishida *et al.*, 1997)
Rp-I *Radianthus (Heteractis)paumotensis*		4β, 6C Type 2	Crust, mammals Muscle & neuron	36 (crab) 1.5 (i.c./mice)	Na_V	(Schweitz *et al.*, 1985)
RpIII	5330(48)	4β, 6C Type 2	Crust, mammals Muscle & neuron	10 (crab) 2 (i.c. /mice)	Na_V	(Schweitz *et al.*, 1985)
ShI *Stichodactyla helianthus*	5137(48)	4β, 6C (1SHI) Type 2	Crust NL (mice)	0.3 (crab) >15000 (i.p./mice)	Na_V	(Kem *et al.*, 1989; Salgado and Kem, 1992)
ShK	4055(35)	2α, 6C (1ROO) SAK-I	Crust, mammals	More toxic than BgK?	K_V1, K_V3	(Pennington *et al.*, 1995; Yan *et al.*, 2005)
ShPI	6110(55)	2β, 1α, 6C SAKII	?	?	?	(Antuch *et al.*, 1993)
SHTXI, SHTXII *Stichodactyla haddonii*	3059(28)	2α, 6C SAK-I	Crust (NL)	1000 (crab) NL, paralytic	K_V1	(Honma *et al.*, 2008)
SHTXIII	7035(62)	2β, 1α, 6C SAKII	Crust (NL)	>1000 (crab) NL, paralytic	K_V?	(Honma *et al.*, 2008)
SHTXIV	5229(48)	4β, 6C Type 2	Crust	93 (crab)	Na_V?	(Honma *et al.*, 2008)

References listed here are not exhaustive but are examples of some structural, pharmacological characterization of toxins and their toxicity studies; Sea anemone *genus* and *species* are indicated at the head of each group of toxin from a same SA. Abbreviations used are: Crust: crustacean, NL:

Non Lethal; NT: Non toxic, i.c.: intracisternal, i.m.: intramuscular; "?" indicates an unknown or proposed target; DL_{50} in crabs were determined after i.m. injections. *Les références citées ici ne constituent pas une liste exhaustive mais sont quelques exemples d'étude de la caractérisation structurale et pharmacologique des toxines et de leur toxicité. Les genres et espèces d'anémones de mer sont indiqués en italique à la tête de chaque groupe de toxine issu d'une même espèce. Les abréviations utilisées sont: Crust: crustacé, NL: Non Létal; NT: Non toxique, i.c.: intracisternale, i.m.: intramusculaire; "?" indique une cible inconnue ou proposée; les DL_{50} chez le crabe sont déterminées après une injection i.m.*

ventricular fibrillation which are the cause of death in mammals (Alsen *et al.*, 1978; Bruhn *et al.*, 2001; Renaud *et al.*, 1986; Shibata *et al.*, 1976). The molecular mechanism implicates a major action on cardiac TTX-resistant Na_V channels, which leads to delayed inactivation (closure) of fast Na^+ currents and a prolongation of the action potential duration. Interestingly, AsIII, a short toxin whose structure is different from type 1 and 2 SA-Na_V toxins, is specifically toxic on crustaceans and active on their Na^+ currents (Warashina *et al.*, 1988). AsIII is completely devoid of toxicity on mice and unable to displace AsII from its receptor site on neuronal Na_V channels (Schweitz *et al.*, 1981).

Structure-function studies using chemical modifications or mutants revealed some crucial aminoacids responsible for species or tissue specificity, toxicity and binding to their receptor. In particular, a cluster of positively charged residues (Arg and Lys) and some hydrophobic residues are essential for the activity of type 1 and 2 toxins (Kelso *et al.*, 1996; Loret *et al.*, 1994). Some examples are given below:

- In AsII, His32, His37, Lys 35, Lys36 and Lys 46, are important for toxicity and also for binding activity (Barhanin *et al.*, 1981) while Asp7 Asp9 and Gln47 are related only to toxicity. Arg14 placed in a flexible loop which is conserved among type 1 and 2 SA toxins is important for toxicity and binding (Seibert *et al.*, 2003).
- Hydrophobic residues like Leu18 and W33 in AP-B are important for binding affinities on Na_V (Dias-Kadambi *et al.*, 1996b; Dias-Kadambi *et al.*, 1996a).
- Lys 37 residue in Ap-B is crucial for Na_V interaction on site3 (Benzinger *et al.*, 1998).
- Examples of toxins sharing both neurotoxic and cardiotoxic properties are AsII, AsV, AP-A, AP-B, APE1-1, AP-C. The presence of Arg13, Pro14 and Lys49 in AP-B allows the discrimination between neuronal and cardiac channels (Kelso *et al.*, 1996).

Moreover, it is supposed that amino acids which determine the mammalian specificity could be His39 and Pro 41 which are found in all mammalian toxins sequenced so far, and are absent in toxins with no activity on mammalian channels (Lazdunski *et al.*, 1986).

Finally, a few number of SA toxins, presenting new structures, have been characterized along with the crustacean toxic SA peptides. AETXII, AETXIII, and gigantoxin I, while being highly toxic to crabs, are structurally distinct from the known SA type 1 or 2 toxins, and share homologies with spider neurotoxins and mammalian EGF factors, respectively (Shiomi *et al.*, 2003; Shiomi *et al.*, 1997). AETXII and AETXIII are longer peptides (59 residues), including 10 half cysteines. Another toxin, AmI displays low toxicity for crabs and presents a new structure. It is a short peptide, having no sequence homologies with any known SA-Na_V toxin, and it could have another target among the large families of voltage-gated ionic channels (Honma *et al.*, 2005).

The purification of "toxic" components from sea anemone species has been largely investigated before 1980, and only a few toxins have been described since then with new structure, pharmacology and sometimes relatively low toxic effects on crustaceans and mammals.

Sea anemone peptides that block voltage-dependent K^+ channels: diversity of structure, toxicities and targets

Besides the nearly 50 SA-Na_V toxins characterized so far, few toxins acting on voltage-dependent K^+ channels (K_V) were discovered after 1990. These K_V channel blockers contribute to the toxic symptoms of envenomation, because they act synergistically with Na_V activators, by prolonging the action potential duration maintaining the membrane hyperexcitability and increasing acetylcholine release at nerve endings. Some of these neurotoxins display paralysing activity only in crab without any lethality (AmII, BgK, SHTX I, *Table 1*). Neurotoxicity after central injections in mammals, have been described for the toxins which target K_V1 channels. These neurotoxic effects include hyperexcitability, trembling, fasciculations, and salivation (Cotton *et al.*, 1997).

Potassium channels are the most diverse class of ion channels and are expressed in a large variety of tissues, in both excitable and non-excitable cells. They are key regulators of neuronal excitability by setting the resting membrane potential and controlling the shape, frequency and repolarization phase of action potentials (Shieh *et al.*, 2000). The cloning of about 80 potassium channel genes has allowed a classification into three structural groups. The six transmembrane segments, one pore domain K^+ channels, which are either voltage-dependent (K_V) or calcium-dependent (K_{Ca}) are targeted by a large number of animal toxins. Due to their high specificity and affinity for K^+ channels, these toxins have facilitated the structure–function studies of K^+ channels (Aiyar *et al.*, 1995; MacKinnon, 1991).

Sea anemones have evolved to produce structurally different peptides that target some of the K_V channel subfamilies and use different binding mechanisms and modes of action. These toxins can be classified into three types, based on their structural homologies (Diochot, 2009; Honma and Shiomi, 2006; *Figure 1*). "Sea Anemone Potassium type 1" (SAK-I) are short peptides (35 to 37 amino acid residues) with 2 α helices ("$\alpha\alpha$-type fold") and 3 disulfide bridges. The SAK-II group includes long peptides (58-59 amino acids) having 3 disulfide bridges. These peptides share homologies with Kunitz-type protease inhibitor and also with dendrotoxin-I (DTX-I, a K_V1 channel inhibitor isolated from black mamba). The third group (SAK-III) of toxins

belong to the β-defensin fold family ("all beta structure") which includes peptides of various origins, including human, snake, *Platypus*, some of them display antimicrobial, or, analgesic activities (Torres and Kuchel, 2004).

The SAK-I group of toxins and their relative toxicities

The pharmacology of SAK-I and SAK-II toxins have been first described with respect to their ability to displace, with subnanomolar affinities, the DTX-I binding to its specific brain membrane receptors, mainly represented by $K_V1.1$, $K_V1.2$, and $K_V1.6$ channels, and also scorpion (charybdotoxin) binding to T lymphocytes expressing the $K_V1.3$ channel (Aneiros *et al.*, 1993; Dauplais *et al.*, 1997; Gendeh *et al.*, 1997; Schweitz *et al.*, 1995; Tudor *et al.*, 1996; Tytgat *et al.*, 1995).

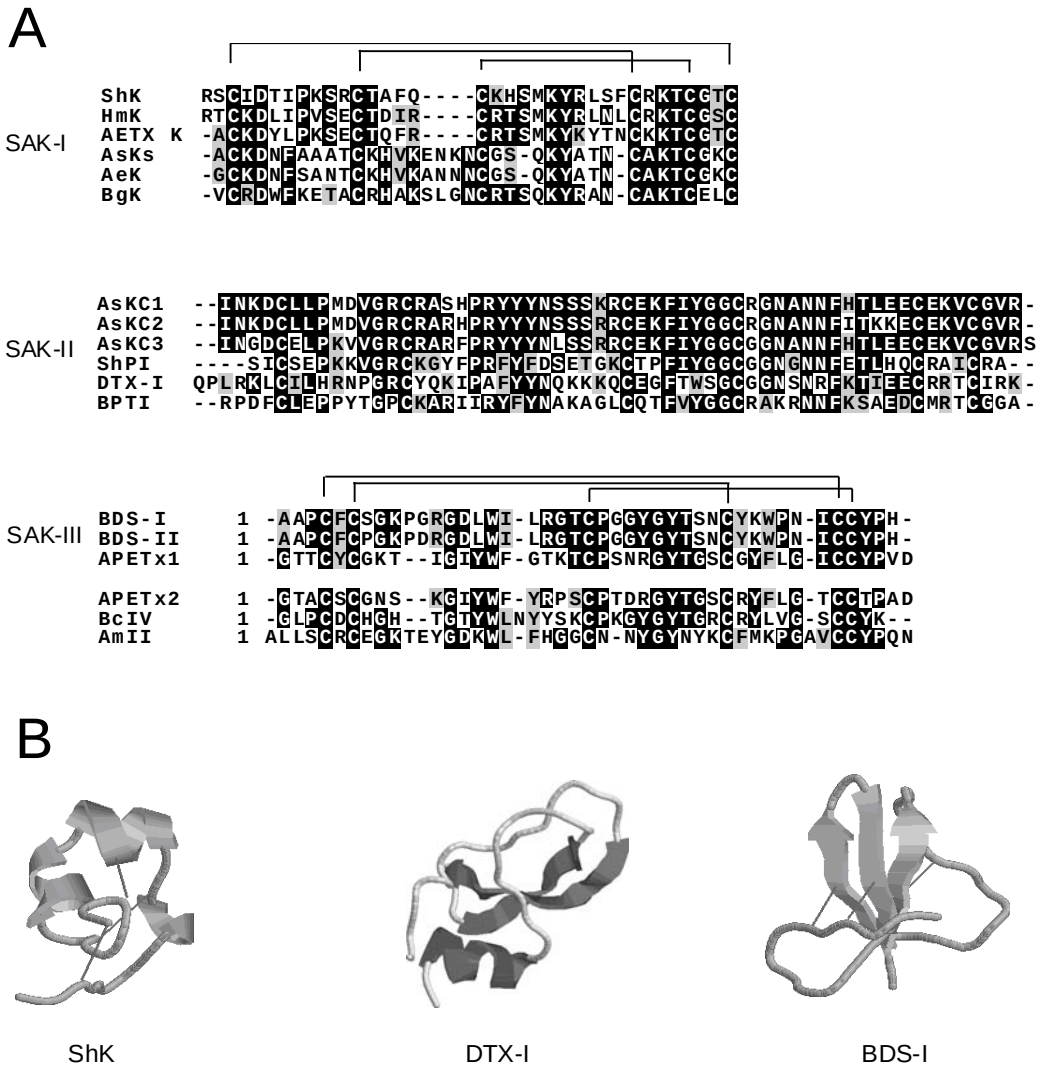

Figure 1. Structure of sea anemone toxins in the different SAK groups. (**A**) Multiple peptide sequence alignment of the three groups of known sea anemone toxins. Amino acid identities (*black boxes*) and homologies (*grey boxes*) are shown. (**B**) The sea anemone K^+ channel inhibitors belong to three different structural groups. The ribbon structures were drawn with the RASMOL program, using coordinates from the Protein Data Bank. In the SAK-I group, peptides with two short α-helices and one helical turn are represented by ShK (PDB code 1ROO). The SAK-II type includes peptides with a two-stranded β-sheet and two α-helices, represented here by DTX-I (PDB code 1DEN). In the SAK-III group are peptides showing a triple-stranded antiparallel β-sheet without α-helix, like BDS-I (PDB code 1BDS). Lines correspond to disulfide bridges. BcIV, and AmII belong to the same structural SAK-III group but their pharmacological activity is not determined. In the same group, APETx2 is active on ASIC3 channels.

Figure 1. *Structure des toxines d'anémones de mer dans les différents groupes SAK. (**A**) Alignements de séquences peptidiques pour les trois groupes connus de toxines d'anémone de mer. Les acides aminés identiques (*carrés noirs*) et homologues (*carrés gris*) sont montrés. (**B**) Les toxines d'anémones de mer inhibitrices des canaux K^+ appartiennent à trois groupes structuraux différents. Les structures ont été élaborées avec le programme RASMOL en utilisant les coordonnées PDB. Dans le groupe SAK-I, les peptides ayant deux hélices α courtes sont représentés par ShK (PDB code 1ROO). Le groupe SAK-II comporte des peptides ayant deux feuillets β et deux hélices α, représenté ici par DTX-I (PDB code 1DEN). Dans le groupe SAK-III se trouvent des peptides ayant un triple feuillet βantiparallèle sans hélice α, tel que BDS-I (PDB code 1BDS). Les lignes correspondent aux ponts disulfures. BcIV et AmII appartiennent à la même famille structurale dans le groupe SAK-III mais leur activité pharmacologique n'est pas encore connue. Dans ce même groupe, APETx2 inhibe les canaux ASIC3.*

In the first of SAK-I group, the best characterized toxins are BgK, a minor component of the sea anemone *Bunodosoma granulifera*, ShK and HmK, peptides isolated from *Stichodactyla helianthus* and *Heteractis magnifica*, respectively, acting from picomolar to nanomolar concentration on different K_V1 channels subtypes, with an inhibition process independent of channel opening (Aneiros *et al.*, 1993; Cotton *et al.*, 1997; Gendeh *et al.*, 1997; Kalman *et al.*, 1998; Pennington *et al.*, 1995; *Figure 1A*). BgK was described as a potent neurotoxin able to induce paralysis, trembling of tail, fasciculations and death in mice (*Table 1*, Cotton *et al.*, 1997). Its affinity for specific neuronal subtypes of K_V1 channels ($K_V1.1$, $K_V1.2$, $K_V1.3$ and $K_V1.6$) is shared with ShK, which has even better affinity (picomolar) for the same channels (Cotton *et al.*, 1997; Kalman *et al.*, 1998). It can be supposed by extension that ShK is also able to induce severe neurotoxic symptoms and lethality as for DTX-I, the most neurotoxic peptide isolated from snake already known to inhibit $K_V1.1$, $K_V1.2$ and $K_V1.6$ with nanomolar affinities (Harvey, 2001). In leukemia cells, ShK and BgK also block the intermediate-conductance Ca^{2+}-activated K^+ current ($IK_{Ca}1$), a current regulating the membrane potential and modulating the calcium signal in many different type of cell types (T lymphocytes, erythrocytes, coloncytes; Rauer *et al.*, 1999). An extended interaction of ShK with other families of K_V channels was also shown. ShK blocks with high affinity (IC_{50} = 0.3-6 nM) the $K_V3.2$ current, which is critical for high-frequency repetitive firing in cortical GABAergic fast-spiking interneurons (Yan *et al.*, 2005).

The SAK-II group of toxins

Only seven SA toxins are described in this group: the 3 kalicludines (AsKC1-3), ShPI isolated from *Stichodactyla helianthus* (Antuch *et al.*, 1993), AEPI-I isolated from *Actinia equina* (Ishida *et al.*, 1997), AXPI-I from *Anthopleura xanthogrammica* (Minagawa *et al.*, 1997) and SHTXIII from *Stichodactyla haddoni* (Honma *et al.*, 2008; *Figure 1*). These toxins are not toxic for crustaceans. Although extensive studies have shown that SAK-I peptides inhibit K_V subtypes in transfected mammalian cells and neuronal preparations, only the kalicludines were tested for their K_V blocking effects in the SAK-II group (Schweitz *et al.*, 1995). AsKC2 inhibits $K_V1.2$ channels with a lower affinity (IC_{50} > 1µM) than DTX-I, and it is not excluded that other K_V1 channels could be targets for kalicludines, but this remains to be determined.

The other peptides ShPI, AEPI-I, AXPI-I and SHTX III have yet no pharmacology described on K^+ channels although one of them (SHTX III) is able to displace DTX-I from its receptor on rat synaptosomal membranes and has been described as a non lethal peptide for crabs (Honma *et al.*, 2008).

The SAK-III group of toxins are not toxic

In the SAK-III type group, the two BDS (Blood Depressing Substances) toxins are very similar 43 amino acid peptides, isolated from *Anemonia sulcata* extracts in 1985 (*Figure 1*). They were patented for their antihypertensive and antiviral activities (against Herpes simplex type I and mouse hepatitis virus) after intravenous injections in mammal (Beress *et al.*, 1985; Driscoll *et al.*, 1989a; Llewellyn and Norton, 1991). BDS-II, the most active, decreased the blood pressure by 50% in cats at a dose of 1 µg/kg. At this time, BDS toxins, which are able to induce negative inotropic effects and also to compete with AP-A binding on rat brain synaptosomes, were considered as antagonists of Na_V channels (Llewellyn and Norton, 1991). However, BDS-I and BDS-II inhibition on K_V channels was described 13 years later on $K_V3.4$ (IC_{50} = 42 nM), $K_V3.1$ and $K_V3.2$ channels (Diochot *et al.*, 1998; Yeung *et al.*, 2005). Both toxins induce a positive shift of the activation curve of $K_V3.1$- and $K_V3.2$-mediated currents, indicating that BDS toxins act as gating modifiers similar to a number of spider toxins acting on K_V2 and K_V4 channels. The BDS peptides would be promising tool to study the role of K_V3 channels in pathologies, since $K_V3.4$ channels may be of particular importance in skeletal muscle periodic paralysis (Abbott *et al.*, 2001), or in Alzheimer's disease where the $K_V3.4$ gene seems to be overexpressed in cerebral cortex (Angulo *et al.*, 2004; Lien and Jonas, 2003) and Parkinson disease (Baranauskas *et al.*, 2003).

In the same SAK-III group, APETx1, a 42 amino acid peptide isolated from *Anthopleura elegantissima,* shares 54% sequence homology with BDS toxins but has a different activity on K^+ channels. APETx1 has moderate effects on $K_V1.4$ currents at high concentrations, but it is a specific blocker of the human *ether a go-go* related gene (human ERG, HERG) K^+ channel (IC_{50} = 34 nM; Diochot *et al.*, 2003). HERG is particularly expressed in mammalian heart where it contributes to the rapidly activating delayed rectifier potassium current (IKr) which controls the duration of the plateau phase of the action potential (Sanguinetti *et al.*, 1995). Several mutations on the HERG gene are responsible for inherited disorders characterized by abnormal slow repolarization of action potentials associated with long QT intervals (Sanguinetti *et al.*, 1996). APETx1 shifts the voltage-dependence of HERG activation towards depolarizing states (Diochot *et al.*, 2003; Zhang *et al.*, 2007), acting as a gating modifier rather than a pore blocker. APETx1, owing to its different and unique structure, has been reported to be selective for the neuronal and cardiac (human and rat) ERG1 channels. It does not compete with the scorpion toxins ErgTx1 and BeKm-1, also known to block ERG1 channels, suggesting binding to another region of the channel (Chagot *et al.*, 2005a; Restano-Cassulini *et al.*, 2006; Wanke and Restano-Cassulini, 2007).

Interestingly, SAK-III peptides are not toxic or lethal after *in vivo* injections in crustaceans or mammals (crabs or mice) unlike sea anemone Na_V and K_V1 toxins previously described (*Table 1*). BDS and APETx1 were isolated from HPLC fractions lacking toxicity after i.m. injection in crabs (Beress, personal communication). Moreover, our experiments using the central i.c. or i.c.v. injections of BDS in rodents were unable to induce any neurotoxic effects (Diochot *et al.*, 1998; Driscoll *et al.*, 1989a).

In the same group, AmII and BcIV purified from *Antheopsis maculata* (Honma *et al.*, 2005) and *Bunodosoma caissarum* (Oliveira *et al.*, 2006), respectively, have no lethal effect on crab or mice. Although

BcIV is supposed to be a Na_V activator because it prolongs the action potential duration on crab nerve, it is less potent than BcIII, a type 1 Na_V toxin. It could also be possible that this toxin acts on K_V, which was not tested.

The SAK-III group includes another peptide, APETx2, which shares 64% sequence identity with APETx1 and blocks a Na^+ permeable Acid-Sensing Ion Channel, ASIC3 (Chagot *et al.*, 2005b; Diochot *et al.*, 2004) and, although with less affinity, a TTX-resistant-Na_V channel (Blanchard *et al.*, 2011). Our recent work has shown the potent peripheral analgesic effect of this peptide.

Non toxic polypeptides with therapeutic perspectives

Use of ShK in autoimmune diseases

The ShK toxin-channel interaction studies allowed the design of new types of toxins, such as ShK-Dap22 a mutant peptide where Lys22 has been replaced by a diaminopropionic acid. Binding and electrophysiological studies have shown that ShK-Dap22 is a highly potent and selective blocker of the $K_V1.3$ channel with a 100-fold decreased affinity for $K_V1.1$, $K_V1.4$ and $K_V1.6$ channels (Kalman *et al.*, 1998). A high expression level of $K_V1.3$ is considered as a marker for activated effector memory T cells (T_{EM} cells) which are involved in the pathogenesis of autoimmune diseases. Therefore, the selective suppression of autoreactive T_{EM} cells with $K_V1.3$ blockers might constitute a novel approach for the treatment of multiple sclerosis and other autoimmune diseases, such as type-1 diabete mellitus or psoriasis. Both ShK and ShK-Dap22 were proven to prevent and treat rat autoimmune encephalomyelitis (Beeton *et al.*, 2001; Norton *et al.*, 2004). In addition, ShK-F6CA, a fluorescein-labelled analogue of ShK, has been reported to have potential applications in the diagnostic of autoimmune diseases (Beeton *et al.*, 2003; Norton *et al.*, 2004). This peptide, containing an additional negatively-charged moiety at the N-terminus, has a higher affinity and selectivity than ShK for $K_V1.3$ channels, allowing a specific detection of activated T_{EM} cells implicated in multiple sclerosis.

Analgesic properties of APETx2, an inhibitor of ASIC3-containing channels

Tissue acidosis is commonly associated with pain and is a factor found in inflammation, ischemia, fractures, haematomas, tumour development, or muscle incisions like for instance after surgical procedures. Tissue acidosis produces pain *via* the depolarization of the peripheral terminals of nociceptive neurons, which detect noxious stimuli. Ion channels gated by protons and present in nociceptors such as TRPV1 (Transient Receptor Potential channels Vanilloid 1) and ASICs, are mediating this depolarization. ASICs are of particular interest since they are particularly sensitive to extracellular protons (the native ASIC-like responses are approximately 10-fold more sensitive to changes in H^+ than the TRPV1 responses), being able to activate for very small acidifications. In addition, some ASICs (ASIC3) generate a sustained depolarizing current compatible to the detection of non-adapting pain (Deval *et al.*, 2010; Deval *et al.*, 2008; Lingueglia, 2007; Yagi *et al.*, 2006).

ASICs belongs to the degenerin/epithelial sodium channel (Deg/ENaC) superfamily (Bianchi and Driscoll, 2002; Kellenberger and Schild, 2002; Waldmann *et al.*, 1996) and are related to the FMRFamide-gated Na^+ channel FaNaC identified from the invertebrate nervous system (Lingueglia *et al.*, 1995; Lingueglia *et al.*, 2006). They are expressed in both mammalian central (CNS) and peripheral (PNS) nervous system, and particularly in nociceptors where they are proposed to detect acidosis to inform the CNS about tissue damages. Six different proteins have now been identified in rodents: ASIC1a, ASIC1b, ASIC2a, ASIC2b, ASIC3 and ASIC4; these proteins are encoded by four genes. Functional channels, generated by the association of 3 subunits (homo- or heterotrimers), are activated by acidic pH to mediate a sodium-selective, amiloride-sensitive, current (Babinski *et al.*, 2000; Bassilana *et al.*, 1997; Hesselager *et al.*, 2004; Jasti *et al.*, 2007; Ugawa *et al.*, 2003; Waldmann *et al.*, 1999). The pharmacology of ASICs is restricted to non selective drugs which activate or inhibit the currents at high concentration ranges. To date, only two peptides isolated from spider and sea anemone venoms were characterized as selective and high affinity blockers of ASIC1a and ASIC3, respectively. The spider toxin PcTx1 proved to behave similarly to a “gating modifier toxin” by changing the H^+ affinity of ASIC1a (Chen *et al.*, 2005; Salinas *et al.*, 2006). The sea anemone peptide APETx2 displays structural elements common to other sea anemone toxins in the SAK-III group but is a specific inhibitor for ASIC3. These two toxins have been of a great utility to dissect the role of ASIC isoforms in functions related to pain in the PNS and CNS.

The sea anemone peptide APETx2 is a major constituent in the venom of *Anthopleura elegantissima*. It is a basic (pI = 9.59) peptide of 42 amino acids crosslinked by three disulfide bridges. APETx2 displays a high sequence homology (76%) with APETx1 but some sequence homologies are also found with BDS peptides (57%) which block $K_V3.4$ channels, and with AP-A, AP-B, AP-C toxins (41-47%) which activate Na_V channels. APETx2 structure was determined by two-dimensional ^{1}H-NMR using the native toxin (Chagot *et al.*, 2005b). It consists of a compact disulfide-bonded core composed of a four stranded β-sheet from which a loop (15-27) and the N- and C-termini emerge. The mode of action of APETx2 remains to be determined.

APETX2 blocks ASIC3 containing channels (IC_{50} of 63 nM on homotrimeric ASIC3 to 2 µM on heterotrimeric channels) in various expression systems (Diochot *et al.*, 2004; *Table 1*). It has been also shown recently that APETx2 inhibits the TTX-resistant $Na_V1.8$-mediated current present in DRG neurons with an IC_{50} of 2.6 µM (Blanchard *et al.*, 2011). In DRG neurons, APETx2 (3 µM) inhibits 50% of an ASIC3-like current, mainly constituted by ASIC3 homomers and heteromers, which was recorded in 26.5% of the neurons. The inhibition of the transient peak ASIC3-mediated current is rapid and fully reversible. The effect of APETx2 on ASIC3 containing channels in the PNS (order of potency ASIC3 > ASIC2b+3 > ASIC1b+3 > ASIC1a+3) prompted us to test its effects on different pain models in rodents since it does not block central ASIC1a or ASIC2a (Deval *et al.*, 2008; Diochot *et al.*, 2004).

APETx2 confers analgesic properties when applied peripherally to rodents. First, APETx2 can suppress bursts of activity induced by moderate tissue acidification (pH around 7.0) in nociceptive C-fibres in a rat nerve-skin preparation (Deval *et al.*, 2008; *Figure 2A*). Second, APETx2 can prevent spontaneous pain behaviour (hindpaw flinches) in rodents when a cocktail of ASIC3 activators (moderate acidification, hypertonic solution, and arachidonic acid) are injected in rat hind paw (*Figure 2B*).

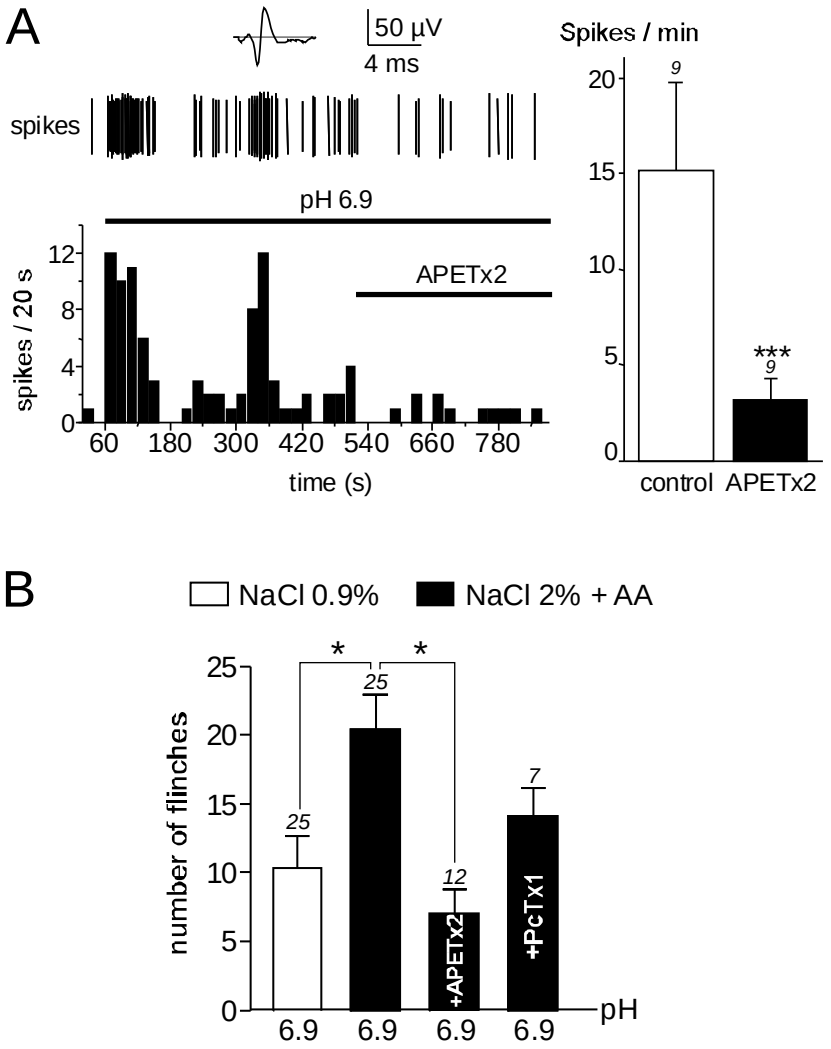

Figure 2. Effect of ASIC3 inhibition by APETx2 on acid and inflammatory pain (according to *Figures 1B* and *3E* from Deval *et al.*, 2008). (**A**) Response of an unmyelinated C-fibre to pH 6.9 (*spikes*) with the corresponding time plot of the spike-frequency shown below. The firing of action potential is maintained at pH 6.9, and application of APETx2 (10 µM) inhibits the response. The *top trace* shows the average action potential. Average spike frequency at pH 6.9 and pH 6.9 with 10 µM APETx2 (n=9) is presented on the *right*. (**B**) Effect on pain behaviour in rat of subcutaneous injections of acid (pH 6.9), hyperosmolarity, and 10 µM arachidonic acid (AA) together are compared with the effect of pH 6.9 alone. Conditions under which 10µM APETx2 or 60nM PcTx1 were added to the injected inflammatory cocktail are indicated on the bargraph. The number of experiments (n) is indicated above each bar (* P<0.05, Kruskal-Wallis test followed by a Dunn's *post hoc* test).

Figure 2. *Effet de l'inhibition de ASIC3 par APETx2 sur la douleur acide et inflammatoire (selon les* Figures 1B *et* 3E *de Deval* et al*., 2008). (**A**) Réponse à pH 6.9 (*pics d'activité*) d'une fibre de type C non myélinisée et tracé montrant la fréquence des signaux au cours du temps (*montré en dessous*). Le déclenchement du potentiel d'action est maintenu à pH 6.9 et l'application d'APETx2 (10 µM) inhibe la réponse. Une* trace au dessus *montre le potentiel d'action. La fréquence des signaux moyennée à pH 6.9 et pH 6.9 en présence de 10 µM d'APETx2 (n=9) est montrée* à droite*. (**B**) Effet de l'injection sous-cutanée d'acide (pH 6.9) d'une solution hyperosmotique, et de 10µM d'acide arachidonique (AA) comparées ensemble à l'effet du pH acide (6.9) seul. Les conditions selon lesquelles 10µM d'APETx2 ou 60nM de PcTx1 ont été rajoutées au cocktail inflammatoire sont indiquées sur la barre de l'histogramme. Le nombre d'expériences (n) est indiqué au dessus de chaque barre (* P<0.05, test Kruskal-Wallis suivi d'un test Dunn's* post hoc*).*

Under the same experimental conditions, the spider toxin PcTx1, which specifically blocks homomeric ASIC1a-mediated currents, is unable to prevent analgesia. In a model of inflammation induced by peripheral injections of Complete Freund's Adjuvant (CFA) in rats, heat hyperalgesia is prevented when APETx2 is co-injected with CFA. This analgesic effect was also obtained by using specific ASIC3 siRNA in rats, strongly

suggesting the implication of ASIC3 as sensors of tissue acidosis and integrators of several signals produced during inflammation, thus contributing to inflammatory hyperalgesia (Deval *et al.*, 2010; Deval *et al.*, 2008; Karczewski *et al.*, 2010). Another study on acidic pain on a rat gastrocnemius muscle model shows that a pre-treatment with APETx2 is able to prevent the development of mechanical hypersensitivity. In the same pain model induced by an inflammation (CFA), local administration of APETx2 has also analgesic properties (Karczewski *et al.*, 2010). In a recent work, our group has shown that the expression of ASIC3 is increased in sensory neurons innervating the hindpaw plantar muscle in a model of rat postoperative pain induced by hindpaw skin and muscle incision in rats (Deval *et al.*, 2011). In this model, spontaneous, thermal, and postural pain behaviours are measured 4 hours after surgery by using flinching, Hargreaves (heat hyperalgesia), and weight bearing tests, respectively. Interestingly, spontaneous pain and heat hyperalgesia behaviours are significantly reduced by a local intra-operative application of 20 µM APETx2, but it has no effect on postural pain (*Figure 3A-C;* Deval *et al.*, 2011). However, the postural pain behaviour is attenuated in animals treated with APETx2, 24 hours after the surgery (*Figure 3D*). In conclusion, peripheral analgesic properties were recently demonstrated for APETx2, both in acidic, inflammatory and postoperative pain. Although analgesic effects of APETx2 cannot exclude the participation of $Na_V1.8$, these effects clearly involve peripheral ASIC3 in skin and muscle nociceptors, as demonstrated by the use of specific ASIC3 siRNA. APETx2 is thus a very interesting tool, with potent therapeutic implications in peripheral pain, and could serve as a model to design future local analgesics.

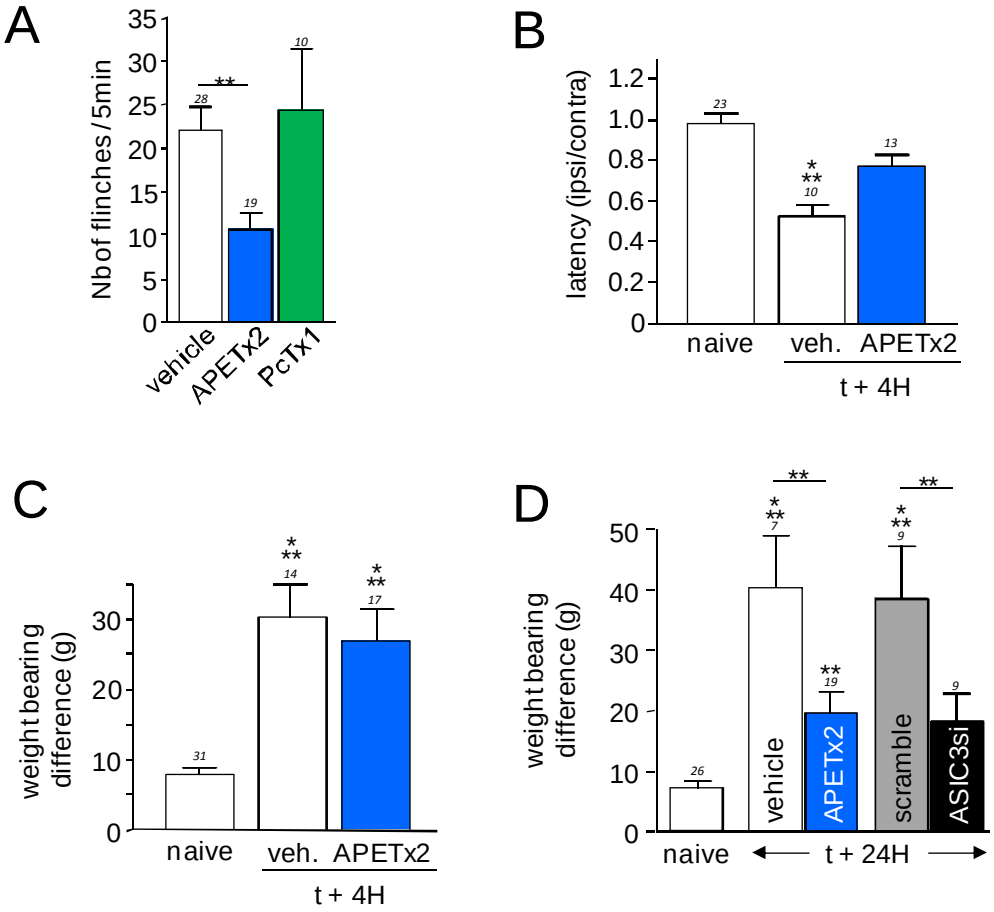

Figure 3. Effect of ASIC3 inhibition by APETx2 on postoperative pain (according to *Figures 3B*, *C*, *E* and *4A* from Deval *et al.*, 2011). (**A**) Effect of APETx2 (20 µM) and PcTx1 (120 nM) on spontaneous pain 4 h after surgery, and measured as the number of flinches of the ipsilateral hindpaw over a period of 5 min (** p<0.01, Kruskal-Wallis test followed by a Dunn's *post hoc* test). (**B**) Effect of local application of 20 µM APETx2 on postoperative thermal hyperalgesia evaluated with the Hargreaves test 4 h after surgery (*** p<0.001 compared to naïve animals, one way ANOVA followed by a Turkey's *post hoc* test). (**C** and **D**) Effect of local application of 20 µM APETx2 on postural pain evaluated with the dynamic weight-bearing test 4 h (**C**) and 24 h (**D**) after surgery (* p<0.05 and *** p<0.001, one way ANOVA followed by a Turkey's *post hoc* test).

Figure 3. *Effet de l'inhibition de ASIC3 par APETx2 sur la douleur post-opératoire (selon les* Figures 3B, C, E *et* 4A *de Deval* et al.*, 2011). (**A**) Effet d'APETx2 (20 µM) et de PcTx1 (120 nM) sur la douleur spontanée 4 h après la chirurgie, mesurée par le nombre de lever de la patte arrière ipsilatérale sur une période de 5 min (** p<0.01, test Kruskal-Wallis suivi d'un test Dunn's* post hoc*). (**B**) Effet de l'application locale de 20 µM d'APETx2 sur l'hyperalgésie thermique post-opératoire évaluée avec le test Hargreaves 4 h après la chirurgie (*** p<0.001 comparé avec les animaux naïfs, one way ANOVA suivi d'un test Turkey's* post hoc*). (**C** et **D**) Effet de l'application locale de 20 µM d'APETx2 sur la douleur posturale évalué avec le test de répartition du poids en dynamique 4 h (**C**) et 24 h (**D**) après la chirurgie (* p<0.05 et *** p<0.001, one way ANOVA suivi d'un test Turkey's* post hoc*).*

Conclusion

Toxins from sea anemone venom do not act only on their natural marine preys, *i.e.* fishes and crustaceans, but also on mammals where a high diversity of sea anemone peptides having different structures have been described with different degrees of toxicity ranging from paralyzing effects to lethality, sometimes associated with cardiotoxic effects. High toxicity is correlated with effects of SA toxins on Na_V channels, while some neurotoxic effects can also be attributed to the action of toxins on K_V1 channels. An increasing number of studies reveal the presence of non-toxic or low-toxic peptides which target new channels related to important sensory functions. Peptides with new structures and unknown targets have also been identified. It is quite surprising that no activity on voltage-gated Ca^{2+} channels was reported yet in SA venoms, since Ca^{2+} channel blockers were largely characterized in other animal venoms like snakes, spiders, cones and scorpions, and can also participate to the paralyzing effects on preys.

Recently, peptidomic and transcriptomic approaches reported the presence of more than 80 toxins in the venom of *Bunodosoma cangicum* and more than 40 new sequences in the venom of *Anemonia sulcata* (Kozlov and Grishin, 2011; Zaharenko *et al.*, 2008). This could predict for the future years an exponential increase of interesting tools, isolated from sea anemones, to study ion channels as well as specific pathologies, and maybe to design new therapeutic agents.

Acknowledgements. *We thank the « Association Française contre les Myopathies » (AFM), the « Fondation pour la Recherche Médicale » (FRM), the « Agence Nationale de la Recherche » (ANR) for financial support. This work is also dedicated to Dr H. Schweitz who deeply contributed to sea anemone toxin research.*

References

Abbott GW, Butler MH, Bendahhou S, Dalakas MC, Ptacek LJ, Goldstein SA (2001) MiRP2 forms potassium channels in skeletal muscle with Kv3.4 and is associated with periodic paralysis. *Cell* **104**: 217-231

Aiyar J, Withka JM, Rizzi JP, Singleton DH, Andrews GC, Lin W, Boyd J, Hanson DC, Simon M, Dethlefs B, *et al.* (1995) Topology of the pore-region of a K^+ channel revealed by the NMR-derived structures of scorpion toxins. *Neuron* **15**: 1169-1181

Alsen C (1983) Biological significance of peptides from *Anemonia sulcata. Fed Proc* **42**: 101-108

Alsen C, Beress L, Tesseraux I (1978) Toxicities of sea anemone (*Anemonia sulcata*) polypeptides in mammals. *Toxicon* **16**: 561-566

Aneiros A, Garcia I, Martinez JR, Harvey AL, Anderson AJ, Marshall DL, Engstrom A, Hellman U, Karlsson E (1993) A potassium channel toxin from the secretion of the sea anemone *Bunodosoma granulifera*. Isolation, amino acid sequence and biological activity. *Biochim Biophys Acta* **1157**: 86-92

Angulo E, Noe V, Casado V, Mallol J, Gomez-Isla T, Lluis C, Ferrer I, Ciudad CJ, Franco R (2004) Up-regulation of the Kv3.4 potassium channel subunit in early stages of Alzheimer's disease. *J Neurochem* **91**: 547-557

Antuch W, Berndt KD, Chavez MA, Delfin J, Wuthrich K (1993) The NMR solution structure of a Kunitz-type proteinase inhibitor from the sea anemone *Stichodactyla helianthus*. *Eur J Biochem* **212**: 675-684

Babinski K, Catarsi S, Biagini G, Seguela P (2000) Mammalian ASIC2a and ASIC3 subunits co-assemble into heteromeric proton-gated channels sensitive to Gd^{3+}. *J Biol Chem* **275**: 28519-28525

Baranauskas G, Tkatch T, Nagata K, Yeh JZ, Surmeier DJ (2003) Kv3.4 subunits enhance the repolarizing efficiency of Kv3.1 channels in fast-spiking neurons. *Nat Neurosci* **6**: 258-266

Barhanin J, Hugues M, Schweitz H, Vincent JP, Lazdunski M (1981) Structure-function relationships of sea anemone toxin II from *Anemonia sulcata*. *J Biol Chem* **256**: 5764-5769

Bassilana F, Champigny G, Waldmann R, de Weille JR, Heurteaux C, Lazdunski M (1997) The acid-sensitive ionic channel subunit ASIC and the mammalian degenerin MDEG form a heteromultimeric H^+-gated Na^+ channel with novel properties. *J Biol Chem* **272**: 28819-28822

Beeton C, Wulff H, Barbaria J, Clot-Faybesse O, Pennington M, Bernard D, Cahalan MD, Chandy KG, Beraud E (2001) Selective blockade of T lymphocyte $K^{(+)}$ channels ameliorates experimental autoimmune encephalomyelitis, a model for multiple sclerosis. *Proc Natl Acad Sci U S A* **98**: 13942-13947

Beeton C, Wulff H, Singh S, Botsko S, Crossley G, Gutman GA, Cahalan MD, Pennington M, Chandy KG (2003) A novel fluorescent toxin to detect and investigate Kv1.3 channel up-regulation in chronically activated T lymphocytes. *J Biol Chem* **278**: 9928-9937

Benzinger GR, Kyle JW, Blumenthal KM, Hanck DA (1998) A specific interaction between the cardiac sodium channel and site-3 toxin anthopleurin B. *J Biol Chem* **273**: 80-84

Beress L, Beress R (1975a) Purification of three polypeptides with neuro- and cardiotoxic activity from the sea anemone *Anemonia sulcata*. *Toxicon* **13**: 359-367

Beress L, Beress R, Wunderer G (1975b) Isolation and characterisation of three polypeptides with neurotoxic activity from *Anemonia sulcata*. *FEBS Lett* **50**: 311-314

Beress L, Doppelfeld I-S, Etschenberg E, Graf E, Henschen A, Zwick J (1985) Federal Republic of Germany Patent DE 3324689 A1

Bianchi L, Driscoll M (2002) Protons at the gate: DEG/ENaC ion channels help us feel and remember. *Neuron* **34**: 337-340

Blanchard MG, Rash LD, Kellenberger S (2011) Inhibition of voltage-gated $Na^{(+)}$ currents in sensory neurons by the sea anemone toxin APETx2. *Br J Pharmacol* (in press)

Bosmans F, Aneiros A, Tytgat J (2002) The sea anemone *Bunodosoma granulifera* contains surprisingly efficacious and potent insect-selective toxins. *FEBS Lett* **532**: 131-134

Bosmans F, Tytgat J (2007) Sea anemone venom as a source of insecticidal peptides acting on voltage-gated Na^+ channels. *Toxicon* **49**: 550-560

Bruhn T, Schaller C, Schulze C, Sanchez-Rodriguez J, Dannmeier C, Ravens U, Heubach JF, Eckhardt K, Schmidtmayer J, Schmidt H, Aneiros A, Wachter E, Beress L (2001) Isolation and characterisation of five neurotoxic and cardiotoxic polypeptides from the sea anemone *Anthopleura elegantissima*. *Toxicon* **39**: 693-702

Catterall WA, Cestele S, Yarov-Yarovoy V, Yu FH, Konoki K, Scheuer T (2007) Voltage-gated ion channels and gating modifier toxins. *Toxicon* **49**: 124-141

Chagot B, Diochot S, Pimentel C, Lazdunski M, Darbon H (2005a) Solution structure of APETx1 from the sea anemone *Anthopleura elegantissima*: a new fold for an HERG toxin. *Proteins* **59**: 380-386

Chagot B, Escoubas P, Diochot S, Bernard C, Lazdunski M, Darbon H (2005b) Solution structure of APETx2, a specific peptide inhibitor of ASIC3 proton-gated channels. *Protein Sci* **14**: 2003-2010

Chen X, Kalbacher H, Grunder S (2005) The Tarantula Toxin Psalmotoxin 1 Inhibits Acid-sensing Ion Channel (ASIC) 1a by Increasing Its Apparent H^+ Affinity. *J Gen Physiol* **126**: 71-79

Cotton J, Crest M, Bouet F, Alessandri N, Gola M, Forest E, Karlsson E, Castaneda O, Harvey AL, Vita C, Menez A (1997) A potassium-channel toxin from the sea anemone *Bunodosoma granulifera*, an inhibitor for Kv1 channels. Revision of the amino acid sequence, disulfide-bridge assignment, chemical synthesis, and biological activity. *Eur J Biochem* **244**: 192-202

Dauplais M, Lecoq A, Song J, Cotton J, Jamin N, Gilquin B, Roumestand C, Vita C, de Medeiros CL, Rowan EG, Harvey AL, Menez A (1997) On the convergent evolution of animal toxins. Conservation of a diad of functional residues in potassium channel-blocking toxins with unrelated structures. *J Biol Chem* **272**: 4302-4309

Deval E, Gasull X, Noel J, Salinas M, Baron A, Diochot S, Lingueglia E (2010) Acid-sensing ion channels (ASICs): pharmacology and implication in pain. *Pharmacol Ther* **128**: 549-558

Deval E, Noel J, Gasull X, Delaunay A, Alloui A, Friend V, Eschalier A, Lazdunski M, Lingueglia E (2011) Acid-sensing ion channels in postoperative pain. *J Neurosci* **31**: 6059-6066

Deval E, Noel J, Lay N, Alloui A, Diochot S, Friend V, Jodar M, Lazdunski M, Lingueglia E (2008) ASIC3, a sensor of acidic and primary inflammatory pain. *Embo J* **27**: 3047-3055

Dias-Kadambi BL, Combs KA, Drum CL, Hanck DA, Blumenthal KM (1996b) The role of exposed tryptophan residues in the activity of the cardiotonic polypeptide anthopleurin B. *J Biol Chem* **271**: 23828-23835

Dias-Kadambi BL, Drum CL, Hanck DA, Blumenthal KM (1996a) Leucine 18, a hydrophobic residue essential for high affinity binding of anthopleurin B to the voltage-sensitive sodium channel. *J Biol Chem* **271**: 9422-9428

Diochot S, Lazdunski M. (2009) Sea anemone Toxins affecting Potassium Channels. In *Marine Toxins as Research Tools.* Fusetani N, Kem W (eds) pp 99-122. Springer-Verlag, Berlin Heidelberg

Diochot S, Baron A, Rash LD, Deval E, Escoubas P, Scarzello S, Salinas M, Lazdunski M (2004) A new sea anemone peptide, APETx2, inhibits ASIC3, a major acid-sensitive channel in sensory neurons. *Embo J* **23**: 1516-1525

Diochot S, Loret E, Bruhn T, Beress L, Lazdunski M (2003) APETx1, a new toxin from the sea anemone *Anthopleura elegantissima*, blocks voltage-gated human ether-a-go-go-related gene potassium channels. *Mol Pharmacol* **64**: 59-69

Diochot S, Schweitz H, Beress L, Lazdunski M (1998) Sea anemone peptides with a specific blocking activity against the fast inactivating potassium channel Kv3.4. *J Biol Chem* **273**: 6744-6749

Driscoll PC, Clore GM, Beress L, Gronenborn AM (1989a) A proton nuclear magnetic resonance study of the antihypertensive and antiviral protein BDS-I from the sea anemone *Anemonia sulcata*: sequential and stereospecific resonance assignment and secondary structure. *Biochemistry* **28**: 2178-2187

Gendeh GS, Young LC, de Medeiros CL, Jeyaseelan K, Harvey AL, Chung MC (1997) A new potassium channel toxin from the sea anemone *Heteractis magnifica*: isolation, cDNA cloning, and functional expression. *Biochemistry* **36**: 11461-11471

Goudet C, Ferrer T, Galan L, Artiles A, Batista CF, Possani LD, Alvarez J, Aneiros A, Tytgat J (2001) Characterization of two *Bunodosoma granulifera* toxins active on cardiac sodium channels. *Br J Pharmacol* **134**: 1195-1206

Harvey AL (2001) Twenty years of dendrotoxins. *Toxicon* **39**: 15-26

Hesselager M, Timmermann DB, Ahring PK (2004) pH Dependency and desensitization kinetics of heterologously expressed combinations of acid-sensing ion channel subunits. *J Biol Chem* **279**: 11006-11015

Honma T, Hasegawa Y, Ishida M, Nagai H, Nagashima Y, Shiomi K (2005) Isolation and molecular cloning of novel peptide toxins from the sea anemone *Antheopsis maculata*. *Toxicon* **45**: 33-41

Honma T, Kawahata S, Ishida M, Nagai H, Nagashima Y, Shiomi K (2008) Novel peptide toxins from the sea anemone *Stichodactyla haddoni*. *Peptides* **29**: 536-544

Honma T, Shiomi K (2006) Peptide toxins in sea anemones: structural and functional aspects. *Mar Biotechnol (NY)* **8**: 1-10

Ishida M, Yokoyama A, Shimakura K, Nagashima Y, Shiomi K (1997) Halcurin, a polypeptide toxin from the sea anemone *Halcurias sp*., with a structural resemblance to type 1 and 2 toxins. *Toxicon* **35**: 537-544

Jasti J, Furukawa H, Gonzales EB, Gouaux E (2007) Structure of acid-sensing ion channel 1 at 1.9 A resolution and low pH. *Nature* **449**: 316-323

Kalman K, Pennington MW, Lanigan MD, Nguyen A, Rauer H, Mahnir V, Paschetto K, Kem WR, Grissmer S, Gutman GA, Christian EP, Cahalan MD, Norton RS, Chandy KG (1998) ShK-Dap22, a potent Kv1.3-specific immunosuppressive polypeptide. *J Biol Chem* **273**: 32697-32707

Karczewski J, Spencer RH, Garsky VM, Liang A, Leitl MD, Cato MJ, Cook SP, Kane S, Urban MO (2010) Reversal of acid-induced and inflammatory pain by the selective ASIC3 inhibitor, APETx2. *Br J Pharmacol* **161**: 950-960

Kellenberger S, Schild L (2002) Epithelial sodium channel/degenerin family of ion channels: a variety of functions for a shared structure. *Physiol Rev* **82**: 735-767

Kelso GJ, Drum CL, Hanck DA, Blumenthal KM (1996) Role for Pro-13 in directing high-affinity binding of anthopleurin B to the voltage-sensitive sodium channel. *Biochemistry* **35**: 14157-14164

Kem WR, Parten B, Pennington MW, Price DA, Dunn BM (1989) Isolation, characterization, and amino acid sequence of a polypeptide neurotoxin occurring in the sea anemone *Stichodactyla helianthus*. *Biochemistry* **28**: 3483-3489

Koh CY, Kini RM (2011) From snake venom toxins to therapeutics - Cardiovascular examples. *Toxicon*. (in press)

Kozlov S, Grishin E (2011) The mining of toxin-like polypeptides from EST database by single residue distribution analysis. *BMC Genomics* **12**: 88

Lazdunski M, Frelin C, Barhanin J, Lombet A, Meiri H, Pauron D, Romey G, Schmid A, Schweitz H, Vigne P, *et al.* (1986) Polypeptide toxins as tools to study voltage-sensitive Na^+ channels. *Ann N Y Acad Sci* **479**: 204-220

Lien CC, Jonas P (2003) Kv3 potassium conductance is necessary and kinetically optimized for high-frequency action potential generation in hippocampal interneurons. *J Neurosci* **23**: 2058-2068

Lingueglia E (2007) Acid-sensing ion channels in sensory perception. *J Biol Chem* **282**: 17325-17329

Lingueglia E, Champigny G, Lazdunski M, Barbry P (1995) Cloning of the amiloride-sensitive FMRFamide peptide-gated sodium channel. *Nature* **378**: 730-733

Lingueglia E, Deval E, Lazdunski M (2006) FMRFamide-gated sodium channel and ASIC channels: a new class of ionotropic receptors for FMRFamide and related peptides. *Peptides* **27**: 1138-1152

Llewellyn LE, Norton RS (1991) Binding of the sea anemone polypeptide BDS II to the voltage-gated sodium channel. *Biochem Int* **24**: 937-946

Loret EP, del Valle RM, Mansuelle P, Sampieri F, Rochat H (1994) Positively charged amino acid residues located similarly in sea anemone and scorpion toxins. *J Biol Chem* **269**: 16785-16788

MacKinnon R (1991) Determination of the subunit stoichiometry of a voltage-activated potassium channel. *Nature* **350**: 232-235

Miljanich GP (2004) Ziconotide: neuronal calcium channel blocker for treating severe chronic pain. *Curr Med Chem* **11**: 3029-3040

Minagawa S, Ishida M, Nagashima Y, Shiomi K (1998) Primary structure of a potassium channel toxin from the sea anemone *Actinia equina*. *FEBS Lett* **427**: 149-151

Minagawa S, Ishida M, Shimakura K, Nagashima Y, Shiomi K (1997) Isolation and amino acid sequences of two Kunitz-type protease inhibitors from the sea anemone *Anthopleura aff. xanthogrammica*. *Comp Biochem Physiol B Biochem Mol Biol* **118**: 381-386

Mouhat S, Andreotti N, Jouirou B, Sabatier JM (2008) Animal toxins acting on voltage-gated potassium channels. *Curr Pharm Des* **14**: 2503-2518

Norton RS (1991) Structure and structure-function relationships of sea anemone proteins that interact with the sodium channel. *Toxicon* **29**: 1051-1084

Norton RS, Pennington MW, Wulff H (2004) Potassium channel blockade by the sea anemone toxin ShK for the treatment of multiple sclerosis and other autoimmune diseases. *Curr Med Chem* **11**: 3041-3052

Norton TR, Kashiwagi, M., Shibata S. (1978) Anthopleurin A, B and C cardiotonic polypeptides fron the sea anemones *Anthopleura xanthogrammica* (Brandt) and *Anthopleura elegantissima* (Brandt). In *Drugs and Food from the Sea: Myth or Reality?* Kaul PN, Sindermann CJ (eds) pp 37-50. University of Oklahoma Press, Norman, OK

Norton TR, Ohizumi Y, Shibata S (1981) Excitatory effect of a new polypeptide (anthopleurin-B) from sea anemone on the guinea-pig vas deferens. *Br J Pharmacol* **74**: 23-28

Oliveira JS, Zaharenko AJ, Ferreira WA, Jr., Konno K, Shida CS, Richardson M, Lucio AD, Beirao PS, de Freitas JC (2006) BcIV, a new paralyzing peptide obtained from the venom of the sea anemone *Bunodosoma caissarum*. A comparison with the Na^+ channel toxin BcIII. *Biochim Biophys Acta* **1764**: 1592-1600

Pennington MW, Byrnes ME, Zaydenberg I, Khaytin I, de Chastonay J, Krafte DS, Hill R, Mahnir VM, Volberg WA, Gorczyca W, *et al.* (1995) Chemical synthesis and characterization of ShK toxin: a potent potassium channel inhibitor from a sea anemone. *Int J Pept Protein Res* **46**: 354-358

Rauer H, Pennington M, Cahalan M, Chandy KG (1999) Structural conservation of the pores of calcium-activated and voltage-gated potassium channels determined by a sea anemone toxin. *J Biol Chem* **274**: 21885-21892

Renaud JF, Fosset M, Schweitz H, Lazdunski M (1986) The interaction of polypeptide neurotoxins with tetrodotoxin-resistant Na^+ channels in mammalian cardiac cells. Correlation with inotropic and arrhythmic effects. *Eur J Pharmacol* **120**: 161-170

Restano-Cassulini R, Korolkova YV, Diochot S, Gurrola G, Guasti L, Possani LD, Lazdunski M, Grishin EV, Arcangeli A, Wanke E (2006) Species diversity and peptide toxins blocking selectivity of ether-a-go-go-related gene subfamily K^+ channels in the central nervous system. *Mol Pharmacol* **69**: 1673-1683

Romey G, Abita JP, Schweitz H, Wunderer G, Lazdunski (1976) Sea anemone toxin:a tool to study molecular mechanisms of nerve conduction and excitation-secretion coupling. *Proc Natl Acad Sci U S A* **73**: 4055-4059

Salgado VL, Kem WR (1992) Actions of three structurally distinct sea anemone toxins on crustacean and insect sodium channels. *Toxicon* **30**: 1365-1381

Salinas M, Rash LD, Baron A, Lambeau G, Escoubas P, Lazdunski M (2006) The receptor site of the spider toxin PcTx1 on the proton-gated cation channel ASIC1a. *J Physiol* **570**: 339-354

Sanguinetti MC, Curran ME, Spector PS, Keating MT (1996) Spectrum of HERG K^+-channel dysfunction in an inherited cardiac arrhythmia. *Proc Natl Acad Sci U S A* **93**: 2208-2212

Sanguinetti MC, Jiang C, Curran ME, Keating MT (1995) A mechanistic link between an inherited and an acquired cardiac arrhythmia: HERG encodes the IKr potassium channel. *Cell* **81**: 299-307

Schweitz H (1984) Lethal potency in mice of toxins from scorpion, sea anemone, snake and bee venoms following intraperitoneal and intracisternal injection. *Toxicon* **22**: 308-311

Schweitz H, Bidard JN, Frelin C, Pauron D, Vijverberg HP, Mahasneh DM, Lazdunski M, Vilbois F, Tsugita A (1985) Purification, sequence, and pharmacological properties of sea anemone toxins from *Radianthus paumotensis*. A new class of sea anemone toxins acting on the sodium channel. *Biochemistry* **24**: 3554-3561

Schweitz H, Bruhn T, Guillemare E, Moinier D, Lancelin JM, Beress L, Lazdunski M (1995) Kalicludines and kaliseptine. Two different classes of sea anemone toxins for voltage sensitive K^+ channels. *J Biol Chem* **270**: 25121-25126

Schweitz H, Vincent JP, Barhanin J, Frelin C, Linden G, Hugues M, Lazdunski M (1981) Purification and pharmacological properties of eight sea anemone toxins from *Anemonia sulcata*, *Anthopleura xanthogrammica*, *Stoichactis giganteus*, and *Actinodendron plumosum*. *Biochemistry* **20**: 5245-5252

Seibert AL, Liu J, Hanck DA, Blumenthal KM (2003) Arg-14 loop of site 3 anemone toxins: effects of glycine replacement on toxin affinity. *Biochemistry* **42**: 14515-14521

Shibata S, Norton TR, Izumi T, Matsuo T, Katsuki S (1976) A polypeptide (AP-A) from sea anemone (*Anthopleura xanthogrammica*) with potent positive inotropic action. *J Pharmacol Exp Ther* **199**: 298-309

Shieh CC, Coghlan M, Sullivan JP, Gopalakrishnan M (2000) Potassium channels: molecular defects, diseases, and therapeutic opportunities. *Pharmacol Rev* **52**: 557-594

Shiomi K, Honma T, Ide M, Nagashima Y, Ishida M, Chino M (2003) An epidermal growth factor-like toxin and two sodium channel toxins from the sea anemone *Stichodactyla gigantea*. *Toxicon* **41**: 229-236

Shiomi K, Qian WH, Lin XY, Shimakura K, Nagashima Y, Ishida M (1997) Novel polypeptide toxins with crab lethality from the sea anemone *Anemonia erythraea*. *Biochim Biophys Acta* **1335**: 191-198

Torres AM, Kuchel PW (2004) The beta-defensin-fold family of polypeptides. *Toxicon* **44**: 581-588

Tudor JE, Pallaghy PK, Pennington MW, Norton RS (1996) Solution structure of ShK toxin, a novel potassium channel inhibitor from a sea anemone. *Nat Struct Biol* **3**: 317-320

Tytgat J, Debont T, Carmeliet E, Daenens P (1995) The alpha-dendrotoxin footprint on a mammalian potassium channel. *J Biol Chem* **270**: 24776-24781

Ugawa S, Yamamoto T, Ueda T, Ishida Y, Inagaki A, Nishigaki M, Shimada S (2003) Amiloride-insensitive currents of the acid-sensing ion channel-2a (ASIC2a)/ASIC2b heteromeric sour-taste receptor channel. *J Neurosci* **23**: 3616-3622

Waldmann R, Champigny G, Lingueglia E, De Weille JR, Heurteaux C, Lazdunski M (1999) H(+)-gated cation channels. *Ann N Y Acad Sci* **868**: 67-76

Waldmann R, Champigny G, Voilley N, Lauritzen I, Lazdunski M (1996) The mammalian degenerin MDEG, an amiloride-sensitive cation channel activated by mutations causing neurodegeneration in *Caenorhabditis elegans*. *J Biol Chem* **271**: 10433-10436

Wanke E, Restano-Cassulini R (2007) Toxins interacting with ether-a-go-go-related gene voltage-dependent potassium channels. *Toxicon* **49**: 239-248

Warashina A, Jiang ZY, Ogura T (1988) Potential-dependent action of *Anemonia sulcata* toxins III and IV on sodium channels in crayfish giant axons. *Pflugers Arch* **411**: 88-93

Yagi J, Wenk HN, Naves LA, McCleskey EW (2006) Sustained currents through ASIC3 ion channels at the modest pH changes that occur during myocardial ischemia. *Circ Res* **99**: 501-509

Yan L, Herrington J, Goldberg E, Dulski PM, Bugianesi RM, Slaughter RS, Banerjee P, Brochu RM, Priest BT, Kaczorowski GJ, Rudy B, Garcia ML (2005) *Stichodactyla helianthus* peptide, a pharmacological tool for studying Kv3.2 channels. *Mol Pharmacol* **67**: 1513-1521

Yeung SY, Thompson D, Wang Z, Fedida D, Robertson B (2005) Modulation of Kv3 subfamily potassium currents by the sea anemone toxin BDS: significance for CNS and biophysical studies. *J Neurosci* **25**: 8735-8745

Zaharenko AJ, Ferreira WA, Jr., Oliveira JS, Richardson M, Pimenta DC, Konno K, Portaro FC, de Freitas JC (2008) Proteomics of the neurotoxic fraction from the sea anemone *Bunodosoma cangicum* venom: Novel peptides belonging to new classes of toxins. *Comp Biochem Physiol Part D Genomics Proteomics* **3**: 219-225

Zhang M, Liu XS, Diochot S, Lazdunski M, Tseng GN (2007) APETx1 from sea anemone *Anthopleura elegantissima* is a gating modifier peptide toxin of the human ether-a-go-go- related potassium channel. *Mol Pharmacol* **72**: 259-268

Toxines et Transferts ioniques – Toxins and Ion transfers
Rencontres en Toxinologie – Meeting on Toxinology, 2011
Editions de la SFET – SFET Editions
Accès libre en ligne sur le site – Free access on line on the site : http://www.sfet.asso.fr

Tools for studying peptide toxin modulation of voltage-gated sodium channels

Stefan H. HEINEMANN*, Enrico LEIPOLD

Center for Molecular Biomedicine, Department of Biophysics, Friedrich Schiller University of Jena and Jena University Hospital, Hans-Knöll-Str. 2, D-07745 Jena, Germany

** Corresponding author ; Tel : +49 (0) 3641 9 395650 ; Fax : +49 (0) 3641 9 395652 ; E-mail : stefan.h.heinemann@uni-jena.de*

Abstract

Voltage-gated sodium channels are of prime importance for rapid neuronal signaling and, therefore, are targets of various types of peptide toxins. In order to understand the molecular mechanisms underlying toxin-channel interaction, detailed functional analysis of channel function upon heterologous expression in host cells is required. Here, we review a couple of methods that proved useful for the identification of interaction sites at the channel protein and for gaining insight into the impact of peptide toxins on channel gating. We describe the construction of sodium channel chimeras and specific mutants, extraction of single-channel data based on macroscopic currents, and methods for the unambiguous identification of current components associated with transiently expressed sodium channel genes.

Des outils pour étudier la modulation des canaux sodium sensibles au potentiel par les toxines peptidiques

Les canaux sodium dépendants du potentiel ont un rôle majeur dans la signalisation neuronale rapide et, de ce fait, sont les cibles de nombreuses espèces de toxines peptidiques. Afin de comprendre le mécanisme moléculaire de l'interaction toxine-canal, une étude précise du fonctionnement de ces canaux, à l'aide d'un système d'expression hétérologue, est nécessaire. Dans cette revue, nous présentons certaines méthodes particulièrement adaptées à l'identification du site d'interaction des toxines avec les canaux sodium et de leur impact sur le fonctionnement de ces canaux. Nous décrivons la construction de canaux sodium chimériques et de mutants spécifiques, l'extraction de données sur le canal unique à partir des courants macroscopiques et les méthodes d'identification, de façon non-ambiguë, des courants ioniques associés à l'expression transitoire des gènes de ces canaux.

Keywords : *Conotoxin, channel gating, patch-clamp, scorpion toxin, sodium channel.*

Introduction

Voltage-gated sodium channels (Na_V channels) are responsible for the rapid upstroke of an action potential and play a pivotal role in electrical signaling of neuronal and muscle cells. Many peptide toxins of venomous animals, such as scorpions, sea anemones, wasps and cone snails, have therefore evolved to specifically interfere with Na_V channels and, hence, to affect electrical signaling of the respective target organism. Depending on the mode of interference, Na_V channel-specific toxins inhibit (*e.g.* µ-conotoxins, µO-conotoxins) or enhance (*e.g.* δ-conotoxins, scorpion α- and β-toxins) Na^+ currents and either block neuronal activity or cause hyperexcitability, respectively – in either case with deleterious consequences for the affected organism (for reviews see, Cestèle and Catterall, 2000; Heinemann and Leipold, 2007).

Like other peptide toxins, Na_V channel toxins have attracted considerable attention because they are very useful experimental tools. On one hand, they have proven very instrumental in studying the molecular mechanisms of Na_V channel function: µ-conotoxins block the channel and therefore are used to probe the outer vestibule of the channel pore; other peptides such as µO-conotoxins, δ-conotoxins, and scorpion α- and β-toxins belong to the class of voltage-sensor toxins, *i.e.* they interfere with the gating machinery of the channel and provide important information on the function of individual voltage-sensors. On the other hand, an even greater potential resides in the ability of some Na_V toxins to distinguish different Na_V channel isoforms. From the nine prototypic Na_V channels in humans ($Na_V1.1$-$Na_V1.9$), most display very similar properties in terms of ion permeation and gating characteristics (voltage dependence and kinetics of activation and inactivation) and, therefore, often only can be distinguished with the aid of pharmacological intervention, such as the application of Na_V-specific peptide toxins.

Some peptide toxins are even promising lead structures for clinical application; for example, toxins

inhibiting peripheral Na_V channels, such as some μ-conotoxins, are considered potential analgesics or muscle relaxants. In particular when addressing clinical applications, subtype specificity is an important issue because off-site effects, such as blockade of cardiac $Na_V1.5$ channels, have to be avoided. Therefore, it is important to understand how peptide toxins affect Na_V channels on a molecular level and which structural features – of the channel and the toxin itself – are responsible for a specific toxin-channel interaction.

In order to reach the above-mentioned goal, several experimental requirements have to be met. Typically, one needs to study the toxin effects on identified channel proteins with electrophysiological methods as to precisely assay channel function. In most cases, it is not sufficient to study wild-type channels only, but Na_V channel structures have to be manipulated systematically. For functional assays, corresponding constructs have to be expressed in host cells. Although expression in *Xenopus* oocytes is the most straightforward approach, several arguments are in favor of mammalian cells as an expression system: when studying mammalian Na_V channels, mammalian host cells may provide a more suited environment, *e.g.* by providing the matching interaction proteins or post-translational modification mechanisms; time resolution and voltage-clamp control are much better in small mammalian cells than in oocytes; strong invaginations of the oocyte membrane may compromise the free access of toxins to all sites of the plasma membrane; finally, oocytes are large (about 1 mm diameter) and, hence, typically much more toxin is required for functional studies – this is a serious limitation when working with native toxins that are only available in very small quantities.

Here, we consider experimental approaches for studying toxin effects on Na_V channels expressed in mammalian cells. We describe various experimental strategies for only one example, namely the investigation of the subtype specificity of μ-conotoxins. In this case, one may meet several technical obstacles. We will try to address some of them and will discuss how to overcome them. (a) For the identification of molecular entities determining the subtype specificity, generation of channel chimeras can be very helpful, but how to make such chimeras in a systematic and economic manner? (b) Toxins may not always block Na_V channels completely – they may block partially and affect open probability; how to determine single-channel parameters from whole-cell recordings? (c) Na^+ current associated with transfected Na_V channel genes may be very small, in particular when considering the residual components after toxin application; how do we discriminate such exogenous signals from currents through Na_V channels endogenous to the host cells?

Mixing and matching of sodium channel modules

Na_V channels are formed by a large α-subunit and up to two small auxiliary β-subunits with only one transmembrane segment. Most functional features of Na_V channels are determined by the α-subunit which is composed of four homologous domains (DI-DIV) comprising voltage-sensors (S1-S4) and pore/gate (S5-S6) modules (*Figure 1a*). Peptide toxins typically interact with Na_V channels *via* the extracellular side, thus the primary interaction epitopes are the extracellular linkers S1/2, S3/4, and the pore loops, also referred to as SS1 and SS2. Such linkers show considerably less conservation than the transmembrane segments (S1-S6) when comparing Na_V channels of various species (paralogs) or all Na_V isoforms of one organism (orthologs). It therefore does not come as a surprise that such linkers most likely determine toxin specificity for a certain channel type. Depending on the class of toxins, only a few linkers may be of relevance. For example, the impact of scorpion α-toxins is largely determined by the S3/4 linker of DIV (*e.g.* Rogers *et al.*, 1996; Leipold *et al.*, 2004) and by the pore loops of DI (Gur *et al.*, 2011). Scorpion β-toxins exert their effect by influencing S3/4 of DII (Cestèle *et al.*, 1998), but the pore loops of DIII are also required for toxin action (Leipold *et al.*, 2006). In this respect, μO-conotoxins share properties with scorpion β-toxins (Zorn *et al.*, 2006; Leipold *et al.*, 2007) and, most likely, δ-conotoxins with scorpion α-toxins (Leipold *et al.*, 2005; for review, see Heinemann and Leipold, 2007). Thus, it appears that there are two main classes of Na_V-specific voltage-sensor toxins: one affects the voltage-sensor in DIV but also requires the pore loops of DI, the other affects the voltage-sensor of DII with secondary contacts in the pore loops of DIII. The situation is different for pore-blocking toxins like μ-conotoxins. They apparently occlude the pore from the extracellular side and, therefore, must make contact with the pore loops of all four domains (*e.g.* Dudley *et al.*, 1995, 2000; Li *et al.*, 2001; Choudhary *et al.*, 2007). Nevertheless, depending on the structural conservation of the individual pore loops, the subtype specificity of μ-conotoxins may be determined by only a few pore loops or only a single residue. As the most prominent example, μ-GIIIA blocks rat skeletal muscle $Na_V1.4$ channels but is about 1000 times less potent for the human paralog. The reason is a single S-to-L difference in the outer pore loop of DII (Cummins *et al.*, 2002). In a more recent study, we could show that μ-SIIIA's preference for rat $Na_V1.4$ over human $Na_V1.7$ channels is also located in the pore loop of DII but one residue toward the N-terminus, A-to-N (Leipold *et al.*, 2011).

For all these studies and for any future question addressing the localization of interaction sites and determinants for subtype specificity, construction and functional evaluation of channel chimeras is very useful. In the following, we briefly describe the experimental approach.

Construction of domain chimeras

Construction of several chimeric Na_V channels has been reported thus far, all of them designed to address specific questions regarding channel function or to study the interactions of the channels with specific modifiers and neurotoxins. Typically, these chimeras consist of a well-characterized background channel in which functional modules, like voltage-sensors, pore-modules, or whole domains, were replaced with those of a Na_V paralog or ortholog. For example, Chahine *et al.* (1996) swapped the large domain-connecting loops between $Na_V1.4$ and $Na_V1.5$ to identify protein parts that determine the different activation and inactivation behavior of both channel subtypes. Whole domains were exchanged between $Na_V1.4$ and $Na_V1.5$ to investigate their slow

inactivation behavior (O´Reilly *et al.*, 1999) and their susceptibility to inhibition by cocaine (Wright *et al.*, 1999). Vijayaragavan *et al.* (2004) used $Na_V1.8/1.7$ chimeras to demonstrate expressional regulation of $Na_V1.8$ *via* the C-terminal structures. A similar set of $Na_V1.8/1.4$ chimeras was utilized by Choi *et al.* (2004) to demonstrate the importance of $Na_V1.8$'s C-terminus for its unique inactivation behavior. Lee and Goldin (2008, 2009) reported on N- and C-terminal chimeras of $Na_V1.2$ and $Na_V1.6$. There are also chimeras of mammalian and insect Na_V channels which were preliminarily used for studying the channel specificities of neurotoxins (*e.g.* Shichor *et al.*, 2002; Gur *et al.*, 2011).

For an efficient scientific exploitation of Na_V channel chimeras, they are ideally generated such that combinations of many isoforms are easily constructed. We chose rat $Na_V1.4$ as a reference channel because it is very well characterized, it expresses well in various host cells, and the handling of the coding DNA is straightforward. Efficient replacement of individual domains of $Na_V1.4$ by those of orthologous or paralogous channel types requires unique restriction sites in the DNA sequence of the corresponding expression constructs, thus enabling easy release and insertion of DNA fragments by enzymatic cleavage and ligation, respectively. For the generation of domain chimeras, five restriction sites are needed: three in the coding sequence, one 5' upstream, and another one 3' downstream of the coding region. In order to avoid structural incompatibilities at the site of ligation, the cleavage sites should be in areas of strong coding-sequence conservation (*Figure 1b*). Transmembrane segments, for example, are highly conserved among Na_V channels and therefore may provide ideal sites for the assembly of chimeras, in most cases without disturbing integrity and function of the resulting channels. An endogenous restriction site (endonuclease BsiWI), satisfying this criterion, is located at position 1328 (S6 in DI) of rat SCN4A. Since no other endogenous cleavage sites were suited for the construction of domain chimeras, we introduced silent mutations into SCN4A that allow cleavage by NheI at position 3120 (S1 in DIII) and ClaI at position 3863 (S6 in DIV) using a PCR-based strategy as described in Zorn *et al.* (2006); cleavage sites and their relation to the channel structure are illustrated in *Figure 1*. DNA fragments coding for individual domains from rat $Na_V1.2$ (Zorn *et al.*, 2006; Leipold *et al.*, 2007) and human $Na_V1.5$ (Leipold *et al.*, 2011) were PCR-amplified and the necessary restriction sites were inserted with the PCR primers. Subsequently, the PCR-amplified donor DNA fragments as well as the $Na_V1.4$ background construct were cleaved with the corresponding restriction enzymes and individual donor domains were ligated into the background construct. This "mixing and matching" strategy resulted in complete sets of fully functional $Na_V1.4/1.2$ and $Na_V1.4/1.5$ domain chimeras.

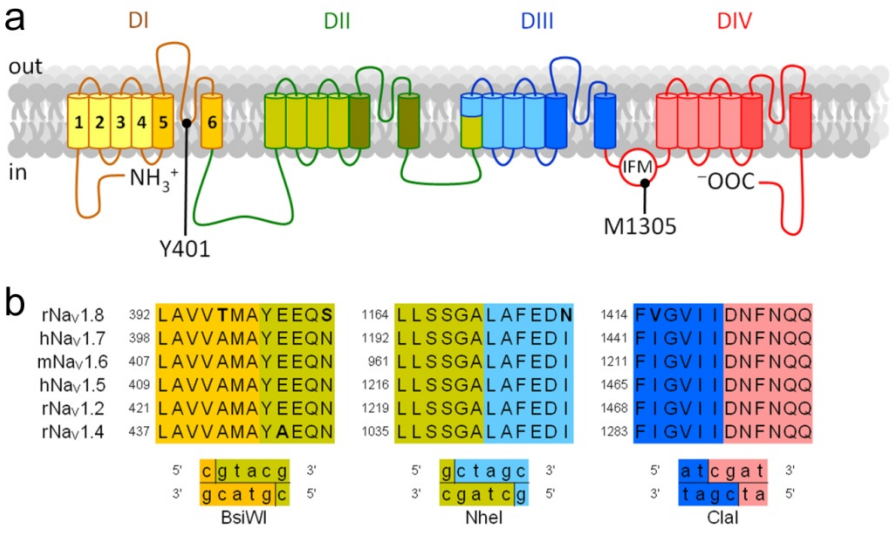

Figure 1. Construction of sodium channel domain chimeras. (**a**) Topological cartoon of a Na_V channel α-subunit with four homologous domains DI-DIV. The color code highlights fractions used to construct domain chimeras. Also shown is a site used to alter tetrodotoxin (TTX) sensitivity of channels (Y401) and the inactivation motif used to render channel inactivation sensitive to oxidative attack (M1305). Residue numbers refer to rat $Na_V1.4$. (**b**) Multiple sequence alignments of the indicated Na_V channel isoforms (r=rat, h=human, m=mouse) around the sites used for domain chimera construction showing high sequence conservation. Short DNA sequences covering the restriction sites were engineered to ease the mixing and matching of domains among different channel isoforms. Appropriate restriction enzymes are indicated.

Figure 1. *Construction de domaines de canaux sodium chimériques. (**a**) Représentation schématique d'une sous-unité alpha de canal sodium avec quatre domaines homologues DI-DIV. Le code couleur met en évidence les régions utilisées dans la construction des domaines chimériques. Les sites impliqués dans la sensibilité à la tétrodotoxine (TTX) des canaux (Y401) et dans celle à l'effet d'une oxydation sur l'inactivation des canaux (M1305) sont indiqués. La numérotation des résidus fait référence au canal $Na_V1.4$ de rat. (**b**) Alignements multiples des séquences de différentes isoformes de Na_V (r=rat, h=humain, m=souris), autour des régions impliquées dans la formation des canaux chimériques, montrant une grande conservation des séquences. Les courtes séquences de DNA couvrant les sites de restrictions ont été construites afin de faciliter l'échange de domaines entre les différentes isoformes de canaux. Les enzymes de restriction appropriés sont indiqués.*

$Na_V1.4/1.2$ chimeras were used to study the channel sensitivity toward µO-conotoxin MrVIA (*Conus marmoreus*). The pore loop in DIII was identified as the molecular determinant responsible for the high

sensitivity of $Na_V1.4$ toward µO-MrVIA and the poor sensitivity of $Na_V1.2$ (Zorn *et al.*, 2006; Leipold *et al.*, 2007). In addition, it could be shown that µO-MrVIA and the scorpion β-toxin Tz1 interact with the same channel epitope, the pore loop in DIII (Leipold *et al.*, 2006). Chimeras between $Na_V1.4$ and $Na_V1.5$ proved useful for the identification of structural components responsible for the differential sensitivity toward µ-conotoxin SIIIA (*Conus striatus*). While $Na_V1.4$ was µ-SIIIA-sensitive, we showed that the pore loop of DII is the major determinant for the µ-SIIIA-insensitivity of $Na_V1.5$ (Leipold *et al.*, 2011).

Specific tuning of channel functions

To study the influence of neurotoxins on Na_V channels, mutations that equip the channels with novel functional properties can be instrumental. For example, µO-MrVIA displays striking voltage dependence, *i.e.* it dissociates from the channels upon strong depolarizations suggesting toxin interaction with the voltage-sensors. To identify which voltage-sensor is involved and which charge may be of particular relevance, we generated and assayed a set of eight $Na_V1.4$ gating charge mutants (Leipold *et al.*, 2007) each with one charge neutralization in either the first or the second position of the S4 segments. This systematic approach led to the conclusion that µO-MrVIA "blocks" Na_V channels by preventing the activation of their voltage-sensor in DII.

When Na_V channels have to be studied in host cells with large endogenous Na_V channel expression, such as in neuronal cells needed for the functional expression of $Na_V1.8$ (Schirmeyer *et al.*, 2009), endogenous Na^+ currents have to be eliminated. If they are sensitive to tetrodotoxin (TTX), like in Neuro-2A cells where 300 nM TTX completely blocks endogenous Na^+ currents, exogenously expressed channels should be made resistant to TTX. Typically, this is easily achieved by mutating residue Y401 in DI (numbering of rat $Na_V1.4$, *Figure 1a*) or the corresponding homologous residues in other channel types to serine – the side chain present in TTX-resistant $Na_V1.8$ and $Na_V1.9$ channels.

Non-stationary noise analysis of sodium currents

Currents mediated by Na_V channels are readily measured with the whole-cell patch-clamp method (Hamill *et al.*, 1981). Provided the electrical pipette capacitance (about 4 pF) and cell capacitance (about 10 pF) are both small and well compensated, a time resolution of about 100 µs is achieved; this is not fast enough to faithfully infer about Na_V channel activation gating transitions at high voltages, but it is sufficient for most purposes to yield reliable estimates of current amplitude, inactivation kinetics, and activation kinetics up to about 0 mV. Compilation of macroscopic current traces thus yields information on channel kinetics and voltage dependence of activation and inactivation. Owing to the relative rapid inactivation, true channel open probability is not readily estimated from macroscopic data, as this would require precise knowledge of how activation and inactivation are coupled. In addition, there is no direct access to the single-channel current size.

This can be a substantial limitation when studying the effect of peptide toxins on Na_V channels. Let us consider a µ-conotoxin applied to HEK 293 cells expressing a specific Na_V isoform. The µ-conotoxin blocks the channel but even at high toxin concentration, a residual steady-state current is measured. This may either mean that the channels are only partially blocked, *i.e.* the single-channel current size is reduced, or a certain fraction of channels is blocked while another one may be resistant to block (*e.g.* a fraction of channels that is post-translationally modified to obtain a smaller sensitivity toward the toxin). In such a case, one will need to obtain direct estimates for the single-channel current size (i) and the maximal open probability ($P_{o,max}$). After Sigworth (1980), such information can be extracted from non-stationary fluctuations of current amplitudes among successive current recordings by analyzing the ensemble current and ensemble variance according to *Equation 1*. Heinemann and Conti (1992) described this method in detail for macroscopic patch-clamp data and Steffan and Heinemann (1997) provided the theoretical framework for a quantitative error estimation of the derived parameters. Here, we address the specific problems when performing non-stationary noise analysis of whole-cell Na^+ currents before and after application of µ-conotoxins.

Pulse protocol and current recording

Non-stationary noise analysis relies on successive recordings of many current traces in response to identical conditions and stimuli. This statement contains two major terms that need to be considered with great care. The meaning of "many" depends on the signal-to-noise ratio; considering wild-type Na_V channels under physiological conditions and a peak current size of about 1 nA, one typically needs at least 100-200 current traces. "Identical conditions" means that for all stimulations there should be the same chance for all channels to open, *i.e.* there should be no drift in the number of channels, no other change in channel properties, and no drift in leak or cell capacitance. Both criteria require the rapid recording of all current traces at invariable intervals. It also means that the repetition interval must be large enough as to avoid cumulative channel inactivation. In addition, current recording has to include reference traces used for leak correction. Thus, we propose a stimulation protocol as outlined in *Figure 2a*. Rather than applying one stimulus per sweep and then alternating the main stimulus with the leak stimulus from time to time (Heinemann and Conti, 1992), we generate one stimulus template containing segments for leak correction and several segments for Na^+ current recording covering a range of depolarizations. In the example shown where the holding potential is -120 mV, there are steps to -140 mV and -100 mV used for generating leak currents, and depolarizing steps to -20, -10, +10, and +20 mV; all steps must have equal lengths. The time between test depolarizations is chosen to allow complete recovery from fast inactivation: here, 40 ms. Such a protocol can be repeated at a rate of 1 Hz without running into cumulative slow inactivation, *i.e.* the recording of 200 sweeps will take 200 s. The sampling rate should be chosen as high as possible; typical values are 20 µs with an 8-pole low-pass Bessel filter set to 5 kHz.

Prior to automatic analysis, one should make sure that there are no obvious artifacts in the recordings, and that the leak, capacitance and Na_V-mediated currents are roughly stable. Elimination of "bad" recordings can also be automated according to objective criteria as described in Heinemann and Conti (1992). As the result of raw data analysis, there will be the mean leak traces, the mean leak-corrected Na^+ current traces (*Figure 2b*) and, based on the differences of successive recordings (*Figure 2a*), the mean ensemble variances of the Na^+ currents (*Figure 2b*).

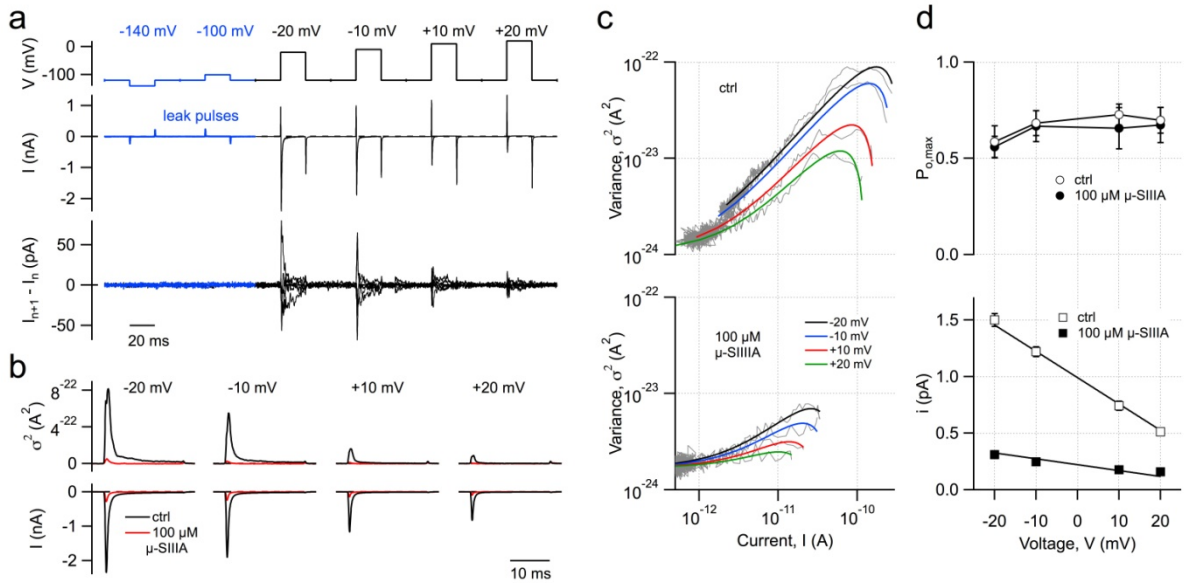

Figure 2. Non-stationary noise analysis of Na^+ currents recorded in the whole-cell configuration from transfected HEK 293 cells. (**a**) Pulse protocol used to activate Na_V channels (*top*). Current traces resulting from the blue stimulation segments are used for correcting leak and capacitive currents. Superposition of 6 raw data traces (*center*) and 5 differences of successive traces (*bottom*). (**b**) Leak-corrected mean current (*bottom*) and mean ensemble variance (*top*) for $Na_V1.4$ channels, before (*black*) and after (*red*) application of 100 µM µ-SIIIA. Mean data are based on 200 individual current sweeps each. (**c**) Mean ensemble variance as a function of mean current for four different voltages (*gray*) with superimposed global fits according to *Equation 1* on a logarithmic scale under control conditions (*top*) and after application of µ-SIIIA (*bottom*). (**d**) Resulting parameters as a function of test-voltage: maximal open probability ($P_{o,max}$, *top*) and single-channel current (*i*, *bottom*) for control conditions (n=6, *open symbols*) and after µ-SIIIA application (n=4, *filled symbols*). $P_{o,max}$ values are connected by straight lines; *i* values are superimposed with linear fits. Error bars indicate standard error of the mean (S.E.M.) values.

Figure 2. *Analyse de bruit non stationnaire des courants Na^+ enregistrés dans la configuration « cellule entière » au niveau de cellules HEK 293 transfectées. (**a**) Protocole d'impulsions utilisé pour activer des canaux Na_V (*en haut*). Traces de courant résultant de la série bleue de stimulations et utilisés pour corriger les courants de fuite et capacitifs. Superposition de 6 traces de données brutes (*au centre*) et de 5 différences de traces successives (*en bas*). (**b**) Courant moyen corrigé du courant de fuite (*en bas*) et moyenne de l'ensemble des variances (*en haut*) pour les canaux $Na_V1.4$, avant (*en noir*) et après (*en rouge*) l'application de 100 µM de µ-SIIIA. Dans chaque cas, les données moyennes sont basées sur 200 balayages de courant individuel. (**c**) Moyenne de l'ensemble des variances en fonction du courant moyen pour quatre potentiel différents (*en gris*) avec superposition des ajustements globaux selon l'*Equation 1 *sur une échelle logarithmique, dans des conditions contrôles (*en haut*) et après l'application de µ-SIIIA (*en bas*). (**d**) Paramètres résultants en fonction de la stimulation test: probabilité maximale d'ouverture ($P_{o,max}$, en haut) et courants via un seul canal (i, en bas) pour les conditions contrôles (n=6, symboles blancs) et après l'application de µ-SIIIA (n=4, symboles noirs). Les valeurs de $P_{o,max}$ sont reliées par des lignes droites; celles de i sont ajustées linéairement. Les barres d'erreur indiquent les valeurs de l'erreur standard de la moyenne (E.S.M.).*

Noise analysis and global data fitting

The next step in non-stationary noise analysis is to plot the mean ensemble variance (σ^2) as a function of the mean current (I). Given the limited time resolution of whole-cell patch-clamp, one should only use those data corresponding to inactivating currents, *i.e.* from the peak current to the end. These data are then fitted with *Equation 1* to yield the background variance (σ^2_b), the single-channel current (i) and the total number of channels (N). The maximal open probability ($P_{o,max}$) is subsequently obtained from $I_{max} = P_{o,max} * i * N$. This procedure only works well if the data contain information about a wide range of P_o values; ideally, P_o should go from zero to greater than 0.5, *i.e.* the parabola defined by *Equation 1* should exceed its maximum. For Na_V channels with their rapid inactivation, however, P_o typically is much smaller than 0.5. Therefore, current recordings at -20 mV or below might be useful for estimating the single-channel current size (i), but such data do not constrain the fit as to allow faithful estimation of N. Therefore, as proposed earlier for the analysis of *Shaker* K^+ channel-mediated current recordings (Starkus *et al.*, 2003), N needs to be constrained by additional data. Rather than fitting σ^2-I relationships for individual test potential, we apply here a global fit to the data of all test potentials simultaneously using individual single-channel currents [$i(V)$] but only one total number of channels N (*Figure 2c*).

$$\sigma^2 = \sigma_b^2 + i\,I - \frac{I^2}{N} \qquad \textit{Equation 1}$$

A corresponding experiment is illustrated in *Figure 2*. $Na_V1.4$ channels were expressed in HEK 293 cells, and single-channel parameters were determined before and after application of 100 µM of µ-SIIIA. For detailed experimental protocols, refer to Leipold *et al.* (2011). Even this saturating toxin concentration does not block the macroscopic current completely (see *Figure 2b*, *red traces*). We thus analyzed control currents and current after toxin application for 200 successive data traces each, and compiled leak-corrected mean current and ensemble variance using PulseTools software (HEKA Elektronik, Lambrecht/Pfalz, Germany). Such data were exported to IgorPro (WaveMetrics, Lake Oswego, OR, USA) and the falling phases of the current traces were plotted in a parametric manner, *i.e.* σ^2 *versus I* (*Figure 2c*). In IgorPro, a global fit according to *Equation 1* was applied to all data of one condition, leaving as free parameters 4 background variances (σ^2_b, for 4 voltages), 4 single-channel currents and only one total number of channels (*N*). The results, based on 4-6 such experiments, are summarized in *Figure 2d*: while the maximal open probabilities only showed some voltage dependence in the range explored, they did not significantly differ between control and toxin conditions. Single-channel current, however, was reduced substantially by µ-SIIIA. The conductance derived from a linear fit to the *i*(*V*) data was reduced from 23.3±1.2 to 5.2±0.3 pS, thus clearly showing that µ-SIIIA does not occlude the Na_V channel pore completely but leaves some "leak" current of about 20% of the original value. In addition, it was noticed that the total number of channels dropped to about 55%, indicating that some channels were either completely blocked or disappeared because of other reasons.

Non-invasive and rapid removal of fast channel inactivation

As shown above, non-stationary noise analysis can be applied to analyze current components that persist upon toxin application. Such a component, however, could also be of alternative origin. Although electrically non-excitable, HEK 293 cells also exhibit some endogenous Na^+ currents. Depending on cell culture conditions and transfection, about 100 pA of peak Na^+ currents can be recorded. Such endogenous currents appear to be particularly apparent when cells are transfected with plasmids (*e.g.* empty vectors). Judged from the voltage dependence of steady-state inactivation, these endogenous currents share some similarity with cardiac $Na_V1.5$-mediated currents; in addition, the currents are not completely blocked with 300 nM TTX (*not shown*). PCR analysis of cDNA from HEK 293 cells suggests some expression of $Na_V1.7$, $Na_V1.5$ and $Na_V1.6$ channels. Thus, HEK 293 cells are a very suited expression system for Na_V channels because most cells do not exhibit endogenous Na^+ currents, although some residual endogenous current components cannot be excluded. Therefore, in particular in experiments where the exogenous channel gene expresses poorly or when only a small fraction of residual current has to be analyzed (*Figure 3*), one may need independent proof for the identity of the respective current component. We have already seen that it can be useful to alter the TTX sensitivity of the channel under investigation in order to discriminate it clearly from endogenous components. However, in some experiments, this method may be insufficient because (a) the endogenous current may contain TTX-sensitive and –insensitive components (such as in dorsal root ganglion neurons, for example), or (b) TTX may interfere with the toxin under investigation. This is particularly relevant when studying µ-conotoxins that target receptor site-1 of Na_V channels much like TTX and saxitoxin. Therefore, specific modulation of channel inactivation may be an alternative option.

Most Na_V channel isoforms share strong similarity regarding their kinetics of inactivation. Deliberate removal of inactivation would therefore be an ideal tool to identify exogenously expressed channels. In addition, removal of fast inactivation will "simplify" the complex gating scheme of Na_V channels and may, therefore, help to understand the molecular mechanisms underlying the specific interaction of some peptide toxins with the channel's voltage-sensors. It therefore appears quite straightforward to generate Na_V channel mutants in which fast channel inactivation is eliminated. Based on the knowledge of the functional relevance of the IFM inactivation motif in the intracellular linker connecting domains III and IV (*Figure 1a*; West *et al.*, 1992), one could alter this motif to IQM or QQQ in order to remove inactivation. However, such mutations apparently have a strong effect on cell function. While inactivation-deficient Na_V channels express reasonably well in *Xenopus* oocytes (*e.g.* Schlief *et al.*, 1996), current amplitudes obtained in mammalian cells are typically very small (Grant *et al.*, 2000). Although not studied in detail, it appears that non-inactivating Na_V channels contribute to cell depolarization and, hence, reduce the likelihood of survival. Besides such technical considerations, expression of inactivation-deficient Na_V variants bears the disadvantage of lacking control conditions, *i.e.* channels with intact inactivation.

Therefore, it would be ideal to use a Na_V channel mutant with functional properties virtually indistinguishable from wild-type channels and whose inactivation can be eliminated during the course of an experiment in a largely non-invasive manner without changing pipette or bath solution. An approach followed here relies on the chemical modification of the IFM inactivation motif. While the methionine alone is already a target for oxidative modification that ultimately leads to loss of inactivation (Kassmann *et al.*, 2008), we previously showed that placement of a cysteine residue inside this motif (ICM) makes channel inactivation very sensitive to oxidative modification (Haenold *et al.*, 2008). Here, we introduce channel mutant "IFC" as also very sensitive but displaying almost complete inactivation under control conditions. Such mutant, when expressed in mammalian cells and assayed in the whole-cell recording configuration, has to be challenged chemically to remove inactivation. This is readily obtained, *e.g.* by the extracellular application of 100 µM of the membrane permeant cysteine-specific modifier DTNP [2,2'-Dithiobis(5-nitropyridin)]. Such an external application, however, may interfere with simultaneous external application of toxins under study. We therefore propose an alternative method.

Rather than using acute application of a chemical that modifies the cysteine in the "IFC" motif to remove inactivation, we make use of the light-sensitive dye Lucifer Yellow. When irradiated with blue light, it decomposes and releases radicals that rapidly react with thiol groups and even remove inactivation of wild-type

Na_V channels when exposed for a long time (Higure *et al.*, 2003; Kassmann *et al.*, 2008). In the experiment shown in *Figure 3*, it is illustrated how Lucifer Yellow, loaded into the cell *via* the patch-pipette, is used to rapidly remove inactivation of "IFC" channels during application of µ-conotoxin SmIIIA (from *Conus stercusmuscarum*) to identify the nature of the small current component remaining after toxin application.

Lucifer Yellow, at a concentration of 250 µM, is supplemented to the pipette solution. A few minutes after establishing a whole-cell configuration, the cell is loaded with the dye. These operations and the acquisition of control current data are performed with dim transmission microscope light. Breakdown of Lucifer Yellow is elicited by application of blue light from a 50-W HBO mercury lamp, directed to the cell *via* a 10x objective and passed through a GFP epifluorescence filter set (492/SP, 495/BS). As can be seen in *Figure 3b*, illumination of the cell removed inactivation of $Na_V1.4$-IFC channels almost completely without any apparent channel deterioration. Inactivation removal occurred with a time constant of about 10 s (*Figure 3c*), *i.e.* a total light exposure of one minute was sufficient to reach saturation. When the same procedure was applied to wild-type $Na_V1.4$ channels, loss of inactivation within one minute was less than 5% (Kassmann *et al.*, 2008).

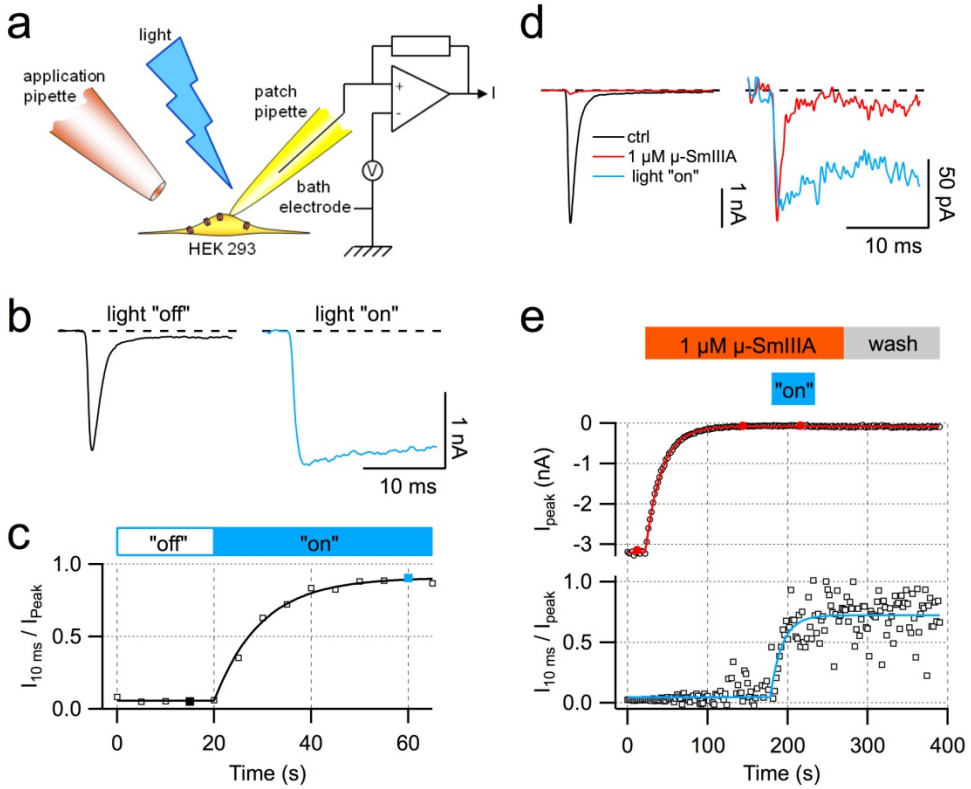

Figure 3. Removal of fast Na_V channel inactivation with light-exposed Lucifer Yellow. (**a**) Experimental design showing a HEK 293 cell under whole-cell patch-clamp control; the cell is loaded with Lucifer Yellow *via* the patch-pipette. Toxin is locally applied *via* a small pipette and Lucifer Yellow is excited by blue light *via* the objective. (**b**) Sample $Na_V1.4$-IFC-mediated current traces at -20 mV, before (*black*) and 40 s after (*blue*) light was turned on. (**c**) Time course of inactivation removal in response to light stimulation. The superimposed curve is a single-exponential fit with a time constant of 9.7±0.6 s. (**d**) $Na_V1.4$-IFC-mediated current traces before (*black*) and after (*red*) application of 1 µM µ-SmIIIA (*left*); the toxin reduces the peak current to a few percents. Magnified current trace after µ-SmIIIA application (*right*) before (*red*) and after (*blue*) the light was turned on; the residual current clearly loses inactivation, indicating that is was no endogenous current but truly results from $Na_V1.4$-IFC. (**e**) Time course of peak inward current (*top*) and fraction of non-inactivating current (*bottom*) with the indicated stimulation with toxin and light. Continuous curves are single-exponential data fits with time constants of 19.9±0.8 s for channel block by µ-SmIIIA (*red*) and 9.5±2.5 s for light-induced removal of inactivation of the toxin-resistant current component (*blue*).

Figure 3. *Suppression de l'inactivation rapide du canal Na_V avec le Jaune Lucifer exposé à la lumière. (**a**) Conception expérimentale montrant une cellule HEK 293 enregistrée en* patch-clamp *dans la configuration « cellule entière »; la cellule est chargée de Jaune Lucifer* via *la pipette de* patch*. La toxine est appliquée localement,* via *une petite pipette, et le Jaune Lucifer est excité par une lumière bleue à travers l'objectif. (**b**) Echantillon de traces de courant médié par les canaux $Na_V1.4$-IFC à -20 mV, avant (*noir*) et 40 s après (*bleu*) que la lumière ait été ouverte. (**c**) Evolution dans le temps de la suppression de l'inactivation, en réponse à une stimulation lumineuse. La courbe superposée est un ajustement selon une seule exponentielle avec une constante de temps de 9,7±0,6 s. (**d**) Traces de courant médié par les canaux $Na_V1.4$-IFC avant (*noir*) et après (*rouge*) l'application de 1 µM de µ-SmIIIA (*gauche*); la toxine réduit le pic de courant quelques pourcents. Trace amplifiée de courant après l'application de µ-SmIIIA (*droite*) avant (*rouge*) et après (*bleu*) que la lumière ait été ouverte; le courant résiduel perd clairement son inactivation, ce qui indique que ce n'était pas un courant endogène mais un courant réellement médié par les canaux $Na_V1.4$-IFC. (**e**) Evolution dans le temps du pic de courant entrant (*haut*) et de la fraction de courant qui ne s'inactive pas (*bas*) avec la stimulation par la toxine et la lumière, comme indiqué. Les courbes continues sont des ajustements mono-exponentiels des données avec des constantes de temps de 19,9±0,8 s pour le blocage du canal par la µ-SmIIIA (*rouge*) et 9,5±2,5 s pour la suppression de l'inactivation, produite par la lumière, de la composante de courant résistante à la toxine (*bleu*).*

In *Figure 3d-e*, currents through $Na_V1.4$-IFC channels were measured under control conditions (black) and during application of 1 µM µ-SmIIIA, which blocks the peak current by about 95% within about 100 s. To reveal the nature of the remaining small current (shown in red in *Figure 3d*), Lucifer Yellow breakdown was initiated with a 60-s episode of blue light illumination. About 30 s after light was turned on, inactivation of the residual current was completely removed (*Figure 3d*, blue trace), clearly showing that the channels responsible for the remaining current component are the exogenously expressed $Na_V1.4$-IFC channels and not channels endogenous to HEK 293 cells.

Conclusion

We conclude that channel chimeras, when constructed in a systematic manner, (a) have a high chance of yielding functional channels, (b) transplant functional channel modules, (c) are useful tools for finding out where/how toxins bind to the channel protein and what causes the subtype specificity of some toxins. Furthermore, we conclude that non-stationary noise analysis, applied to voltage-gated ion channels, is tricky because of the limited time resolution. However, when simultaneously applied for several voltages and using global fit procedures, it provides a rapid and easy access to single-channel parameters otherwise not attainable. Finally, light-induced removal of rapid inactivation is a useful tool for the identification of "foreign" current components in HEK 293 cells. In addition, deliberate removal of fast inactivation provides access to kinetic studies otherwise hard to perform because non-inactivating sodium channels typically do not result in sizable currents in mammalian cells.

Acknowledgements. *We like to acknowledge support* via *the CONCO cone snail genome project for health within the 6th Framework Program (LSHB-CT-2007) and DFG HE2993/5, O. Hartley (Univ. Geneva) for providing us with µ-SmIIIA, and D. Imhof (Univ. Bonn) for µ-SIIIA.*

References

Chahine M, Deschene I, Chen LQ, Kallen RG (1996) Electrophysiological characteristics of cloned skeletal and cardiac muscle sodium channels. *Am J Physiol* **271**: 498-506

Cestèle S, Catterall WA (2000) Molecular mechanisms of neurotoxin action on voltage-gated sodium channels. *Biochemie* **82**: 883-892

Cestèle S, Qu Y, Rogers JC, Rochat H, Scheuer T, Catterall WA (1998) Voltage sensor-trapping: enhanced activation of sodium channels by beta-scorpion toxin bound to the S3-S4 loop in domain II. *Neuron* **21**: 919-931

Choi JS, Tyrrell L, Waxman SG, Dib-Hajj SD (2004) Functional role of the C-terminus of voltage-gated sodium channel Na(v)1.8. *FEBS Lett* **572**: 256-260

Choudhary G, Aliste MP, Tieleman DP, French RJ, Dudley SC Jr (2007) Docking of µ-conotoxin GIIIA in the sodium channel outer vestibule. *Channels* **1**: 344-352

Cummins TR, Aglieco F, Dib-Hajj SD (2002) Critical molecular determinants of voltage-gated sodium channel sensitivity to µ-conotoxins GIIIA/B. *Mol Pharmacol* **61**: 1192-1201

Dudley SC Jr, Chang N, Hall J, Lipkind G, Fozzard HA, French RJ (2000) µ-conotoxin GIIIA interactions with the voltage-gated Na^+ channel predict a clockwise arrangement of the domains. *J Gen Physiol* **116**: 679-690

Dudley SC Jr, Todt H, Lipkind G, Fozzard HA (1995) A µ-conotoxin-insensitive Na^+ channel mutant: possible localization of a binding site at the outer vestibule. *Biophys J* **69**: 1657-1665

Grant AO, Chandra R, Keller C, Carboni M, Starmer CF (2000) Block of wild-type and inactivation-deficient cardiac sodium channels IFM/QQQ stably expressed in mammalian cells. *Biophys J* **79**: 3019-3035

Gur M, Kahn R, Karbat I, Regev N, Wang J, Catterall WA, Gordon D, Gurevitz M (2011) Elucidation of the molecular basis of selective recognition uncovers the interaction site for the core-domain of scorpion alpha-toxins on sodium channels. *J Biol Chem* 2011 [Epub ahead of print] doi: 10.1074/jbc.M111.259507

Haenold R, Wassef R, Brot N, Neugebauer S, Leipold E, Heinemann SH, Hoshi T (2008) Protection of vascular smooth muscle cells by methionine sulfoxide reductase A – Role of intracellular localization and substrate availability. *Free Radic Res* **42**: 978–988

Hamill OP, Marty A, Neher E, Sakmann B, Sigworth FJ (1981) Improved patch-clamp techniques for high-resolution current recording from cells and cell-free membrane patches. *Pflügers Arch* **391**: 85-100

Heinemann SH, Conti F (1992) Non-stationary noise analysis and its application to patch clamp recordings. In: B. Rudy, L.E. Iverson (Edts) Academic Press, Ion Channels*, Methods Enzymol.* **207**: 131-148

Heinemann SH, Leipold E (2007) Conotoxins of the O-superfamily affecting voltage-gated sodium channels. *Cell Mol Life Sci* **64**: 1329-1340

Higure Y, Katayama Y, Takeuchi K, Ohtubo Y, Yoshii K (2003) Lucifer Yellow slows voltage-gated Na^+ current inactivation in a light-dependent manner in mice. *J Physiol* **550**: 159-167

Kassmann M, Hansel A, Leipold E, Birkenbeil J, Lu SQ, Hoshi T, Heinemann SH (2008) Oxidation of multiple methionine residues impairs rapid sodium channel inactivation. *Pflügers Arch* **456**: 1085-1095

Leipold E, DeBie H, Zorn S, Borges A, Olivera BM, Terlau H, Heinemann SH (2007) µO-conotoxins inhibit Na_V channels by interfering with their voltage sensors in domain-2. *Channels* **1**: 253-262

Leipold E, Hansel A, Borges A, Heinemann SH (2006) Subtype specificity of scorpion β-toxin Tz1 interaction with voltage-gated sodium channels is determined by the pore loop of domain 3. *Mol Pharmacol* **70**: 340-347

Leipold E, Hansel A, Olivera BM, Terlau H, Heinemann SH (2005) Molecular interaction of δ-conotoxins with voltage-gated sodium channels. *FEBS Lett* **579**: 3881-3884

Leipold E, Lu SQ, Gordon D, Hansel A, Heinemann SH (2004) Combinatorial interaction of scorpion α-toxins Lqh-3, Lqh-2 and LqhαIT with sodium channel receptor sites-3. *Mol Pharmacol* **65**: 685-691

Leipold E, Markgraf R, Miloslavina A, Kijas M, Schirmeyer J, Imhof D, Heinemann SH (2011) Molecular determinants of the subtype specificity of μ-conotoxin SIIIA targeting neuronal voltage-gated sodium channels. *Neuropharmacology* **61**: 105-111

Li RA, Ennis IL, French RJ, Dudley SC Jr, Tomaselli GF, Marban E (2001) Clockwise domain arrangement of the sodium channel revealed by μ-conotoxin (GIIIA) docking orientation. *J Biol Chem* **276**: 11072-11077

Lee A, Goldin AL (2009) Role of the terminal domains in sodium channel localization. *Channels* **3**: 171-180

Lee A, Goldin AL (2008) Role of the amino acid and carboxy termini in isoform-specific sodium channel variation. *J Physiol* **586**: 3917-3926

O´Reilly JP, Wang SY, Kallen RG, Wang GK (1999) Comparison of slow inactivation in human heart and rat skeletal muscle Na^+ channel chimaeras. *J Physiol* **515**: 61-73

Rogers JC, Qu Y, Tanada TN, Scheuer T, Catterall WA (1996) Molecular determinants of high affinity binding of α-scorpion toxin and sea anemone toxin in the S3-S4 extracellular loop of domain IV of the Na^+ channel α subunit. *J Biol Chem* **217**: 15950-15962

Schirmeyer J, Szafranski K, Leipold E, Mawrin C, Platzer M, Heinemann SH (2010) A subtle alternative splicing event of the $Na_v1.8$ voltage-gated sodium channel is conserved in human, rat, and mouse. *J Mol Neurosci* **41**: 310-314

Schlief, T, Schönherr R, Imoto K, Heinemann SH (1996) Pore properties of rat brain II sodium channels mutated in the selectivity filter domain. *Eur Biophys J* **25**: 75-91

Shichor I, Zlotkin E, Ilan N, Chikashvili D, Stühmer W, Lotan I (2002) Domain 2 of *Drosphila para* voltage-gated sodium channel confers insect properties to a rat brain channel. *J Neurosci* **22**: 4364-4371

Sigworth FJ (1980) The variance of sodium current fluctuations at the node of Ranvier. *J Physiol* **307**: 97-129

Starkus JG, Varga Z, Schönherr R, Heinemann SH (2003) Mechanisms for the inhibition of *Shaker* potassium channels by protons. *Pflügers Arch* **447**: 44-54

Steffan R, Heinemann SH (1997) Error estimates for results of nonstationary noise analysis derived with linear least squares methods. *J Neurosci Methods* **78**: 51-63

Vijayaragavan K, Acharfi S, Chahine M (2004) The C-terminal region as a modulator of rNa(v)1.7 and rNa(v)1.8 expression levels. *FEBS Lett* **559**: 39-44

West JW, Patton DE, Scheuer T, Wang Y, Goldin AL, Catterall WA (1992) A cluster of hydrophobic amino acid residues required for fast Na^+-channel inactivation. *Proc Natl Acad Sci USA* **89**: 10910-10914

Wright SW, Wang S-Y, Xiao Y-F, Wang GK (1999) State-dependent cocaine block of Na channel isoforms, chimeras, and channels coexpressed with the β1-subunit. *Biophys J* **76**: 233-245

Zorn S, Leipold E, Hansel A, Bulaj G, Olivera BM, Terlau H, Heinemann SH (2006) The μO-conotoxin MrVIA inhibits voltage-gated sodium channels by associating with domain-3. *FEBS Lett* **580**: 1360-1364

Toxines et Transferts ioniques – Toxins and Ion transfers
Rencontres en Toxinologie – Meeting on Toxinology, 2011
Editions de la SFET – SFET Editions
Accès libre en ligne sur le site – Free access on line on the site : http://www.sfet.asso.fr

An overview of the ion channel modulation and neurocellular disorders induced by ciguatoxins

César MATTEI[1,2*], Jordi MOLGÓ[1], Evelyne BENOIT[1]

[1] CNRS, Institut de Neurobiologie Alfred Fessard - FRC2118, Laboratoire de Neurobiologie et Développement – UPR3294, 1 avenue de la Terrasse, F-91198 Gif sur Yvette cedex, France ; [2] Laboratoire Récepteurs et Canaux ioniques Membranaires, UFR Sciences, Université d'Angers, Angers, France

** Corresponding author ; E-mail : cesar.mattei@univ-angers.fr*

Abstract

*Numerous toxins bind central and peripheral nervous system receptors, including ion channels. Among them, ciguatoxins are non-peptidic compounds produced by tropical dinoflagellates (*Gambierdiscus *genus). They are responsible for a human intoxication, named ciguatera fish poisoning, mediated through seafood and fish. These toxins were initially described as voltage-gated sodium channel activators. Hence, they are responsible for various perturbations of the biophysical properties of these channels, such as inhibition of part of their inactivation and shift of their activation towards more negative potentials. In addition, ciguatoxins target and block voltage-dependent potassium channels in excitable membranes. These modifications of sodium and potassium voltage-gated channel properties result in a variety of neurocellular perturbations, such as massive Na^+ entry, increase in intracellular Ca^{2+}, enhancement of neuronal excitability, sustained increase in spontaneous and transient increase in evoked neurotransmitter release from the motor nerve terminals, and uncoordinated muscular fibres contraction. However, the interaction between ciguatoxins and ion channels does not account for all the symptoms associated with ciguatera fish poisoning. Recent data strongly suggest that these toxins can also target, at low concentrations, other membrane receptors. Such interactions could be explained by the non-peptidic nature of these toxins and their low molecular weight.*

Une vue d'ensemble de la modulation des canaux ioniques et des altérations neurocellulaires produites par les ciguatoxines

De nombreuses toxines interagissent avec des récepteurs des systèmes nerveux central et périphérique, dont les canaux ioniques. Parmi elles, les ciguatoxines sont des toxines non-peptidiques, issues de dinoflagellés (genre Gambierdiscus*) des zones tropicales et responsables d'une intoxication humaine, nommée ciguatéra, par la contamination de poissons et de fruits de mer. Ces toxines ont été initialement décrites comme des activateurs des canaux sodium sensibles au potentiel de membrane. A ce titre, elles sont responsables de modifications importantes des propriétés biophysiques de ces canaux, telles que l'inhibition partielle de leur inactivation et le déplacement de leur activation vers des potentiels de membrane plus négatifs. De plus, les ciguatoxines ciblent et bloquent les canaux potassium dépendants du potentiel dans les membranes excitables. Ces altérations fonctionnelles des canaux sodium et potassium, sensibles au potentiel, se traduisent par un ensemble de perturbations neurocellulaires, telles que l'entrée massive d'ions Na^+, l'augmentation du Ca^{2+} intracellulaire, l'augmentation de l'excitabilité neuronale, l'accroissement maintenu de la libération spontanée et celui transitoire de la libération évoquée de neurotransmetteur au niveau des terminaisons nerveuses motrices, ainsi que la contraction incoordonnée des fibres musculaires. Cependant, l'interaction des ciguatoxines avec les canaux ioniques ne suffit pas à rendre compte de la totalité des symptômes associés à la ciguatéra. Des travaux récents suggèrent fortement que ces toxines se lient également, à faibles concentrations, à d'autres récepteurs membranaires. De telles liaisons pourraient s'expliquer par la nature non-peptidique des toxines et leur faible poids moléculaire.*

Keywords : *Brevenal, ciguatoxins, dinoflagellate, neurological symptoms, neuronal excitability, neurotransmitter release, voltage-gated ion channels.*

Introduction

Ciguatoxins (CTXs) are responsible for ciguatera fish poisoning, a human syndrome acquired through the marine food chain. Poisoning appears after the consumption of tropical and subtropical fish which contain at least one form of CTXs (Achaibar *et al.*, 2007; Isbister and Kiernan, 2005). CTXs are cyclic polyether compounds produced by different dinoflagellates of the genus *Gambierdiscus (G. toxicus*, *G. Pacificus*, *G.*

australes, *G. polynesiensis*, and *G. Belizeanus;* Chinain *et al.*, 2010; Roeder *et al.*, 2010) which colonizes the coral reef and gets eaten by herbivorous fish (for a review, see Molgó *et al.*, 2010). The disease's symptoms include gastro-intestinal, cardiac, dermatological, neurological and muscle disorders (Friedman *et al.*, 2008). Variations in symptoms depend on the geographical area of the intoxication, as well as on the nature and concentration of toxins, and on individual susceptibility (Achaibar *et al.*, 2007). Ciguatera is considered as a major public health issue since up to 50,000 cases can be recorded in a single year. It concerns mainly the endemic areas, but ciguatera appeared recently under temperate latitudes, in Spanish and Portuguese Islands, as well as in the Mediterranean, probably through the development of the fishing industry and the modifications of the climate (Otero *et al.*, 2010; Alfonso *et al.*; 2010). No cure is available yet, and symptomatic treatment is administered to people exhibiting ciguatoxic symptoms. It consists in intravenous perfusion of D-mannitol to counter-balance neurological symptoms, in analgesics against muscle pain troubles, in antihistaminics for dermatological allergies and, in acute cases, in monitoring vital parameters (Achaibar *et al.*, 2007). The ecological role of CTXs remains unknown, but recent data on *Karenia brevis*, a dinoflagellate which produces CTX-structurally related toxins, named brevetoxins (PbTxs), strongly suggest that salinity modification of marine medium enhances PbTx production from *K. brevis*. Hypo-osmotic stress induces the dinoflagellate to produce PbTxs and then, to resist to these important osmotic changes (Errera and Campbell, 2011).

Increased neuronal excitability

CTXs bind to the α subunit of voltage-sensitive sodium channels (VSSCs) at their receptor site 5 and trigger the opening of the pore at the resting membrane potential (Bidart *et al.*, 1984; Lombet *et al.*, 1987; Benoit *et al.*, 1996). The toxins are responsible for alteration of the biophysical properties of the channels: CTXs inhibit, in part, their inactivation process (*Figure 1A*) and shift the voltage-dependence of their activation to more negative membrane potentials (Benoit *et al.*, 1986, 1996). These modifications were observed on both sensory and motor nerve fibres and led to the appearance of spontaneous and repetitive action potentials (Benoit *et al.*, 1996; Strachan *et al.*, 1999; Mattei *et al.*, 1999). CTXs, like PbTxs, target the receptor site 5 of VSSCs and exhibit an affinity for, at least, $Na_V1.2$ (brain), $Na_V1.4$ (skeletal muscle), $Na_V1.5$ (heart), $Na_V1.6$ (motor neuron) and $Na_V1.8$ (sensory neurons) in heterologous or native systems (Caldwell *et al.*, 2000; Yamaoka *et al.*, 2004, 2009; Lombet *et al.*, 1987; Mattei *et al.*, 2010). Although CTXs have been shown to activate VSSCs by altering their inactivation mechanism, other data strongly suggest that they are also able to down-regulate VSSC activation. Inhibition of Na^+ currents was described using different CTXs, in a concentration-dependent manner (Yamaoka *et al.*, 2004; Schlumberger *et al.*, 2010). This led authors to speculate about a multimodal effect of CTXs on VSSCs, with both stimulatory and inhibitory aspects, which could be due to the chemical nature of these toxins: (i) their lipophilic properties enable CTXs to insert within the membrane and (ii) their relatively high molecular size (Yamaoka *et al.*, 2004).

Other membrane receptors are thought to be targeted by CTXs and may contribute to the increased neuronal excitability. The fact that CTXs could act on voltage-sensitive K^+ channels was first proposed when it was observed that CTXs produce an increase in the duration of action potentials recorded from single frog myelinated axons and DRG neurons (Mattei *et al.*, 1999; Birinyi-Strachan *et al.*, 2005). Then, in various cellular preparations – frog myelinated nerve fibre (*Figure 1B*), rat myotubes and DRG neurons – CTXs were shown to decrease K^+ currents (Hidalgo *et al.*, 2002; Birinyi-Strachan *et al.*, 2005; Schlumberger *et al.*, 2010). Thus, CTXs increase the neuronal excitability of both sensory and motor nerve fibres through a dual action on Na^+ and K^+ channels at nanomolar concentrations.

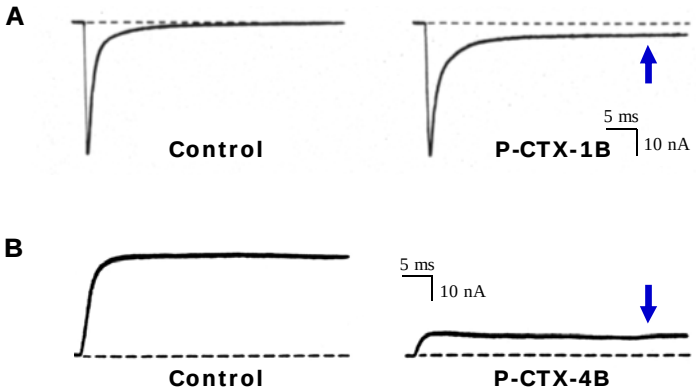

Figure 1. Effects of ciguatoxins on ionic currents recorded from frog single myelinated axons, during 40 ms depolarizations to 0–50 mV from a holding potential of -120 mV. (**A**) Representative traces of sodium current before (control) and after addition of 10 nM Pacific ciguatoxin-1B (P-CTX-1B). (**B**) Representative traces of potassium current before (control) and after addition of 24 nM Pacific ciguatoxin-4B (PCTX-4B). Dashed lines indicate the zero current level.

Figure 1. *Effets des ciguatoxines sur les courants ioniques enregistrés sur des axons myélinisés isolés de grenouille, au cours de dépolarisations de 40 ms à 0–50 mV à partir d'un potentiel de maintien de -120 mV. (**A**) Traces représentatives de courant sodium avant (contrôle) et après l'addition de 10 nM de ciguatoxine-1B du Pacifique (P-CTX-1B). (**B**) Traces représentatives de courant potassium avant (contrôle) et après l'addition de 24 nM de ciguatoxine-4B du Pacifique (PCTX-4B). Les lignes en traits discontinus indiquent le niveau zéro de courant.*

Morphological disturbances

The up-regulation of VSSCs by CTXs promotes an increase in intracellular Na^+ concentration (Na^+_i), which may saturate all the cellular pumps and exchangers that are activated to reduce Na^+_i (Mattei *et al.*, 2008). The intracellular osmotic disorders induced by this Na^+ entry are compensated by an influx of water which causes an increase in cellular volume. To assess the morphological modifications of neuronal preparations induced by CTXs, the styryl FM1-43, classically used as an endo-exocytosis dye, was used. In myelinated nerve fibres and nerve terminals, CTXs, like PbTxs, elicit an about 2-fold volume increase (Benoit *et al.*, 1996; Mattei *et al.*, 1999, 2010). Evidence of an osmotic disorder was brought by the observation that addition of hyperosmotic D-mannitol reverses CTX-induced cellular swelling. Furthermore, in cells where CTXs did not trigger spontaneous and repetitive action potentials, the raise of Na^+_i is not sufficient to induce a volume increase (Bidart *et al.*, 1984; Benoit *et al.*, 1998).

Intracellular Ca^{2+} perturbations

The activation of VSSCs by CTXs has been shown to increase intracellular concentration of Ca^{2+} (Ca^{2+}_i). This is due to a direct mobilisation of these ions from intracellular Ca^{2+} stores and to an indirect activation of the Na^+/Ca^{2+} exchanger in the reversed mode, allowing Ca^{2+} influx against Na^+ efflux (Molgó *et al.*, 1993; Hidalgo *et al.*, 2002; Mattei *et al.*, 2008). Voltage-sensitive Ca^{2+} channels are also probably opened by the depolarizing effect of CTXs, allowing Ca^{2+} to enter into cells. This tetrodotoxin (TTX)-sensitive Ca^{2+} mobilization is thought to be mediated by IP_3 receptors because it prevented a subsequent action of bradykinin (Molgó *et al.*, 1993). Direct evidence for the increase in IP_3 mass levels following Na^+-entry has been obtained with PbTX-3 (Liberona et al.,2008). Then, Ca^{2+}_i increase is supposed to initiate exocytosis of neurotransmitter-containing vesicles.

Neurotransmitter release and hormonal secretion enhancement

The CTX-induced up-regulation of VSSCs and inhibition of K^+ channels are followed by a variety of consequences on neurotransmission and neurosecretion. When bathed with CTXs, the neuromuscular junction exhibit a post-synaptic depolarization and trains of repetitive action potentials (Molgó *et al.*, 1990; Mattei *et al.*, 2010). CTXs first increase, then reduce and eventually block Ca^{2+}-dependent nerve-evoked transmitter release. However, they also enhance Ca^{2+}-independent spontaneous quantal acetylcholine release from neuromuscular junctions. This is followed by the depletion of acetylcholine-containing synaptic vesicles and, consecutively, by a complete blockade of neurotransmitter release. Electron microscopy revealed that CTXs inhibited the recycling of synaptic vesicles (Molgó *et al.*, 1991). Therefore, CTXs increase synaptic transmission through both spontaneous and repetitive synchronous release of neurotransmitter. Subsequent membrane depolarisation and impairment of action potential generation contribute to the neurotransmission decrease (Molgó *et al.* 1990). In bovine chromaffin cells, CTXs exhibit a potent secretory effect. In fact, the activation of VSSCs and the subsequent Ca^{2+}_i increase trigger exocytosis of catecholamine-containing vesicles. This CTX-induced secretion relies on both extra- and intracellular Ca^{2+}, and was abolished by previous intoxication of chromaffin cells with the botulinum neurotoxin A (Mattei *et al.*, 2008).

Inhibition of ciguatoxin actions

TTX, a potent Na^+ channel inhibitor, was used to prevent almost all the CTX-induced effects on excitable cells (Molgó *et al.*, 1991; Benoit *et al.*, 1996; Mattei *et al.*, 2008). In addition, because of the osmotic perturbations they generate – *i.e.* Na^+ influx and subsequent cellular volume increase – a hyperosmolar solution of D-mannitol either reverses or prevents the neurocellular actions of CTXs. Hence, D-mannitol inhibits bursts of CTX-induced spontaneous action potentials in myelinated nerve fibres and thus decreases the cellular swelling of nodes of Ranvier and nerve terminals (Benoit *et al.*, 1996; Mattei *et al.*, 2010). For years, intravenous D-mannitol was considered as a beneficial treatment in human ciguatera intoxications (Palafox *et al.*, 1988), but more recent epidemiological data show that patients improved without treatment (Isbister and Kiernan, 2005). Finally, brevenal, a natural molecule isolated from the dinoflagellate *K. brevis*, was shown to inhibit the stimulatory effect of CTXs, in a range of physiological concentrations (Mattei *et al.*, 2008; Nguyen-Huu *et al.*, 2010). Brevenal was initially shown to displace PbTx binding to receptor site 5 of VSSCs (Bourdelais *et al.*, 2004). Its blocking effect towards CTX-induced neurosecretion through an allosteric effect on VSSCs could be useful in a future treatment of ciguatera.

References

Achaibar KC, Moore S, Bain PG (2007) Ciguatera poisoning. *Pract Neurol* **7**: 316-322

Alfonso A, Rodriguez P, Otero P, Pasconcellos V, Azevedo J, *et al.* (2010) The changing profile of marine neurotoxins in Europe. In *Advances and new technologies in Toxinology*. Barbier J, Benoit E, Marchot P, Mattéi C, Servent D (eds) pp 167-174. SFET Editions, Gif-sur-Yvette, France, Epub on http://www.sfet.asso.fr (ISSN 1760-6004)

Benoit E, Legrand AM, Dubois JM (1986) Effects of ciguatoxin on current and voltage clamped frog myelinated nerve fibre. *Toxicon* **24**: 357-364

Benoit E, Juzans P, Legrand AM, Molgó J (1996) Nodal swelling produced by ciguatoxin-induced selective activation of sodium channels in myelinated nerve fibers. *Neuroscience* **71**: 1121-1131

Benoit E, Meunier FA, Mattei C, Juzans P, Legrand AM, Molgó J (1998) Do sodium ion influx through ciguatoxin-modified voltage-dependent sodium channels induce swelling of the myelinated nerves and neuroblastoma cells? In *Harmful Algae*. Reguera B, Blanco J, Fernández ML, Wyatt T (eds) pp 590-593. Xunta de Galicia and Intergovernmental Oceanographic Commission of UNESCO Publishers

Bidard JN, Vijverberg HP, Frelin C, Chungue E, Legrand AM, Bagnis R, Lazdunski M (1984) Ciguatoxin is a novel type of Na^+ channel toxin. *J Biol Chem* **259**: 8353-8357

Birinyi-Strachan LC, Gunning SJ, Lewis RJ, Nicholson GM (2005) Block of voltage-gated potassium channels by Pacific ciguatoxin-1 contributes to increased neuronal excitability in rat sensory neurons. *Toxicol Appl Pharmacol* **204**: 175-186

Bourdelais AJ, Campbell S, Jacocks H, Naar J, Wright JL, *et al.* (2004) Brevenal is a natural inhibitor of brevetoxin action in sodium channel receptor binding assays. *Cell Mol Neurobiol* **24**: 553-563

Caldwell JH, Schaller KL, Lasher RS, Peles E, Levinson SR (2000) Sodium channel Na(v)1.6 is localized at nodes of ranvier, dendrites, and synapses *Proc Natl Acad Sci USA* **97**: 5616-5620

Chinain M, Darius HT, Ung A, Cruchet P, Wang Z, Ponton D, Laurent D, Pauillac S (2010) Growth and toxin production in the ciguatera-causing dinoflagellate *Gambierdiscus polynesiensis* (Dinophyceae) in culture. *Toxicon* **56**: 739-750

Errera RM, Lisa Campbell L (2011) Osmotic stress triggers toxin production by the dinoflagellate *Karenia brevis*. *Proc Natl Acad Sci USA* **108:** 10597-10601

Friedman MA, Fleming LE, Fernandez M, Bienfang P, Schrank K, *et al.* (2008) Ciguatera fish poisoning: treatment, prevention and management. *Mar Drugs* **6**: 456-479

Hidalgo J, Liberona JL, Molgó J, Jaimovich E (2002) Pacific ciguatoxin-1b effect over Na^+ and K^+ currents, inositol 1,4,5-triphosphate content and intracellular Ca^{2+} signals in cultured rat myotubes. *Br J Pharmacol* **137**: 1055-1062

Isbister GK, Kiernan MC (2005) Neurotoxic marine poisoning. *Lancet Neurol* **4**: 219-228

Lewis RJ (2001) The changing face of ciguatera. *Toxicon* **39**: 97-106

Liberona JL, Cardenas C, Reyes R, Hidalgo J, Molgó J, Jaimovich E (2008) Sodium dependent action potentials induced by brevetoxin-3 trigger both IP3 increase and intracellular Ca^{2+} release in rat skeletal myotubes. *Cell Calcium* **44**: 289-297

Lombet A, Bidard JN, Lazdunski M (1987). Ciguatoxin and brevetoxins share a common receptor site on the neuronal voltage-dependent Na^+ channel. *FEBS Lett* **219**: 355-359

Mattei C, Molgó J, Marquais M, Vernoux JP, Benoit E (1999) Hyperosmolar D-mannitol reverses the increased membrane excitability and the nodal swelling caused by Caribbean ciguatoxin-1 in single frog myelinated axons. *Brain Res* **847**: 50-58

Mattei C, Dechraoui MY, Molgó J, Meunier FA, Legrand AM, Benoit E (1999) Neurotoxins targetting receptor site 5 of voltage-dependent sodium channels increase the nodal volume of myelinated axons. *J Neurosci Res* **55**: 666-673

Mattei C, Wen PJ, Nguyen-Huu TD, Alvarez M, Benoit E, Bourdelais AJ, Lewis RJ, Baden DG, Molgó J, Meunier FA (2008) Brevenal inhibits pacific ciguatoxin-1B-induced neurosecretion from bovine chromaffin cells. *PLoS One* **3**: e3448

Mattei C, Marquais M, Schlumberger S, Molgó J, Vernoux JP, Lewis RJ, Benoit E (2010) Analysis of Caribbean ciguatoxin-1 effects on frog myelinated axons and the neuromuscular junction. *Toxicon* **56**: 759-767

Molgó J, Comella JX, Legrand AM (1990) Ciguatoxin enhances quantal transmitter release from frog motor nerve terminals. *Br J Pharmacol* **99**: 695-700

Molgó J, Comella JX, Shimahara T, Legrand AM (1991) Tetrodotoxin-sensitive ciguatoxin effects on quantal release, synaptic vesicle depletion, and calcium mobilization. *Ann NY Acad Sci* **635**: 485-488

Molgó J, Laurent D, Pauillac S, Chinain M, Yeeting B (2010) Ciguatera and related biotoxins. *Toxicon* **56**: Issue 9 (Special issue)

Molgó J, Shimahara T, Legrand AM (1993) Ciguatoxin, extracted from poisonous morays eels, causes sodium-dependent calcium mobilization in NG108-15 neuroblastoma x glioma hybrid cells. *Neurosci Lett* **158**: 147-150

Nguyen-Huu TD, Mattei C, Wen PJ, Bourdelais AJ, Lewis RJ, Benoit E, Baden DG, Molgó J, Meunier FA (2010) Ciguatoxin-induced catecholamine secretion in bovine chromaffin cells: mechanism of action and reversible inhibition by brevenal. *Toxicon* **56**: 792-796

Otero P, Pérez S, Alfonso A, Vale C, Rodríguez P, Gouveia NN, Gouveia N, Delgado J, Vale P, Hirama M, Ishihara Y, Molgó J, Botana LM (2010). First toxin profile of ciguateric fish in Madeira Arquipelago (Europe). *Anal Chem* **82**: 6032-6039

Roeder K, Erler K, Kibler S, Tester P, Van The H, Nguyen-Ngoc L, Gerdts G, Luckas B (2010) Characteristic profiles of Ciguatera toxins in different strains of *Gambierdiscus* spp. *Toxicon* **56**: :731-738

Schlumberger S, Mattei C, Molgó J, Benoit E (2010) Dual action of a dinoflagellate-derived precursor of Pacific ciguatoxins (P-CTX-4B) on voltage-dependent K(+) and Na(+) channels of single myelinated axons. *Toxicon* **56**: 768-775

Strachan LC, Lewis RJ, Graham M. Nicholson GH (1999) Differential actions of Pacific Ciguatoxin-1 on sodium channel subtypes in mammalian sensory neurons *J Pharm Exp Ther* **288**: 379-388

Trainer VL, Baden DG, Catterall WA (1994) Identification of peptide components of the brevetoxin receptor site of rat brain sodium channels. *J Biol Chem* **269**: 19904-19909

Yamaoka K, Inoue M, Miyahara H, Miyazaki K, Hirama M (2004) A quantitative and comparative study of the effects of a synthetic ciguatoxin CTX3C on the kinetic properties of voltage-dependent sodium channels. *Br J Pharmacol* **142** : 879-889

Yamaoka K, Inoue M, Miyazaki K, Hirama M, Kondo C, Kinoshita E, Miyoshi H, Seyama I (2009) Synthetic ciguatoxins selectively activate $Na_V1.8$-derived chimeric sodium channels expressed in HEK293 cells. *J Biol Chem* **284**: 7597-7605

Toxines et Transferts ioniques – Toxins and Ion transfers
Rencontres en Toxinologie – Meeting on Toxinology, 2011
Editions de la SFET – SFET Editions
Accès libre en ligne sur le site – Free access on line on the site : http://www.sfet.asso.fr

Pinnatoxins : an emergent family of marine phycotoxins targeting nicotinic acetylcholine receptors with high affinity

Rómulo ARÁOZ[1], Denis SERVENT[2], Jordi MOLGÓ[1*], Bogdan I. IORGA[3], Carole FRUCHART-GAILLARD[2], Evelyne BENOIT[1], Zhenhua GU[4], Craig STIVALA[4], Armen ZAKARIAN[4]

[1] CNRS, Centre de Recherche de Gif-sur-Yvette - FRC3115, Institut de Neurobiologie Alfred Fessard - FRC2118, Laboratoire de Neurobiologie et Développement - UPR3294, F-91198 Gif-sur-Yvette, France ; [2] CEA, iBiTec-S, Service d'Ingénierie Moléculaire des Protéines, Laboratoire de Toxinologie Moléculaire et Biotechnologies, F-91191 Gif-sur-Yvette, France ; [3] CNRS, Centre de Recherche de Gif-sur-Yvette - FRC3115, Institut de Chimie des Substances Naturelles - UPR 2301, F-91198 Gif-sur-Yvette, France ; [4] Department of Chemistry and Biochemistry, University of California, Santa Barbara, California 93106-9510, USA

** Corresponding author ; Tel : +33 (0) 1 6982 3642 ; Fax : +33 (0) 1 6982 3447 ; E-mail : molgo@inaf.cnrs-gif.fr*

Abstract

Pinnatoxins belong to an emerging class of phycotoxins of the cyclic imine group. Detailed studies of their biological effects have been impeded for a long time due to unavailability of both the complex natural product and its natural source. Recent studies point out that the dinoflagellate Vulcanodinium rugosum *Nézan* et *Chomérat, gen. nov., sp. nov., first discovered in France, is responsible for the production of pinnatoxins E, F and G in New Zealand, Australia, Japan and France. With synthetic pinnatoxin A, a detailed study has been performed, providing conclusive evidence for its mode of action as a potent inhibitor of nicotinic acetylcholine receptors (nAChRs), more selective for the human neuronal $\alpha 7$ subtype than for $\alpha 4\beta 2$ or $\alpha 1_2\beta\gamma\delta$ muscle subtypes. Such studies resulted in the revision of the mode of action of pinnatoxin A from calcium channel activation (originally proposed) to the inhibition of nAChRs with a notable selectivity for the neuronal human $\alpha 7$ subtype. Electrophysiological and competition binding studies confirmed the hypothesis that the spiroimine component of pinnatoxins is an important structural factor for blocking nAChRs.*

Pinnatoxins : une famille émergente de phycotoxines marines ciblant les récepteurs nicotiniques de l'acétylcholine avec une haute affinité

Les pinnatoxines appartiennent à une classe émergente de phycotoxines du groupe des imines cycliques. Les études détaillées de leurs effets biologiques ont été entravées, pendant une longue période, par l'indisponibilité à la fois du produit complexe naturel et de sa source naturelle. Des études récentes soulignent que le dinoflagellé Vulcanodinium rugosum *gen. nov., sp. nov. Nezan* et *Chomérat, d'abord découvert en France, est responsable de la production de pinnatoxines E, F et G en Nouvelle-Zélande, Australie, Japon et France. Avec la pinnatoxine A synthétique, une étude détaillée a été effectuée, fournissant une preuve concluante de son mode d'action comme inhibiteur puissant des récepteurs nicotiniques de l'acétylcholine (nAChR), plus sélectif pour le sous-type neuronal humain $\alpha 7$ que pour les sous-types musculaires $\alpha 4\beta 2$ ou $\alpha 1_2\beta\gamma\delta$. De telles études ont abouti à la révision du mode d'action de la pinnatoxine A, de l'activation des canaux calciques (proposée initialement) à l'inhibition des nAChR avec une sélectivité remarquable pour le sous-type neuronal humain $\alpha 7$. Des études d'électrophysiologie et de fixation compétitive ont confirmé l'hypothèse selon laquelle la composante spiro-imine des pinnatoxines est un facteur structural important pour le blocage des nAChR.*

Keywords : *Pinnatoxins*, Vulcanodinium rugosum *dinoflagellate*, *toxicity*, *voltage-clamp electrophysiology*, Xenopus laevis.

Introduction

Marine environments are massively complex and contain diverse assemblage of life forms which occur in environments with extreme variations in pressure, salinity and temperature. As a result, marine microorganisms have developed unique metabolic and physiological capabilities to survive in such extreme habitats that led them to produce different kind of metabolites. Human poisoning by toxins of marine origin is a substantial worldwide hazard that may occur by the ingestion of contaminated finfish or shellfish, and through

water or aerosol exposure. Shellfish constitute a worldwide rich food resource that may be contaminated by toxins produced by harmful dinoflagellates upon which filter-feeding bivalve mollusks (such as clams, mussels, oysters or scallops) feed. Shellfish can concentrate these phycotoxins in their edible tissues and act as vectors for transferring these toxic chemical compounds to fish, crabs, birds and humans. The increased frequency and wide distribution of toxic algal blooms has become an environmental and economic problem that menaces wildlife and human health.

Pinnatoxins an emerging class of phycotoxins

Pinnatoxins (*Figure 1*) are toxins that were originally identified in shellfish of the genera *Pinna* and *Pteria* in Japan, after food poisoning incidents in China (Zheng *et al*., 1990) linked to consumption of Pinna spp (*Pinna attenuate*). However, it is still uncertain whether these toxins were the cause of these events. Pinnatoxin A was the first pinnatoxin to be chemically characterized. It was isolated from the bivalve *Pinna muricata* from the sub-tropical Okinawa region in Japan (Uemura *et al*., 1995). This was followed by the further chemical description of pinnatoxins B-D from the same bivalve material (Chou *et al*., 1996a,b; Takada *et al.*, 2001). More recently, three novel analogues of pinnatoxin A, the pinnatoxins E, F and G, were isolated and structurally characterized from the digestive glands of two bivalves: Pacific oysters (*Crassostrea gigas*) and the razorfish (*Pinna bicolor*; McNabb *et al.*, 2008; Selwood *et al.*, 2010). Pinnatoxins F and G were proposed as the progenitors of all the known pinnatoxins and pteriatoxins, *via* metabolic and hydrolytic transformations in shellfish (Selwood *et al.*, 2010). Pinnatoxins are a family of toxins belonging to a heterogeneous group of macrocyclic compounds called cyclic imines (for reviews see Molgó *et al.*, 2007; Cembella and Krock, 2008; Guéret and Brimble, 2010). The distinguishing feature of these compounds is the presence of a cyclic imine moiety which has also been found in other marine toxins like gymnodimines (Seki *et al*., 1995), spirolides (Hu *et al*., 2001), pteriatoxins (Takada *et al.*, 2001), prorocentrolides (Chou *et al*., 1996a,b), and spiro-prorocentrimines (Lu *et al*., 2001).

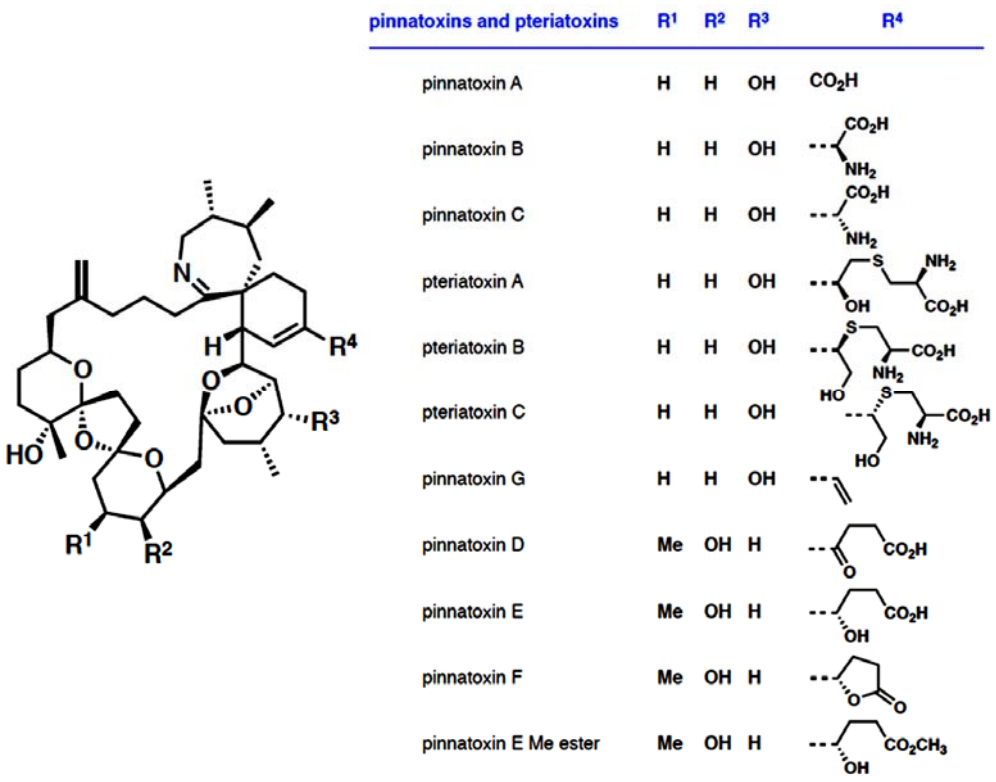

Figure 1. Chemical structure of all pinnatoxins known to date, and pteriatoxin structure shown for comparison.

Figure 1. *Structure chimique des pinnatoxines connues à ce jour et celle des ptériatoxines montrée pour comparaison.*

A new species of dinoflagellate responsible for pinnatoxin production and contamination

Dinoflagellate cysts were isolated from surface sediments in mangrove habitats in both New Zealand and South Australia, where shellfish were reported positive for pinnatoxins. Analysis of these sediment samples resulted in the discovery of a peridinoid dinoflagellate producing pinnatoxins E and F in New Zealand, and pinnatoxins E, F and G in South Australia (Rhodes *et al*., 2010a,b, 2011a). Recent studies on surface sediment samples obtained from Ishigakijima (Okinawa, Japan) have also reported the presence of a thecate dinoflagellate (Peridiniales, Dinophyceae) which appeared under the light and scanning electron microscope morphologically identical to those isolated from New Zealand and Australian waters. The Japanese cultured cells produced only

pinnatoxin G, as determined by liquid chromatography-mass spectrometry, and further confirmed by collision induced dissociation experiments (Smith *et al.*, 2011).

Morphological and phylogenetic similarities were observed between the Japanese dinoflagellate and a recently described new peridinoid dinoflagellate named *Vulcanodinium rugosum* (Nézan and Chomérat, 2011). This new armoured marine dinoflagellate, obtained in water samples of Mediterranean lagoons in the coast of France, *V. rugosum* Nézan *et* Chomérat, gen. nov., sp. nov., exhibits a morphology that looks like either peridinioid or gonyaulacoid species (see *Figure 2*). A phylogenetic study, based on the large subunit (LSU) rDNA sequence data, confirmed that this taxon is new and belongs to the order Peridiniales. However, its affiliation to a particular family or to a known genus was not possible. Therefore, a new generic name, *Vulcanodinium*, was proposed (Nézan and Chomérat, 2011). Interestingly, the dinoflagellate *V. rugosum* has recently been reported not only to be morphologically identical to the previously reported dinoflagellates from New Zealand, Australia and Japan, but also to have large similarities in the LSU rDNA (96–97%) and internal transcribed spacer (ITS) sequences (84-88%) compared to the French material (Rhodes *et al.*, 2011b). These results indicate that this dinoflagellate is responsible for the production of pinnatoxins E, F and G in New Zealand, Australia and Japan and also in France (Philipp Hess, Ifremer, personal communication).

Shellfish contamination (mussels and clams) by pinnatoxins and the link to the dinoflagellate *V. rugosum* have been first reported in France in 2011 (Hess, 2011), but retro-analysis of contaminated shellfish samples indicates high levels of pinnatoxin G since 2006. However, due to the lack of certified standards for pinnatoxins, these toxins have not been reported in Europe until recently. A survey of Norwegian blue mussels for the presence of pinnatoxins by LC-MS/MS analysis of extracts, obtained as part of Norway's routine monitoring program for regulated micro-algal toxins, revealed that pinnatoxin G was widespread and present in 69% of the shellfish samples analyzed (Rundberget *et al.*, 2011). These results suggest that pinnatoxins may be much widespread than previously suspected, and indicate that they could be responsible for sporadic incidents of rapid-onset symptoms during mouse bioassays of shellfish in Europe and elsewhere. However, their toxicological significance remains at present unclear.

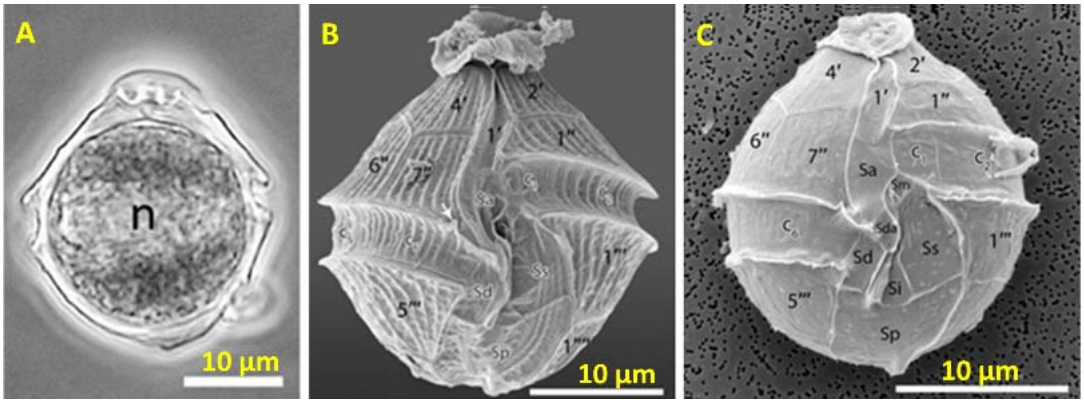

Figure 2. Contrast phase (**A**) and scanning electron micrographs (**B** and **C**) of the dinoflagellate *Vulcanodinium rugosum* Note in (**A**), the cell nucleus (*n*). (**B**) Ventral view of the dinoflagellate. Note the small indentation in the c6 plate (*white arrow*). (**C**) Smaller form of the dinoflagellate revealing the arrangement of its thecal surface. Adapted with permission from Nézan and Chomérat (2011; Figures 4, 7 and 25).

Figure 2. *Observations en contraste de phase (**A**) et en microscopie électronique à balayage (**B** et **C**) du dinoflagellé* Vulcanodinium rugosum*. Notez en (**A**) le noyau (*n*) de la cellule. (**B**) Vue ventrale du dinoflagellé. Notez la petite indentation sur le bord antérieur de la plaque c6 (*flèche blanche*). (**C**) Petite forme du dinoflagellé montrant l'arrangement de sa surface thécale. Reproduit avec permission de Nézan et Chomérat (2011; Figures 4, 7 et 25).*

Pinnatoxins exhibit fast-acting toxicity in rodents

Pinatoxins exhibit fast-acting toxicity in rodent bioassays. The symptoms following intraperitoneal (i.p.) injection of a lethal dose of pinnatoxin A to mice give a toxicological profile characterized by transient mouse hyperactivity followed by a decrease in respiratory rate with prominent abdominal breathing, leading to death due to respiratory paralysis. Such a toxicological profile is also seen with most cyclic imine toxins that are highly toxic to mice by i.p injection, causing death in as little as 5 min (Munday, 2008). Crude extracts of mass dinoflagellate cultures containing pinnatoxins G, E, F and A, or pinnatoxin G only, when tested for toxicity in mice by i.p. injection, gavage and voluntary consumption, revealed toxicity ratios of 1.0:1.8:4.5 for the former and 1.0:2.9:7.8 for the latter, respectively (Rhodes *et al.*, 2011a). This is similar to the ratios obtained for New Zealand dinoflagellate isolates (Rhodes *et al.*, 2010b), but differs from other cyclic imines for which oral toxicity was reported to be 10-1000-fold less by i.p. administration (Munday, 2008). If this is confirmed with pure pinnatoxins, a re-appraisal of the current process would be necessary for establishing the "toxic equivalency factor" values (EFSA, 2009), in which i.p. toxicities are used to estimate the relative oral toxicities of marine micro-algal toxins in sea food.

Pinnatoxin A targets nicotinic acetylcholine receptors with high affinity

It has been initially suggested that the mode of action of pinnatoxins involved calcium channel activation

(Zheng *et al.*, 1990; Uemura *et al.*, 1995). However, the symptoms following an i.p. injection of a lethal dose of pinnatoxin A to mice gave a toxicological profile that suggested affecting nicotinic acetylcholine receptors (nAChRs) at the skeletal neuromuscular junction and in the central nervous system. Furthermore, there is growing evidence that other structurally related cyclic imine toxins (gymnodimine A and 13-desmethyl spirolide C) affect both muscle and neuronal nAChR subtypes (Kharrat *et al.*, 2008; Bourne *et al.*, 2010).

Thanks to a robust multi-step and scalable synthetic access to pinnatoxin A, that delivered large quantities of the toxin, it was possible to perform a detailed study of its mode of action (Stivala and Zakarian, 2008; Aráoz *et al.*, 2011a). As shown in a representative recording (*Figure 3A*), in oocytes expressing the human $\alpha 7$ nAChR, the perfusion of 350 µM acetylcholine (ACh; corresponding to the EC_{50} determined experimentally) elicited peak currents of 1 to 3 µA amplitude at a holding membrane potential of –60 mV.

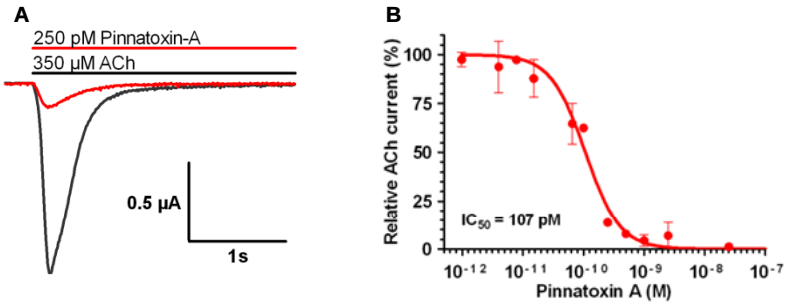

Figure 3. Effect of pinnatoxin A on $\alpha 7$ nAChR subtype expressed in *Xenopus oocytes*. (**A**) ACh-evoked current recorded at a holding potential of -60 mV on the same oocyte, before (*black tracing*) and after (*red tracing*) addition of 250 pM pinnatoxin A. (**B**) Concentration-dependent inhibition of ACh-evoked currents by pinnatoxin A for human $\alpha 7$ nAChR subtype. Adapted with permission from Aráoz *et al.* (2011a) [Copyright (2011) American Chemical Society].

Figure 3. *Effet de la pinnatoxine A sur le sous-type $\alpha 7$ de nAChR exprimé dans des ovocytes de xénope. (**A**) Courant évoqué par l'ACh et enregistré à un potentiel de maintien de -60 mV sur un même ovocyte, avant (*noir*) et après (*rouge*) l'addition de 250 pM de pinnatoxin A. (**B**) Inhibition dépendante de la concentration de pinnatoxine A des courants évoqués par l'ACh pour le sous-type humain $\alpha 7$ de nAChR. Reproduit avec permission d'Aráoz* et al. *(2011a) [Copyright (2011) American Chemical Society].*

The ACh-evoked currents started to desensitize within about 300 ms, but pinnatoxin A did not appear to affect the rate of receptor desensitization. However, ACh-evoked currents were markedly reduced in amplitude by pico- to nanomolar pinnatoxin A concentrations, as shown in the concentration-inhibition curve (*Figure 3B*). Pinnatoxin A (0.1-50 nM), when applied on its own, did not evoke any inward current, indicating that it has no agonist effect on the $\alpha 7$ nAChR subtype. Pinnatoxin A also blocked the human $\alpha 4\beta 2$ nAChR subtype expressed in *Xenopus* oocytes, but higher concentrations were needed to block the ACh-evoked currents, indicating that the toxin was less potent for this neuronal receptor subtype compared to the $\alpha 7$ subtype. In oocytes in which the *Torpedo* $\alpha 1_2\beta\gamma\delta$ muscle nAChR subtype has been incorporated into their membranes, pinnatoxin A also blocked the ACh-evoked nicotinic currents, in a concentration-dependent manner, with an IC_{50} of 5.53 nM (4.5-6.8 nM, 95% confidence intervals). The electrophysiological and competition binding studies demonstrated the ability of pinnatoxin A to interact efficiently with various nAChR subtypes. The selectivity profile and affinity values determined by the two approaches were similar: human $\alpha 7$ (0.1-0.3 nM) > $\alpha 1_2\beta\gamma\delta$ muscle-type *Torpedo* (3-5 nM) > human $\alpha 3\beta 2$ = $\alpha 4\beta 2$ (10-30 nM), demonstrating the ability of this toxin to recognize muscle as well as neuronal subtypes (Aráoz *et al.*, 2011a).

To determine whether the spiroimine fragment in pinnatoxin A was required for blocking nAChR subtypes, experiments were performed with a pinnatoxin A analog containing an acyclic form of the imine ring (pinnatoxin AK). Both electrophysiological and competition binding assays showed the inactivity of pinnatoxin AK with different nAChR subtypes, highlighting the crucial role of the cyclic imine for the biological activity of pinnatoxin A. This inactivity can be explained by the existence of conformers strongly stabilized by an intramolecular ionic interaction between the ammonium and carboxylate groups of pinnatoxin AK in solution (for further details see Aráoz *et al.*, 2011b).

Conclusion

A considerable advance has been obtained during the last two decades in pinnatoxin research, following the first report on pinnatoxin toxicity. This family of phycotoxins has been not only well characterized from the chemical point of view, but also the dinoflagellate *V. rugosum* Nézan et Chomérat, *gen. nov., sp. nov.*, has been identified as *responsible* for the production of pinnatoxin E, F and G in New Zealand, Australia, Japan and France. Electrophysiological and competition binding studies confirmed the hypothesis that the spiroimine component of pinnatoxins is an important structural factor for blocking nAChRs. Finally, the success in the total synthesis of pinnatoxin A and pinnatoxin G (Aráoz *et al.*, 2011a), and the knowledge of their revisited mode of action, pave the way for both the production of certified standards to be used for mass spectrometry determination of toxins in marine matrices and the development of tests to detect these toxins in contaminated shellfish.

Acknowledgements. *This work was supported in part by US National Institutes of Health (NIGMS, GM077379 to A.Z. with subcontract KK1036 to J.M.) and by grants from EU 7th Frame Program STC-CP2008-1-555612 (ATLANTOX) and 2009-1/117*

PHARMATLANTIC (to J.M.). Authors want to thank Mrs Patricia Villeneuve for her excellent technical assistance and for taking care of the Xenopus laevis *frogs used in our studies.*

References

Aráoz R, Servent D, Molgó J, Iorga BI, Fruchart-Gaillard C, Benoit E, Gu Z, Stivala C, Zakarian A (2011a) Total synthesis of pinnatoxins A and G and revision of the mode of action of pinnatoxin A. *J Am Chem Soc* **133**: 10499-10511

Aráoz R, Zakarian A, Molgó J, Iorga BI (2011b) Insights into the interaction of pinnatoxin A with nicotinic acetylcholine receptors using molecular modeling. In *Toxins and Ion transfers*. Barbier J, Benoit E, Gilles N, Ladant D, Martin-Eauclaire M-F, Mattéi C, Molgó J, Popoff M, Servent D (eds) pp 49-54. SFET Editions, Gif-sur-Yvette, France, Epub on http://www.sfet.asso.fr (ISSN 1760-6004)

Bourne Y, Radic Z, Aráoz R, Talley TT, Benoit E, Servent D, Taylor P, Molgó J, Marchot P (2010) Structural determinants in phycotoxins and AChBP conferring high affinity binding and nicotinic AChR antagonism. *Proc Natl Acad Sci USA* **107**: 6076-6081

Cembella A, Krock B (2008) Cyclic imine toxins: chemistry, biogeography, biosynthesis, and pharmacology. In *Seafood and Freshwater Toxins: Pharmacology, Physiology and Detection*. Botana LM (ed) pp 561-580. CRC Press, Boca Raton, FL

Chou T, Haino T, Kuramoto M, Uemura D (1996b) Isolation and structure of pinnatoxin D, a new shellfish poison from the Okinawan bivalve *Pinna muricata*. *Tetrahedron Lett* **37**: 4027-4030

Chou TT, de Freitas ASW, Curtis JM, Oshima Y, Walter JA, Wright JLC (1996a) Isolation and structure of prorocentrolide B a fast–acting toxin from *Prorocentrum maculosum*. *J Nat Prod* **59**: 1010–1014

EFSA - The European Food Safety Authority (2009) Scientific opinion of the panel on contaminants in the food chain on a request from the European Commission on marine biotoxins in shellfish. Summary on Regulated Marine Biotoxins. *EFSA J* **1306**: 1–23

Guéret SM, Brimble MA (2010) Spiroimine shellfish poisoning (SSP) and the spirolide family of shellfish toxins: Isolation, structure, biological activity and synthesis. *Nat Prod Rep* **27**: 1350-1366

Hess P (2011). First report of pinnatoxin in mussels and a novel dinoflagellate, *Vulcanodinium rugosum*, from France. 8th *International Conference on Molluscan Shellfish Safety*, Charlottetown, Prince Edwards Island, Canada (June, 12-17, 2011)

Hu T, Burton IW, Cembella AD, Curtis JM, Quilliam MA, Walter JA, Wright JLC (2001) Characterization of spirolides a, c, and 13-desmethyl c, new marine toxins isolated from toxic plankton and contaminated shellfish. *J Nat Prod* **64**: 308-312

Kharrat R, Servent D, Girard E, Ouanounou G, Amar M, Marrouchi R, Benoit E, Molgó J (2008) The marine phycotoxin gymnodimine targets muscular and neuronal nicotinic acetylcholine receptor subtypes with high affinity. *J Neurochem* **107**: 952–963.

Lu CK, Lee GH, Huang R, Chou HN (2001) Spiro-prorocentrimine, a novel macrocyclic lactone from a benthic *Prorocentrum* sp. of Taiwan. *Tetrahedron Lett* **42**: 1713-1716

McNabb P, Rhodes L, Selwood A (2008) Results of analyses for brevetoxins and pinnatoxins in Rangaunu Harbour oysters, 1993-2008. *Cawthron Report* No1453, 18 pp

Molgó J, Girard E, Benoit E (2007) Cyclic imines: an insight into this emerging group of bioactive marine toxins. In *Phycotoxins: Chemistry and Biochemistry*. Botana LM (ed) pp 319-335. Blackwell Publishing, Iowa

Munday R (2008) Toxicology of cyclic imines: gymnodimine, spirolides, pinnatoxins, pteriatoxins, prorocentrolide, spiro-prorocentrimine, and symbioimines. In *Seafood and Freshwater Toxins: Pharmacology, Physiology and Detection*. Botana LM (ed) 2nd edition, pp 581-594. CRC Press, Boca Raton, FL

Nézan E, Chomérat N (2011). *Vulcanodinium rugosum* gen. et sp. nov. (Dinophyceae), un nouveau dinoflagellé marin de la côte méditerranéenne française. *Cryptogam Algol* **32**: 3-18

Rhodes L, Selwood A, McNabb P, Smith K (2010a) Pinnatoxin in Rangaunu Harbour, Northland, New Zealand. In *Harmful Algae 2008*. Ho K *et al.* (eds) pp 151-154. Proceedings 13th International Conference on Harmful Algae, Hong Kong, China, (November 2008). Env Pub House, Hong Kong

Rhodes L, Smith K, Selwood A, McNabb P, Molenaar S, Munday R, Wilkinson C, Hallegraeff G (2011a) Production of pinnatoxins E, F and G by scrippsielloid dinoflagellates isolated from Franklin Harbour, South Australia. New Zealand. *J Mar Freshwater Res* **45**: 703-709

Rhodes L, Smith K, Selwood A, McNabb P, Munday R, Suda S, Molenaar S, Hallegraeff G (2011b) Dinoflagellate *Vulcanodinium rugosum* identified as the causative organism of pinnatoxins in Australia, New Zealand and Japan. *Phycologia* **50**: 624-628

Rhodes L, Smith K, Selwood A, McNabb P, van Ginkel R, Holland P,Munday R (2010b) Production of pinnatoxins by a peridinoid dinoflagellate isolated from Northland, New Zealand. *Harmful Algae* **9**: 384-389

Rundberget T, Aasen JAB, Selwood AI, Miles CO (2011) Pinnatoxins and spirolides in Norwegian blue mussels and seawater. *Toxicon* (in press) doi:10.1016/j.toxicon.2011.08.008

Seki T, Satake M, Mackenzie L, Kaspar H F, Yasumoto T (1995) Gymnodimine, a new marine toxin of unprecedented structure isolated from New Zealand oysters and the dinoflagellate *Gymnodinium* sp. *Tetrahedron Lett* **36**: 7093-7096

Selwood AI, Miles CO, Wilkins AL, van Ginkel R, Munday R, Rise F, McNabb P (2010) Isolation, structural determination, and acute toxicity of novel pinnatoxins E, F and G. *J Agric Food Chem* **58**: 6532-6542

Smith KF, Rhodes LL, Suda S, Andrew I. Selwood AI (2011) A dinoflagellate producer of pinnatoxin G, isolated from sub-tropical Japanese waters. *Harmful Algae* **10**: 702-705

Stivala CE, Zakarian A (2008) Total synthesis of (+)-pinnatoxin A. *J Am Chem Soc* **130**: 3774-3776

Takada N, Umemura N, Suenaga K, Uemura D (2001) Structural determination of pteriatoxins A, B and C, extremely potent toxins from the bivalve *Pteria penguin*. *Tetrahedron Lett* **42**: 3495-3497

Uemura D, Chou T, Hainao T, Nagatsu A, Fukuzawa S, Zheng SZ, Chen HS (1995) Pinnatoxin A: a toxic amphoteric macrocycle from the Okinawan bivalve *Pinna muricata*. *J Am Chem Soc* **117**: 1155–1156

Zheng SZ, Huang FL, Chen SC, Tan XF, Zuo JB, Peng J, Xie RW (1990) The isolation and bioactivities of pinnatoxin. *J Mar Drugs* **33**: 33-35 (*in Chinese*)

Toxines et Transferts ioniques – Toxins and Ion transfers
Rencontres en Toxinologie – Meeting on Toxinology, 2011
Editions de la SFET – SFET Editions
Accès libre en ligne sur le site – Free access on line on the site : http://www.sfet.asso.fr

Insights into the interaction of pinnatoxin A with nicotinic acetylcholine receptors using molecular modeling

Rómulo ARÁOZ[1], Armen ZAKARIAN[2], Jordi MOLGÓ[1], Bogdan I. IORGA[3*]

[1] CNRS, Centre de Recherche de Gif-sur-Yvette - FRC 3115, Institut de Neurobiologie Alfred Fessard - FRC 2118, Laboratoire de Neurobiologie et Développement - UPR 3294, 1 avenue de la Terrasse, 91198 Gif-sur-Yvette, France ; [2] Department of Chemistry and Biochemistry, University of California, Santa Barbara, California, 93106-9510, USA ; [3] Institut de Chimie des Substances Naturelles - CNRS UPR 2301, Centre de Recherche de Gif-sur-Yvette - FRC 3115, 1 avenue de la Terrasse, 91198 Gif-sur-Yvette, France

** Corresponding author ; Tel : +33 (0) 1 6982 3094 ; Fax : +33 (0) 1 6907 7247 ;*
E-mail : bogdan.iorga@icsn.cnrs-gif.fr

Abstract

The interaction between a macrocyclic spiroimine phycotoxin, pinnatoxin A, with three different subtypes of nicotinic acetylcholine receptors (nAChRs) has been explored using molecular modeling techniques. A two-step protocol has been used for flexible docking of the macrocyclic toxin at the nAChR subunit interface. The protein-ligand interactions identified are in good agreement with the selectivity profile determined experimentally. A particular conformation has been evidenced for the acyclic amino-ketone form of the pinnatoxin A, which explains the lack of biological activity observed for this derivative and emphasizes the importance of the spiroimine pharmacophore within this phycotoxin family.

Etude de l'interaction de la pinnatoxin A avec les récepteurs nicotiniques de l'acétylcholine par modélisation moléculaire

L'interaction d'une phycotoxine macrocyclique de type spiroimine, pinnatoxine A, avec trois sous-types de récepteurs nicotiniques de l'acétylcholine (nAChRs) a été étudiée par différentes techniques de modélisation moléculaire. Une procédure en deux étapes a été utilisée pour le « docking » flexible de ces toxines macrocycliques à l'interface de deux sous-unités de nAChR. Les interactions protéine-ligand ainsi identifiées sont en accord avec le profil de sélectivité déterminé expérimentalement. Une conformation particulière a été mise en évidence pour la forme acyclique amino-cétone de la pinnatoxine A, qui explique le manque d'activité biologique observé pour ce dérivé et souligne l'importance du pharmacophore spiroimine dans cette famille de phycotoxines.

Keywords : *Conformational analysis, homology modeling, molecular docking, nicotinic acetylcholine receptors, pinnatoxin A, spiroimine toxins.*

Introduction

Macrocyclic spiroimine phycotoxins represent a newly emerging group of marine toxins with worldwide distribution, associated with marine algal blooms and shellfish toxicity (Molgó *et al.*, 2007). This family comprises five different classes of toxins: gymnodimines, spirolides, pinnatoxins, pteriatoxins, and spiro-prorocentrimines. Among them, pinnatoxins (**1**, *Figure 1*) are of special interest since, unlike the other phycotoxins, they have been shown to retain their toxicity following oral administration at a level similar to that observed for intraperitoneal injection (Rhodes *et al.*, 2010; Selwood *et al.*, 2010). Additionally, limited information about pinnatoxin A is available due to the low and unreliable availability from natural sources, undermined by the fact that their producing organism has not been identified until recently (Rhodes *et al.*, 2010). A robust and scalable synthetic access to pinnatoxin A described very recently provided the required quantities for the validation of a new mechanism of action, as a potent inhibitor of nicotinic acetylcholine receptors, with a selectivity for the human neuronal α7 subtype (Stivala and Zakarian, 2008; Aráoz *et al.*, 2011).

In this work, we present a detailed discussion of the structural determinants of the interaction between pinnatoxin A (**1**) and its acyclic amino-ketone form (**2**) and three subtypes of nicotinic acetylcholine receptors (nAChRs). These interactions were identified using molecular modeling techniques and are in very good agreement with the selectivity profile previously determined experimentally (Aráoz *et al.*, 2011).

Materials and methods

Three-dimensional coordinates of the ligands were generated using Corina software v3.44

(http://www.molecular-networks.com/). All conformational search calculations were carried out using MacroModel v9.7 (http://www.schrodinger.com/) with the default values, with the exception of a conformer energy window of 42 kJ/mol within the Mixed MCMM/Low-Mode search protocol.

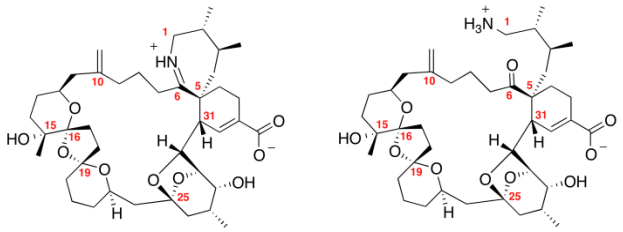

1 2

Figure 1. Chemical structures of pinnatoxin A (**1**) and its acyclic amino-ketone form (**2**).

Figure 1. *Structures chimiques de la pinnatoxine A (**1**) et de sa forme acyclique amino-cétone (**2**).*

Three-dimensional structures for the three nAChRs subtypes were built by homology modelling with Modeller v9.7 (Eswar *et al.*, 2008), using the crystal structure (PDB code 2WZY) of AChBP in complex with 13-desmethyl spirolide C (Bourne *et al.*, 2010) as template.

Gold software v4.1 (Verdonk *et al.*, 2003) was used for molecular docking calculations, the binding site being defined as a sphere with a 15 Å radius centered at half-distance between backbone oxygen atoms of residues W147 and C190 and the GoldScore scoring function was used, all other parameters having default values. Whenever it was possible, side chain flexibility was introduced in key positions of the binding site in order to optimize the establishment of protein-ligand interactions. AutoDock 4.0 (Morris *et al.*, 1998) was also used for testing an approach described in the literature dealing with the flexibility of macrocyclic systems (Forli and Botta, 2007). Images were generated with Chimera (Pettersen *et al.*, 2004).

Results and Discussion

Three-dimensional structures of various nAChR subtypes have been previously described in the literature, built by homology modeling with a soluble analogue of nAChRs, the Acetylcholine Binding Protein (AChBP): human α7 (Schapira *et al.*, 2002; Henchman *et al.*, 2003; Espinoza-Fonseca, 2004; Law *et al.*, 2005; Taly *et al.*, 2005; Iorga *et al.*, 2006), chick α7 (Le Novere *et al.*, 2002), rat α7 (Dutertre and Lewis, 2004), human α4β2 (Schapira *et al.*, 2002; Iorga *et al.*, 2006; Pedretti *et al.*, 2008; Henderson *et al.*, 2010), rat α4β2 (Le Novere *et al.*, 2002), human α4β4 (Pedretti *et al.*, 2008), human α3β4 (Iorga *et al.*, 2006; Gonzalez-Cestari *et al.*, 2009), human α3β2 (Schapira *et al.*, 2002), rat α3β2 (Everhart *et al.*, 2003; Dutertre and Lewis, 2004), rat α3β4 (Costa *et al.*, 2003), rat α3β2 (Everhart *et al.*, 2003), human $\alpha 1_2\beta 1\gamma\delta$ (Sine *et al.*, 2002), mouse $\alpha 1_2\beta 1\gamma\delta$ (Molles *et al.*, 2002; Willcockson *et al.*, 2002), *Torpedo* $\alpha 1_2\beta 1\gamma\delta$ (Le Novere *et al.*, 2002; Samson *et al.*, 2002; Sullivan *et al.*, 2002). In this work, homology models of human α7, α4β2 and *Torpedo marmorata* $\alpha 1_2\beta 1\gamma\delta$ nAChR pentamers were built using the standard protocol implemented in Modeller (Eswar *et al.*, 2008). Among the available AChBP crystal structures, the recently published (Bourne *et al.*, 2010) complex with 13-desmethyl spirolide C (PDB code 2WZY) was chosen as template, given the structural similarity between this ligand and pinnatoxin A. The sequence alignment described previously (Bourne *et al.*, 2010) was used for building homology models. However, the models of the $\alpha 1_2\beta 1\gamma\delta$ subtype contained the loop F positioned in the main binding site, which obviously was not compatible with the subsequent docking of pinnatoxin A at the same site. For this subtype, a new generation of protein conformers was generated using the Modeller's module capable of building models in the presence of a bound ligand, in this case 13-desmethyl spirolide C (PDB code 2WZY). Additionally, a particular attention was directed to the conformation of the loop F of the δ subunit, which contains a relatively big insertion compared to the AChBP template, and which is probably very flexible. This loop remained unresolved in the Unwin's electron microscopy structure of *Torpedo* nAChR (Unwin, 2005). The conformation of this loop was thus optimized using the Modeller's "loop refine" module and the "very slow" refinement method. For each homology modeling calculation, 100 conformers were generated, and the one with the best DOPE (Discrete Optimized Protein Energy) score was retained.

Direct docking (Verdonk *et al.*, 2003) of the pinnatoxin A structure generated with Corina on these homology models, at the subunit interface, were unsuccessful, mainly because the most stable conformation of pinnatoxin A in vacuum was not able to fit into the receptor binding site. It was clear that we would need to use a docking protocol capable of introducing flexibility for the macrocyclic system of pinnatoxin A.

Presently, to the best of our knowledge, no docking software is able to deal directly with the problem of ligand flexibility in macrocyclic structures. A workaround has been recently proposed (Forli and Botta, 2007) using AutoDock (Morris *et al.*, 1998), but unfortunately in our hands this protocol was ineffective, resulting in conformations that are too distorted to be useful. We propose here a new, two-step procedure which involves the initial generation of an ensemble of conformers probing macrocycle flexibility followed by docking of this ensemble to identify the most suitable macrocycle conformation for a given target. Flexibility of ligand fragments other than the macrocycle is properly handled by the standard docking protocol implemented in Gold. This procedure is general, and can be successfully applied to any macrocyclic ligand.

An ensemble containing 47 pinnatoxin A conformers was obtained by conformational search, using dihedral restraints extracted from the common pattern of ligand X-ray structures for gymnodimine A and 13-desmethyl

spirolide C (Bourne *et al.*, 2010). This ensemble was subsequently docked using Gold (Verdonk *et al.*, 2003) at the subunit interface of the three homology models generated previously. Overall, the docking protocol used in this work introduces flexibility at the level of both ligand (including macrocycle) and binding site protein side chains, in order to generate realistic protein-ligand complexes.

A detailed analysis of interactions between pinnatoxin A and various subtypes of nAChRs is presented in *Figure 2* and *Table 1*. The ligand is positioned in a similar manner in all three complexes, with differences in binding affinity arising mainly from the residue variability in key positions of the binding site. Pinnatoxin A establishes an important number of hydrogen bonds (seven) with $\alpha 7$ nAChR, which are well distributed in the binding site and involve most of the ligand's functional groups. Conversely, only five hydrogen bonds are observed in the $\alpha 4\beta 2$ complex, covering approximately 50% of the binding site at a close distance. The $\alpha 1_2\beta 1\gamma\delta$ complex shows intermediate behavior, with the five hydrogen bonds more equally distributed in the binding site. The latter complex also benefits from important hydrophobic contacts with the complementary δ subunit; these interactions are substantially reduced in the $\alpha 4\beta 2$ complex. Most of the residues present in the binding site are conserved among the three nAChRs subtypes considered (residues 93, 143, 147, 149, 188, 190, 191 and 195 from the principal side and residues 55, 79, and 118 from the complementary side, highlighted in *Table 1*). At the same time, in a few positions with amino acid variability the neighboring residues are able to compensate for the missing interaction (*e.g.* in $\alpha 1_2\beta 1\gamma\delta$, the carboxylate group of pinnatoxin A is not able to establish an ionic interaction with V186 as it does with the equivalent residue R186 in the $\alpha 7$ and $\alpha 4\beta 2$ nAChR subtypes; instead, it interacts with K143). However, in some cases, differences in amino acid sequence are responsible for changes in the protein-ligand interaction pattern. One example is Q116 from the $\alpha 7$ subtype, which interacts with an oxygen atom from the bis-spiroketal core, while the equivalent residues F116 from $\alpha 4\beta 2$ and T116 from the $\alpha 1_2\beta 1\gamma\delta$ subtype are unable to establish similar interactions. Similarly, Q57 from the $\alpha 7$ subtype and D57 from the $\alpha 1_2\beta 1\gamma\delta$ subtype form hydrogen bonds with a hydroxy group at the C28 position of pinnatoxin A near the solvent-exposed site, whereas the side chain of the equivalent T57 residue from the $\alpha 4\beta 2$ subtype is too short to form analogous interactions. Overall, the protein-ligand interactions identified in these three complexes are in very good agreement with the experimental biological data, with pinnatoxin A showing significantly stronger interactions with the $\alpha 7$ nAChR subtype compared to the $\alpha 4\beta 2$ subtype, while the $\alpha 1_2\beta 1\gamma\delta$ subtype displayed intermediate interactions, showing significant hydrophobic contribution from the complementary side.

Table 1. Protein-ligand interactions within a 4 Å distance between atoms in pinnatoxin A and various subtypes of nAChRs. Residues that are conserved in the alignment of subunits $\alpha 7$, $\alpha 4$, $\alpha 1$ and $\alpha 7$, $\beta 2$, δ are represented in *bold*, and those establishing hydrogen bonds with the ligand are colored in *blue*. Residue numbering is the same as previously described (Bourne *et al.*, 2010). Reprinted with permission from Aráoz *et al.,* Total synthesis of pinnatoxin A and G and revision of the mode of action of pinnatoxin A. Journal of the American Chemical Society 133: 10499-10511 [Copyright (2011) American Chemical Society].

Tableau 1. *Interactions protéine-ligand dans un rayon de 4 Å par rapport au ligand, entre la pinnatoxine A et différents sous-types de récepteurs nicotiniques de l'acétylcholine. Les résidus conservés dans l'alignement de séquences des sous-unités $\alpha 7$, $\alpha 4$, $\alpha 1$ et $\alpha 7$, $\beta 2$, δ sont représentés en gras, et ceux qui forment des liaisons hydrogène avec le ligand sont colorés en bleu. La numérotation des résidus est la même que celle décrite précédemment (Bourne et al., 2010). Reproduit avec permission de l'article Aráoz* et al.*, Total synthesis of pinnatoxin A and G and revision of the mode of action of pinnatoxin A. Journal of the American Chemical Society 133: 10499-10511. [Copyright (2011) American Chemical Society].*

Ligand fragment	α7/α7 interface		α4/β2 interface		α1/δ interface	
	(+)-subunit	(–)-subunit	α subunit	β subunit	α subunit	δ subunit
carboxylate	R186, **Y188**	–	R186	–	**K143**	**W55**, I161(+9)*
cyclohexene ring	**Y93**, R186, **Y188**	**W55**	**Y93**, **W147**, R186	**W55**	**Y93**, **K143**, **W147**	**W55**, I161(+9)*
7-membered imine ring	**Y93**, **W147**, S148, G150, **Y188**, **Y195**	–	**Y93**, S146, **W147**, **Y149**, D150, R186, **Y195**	–	**Y93**, I148, **W147**, T148, **Y149**, **Y188**, **Y195**	–
solvent-buried branch	**W147**	**W55**, Q116, **L118**	**W147**	**W55**, **L118**	**Y93**, **W147**, T148	**W55**, Y103, L108, **L118**
bis-spiroacetal core	**W147**, S148, **Y188**, **C190**, **C191**, **Y195**	**R79**, L108, Q116	D150, **Y188**, **C190**, **C191**, E193, **Y195**	–	**W147**, T148, K153, **Y188**, **C190**, **C191**, D193, **Y195**	L108, R110
Solvent-exposed branch	–	**W55**, Q57, Q116, **L118**	–	S36, **W55**, T57, **L118**	**Y188**	**W55**, D57, **L118**

* This isoleucine residue belongs to the main insertion on the δ subunit's loop F, 9 residues after D161.

* *Ce résidu isoleucine appartient à l'insertion principale sur la boucle F de la sous-unité δ, 9 résidus après D161.*

A similar protocol (conformational search producing an ensemble containing 280 conformers followed by docking) was applied to the acyclic amino-ketone form of pinnatoxin A (**2**, *Figure 1*). Docking analysis showed that this compound binds non-specifically at the subunit interface, the main interaction observed being between

the ammonium group of **2** and the side chain of D197. To determine whether the spiroimine fragment in pinnatoxin A is required for its potent blockage of nAChR subtypes, experiments were performed with compound **2** and both electrophysiological and binding assays showed its inactivity with different nAChRs, highlighting the crucial role of the cyclic imine for the biological activity of pinnatoxin A (Aráoz *et al.*, 2011). This inactivity can be explained by the existence of conformers strongly stabilized by an intramolecular ionic interaction between the ammonium and carboxylate groups of **2** in solution (*Figure 3*). These conformers, which are unable to bind directly to the nAChR subunit interface, would require an energetically unfavorable disruption of the intramolecular ion pair to produce an "open" form of the ligand, which could potentially interact with the binding site.

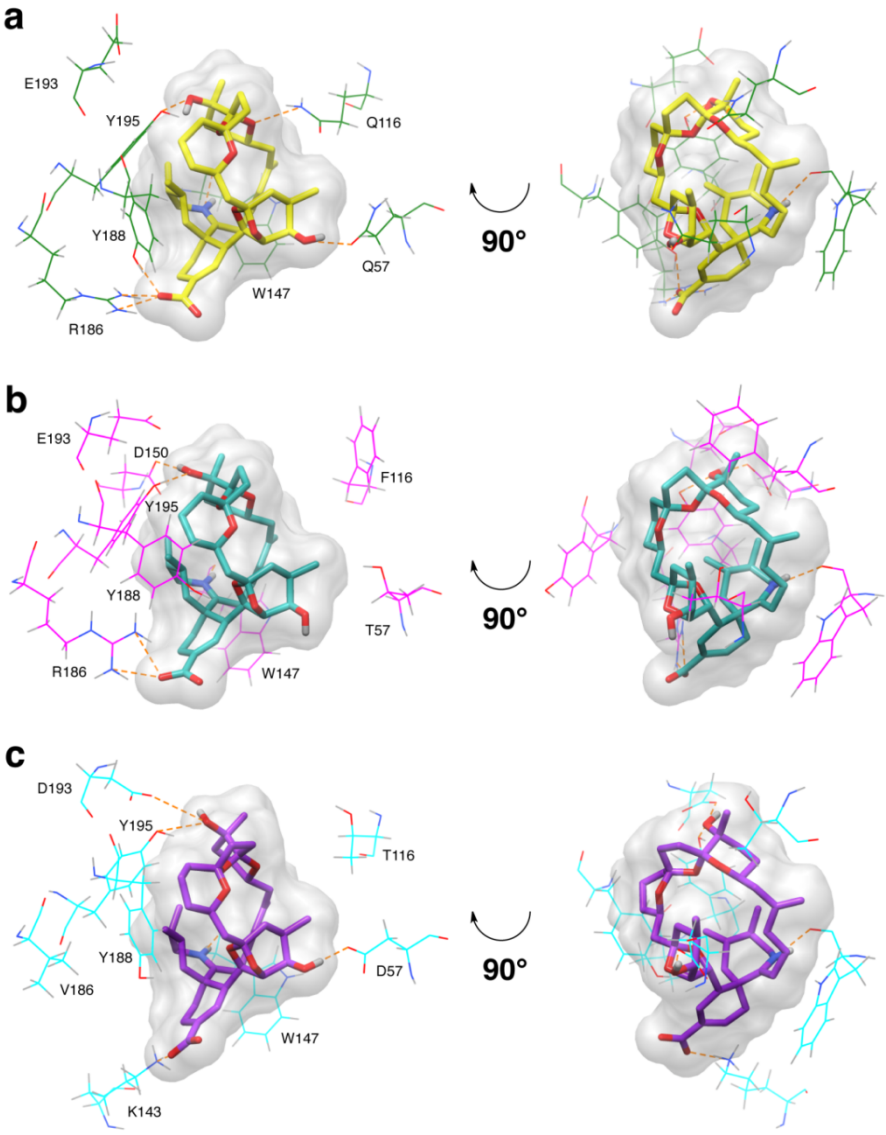

Figure 2. Representative protein-ligand interactions in pinnatoxin A-nAChR complexes obtained by molecular modeling: (**a**) human α7 (*green*, α7-α7 interface), (**b**) human α4β2 (*magenta*, α4-β2 interface), and (**c**) *Torpedo* α1β1γδ (*cyan*, α1-δ interface). Only amino acids interacting through hydrogen bonds with the ligand (and the residues from equivalent positions in the sequence alignment) are shown (see *Table 1* for further information). Pinnatoxin A is colored in (**a**) *yellow*, (**b**) *light blue*, and (**c**) *violet*. For each complex, two different views, rotated by 90°, are presented. Non-polar hydrogen atoms of the ligand are not shown for clarity. Adapted with permission from Aráoz *et al.*, Total synthesis of pinnatoxin A and G and revision of the mode of action of pinnatoxin A. Journal of the American Chemical Society 133: 10499-10511 [Copyright (2011) American Chemical Society].

Figure 2. *Interactions représentatives protéine-ligand dans les complexes pinnatoxine A-récepteurs nicotiniques de l'acétylcholine, générés par modélisation moléculaire: (**a**) sous-type humain α7 (*vert, *interface α7-α7), (**b**) sous-type humain α4β2 (*magenta, *interface α4-β2), et (**c**) sous-type* Torpedo *α1β1γδ (*cyan, *interface α1-δ). Seuls les acides aminés qui forment des liaisons hydrogène avec le ligand (et les résidus dans les positions équivalentes de l'alignement de séquences) sont représentés (voir le* Tableau 1 *pour plus d'informations). La pinnatoxine A est colorée en (**a**)* jaune, *(**b**)* bleu clair, *et (**c**)* violet. *Pour chaque complexe, deux vues différentes, avec une rotation de 90°, sont présentées. Les atomes d'hydrogène non-polaires du ligand sont cachés pour plus de clarté. Reproduit avec permission de l'article Aráoz* et al., *Total synthesis of pinnatoxin A and G and revision of the mode of action of pinnatoxin A. Journal of the American Chemical Society 133: 10499-10511. [Copyright (2011) American Chemical Society].*

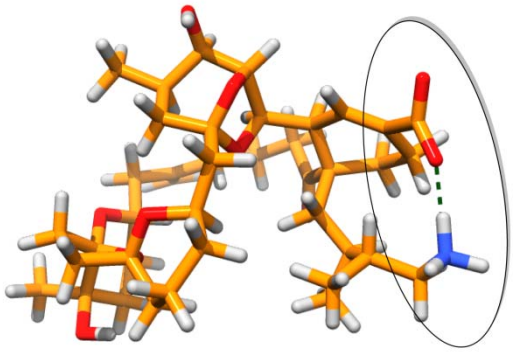

Figure 3. Three-dimensionnal structure of the pinnatoxin A acyclic amino-ketone form (**2**) showing strong ionic interaction between the ammonium and carboxylate groups. Adapted with permission from from Aráoz *et al.,* Total synthesis of pinnatoxin A and G and revision of the mode of action of pinnatoxin A. Journal of the American Chemical Society 133: 10499-10511 [Copyright (2011) American Chemical Society].

Figure 3. *Structure tridimensionnelle de la forme acyclique amino-cétone de la pinnatoxine A (**2**) montrant une forte interaction ionique entre les groupes ammonium et carboxylate. Reproduit avec permission de l'article Aráoz* et al.*, Total synthesis of pinnatoxin A and G and revision of the mode of action of pinnatoxin A. Journal of the American Chemical Society 133: 10499-10511. [Copyright (2011) American Chemical Society].*

These observations reinforce the functional role of the cyclic imine and the importance of its structural integrity for the interaction with nAChRs. The cyclic imine moiety represents the key feature in this family of phycotoxins and its role in binding of pinnatoxin A to nAChRs, according to the modeling, is dual. First, in conjunction with the C28 hydroxy group of the bridged EF-ketal, it anchors the ligand to the binding site through hydrogen bonds in a conformation ideally poised to optimize the interactions with neighboring residues. Moreover, the hydrogen bond established by this group with the backbone carbonyl of W147 is observed not only in all three docking complexes obtained in this work, but also in the two crystal structures of the complexes between AChBP and gymnodimine A or 13-desmethyl spirolide C (Bourne *et al.*, 2010). Second, binding of the closed imino ring A in pinnatoxin A (**1**) appears to be more favorable, both sterically and energetically, than that of the corresponding open amino ketone form (**2**).

The presence of a protonated imine nitrogen might represent a common functional feature in the cyclic imine phycotoxins interacting with nicotinic receptors, as has been shown for pinnatoxin A (Aráoz *et al.*, 2011), gymnodimine A, and 13-desmethyl spirolide C (Kharrat *et al.*, 2008; Bourne *et al.*, 2010) and that has yet to be demonstrated for pteriatoxins and prorocentrolides.

Conclusion

In this work, molecular modeling studies provided further detailed insight into the structural determinants of the interaction between a macrocyclic spiroimine phycotoxin, pinnatoxin A, with three different subtypes of nAChRs. A two-step protocol has been established for flexible docking of the macrocyclic toxin at the nAChR subunit interface. The protein-ligand interactions identified are in good agreement with the selectivity profile determined experimentally. A particular conformation has been evidenced for the acyclic amino-ketone form of the pinnatoxin A, which explains low, if any, biological activity observed for this derivative and emphasizes the importance of the spiroimine pharmacophore within this phycotoxin family.

Acknowledgements. *This work was supported in part by US National Institutes of Health (NIGMS, GM077379 to A.Z. with subcontract KK1036 to J.M.). R.A. was supported by a grant from EU 7th Frame Program STC-CP2008-1-555612 (ATLANTOX).*

References

Aráoz R, Servent D, Molgó J, Iorga BI, Fruchart-Gaillard C, Benoit E, Gu Z, Stivala C, Zakarian A (2011) Total synthesis of pinnatoxins A and G and revision of the mode of action of pinnatoxin A. *J Am Chem Soc* **133**: 10499-10511

Bourne Y, Radic Z, Aráoz R, Talley TT, Benoit E, Servent D, Taylor P, Molgó J, Marchot P (2010) Structural determinants in phycotoxins and AChBP conferring high affinity binding and nicotinic AChR antagonism. *Proc Natl Acad Sci USA* **107**: 6076-6081

Costa V, Nistri A, Cavalli A, Carloni P (2003) A structural model of agonist binding to the alpha3beta4 neuronal nicotinic receptor. *Br J Pharmacol* **140**: 921-931

Dutertre S, Lewis RJ (2004) Computational approaches to understand alpha-conotoxin interactions at neuronal nicotinic receptors. *Eur J Biochem* **271**: 2327-2334

Espinoza-Fonseca LM (2004) Base docking model of the homomeric alpha7 nicotinic receptor-beta-amyloid(1-42) complex. *Biochem Biophys Res Commun* **320**: 587-591

Eswar N, Eramian D, Webb B, Shen MY, Sali A (2008) Protein structure modeling with MODELLER. *Methods Mol Biol* **426**: 145-159

Everhart D, Reiller E, Mirzoian A, McIntosh JM, Malhotra A, Luetje CW (2003) Identification of residues that confer alpha-conotoxin-PnIA sensitivity on the alpha 3 subunit of neuronal nicotinic acetylcholine receptors. *J Pharmacol Exp Ther* **306**: 664-670

Forli S, Botta M (2007) Lennard-Jones potential and dummy atom settings to overcome the AUTODOCK limitation in treating flexible ring systems. *J Chem Inf Model* **47**: 1481-1492

Gonzalez-Cestari TF, Henderson BJ, Pavlovicz RE, McKay SB, El-Hajj RA, Pulipaka AB, Orac CM, Reed DD, Boyd RT, Zhu MX, Li C, Bergmeier SC, McKay DB (2009) Effect of novel negative allosteric modulators of neuronal nicotinic receptors on cells expressing native and recombinant nicotinic receptors: implications for drug discovery. *J Pharmacol Exp Ther* **328**: 504-515

Henchman RH, Wang HL, Sine SM, Taylor P, McCammon JA (2003) Asymmetric structural motions of the homomeric alpha7 nicotinic receptor ligand binding domain revealed by molecular dynamics simulation. *Biophys J* **85**: 3007-3018

Henderson BJ, Pavlovicz RE, Allen JD, Gonzalez-Cestari TF, Orac CM, Bonnell AB, Zhu MX, Boyd RT, Li C, Bergmeier SC, McKay DB (2010) Negative allosteric modulators that target human alpha4beta2 neuronal nicotinic receptors. *J Pharmacol Exp Ther* **334**: 761-774

Iorga B, Herlem D, Barre E, Guillou C (2006) Acetylcholine nicotinic receptors: finding the putative binding site of allosteric modulators using the "blind docking" approach. *J Mol Model* **12**: 366-372

Kharrat R, Servent D, Girard E, Ouanounou G, Amar M, Marrouchi R, Benoit E, Molgó J (2008) The marine phycotoxin gymnodimine targets muscular and neuronal nicotinic acetylcholine receptor subtypes with high affinity. *J Neurochem* **107**: 952-963

Law RJ, Henchman RH, McCammon JA (2005) A gating mechanism proposed from a simulation of a human alpha7 nicotinic acetylcholine receptor. *Proc Natl Acad Sci U S A* **102**: 6813-6818

Le Novere N, Grutter T, Changeux JP (2002) Models of the extracellular domain of the nicotinic receptors and of agonist- and Ca^{2+}-binding sites. *Proc Natl Acad Sci U S A* **99**: 3210-3215

Molgó J, Girard E, Benoit E (2007) The cyclic imines: an insight into this emerging group of bioactive marine toxins. In *Phycotoxins: Chemistry and Biochemistry*. Hui YH, Botana LM (eds) pp 319-355. Oxford: Balckwell Publishing

Molles BE, Tsigelny I, Nguyen PD, Gao SX, Sine SM, Taylor P (2002) Residues in the epsilon subunit of the nicotinic acetylcholine receptor interact to confer selectivity of waglerin-1 for the alpha-epsilon subunit interface site. *Biochemistry* **41**: 7895-7906

Morris GM, Goodsell DS, Halliday RS, Huey R, Hart WE, Belew RK, Olson AJ (1998) Automated docking using a Lamarckian genetic algorithm and an empirical binding free energy function. *J Comput Chem* **19**: 1639-1662

Pedretti A, Marconi C, Bolchi C, Fumagalli L, Ferrara R, Pallavicini M, Valoti E, Vistoli G (2008) Modelling of full-length human alpha4beta2 nicotinic receptor by fragmental approach and analysis of its binding modes. *Biochem Biophys Res Commun* **369**: 648-653

Pettersen EF, Goddard TD, Huang CC, Couch GS, Greenblatt DM, Meng EC, Ferrin TE (2004) UCSF Chimera-a visualization system for exploratory research and analysis. *J Comput Chem* **25**: 1605-1612

Rhodes L, Smith K, Selwood A, McNabb P, van Ginkel R, Holland P, Munday R (2010) Production of pinnatoxins by a peridinoid dinoflagellate isolated from Northland, New Zealand. *Harmful Algae* **9**: 384-389

Samson A, Scherf T, Eisenstein M, Chill J, Anglister J (2002) The mechanism for acetylcholine receptor inhibition by alpha-neurotoxins and species-specific resistance to alpha-bungarotoxin revealed by NMR. *Neuron* **35**: 319-332

Schapira M, Abagyan R, Totrov M (2002) Structural model of nicotinic acetylcholine receptor isotypes bound to acetylcholine and nicotine. *BMC Struct Biol* **2**: 1

Selwood AI, Miles CO, Wilkins AL, van Ginkel R, Munday R, Rise F, McNabb P (2010) Isolation, structural determination and acute toxicity of pinnatoxins E, F and G. *J Agric Food Chem* **58**: 6532-6542

Sine SM, Wang HL, Bren N (2002) Lysine scanning mutagenesis delineates structural model of the nicotinic receptor ligand binding domain. *J Biol Chem* **277**: 29210-29223

Stivala CE, Zakarian A (2008) Total synthesis of (+)-pinnatoxin A. *J Am Chem Soc* **130**: 3774-3776

Sullivan D, Chiara DC, Cohen JB (2002) Mapping the agonist binding site of the nicotinic acetylcholine receptor by cysteine scanning mutagenesis: antagonist footprint and secondary structure prediction. *Mol Pharmacol* **61**: 463-472

Taly A, Delarue M, Grutter T, Nilges M, Le Novere N, Corringer PJ, Changeux JP (2005) Normal mode analysis suggests a quaternary twist model for the nicotinic receptor gating mechanism. *Biophys J* **88**: 3954-3965

Unwin N (2005) Refined structure of the nicotinic acetylcholine receptor at 4A resolution. *J Mol Biol* **346**: 967-989

Verdonk ML, Cole JC, Hartshorn MJ, Murray CW, Taylor RD (2003) Improved protein-ligand docking using GOLD. *Proteins* **52**: 609-623

Willcockson IU, Hong A, Whisenant RP, Edwards JB, Wang H, Sarkar HK, Pedersen SE (2002) Orientation of d-tubocurarine in the muscle nicotinic acetylcholine receptor-binding site. *J Biol Chem* **277**: 42249-42258

Toxines et Transferts ioniques – Toxins and Ion transfers
Rencontres en Toxinologie – Meeting on Toxinology, 2011
Editions de la SFET – SFET Editions
Accès libre en ligne sur le site – Free access on line on the site : http://www.sfet.asso.fr

VacA from Helicobacter pylori *: journey and action mechanism in epithelial cells*

Vittorio RICCI[1*], Patrice BOQUET[2]

[1] Department of Physiology, Human Physiology Section, University of Pavia Medical School, Via Forlanini 6, 27100 Pavia, Italy ; [2] Department of Clinical Bacteriology, Nice University Hospital, 151 route de Saint Antoine de Ginestière, 06202 Nice cedex 03, France

** Corresponding author ; Tel : +39 0382 987254 ; Fax : +39 0382 987664 ; E-mail : vricci@unipv.it*

Abstract

The VacA toxin from Helicobacter pylori *is composed by a N-terminal 33-kDa and a C-terminal 55-kDa fragment (named p33 and p55, respectively), thus structurally resembling an A-B toxin. Through its p55 fragment, VacA binds to lipid rafts of host cells and, upon hexamerization, inserts its p33 domain into the lipid bilayer of plasma membrane forming an anion-selective channel, being thus currently classified as a pore-forming toxin. VacA is then internalized by the GEEC (GPI-enriched Early Endosomal Compartment) endocytic pathway (specialized in the endocytosis of glycosylphosphatidylinositol-anchored proteins). Exploiting the peculiar actin-comet-tail-dependent motility of a subpopulation of early endosomes, VacA partly reaches mitochondria (where its pore-forming activity is transferred into the inner mitochondrial membrane and triggers cell death), while the most part reaches a late endosomal compartment whose osmotic swelling leads to cytoplasmic vacuolation. Considering its structure-function relationship, VacA might be a new type of A-B toxin in which the enzymatic activity of A subunit has been replaced by a pore-forming one.*

*Trafic intracellulaire et mécanisme d'action de la toxine VacA d'*Helicobacter pylori *dans les cellules épithéliales*

*La toxine VacA d'*Helicobacter pylori *est composée d'un fragment N-terminal de 33 kDa et d'un fragment C-terminal de 55 kDa (appelés p33 et p55, respectivement). Elle ressemble donc, structuralement, à une toxine A-B. Par son fragment p55, VacA se lie aux radeaux lipides («lipid rafts») des cellules hôtes et, après hexamérisation, insère son domaine p33 dans la bicouche lipidique en induisant la formation d'un canal sélectif aux anions, étant ainsi actuellement classée comme une toxine formant des pores. Elle est alors internalisée par la voie endocytaire dépendante des compartiments endosomaux précoces enrichis en GPI (GEEC) et spécialisée dans l'endocytose des protéines ancrées au glycosylphosphatidylinositol. Grâce à l'actine qui est responsable de la motilité d'une sous-population des endosomes précoces, une partie de VacA rejoint les mitochondries (où son activité de formation des pores est transférée dans la membrane mitochondriale interne et déclenche la mort cellulaire), tandis que la plupart de VacA atteint un compartiment endosomal tardif dont le gonflement osmotique entraîne une vacuolisation cytoplasmique. Compte tenu de sa relation structure-fonction, VacA pourrait être un nouveau type de toxine A-B dans laquelle l'activité enzymatique de la sous-unité A serait remplacée par une activité porogène.*

Keywords : *A-B Toxins,* Helicobacter pylori, *intracellular trafficking, VacA/CagA relationship, VacA toxin.*

Introduction

VacA toxin, one of the most important virulence factors of *Helicobacter pylori*, is a protein which apparently exerts pleiotropic effects on mammalian cells and tissues. In 2005, *Nature Rev Microbiol* published a landmark paper by Cover and Blanke in which VacA was thus proposed as a paradigm for toxin multifunctionality (Cover and Blanke, 2005). However, an increasing body of evidence now suggests that VacA may rather be the prototype of a new class of monofunctional A-B toxins. The present paper is devoted to discuss the characteristics of VacA as a new type of A-B toxin depicting its journey and action mechanism in epithelial cells where *H. pylori* is however modulating VacA-induced toxicity by means of another virulence factor such as CagA.

The pleiotropic effects of VacA

Since the discovery that *H. pylori* (at that time named *Campylobacter pylori*) releases in its broth culture supernatant a toxin (later identified as VacA) causing a unique cytoplasmic vacuolation in cultured cells (Leunk

et al., 1988), a flurry of quite different cellular activities has been attributed to VacA which is to date consequently qualified in the literature as a multifunctional toxin (Cover and Blanke, 2005; Isomoto *et al.*, 2010). However, a careful analysis of VacA cellular effects described so far shows that only three toxin activities have been repetitively confirmed by independent laboratories suggesting that they are true biological effects. These activities are (i) osmotic swelling of late endocytic compartments (by indirect overactivation of their V-ATPase) which leads to cell vacuolation (Szabò *et al.*, 1999), (ii) induction of apoptosis by triggering the so-called intrinsic pathway (*i.e.* mitochondria-dependent; Galmiche *et al.*, 2000), and (iii) inhibition of the proliferation of T lymphocytes by blockage of the nuclear transcription factor NFAT activation (Gebert *et al.*, 2003). Worth noting, all these three activities rely totally on one single property of VacA, namely its pore-forming activity (Szabò *et al.*, 1999; Boncristiano *et al.*, 2003; Cover *et al.*, 2003). Nevertheless, many other disparate VacA activities on different cell types have been described, but all these effects are still waiting for independent confirmation and the possibility arises that at least some of them, if confirmed, might simply be epiphenomena of a single primary toxin action. In particular, VacA has been reported to cause (for a review see Ricci *et al.*, 2000; Cover and Blanke, 2005; Isomoto *et al.*, 2010): (1) increase in the permeability of the epithelial paracellular route, (2) selective inhibition of Ii-dependent antigen presentation, (3) increased transport of urea across epithelia, (4) binding of the toxin to a putative intermediate filament-interacting protein and disorganization of the cytoskeletal architecture of gastric epithelial cells, (5) activation of Ca^{2+}-dependent Cl^- channels which may result in enterotoxic effect and diarrhea, (6) interaction with RACK1 protein, (7) increase in bicarbonate and pepsinogen secretion by gastric mucosa and, by contrast, decrease in bicarbonate secretion by duodenal mucosa, (8) increased extracellular secretion of acidic hydrolases, (9) induction of cytosolic calcium oscillations and activation of mast cells, (10) blockade of phagosome maturation and impairment of the degradative power of late endosomes and lysosomes, (11) interaction with extracellular matrix adhesive proteins (such as fibronectin) altering cell adhesion and spreading, (12) activation of the p38 MAPK/ATF-2 cell signalling pathway, and (13) through activation of the PI3K/Akt signalling pathway, inhibition of glycogen synthase kinase (GSK)-3, with subsequent translocation of beta-catenin to the nucleus.

Thus, is VacA really a paradigm for toxin multifunctionality as previously suggested (Cover and Blanke, 2005; Isomoto *et al.*, 2010), taking that all the fully-documented activities of VacA closely depends on its pore-forming action? Or, alternatively, might VacA be better considered as a monofunctional toxin? In this respect, we are now focusing on the interactions of VacA with epithelial cells.

VacA structure / function relationship

According to their action strategy on target cells, bacterial protein toxins are commonly classified into three classes (Boquet and Gill, 1991; Montecucco *et al.*, 1994): (a) interfering with transmembrane signalling cascade, (b) affecting plasma membrane permeability (*i.e.* the so-called pore-forming toxins), and (c) acting inside the cell. As the prototype of the aforementioned first-class toxins, we can consider the heat-stable toxin STa from enterotoxigenic *Escherichia coli*. Indeed, STa acts on the surface of target cells binding to an endogenous ligand surface receptor so as to trigger an intracellular signaling cascade ultimately resulting in an increased Cl^- intestinal secretion and watery diarrhea (Schiavo and van der Goot, 2001; Taxt *et al.*, 2010). As prototypes of the second class, we can consider streptolysin O from *Streptococcus pyogenes* and alpha toxin from *Staphylococcus aureus* (Schiavo and van der Goot, 2001), that form holes into cell membranes. Finally, the A-B toxins (whose the most well-known are diphtheria toxin and Shiga toxin) represent the third-class toxins (Schiavo and van der Goot, 2001). The action strategy of an A-B toxin is to induce the highest cell damage with the lowest dose of toxin by exploiting its enzymatic activity on a key cytosolic regulatory protein. However, to reach its cytosolic target, an A-B toxin is obliged to cross cell membranes (the plasma membrane and/or the limiting membrane of cytoplasmic organelles). To this purpose, A-B toxins are organized into two different subunits (named A and B, respectively). The A subunit is the toxic part of the toxin and is linked to the B one in turn committed to bind the target cells and to allow the A subunit to translocate into the cytosol where exerting its enzymatic activity.

In its mature form (*Figure 1A*), VacA is a 88-kDa protein which encompasses an N-terminal and a C-terminal subunits (named p33 and p55, respectively) linked by a protease-sensitive loop (Cover and Blanke, 2005; Isomoto *et al.*, 2010). The p33 subunit has been shown to form anion-selective channels in membranes (*i.e.* it exhibits a pore-forming activity) of host cells while the p55 one allows toxin binding to target cells (Cover and Blanke, 2005; Isomoto *et al.*, 2010). Apparently, VacA is thus presenting all the characteristics of a typical A-B toxin in which, however, the pore-forming activity of A subunit (p33) would replace the classical enzymatic one. However, a pore-forming activity seems to be much less potent than an enzymatic one to affect cell homeostasis because holes in membranes may be efficiently repaired by the cell (Bischofberger *et al.*, 2009). Nevertheless, among the different cell membranes, the most fragile one seems to be the inner mitochondrial membrane (IMM) whose alteration rapidly lead to cell death (Galmiche and Boquet, 2006). The VacA p33 subunit has been shown to target mitochondria, to localize in the IMM, to drop cellular ATP, and to cause cell death (Kimura *et al.*, 1999; Galmiche *et al.*, 2000; Domanska *et al.*, 2010). Taken together, these findings thus suggest that VacA might represent the prototype of a new class of bacterial A-B toxins that associates a specific mitochondrial pore-forming subunit (p33) to a cell binding component (p55). However, how does this A-B toxin reach its target with a maximum of efficiency?

VacA intracellular trafficking

To deliver its enzymatic subunit into the cytosol, a canonical A-B toxin may usually follow two different approaches.

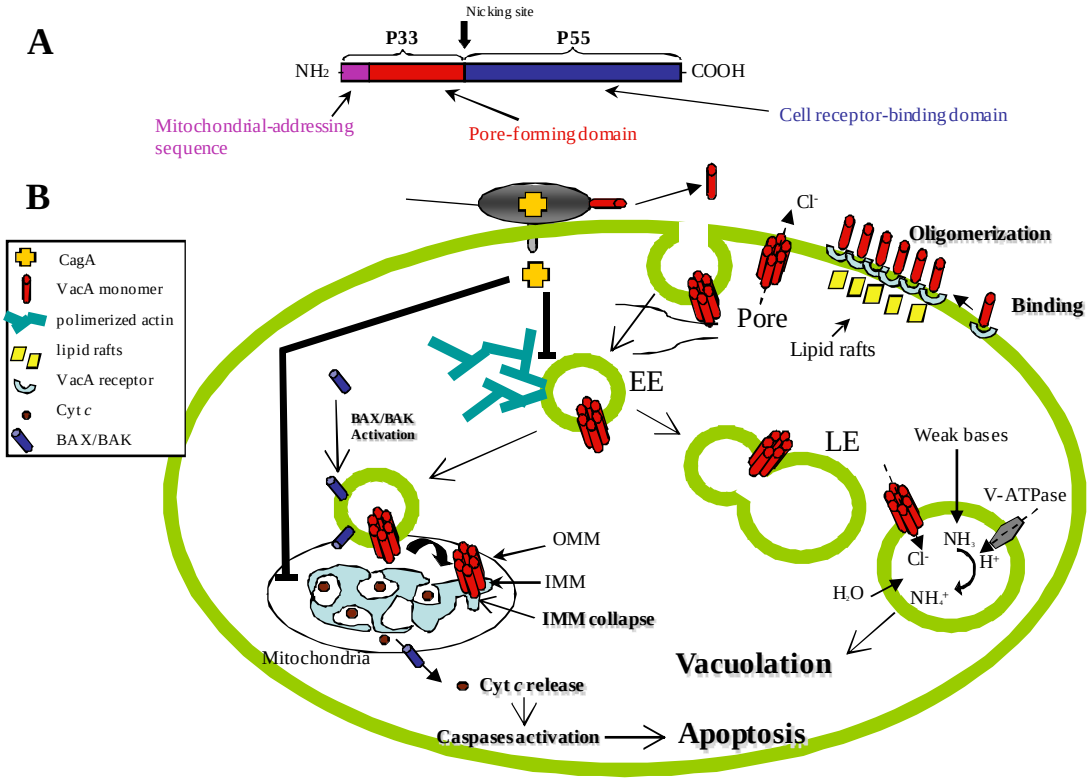

Figure 1. (**A**) **Structure of the VacA toxin.** The large vertical arrow shows the possible nicking, by proteolysis, of the mature 88-kDa toxin into two separated A and B subunits of 33 kDa (p33) and 55 kDa (p55), respectively. (**B**) **Action mechanism of VacA and the interfering effects of CagA.** The toxin is secreted by the bacterium but remains attached to the bacterial surface and is slowly released in the extracellular medium. VacA binds to its cell surface receptor, oligomerizes and is inserted into the plasma membrane at the level of lipid rafts forming a pore endowed with anionic transport properties. The toxin is endocytosed and reaches early endosomal compartments (EE) which can move due to the formation of actin comet tails. These VacA-containing endosomes, which may activate the proapoptotic molecules BAX/BAK by the presence of the toxin, then fuse their membrane with those of mitochondria, favored by the presence of the mitochondrial-addressing sequence at the N-terminus of p33 (this sequence being also involved in the transport of the toxin to the inner mitochondrial membrane (IMM)) but possibly also facilitated by activated proapoptotic molecules. In the IMM the toxin pore disrupts the electrical proton gradient required for the integrity of mitochondrial activity and opens IMM pockets releasing cytochrome *c* (Cyt *c*) in the mitochondrial intermembrane space. This is followed by release of Cyt *c* in the cytosol through outer mitochondrial membrane (OMM)-inserted proapoptotic BAX/BAK channels leading to caspase 9 and 3 activation and apoptosis. Remarkably, few toxin pores inserted in the IMM can be enough for triggering such an effect. The mobile early endosomes can also fuse with late endosomes (LE) where most part of VacA is delivered. Overactivation of the endosomal proton pump (*i.e.* V-ATPase) through intraluminal transport of anions (*i.e.* Cl^-) results in accumulation of weak bases (such as ammonia) by protonation that gives rise to the osmotic swelling finally leading to the typical VacA-dependent cell vacuolation. CagA is injected into the host gastric epithelial cell by a type IV secretion system. This protein can block the intracellular trafficking of VacA by interfering with the formation of actin comet tails at the surface of VacA-containing endosomes, inhibiting their motility and thereby their fusion with either mitochondria (blocking VacA-induced apoptosis) or LE (blocking VacA-induced vacuolation). In addition, CagA may also directly block VacA-induced apoptosis at the level of mitochondria (for instance, by raising the level of anti-apoptotic factors such as Bcl2).

Figure 1. *(**A**) **Structure de la toxine VacA.** La large fleche verticale montre une possible coupure, par protéolyse, de la toxine mature (88 kDa) en deux sous-unités séparées de 33 kDa (p33) et 55 kDa (p55), respectivement. (**B**) **Mécanisme d'action de VacA et ses interactions avec CagA.** La toxine est secrétée par la bactérie, mais elle reste attachée à la surface bactérienne et elle est relarguée lentement dans le milieu extérieur. VacA se lis à son récepteur à la surface cellulaire, s'oligomérise et s'insère dans la membrane plasmatique au niveau des radeaux lipidiques en formant un pore ayant des propriétés de transport anionique. La toxine est endocytosée et gagne les endosomes précoces (EE) qui peuvent migrer grâce à la formation de queues de comète d'actine. Les endosomes contenant VacA, qui peuvent activer les molécules pro-apoptotiques BAX/BAK en présence de la toxine, fusionnent leur membrane avec celle des mitochondries, grâce à la séquence d'adressage aux mitochondries dans la séquence N-terminale de p33 (cette séquence étant aussi impliquée dans le transport de la toxine à la membrane interne des mitochondries (IMM)), mais aussi peut-être grâce aux molécules pro-apoptotiques activées. Dans la IMM le pore formée par la toxine supprime le gradient électrique de protons qui est nécessaire pour l'intégrité de l'activité mitochondriale, et il ouvre les poches de IMM et induit la fuite de cytochrome c (Cyt c) dans l'espace intermembranaire mitochondrial. Ceci est suivi par le relargage de Cyt c dans le cytosol à travers les canaux des molécules pro-apoptotiques insérés dans la membrane externe mitochondirale (OMM) et conduit à l'activation des caspases 3 et 9 et à l'apoptose. Il faut noter que quelques pores de toxine insérés dans l'IMM sont suffisants pour déclencher cet effet. Les endosomes précoces mobiles peuvent aussi fusionner avec les endosomes tardifs (LE) où la plupart de VacA est relâchée. La suractivaition de la pompe à proton endosomale (*i.e. V-ATPase) dans le transport d'anions (*i.e. Cl^-) vers la lumière de l'endosome aboutit à l'accumulation de bases faibles (telles que l'ammoniaque) par protonation qui élève la pression osmotique entraînant une augmentation de volume cellulaire et une vacuolisation typique de VacA. CagA est injectée dans la cellule épithéliale gastrique par un système de sécrétion de type IV. Cette protéine peut bloquer le trafic intracellulaire de VacA en interférant avec la formation des queues de comète d'actine à la surface des endosomes contenant VacA, et en inhibant leur mobilité et ainsi leur fusion avec soit les mitochondries (bloquant l'apoptose induite par VacA) ou les LE (bloquant la vacuolisation induite par VacA). De plus, CagA peut directement bloquer l'apoptose induite par VacA au niveau des mitochondries (par exemple en élevant le niveau des facteurs anti-apoptotiques tels que Bcl2).*

In the first one (it is the case, for instance, of diphtheria toxin), upon endocytosis of the toxin-receptor complex, the entire toxin reaches early endosomes where, because of the acidic pH of this compartment, undergoes a conformational change of a translocating domain located in the B subunit. This leads the fusion of the B subunit of the toxin with the endosomal membrane followed by transport of the enzymatic A subunit into the cytosol where it targets its prey protein. Toxins exploiting such an intracellular trafficking pathway are defined as "short-trip toxins" (Pei *et al.*, 2001).

In the second approach (it is the case, for instance, of Shiga toxin), the toxin undergoes a longer journey inside the cell before the A subunit may enter the cytosol. These "long-trip toxins" (Pei *et al.*, 2001) have to progressively pass through early endosomes, the Golgi apparatus and the endoplasmic reticulum (ER). The enzymatic subunit of the toxin then reaches the cytosol by exploiting the ER-associated degradation (ERAD) machinery through which misfolded proteins are normally retrotranslocated from ER into the cytosol for proteasomal degradation (Johannes and Römer, 2010).

VacA would follow an alternative pathway (*Figure 1B*). There is no cytosolic release of the pore-forming subunit because it would be poorly effective. The toxin pore is directly formed in the lipid bilayers of cell plasma membrane upon hexamerization of VacA monomers after binding to the receptor (Cover and Blanke, 2005; Isomoto *et al.*, 2010). After clathrin-independent internalization through the GEEC endocytic pathway (specialized in the endocytosis of glycosylphosphatidylinositol-anchored proteins), the toxin is then transported to early endosomes which acquire a high motility because of the formation of actin comet tails at their surface (Gauthier *et al.*, 2007). This motility allows such endosomes to reach mitochondria (Oldani *et al.*, 2009) and, as recently shown, by endosomes-mitochondria juxtaposition exchange the transfer of a small amount of VacA to mitochondria together with the activation of the proapoptotic BAX and BAK molecules (Calore *et al.*, 2010). It has been furthermore suggested that the presence of activated BAX and BAK at the surface of VacA-containing endosomes might be involved in the docking of these endosomes to mitochondria (Calore *et al.*, 2010). Translocation of the p33 subunit or of the entire toxin to the IMM is achieved through its N-terminal stretch of 32 hydrophobic amino acids that, acting as a novel mitochondrial-addressing sequence, exploits the mitochondrial import machinery by which exogenous proteins enter this organelle (*i.e.* the TOM complex) (Domanska *et al.*, 2010). By this way, VacA can disrupt the transmembrane electrical potential of the IMM resulting in cell death. The swelling of late endosomal compartments (*i.e.* cell vacuolation) would simply be a side-effect of the toxin which is mostly routed to these compartments (Ricci *et al.*, 1997). This is a quite common behaviour for an A-B toxin in which the A subunit is so powerful that also a very small amount reaching its intracellular target is sufficient to fully intoxicate the cell.

VacA / CagA relationship

Apparently, the role of VacA in *H. pylori* pathogenic action is confined to the early phase of bacterial infection (Salama *et al.*, 2001). Secreted through a type V (*i.e.* autotransporter-dependent) secretion system (Schmitt and Haas, 1994), the toxin is progressively released from the bacterial surface upon detachment by limited proteolysis from its autotransporter moiety (Nguyen *et al.*, 2001). *H. pylori* has developed the capacity to live in the human stomach which is characterized by an extremely low luminal pH. A pivotal bacterial mechanism to maintain a neutral pH within the bacteria is the utilization of urea by means of a powerful urease system (Sachs *et al.*, 2006). Moreover, parietal cells (*i.e.* the producer of the hydrochloric acid responsible for the low gastric pH) are highly sensitive to VacA (Kobayashi *et al.*, 1996; Wang *et al.*, 2008). We have shown that VacA targets and impairs mitochondria (Galmiche *et al.*, 2000). Mitochondria are highly abundant in parietal cells which necessitate a large amount of ATP to secrete hydrochloric acid via the gastric proton pump (Helander and Keeling, 1993). Taking into account the activity of VacA on mitochondria, the toxin is thus ideally suited to shut down the gastric acid production by parietal cells, in particular during the early step of *H. pylori* gastric colonization, when the bacteria (which are neutralophiles able of acid-acclimation, and not acidophiles (Sachs *et al.*, 2005 and 2006)) are exposed to the high acidity characterizing the gastric lumen. Once *H. pylori* is attached to the gastric surface epithelium, it is now partially protected from acidic pH by the mucus-bicarbonate layer rich in urea overlying the gastric epithelium and thus the activity of VacA is no longer required. In addition, after bacterial adherence to the gastric epithelial cells, VacA activity might be deleterious for the persistence of colonization since it would lead to epithelial cell death.

We and others have recently shown that by injecting CagA through a type IV secretion system *H. pylori* protects the colonized gastric epithelial cells against VacA injuring action (*Figure 1B*) (Oldani *et al.*, 2009; Akada *et al.*, 2010). This might explain the virtually constant association of VacA with CagA in highly pathogenic *H. pylori* (*i.e.* the so-called type I strains) even though the respective genes are far apart on the *H. pylori* chromosome and their expression levels are not mutually related (Peek and Blaser, 2002). Worth noting, acquisition of VacA and CagA genes by *H. pylori* has been achieved probably together and positive selection has shaped the structure of both VacA and CagA separately from the core genome of the bacterium (Gangwer *et al.*, 2010). This selection could arise by a form of pseudolinkage of functionally interacting genes in order to balance bacterial damaging action on the host and thus facilitating a persistent gastric colonization (Gangwer *et al.*, 2010). This further supports the idea that CagA may control the cytotoxic action of VacA.

Conclusions

The journey and action mechanism of VacA (as a new type of A-B toxin) in gastric epithelial cells can thus be summarized in a scheme (panel B of *Figure 1*) which is simple, maybe incomplete, but nevertheless helpful for designing new experiments to completely decipher the action strategy of this important bacterial toxin. As

stated by the famous French poet and essayist Paul Valéry "what is simple might be not exact, but what is complicated is useless".

Acknowledgements. *This work was supported in part by grants from the Italian Ministry for University and Research (Progetto di Ricerca di Interesse Nazionale 2009A37C8C_002) and from Regione Lombardia (Progetto SAL-45). The authors declare they have no conflicts of interest to disclose.*

References

Akada JK, Aoki H, Torigoe Y, *et al.* (2010) *Helicobacter pylori* CagA inhibits endocytosis of cytotoxin VacA in host cells. *Dis Model Mech* **3**: 605-617

Boncristiano M, Rossi Paccani S, Barone S, *et al.* (2003) The *Helicobacter pylori* vacuolating toxin inhibits T cell activation by two independent mechanisms. *J Exp Med* **198**: 1887-1897

Boquet P, Gill DM (1991) Modulation of cell functions by ADP-ribosylating bacterial toxins. In: The Comprehensive Sourcebook of Bacterial Protein Toxins, 1st edition, Alouf J and Freer J eds., Academic Press, New York (NY), pp 23-44

Bischofberger M, Gonzalez MR, van der Goot FG (2009) Membrane injury by pore-forming proteins. *Curr Opin Cell Biol* **21**: 589-595

Calore F, Genisset C, Casellato A, *et al.* (2010) Endosome-mitochondria juxtaposition during apoptosis induced by *H. pylori* VacA. *Cell Death Diff.* **17**: 1707-1716

Cover TL, Blanke SR (2005) *Helicobacter pylori* VacA, a paradigm for toxin multifunctionality. *Nature Rev Microbiol* **3**: 320-322

Cover TL, Blaser MJ (1992) Purification and characterization of the vacuolating toxin from *Helicobacter pylori*. *J Biol Chem* **267**: 10570-10575

Cover TL, Krishna US, Israel DA, Peek RM Jr (2003) Induction of gastric epithelial cell apoptosis by *Helicobacter pylori* vacuolating cytotoxin. *Cancer Res* **63**: 951-957

Domanska G, Motz C, Meinecke M, *et al.* (2010) *Helicobacter pylori* VacA toxin/subunit p34 : targeting of an anion channel to the inner mitochondrial membrane. *PLoS Pathog* **6**: e1000878

Galmiche A, Boquet P (2006) Bacterial toxins and mitochondria. In « The Comprehensive Sourcebook of Bacterial Protein Toxins », third edition, Alouf, J.E and Popoff, M.R. Eds, Academic Press, London. pp 188-201

Galmiche A, Rassow J, Doye A, *et al.* (2000) The N-terminal 34 kDa fragment of *Helicobacter pylori* vacuolating cytotoxin targets mitochondria and induces cytochrome c release. *EMBO J* **23**: 6361-6370

Gangwer KA, Shaffer CL, Suerbaum S, *et al.* (2010) Molecular evolution of the *Helicobacter pylori* vacuolating toxin gene (*vacA*). *J Bacteriol* **192**: 6126-6135

Gauthier NC, Monzo P, Gonzales T, *et al.* (2007) Early endosomes associated with dynamics F-actin structures are required for late trafficking of *H. pylori* toxin. *J Cell Biol* **177**: 343-354

Gebert B, Fisher W, Weiss E, Hoffmann R, Haas R (2003) *Helicobacter pylori* vacuolating cytotoxin inhibits T lymphocyte activation. *Science* **301**: 1099-1102

Helander HF, Keeling DJ (1993) Cell biology of gastric acid secretion. *Baillieres Clin Gastroenterol* **7**: 1-21

Isomoto M, Moss J, Hiramaya T (2010) Pleiotropic actions of *Helicobacter pylori* vacuolating cytotoxin VacA. *Tohoku J Exp Med* **220:** 3-14

Johannes L, Römer W (2010) Shiga toxin – from cell biology to biomedical applications. *Nature Rev Microbiol* **8**: 105-116

Kimura M, Goto S, Wada A *et al.* (1999) Vacuolating cytotoxin purified from *Helicobacter pylori* causes mitochondrial damage in human gastric cells. *Microb Pathog* **26**: 45-52

Kobayashi H, Kamiya S, Suzuki T, *et al.* (1996) The effect of *Helicobacter pylori* on gastric acid secretion by isolated parietal cells from a guinea pig. Association with production of vacuolating toxin by *H. pylori*. *Scand J Gastroenterol* **31**: 428-433

Leunk RD, Johnson PT, David BC, Kraft WG, Morgan DR (1988) Cytotoxic activity in broth-culture filtrates of *Campylobacter pylori*. *J Med Microbiol* **26**: 93-99

Montecucco C, Papini E, Schiavo G (1994) Bacterial protein toxins penetrate cells via a four-step mechanism. *FEBS Lett* **346**: 92-98

Nguyen VQ, Caprioli RM, Cover TL (2001) Carboxy-terminal proteolytic processing of *Helicobacter pylori* vacuolating toxin. *Infect. Immun* **69**: 543-546

Oldani A, Cormont M, Hofman V, *et al.* (2009) *Helicobacter pylori* conteracts the apoptotic action of its VacA toxin by injecting the CagA protein into gastric epithelial cells. *PLoS Pathog* **5:** e1000603

Peek RM Jr, Blaser MJ (2002) *Helicobacter pylori* and gastrointestinal tract adenocarcinomas. *Nature Rev Cancer* **2**: 28-37

Pei S, Doye A, Boquet P (2001) Mutation of specific acidic residues of the CNF1 T domain into lysine alters cell membrane translocation of the toxin. *Mol Microbiol* **41**: 1237-1247

Ricci V, Sommi P, Fiocca R, *et al.* (1997) *Helicobacter pylori* vacuolating toxin accumulates within the endosomal-vacuolar compartment of cultured gastric cells and potentiates the vacuolating activity of ammonia. *J. Pathol* **183**: 453-459

Ricci V, Sommi P, Romano M (2000) The vacuolating toxin of *Helicobacter pylori*: a few answer, many questions. *Digest Liver Dis* **32** (Suppl 3): S178-S181

Sachs G, Weeks DL, Wen Y, *et al.* (2005) Acid acclimation by *Helicobacter pylori*. *Physiology* **20**: 429-438

Sachs G, Kraut JA, Wen Y, Feng J, Scott DR (2006) Urea transport in bacteria : acid acclimatation by gastric *Helicobacter spp*. *J Membrane Biol* **212**: 71-82

Salama NR, Otto G, Tompkins L, Falkow S (2001) Vacuolating cytotoxin of *Helicobacter pylori* plays a role during colonization in a mouse model of infection. *Infect Immun* **69**: 730-736

Schiavo G, van der Goot FG (2001) The bacterial toxins toolkit. *Nature Rev Mol Cell Biol* **42:** 1-6

Schmitt W, Haas R (1994) Genetic analysis of the *Helicobacter pylori* vacuolating cytotoxin: structural similarities with IgA protease type of exported proteins. *Mol Microbiol* **12**: 307-319

Szabò I, Brutsche S, Tombola F, *et al.* (1999) Formation of anion selective channels in cell plasma membrane by the toxin VacA of *Helicobacter pylori* is required for its biological activity. *EMBO J* **18**: 5517-5527

Taxt A, Aasland R, Sommerfelt H, Nataro J, Puntervoll P (2010) Heat-stable enterotoxin of enterotoxigenic *Escherichia coli* as a vaccine target. *Infect Immun* **78**: 1824-1831

Wang F, Xia P, Wu F, *et al.* (2008) *Helicobacter pylori* VacA disrupts apical membrane-cytoskeletal interaction in gastric parietal cells. *J Biol Chem* **283**: 26714-26725

Toxines et Transferts ioniques – Toxins and Ion transfers
Rencontres en Toxinologie – Meeting on Toxinology, 2011
Editions de la SFET – SFET Editions
Accès libre en ligne sur le site – Free access on line on the site : http://www.sfet.asso.fr

Known and unknown mitochondrial targeting signals

Joachim RASSOW

Ruhr-University Bochum, Institute for Physiological Chemistry, Gebaeude MA3, 44780 Bochum, Germany
Tel : +49 (0)234 32 29079 ; Fax : +49 (0)234 32 14266 ; E-mail : joachim.rassow@rub.de

Abstract

About 60% of newly synthesized mitochondrial proteins carry a presequence which acts as a targeting signal. Presequences are positively charged amino-terminal extensions which are cleaved upon import into the organelle. Several computer programs are available for the identification of presequences on the basis of the amino acid sequence. However, the import of all other mitochondrial proteins, about 40%, is independent of a classical presequence. In many cases, the alternative targeting signals are unknown. Correspondingly, it is often difficult to identify a mitochondrial targeting signal in a toxin of obvious mitochondrial localization. Recent work on the Helicobacter pylori *VacA toxin revealed a peculiar mitochondrial targeting signal that had never been observed in any endogenous mitochondrial protein.*

Signaux d'adressage mitochondriaux connus et inconnus

Près de 60% des protéines mitochondriales synthétisées dans le cytoplasme présentent une préséquence qui sert de signal d'adressage. Les préséquences sont des extensions amino-terminales chargées positivement qui sont clivées lors de l'import vers les organites. Il existe de nombreux programmes informatiques permettant d'identifier des préséquences sur la base de leur séquence en acides aminés. Néanmoins, l'import de toutes les autres protéines mitochondriales, environ 40%, est indépendant de toute préséquence classique. Souvent, les signaux d'adressage alternatifs sont inconnus. C'est pour cette raison qu'il est généralement difficile d'identifier le signal d'adressage mitochondrial d'une toxine de localisation mitochondriale évidente. Des travaux récents sur la toxine VacA de Helicobacter pylori *ont révélés un signal d'adressage mitochondrial étonnant qui n'a été observé dans aucune protéine mitochondriale endogène.*

Keywords : *β-barrel proteins, mitochondria, prediction programs, presequence, protein targeting.*

Introduction

An increasing number of toxins and effector proteins is recognized to target mitochondria (Boya *et al*., 2004; Kozjak-Pavlovic *et al*., 2008; Arnoult and Castanier, 2010; Lamkanfi and Dixit, 2010). In all these cases, the question arises if the interaction is specific. An answer is facilitated if a specific mitochondrial targeting signal can be identified in the primary structure of the protein. Several prediction programs are available to detect such targeting signals. Unfortunately, these programs often fail to detect distinct targeting sequences, even if experiments have provided compelling evidence of a mitochondrial location.

In fact, mitochondrial import of authentic cellular proteins is mediated by several different mechanisms and thus dependent on different targeting sequences. The algorithms that are provided in the internet are restricted to the identification of the most abundant type of mitochondrial targeting sequences, the positively charged N-terminal presequence. It is therefore important to consider alternative systems of specific mitochondrial targeting if the intracellular distribution of a protein is investigated.

N-terminal presequences

Human mitochondria contain about 1500 different proteins, but the mitochondrial genome encodes only 13 polypeptides. All other proteins are encoded in the nucleus, synthesized in the cytosol, and eventually imported into the mitochondria. About 60% of these proteins are targeted to the mitochondria by positively charged presequences (Schmidt *et al*., 2010). These are N-terminal extensions of 10-80 amino acid residues with a tendency to form α-helical structures. Under these conditions, the positively charged residues are often concentrated at one side of the helix, with uncharged residues located at the opposing side. Presequences are usually completely devoid of negative charges. Highly conserved motifs of distinct amino acid residues are not contained in these sequences (Allison and Schatz, 1986). However, in some proteins, a single amino acid exchange can be sufficient to inactivate the presequence (Messmer *et al*., 2011). An example of a presequence contained in a bacterial protein is shown in *Figure 1*.

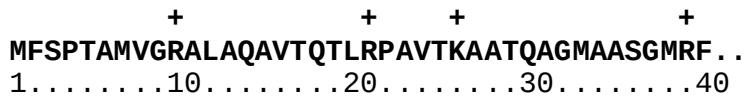

Figure 1. N-terminal presequence of Map, the mitochondria associated protein secreted by EPEC strains. The protein is injected into host cells by a type III secretion system. Inside mitochondria, the protein accumulates in the matrix (Papatheodorou *et al*., 2006).

***Figure 1**. Préséquence N-terminale de Map (*mitochondria associated protein) *sécrétée par les souches EPEC. La protéine est injectée dans la cellule hôte par le système de sécrétion de type III. Dans les mitochondries, la protéine s'accumule dans la matrice (Papatheodorou* et al*., 2006).*

To identify mitochondrial presequences, several excellent prediction programs were developed (Habib *et al*., 2007; Neupert and Herrmann, 2007):

TargetP	http://www.cbs.dtu.dk/services/TargetP/
PSORT II	http://psort.ims.u-tokyo.ac.jp/
MITOPRED	http://bioinformatics.albany.edu/~mitopred/
MitoProt II	http://ihg.gsf.de/ihg/mitoprot.html
Predotar	http://urgi.versailles.inra.fr/predotar/predotar.html

The programs easily detect typical mitochondrial presequences with high probability. Remarkably, most of these proteins are imported into the matrix (*i.e.* the inner compartment of the mitochondria). Presequence-mediated import is probably the only possibility for a protein to enter the matrix compartment. In this pathway, presequences have at least seven different functions:

1. Presequences can increase the solubility of newly synthesized proteins in the cytosol, prior to interactions with the mitochondria (Zara *et al*., 2003).

2. mRNAs encoding mitochondrial proteins have a tendency to accumulate at the surface of mitochondria. Recent data show that ribosomes, together with mRNAs, are recruited to the mitochondrial surface if they synthesize proteins containing N-terminal presequences (Garcia *et al*., 2010).

3. Presequences mediate binding to import receptors (Tom20 and Tom22) that are exposed at the mitochondrial outer surface (Neupert and Herrmann, 2007; Chacinska *et al*., 2009; Endo *et al*., 2011).

4. They mediate an insertion of the preprotein into the general import pore (formed by Tom40, the central component of the outer membrane TOM complex).

5. They interact with receptor structures provided by proteins of the inner membrane (components of the TIM23 complex).

6. Due to their positively charged residues, presequences are pulled into the matrix, driven by the electric potential difference across the mitochondrial inner membrane (the matrix is negatively charged).

7. Inside the matrix, mitochondrial heat shock proteins (mtHsp70) bind to the presequences and mediate the import of the entire protein.

Following translocation across the inner membrane, presequences are no longer required and they are usually quickly cleaved at defined sites (Vögtle *et al*., 2009) and degraded (Falkevall *et al*., 2006). Because of their involvement in the membrane potential-dependent step, presequences are essential in the translocation of proteins across the inner membrane. Some proteins contain structures that prevent a complete translocation of the entire protein. The biogenesis of these proteins is similarly dependent on their presequence, but they accumulate in the inner membrane or in the intermembrane space (Reif *et al*., 2005).

Presequences are often thought to represent the general targeting signal of mitochondrial proteins. However, targeting is only one of several different functions of these sequences. In the case of the rat mitochondrial citrate carrier (CIC), the presequence is even dispensable for targeting. In this protein, the presequence is only required to improve the solubility of the newly synthesized protein (Zara *et al*., 2003). Similarly, in the citrate carrier of the eel, the positive charges of the presequence can be exchanged against negative charges without loss of activity (Zara *et al*., 2007). Moreover, the biogenesis of about 40% of all mitochondrial proteins is completely independent of a presequence (Schmidt *et al*., 2010).

Alternative mitochondrial targeting signals

As presequence-dependent import is characteristic of matrix-targeting, alternative targeting is characteristic of proteins that have their functional location in other mitochondrial compartments. In particular, proteins of the mitochondrial outer membrane and of the intermembrane space are lacking presequences (Neupert and Herrmann, 2007, Chacinska *et al*., 2009):

Tail-anchored proteins. Members of the Bcl-2 family are known to target the outer membrane. Their essential targeting signal is provided by their hydrophobic C-terminus (Motz *et al*., 2003; Rapaport, 2003; Ott *et al*., 2007). The hydrophobic segment is flanked by positive charges and responsible both for targeting and for membrane insertion. Bcl-2 and similar proteins are tail-anchored membrane proteins.

N-terminally anchored proteins. Other outer membrane proteins, such as the major import receptors Tom20 and Tom70, are N-terminally anchored. Similar as with tail-anchored proteins, their targeting is dependent on a hydrophobic transmembrane segment (*Figure 2*; Waizenegger *et al*., 2003; Rapaport, 2003).

```
+                    -++++
MVGRNSAIAAGVCGALFIGYCIYFDRKRRS...
1........10........20........30..
```

Figure 2. N-terminal amino acid sequence of human Tom20 (Hanson *et al*., 1996).

***Figure 2**. Séquence en acides aminés de l'extrémité N-terminale de la protéine humaine Tom 20 (Hanson* et al*., 1996).*

β-barrel proteins. The β-barrel proteins of the mitochondrial outer membrane are of particular interest because both in their structure and in their biogenesis they closely resemble the β-barrel proteins of their bacterial relatives (Dolezal *et al*., 2006; Neupert and Herrmann, 2007; Chacinska *et al*., 2009). Examples of endogenous β-barrel proteins of the mitochondria are Tom40 (the central component of the TOM complex), and porin (an abundant pore-forming protein, often named VDAC). Unfortunately, the structural elements have not yet been identified that determine if a β-barrel protein is imported into mitochondria. In the yeast *Saccharomyces cerevisiae*, any bacterial β-barrel protein seems to be imported into the mitochondria if expressed in the cytosol of intact cells (Walther *et al*., 2009). However, recently published data show that human mitochondria import only a very limited subset of β-barrel proteins (Kozjak-Pavlovic *et al*., 2011). Remarkably, β-barrel proteins do not contain a single defined segment in their amino acid sequence that could act as a mitochondrial targeting signal (Müller *et al*., 2002). The requirements of mitochondrial targeting in human cells were investigated in detail in a study on the pore-forming β-barrel protein PorB of *Neisseria gonorrhoeae*. The results indicated that the mitochondrial protein import machinery does not recognize a specific sequence of the primary structure, but a long part of the protein that has retained the capability to form a distinct tertiary structure (Müller *et al*., 2002). This conclusion was recently confirmed by a study on the expression of the protein YadA from *Yersinia enterocolitica* in yeast (Müller *et al*., 2011). Unfortunately, no algorithm is available to predict mitochondrial targeting of a β-barrel protein.

Intermembrane space proteins. The mitochondrial intermembrane space contains some proteins that are synthesized with a presequence, but most intermembrane space proteins are imported by other mechanisms. Similar as with the outer membrane proteins, it is currently impossible to predict if a protein may belong to this compartment. No intermembrane space targeting signal has been identified. Interestingly, several intermembrane space proteins are imported by a "folded trap mechanism" (Neupert and Herrmann, 2007). The proteins insert into the general import pore (formed by the outer membrane TOM complex) by an unknown mechanism, get transiently exposed to the intermembrane space, and are trapped in this compartment by special means. The polypeptide of cytochrome c interacts with the cytochrome c heme lyase, binds a heme group, and by adopting its native structure, it is trapped inside the mitochondrion (Diekert *et al*., 2001; Neupert and Herrmann, 2007; Giegé *et al*., 2008). A subset of intermembrane space proteins is trapped by redox reactions. These proteins contain two cysteine residues forming a twin Cx_9C motif. The proteins catalysing the redox reactions show obvious similarities to proteins in the periplasmic space of bacteria (Chacinska *et al*., 2009).

Inner membrane metabolite carrier proteins. The mitochondrial inner membrane does not contain any pore-forming proteins because it has to keep the mitochondrial membrane potential $\Delta\Psi$. All exchange of metabolites across this membrane depends on carrier proteins. They are the most abundant proteins of the inner membrane. Import of newly synthesized carrier proteins is dependent on the membrane potential (which is required for protein insertion into the membrane), but the membrane potential-dependent step is independent of any presequence. For a long time, the targeting signals of these proteins have been enigmatic. However, it was shown that the membrane-spanning segments of the carrier proteins, with some assistance by flanking residues, mediate binding to the mitochondria and subsequent translocation across the mitochondrial outer membrane (Curran *et al*., 2002; Chacinsca *et al*., 2009). The carrier proteins constitute a family of about 40 related proteins. The amino acid sequences do not reveal any consensus targeting signal. A mitochondrial location is only indicated by the overall similarity of the proteins. Due to this similarity, it was possible to identify the gene of a metabolite carrier (VMC1) in the genome of the mimivirus (a large DNA virus replicating in *Acanthamoeba polyphaga*; Monné *et al*., 2007).

Known and unknown mitochondrial targeting signals in toxins and effector proteins

While at least 60% of all endogenous mitochondrial proteins are imported with the help of a presequence (Schmidt *et al*., 2010), the abundance of presequences in the proteins of mitochondrial location encoded by pathogenic bacteria and viruses seems to be even lower. Up to now, only a few examples are known (Kozjak-Pavlovic *et al*., 2008). Well established is the function of the N-terminal presequence of the mitochondria associated protein (Map) of enteropathogenic *Escherichia coli* strains (EPEC; Papatheodorou *et al*., 2006). The same bacteria secrete the protein EspF which is similarly targeted by a classical presequence (Papatheodorou *et al*., 2006).

Most toxins and effector proteins are devoid of an obvious mitochondrial targeting signal and their mitochondrial location has to be investigated experimentally: (i) Fusion proteins containing a GFP moiety can be expressed in the cytosol and tested for their distribution in the cell. (ii) The authentic proteins can be expressed in the cytosol, and their distribution can subsequently be monitored by cell fractionation, including the isolation of purified mitochondria. (iii) The proteins can be synthesized in commercially available reticulocyte lysate in the presence of ^{35}S-labelled methionine and tested for import into isolated mitochondria. (iv) If import into isolated yeast mitochondria is possible, mitochondria can be isolated from mutant strains lacking defined components of the mitochondrial import machinery. It is then possible to investigate details of the mitochondrial import pathway (Papatheodorou *et al*., 2007).

In a project on the VacA toxin of *Helicobacter pylori*, we observed that the N-terminal domain of the toxin accumulated in mitochondria if expressed in the cytosol of HeLa cells (Galmiche *et al*., 2000). Unfortunately, the primary structure of the toxin did not reveal any similarity to a mitochondrial protein or to a mitochondrial targeting sequence. In a series of experiments we found that the 32 N-terminal residues of VacA were necessary and sufficient for mitochondrial targeting (Domanska *et al*., 2010). The VacA N-terminus is devoid of any charged residue (*Figure 3*). A targeting signal of this type has never been observed in any endogenous mitochondrial protein: N-terminally anchored proteins (such as Tom20 and Tom70) contain shorter hydrophobic segments, they always contain some positively charged residues, and they are targeted to the mitochondrial outer membrane. The VacA N-terminus differs in its structure, and it directs the toxin to the mitochondrial inner membrane (Domanska *et al*., 2010). Initially it was difficult to reconcile these observations with the fact, that VacA enters host cells by endocytosis and accumulates in endosomes (Boquet *et al*., 2003; Cover and Blanke, 2005). Interestingly, there seems to be a mechanism to transfer VacA from the endosomes to mitochondria, depending on direct contact of both membranes (Gauthier *et al*., 2007; Calore *et al*., 2010). The VacA N-terminus is essential in the transfer of the toxin from the endosomes to the mitochondria (Calore *et al*., 2010). It is tempting to speculate that the 32 residues of the VacA toxin act as a mitochondrial targeting signal, specifically to mediate this transfer between the two different membrane systems (Galmiche and Rassow, 2010).

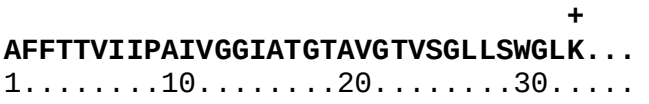

Figure 3. N-terminal amino acid sequence of the *Helicobacter pylori* VacA toxin (Domanska *et al*., 2010).

Figure 3*. Séquence en acides aminés de l'extrémité N-terminale de la toxine VacA d'*Helicobacter pylori *(Domanska et al., 2010).*

Moreover, it is remarkable that the specificity for the transfer of VacA to mitochondria is merely encoded in the length of an unpolar and hydrophobic sequence. In this respect, the situation resembles the targeting system of Kesv, a potassium channel encoded by EsV-1 (a virus isolated from the brown algae *Ectocarpus siliculosus*). Kesv is a small polypeptide of only 124 amino acid residues. The specificity for import into mitochondria is defined by the length of the second of its two membrane-spanning domains (Balss *et al*., 2008).

Conclusion

Mitochondria are an attractive target for pathogens because mitochondria play a central role in the regulation of cell death and survival (Boya *et al*., 2004; Kozjak-Pavlovic *et al*., 2008; Rudel *et al*., 2010; Lamkanfi and Dixit, 2010). Mitochondria can be involved not only in apoptosis, but also in necrotic cell death (Carneiro *et al*., 2009). The proteins that have so far been identified to target mitochondria are extraordinarily heterogenous, and it is difficult to discern common principles of targeting or function. To further elucidate the interactions between virulence factors and mitochondria, it will be necessary to investigate the different systems that determine the specificity of mitochondrial targeting. In these systems, N-terminal presequences appear to be of only minor relevance. To confirm interactions of proteins with mitochondria, it can be misleading to rely on prediction programs, because these programs are usually designed to detect presequences as the only type of targeting signals. Considering alternative systems of targeting may be helpful to identify additional toxins and effector proteins that interact with mitochondria.

Acknowledgements. *Work in the authors laboratory is supported by the Deutsche Forschungsgemeinschaft, grant RA 702/4.*

References

Allison DS, Schatz G (1986) Artificial mitochondrial presequences. *Proc Natl Acad Sci USA* **83**: 9011-9005

Arnoult D, Castanier C (2010) Mitochondrial localization of viral proteins as a means to subvert host defense. *Biochim Biophys Acta* **1831**: 575-583

Balss J, Papatheodorou P, Mehmel M, Baumeister D, Hertel B, Delaroque N, Chatelain FC, Minor DL, van Etten JL, Rassow J, Moroni A, Thiel G (2008) Transmembrane domain length of viral K^+ channels is a signal for mitochondrial targeting. *Proc. Natl. Acad. Sci USA* **105**: 12313-12318

Boya P, Pauleau AL, Poncet D, Gonzalez-Polo RA, Zamzami N, Kroemer G (2004) Viral proteins tarting mitochondria: controlling cell death. *Biochim Biophys Acta* **1659**: 178-189

Calore F, Genisset C, Casellato A, Rossato M, Codolo G, Esposti MD, Scorrano L, de Bernard M (2010) Endosome-mitochondria juxtaposition during apoptosis induced by *H. pylori* VacA. *Cell Death Differ* **17**: 1707-1716

Carneiro LA, Travassos LH, Soares F, Tattoli I, Magalhaes JG, Bozza MT, Plotkowski MC, Sansonetti PJ, Molkentin JD, Philpott DJ, Girardin SE (2009) Shigella induces mitochondrial dysfuntion and cell death in nonmyeloid cells. *Cell Host Microbe* **5**: 123-136

Chacinska A, Koehler CM, Milenkovic D, Lithgow T, Pfanner N (2009) Importing mitochondrial proteins: machineries and mechanisms. *Cell* **138**: 628-644

Cover TL, Blanke SR (2005) *Helicobacter pylori* VacA, a paradigm for toxin multifunctionality. *Nat Rev Microbiol* **3**: 320-332

Curran SP, Leuenberger D, Oppliger W, Koehler CM (2002) The Tim9p-Tim10p complex binds to the transmembrane domains of the ADP/ATP carrier. *EMBO J* **21**: 942-953

Diekert K, de Kroon AI, Ahting U, Niggemeyer B, Neupert W, de Kruijff B, Lill R (2001) Apocytochrome c requires the TOM complex for translocation across the mitochondrial outer membrane. *EMBO J* **20**: 5626-5635

Dolezal P, Likic V, Tachezy J, Lithgow T (2006) Evolution of the molecular machines for protein import into mitochondria. *Science* **313**: 314-318

Domanska G, Motz C, Meinecke M, Harsman A, Papatheodorou P, Reljic B, Dian-Lothrop EA, Galmiche A, Kepp O, Becker L, Günnewig K, Wagner R, Rassow J (2010) *Helicobacter pylori* VacA toxin/subunit p34: targeting of an anion channel to the inner mitochondrial membrane. *PLoS Pathog* **6**: e1000878

Endo T, Yamano K, Kawano S (2011) Structural insight into the mitochondrial protein import system. *Biochim Biophys Acta* **1808**: 955-970

Falkevall A, Alikhani N, Bhushan S, Pavlov PF, Busch K, Johnson KA, Eneqvist T, Tjernberg L, Ankarcrona M, Glaser E (2006) Degradation of the amyloid β-protein by the novel mitochondrial peptidasome, PreP. *J Biol Chem* **281**: 29096-29104

Galmiche A, Rassow J, Doye A, Cagnol S, Contamin S, de Thillot V, Just I, Ricci V, Solcia E, Boquet P (2000) The N-terminal 34 kDa fragment of *Helicobacter pylori* vacuolating cytotoxin targets mitochondria and induces cytochrome c release. *EMBO J* **19**: 6361-6370

Galmiche A, Rassow J (2010) Targeting of *Helicobacter pylori* VacA to mitochondria. *Gut Microbes* **1**: 392-395

Garcia M, Delaveau T, Goussard S, Jacq C (2010) Mitochondrial presequences and open reading frame mediate asymmetric localization od messenger RNA. *EMBO reports* **11**: 285-291

Gauthier NC, Monzo P, Gonzalez T, Doye A, Oldani A, Gounon P, Ricci V, Cormont M, Boquet P (2007) Early endosomes associated with dynamic F-actin structures are required for late trafficking of *H. pylori* VacA toxin. *J Cell Biol* **177**: 343-354

Giegé P, Grienenberger JM, Bonnard G (2008) Cytochrome c biogenesis in mitochondria. *Mitochondrion* **8**: 61-73

Habib SJ, Neupert W, Rapaport D (2007) Analysis and prediction of mitochondrial targeting signals. *Methods Cell Biol* **80**: 761-781

Hanson B, Nuttall S, Hoogenraad N (1996) A receptor for the import of proteins into human mitochondria. *Eur J Biochem* **235**: 750-753

Kozjak-Pavlovic V, Ross K, Rudel T (2008) Import of bacterial pathogenicity factors into mitochondria. *Curr Opin Microbiol* **11**: 1-6

Kozjak-Pavlovic V, Ott C, Götz M, Rudel T (2011) Neisserial Omp85 protein is selectively recognized and assembled into functional complexes in the outer membrane of human mitochondria. *J Biol Chem* **286**: 27019-27026

Lamkanfi M, Dixit VM (2010) Manipulation of host cell death pathways during microbial infections. *Cell Host Microbe* **8**: 44-54

Messmer M, Florentz C, Schwenzer H, Scheper GC, van der Knaap MS, Maréchal-Drouard L, Sissler M (2011) A human pathology-related mutation prevents import of an aminoacyl-tRNA synthetase into mitochondria. *Biochem J* **433**: 441-446

Monné M, Robinson AJ, Boes C, Harbour ME, Fearnley IM, Kunji ERS (2007) The mimivirus genome encodes a mitochondrial carrier that transports dATP and dTTP. *J Biol Chem* **81**: 3181-3186

Motz C, Martin H, Krimmer T, Rassow J (2003) Bcl-2 and porin follow different pathways of TOM-dependent insertion into the mitochondrial outer membrane. *J Mol Biol* **323**: 729-738

Müller A, Rassow J, Grimm J, Machuy N, Meyer TF, Rudel T (2002) VDAC and the bacterial porin PorB of *Neisseria gonorrhoeae* share mitochondrial import pathways. *EMBO J* **21**: 1916-1929

Müller JEN, Papic D, Ulrich T, Grin I, Schütz M, Oberhettinger P, Tommassen J, Linke D, Dimmer KS, Autenrieth IB, Rapaport D (2011) Mitochondria can recognize and assemble fragments of a β-barrel structure. *Mol Biol Cell* **22**: 1638-1647

Neupert W, Herrmann JM (2007) Translocation of proteins into mitochondria. *Annu Rev Biochem* **76**: 723-749

Rapaport D (2003) Finding the right organelle. Targeting signals in mitochondrial outer-membrane proteins. *EMBO reports* **4**: 948-952

Ott M, Norberg E, Walter KM, Schreiner P, Kemper C, Rapaport D, Zhivotovsky B, Orrenius S (2007) The mitochondrial TOM complex is required for tBid/Bax-induced cytochrome c release. J Biol Chem 282: 27633-27639

Papatheodorou P, Domanska G, Öxle M, Mathieu J, Selchow O, Kenny B, Rassow J (2006) The enteropathogenic *E. coli* (EPEC) Map effector is imported into the mitochondrial matrix by the TOM/Hsp70 system and alters organelle morphology. *Cell* Microbiol **8**: 677-689

Papatheodorou P, Domanska G, Rassow J (2007) Protein targeting to mitochondria of *Saccharomyces cerevisiae* and *Neurospora crassa*. In: Protein Targeting Protocols: Second Edition, van der Giezen M (ed), Humana Press inc. Totowa, NJ, Methods in Molecular Biology 390: 151-166

Boquet P, Ricci A, Galmiche A, Gauthier NC (2003) Gastric cell apoptosis and *H. pylori*: has the main function of VacA finally been identified? *Trends Microbiol* **11**: 410-413

Reif S, Randelj O, Domanska G, Dian E, Krimmer T, Motz C, Rassow J (2005) Conserved mechanism of Oxa1p insertion into the mitochondrial inner membrane. *J Mol Biol* **354**: 520-528

Rudel T, Kepp O, Kozjak-Pavlovic V (2010) Interactions between bacterial pathogens and mitochondrial cell death pathways. *Nat Rev Microbiol* **8**: 693-705

Schmidt O, Pfanner N, Meisinger C (2010) Mitochondrial protein import: from proteomics to functional mechanisms. *Nat Rev Mol Cell Biol* **11**: 655-667

Vögtle F-N, Wortelkamp S, Zahedi R, Becker D, Leidhold C, Gevaert K, Kellermann J, Voos W, Sickmann A, Pfanner N, Meisinger C (2009) Global analysis of the mitochondrial N-proteome identifies a processing peptidase critical for protein stability. *Cell* **139**: 428-439

Waizenegger T, Stan T, Neupert W, Rapaport D (2003) Siganl-anchored domains of proteins of the outer membrane of mitochondria - Structural and functional characteristics. *J Biol Chem* **278**: 42064-42071

Zara V, Ferramosca A, Palmisano I, Palmieri F, Rassow J (2003) Biogenesis of rat mitochondrial citrate carrier (CIC): The N-terminal presequence facilitates the solubility of the preprotein but does not act as a targeting signal. *J Mol Biol* **325**: 399-408

Zara V, Dolce V, Capobianco L, Ferramosca A, Papatheodorou P, Rassow J, Palmieri F (2007) Biogenesis of eel liver citrate carrier (CIC): ngeative charges can substitute for positive charges in the presequence. *J Mol Biol* **365**: 958-967

Toxines et Transferts ioniques – Toxins and Ion transfers
Rencontres en Toxinologie – Meeting on Toxinology, 2011
Editions de la SFET – SFET Editions
Accès libre en ligne sur le site – Free access on line on the site : http://www.sfet.asso.fr

Clostridium perfringens *epsilon toxin : a fascinating toxin*

Michel R. POPOFF

Institut Pasteur, Unité des Bactéries anaérobies et Toxines, 25 rue du Dr Roux, 75724 Paris cedex15, France
Tel : +33 1 4568307 ; E-mail : mpopoff@pasteur.fr

Abstract

Epsilon toxin (ETX) is produced by strains of Clostridium perfringens *classified as type B or D. ETX belongs to the heptameric β-pore-forming toxins including aerolysin and* C. septicum *alpha toxin, which are characterized by the formation of a pore through the plasma membrane of eukaryotic cells consisting in a β-barrel of 14 amphipatic β-strands. In contrast to aerolysin and* C. septicum *alpha toxin, ETX is a much more potent toxin, which is responsible for enterotoxemia in animals, mainly in sheep. ETX induces perivascular edema in various tissues and accumulates particularly in the kidneys and in the brain, where it causes edema and necrotic lesions. ETX is able to pass through the blood brain barrier and to stimulate the release of glutamate, which accounts for the nervous excitation symptoms observed in animal enterotoxemia. At the cellular level, ETX causes a rapid swelling followed by a cell death involving necrosis. The precise mode of action of ETX remains to be determined. Therefore, ETX is a powerful toxin. However, it also represents a unique tool to vehicle drugs into the central nervous system or to target glutamatergic neurons.*

Toxine epsilon de Clostridium perfringens *: une toxine fascinante*

La toxine epsilon (ETX) est produite par les souches de Clostridium perfringens *classées en type B ou D. ETX appartient à la famille des toxines qui forment des pores heptamériques comprenant l'aérolysine et la toxine alpha de* C. septicum*. Ces toxines se caractérisent par la formation de pores à travers la membrane plasmique des cellules eucaryotes qui consistent en une structure en tonneau comprenant 14 feuillets β amphipatiques. Contrairement à l'aérolysine et à la toxine alpha de* C. septicum*, ETX est une toxine beaucoup plus puissante. Elle est responsable d'entérotoxémie chez les animaux, principalement les ovins. ETX induit des oedèmes périvasculaires dans divers tissus et s'accumule particulièrement dans les reins et le cerveau où elle provoque une libération de glutamate à l'origine des signes nerveux d'excitation observés au cours de l'entérotoxémie. Au niveau cellulaire, ETX induit des effets rapides de gonflement suivis d'une mort par nécrose. Le mode précis d'action d'ETX reste à déterminer. ETX est une puissante toxine qui représente un outil unique pour véhiculer des composés thérapeutique au système nerveux central et cibler les neurones glutamatergiques.*

Keywords : *Aerolysin, cell necrosis,* Clostridium perfringens*, C. septicum alpha toxin, epsilon toxin, pore-forming toxin.*

Introduction

Clostridium perfringens is a Gram positive, rod-shaped, anaerobic and sporulating bacterium which produces the largest number of toxins compared to other bacteria. It is a proteolytic and glucidolytic *Clostridium* which grows rapidly in complex medium. According to the main lethal toxins (alpha, beta, epsilon, and iota toxins), *C. perfringens* is divided into 5 toxinotypes (A to E). Epsilon toxin (ETX) is synthesized by toxinotypes B and D. However, the high diversity of toxin combinations, which can be produced by *C. perfringens* strains, makes more complex the classification in 5 toxinotypes (Petit *et al.*, 1999).

Based on the toxins produced, *C. perfringens* is responsible for diverse pathologies in man and animals, resulting from a gastro-intestinal or wound contamination and including food poisoning, enteritis, necrotic enteritis, enterotoxemia, gangrene, and puerperal septicemia. Toxinotype B is the causative agent of lamb dysenteria which is only found in some countries like the UK, whereas toxinotype D is responsible for a fatal, economically important disease of sheep worldwide, called enterotoxemia. ETX contributes with beta toxin to the pathogenesis of toxinotype B, and it is the causative virulence factor of all symptoms and lesions due to toxinotype D. ETX is one of the most potent toxins known. Its lethal activity ranges just below the botulinm neurotoxins. Indeed, the lethal dose by intraperitoneal injection in mice is 1.2 ng/kg for botulinum neurotoxin A and 70 ng/kg for ETX (Gill, 1987; Minami *et al.*, 1997). For this reason, ETX is considered as a potential biological weapon classified as biological agent of the category B, although very few ETX-mediated natural

disease has been reported in humans (Mantis, 2005). ETX belongs to the family of aerolysin pore-forming toxins. However, its precise mode of action accounting for its high potency remains to be defined (Knapp *et al.*, 2010b).

ETX structure

At the amino acid sequence level, ETX shows some homology with the *Bacillus sphaericus* mosquitocidal toxins Mtx2 and Mtx3, with 26 and 23% sequence identity, respectively (Hunter *et al.*, 1992). Mtx2 and Mtx3 are toxins specific of mosquito larvae, which are activated by proteolytic cleavage and which probably act by pore formation (Phannachet *et al.*, 2011). In addition, a hypothetical protein encoded by a gene located in the vicinity of the C2 toxin genes on a large plasmid in *C. botulinum* type D shows a sequence similarity with that of ETX (Sakaguchi *et al.*, 2009).

ETX retains an elongated form and contains three domains, which are mainly composed of β-sheets (Cole *et al.*, 2004). Despite poor sequence identity (14%), the ETX overall structure is significantly related to that of the pore forming toxin aerolysin produced by *Aeromonas* species (Gurcel *et al.*, 2006; Parker *et al.*, 1994), and to the model of alpha-toxin from *Clostridium septicum*, an agent of gangrene (Melton *et al.*, 2004). However, ETX is a much more potent toxin with a 100 times more lethal activity in mouse, than aerolysin and *C. septicum* alpha-toxin (Gurcel *et al.*, 2006; Minami *et al.*, 1997; Tweten, 2001). The main difference between toxins is that the aerolysin domain I, which is involved in initial toxin interaction with cells, is missing in ETX. Domain 1 of ETX consists in a large α-helix followed by a loop and three short α-helices and is similar to domain 2 of aerolysin which interacts with the glucosyl phosphatidylinositol (GPI) anchors of proteins. This domain of ETX could have a similar function of binding to receptor. A cluster of aromatic residues (Tyr49, Tyr43, Tyr42, Tyr209, and Phe212) in ETX domain 1 could be involved in receptor binding (Cole *et al.*, 2004). Domain 2 is a β-sandwich structurally related to domain 3 of aerolysin. This domain contains a two-stranded sheet with an amphipatic sequence predicted to be the channel-forming domain (see below). In contrast to the cholesterol-dependent cytolysins, only one amphipathic β–hairpin from each monomer is involved in the pore structure of ETX and other heptameric β-pore-forming toxins (β-PFTs) like aerolysin. Domain 3 is also a β-sandwich analogous to domain 4 of aerolysin and contains the cleavage site for toxin activation. Domain 3, after removing of the C-terminus, is likely involved in monomer-monomer interaction required for oligomerization (Cole *et al.*, 2004; Knapp *et al.*, 2010b).

The pore-forming domain has been identified in domain 2. The segment His151-Ala181 contains alternate hydrophobic-hydrophilic residues, which are characteristic of membrane-spanning β-hairpins, and forms two amphipatic β-strands on ETX structure. Site-directed mutagenesis confirmed that this segment is involved in ETX channel activity in lipid bilayers (Knapp *et al.*, 2009). Interestingly, the ETX pore-forming domain shows higher sequence similarity to those of the binding components (Ib, C2-II, CDTb, CSTb) of clostridial binary toxins [iota toxin, C2 toxin, *C. difficile* transferase (CDT), *C. spiroforme* toxin (CST), respectively], and to a lesser extent to *B. anthracis* protective antigen (PA, the binding component of anthrax toxins), than with that of aerolysin. However, the ETX segment Lys162 to Glu169, which is exposed to the transmembrane side of the channel and forms the loop linking the two β-strands forming the transmembrane β-hairpin, is unrelated at the amino acid sequence level to those of other β-PFTs. The ETX loop is flanked by two charged residues, Lys-162 and Glu-169, and contains a proline in the central part, similarly to the sequence of the corresponding aerolysin loop. Binding components share a similar structure organization with that of β-pore-forming toxins and notably contain an amphipathic flexible loop that forms a β-hairpin, playing a central role in pore formation (Geny and Popoff, 2006; Schleberger *et al.*, 2006). This suggests that binding components and β-PFTs have evolved from a common ancestor. However, β-PFTs have acquired a specific function consisting in the translocation of the corresponding enzymatic components of binary toxins through the membrane of endosomes at acidic pH. In contrast, β-PFTs such as ETX and aerolysin can form pores in plasma membrane at neutral pH, which are responsible for cytotoxicity.

Essential amino acids for the lethal activity have been identified by biochemistry and mutagenesis. A previous work with chemical modifications shows that His residues are required for the active site, and Trp and Tyr residues are necessary for the binding to target cells (Sakurai, 1995). The molecule contains a unique Trp and two His. Amino acid substitutions showed that His106 is important for the biological activity, whereas His149 and Trp190 probably are involved to maintain the structure of ETX but are not essential for the activity (Oyston *et al.*, 1998).

Molecular and cellular mechanism of action

Specific activity of ETX is also observed in cultured cells. Only very few cell lines including renal cell lines from various species such as Madin-Darby canine kidney (MDCK), mouse kidney cortical collecting duct ($mpkCCD_{cl4}$), and to a lesser extent the human leiomyoblastoma (G-402) cells are sensitive to ETX (Payne *et al.*, 1994; Shortt *et al.*, 2000). Surprisingly, kidney cell lines from ETX-susceptible animal species like lamb and cattle, are ETX resistant suggesting that the ETX receptor in primary cells is lost in cultured cell lines (Payne *et al.*, 1994 and unpublished data).

A marked swelling is observed in the first phase of intoxication, followed by mitochondria disappearance, blebbing and membrane disruption. The cytotoxicity can be monitored by using an indicator of lysosomal integrity (neutral red) or mitochondrial integrity [3-(4,5-dimethylthiazol-2-yl)-2,5-diphenyltetrazolium bromide MTT] (Borrmann *et al.*, 2001; Heine *et al.*, 2008; Lindsay *et al.*, 1995; Payne *et al.*, 1994; Petit *et al.*, 1997; Shortt *et al.*, 2000).

ETX binds to MDCK cell surface, preferentially to the apical site, and recognizes a specific membrane receptor which is not present in insensitive cells. Binding of the toxin to its receptor leads to the formation of large membrane complexes which are very stable when the incubation is performed at 37°C. In contrast, the complexes formed at 4°C are dissociated by sodium dodecyl sulfate (SDS) and heating. This suggests a maturation process like a prepore and then a functional pore formation. Endocytosis and internalization of the toxin into the cell were not observed, and the toxin remains associated to the cell membrane throughout the intoxication process (Petit *et al.*, 1997). The ETX large membrane complex in MDCK cells and synaptosomes correspond to the heptamerization of toxin molecules within the membrane and pore formation (Miyata *et al.*, 2001; Miyata *et al.*, 2002; Petit *et al.*, 1997). ETX prototoxin is able to bind to sensitive cells but does not oligomerize, in contrast to activated ETX. Thus, the 23 C-terminal residues of the prototoxin control the toxin activity by preventing the heptamerization. These amino acids are removed in the active toxin molecule (Miyata *et al.*, 2001).

ETX binding to susceptible cells or synaptosomes and subsequent complex formation are prevented by protease treatment but not or weakly by phospholipase C, glycosidases or neuraminidase, indicating a protein nature of ETX receptor (Dorca-Arevalo *et al.*, 2008; Nagahama and Sakurai, 1992; Payne *et al.*, 1997; Petit *et al.*, 1997). ETX receptor could be related to a 34 or 46 kDa protein or glycoprotein in MDCK cells (Payne *et al.*, 1997; Petit *et al.*, 1997) and to a 26 kDa sialyglycoprotein in rat brain (Nagahama and Sakurai, 1992). Hepatitis A virus cellular receptor 1 (HAVCR1) has been identified to facilitate ETX cytotoxicity in MDCK cells and the human kidney cell line ACHN. ETX binds to HAVCR1 *in vitro* (Ivie *et al.*, 2011). However, it is not yet clear whether HAVCR1 is a functional ETX receptor. Moreover, although ETX does not directly interact with a lipid, the lipid environment of ETX receptor is critical for the binding of ETX to cell surface, since detergent treatment prevents ETX binding to the cell surface (Payne *et al.*, 1997; Petit *et al.*, 1997). It is noteworthy that ETX can interact with artificial lipid bilayers and form functional channels, without the requirement of a specific receptor in contrast to cell membrane, albeit less efficiently compared to MDCK cells. Lipid bilayers have smooth surfaces without any surface structure including the surface-exposed carbohydrates and proteins of biological membranes, which means that the toxins can interact with the hydrocarbon core of the lipid bilayer and can insert without the help of receptors, whereas receptors are required to promote such an interaction in cell membrane (Petit *et al.*, 2001).

In synaptosomes and MDCK cells, the ETX receptor has been localized in lipid raft microdomains, which are enriched in certain lipids such as cholesterol and sphingolipids as well as in certain proteins like GPI-anchored proteins, suggesting that such a protein could be an ETX receptor (Chassin *et al.*, 2007; Miyata *et al.*, 2002). However, in contrast to aerolysin and *C. septicum* alpha-toxin, ETX does not interact with a GPI-anchored protein as receptor, since phosphatidylinositol-specific phospholipase C did not impair binding or ETX complex formation (Chassin *et al.*, 2007). Localization of ETX receptor in lipid microdomains is further supported by the fact that ETX prototoxin and active form bind preferentially to detergent-resistant membrane fractions (DRM) and only activated ETX forms heptamers in DRM (Miyata *et al.*, 2002). In addition, membrane cholesterol removal with methyl-beta-cyclodextrin (MβCD) impairs ETX binding and pore formation (Chassin *et al.*, 2007; Lonchamp *et al.*, 2011; Miyata *et al.*, 2002). The composition of lipid rafts in sphingomyelin and gangliosides, as well as membrane fluidity, influence ETX binding to sensitive cells, heptamerization, and cytotoxicity (Nagahama *et al.*, 2006; Shimamoto *et al.*, 2005). Thus, inhibitors of sphingolipid or glycosphingolipid synthesis increase cell susceptibility to ETX, whereas inhibitors of sphingomyelin synthesis or addition of monosialotetrahexosylganglioside (GM1) dramatically decreases ETX binding and subsequent heptamerization (Shimamoto *et al.*, 2005). Moreover, phosphatidylcholine (PC) molecules, which increase membrane fluidity, facilitate ETX binding and assembly (Nagahama *et al.*, 2006). ETX bound to its receptor shows a confined mobility on cell membrane probably permitting interaction between ETX monomers and subsequent oligomerization (Masson *et al.*, 2009). Local lipid composition and membrane fluidity likely control ETX bound to receptor in cell membrane. In addition, lipids such as diacylglycerol and phosphatidyl ethanolamine, which induce a negative membrane curvature, increase ETX pore formation in liposome, whereas lipids having an opposite effect like lyso-PC, impair ETX activity (Nagahama *et al.*, 2006). This is consistent with the model of a ETX prepore formation and subsequent insertion into the membrane to form a functional channel. The structure of ETX pore has been defined as a cone shape (Nestorovich *et al.*, 2011), and thus its insertion in lipid bilayer might be favored by a specific lipid membrane organization. Therefore, although ETX does not directly bind to a lipid receptor, the lipid composition and physical properties of membrane influence ETX access to the receptor, ETX monomer assembly and insertion of ETX pore in membrane.

The cytotoxicity is associated to a rapid loss of intracellular K^+, and an increase in Cl^- and Na^+, whereas an increase in Ca^{++} occurs later. In addition, the loss of viability also correlates with the entry of propidium iodide, indicating that ETX forms large pores in cell membrane. Pore formation is evident in artificial lipid bilayer. ETX induces water-filled channels permeable to hydrophilic solutes up to a molecular mass of 1 kDa, which represent general diffusion pores slightly selective for anions (Petit *et al.*, 2001). In polarized MDCK cells, ETX induces a rapid and dramatic increase in permeability. Pore formation in the cell membrane is likely responsible for the permeability change of cell monolayers. Actin cytoskeleton and organization of tight and adherens junctions are not altered, and the paracellular permeability to macromolecules is not significantly increased upon ETX treatment (Chassin *et al.*, 2007; Petit *et al.*, 2003). ETX causes a rapid cell death by necrosis, characterized by a marked reduction in nucleus size without DNA fragmentation. Toxin-dependent cell signaling leading to cell necrosis is not yet fully understood and includes ATP depletion, AMP-activated protein kinase stimulation, mitochondrial membrane permeabilization, and mitochondrial-nuclear translocation of apoptosis-inducing factor, which is a potent caspase-independent cell death factor (Chassin *et al.*, 2007). The early and

rapid loss of intracellular K^+ induced by ETX, and also by *C. septicum* alpha toxin, seems to be the early event leading to cell necrosis (Knapp *et al.*, 2010a). It is intriguing that ETX, which has a pore-forming activity related to that of aerolysin and *C. septicum* alpha toxin, is much more active. Does ETX induce a specific intracellular signal responsible for a rapid cell death? MβCD, which prevents ETX pore formation in lipid rafts, does not inhibit the sudden decrease in cellular ATP and cell necrosis (Chassin *et al.*, 2007). A subset of ETX channels unaffected by MβCD might be sufficient to trigger an intracellular signal leading to cell necrosis, excluding the requirement of a large diffusion pore to induce the intracellular toxic program. Therefore, ETX is a very potent toxin which alters the permeability of cell monolayers such as epithelium and endothelium, causing edema and cell death. However, its precise mode of action remains unclear.

Conclusion

ETX belongs to the heptameric β-PFTs family including aerolysin and *C. septicum* alpha toxin which are characterized by the formation of a pore consisting in a β-barrel resulting from the arrangement of 14 amphipatic β-strands (Knapp *et al.*, 2010b). Although these toxins share a similar mechanism of pore formation, ETX is much more potent than aerolysin and *C. septicum* alpha toxin. A main difference is that aerolysin and *C. septicum* alpha toxin recognizes GPI-anchored proteins as receptors, whereas ETX receptor, although localized in lipid rafts, is distinct from GPI-anchored proteins and is distributed in a limited number of cell types. The specific ETX receptor possibly accounts for the high potency of ETX, which also might be dependent of a specific intracellular signaling induced by the toxin. Another particularity of ETX, compared to the other β-PFTs, is its ability to cross the blood brain barrier, likely mediated by the interaction with its specific receptor. ETX can be considered as a neurotoxin since it targets specific neurons which are glutamatergic neurons. In contrast to the other bacterial neurotoxins which inhibit the release of neurotransmitter, ETX has an opposite effect by stimulating the release of glutamate and also acts on other non-neuronal cells. This opens the door to design ETX molecules as delivery system to address compounds into the central nervous system. Thereby, ETX has been used to facilitate the transport of the drug, bleomycin, through the blood brain barrier for the treatment of experimental malignant brain tumor in mice (Hirschberg *et al.*, 2009). Whether ETX is a powerful toxin, which requires a medical vigilance for the prevention of animals, this toxin also represents a unique tool to vehicle drugs in the central nervous system and/or to target glutamatergic neurons.

References

Borrmann E, Günther H, Köhler H (2001) Effect of *Clostridium perfringens* epsilon toxin on MDCK cells. *FEMS Immunol Med Microbiol* **31**: 85-92

Chassin C, Bens M, de Barry J, Courjaret R, Bossu, JL, Cluzeaud F, Ben Mkaddem S, Gibert M, Poulain B, Popoff MR, Vandewalle A (2007) Pore-forming epsilon toxin causes membrane permeabilization and rapid ATP depletion-mediated cell death in renal collecting duct cells. *Am J Physiol Renal Physiol* **293**: F927-937

Cole AR, Gibert M, Popoff MR, Moss DS, Titball RW, Basak A (2004) *Clostridium perfringens* ε-toxin shows structural similarity to the pore-forming toxin aerolysin. *Nat Struct Mol Biol* **11**: 797-798

Dorca-Arevalo J, Soler-Jover A, Gibert M, Popoff MR, Martin-Satue M, Blasi J (2008) Binding of epsilon-toxin from *Clostridium perfringens* in the nervous system. *Vet Microbiol* **131**: 14-25

Geny B, Popoff MR (2006) Bacterial protein toxins and lipids: pore formation or toxin entry into cells. *Biol Cell* **98**: 667-678

Gill DM (1987) Bacterial toxins: lethal amounts. In *Toxins and Enzymes*. Laskin AI, Lechevalier HA (eds) Vol 8, pp 127-135. CRC Press, Cleveland

Gurcel L, Iacovache I, van der Goot FG (2006) Aerolysin and related *Aeromonas* toxins. In *The Source Book of Bacterial Protein Toxins*. Alouf JE, Popoff MR (eds) Vol in press, pp 606-620. Elsevier, Academic Press, Amsterdam

Heine K, Pust S, Enzenmuller S, Barth H (2008) ADP-ribosylation of actin by the *Clostridium botulinum* C2 toxin in mammalian cells results in delayed caspase-dependent apoptotic cell death. *Infect Immun* **76**: 4600-4608

Hirschberg H, Zhang MJ, Gach HM, Uzal FA, Peng Q, Sun CH, Chighvinadze D, Madsen SJ (2009) Targeted delivery of bleomycin to the brain using photo-chemical internalization of *Clostridium perfringens* epsilon prototoxin. *J Neurooncol* **95**: 317-329

Hunter SE, Clarke IN, Kelly DC, Titball RW (1992) Cloning and nucleotide sequencing of the *Clostridium perfringens* epsilon-toxin gene and its expression in *Escherichia coli*. *Infect Immun* **60**: 102-110

Ivie SE, Fennessey CM, Sheng J, Rubin DH, McClain MS (2011) Gene-trap mutagenesis identifies mammalian genes contributing to intoxication by *Clostridium perfringens* epsilon-toxin *PLoS One* **6**: e17787

Knapp O, Maier E, Benz R, Geny B, Popoff MR (2009) Identification of the channel-forming domain of *Clostridium perfringens* Epsilon-toxin (ETX). *Biochim Biophys Acta* **1788**: 2584-2593

Knapp O, Maier E, Mkaddem SB, Benz R, Bens M, Chenal A, Geny B, Vandewalle A, Popoff MR (2010a) *Clostridium septicum* alpha-toxin forms pores and induces rapid cell necrosis. *Toxicon* **55**: 61-72

Knapp O, Stiles BG, Popoff MR (2010b) The aerolysin-like toxin family of cytolytic, pore-forming toxins. *Open Toxinol J* **3**: 53-68

Lindsay CD, Hambrook JL, Upshall DG (1995) Examination of toxicity of *Clostridium perfringens* ε-toxin in the MDCK cell line. *Toxic In Vitro* **9**: 213-218

Lonchamp E, Dupont JL, Wioland L, Courjaret R, Mbebi-Liegeois C, Jover E, Doussau F, Popoff MR, Bossu JL, de Barry J, Poulain B (2011) *Clostridium perfringens* epsilon toxin targets granule cells in the mouse cerebellum and stimulates glutamate release. *PLoS One* **5**: e13046

Mantis NJ (2005) Vaccines against the category B toxins: Staphylococcal enterotoxin B, epsilon toxin and ricin. *Adv Drug Deliv Rev* **57**: 1424-1439

Masson JB, Casanova D, Turkcan S, Voisinne G, Popoff MR, Vergassola M, Alexandrou A (2009) Inferring maps of forces inside cell membrane microdomains. *Phys Rev Lett* **102**: 048103

Melton JA, Parker MW, Rossjohn J, Buckley JT, Tweten RK (2004) The identification and structure of the membrane-spanning domain of the *Clostridium septicum* alpha toxin. *J Biol Chem* **279**: 14315-14322

Minami J, Katayama S, Matsushita O, Matsushita C, Okabe A (1997) Lambda-toxin of *Clostridium perfringens* activates the precursor of epsilon-toxin by releasing its N- and C-terminal peptides. *Microbiol Immunol* **41**: 527-535

Miyata S, Matsushita O, Minami J, Katayama S, Shimamoto S, Okabe A (2001) Cleavage of C-terminal peptide is essential for heptamerization of *Clostridium perfringens* ε-toxin in the synaptosomal membrane. *J Biol Chem* **276**: 13778-13783

Miyata S, Minami J, Tamai E, Matsushita O, Shimamoto S, Okabe A (2002) *Clostridium perfringens* ε-toxin forms a heptameric pore within the detergent-insoluble microdomains of Madin-Darby Canine Kidney Cells and rat synaptosomes. *J Biol Chem* **277**: 39463-39468

Nagahama M, Hara H, Fernandez-Miyakawa M, Itohayashi Y, Sakurai J (2006) Oligomerization of *Clostridium perfringens* epsilon-toxin is dependent upon membrane fluidity in liposomes. *Biochemistry* **45**: 296-302

Nagahama M, Sakurai J (1992) High-affinity binding of *Clostridium perfringens* epsilon-toxin to rat brain. *Infect Immun* **60**: 1237-1240

Nestorovich EM, Karginov VA, Bezrukov SM (2011) Polymer partitioning and ion selectivity suggest asymmetrical shape for the membrane pore formed by epsilon toxin. *Biophys J* **99**: 782-789

Oyston PCF, Payne DW, Havard HL, Williamson ED, Titball RW (1998) Production of a non-toxic site-directed mutant of *Clostridium perfringens* e-toxin which induces protective immunity in mice. *Microbiol* **144**: 333-341

Parker MW, Buckley JT, Postma JP, Tucker AD, Leonard K, Pattus F, Tsernoglou D (1994) Structure of the Aeromonas toxin proaerolysin in its water-soluble and membrane-channel states. *Nature* **367**: 292-295

Payne D, Williamson ED, Titball RW (1997) The *Clostridium perfringens* epsilon-toxin. *Rev Med Microbiol* **8**: S28-S30

Payne DW, Williamson ED, Havard H, Modi N, Brown J (1994) Evaluation of a new cytotoxicity assay for *Clostridium perfringens* type D epsilon toxin. *FEMS Microbiol Lett* **116**: 161-168

Petit L, Gibert M, Gillet D, Laurent-Winter C, Boquet P, Popoff MR (1997) *Clostridium perfringens* epsilon-toxin acts on MDCK cells by forming a large membrane complex. *J Bacteriol* **179**: 6480-6487

Petit L, Gibert M, Gourch A, Bens M, Vandewalle A, Popoff MR (2003) *Clostridium perfringens* Epsilon Toxin rapidly decreases membrane barrier permeability of polarized MDCK Cells. *Cell Microbiol* **5**: 155-164

Petit L, Gibert M, Popoff MR (1999) *Clostridium perfringens*: toxinotype and genotype. *Trends Microbiol* **7**: 104-110

Petit L, Maier E, Gibert M, Popoff MR, Benz R (2001) *Clostridium perfringens* epsilon-toxin induces a rapid change in cell membrane permeability to ions and forms channels in artificial lipid bilayers. *J Biol Chem* **276**: 15736-15740

Phannachet K, Raksat P, Limvuttegrijeerat T, Promdonkoy B (2011) Production and characterization of N- and C-terminally truncated Mtx2: a mosquitocidal toxin from Bacillus sphaericus. *Curr Microbiol* **61**: 549-553

Sakaguchi Y, Hayashi T, Yamamoto Y, Nakayama K, Zhang K, Ma S, Arimitsu H, Oguma K (2009) Molecular analysis of an extrachromosomal element containing the C2 toxin gene discovered in *Clostridium botulinum* type C. *J Bacteriol* **191**: 3282-3291

Sakurai J (1995) Toxins of *Clostridium perfringens*. *Rev Med Microbiol* **6**: 175-185

Schleberger C, Hochmann H, Barth H, Aktories K, Schulz GE (2006) Structure and action of the binary C2 toxin from *Clostridium botulinum*. *J Mol Biol* **364**: 705-715

Shimamoto S, Tamai E, Matsushita O, Minami J, Okabe A, Miyata S (2005) Changes in ganglioside content affect the binding of *Clostridium perfringens* epsilon-toxin to detergent-resistant membranes of Madin-Darby canine kidney cells. *Microbiol Immunol* **49**: 245-253

Shortt SJ, Titball RW, Lindsay CD (2000) An assessment of the in vitro toxicology of *Clostridium perfringens* type D epsilon-toxin in human and animal cells. *Hum Experim Toxicol* **19**: 108-116

Tweten RK (2001) *Clostridium perfringens* beta toxin and *Clostridium septicum* alpha toxin: their mechanisms and possible role in pathogenesis. *Vet Microbiol* **82**: 1-9

Toxines et Transferts ioniques – Toxins and Ion transfers
Rencontres en Toxinologie – Meeting on Toxinology, 2011
Editions de la SFET – SFET Editions
Accès libre en ligne sur le site – Free access on line on the site : http://www.sfet.asso.fr

Binding partners of protective antigen from Bacillus anthracis *share certain common motives*

Christoph BEITZINGER[1§], Angelika KRONHARDT[1§], Roland BENZ[1,2*]

[1] *Rudolf-Virchow-Center, DFG-Research Center for Experimental Biomedicine, University of Würzburg, Versbacher Str. 9 D-97078 Würzburg, Germany ;* [2] *School of Engineering and Science, Jacobs University Bremen, Campusring 1, D-28759 Bremen, Germany*

[§] *These authors contributed equally to the paper*
* *Corresponding author ; Tel : +49 421 200 3151 ; E-mail : r.benz@jacobs-university.de*

Abstract

Binary toxins of the AB_7-type are of special interest for scientific investigations as they are among the most potent and specialized bacterial protein toxins. Initiated with the purpose to find cure against anthrax toxin intoxication, nowadays the focus shifted to the investigation of the sophisticated transport mechanism of these molecular syringes. In the intoxication process, the B-subunits multimerize to form a pore that binds with high affinity to host cell receptors and the A-subunits. Followed by endocytosis of the complex into cells the translocation of the enzymatic component into the cytosol occurs upon acidification of the endosomes. Recent publications elucidate that the forces involved in transport include binding affinity, proton gradient and voltage across the endosomal membrane. The data presented here focus on different binding partners of Bacillus anthracis *protective antigen (PA), which range from ions and small molecule inhibitors to effector proteins related or unrelated to the AB_7-type of toxins. Thereby, possible ways to block intoxication by anthrax toxin or to use anthrax PA as specific transportation system are discussed.*

Les différents partenaires de liaison à l'antigène protecteur (PA) de Bacillus anthracis *partagent des structures semblables*

Les toxines binaires de type AB_7 sont d'un grand intérêt scientifique du fait qu'elles sont parmi les plus puissantes et les plus spécialisées des toxines bactériennes. Initialement l'objectif était de trouver un traitement contre l'intoxication à la toxine du charbon, actuellement les recherches se sont portées sur l'étude du mécanisme de transport très sophistiqué de ces seringues moléculaires. Au cours du processus d'intoxication, les sous-unités B se multimérisent pour former un pore qui se lie avec une haute affinité à des récepteurs cellulaires et aux sous-unités A. Après endocytose du complexe dans la cellule, la translocation du composant enzymatique dans le cytosol intervient à la suite de l'acidification des endosomes. Des publications récentes ont mis en évidence que les forces impliquées dans le transport incluent l'affinité de liaison, le gradient de proton et la différence de potentiel à travers la membrane endosomale. Les données présentées ici concernent les différents partenaires de liaison à l'antigène protecteur (PA) de la toxine du charbon, qui comprennent des ions et des petites molécules inhibitrices jusqu'à des protéines effectrices reliées ou non aux toxines de type AB_7. Ainsi, les voies possibles pour bloquer l'intoxication par la toxine du charbon ou pour utiliser l'antigène protecteur PA comme système de transport spécifique sont discutées.

Keywords : Bacillus anthracis, *cationic binding, protective antigen, voltage-dependence.*

Introduction

Anthrax toxin represents one of the main virulence factors of *Bacillus anthracis*. The plasmid-encoded tripartite toxin comprises a receptor-binding moiety termed protective antigen (PA) and two intracellular active enzymes, edema factor (EF) and lethal factor (LF) (Friedlander, 1986; Mock and Fouet, 2001; Collier and Young, 2003). EF is a calcium and calmodulin-dependent adenylate-cyclase (89 kDa) that causes a dramatic increase of intracellular cAMP level, upsetting water homeostasis and destroying the balance of intracellular signaling pathways (Dixon *et al.*, 1999; Mock and Fouet, 2001; Lacy and Collier, 2002). LF is a highly specific zinc metalloprotease (90 kDa) that removes specifically the N-terminal tail of mitogen-activated protein kinase kinases (MAPKKs) (Collier and Young, 2003; Turk, 2007; Rolando *et al.*, 2010). This cleavage leads to subsequent cell death by apoptosis.

Protective antigen (PA) is a cysteine-free 83 kDa protein that binds to two possible receptors, a ubiquitously expressed integral membrane receptor (ATR) and also to the LDL receptor-related protein LRP6, which can both

be involved in anthrax toxin internalization (Scobie and Young, 2005; Wei *et al.*, 2006). PA_{83} present in the serum or bound to receptors is processed by furin to a 63 kDa protein PA_{63} (Ezzell and Abshire, 1992; Petosa *et al.*, 1997). PA_{63} spontaneously oligomerizes in the serum and/or on the cell surface into a heptamer or octamer (Petosa *et al.*, 1997; Feld *et al.*, 2010) and binds EF and/or LF with very high affinity (Escuyer and Collier, 1991; Elliott *et al.*, 2000; Cunningham *et al.*, 2002). The assembled toxic complexes are then endocytosed and directed to endosomes. There, low pH results in the translocation of EF and LF across the endosomal membrane. Combined with acidification is channel formation by PA_{63}, which could represent the mechanism for the translocation scheme of the toxins (Finkelstein, 1994; Miller *et al.*, 1999; Zhang *et al.*, 2004; Abrami *et al.*, 2005).

Recombinant, nicked anthrax protein PA_{63} from *B. anthracis* was obtained from List Biological Laboratories Inc., Campbell, CA. One mg of lyophilized protein was dissolved in 1 ml 5 mM HEPES, 50 mM NaCl, pH 7.5 complemented with 1.25% trehalose. Aliquots were stored at -20°C.

Black lipid bilayer membranes were formed as described previously (Benz *et al.*, 1978). The instrumentation consisted of a Teflon chamber with two aqueous compartments connected by a small circular hole. The hole had a surface area of about 0.4 mm^2. Membranes were formed by painting onto the hole a 1% solution of diphytanoyl phosphatidylcholine (Avanti Polar Lipids, Alabaster, AL) in n-decane. The aqueous salt solutions (Merck, Darmstadt, Germany) were buffered with 10 mM MES-KOH, pH 6. Control experiments revealed that the pH was stable during the time course of the experiments. PA_{63} was reconstituted into the lipid bilayer membranes by adding concentrated stock solutions to the aqueous phase to the *cis*-side of a membrane in the black state. Channel reconstitution reached its maximum between 60 to 120 minutes after addition of PA to the *cis*-side.

Membrane conductance was measured after application of a fixed membrane potential from a battery-operated voltage source with a pair of silver/silver chloride electrodes with salt bridges inserted into the aqueous solutions on both sides of the membrane. The membrane current was measured with a home-made current-to-voltage converter using a Burr Brown operational amplifier with feedback resistors between 0.1 and 10 GΩ. The potentials applied to the membranes throughout the study always refer to those applied to the *cis*-side, the side of addition of PA. Similarly, positive currents were caused by positive potentials at the *cis*-side and negative ones by negative potentials at the same side. The temperature was kept at 20°C throughout.

Titration experiments were performed with membranes containing only a few or many PA_{63}-channels. The amplified signal was recorded with a strip chart recorder to measure the absolute magnitude of the membrane current and to calculate the stability constant *K* for substrate binding to PA. The conductance data of the titration experiments were analyzed using a formalism derived earlier for the carbohydrate-induced block of the maltoporin and CymA-channels (Benz *et al.*, 1987; Orlik *et al.*, 2002; Orlik *et al.*, 2003) and the block of the PA_{63}-channels with LF and EF (Neumeyer *et al.*, 2006a; Neumeyer *et al.*, 2006b). The conductance, G(c), at a given concentration c of substrates relative to the initial conductance, G_{max} (in the absence of substrates), was analyzed using the following equation:

$$\frac{G_{\max} - G(c)}{G_{\max}} = \frac{K \cdot c}{K \cdot c + 1} \qquad \textit{Equation 1}$$

where *K* is the stability constant for the binding of substrates to the PA_{63}-channel. The half saturation constant, K_s, of its binding is given by the inverse stability constant 1/*K*.

Results : Known binding substrates of protective antigen

There are different substrates which are characterized to bind to protective antigen. These are proteins, related or not related to the AB_7-type toxins, and small molecule inhibitors.

Native effector proteins of protective antigen

Full length EF and LF

Anthrax toxin consists of the binding and translocation component protective antigen (PA) and the two enzymatic components edema factor (EF) and lethal factor (LF). They both bind to the same motif located in domain 1 of the PA_{63}-prepore (Lacy and Collier, 2002; Pimental *et al.*, 2004). As two monomers of the heptameric prepore are required to bind one enzymatic component (Cunningham *et al.*, 2002) the heptameric form of the PA-channel is able to bind up to three molecules at the same time (Mogridge *et al.*, 2002), whereas the PA octamer provides up to four binding sites (Feld *et al.*, 2010). Both EF and LF attach with their N-terminal end to PA. Arora and Leppla (1993) could show that the N-terminal domain is sufficient to bind to PA and also to translocate fusion proteins. Recently, Feld and colleagues demonstrated that LF initially binds with its N-terminal domain to an amphipatic cleft on the surface of the PA_{63}-prepore, the so called α-cleft (Feld *et al.*, 2010).

In lipid bilayer membranes titration experiments revealed that binding only occurred when EF and LF were added to the same side as PA_{63} (the *cis*-side of the membrane), substrate given to the *trans*-side did not show any effect indicating that the PA-pore only possesses one binding site within the mushroom body (Neumeyer *et al.*, 2006a; Neumeyer *et al.*, 2006b). The conductance decreased in a dose-dependent manner. The affinity to

the PA-pore is in the low nanomolar range and it could be shown that the block of PA is a single hit process. As the binding is ionic strength-dependent the K_s values increase by a factor of about 500 from 50 mM to 1000 mM KCl electrolyte concentration.

EF_N and LF_N

EF's and LF's N-terminal fragments called EF_N and LF_N as well as fusion proteins are able to bind to PA-channels, e.g. LF_N-DTA (LF fused to diphtheria toxin), and are translocated through the pore into the cytosol of target cells (Blanke *et al.*, 1996). Therefore, the truncated components EF_N and LF_N were supposed to have similar binding properties as full length EF and LF. However, the affinity of the truncated proteins is tenfold weaker compared to full length EF and LF indicating that further interactions of the C-terminal region of EF and LF are involved in the binding process (Leuber *et al.*, 2008).

His-tagged proteins

Several studies elucidated that an N-terminal His_6-tag attached to EF or LF increases the binding affinity to the PA-channel (Blanke *et al.*, 1996; Neumeyer *et al.*, 2006a; Neumeyer *et al.*, 2006b). As the binding is due to interactions between negative charges of the PA-pore and positive charges of the enzymatic components, additional positive charges of the His_6-tag enhance the binding of the truncated EF_N and LF_N to the PA-channel as well by a factor of about 10 (Leuber *et al.*, 2008).

Cross-reactivity of anthrax- and C2-toxin

Binding of close related proteins

Another prominent member of the AB_7-toxin family is the C2-toxin of *Clostridium botulinum*. It performs a very similar mode of intoxication and the channel forming components C2II and PA exhibit about 35% amino acid homology. To test if these two toxins are also functionally interchangeable, cross-reaction experiments were performed by combining the channel forming component of one toxin with the respective enzymatic component of the other toxin (Kronhardt *et al.*, 2011). In lipid bilayer experiments binding could be observed for each combination, however, anthrax EF and LF had higher binding affinities to the C2II-channel than C2I to the PA-channel. *In vitro* experiments revealed that PA is not only able to bind but also to translocate the enzymatic component C2I of C2-toxin resulting in intoxication and cell death. The combination of C2II and EF or LF, respectively, merely led to toxic effects when exposed to HUVEC cells (Kronhardt *et al.*, 2011). Due to this high flexibility PA is an extremely interesting protein for a general transport system across membranes.

Binding of unrelated proteins is enabled by His_6-tag

It was shown before that polycationic peptides fused to diphtheria toxin (DTA) enhances the uptake of this protein *via* PA-pores (Blanke *et al.*, 1996). This work focused on different, charged tags, which exhibited either no change in affinity for Glu_6-tag and random sequence (compared to untagged DTA) or increased binding for His_6-, Arg_6- and Lys-tags of different length. With the knowledge of the binding properties of his-tagged native effectors, the DTA experiments and cross-reactivity of C2I, the next step was to check for His_6-C2I. The affinity to PA *in vivo* and *in vitro* was strongly increased as expected (Beitzinger *et al.*, 2011). Following this set of experiments a protein fragment of Lambda phage protein (gPJ) not related to any toxins was tested. Whereas gpJ was not able to bind to PA, its affinity towards the PA-channel was in the range of EF and LF when it was coupled to a His_6-tag (Beitzinger *et al.*, 2011). Finally, the authors could show similar results for EDIN of *Staphylococcus aureus*, which ADP-ribosylates and inactivates Rho-GTP binding proteins. His_6-EDIN binds to the PA-channel in titration experiments and is transported through the PA-channel in intoxication assays. Additionally, it has been found that the process is highly voltage-dependent. This means that PA-pores may be used as molecular syringes, which deliver His_6-tagged target proteins into cells possessing the known receptors for PA (Lang *et al.*, 2010).

Small molecule inhibitors

Chloroquine and other 4-aminoquinolones block protective antigen

Anthrax toxin is one of the most potent bacterial toxins and could be used as a biological weapon or for terroristic activities by spreading spores of multi resistant *B. anthracis* bacteria (Keim *et al.*, 2001; Inglesby *et al.*, 2002; Jernigan *et al.*, 2002). This threat could be handled by introducing small molecules which are able to block PA-pores and efficiently prohibit translocation of the effectors, therefore buying time to deal with the bacterial infection. First results were found for chloroquine and other 4-aminoquinolones formerly used as antibiotics (Lewis *et al.*, 1973; Vedy, 1975). These substrates depicted high affinity binding in titration experiments to PA (Orlik *et al.*, 2005). Additionally, it is well known that chloroquine acquires positive charges under acidic condition and accumulates in endosomes (Neumeyer *et al.*, 2008). Both effects would enhance the blockage of PA *in vivo*. Concerning the side effects of chloroquine and related substances on humans, there is the urge for blocker-molecules with homologous structure, which do not exhibit cell toxicity.

Cyclodextrin-complexes form a plug for the PA-pore

Cyclodextrins have been found to bind to CymA-porin of *Klebsiella oyxtoca* (Pajatsch *et al.*, 1999; Orlik *et al.*, 2003). The ring-shaped complex of seven glucose units in β-cyclodextrin happens to be in a perfect size for the blockage of binary toxin channels and is itself not toxic at all. Additionally, β-cyclodextrin and PA share a sevenfold symmetry, which offers one side chain of β-cyclodextrin for each PA_{63} monomer. Therefore, β-cyclodextrin has been tested as a basis drug for PA blockage (Nestorovich *et al.*, 2010). Recently, experiments with β-cyclodextrin

and C2II – a very homologous AB_7-toxin-channel as described before – were performed in a trial of modern, literature based drug design. In this study, changes in the outward facing part of the rings functional groups led to enhanced binding stabilities. Interestingly, the introduction of a positive charge and some aromatic residues were found to be responsible for this effect (Nestorovich *et al.*, 2011). The possible seven charges in the β-cyclodextrin structure seem to match with the PA binding pocket. Even though the authors could show blockage of intoxication in cell-based assays, the seven permanent charges could avoid specificity or passage through membranes *in vivo*, which reasons in the necessity of further pharmacological studies.

Results : Binding of divalent and trivalent cations to protective antigen

The PA-channel is known to be highly cation selective (Blaustein *et al.*, 1989) and additional positive charges of His_6-tags increase the binding properties of several proteins (Blanke *et al.*, 1996; Neumeyer *et al.*, 2006a; Neumeyer *et al.*, 2006b; Leuber *et al.*, 2008; Beitzinger *et al.*, 2011). Therefore, we addressed the question if also divalent and trivalent cations are able to bind and to block the PA_{63}-channel.

The binding of $CuSO_4$, $ZnCl_2$, $NiCl_2$ and $LaCl_3$ to the PA_{63}-channel was investigated by performing titration experiments similar to those described for binding of EF and LF (Boquet and Lemichez, 2003; Neumeyer *et al.*, 2006a; Neumeyer *et al.*, 2006b). After reconstitution of the PA-channels added to the *cis*-side of a lipid bilayer membrane, the rate of insertions became very small. Then, concentrated solutions of divalent or trivalent cations were added to the *cis*- or the *trans*-side of the membrane, respectively, while stirring to allow equilibration. The membrane conductance decreased in a dose-dependent manner meaning that the cations bound to the PA-channel and thereby reduced the conductance. Analysis of the titration experiments by Lineweaver-Burke plots according to equation (1) indicated that the interaction between the cations and the PA-channel represents a single hit binding process. The results shown in *Table 1* reveal that there are considerable differences concerning the stability constants of the respective cations to the PA-pore. Highest binding affinity was observed for Cu^{2+}, followed by La^{3+}, which was in the micromolar range, whereas the binding affinity of Ni^{2+} and Zn^{2+} were in the millimolar range. The binding constants of the divalent and trivalent cations to the PA-channel decreased in the series $K_{Cu} > K_{La} > K_{Zn} > K_{Ni}$ from about 10,000 M^{-1} to about 100 M^{-1} in 150 mM KCl (see *Table 1*).

Table 1. Stability constants *K* and half saturation constants K_s for the binding of divalent and trivalent cations to the PA_{63} channel.

***Tableau 1**. Constantes de stabilité K et de demi-saturation Ks pour la liaison de cations bivalents et trivalents au canal PA_{63}*

PA_{63} with		*K* [M^{-1}]	K_s [mM]
Cu^{2+}	cis +10mV	9237	0.11
	cis -10mV	7244	0.14
	trans +10mV	5254	0.19
Ni^{2+}	cis +10mV	122	8.2
	cis -10mV	47	21.3
	trans +10mV	65	15.4
Zn^{2+}	cis +10mV	1246	0.8
	cis -10mV	307	3.3
	trans +10mV	244	4.1
La^{3+}	cis +10mV	1383	0.7
	cis -10mV	654	1.5

Stability constants *K* of Cu^{2+}, Ni^{2+}, Zn^{2+} and La^{3+} to PA_{63}-channels reconstituted in lipid bilayer membranes formed from diphytanoyl phosphatidylcholine/n-decane. The aqueous phase contained 150 mM KCl, 10 mM MES-KOH pH 6.0; T=20°C. The voltage was applied as indicated. The data represent the means of at least three individual experiments. K_s is the half saturation constant, calculated as 1/*K*.

Constantes de stabilité K *du* Cu^{2+}, *du* Ni^{2+}, *du* Zn^{2+} *et du* La^{3+} *aux canaux* PA_{63} *reconstitués dans des bicouches lipidiques formées à partir de diphytanoyl phosphatidylcholine/n-décane. La phase aqueuse contient 150 mM de KCl, 10 mM de MES-KOH pH 6,0; T=20°C. La différence de potentiel a été appliquée comme indiqué dans le tableau. Les données correspondent aux moyennes d'au moins trois expériences indépendantes.* K_s *est la constante de demi-saturation et est égale à 1/*K.

Binding to the PA-channel is generally supposed to rely on ion-ion interaction. Therefore, we performed titration experiments for binding of Cu^{2+} in various electrolyte concentrations to check if this was also true for the binding of the divalent cations. The stability constants *K* for Cu^{2+} binding to the PA-channel decreased with increasing electrolyte concentration from about 80,000 M^{-1} at 50 mM KCl to about 1,500 M^{-1} at 1 M KCl (see *Table 2*). That means that the stability constant of copper ion binding to the PA-channel is strongly ionic-strength dependent.

Interestingly, the binding of the cations was barely influenced by the side of addition. Irrespectively of the side of addition, the stability constants were nearly stable. Additionally, the binding affinities of the cations to the PA-channel were not changed when negative voltage in the physiological range was applied. This indicates that the cations were able to equilibrate rapidly across the PA-channel irrespective of the applied voltage.

Table 2. Ionic-strength dependence of the binding of Cu^{2+} to the PA_{63}-channel.

***Tableau 2**. La liaison du Cu^{2+} au canal PA_{63} est dépendante de la force ionique.*

PA_{63} with		K [M^{-1}]	K_s [mM]
Cu^{2+}	50 mM	87935	0.01
	150 mM	9237	0.11
	300 mM	3638	0.27
	1 M	1626	0.62

Stability constants K of Cu^{2+} to PA_{63}-channels reconstituted in lipid bilayer membranes formed from diphytanoyl phosphatidylcholine/n-decane. The aqueous phase contained four different KCl-concentrations, 10 mM MES-KOH pH 6.0; T=20°C. The data represent means of at least three titration experiments. K_s is the half saturation constant, calculated as $1/K$. Note that the ionic strength had a considerable influence on the stability constant of binding of copper ions to the PA_{63}-channel.

Constantes de stabilité K *du Cu^{2+} aux canaux PA_{63} reconstitués dans des bicouches lipidiques formées à partir de diphytanoyl phosphatidylcholine/n-décane. La phase aqueuse contient quatre concentrations différentes de KCl, en présence de 10 mM de MES-KOH pH 6,0; T=20°C. Les données correspondent aux moyennes d'au moins trois expériences de titration.* K_s *est la constante de demi-saturation et est égale à 1/*K*. Il est à noter que la force ionique a une influence considérable sur la liaison des ions cuivre aux canaux PA_{63} comme indiqué par les valeurs des constantes de stabilité* K*.*

The results of the titration experiments suggested that the PA-channel either contains two different binding sites for divalent and trivalent cations, one at the *cis*- and one at the *trans*-side of the channel, or just one binding site which is accessible from both sides of the channel. This could be the case, as the small cations are able to cross the channel rapidly and equilibrate in the aqueous solution. Titration experiments with copper ions on both sides of the membrane led to subsequent decrease of PA-induced conductance. Then, 5 mM EDTA was added to the *trans*-side of the membrane. No effect on the conductance could be observed. However, addition of EDTA to the *cis*-side of the membrane resulted in increasing conductance. The copper induced blockage of the PA-channels could be fully restored meaning that the PA-pore only contains one binding site for copper ions which is localized at the *cis*-side of the channel.

Conclusion

Binding substrates of protective antigen share common motives

Positive charges play a crucial role in binding to PA_{63}-channels

It is well known that PA-pores are strongly cation selective up to a factor of 20 p_c/p_a (Blaustein *et al.*, 1989). Additionally, recent studies found proof, that negatively charged amino acids in the vestibule of PA-channels play a crucial role in the binding of EF and LF (Orlik *et al.*, 2005; Leuber *et al.*, 2008). These findings already indicate the importance of ion-ion interaction for binding and translocation events to PA. The data presented here underline this assumption by depicting the existence of positive charges in high affinity substrates ranging from simple ions, over small inhibitor molecules and molecule complexes as well as peptides, to related proteins and finally protein effectors only containing chargeable tags.

First time evidence that different cationic electrolytes serve as a binding partner to PA-channels is presented in this work. This is of special interest, as the ions themselves seem to be too small to block the channel conductance. The sevenfold symmetry of the pore provides seven possible negative charges for each acidic amino acid facing the lumen of PA_{63}. On top of that, the constriction site of PA, the so-called Φ-clamp is surrounded by these rings of negative charges. Therefore, a plug consisting of more and more cations may form around this site explaining the results. Additional support for this theory is provided by the studies with sevenfold charged β-cyclodextrin and the length dependent binding of positive charged tags (Blanke *et al.*, 1996; Nestorovich *et al.*, 2010). Binding of cations could be possible from both sides of PA-channels out of two reasons. First, ions might be small enough to pass the Φ-clamp and bind from the opposite side. Second, multiple rings of acidic amino acids exist in the lumen of the channel on both sides of the Φ-clamp forming more than one binding site. It has been shown that this is not the case as only one binding site could be identified for all the substrates.

Aromatic residues enhance affinities towards PA-pores

Another important function is represented by aromatic ring-systems. Especially when the affinity of blocker-substrates is discussed, it becomes obvious that the existence of aromatic residues strengthens the binding to toxin channels (Nestorovich *et al.*, 2011). This could found on the existence of the Φ-clamp, too. As the on-rate derived by current noise analysis is in the range of diffusion for molecules like chloroquine, the off-rate

contributes to a larger extend to the stability constant (Orlik *et al.*, 2005). That reasons that molecules which are directed directly to the constriction site and settle there should form the most stable block. Considering the Φ-clamps composition out of seven phenylalanine residues, it is easy to understand, that aromatic side-chains serve this purpose best (Orlik *et al.*, 2005). Taken the pharmacological use of those substrates into consideration, the aromatic residues could provide a further purpose in enabling these molecules to cross membranes and reach the endosome, where they are charged due to acidic pH. This trapping-effect known from chloroquine and other 4-aminoquinolones further increases blockage of PA-channels.

Binding of charged substrates is voltage-dependent

Recently a change in voltage-dependency of the PA-channel after His_6-EDIN titration has been found (Beitzinger *et al.*, 2011). The stability constants for binding are influenced when positive voltages are applied. It seems to be the case, that the force of the electric field pulls the tagged N-terminus of the protein deeper into the pore, thereby increasing the stability constant for binding of these His_6-tagged polypeptides. This finding partially serves as an explanation for the translocation of foreign substrates *in vivo*, which possess positively charged tags, as the acidic endosome exhibits this field direction. Further studies are necessary to fully elucidate this voltage-dependent binding and translocation process of all charged substrates to the PA-pore mentioned here.

Outview

Considering the data provided and summed up here, it is obvious, that binding and translocation concerning PA is of special interest. Not only for understanding one of the most potent bacterial toxins in more detail, but in order to cure anthrax intoxication in the context of biological terrorism and the potential usage of PA as a versatile molecular syringe for various purposes, further work has to be done in this vital field of studies.

Acknowledgements. *This work was funded by the Deutsche Forschungsgemeinschaft (SFB 487, project A5) and the Rudolf-Virchow-Center, DFG-Research Center for Experimental Biomedicine, University of Würzburg. The authors would like to thank Emmanuel Lemichez and Monica Rolando, Inserm Nice for helpful discussions and Michel R. Popoff for his help with the preparation of the manuscript.*

References

Abrami L, Reig N, van der Goot FG (2005) Anthrax toxin: the long and winding road that leads to the kill. *Trends Microbiol* **13**: 72-78

Arora N, Leppla SH (1993) Residues 1-254 of anthrax toxin lethal factor are sufficient to cause cellular uptake of fused polypeptides. *J Biol Chem* **268**: 3334-3341

Beitzinger C, Rolando M, Kronhardt A, Flatau G, Popoff MR, Lemichez E, Benz R (2011) Anthrax toxin protective antigen uptake of N-terminal His-tagged proteins into cells is voltage-dependent. *(Manuscript)*

Benz R, Janko K, Boos W, Lauger P (1978) Formation of large, ion-permeable membrane channels by the matrix protein (porin) of Escherichia coli. *Biochim Biophys Acta* **511**: 305-319

Benz R, Schmid A, Vos-Scheperkeuter GH (1987) Mechanism of sugar transport through the sugar-specific LamB channel of Escherichia coli outer membrane. *J Membr Biol* **100**: 21-29

Blanke SR, Milne JC, Benson EL, Collier RJ (1996) Fused polycationic peptide mediates delivery of diphtheria toxin A chain to the cytosol in the presence of anthrax protective antigen. *Proc Natl Acad Sci U S A* **93**: 8437-8442

Blaustein RO, Koehler TM, Collier RJ, Finkelstein A (1989) Anthrax toxin: channel-forming activity of protective antigen in planar phospholipid bilayers. *Proc Natl Acad Sci U S A* **86**: 2209-2213

Boquet P, Lemichez E (2003) Bacterial virulence factors targeting Rho GTPases: parasitism or symbiosis? *Trends Cell Biol* **13**: 238-246

Collier RJ, Young JA (2003) Anthrax toxin. *Annu Rev Cell Dev Biol* **19**: 45-70

Cunningham K, Lacy DB, Mogridge J, Collier RJ (2002) Mapping the lethal factor and edema factor binding sites on oligomeric anthrax protective antigen. *Proc Natl Acad Sci U S A* **99**: 7049-7053

Dixon TC, Meselson M, Guillemin J, Hanna PC (1999) Anthrax. *N Engl J Med* **341**: 815-826

Elliott JL, Mogridge J, Collier RJ (2000) A quantitative study of the interactions of Bacillus anthracis edema factor and lethal factor with activated protective antigen. *Biochemistry (Mosc)* **39**: 6706-6713

Escuyer V, Collier RJ (1991) Anthrax protective antigen interacts with a specific receptor on the surface of CHO-K1 cells. *Infect Immun* **59**: 3381-3386

Ezzell JW, Jr., Abshire TG (1992) Serum protease cleavage of Bacillus anthracis protective antigen. *J Gen Microbiol* **138**: 543-549

Feld GK, Thoren KL, Kintzer AF, Sterling HJ, Tang, II, Greenberg SG, Williams ER, Krantz BA (2010) Structural basis for the unfolding of anthrax lethal factor by protective antigen oligomers. *Nat Struct Mol Biol* **17**: 1383-1390

Finkelstein A (1994) The channel formed in planar lipid bilayers by the protective antigen component of anthrax toxin. *Toxicology* **87**: 29-41

Friedlander AM (1986) Macrophages are sensitive to anthrax lethal toxin through an acid-dependent process. *J Biol Chem* **261**: 7123-7126

Inglesby TV, O'Toole T, Henderson DA, Bartlett JG, Ascher MS, Eitzen E, Friedlander AM, Gerberding J, Hauer J, Hughes J, McDade J, Osterholm MT, Parker G, Perl TM, Russell PK, Tonat K (2002) Anthrax as a biological weapon, 2002: updated recommendations for management. *JAMA* **287**: 2236-2252

Jernigan DB, Raghunathan PL, Bell BP, Brechner R, Bresnitz EA, Butler JC, Cetron M, Cohen M, Doyle T, Fischer M, Greene C, Griffith KS, Guarner J, Hadler JL, Hayslett JA, Meyer R, Petersen LR, Phillips M, Pinner R, Popovic T, Quinn CP, Reefhuis J, Reissman D, Rosenstein N, Schuchat A, Shieh WJ, Siegal L, Swerdlow DL, Tenover FC, Traeger M, Ward JW, Weisfuse I, Wiersma S, Yeskey K, Zaki S, Ashford DA, Perkins BA, Ostroff S, Hughes J, Fleming D, Koplan JP, Gerberding JL (2002) Investigation of bioterrorism-related anthrax, United States, 2001: epidemiologic findings. *Emerg Infect Dis* **8**: 1019-1028

Keim P, Smith KL, Keys C, Takahashi H, Kurata T, Kaufmann A (2001) Molecular investigation of the Aum Shinrikyo anthrax release in Kameido, Japan. *J Clin Microbiol* **39**: 4566-4567

Kronhardt A, Rolando M, Beitzinger C, Stefani C, Leuber M, Flatau G, Popoff MR, Benz R, Lemichez E (2011) Cross-Reactivity of Anthrax and C2 Toxin: Protective Antigen Promotes the Uptake of Botulinum C2I Toxin into Human Endothelial Cells. *PLoS One* **6**: e23133

Lacy DB, Collier RJ (2002) Structure and function of anthrax toxin. *Curr Top Microbiol Immunol* **271**: 61-85

Lang AE, Schmidt G, Schlosser A, Hey TD, Larrinua IM, Sheets JJ, Mannherz HG, Aktories K (2010) Photorhabdus luminescens toxins ADP-ribosylate actin and RhoA to force actin clustering. *Science* **327**: 1139-1142

Leuber M, Kronhardt A, Tonello F, Dal Molin F, Benz R (2008) Binding of N-terminal fragments of anthrax edema factor (EF(N)) and lethal factor (LF(N)) to the protective antigen pore. *Biochim Biophys Acta* **1778**: 1436-1443

Lewis AN, Dondero TJ, Jr., Ponnampalam JT (1973) Letter: Falciparum malaria resistant to chloroquine suppression but sensitive to chloroquine treatment in West Malaysia. *Trans R Soc Trop Med Hyg* **67**: 310-312

Miller CJ, Elliott JL, Collier RJ (1999) Anthrax protective antigen: prepore-to-pore conversion. *Biochemistry (Mosc)* **38**: 10432-10441

Mock M, Fouet A (2001) Anthrax. *Annu Rev Microbiol* **55**: 647-671

Mogridge J, Cunningham K, Collier RJ (2002) Stoichiometry of anthrax toxin complexes. *Biochemistry (Mosc)* **41**: 1079-1082

Nestorovich EM, Karginov VA, Berezhkovskii AM, Bezrukov SM (2010) Blockage of anthrax PA63 pore by a multicharged high-affinity toxin inhibitor. *Biophys J* **99**: 134-143

Nestorovich EM, Karginov VA, Popoff MR, Bezrukov SM, Barth H (2011) Tailored ss-cyclodextrin blocks the translocation pores of binary exotoxins from C. Botulinum and C. Perfringens and protects cells from intoxication. *PLoS One* **6**: e23927

Neumeyer T, Schiffler B, Maier E, Lang AE, Aktories K, Benz R (2008) Clostridium botulinum C2 toxin. Identification of the binding site for chloroquine and related compounds and influence of the binding site on properties of the C2II channel. *J Biol Chem* **283**: 3904-3914

Neumeyer T, Tonello F, Dal Molin F, Schiffler B, Benz R (2006a) Anthrax edema factor, voltage-dependent binding to the protective antigen ion channel and comparison to LF binding. *J Biol Chem* **281**: 32335-32343

Neumeyer T, Tonello F, Dal Molin F, Schiffler B, Orlik F, Benz R (2006b) Anthrax lethal factor (LF) mediated block of the anthrax protective antigen (PA) ion channel: effect of ionic strength and voltage. *Biochemistry (Mosc)* **45**: 3060-3068

Orlik F, Andersen C, Benz R (2002) Site-directed mutagenesis of tyrosine 118 within the central constriction site of the LamB (maltoporin) channel of Escherichia coli. II. Effect on maltose and maltooligosaccharide binding kinetics. *Biophys J* **83**: 309-321

Orlik F, Andersen C, Danelon C, Winterhalter M, Pajatsch M, Bock A, Benz R (2003) CymA of Klebsiella oxytoca outer membrane: binding of cyclodextrins and study of the current noise of the open channel. *Biophys J* **85**: 876-885

Orlik F, Schiffler B, Benz R (2005) Anthrax toxin protective antigen: inhibition of channel function by chloroquine and related compounds and study of binding kinetics using the current noise analysis. *Biophys J* **88**: 1715-1724

Pajatsch M, Andersen C, Mathes A, Bock A, Benz R, Engelhardt H (1999) Properties of a cyclodextrin-specific, unusual porin from Klebsiella oxytoca. *J Biol Chem* **274**: 25159-25166

Petosa C, Collier RJ, Klimpel KR, Leppla SH, Liddington RC (1997) Crystal structure of the anthrax toxin protective antigen. *Nature* **385**: 833-838

Pimental RA, Christensen KA, Krantz BA, Collier RJ (2004) Anthrax toxin complexes: heptameric protective antigen can bind lethal factor and edema factor simultaneously. *Biochem Biophys Res Commun* **322**: 258-262

Rolando M, Stefani C, Flatau G, Auberger P, Mettouchi A, Mhlanga M, Rapp U, Galmiche A, Lemichez E (2010) Transcriptome dysregulation by anthrax lethal toxin plays a key role in induction of human endothelial cell cytotoxicity. *Cell Microbiol* **12**: 891-905

Scobie HM, Young JA (2005) Interactions between anthrax toxin receptors and protective antigen. *Curr Opin Microbiol* **8**: 106-112

Turk BE (2007) Manipulation of host signalling pathways by anthrax toxins. *Biochem J* **402**: 405-417

Vedy MJ (1975) [Retinopathy caused by chloroquine in the prevention of malaria in children]. *Bull Soc Ophtalmol Fr* **75**: 609-611

Wei W, Lu Q, Chaudry GJ, Leppla SH, Cohen SN (2006) The LDL receptor-related protein LRP6 mediates internalization and lethality of anthrax toxin. *Cell* **124**: 1141-1154

Zhang S, Finkelstein A, Collier RJ (2004) Evidence that translocation of anthrax toxin's lethal factor is initiated by entry of its N terminus into the protective antigen channel. *Proc Natl Acad Sci U S A* **101**: 16756-16761

Toxines et Transferts ioniques – Toxins and Ion transfers
Rencontres en Toxinologie – Meeting on Toxinology, 2011
Editions de la SFET – SFET Editions
Accès libre en ligne sur le site – Free access on line on the site : http://www.sfet.asso.fr

Ways for partial and total inhibition of staphylococcal bicomponent leucotoxins

Gilles PREVOST[1*], Mira TAWK[1], Mauro DALLA SERRA[2], Bernard POULAIN[3], Sarah CIANFERANI[4], Benoît-Joseph LAVENTIE[1], Emmanuel JOVER[3]

[1] Université de Strasbourg, Physiopathologie et Médecine Translationnelle, EA-4438, Strasbourg, France ; [2] Fondazione Bruno Kessler-Consiglio Nazionale delle Ricerche-Istituto di Biofisica – Trento, Italy ; [3] Institut des Neurosciences cellulaires et Intégratives, UPR 3212, Neurotransmission et sécrétion neuroendocrine ; Institut Hubert Curien – Université de Strasbourg, UMR 7178, Strasbourg, France

** Corresponding author ; Tel : +33 (0)3 6885 3757 ; Fax : +33 (0)3 6885 3808 ; E-mail : prevost@unistra.fr*

Abstract

Staphylococcal leucotoxins operate by two distinct proteins of approximately 31 kDa and 35 kDa. The components associate with the targeted membranes before stabilising oligomers that are able to activate cell, i.e. *human polymorphonuclear cells, Ca^{2+} metabolism, and thereafter pores become functional lyze cells by huge loss of water and mainly monovalent cations. We found that some peptides may block up pores and induce loss of the lytic leucotoxin activity. Such peptides were useful to analyze the calcium entry in hPMNs. In such a context, some calcium channels activated by leucotoxins HlgC-HlgB and Panton-Valentine leucocidin were identified using some inhibitors, thus leading to absolute inhibition of their biological activity. We then evidence the involvement of calcium store release* via *IP3 receptors, and some linked calcium channels at the membrane. Other ways exist to completely inhibit these leucotoxins and these inhibitors might gain application when they efficiently target the largest number of leucotoxins. This is the case of new humanized antibodies and other organic compounds derivatives from calixarenes. Both these molecules interact with and neutralize leucotoxins, thus antagonizing their binding to membranes. These products have shown efficacy in blocking the inflammatory role of leucotoxins* in vivo.

Différentes approches pour l'inhibition partielle ou totale des leucotoxines de staphylocoques

Les leucotoxines staphylococciques opèrent via *deux protéines distinctes d'environ 31 et 35 kDa Ces composés s'associent à la surface de la membrane avant de se stabiliser en oligomères responsables d'une activation du métabolisme calcique des cellules cibles,* i.e. *les polynucléaires humains. Ensuite, des pores deviendront fonctionnels et lyseront les cellules après la perte d'eau et de cations monovalents. Des peptides synthétiques sont capables d'obturer le pore et induisent une perte de l'activité lytique. Ces peptides sont utilisés pour identifier des canaux calciques activés par les leucotoxines. Ainsi, certaines voies et canaux calciques comme la voie de l'IP3 et certains canaux associés ont été identifiés après l'action de la gamma-hémolysine HlgC-HlgB et de la leucocidine de Panton et Valentine grâce à différents inhibiteurs, bloquant alors toute l'activité biologique. Il existe cependant d'autres approches séduisantes pour bloquer l'activité biologique de l'éventail le plus large possible de leucotoxines. C'est le cas d'anticorps humanisés, mais aussi de composés organiques dérivés des calixarènes. Ces composés interagissent et neutralisent la capacité des leucotoxines à se fixer sur les membranes. Leurs propriétés anti-inflammatoires sélectives ont pu être vérifiées* in vivo.

Keywords : *Binding inhibition, calcium channels, pathogenicity, staphylococcal leucotoxins, therapeutics.*

Introduction

Staphylococcal leucotoxins now gather a cohort of bi-component pore-forming toxins (PFTs) active against human leucocytes that are secreted by *Staphylococcus aureus* (SA), *Staphylococcus intermedius and Staphylococcus pseudointermedius* (Prévost, 2005; Ventura *et al.*, 2010; Riegel *et al.*, 2011). The alpha-toxin from SA is an example of a related one-component pore-forming toxin (Song *et al.*, 1996). The bipartite character is supported by the interaction of two distinct proteins distinguished as class S and class F proteins of 31-32 and 34-35 kDa, respectively. These secreted PFTs may be constant or not according to the leucotoxin and, thus, may have more or less clinical significance. After a decade of controversies, it appears that one of them, the Panton-Valentine leucotoxin (PVL) is a gravity factor for a number of necrotizing infections including

pneumonia, osteomyelitis, ... and is a determinant factor for furuncles (Prévost, 2005; Baba Moussa *et al.*, 2011). Finally, the complementary features of these leucotoxins, and their role in the acuteness in infections is mostly admitted. Because these proteins have to assemble to target membranes and form a pore, the bipartite model has longer been studied to determine its specificity, possibility to combine proteins (Prévost, 2005), difference in the ion selectivity of pores (Comai *et al.*, 2002), sandwich position of the two proteins inside the pore (Viero *et al.*, 2006), mode of the deployment of the central domain that form the β-hairpins, the basic elements of the trans-membrane β-barrel forming the pore (Viero *et al.*, 2008). Several reports suggested a stoichiometry of the pore reaching an octamer (Miles *et al.*, 2002; Joubert *et al.*, 2006), and the publication of the three-dimensional structure of HlgA-HlgB, *i.e.* gamma-hemolysin has recently confirmed the previous data (Yamashita *et al.*, 2011).

After the formation of an octameric prepore constituted of 4 alternating class S and class F proteins, the central domains of each monomer will participate to the building of a transmembrane β-barrel. While most of leucotoxins are not equivalent for their cell spectra, polymorphonuclear cells (PMNs) remain common target cells. The other common features meet the biological activities that are mainly composed of a cell activation consisting in the calcium entry into cytoplasm of target cells, and secondarily to the formation of pores leading to the equilibrium of monovalent cations and to the osmotic exchange involving water that leads to cell necrosis (Genestier *et al.*, 2005). As leucotoxins probably are involved in human pathology, the various possibilities to inhibit leucotoxins may have interest and possible applications. Thus, in this short review we will meet some possibilities to block biological activities of these toxins, or to selectively block the calcium activation or the pore function following the formation of oligomers. Moreover, even classified as pore-forming toxins, we do not have evaluation of the effects of leucotoxins at low concentrations on cell signaling. Whereas the pore formation can be detected within few minutes following applications of toxins, Ca^{2+} entry rises faster and with large amplitude into cells.

Blocking the whole activity of staphylococcal leucotoxins

These approaches might be dedicated to possible future therapeutics in case of acute SA infections and risk of non response to treatment even if dedicated antimicrobials were administered. Indeed, by blocking the largest number of pore-forming leucotoxins that SA may produce, this might result in a lesser inflammatory response and tissues necrosis, thus giving an advantage to antimicrobial therapy. We got the opportunity to test innovative antibodies against staphylococcal leucotoxins, and tentatively try to understand and develop some chemicals that specifically interact with staphylococcal leucotoxins. The main interest of these two approaches is, while constituting promising inhibitors, they might offer tools to target all or almost all leucotoxins and project the ability to totally suppress a family of toxins produced by a pathogenic micro-organism.

Blocking the biological activity by humanized antibodies

Humanized Heavy Chain only Antibodies (HCAb) were generated against the *S. aureus* Panton-Valentine leucotoxin (PVL) from immunized transgenic mice to neutralize toxin activity (*Figure 1A*). Genes encoding antibodies were in fact cloned from llama heavy chains from immunoglobulins into a phage display system and mutated to be humanized, selected after panning reactive antibodies, and further stably transfected into Human Embryogenic Kidney cells (HEK)(Laventie *et al.*, 2011). One anti-LukS-PV HCAb, three anti-LukF-PV HCAbs with nanomolar affinities and one engineered tetravalent (*Figure 1B*) and bi-specific HCAb were tested *in vitro* (*Figure 1C*) and *in vivo* (*Figure 1D*). They all prevent toxin binding and pore formation. After their incubation with a non immune serum, these antibodies remained almost fully active.

HCAbs against LukS-PV do not recognize LukF-PV. Conversely, HCAbs against LukF-PV do not detect LukS-PV (*Figure 1C*). This excludes the possibility that the antibodies recognize common epitopes present in both recombinant proteins. The bi-specific HCAb obviously detects both LukS-PV and LukF-PV. Further analysis showed that other bi-component leucotoxins (HlgA-HlgB, HlgC-HlgB, LukE-LukD) are not inhibited except anti-LukS-PV HCAb which also inhibited the gamma-hemolysin couple HlgC-HlgB (*Figure 1C*). Anti-LukS-PV HCAb also binds to gamma hemolysin C (HlgC) and inhibits HlgC-HlgB pore formation. The IC_{50} of the anti-LukS-PV 3A11 and the bi-specific antibody were 1.14 nM and 0.31 nM (Laventie *et al.*, 2011), respectively for the PVL (LukS-PV 0.1 nM / LukF-PV 5 nM) and 0.10 and 0.12 nM respectively against HlgC-HlgB (HlgC 0.1 nM / HlgB 0.5 nM) as measured by Biacore™. The IC_{50} of anti-LukF-PV 4, 82, 125 and the bi-specific antibody 3A11-4 were 0.93, 0.91, 0.65 and 1.44 nM, respectively for PVL (LukS-PV 1 nM / LukF-PV 1 nM). Complete PVL inhibition was reached >3 nM of anti-LukS-PV, and 0.3 nM for gamma-hemolysin. This inhibition remains stable in time (maximum tested: 2 h). Complete PVL inhibition was reached with ~8 nM of anti-LukF-PV. If a higher amount of anti-LukS-PV 3A11 or anti-LukF-PV 4 (7 nM) is added 5 or 15 min after toxin application onto hPMNs, it stabilizes but does not reduce the ethidium entry slope. Thus, the antibodies block neo-pore formation, but for already formed pores we are not sure that the residual signal correspond to ethidium already stored into cells or reflect a somewhat equilibrium between cells loosing ethidium due to necrosis and a reduced entry of the molecule into permeated cells (see Laventie *et al.*, 2011). Strictly parallel observations were made for calcium entry. Finally, the observed neutralization was operating onto the binding of the targeted component in almost a 1:1 ratio.

Experiments *in vivo* in a toxin-induced rabbit endophthalmitis model showed these HCAbs inhibit inflammatory reactions and tissue destruction caused by leucotoxins. HCAbs are also biologically active *in vivo* by neutralizing the PVL effect in rabbit eye vitreous. While the inflammatory condition of eyes injected with PVL rapidly aggravate within 48hrs, the inhibition achieved with antibodies is stable in time (48 to > 96h) without apparent default in vision or behavior (*Figure 1D*). The same molar amount of tetravalent antibody dimer is

more effective than the HCAb dimers. Thus, the tetravalent complex offers advantage, because more effective at lower dose and, since it consists of a single chain, easier to produce. Our results suggest the possibility of antibody application in combination with intravitreal antimicrobial management strategy for post cataract surgery endophthalmitis and possibly other infections.

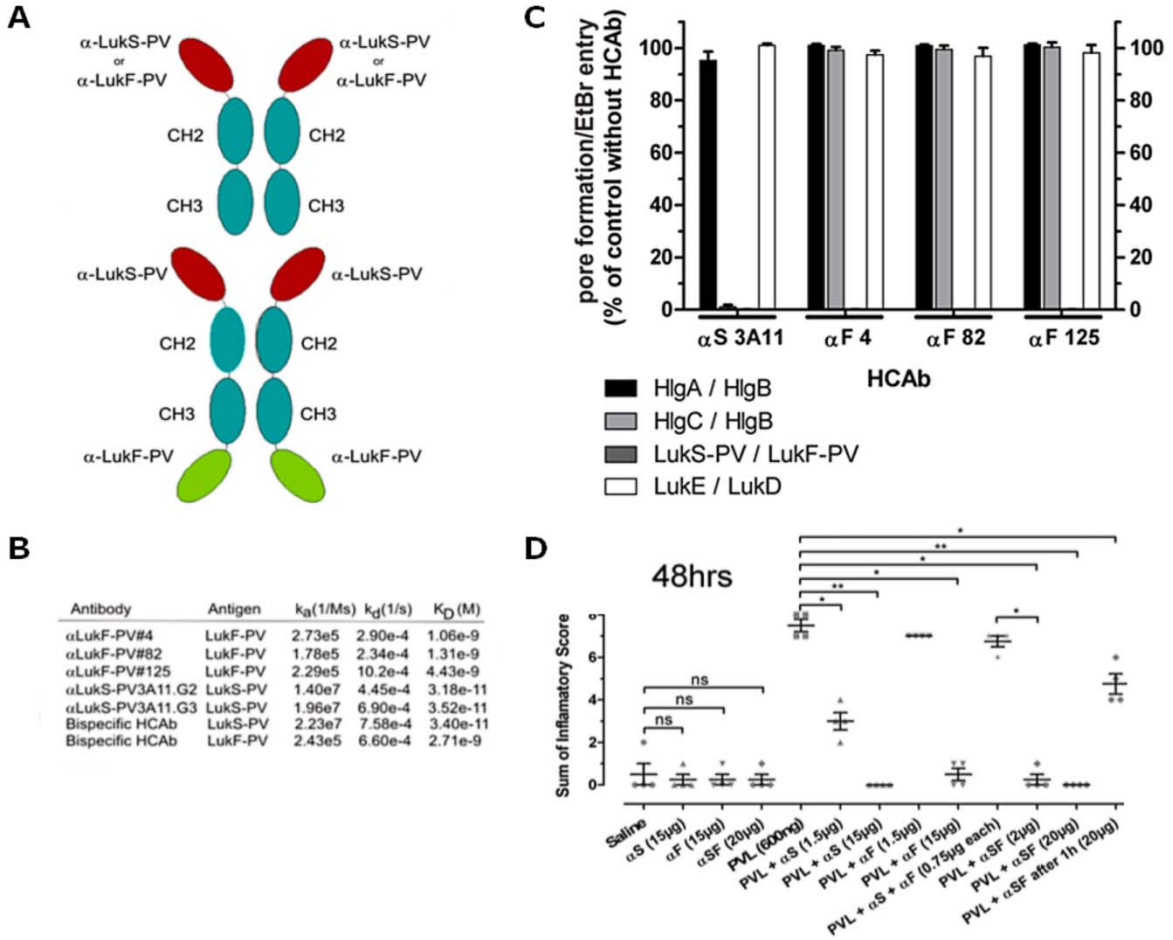

Antibody	Antigen	k_a(1/Ms)	k_d(1/s)	K_D(M)
αLukF-PV#4	LukF-PV	2.73e5	2.90e-4	1.06e-9
αLukF-PV#82	LukF-PV	1.78e5	2.34e-4	1.31e-9
αLukF-PV#125	LukF-PV	2.29e5	10.2e-4	4.43e-9
αLukS-PV3A11.G2	LukS-PV	1.40e7	4.45e-4	3.18e-11
αLukS-PV3A11.G3	LukS-PV	1.96e7	6.90e-4	3.52e-11
Bispecific HCAb	LukS-PV	2.23e7	7.58e-4	3.40e-11
Bispecific HCAb	LukF-PV	2.43e5	6.60e-4	2.71e-9

Figure 1. Blocking effect of recombinant humanized HCAbs onto staphylococcal leucotoxins. (**A**) Schematic structure of Heavy Chains only Antibodies and the constructed Tetravalent antibody directed against both LukS-PV and LukF-PV. (**B**) Affinity constants obtained by Surface Plasmon Resonance of the antibodies for targeted PVL components; the given values are means of three independant experiments. (**C**) Neutralization of the pore-forming activity onto human PMNs of the four tested HCAbs against various staphylococcal leucotoxins; errors barrs were obtained from 3 distinct experiments. (**D**) An inflammatory score of both the posterior and anterior chambers of rabbit eyes injected by PVL and/or HCAbs evidenced their power to neutralize the toxin effects; significant differences were established from three sets of data by the Mann-Whitney test.

Figure 1. *Les HCAbs humanisés recombinants anti-leucotoxines ont un effet neutralisant. (**A**) Structure schématique des HCAbs et de l'anticorps tétravalent reconstruit, dirigés contre LukS-PV et LukF-PV. (**B**) Constantes d'affinité déterminées en Résonance Plasmonique de Surface des anticorps pour les composés de la leucocidine de Panton et Valentine; les valeurs sont des valeurs moyennes issues de 3 expériences indépendantes. (**C**) Neutralisation de la formation des pores de 4 leucotoxines staphylococciques par les HCAbs; les barres d'erreurs sont issues de 3 expériences indépendantes réalisées sur des polynucléaires humains provenant de donneurs différents. (**D**) Scores inflammatoires combinés des chambres postérieure et antérieure d'yeux de lapin injectés par la PVL en présence ou non d'HCAbs ; les différences statistiques sont obtenues sur la base de trois séries d'analyses par le test de Mann-Whitney.*

Blocking the biological activity by small chemicals : calixarenes

Based on the rapid screening of molecules that would present a hydrodynamic diameter compatible with the entry of the pore of leucotoxins, we finally retain three cyclic compounds that differ by their complexity. They are *para*-sulfonato-calix[4 or 6 or 8]arenes (SCn; *Figure 2A*). These molecules were able to inhibit the full activity of most staphylococcal leucotoxins at a concentration of 30 µM when toxins were applied at nM concentrations onto synthetic membranes or liposomes or erythrocytes or human PMNs (Potrich G, personal communication). These calixarenes were not significantly hemolytic to human erythrocytes compared to the concentration cited. Also, they were not able to modify both the width and the granularity of human PMNs. Thus, no displacement and no necrosis were observed for these compounds applied onto PMNs in concentrations corresponding to a therapeutic index of 5 to 10. While the entry of calcium promptly promoted by leucotoxins was inhibited as well as that of the delayed entry of ethidium into the cells, we questioned whether these molecules may interfere with the binding of

toxins onto targeted cells. In fact, these molecules did not interact with membranes by themselves, since the calixarenes first applied, then washed by centrifugation from cells have no effect onto the further application of leucotoxins onto PMNs. By using fluorescent class S proteins and calixarenes and flow cytometry, we observed that the presence of calixarenes strongly inhibit this binding onto live cells compared with a competition with non fluorescent class proteins. This binding appeared sensitive to the presence of calixarenes, but SC4 has almost no influence while the two other molecules are effective. The binding of class F proteins was only affected with concentrations of SC6 or SC8 20-50-fold larger than those sufficient to inhibit class S proteins (*Figure 2C*). Moreover, SC6 and SC8 were able to interact with the class S protein bound to membranes that renders non effective a further application of the class F protein to operate an oligomer (*Figure 2D*). The application of calixarenes on already formed pores into PMNs led us to observe that neither calcium nor ethidium continued to accumulate into cells evoking that pores were arrested. In order to evidence a possible and direct interaction between class S protein and calixarenes, we used Electrospray mass spectrometry and Surface Plasmon Resonance (SPR; Anderluh G, personal communication). Electrospray mass spectrometry (ESI-MS/MS) allows to evidence that leucotoxins, placed in 50 mM ammonium acetate, pH 4.8 acquired, in the presence of SCn, bound SC8>SC6>>SC4 with some differences according to the class S proteins that were tested at a 1/1 ratio that may be displaced with an excess of SCn (*Figure 2B*).

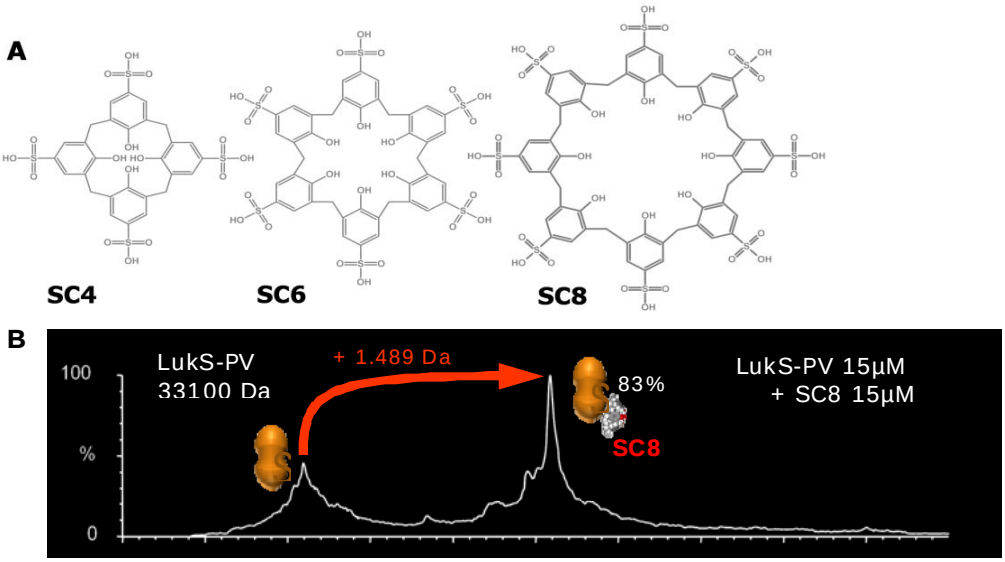

C

* n=3 SD<±8%	PVL : LukS-PV 0.1 nM / LukF-PV 5 nM			
	Ethidium entry		Fluorescent S binding	
	IC_{50} (µM)	IC_{90} (µM)	IC_{50} (µM)	IC_{90} (µM)
SC4	209	Nd	60	Nd
SC6	1.2	12.3	4.8	13.6
SC8	1.6	4.0	2.6	17.1
SC4*-1	210	1400	170	2900
SC4*-2	20.7	94	8.1	76
SC4*-3	14.6	52	6.3	47.4

D

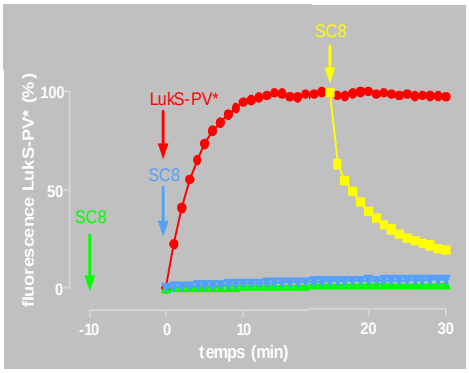

Figure 2. Some para-sulfonato calixarenes interact directly with class S leucotoxin proteins and inhibit their binding to membranes and biological activity. (**A**) Schematic plane structure of SC4, SC6 and SC8. (**B**) Acquisition of mass of LukS-PV after its incubation with SC8 as measured by using Electrospray Ionisation Mass Spectrometry corresponds to the interaction at a ratio 1:1. (**C**) Values of inhibitory concentrations 50% and 90% for the pore-forming activity onto human PMNs by flow cytometry and the binding of PVL and LukS-PV, respectively for six calixarenes; the given IC_{50}, IC_{90} (µM) values are direct means of three independant sets of data, standard errors never exceed 8%. (**D**) When the SC8 was applied after that of fluorescent LukS-PV onto human PMNs, there was a decrease of the bound LukS-PV indicating the displacement of the protein.

Figure 2. *Certains para-sulfonato calixarènes interagissent directement avec les leucotoxines et inhibent leur fixation sur les membranes et leurs fonctions biologiques. (**A**) Représentation schématique plane des SC4, SC6, et SC8. (**B**) La co-incubation de LukS-PV avec le SC8 implique une acquisition de masse, mesurée par spectrométrie de masse electrospray correspondant à celle de SC8. (**C**) Valeurs moyennes obtenues en cytométrie en flux de trois expériences indépendantes à partir des PMNs de donneurs différents de concentrations inhibitrices 50% et 90% (µM) pour la fonction de perméation des membranes révélée par l'entrée d'éthidium et pour la fixation aux membranes de LukS-PV fluorescent. (**D**) L'application de SC8 ultérieure à l'incubation de LukS-PV fluorescent sur les PMNs humains révèle en cytométrie en flux une chute de la fluorescence associée aux cellules.*

Once again, class F proteins did not significantly interact with calixarenes. SPR confirmed these data, and the resonance signal was disturbed when calixarenes or leucotoxins class S proteins were immobilised. Moreover, when liposomes were deposited onto SPR-chips, the binding of HlgA was decreased when we submit a flow of class S protein mixed with SCn. Finally, SC6 or SC8 demonstrated their efficacy *in vivo* by the proof that SC6 or SC8 are able to control the inflammation induced by the intra-vitreal injection of leucotoxins into the rabbit eye.

The development of new calixarenes (SC4-1, -2, -3) is now starting with the emergence of new SC4 derivatives that finally, are still non toxic, but can inhibit leucotoxins in a comparable manner and intensity as did SC6 and SC8 (*Figure 2C*). Such molecules may have interest due to their relatively low molecular weight and their relative solubility.

Blocking the pore of staphylococcal leucotoxins

In the screening cited above, a cyclic peptide had some influence onto the pore formation induced by HlgA-HlgB into liposomes and rabbit red blood cells. As such a peptide may have the interest to harbour a hydrodynamic diameter compatible with the upper side of the leucotoxin pore, it was evaluated onto human PMNs further incubated with HlgC-HlgB or with the PVL. In both cases, while the entry of ethidium was strongly reduced, the calcium entry remained comparable as for the toxin alone, despite low toxin concentrations (*Figure 3A, B*). Cells are naturally tight to ethidium, the two constitutive leucotoxin components are required to induce the entries of both calcium, then ethidium, thus this cyclic peptide can be considered as a tool for the further investigation of cell signaling mediated by leucotoxins.

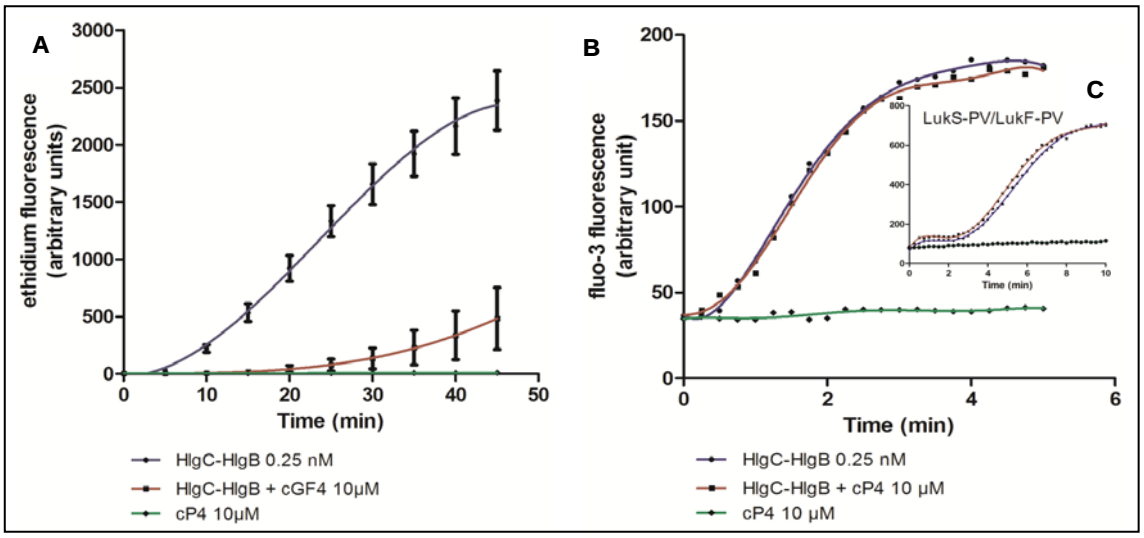

Figure 3. A cyclic peptide, cP4, is able to selectively block the pore-forming activity of staphylococcal leucotoxins in human PMNs. (**A**) When added at 10 µM, the cP4 peptide dramatically reduced the entry of ethidium induced by HlgC-HlgB in human PMNs; only a weak activity was recorded after 20 min of toxin application, whereas it is prominent in the control at the same time. (**B**) Inversely, the entry of Ca^{2+} remained at the same level as for the control. (**C**) The same influence of the peptide was observed on the PVL (LukS-PV 0.05 nM – LukF-PV 0.5 nM).

Figure 3. *Un peptide cyclique, cP4, bloque sélectivement l'activité de formation de pores des leucotoxines de staphylocoques sur les PMNs humains. (**A**) Lorsque le peptide est ajouté à 10 µM, il provoque un important retard de l'entrée d'éthidium dans les PMNs humains traités par HlgC-HlgB, dont le temps de latence est d'environ 20 min contre 5 min pour le contrôle. (**B**) Inversement, l'entrée de Ca^{2+} dans les mêmes cellules traitées par la même toxine n'est pas affectée. (**C**) Une influence similaire du peptide a été observée pour la leucocidine de Panton et Valentine.*

Blocking the calcium activation of staphylococcal leucotoxins

The use of the cyclic peptide described above allows the observation of Ca^{2+} signaling without the disastrous damage of pores that disturb evolution of cell signaling pathways. The origin of the rise of the intracellular Ca^{2+} induced by the leucotoxins is investigated by using flow cytometry and Ca^{2+} probes Fura-2 or Fluo-3, in order to identify the signaling pathways activated by these leucotoxins in human PMNs. Calcium channels were challenged with inhibitors to identify those channels activated in the presence of leucotoxins (Bird *et al.*, 2008). The 2-Aminoethoxydiphenyl borate (2-APB) is an inhibitor of IP_3-induced Ca^{2+} release and a blocker of store-operated Ca^{2+} entry (SOCE). When used in absence of extracellular Ca^{2+} (*Figure 4*), the 2-APB strongly inhibited the intracellular Ca^{2+} rise induced by HlgC-HlgB but not by the PVL. These results suggest that in the case of HlgC-HlgB, the IP_3-induced Ca^{2+} release is implicated in the Ca^{2+} signaling pathway. The use of Ryanodine, an inhibitor of the ryanodine receptor, has no effect on intracellular Ca^{2+} rise, thus allowing to conclude that the ryanodine receptors are not involved. In presence of extracellular Ca^{2+} (see *Figure 4*), the 2-APB also inhibited the intracellular Ca^{2+} rise induced by HlgC-HlgB but again not that of the PVL. In presence of extracellular Ca^{2+}, the 2-APB effect must be due to the inhibition of store-operated Ca^{2+} entry (SOCE) as well.

To prove the involvement of the SOCE in the leucotoxins induced Ca^{2+} signaling pathway in human PMNs, we used specific antibodies targeting the reticular Ca^{2+} sensor stromal interacting molecule (Stim), a component of the SOCE complex, and confocal microscopy (Staali *et al.*, 1998; Collins *et al.*, 2011; Roos *et al.*, 2005; Vamai *et al.*, 2009). The goat polyclonal N-19 antibody and the mouse monoclonal A-8 antibody were used to check the subcellular location of Stim-1 compared to the location of HlgC-HlgB and PVL tagged with Alexa-488 on HlgB and LukF-PV, respectively. *Figure 4* shows that the toxin localizes in an internal compartment which is also labeled by the anti Stim-1 antibodies.

In addition to these data, the use of other inhibitors such as N-(p-amylcinnamoyl)anthranilic acid (ACA), a direct blocker of several Transient Receptor Potential channels (TRP), suggest the involvement of TRPs in the intracellular Ca^{2+} rise induced by HlgC-HlgB.

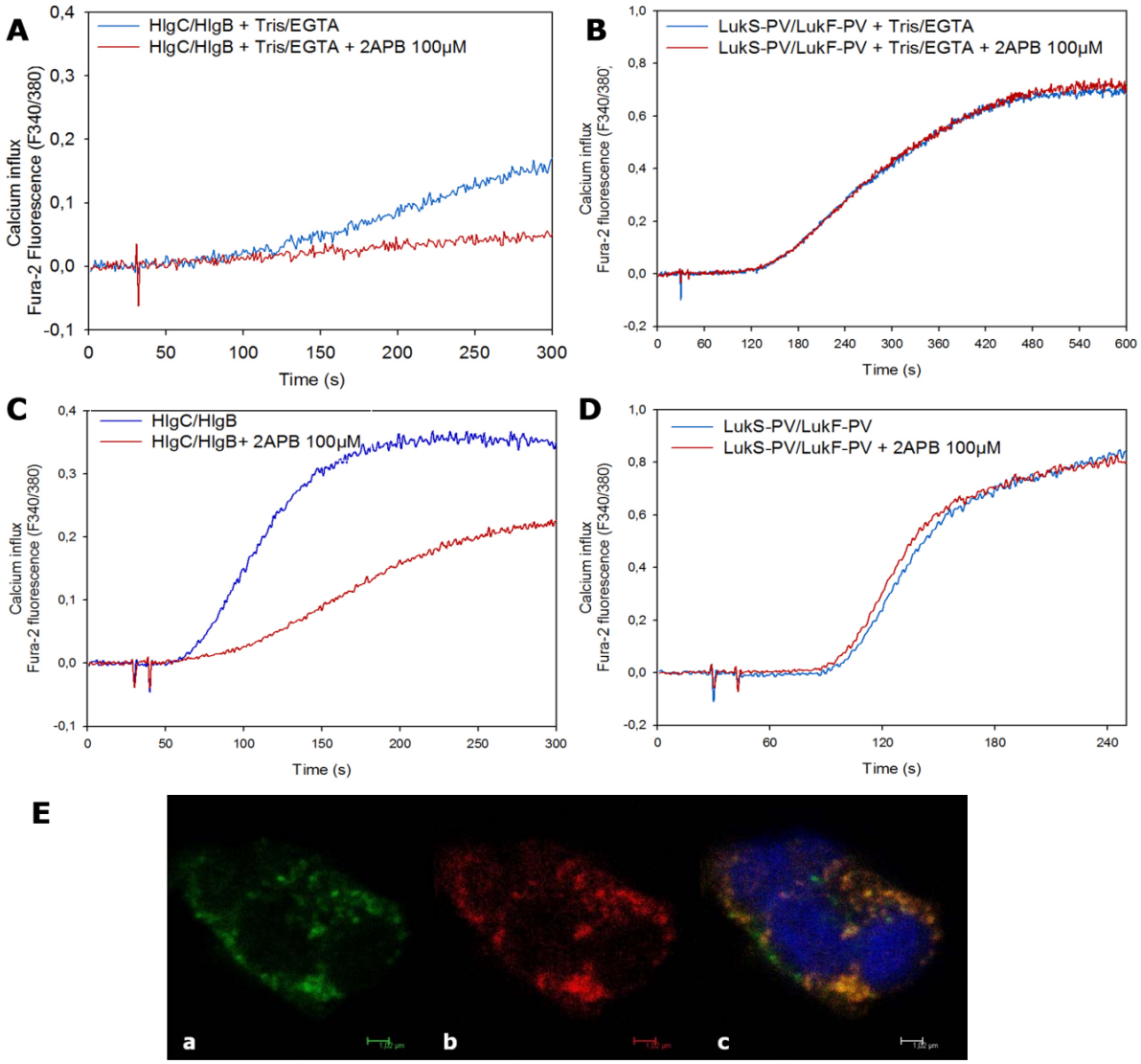

Figure 4. Effect of 2-APB on the increase in $[Ca^{2+}]_i$ due to HlgC- HlgB and PVL. In the absence of extracellular Ca^{2+}, 2-APB strongly inhibited the increase in $[Ca^{2+}]_i$ in the presence of (**A**) HlgC-HlgB, but not (**B**) PVL. Similarly, in the presence of extracellular Ca^{2+}, 2-APB inhibited the increase in $[Ca^{2+}]_i$ after treatment of cells with (**C**) HlgC-HlgB, but not (**D**) PVL. These results indicate that IP_3R, SOCs, and thus IP_3 pathway of hPMNs, are involved in calcium signaling of HlgC-HlgB. (**E**) Confocal microscopy of PMNs labelled with leucotoxin HlgC-HlgB-Alexa-488 (*green*) and the anti Stim-1 A-8 antibody (*red*). Photographs correspond to pixels labeled with both markers; (**a**) HlgC/HlgB, (**b**) A-8, and (**c**) merge. The nucleus is labeled with Hoesht 33258 (*blue*). Bars size = 1.02 µm.

Figure 4. *Effet du 2-APB sur l'influx de Ca^{2+} induit par HlgC-HlgB dans les PMNs humains. En l'absence de Ca^{2+} extracellulaire, le 2-APB inhibe très fortement l'augmentation de Ca^{2+} intra-cellulaire dans les cellules traitées par (**A**) HlgC-HlgB, (**B**) mais n'a pas d'influence si les PMNs sont traités par la PVL. De manière similaire, en présence de Ca^{2+} extra-cellulaire, le 2-APB inhibe l'influx de Ca^{2+} après le traitement des cellules par (**C**) HlgC-HlgB, mais pas (**D**) la PVL. Ces résultats indiquent que les récepteurs IP_3, les SOCs, et donc la voie IP_3, est mise en jeu dans les PMNs humains par la leucotoxine HlgC-HlgB, mais pas par la PVL. (**E**) Microscopie confocale des PMNs humains marqués par la leucotoxine HlgC-HlgB-Alexa-488* (vert), *et par l'anticorps A-8 anti-Stim-1* (rouge). *Les photographies correspondent aux pixels colorés par les deux marqueurs : (**a**) HlgC-HlgB*, (**b**) A-8µ, (**c**) la superposition des deux colorations. Les noyaux sont colorés au Hoechst 32528* (bleu). *Les barres représentent une échelle de 1,02 µm.*

In conclusion, our results suggest that following the binding of the leucotoxins to their membrane specific ligand at the plasma membrane, they can be internalized with Stim-1 into intracellular compartments triggering the intracellular Ca^{2+} increase as a result of calcium channels activation. Additional experiments should be done to decipher the internal distribution of the leucotoxins into cell compartments and the chronology and role of Ca^{2+} signals. One hypothesis would be that the internalised leucotoxin, by its presence in endosomes carrying Stim1, starts a process which includes the Ca^{2+} release from the endosome and that may be followed by the formation of the Stim1/ORAI1 complex. More work is needed to identify the signalling pathways and cell responses generated by leucotoxins.

Conclusion

We now have acquired different means to block both functions of staphylococcal leucotoxins or to selectively block pore-formation or Ca^{2+} activation in human PMNs, or into sensitive neurons (see Jover *et al.*, 2011). Both HCAbs and calixarenes approaches are exciting because they may give opportunity to block most or all bipartite leucotoxins and may be few other related toxins. They are now about to be evaluated in infectious models where they might provide some beneficial effects in the context of acute infections due to particular virulent strains where antimicrobial treatment only is not sufficient to eradicate infection or not satisfying enough to avoid irreversible tissue damage. The possibility to block pores really allows a more significant study of signal pathways involved by the action of low concentrations of leucotoxins or particular ones. At evidence this suggests the translocation of these toxin and their cell trafficking into endoplasm. This feature is now completed by a dissection of Ca^{2+} channels and pathways involved in the rise of divalent cation, and strongly the role of the complex Stim-1 / Orai1, which a novel concept of the action of these leucotoxins. Finally, it appeared that some of the Ca^{2+} inhibitors have no similar efficacies according to the leucotoxin analyzed, and again they appear more complex than speculated. Such studies applied on different target cells will evoke the complex proteomics operated according to tissues and may emphasize new knowledge in the understanding of some infections and associated inflammation.

Acknowledgements. *We thank Daniel Keller for toxins preparations and Raymonde Girardot for the skillful assistance at flow cytometry and spectrofluorimetry. Mira Tawk and Benoit Laventie were supported by doctoral fellowships from the Fondation Fouassier and the French Ministery of Superior Education, respectively. This study was supported by CNRS, Direction de la Recherche et des Etudes Doctorales, and authors greatly acknowledge a specific award from the "Conseil Scientifique de l'Université de Strasbourg".*

References

Baba-Moussa L, Sina H, Scheftel JM, Moreau B, Sainte-Marie D, Kotchoni SO, Prévost G, Couppié P (2011) Staphylococcal Panton-Valentine Leucocidin as a major virulence factor associated to furuncles. *PLoS ONE* **6**: e25716

Bird GS, DeHaven WI, *et al.* (2008) Methods for studying store-operated calcium entry. *Methods* **46**: 204-212

Collins SR, Meyer T (2011) Evolutionary origins of STIM1 and STIM2 within ancient Ca^{2+} signaling systems. *Trends Cell Biol* **21**: 202-211

Comai M, Dalla Serra M, Coraiola M, Werner S, Colin DA, Monteil H, Prévost G, Menestrina G (2002) Protein engineering modulates the transport properties and ion selectivity of the pores formed by staphylococcal gamma-haemolysins in lipid membranes. *Mol Microbiol* **44**: 1251-1267

Genestier AL, Michallet MC, Prévost G, *et al.* (2005) *Staphylococcus aureus* Panton-Valentine leukocidin directly targets mitochondria and induces Bax-independent apoptosis of human neutrophils. *J Clin Invest* **115**: 3117-3127

Jover E, Laventie B-J, Tawk M, Poulain B, Prévost G (2011) Neurotoxicity of *Staphylococcus aureus* leucotoxins : interaction with the store operated calcium entry complex in central and sensory neurons. In *Toxins and Ion transfers*. Barbier J, Benoit E, Gilles N, Ladant D, Martin-Eauclaire M-F, Mattéi C, Molgó J, Popoff M, Servent D (eds) pp 139-143. SFET Editions, Gif-sur-Yvette, France, Epub on http://www.sfet.asso.fr (ISSN 1760-6004)

Joubert O, Viero G, Keller D, *et al.* (2006) Engineered covalent leucotoxin heterodimers form functional pores: insights into S-F interactions. *Biochem J* **396**: 381-389

Laventie BJ, Rademaker R, Saleh M, de Boer E, Janssens R, Bourcier T, Subilia A, Marcellin L, van Haperen R, Lebbink JHG, Chen T, Prévost G, Grosveld F, Drabek D (2005) Heavy chain only antibodies and tetravalent bi-specific antibody neutralizing *Staphylococcus aureus* leucotoxins. *PNAS* **108**: 16404-16409

Miles G, Movileanu L, Bayley H (2002) Subunit composition of a bicomponent toxin: staphylococcal leukocidin forms an octameric transmembrane pore. *Protein Sci* **11**: 894-902

Prévost G (2005) Toxins in *Staphylococcus aureus* pathogenesis. In *Microbial Toxins: Molecular and Cellular Biology*. Proft T (ed) pp 243-284. Horizon Bioscience Press, Norfolk (UK)

Riegel P, Jesel-Morel L, Laventie B, Vandenesch F, Prévost G (2011) Coagulase-positive *Staphylococcus pseudintermedius* from animals causing human endocarditis and producing leukotoxins. *Int J Med Microbiol* **301**: 237-239

Roos J, DiGregorio PJ, *et al.* (2005) STIM1, an essential and conserved component of store-operated Ca^{2+} channel function. *J Cell Biol* **169**: 435-445

Varnai P, Hunyady L, *et al.* (2009) STIM and Orai: the long-awaited constituents of store-operated calcium entry. *Trends Pharmacol Sci* **30**: 118-128

Song L, Hobaugh MR, Shustak C, Cheley S, Bayley H, Gouaux, JE (1996) Structure of staphylococcal alpha-hemolysin, a heptameric transmembrane pore. *Science* **274**: 1859-1866

Staali L, Monteil H, Colin DA (1998) The staphylococcal pore-forming leukotoxins open Ca^{2+} channels in the membrane of human polymorphonuclear neutrophils. *J Membr Biol* **162**: 209-216

Ventura CL, Malachowa N, Hammer CH, Nardone GA, Robinson MA, Kobayashi SD, DeLeo FR (2010) Identification of a novel *Staphylococcus aureus* two-component leukotoxin using cell surface proteomics. *PLoS ONE* **5**: e11634

Viero G, Cunaccia R, Prévost G, Werner S, Monteil H, Keller D, Joubert O, Menestrina G, Dalla Serra (2006) Homologous *versus* heterologous interactions in the bicomponent staphylococcal gammahaemolysin pore. *Biochem J* **394**: 217-225

Viero G, Gropuzzo A, Joubert O, Keller D, Prévost G, Dalla Serra M (2008) A molecular pin to study the dynamics of beta-barrel formation in pore-forming toxins on erythrocytes: a sliding model. *Cell Mol Life Sci* **65**: 312-323

Yamashita K, Kawai Y, Tanaka Y, Hirano N, Kaneko J, Tomita N, Ohta M, Kamio Y, Yao M, Tanaka I (2011) Crystal structure of the octameric pore of staphylococcal γ-hemolysin reveals the β-barrel pore formation mechanism by two components. *PNAS* **108**: 17314-17319

Toxines et Transferts ioniques – Toxins and Ion transfers
Rencontres en Toxinologie – Meeting on Toxinology, 2011
Editions de la SFET – SFET Editions
Accès libre en ligne sur le site – Free access on line on the site : http://www.sfet.asso.fr

The cholesterol-dependent cytolysins : molecular mechanism to vaccine development

Rodney TWETEN

Department of Microbiology and Immunology, the University of Oklahoma Health Sciences Center, Oklahoma City, Oklahoma 73104, USA

Tel : +1 405 271-1205 ; Fax : +1 405 271-3117 ; E-mail : rod-tweten@ouhsc.edu

Abstract

The cholesterol-dependent cytolysins (CDCs) are a large family of pore forming toxins that contribute to the pathogenesis of many Gram-positive pathogenic bacteria. The study of the pore forming mechanism of these toxins has revealed that they undergo a series of remarkable structural transitions during their transition from soluble monomers to a membrane-embedded oligomeric pore complex. These studies have led to the discovery that the family of eukaryotic and prokaryotic membrane attack complex/perforin (MACPF) proteins may use a CDC-like mechanism to form pores and may be ancient ancestors of the CDCs. Finally, understanding the molecular mechanism of the CDCs has allowed the rational design of potential vaccine derivatives of the CDCs that maintain the antigenic structure of their soluble form.

Les cytolysines dépendantes du cholestérol : du mécanisme moléculaire au développement de vaccins

Les cytolysines dépendantes du cholestérol (CDC) constituent une grande famille de toxines formant des pores qui contribuent à la pathogenèse de nombreuses bactéries pathogènes à Gram-positif. L'étude du mécanisme de formation de pores de ces toxines a révélé qu'elles subissent une série de transitions structurelles remarquables pendant leur transition de monomères solubles en complexes oligomériques formant des pores insérés dans la membrane. Ces études ont mené à la découverte que la famille de protéines, procaryotes et eucaryotes, qui forment des complexes attaquant ou perforant les membranes (membrane attack complex/perforin; MACPF) peuvent utiliser un mécanisme similaire à celui des CDC pour former des pores et pourraient être les ancêtres des CDC. Enfin, la compréhension du mécanisme moléculaire des CDC a permis une conception rationnelle de vaccins potentiels dérivés des CDC qui maintiennent la structure antigénique de leur forme soluble.

Keywords : *Cholesterol-dependent cytolysins, intermedilysin, membrane attack complex/perforin, perfringolysin O, pneumolysin, pore-forming toxin*.

Introduction

The CDCs constitute a large class of cytolytic pore-forming proteins that contribute to the pathogenesis of many Gram-positive bacteria. The CDCs are secreted as soluble monomers, which then bind to cholesterol-rich membranes and assemble a large β-barrel pore (Hotze and Tweten, 2011). The CDCs have been shown to function as primary or ancillary pathogenesis factors in those bacterial pathogens where the role of the CDC has been studied. Whether they also serve other roles remains unclear. Many CDC producing bacteria are infrequent opportunistic pathogens and spend most of their life as commensals. Hence, it is possible that CDCs may also contribute to the maintenance of the commensal state of many bacterial species in ways that remain unclear.

Although the CDCs are termed β-hemolytic toxins, it is unlikely that CDC-mediated hemolysis is a primary feature of CDCs during pathogenesis. In fact, the use of CDCs as general cytolytic agents has not been rigorously shown to be a primary function of any CDC. It is not necessary to form a pore comprised of 30-40 monomers with a diameter 20-30 nM, as is formed by the CDCs (Czajkowsky *et al*., 2004), to lyse a cell. A much smaller pore would function as an efficient lytic agent at a significantly lower energy cost to the cell. Presumably, the large pore formed by the CDC is used in more sophisticated ways by bacteria than as a brute force cytolytic agent, although how bacterial pathogens employ the large pore to cause a myriad of cellular effects remains less well understood.

The CDCs, formerly known by various names including the thiol-activated cytolysins, oxygen labile toxins or cholesterol binding toxins, exhibit several hallmark characteristics that include a complete dependence on

cholesterol for their cytolytic activity, the formation of extraordinarily large pore complexes and the presence of an 11 residue signature peptide motif termed the undecapeptide or tryptophan-rich motif. Many bacterial pore-forming toxins assemble β-barrel pores (Olson and Gouaux, 2005; Olson *et al.*, 1999; Song *et al.*, 1996): the mechanism by which the CDCs assemble their β-barrel pore, however, exhibits many novel features not previously observed in other β-barrel pore forming toxins. Herein the focus will be on the current state of understanding of the structure and pore forming mechanism of the CDCs.

Membrane recognition by the CDCs

For nearly 60 years the CDC cytolytic mechanism was known to be sensitive to the presence of membrane cholesterol (Howard *et al.*, 1953): membranes that lack cholesterol are not sensitive to pore formation by the CDCs. The ability to inhibit the lytic activity of the CDCs with added cholesterol has been one measure of whether a pore forming protein may be a CDC. Many studies have been performed on the interaction of the CDCs with cholesterol. It has been assumed that cholesterol inhibited the CDCs by occupying a receptor binding site that specifically bound membrane cholesterol. However, as described below, the nature of the cholesterol binding motif has been elusive and only recently has its structure been identified.

The structural requirements of the sterol for CDC recognition and binding are fairly rigid. Prigent and Alouf (1976) initially performed a series of analyses that elucidated these requirements, which showed that the CDCs primarily bind to cholesterol and closely related sterols that maintain an intact 3-β-hydroxy headgroup. It is clear that the 3-β-hydroxyl is a key determinant for binding as any perturbation of this structure, even a change in its stereochemistry, abrogates binding. The surrounding lipid structure also has a significant influence on the ability of CDCs to recognize and bind to cholesterol: studies have shown that lipids that pack tightly with cholesterol or that have large headgroups can decrease the ability of the CDCs to recognize and bind cholesterol (Flanagan *et al.*, 2009; Nelson *et al.*, 2008), presumably by steric occlusion of the small 3-β-hydroxy headgroup of cholesterol.

Until recently it was generally accepted that the conserved undecapeptide signature motif (*Figure 1*) of the CDCs was the cholesterol-recognition/binding motif (CRM). Mutations or chemical modification of the undecapeptide residues often affected binding affinity, but never completely abrogated binding (Nakamura *et al.*, 1995; Ohno-Iwashita *et al.*, 1988). More recently, Soltani *et al.* (2007) showed that membrane insertion of the three domain 4 loops (L1-L3, *Figure 1*) was cholesterol dependent, but membrane insertion of the undecapeptide was not, which suggested that the CRM was located in one or more of these three loops. Farrand *et al.* (2010) recently identified the CRM in loop L1 (*Figure 1*) and showed that it is comprised of a threonine-leucine pair. The structure of the CRM was surprisingly simple, but then the structure of the cholesterol headgroup exposed at the surface of the bilayer is also comparatively limited since it is comprised of the 3-β-hydroxy. The Thr-Leu pair is conserved in all known CDCs suggesting that its structure cannot be changed, even by substitution of conservative mutations. Farrand *et al.* (2010) confirmed this by showing that the most conservative mutations of these residues resulted in dramatic loss of binding activity on cells.

A small, but growing family of CDCs use human CD59 as their receptor rather than cholesterol: these CDCs include *Streptococcus intermedius* intermedilysin (ILY; Giddings *et al.*, 2004), *Gardnerella vaginalis* vaginolysin (VLY; Gelber *et al.*, 2008) and *Streptococcus mitis* lectinolysin (LLY; Wickham *et al.*, 2011). The pore-forming activity of these CDCs, however, remains cholesterol dependent. LaChapelle *et al.* and Farrand *et al.* solved the basis for the cholesterol-dependence of these toxins (Farrand *et al.*, 2010; LaChapelle *et al.*, 2009). LaChapelle *et al.* showed that ILY disengaged from CD59 upon prepore to pore conversion. Farrand *et al.* subsequently demonstrated that if the CRM was knocked out in ILY it dissociated from the membrane upon prepore to pore conversion. Hence, to maintain contact with the membrane during prepore to pore conversion the CRM of the CD59 binding CDCs must initiate the cholesterol dependent membrane insertion of loops L1-L3, which firmly anchors the prepore complex to the membrane.

Formation of the CDC prepore structure

Upon membrane binding the CDC monomers interact with each other to form the prepore complex. The assembly of the large CDC pore complex is a complex process that is only partially understood. The oligomeric complex of perfringolysin O (PFO) is assembled from 34-37 monomers (Czajkowsky *et al.*, 2004). It was demonstrated by Shepard *et al.* (2000) that PFO formed a prepore complex prior to the insertion of the β-barrel pore and subsequently Hotze *et al.* (2001) showed that PFO could be engineered with a disulfide to trap it in the prepore state and upon its reduction the β-barrel pore rapidly inserted into the membrane. These studies also showed that the oligomerization of the membrane bound monomers of PFO into the prepore complex was the rate-limiting step in the assembly of the pore complex. It is currently unknown if the β-barrel pore forms prior to its insertion into the membrane, but it seems likely since the formation of interstrand hydrogen bonds would greatly reduce the energy cost of their insertion by satisfying the hydrogen bond potential of the polar atoms of the β-hairpin backbone.

The soluble monomers of PFO do not oligomerize in solution, even at the high concentrations required for crystallization. At high concentrations head-to-tail dimers are formed, but it is not clear if these are present at the concentrations expressed by bacteria during infections. One reason that soluble monomers cannot oligomerize is the edge-on interaction of β-strand 5 (β5) with β4 (*Figure 1*), which blocks the intermolecular interaction of β1 of one monomer with β4 of another monomers. In membrane bound monomers β5 must break its edge-on interaction with β4 and swing out of the way to allow the formation backbone hydrogen bonds between β4 and β1 of another monomer. The disruption of this interaction appears to be initiated by the

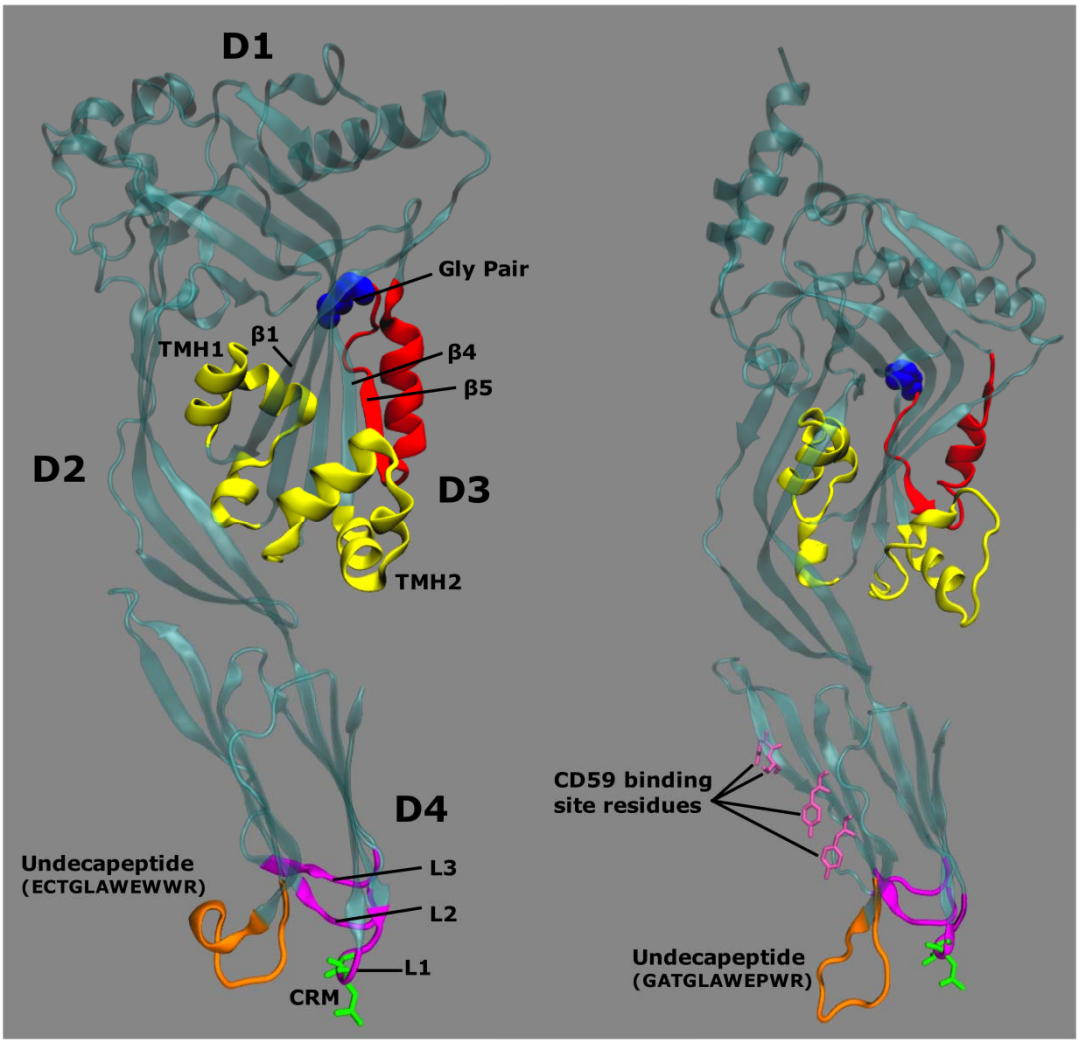

Figure 1. Crystal structures of perfringolysin O and intermedilysin monomers. Shown are some of the features of the soluble monomer structures of perfringolysin O (PFO, *left panel*; Rossjohn *et al.*, 1997) and intermedilysin (ILY, *right panel*; Polekhina *et al.*, 2005). The locations are shown of the α-helices (*yellow*) that ultimately form the transmembrane hairpins (TMHs) that comprise the membrane spanning β-barrel pore. Also shown are the following structures: β5, which swings away from β4 to allow edge-on interactions between β4 of one monomer with β1 of another monomer, the location of the glycine pair (*blue space-filled atoms*) between β4 and β5 that are conserved in all CDCs and are also conserved in the MACPF proteins, loops 1-3 (L1-L3) that insert into the bilayer to anchor the monomers perpendicular to the membrane surface (*magenta*), the Thr-Leu pair (*green*) that comprise the cholesterol recognition/binding motif (CRM) and the location of the conserved undecapeptide motif (*orange*). *On the right* the same structures are shown in the CD59 binding CDC, ILY. In addition, the residues that comprise the CD59 binding motif and the undecapeptide, are different from that of PFO.

Figure 1. Structures cristallines des monomères de perfringolysine O et d'intermedilysine*. La figure montre quelques-unes des caractéristiques structurales du monomère soluble de la perfringolysine O (PFO,* panneau de gauche*; Rossjohn* et al.*, 1997) et d'intermédilysine (ILY,* panneau de droite*; Polekhina* et al.*, 2005). Les localisations des hélices alpha (*jaune*), qui forment finalement les épingles transmembranaires (TMH) constituant la structure du pore en cylindre-béta s'insérant dans la membrane, sont indiquées. Les structures suivantes sont aussi montrées: β5, qui oscille loin de β4 pour permettre l'interaction bord à bord entre β4 d'un monomère et β1 d'un autre monomère, l'emplacement de la paire de glycine (*atomes bleus*) entre β4 et β5 qui sont conservées dans tous les CDC et qui sont également conservées dans les protéines MACPF, les boucles 1-3 (L1-L3) qui s'insèrent dans la bicouche pour ancrer les monomères perpendiculairement à la surface de la membrane (*magenta*), la paire Thr-Leu (*vert*) qui compose le motif de reconnaissance du cholestérol (CRM), et l'emplacement du motif conservé de 11 résidus (undécapeptide;* orange*).* Sur la droite *sont présentées les mêmes structures de la CDC liant CD59, l'ILY. De plus, les résidus qui constituent le motif de liaison à CD59 et l'undécapeptide, sont différents de ceux de PFO.*

interaction of the monomers with the membrane (Ramachandran *et al.*, 2004). The formation of a π-stacking interaction of two aromatic residues in β1 (Tyr-181) and β4 (Phe-318) is also necessary to the formation of the pore complex. Loss of either aromatic resulted in a cytolytically inactive oligomeric complex. We have proposed that the stacking of these two residues maintains the correct intermolecular pairing of transmembrane hairpins (TMHs; Ramachandran *et al.*, 2004), but this may not be the entire story. These two residues are conserved in most CDCs but they are not conserved in all CDCs, which suggests that their function(s) has been accomplished in a different way in these CDCs.

Conversion of the prepore to the pore complex

A key structural transition in the formation of the β-barrel pore is the disruption of the domain 2-3 interface where the α-helical bundle that ultimately forms TMH1 (*Figure 1*) is buried. This interface is not complementary suggesting it has evolved to be easily disrupted (Rossjohn *et al.*, 1997). Using a variety of fluorescence spectroscopic methods Shepard *et al.* (1998) and Shatursky *et al.* (1999) demonstrated that the two sets of α-helical bundles in domain 3 were converted into membrane spanning amphipathic β-hairpins (TMH1 and TMH2, *Figure 1*). As indicated above, it is likely that TMH1 and TMH2 assemble into a partially or wholly formed pre-β-barrel prior to membrane insertion. In membrane bound monomers domain 3 is positioned about 40 Å above the membrane, thus when TMH1 and TMH2 are extended into hairpins this would allow them to form a pre-β-barrel above the bilayer. This scenario, however, also engendered a problem: Shepard *et al.* (1998) and Shatursky *et al.* (1999) clearly showed the TMHs extended across the membrane, yet the fact that domain 3 was suspended 40 Å above the membrane showed that the extended TMHs were only long enough to reach the membrane surface but not cross it. This conundrum was resolved by Czajkowsky *et al.* (2004) who showed by atomic force microscopy that the prepore complex underwent a 40 Å vertical collapse that brought domains 1 and 3 sufficiently close to the membrane to allow the TMHs to span the bilayer. This was subsequently confirmed by Ramachandran *et al.* (2005) using fluorescence resonance energy transfer (FRET) based distance measurements. Hence, these studies suggest that the CDCs assemble the β-barrel pore above the bilayer, thereby satisfying the hydrogen bond potential of the TMH peptide backbone and decreasing the energetic cost of their membrane insertion, and then undergoing a vertical collapse that plunges the β-barrel pore into the membrane.

The membrane attack complex/perforin family of proteins

The molecular structure of the CDCs exhibits many distinct features: the most notable of these is the structure of domain 3, which forms the transmembrane β-barrel (*Figure 1*). The domain 3 protein fold was not found in another family of proteins until the solution of several membrane attack complex/perforin (MACPF) family proteins. The crystal structures of the soluble monomers of several MACPF family proteins (*Figure 2*) revealed a protein fold that exhibited a remarkable similarity to the domain 3 of the CDCs. Based on this structural similarity it has been suggested that the MACPF family proteins form a β-barrel pore that originates from the unfolding of the α-helical bundles found in the domain 3-like protein fold of the MACPF proteins. Whether this is true remains to be proven, but seems likely given the fact that the CDC domain 3 fold exhibits several unique features that are designed to form its β-barrel pore and these features appear to be maintained in the MACPF proteins.

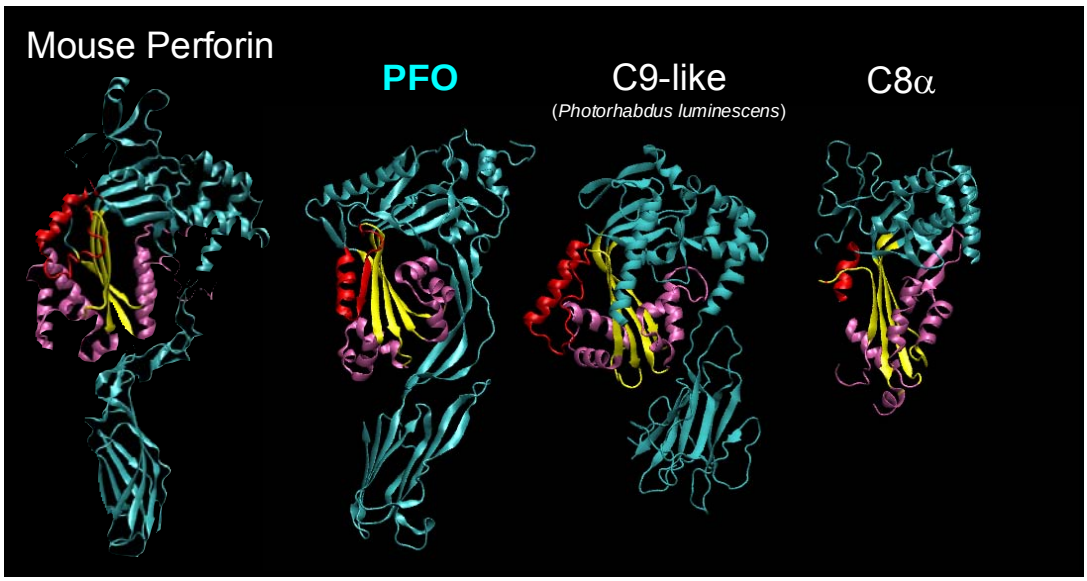

Figure 2. Structure of MACPF monomers. Shown are the crystal structures of three MACPF family proteins: mouse perforin (Law *et al.*, 2010), a complement C9-like protein from *Photorhabdus luminescens* (Rosado *et al.*, 2007) and human complement C8α (Hadders *et al.*, 2007; Slade *et al.*, 2008), compared to that of PFO (Rossjohn *et al.*, 1997). Shown are the structures in the MACPF proteins that exhibit a similar structural fold to domain 3 of PFO which forms the TMHs (*magenta*), the domain 3 core β-sheet (*yellow*) and the short loop (*red*) comprised of β5 and a short α-helix.

Figure 2. Structure des monomères MACPF. *La figure montre les structures cristallines de trois protéines de la famille MACPF: la perforine de souris (Law* et al.*, 2010), une protéine de* Photorhabdus luminescens *similaire au complément C9 (Rosado* et al.*, 2007) et le complément humain C8α (Hadders* et al.*, 2007; Slade* et al.*, 2008), comparées à celle de la PFO (Rossjohn* et al.*, 1997). La figure montre les structures des protéines MACPF qui présentent un repliement structural similaire à celui du domaine 3 de la PFO qui forme les TMHs (*magenta*), le domaine 3 du cœur du feuillet β (*jaune*) et la boucle courte (*rouge*) composée de β5 et d'une courte hélice α.*

Designing a better *Streptococcus pneumoniae* vaccine

S. pneumoniae is a major cause of pneumonia worldwide and in developing countries children are especially vulnerable to this infection. Current *S. pneumoniae* vaccines are based on the polysaccharide capsule, of which there are over 90 different variations. Current vaccines of capsule cover 23 serotypes and conjugate vaccines for children under 2 years cover 13 serotypes. These vaccines are complex and costly to produce, and it has been shown that serotype shifts can occur (Gladstone *et al.*, 2011; Park *et al.*, 2008). Furthermore, the genome of *S. pneumoniae* exhibits a remarkable plasticity (Croucher *et al.*, 2011), suggesting it is capable of significant adaptation to vaccine and antibiotic pressure. A protein-only vaccine has not been developed for *S. pneumoniae*, but would be advantageous if one could be developed that was comprised of conserved proteins that covered most or all serotypes. Surprisingly a conserved pathogenesis factor, the *S. pneumoniae* CDC pneumolysin (PLY), has never been incorporated into vaccine formulations. This has been in part due to residual toxicity of genetically inactivated variants of PLY.

The problem of residual toxicity can now be overcome by a variety of methods now that we have a much better understanding of the mechanism of the CDCs and how they can be inactivated. We have developed several different approaches to inactivating CDCs (Hotze *et al.*, 2002; Hotze *et al.*, 2001; Ramachandran *et al.*, 2004). Decreasing toxicity of PLY, however, is only the first part of generating a better vaccine version of this toxin: how it is accomplished and the nature of the resulting toxoid may also be important. As is evident from the above discussion once the CDC binds to the cell surface via cholesterol a series of conformational changes are initiated and the monomers oligomerize. These processes change the epitope structure of the CDC monomer and occlude epitopes at interacting protein surfaces. Based on our studies all potential PLY vaccine candidates reported to date still retain the capacity to bind the cell in a cholesterol-dependent fashion and undergo some oligomerization. The best version of a CDC vaccine would theoretically prevent binding thereby preventing these structural changes, which would preserve the structure and solubility of the monomer. This would preserve all of the epitopes that would be potentially neutralizing, which would include regions of the CDC involved in binding, oligomerization and insertion of the β-barrel pore. Until recently this type of mutant was not possible since the true identity of the cholesterol-binding motif was not known. Only with the discovery of the cholesterol recognition/binding motif (Farrand *et al.*, 2010) could we generate this mutant. By altering the cholesterol cholesterol-binding motif of PLY to prevent binding, we were able to generate a non-binding mutant that was >20,000-fold less toxic than native PLY and that preserved the solubility and structure of the monomer. Studies with this mutant have demonstrated that this mutant performs well in animal challenge studies and is significantly more protective than native PLY.

Conclusions

The study of the CDC pore forming mechanism has revealed a pore forming mechanism that established many new paradigms and has provided a deep understanding into the molecular transitions that occur as the CDCs make the transition from a soluble monomer to the large membrane embedded pore complex. Furthermore, our understanding of the pore forming mechanism of the CDCs has enable us to rationally design better CDC-based vaccines and has allowed others to propose a pore forming mechanism for the large family of MACPF proteins that play key roles in immune defense and in the pathogenesis of eukaryotic organisms such as *Toxoplasma* and malaria. It is likely that the continued studies of the large family of CDCs will reveal new paradigms and will broaden our understanding of their roles in bacterial pathogenesis.

References

Croucher NJ, Harris SR, Fraser C, Quail MA, Burton J, van der Linden M, McGee L, von Gottberg A, Song JH, Ko KS, Pichon B, Baker S, Parry CM, Lambertsen LM, Shahinas D, Pillai DR, Mitchell TJ, Dougan G, Tomasz A, Klugman KP, Parkhill J, Hanage WP, Bentley SD (2011) Rapid pneumococcal evolution in response to clinical interventions. *Science* **331**: 430-434

Czajkowsky DM, Hotze EM, Shao Z, Tweten RK (2004) Vertical collapse of a cytolysin prepore moves its transmembrane β-hairpins to the membrane. *EMBO J* **23**: 3206-3215

Farrand AJ, LaChapelle S, Hotze EM, Johnson AE, Tweten RK (2010) Only two amino acids are essential for cytolytic toxin recognition of cholesterol at the membrane surface. *Proc Natl Acad Sci USA* **107**: 4341-4346

Flanagan JJ, Tweten RK, Johnson AE, Heuck AP (2009) Cholesterol exposure at the membrane surface is necessary and sufficient to trigger perfringolysin O binding. *Biochemistry* **48**: 3977-3987

Gelber SE, Aguilar JL, Lewis KL, Ratner AJ (2008) Functional and phylogenetic characterization of Vaginolysin, the human-specific cytolysin from *Gardnerella vaginalis*. *J Bacteriol* **190**: 3896-3903

Giddings KS, Zhao J, Sims PJ, Tweten RK (2004) Human CD59 is a receptor for the cholesterol–dependent cytolysin intermedilysin. *Nat Struct Mol Biol* **11**: 1173-1178

Gladstone RA, Jefferies JM, Faust SN, Clarke SC (2011) Continued control of pneumococcal disease in the UK - the impact of vaccination. *J Med Microbiol* **60**: 1-8

Hadders MA, Beringer DX, Gros P (2007) Structure of C8alpha-MACPF reveals mechanism of membrane attack in complement immune defense. *Science* **317**: 1552-1554

Hotze EM, Heuck AP, Czajkowsky DM, Shao Z, Johnson AE, Tweten RK (2002) Monomer-monomer interactions drive the prepore to pore conversion of a beta-barrel-forming cholesterol-dependent cytolysin. *J Biol Chem* **277**: 11597-11605

Hotze EM, Tweten RK (2011) Membrane assembly of the cholesterol-dependent cytolysin pore complex. *Biochim Biophys Acta*

Hotze EM, Wilson-Kubalek EM, Rossjohn J, Parker MW, Johnson AE, Tweten RK (2001) Arresting pore formation of a cholesterol-dependent cytolysin by disulfide trapping synchronizes the insertion of the transmembrane beta-sheet from a prepore intermediate. *J Biol Chem* **276**: 8261-8268

Howard JG, Wallace KR, Wright GP (1953) The inhibitory effects of cholesterol and related sterols on haemolysis by streptolysin. *Br J Exp Pathol* **34**: 174-180

LaChapelle S, Tweten RK, Hotze EM (2009) Intermedilysin-receptor interactions during assembly of the pore complex: assembly intermediates increase host cell susceptibility to complement-mediated lysis. *J Biol Chem* **284**: 12719-12726

Law RH, Lukoyanova N, Voskoboinik I, Caradoc-Davies TT, Baran K, Dunstone MA, D'Angelo ME, Orlova EV, Coulibaly F, Verschoor S, Browne KA, Ciccone A, Kuiper MJ, Bird PI, Trapani JA, Saibil HR, Whisstock JC (2010) The structural basis for membrane binding and pore formation by lymphocyte perforin. *Nature* **468**: 447-451

Nakamura M, Sekino N, Iwamoto M, Ohno-Iwashita Y (1995) Interaction of theta-toxin (perfringolysin O), a cholesterol-binding cytolysin, with liposomal membranes: change in the aromatic side chains upon binding and insertion. *Biochemistry* **34**: 6513-6520

Nelson LD, Johnson AE, London E (2008) How interaction of perfringolysin O with membranes is controlled by sterol structure, lipid structure, and physiological low pH: insights into the origin of perfringolysin O-lipid raft interaction. *J Biol Chem* **283**: 4632-4642

Ohno-Iwashita Y, Iwamoto M, Mitsui K, Ando S, Nagai Y (1988) Protease-nicked theta-toxin of Clostridium perfringens, a new membrane probe with no cytolytic effect, reveals two classes of cholesterol as toxin-binding sites on sheep erythrocytes. *Eur J Biochem / FEBS* **176**: 95-101

Olson R, Gouaux E (2005) Crystal structure of the Vibrio cholerae cytolysin (VCC) pro-toxin and its assembly into a heptameric transmembrane pore. *J Mol Biol* **350**: 997-1016

Olson R, Nariya H, Yokota K, Kamio Y, Gouaux E (1999) Crystal structure of Staphylococcal LukF delineates conformational changes accompanying formation of a transmembrane channel. *Nature Struct Biol* **6**: 134-140

Park SY, Moore MR, Bruden DL, Hyde TB, Reasonover AL, Harker-Jones M, Rudolph KM, Hurlburt DA, Parks DJ, Parkinson AJ, Schuchat A, Hennessy TW (2008) Impact of conjugate vaccine on transmission of antimicrobial-resistant *Streptococcus pneumoniae* among Alaskan children. *Pediatr Infect Dis J* **27**: 335-340

Polekhina G, Giddings KS, Tweten RK, Parker MW (2005) Insights into the action of the superfamily of cholesterol-dependent cytolysins from studies of intermedilysin. *Proc Natl Acad Sci USA* **102**: 600-605

Prigent D, Alouf JE (1976) Interaction of streptolysin O with sterols. *Biochem Biophys Acta* **433**: 422-428

Ramachandran R, Tweten RK, Johnson AE (2004) Membrane-dependent conformational changes initiate cholesterol-dependent cytolysin oligomerization and intersubunit β-strand alignment. *Nat Struct Mol Biol* **11**: 697-705

Ramachandran R, Tweten RK, Johnson AE (2005) The domains of a cholesterol-dependent cytolysin undergo a major FRET-detected rearrangement during pore formation. *Proc Natl Acad Sci USA* **102**: 7139-7144

Rosado CJ, Buckle AM, Law RH, Butcher RE, Kan WT, Bird CH, Ung K, Browne KA, Baran K, Bashtannyk-Puhalovich TA, Faux NG, Wong W, Porter CJ, Pike RN, Ellisdon AM, Pearce MC, Bottomley SP, Emsley J, Smith AI, Rossjohn J, Hartland EL, Voskoboinik I, Trapani JA, Bird PI, Dunstone MA, Whisstock JC (2007) A common fold mediates vertebrate defense and bacterial attack. *Science* **317**: 1548-1551

Rossjohn J, Feil SC, McKinstry WJ, Tweten RK, Parker MW (1997) Structure of a cholesterol-binding thiol-activated cytolysin and a model of its membrane form. *Cell* **89**: 685-692

Shatursky O, Heuck AP, Shepard LA, Rossjohn J, Parker MW, Johnson AE, Tweten RK (1999) The mechanism of membrane insertion for a cholesterol dependent cytolysin: A novel paradigm for pore-forming toxins. *Cell* **99**: 293-299

Shepard LA, Heuck AP, Hamman BD, Rossjohn J, Parker MW, Ryan KR, Johnson AE, Tweten RK (1998) Identification of a membrane-spanning domain of the thiol-activated pore-forming toxin *Clostridium perfringens* perfringolysin O: an α-helical to β-sheet transition identified by fluorescence spectroscopy. *Biochemistry* **37**: 14563-14574

Shepard LA, Shatursky O, Johnson AE, Tweten RK (2000) The mechanism of assembly and insertion of the membrane complex of the cholesterol-dependent cytolysin perfringolysin O: Formation of a large prepore complex. *Biochemistry* **39**: 10284-10293

Slade DJ, Lovelace LL, Chruszcz M, Minor W, Lebioda L, Sodetz JM (2008) Crystal structure of the MACPF domain of human complement protein C8 alpha in complex with the C8 gamma subunit. *J Mol Biol* **379**: 331-342

Soltani CE, Hotze EM, Johnson AE, Tweten RK (2007) Structural elements of the cholesterol-dependent cytolysins that are responsible for their cholesterol-sensitive membrane interactions. *Proc Natl Acad Sci USA* **104**: 20226-20231

Song LZ, Hobaugh MR, Shustak C, Cheley S, Bayley H, Gouaux JE (1996) Structure of staphylococcal alpha-hemolysin, a heptameric transmembrane pore. *Science* **274**: 1859-1866

Wickham SE, Hotze EM, Farrand AJ, Polekhina G, Nero TL, Tomlinson S, Parker MW, Tweten RK (2011) Mapping the intermedilysin-human CD59 receptor interface reveals a deep correspondence with the binding site on CD59 for complement binding proteins C8alpha and C9. *J Biol Chem* **286**: 20952-20962

Toxines et Transferts ioniques – Toxins and Ion transfers
Rencontres en Toxinologie – Meeting on Toxinology, 2011
Editions de la SFET – SFET Editions
Accès libre en ligne sur le site – Free access on line on the site : http://www.sfet.asso.fr

Heat-stable enterotoxin b produced by Escherichia coli *induces apoptosis in rat intestinal epithelial cells*

H. Claudia SYED, J. Daniel DUBREUIL*

Groupe de Recherche sur les Maladies Infectieuses du Porc (GREMIP), Faculté de médecine vétérinaire, Université de Montréal, Québec, Canada

** Corresponding author ; Tel : (450) 773-8521 # 8433 ; Fax : (450) 778-8108 ;*
E-mail : daniel.dubreuil@umontreal.ca

Abstract

A previous study conducted in our laboratory revealed that cultured cells having internalized heat-stable enterotoxin b (STb) displayed apoptotic-like morphology. We therefore investigated if STb induces apoptosis in the IEC-18 cell line (rat ileum epithelial cells) by verifying the activation of caspases-9, -3 and -8 as well as DNA fragmentation of cells treated with purified toxin. We observed activation of caspases-9 and -3 as well as DNA laddering, indicating that STb induces apoptosis in IEC-18 cells.

L'entérotoxine STb produite par Escherichia coli *induit l'apoptose des cellules intestinales épithéliales de rat*

Une étude antérieure menée dans notre laboratoire a révélé que des cellules en culture ayant internalisé l'entérotoxine STb démontraient une morphologie rappelant celle de l'apoptose. Nous avons évalué l'apopotose des cellules IEC-18 (cellules épithéliales de l'iléon de rat) traitées avec la toxine STb purifiée, en vérifiant l'activation des caspases-9, -3 et -8 et la fragmentation de l'ADN. L'observation de l'activation des caspases-9 et -3 et de la fragmentation de l'ADN indique que STb induit l'apoptose des cellules IEC-18.

Keywords : *Apoptosis, caspase, DNA fragmentation,* Escherichia coli*, STb enterotoxin.*

Introduction

Heat-stable enterotoxin b (STb) is one of the toxins produced by enterotoxigenic *Escherichia coli* (ETEC) strains shown to be responsible for the induction of diarrhea and is most commonly associated with post-weaning diarrhea in piglets (Dubreuil, 2008). STb toxin is capable of forming non-specific pores in pig jejunal brush border membrane vesicles (Gonçalves *et al.*, 2007) and of inducing histological damages of the intestine characterized by shortening and atrophy of the villi and thus reduction of the mucosal surface (Rose *et al.*, 1987). These damages have been associated with diminished absorptive ability of the villi and secretion of electrolytes and water during diarrhea.

A previous study conducted in our laboratory demonstrated that cells having internalized STb displayed mitochondrial potential changes and an apoptotic-like morphology (Gonçalves *et al.*, 2009). Indeed, the ability of pore-forming toxins to induce apoptosis is well documented (Braun *et al.*, 2007; Saka *et al.*, 2008; Tran *et al.*, 2011). Apoptosis is a form of programmed cell death characterized by membrane blebbing, chromatin condensation, and DNA fragmentation. Apoptosis can be induced through either an extrinsic or intrinsic pathway.

Extrinsic apoptosis is activated following the interaction of a ligand and a membrane-bound receptor belonging to the Tumor Necrosis Factor Receptor (TNFR) family. This results in the formation of DISC (Death Inducing Signalling Complex) and the activation of caspase-8. Intrinsic apoptosis is the result of intracellular stress causing a change in mitochondrial membrane potential leading to the formation of the apoptosome and the activation of caspase-9. Both caspases-8 and -9 activate caspase-3 which targets downstream substrates leading to DNA fragmentation and eventual cell death.

As STb has been shown to cause apoptotic-like morphology in cultured cells and as rats are used as an animal model for the study of STb, we investigated the ability of STb to induce apoptosis in rat intestinal epithelial cells in culture.

Material and methods

In order to determine if STb induces apoptosis in intestinal epithelial cells of rats, we treated the IEC-18 cell line (rat ileum epithelial cells) with various quantities (nanomole) of purified STb toxin for a period of 24 hours.

Harvested cells were then assessed for caspases activation and DNA fragmentation. The implication of caspases-9, -3 and -8 was verified using fluorescent substrates specific for each of these caspases. Fluorescence emitted from the cleaved substrates was measured with a fluorescence microplate reader at 500 nm. Extracted DNA of toxin-treated IEC-18 cells was migrated on a 1.8% agarose gel and then visualized under a UV lamp at 260 nm. Staurosporine was used at 2 µM (final concentration) as a positive control for apoptosis.

Results

Activation of caspases-9 and -3 (*Figure 1*) was observed in IEC-18 cells treated with 0.05 and 0.5 nmol of STb, similarly to cells treated with staurosporine, our positive control for apoptosis. As caspases-9 and -8 are initiator caspases of the intrinsic and extrinsic pathways, respectively, the evaluation of their activation allowed us to determine the precise pathway targeted by STb. Activation of caspase-3 was also assessed to ensure the implication of the caspase cascade in STb-mediated apoptosis. The activation of caspase-9 in our study indicates that the intrinsic pathway is targeted by STb. Treatment of cells with the same amount of toxin yielded similar activation levels of either caspase-9 or -3 but not of caspase-8 (*Figure 1*), a caspase activated when the extrinsic pathway is involved. The induction of apoptosis by STb through the intrinsic pathway is in accordance with other pore-forming toxins (Génestier *et al.*, 2005; Manente *et al.*, 2008).

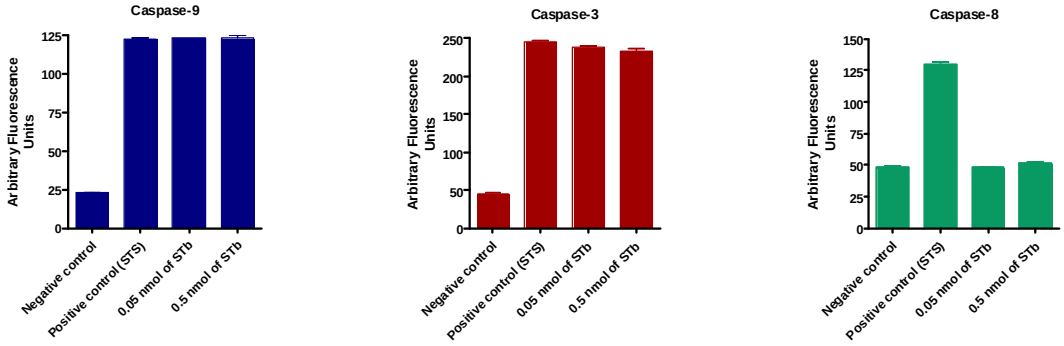

Figure 1. Activation of caspases-9, -3 and -8 in IEC-18 cells treated with 0.05 and 0.05 nmol of STb toxin. Negative control consisted of untreated cells whereas our positive control consisted of cells treated with staurosporine (STS). Mean ± standard error of the mean of 2 experiments.

Figure 1. *L'activation des caspases-9, -3 et -8 dans les cellules IEC-18 traitées avec 0,05 et 0,5 nmol de toxine STb. Les cellules non-traitées représentent le témoin négatif tandis que les cellules traitées avec la staurosporine (STS) représentent le témoin positif. Moyenne ± erreur standard de la moyenne de 2 expériences.*

Extracted DNA from IEC-18 cells treated with 0.25 and 0.5 nmol of STb revealed a similar laddering pattern as observed with extracted DNA of cells treated with staurosporine (*Figure 2*). DNA fragmentation is the result of cleavage by endonucleases of internucleosomal DNA into 180 bp – 200 bp multiples. The fragments of extracted DNA of cells treated with STb are 1000 bp or smaller. Each ladder step is approximately a multiple of 200 bp, indicating the DNA cleavage at internucleosomal sites.

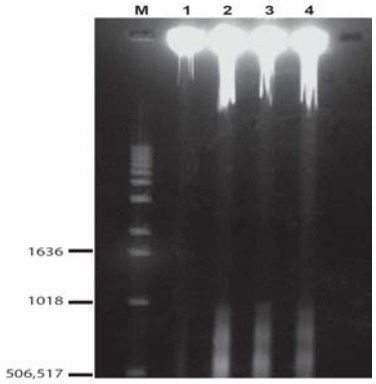

Figure 2. Extracted DNA of IEC-18 cells treated with STb toxin migrated on an agarose gel. **M**: molecular markers in base pairs; **1**: Untreated cells (negative control); **2** and **3**: Cells treated with 0.25 and 0.5 nmol of STb, respectively; **4**: Cells treated with staurosporine (positive control for apoptosis).

Figure 2. *ADN extrait des cellules IEC-18 traitées avec la toxine STb et migré sur gel d'agarose.* ***M****: Marqueurs moléculaires en paires de bases;* ***1****: Cellules non-traitées (contrôle négatif);* ***2*** *et* ***3****: Cellules traitées avec 0,25 et 0,5 nmol de STb, respectivement;* ***4****: Cellules traitées avec la staurosporine (contrôle positif pour l'apoptose).*

Conclusion

We showed for the first time that STb enterotoxin induces apoptosis in rat intestinal epithelial cells. The activation of caspase-9 and -3, but not of caspase-8, in our study is an indication of STb-mediated intrinsic

apoptosis in IEC-18 cells. This pathway involves a change in mitochondrial membrane potential as it was observed in a previous study conducted in our laboratory but using the NIH-3T3 cell line. DNA fragmentation confirms that apoptosis is occurring in rat intestinal epithelial cells following treatment with STb. Apoptosis of villus epithelial cells can explain, at least in part, the accumulation of fluid observed in pig ligated loops. The death of these cells could be related to a loss of absorptive capacity of the intestine intoxicated by STb toxin.

References

Braun JS, Hoffmann O, Schickhaus M, Freyer D, Dagand E, *et al.* (2007) Pneumolysin causes neuronal cell death through mitochondrion damage. *Infect Immun* **75**: 4245-4254

Dubreuil JD (2008) *Escherichia coli* STb toxin and collibacillosis: knowing is half the battle. *FEMS Microbiol Lett* **278**: 137-145

Génestier AL, Michallet M-C, Prevost G, Bellot G, Chalabreysse L, *et al.* (2005) *Staphylococcus aureus* Panton-Valentine leukocidin directly targets mitochondria and induces Bax-independent apoptosis of human neutrophils. *J Clin Invest* **115**: 3117-3127

Gonçalves C, Dubreuil JD (2009) Effect of *Escherichia coli* STb toxin on NIH-3T3 cells. *FEMS Immunol Med Microbiol* **55**: 432-445

Gonçalves C, Vachon V, Schwartz JL, Dubreuil JD (2007) The *Escherichia coli* enterotoxin b permeabilizes piglet jejunal brush border membrane vesicles. *Infect Immun* **75**: 2208-2213

Manente L, Perna A, Buommino E, Altucci L, Lucariello A, *et al.* (2008) The *Helicobacter pylori*'s VacA has direct effects on the regulation of cell cycle and apoptosis in gastric epithelial cells. *J Cell Physiol* **214**: 582-587

Rose R, Whipp SC, Moon HW (1987) Effects of *Escherichia coli* heat-stable enterotoxin b on small intestinal villi in pigs, rabbits, and lambs. *Vet Pathol* **24**: 71-79

Saka HA, Bidinost C, Sola C, Carranza P, Collino C, *et al.* (2008) *Vibrio cholerae* cytolysin is essential for high enterotoxicity and apoptosis induction produced by a cholera toxin gene-negative *V. cholerae* non-O1, non-O139 strain. *Microbial Pathogen* **44**: 118-128

Tran SL, Guillemet E, Ngo-Camus M, Clybouw C, Lereclus D, *et al.* (2011) Haemolysin II is a *Bacillus cereus* virulence factor that induces apoptosis of macrophages. *Cell Microbiol* **13**: 92-108

Toxines et Transferts ioniques – Toxins and Ion transfers
Rencontres en Toxinologie – Meeting on Toxinology, 2011
Editions de la SFET – SFET Editions
Accès libre en ligne sur le site – Free access on line on the site : http://www.sfet.asso.fr

On the mode of entry of clostridial neurotoxins into the cytosol of nerve terminals

Paolo BOLOGNESE[1], Fulvio BORDIN[1], Cesare MONTECUCCO[1*], Marco PIRAZZINI[1], Ornella ROSSETTO[1], Clifford C. SHONE[2]

[1] *Department of Biomedical Sciences and CNR Institute of Neuroscience, University of Padova, Viale G. Colombo 3, 35131 Padova, Italy ;* [2] *Health Protection Agency, Porton Down, Salisbury,Wiltshire, SP4 OJG, UK*

** Corresponding author ; Tel : +39.0498276058 ; Fax : +39.0498276049 ;*
E-mail : cesare.montecucco@unipd.it

Abstract

Tetanus and botulinum neurotoxins enter nerve terminals via *endocytosis inside acidic vesicles. Using a novel cellular assay, we have found that (1) these neurotoxins have to be bound to the membrane* via *at least two anchorage sites for a productive low-pH induced membrane translocation of the active chain to occur, (2) this only happens if the single inter-chain disulfide bond is intact, and (3) the pH dependence of membrane translocation is similar for the various toxins.*

Sur le mode d'entrée des neurotoxines clostridiales dans le cytosol des terminaisons nerveuses

Les neurotoxines tétanique et botuliques entrent dans les terminaisons nerveuses par endocytose dans des vésicules acides. En utilisant un nouveau test cellulaire, nous avons démontré que (1) ces neurotoxines doivent être liées à la membrane par au moins deux sites d'ancrage pour une translocation membranaire efficace du domaine enzymatique à pH acide, (2) ceci n'intervient que si le pont disulfure reliant les deux chaînes est intact, et (3) la translocation membranaire est dépendante du pH de manière similaire pour ces toxines.

Keywords : *Botulism, membrane translocation, molecular model, tetanus.*

Tetanus neurotoxin (TeNT) and botulinum neurotoxins (seven different serotypes: BoNT/A, /B, /C, /D, /E, /F and /G) cause a prolonged blockade of neuroexocytosis by entering into nerve terminals and cleavage of the SNARE (soluble N-ethylmaleimide-sensitive factor-attachment protein-receptor) proteins which form the core of the nanomachine which mediates neurotransmitter release. They are dichain (H, heavy chain and L, light chain) toxins with a single interchain disulfide bond (Rossetto *et al*., 2006; Binz and Rummel, 2009; Montal, 2010). Their cellular mechanism of intoxication consists of four steps: (1) binding, (2) endocytosis inside acidic vesicles, (3) membrane translocation of the metalloprotease L chain, (4) cleavage of either VAMP, or SNAP-25 or syntaxin (Montecucco and Schiavo, 1995). The third step is the least understood because it takes place inside the lumen of a vesicle which is acidified by the v-ATPase proton pump, specifically inhibited by bafilomycin A1 which is a strong inhibitor of TeNT and of BoNTs (Simpson *et al*., 1994; Williamson and Neale, 1994). It is established that, at low pH, the H chain inserts into the membrane and chaperones the partially unfolded L chain on the cytosol side where the SS bond is reduced and displays its metalloprotease activity: TeNT, BoNT/B, /D, /F and /G cleave VAMP/synaptobrevin; BoNT/A, /C and /E cleave SNAP-25; and BoNT/C also cleaves syntaxin (Rossetto *et al*., 2006; Montal, 2010). How low pH converts a highly water soluble molecule into a transmembrane protein conducting channel is not understood.

To tackle this problem at the cellular level, we decided to "export" the site of membrane translocation by making it to occur at the plasma membrane of nerve terminals. We used two types of neurons in culture: cerebellar granular neurons (CGN) because they are a pure culture of primary neurons and NGF-differentiated PC12 cells because they are a cell line. These neurons resist to exposure to short incubation at media of pH as low as 4.5 without any loose of viability or detachment from the substrate. The normal pathway of entry *via* acidic vesicles was blocked by the presence of bafilomycin A1. The presence of the metalloprotease chain in the cytosol was deduced by their metalloprotease activity measured by blotting with specific antibodies the three SNARE proteins and determining the ratio of the cleaved SNARE and of the uncleaved one, an internal "ratiometric" method which compensates for any heterogeneity among samples. Using this method, we found that neither BoNT/A nor BoNT/B were induced by the external low pH to enter neurons and cleave their respective substrates. We reasoned that this was due to the fact that they would bind to the cells only *via* the polysialoganglioside binding site (Binz and Rummel, 2009) and that this single anchorage would leave to the molecule a too high degree of freedom of movement with respect to the membrane with the result that the

toxin molecule would have the possibility of interacting with the membrane surface in many unproductive ways. As one special feature of these neurotoxins is that of having two binding sites in their C-terminal binding domain (Montecucco, 1986; Binz and Rummel, 2009), we reasoned that it was possible that two anchorage points would be needed in order for a productive entry into the membrane to occur. Beginning with TeNT (Rummel *et al*., 2003), BoNT/C and /D were also shown to have two polysialoganglioside binding sites in their binding domain. Accordingly to these reports and to our hypothesis, TeNT, BoNT/C and /D should enter into the two types of neurons used here in a low pH dependent way and cleave their respective substrates. Indeed, *Figure 1* shows that this is the case and, even more remarkably, the three toxins did with the same pH dependence (Pirazzini *et al*., 2011).

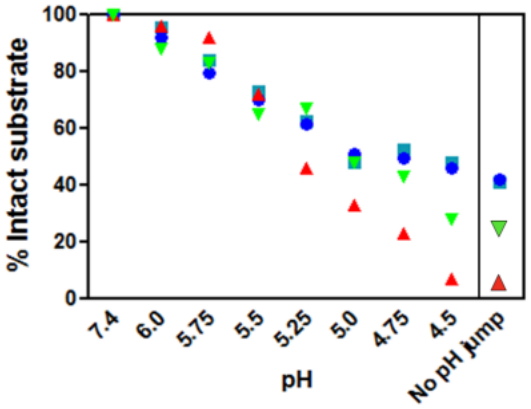

Figure 1. pH dependence of the cleavage of intracellular SNARE proteins by tetanus and botulinum neurotoxins in cerebellar granular neurons in culture after 5 min incubation in extracellular media of the indicated pH value and further incubation at neutral pH in the presence of bafilomycin A1. The percentage of intact SNARE proteins is reported as a function of the pH of the extracellular medium for TeNT (*green triangles*, target protein: VAMP/synaptobrevin), for BoNT/C (*blue rounds* refer to syntaxin, *dark green squares* to SNAP-25) and BoNT/D (*red triangles* refer to the target protein VAMP/synaptobrevin). No pH jump refers to neurons intoxicated *via* the normal route of endocytosis in the absence of bafilomycin A1

Figure 1. *Coupure des protéines SNARE intracellulaires des neurones en grain du cervelet en culture par les neurotoxines tétanique et botuliques en fonction du pH, après 5 min d'incubation en présence de milieux extracellulaires dont la valeur du pH est indiquée, puis d'une incubation supplémentaire à pH neutre en présence de bafilomycine A1. Le pourcentage de protéines SNARE intactes est indiqué pour chaque valeur de pH du milieu extracellulaire en présence de TeNT (*triangles verts*, protéine cible: VAMP/synaptobrévine), de BoNT/C (*ronds bleus *pour la syntaxine,* carrés verts foncés *pour SNAP-25) et BoNT/D (*triangles rouges*, protéine cible: VAMP/synaptobrévine). L'absence de saut de pH signifie que les neurones ont été intoxiqués par la voie normale d'endocytose en l'absence de bafilomycine A1.*

If this "two feet on the ground" explanation is correct, then the exposure of the synaptotagmin binding domain of BoNT/B on the surface of neurons should make the cell sensitive to BoNT/B. Indeed, this was found to be the case (Pirazzini *et al*., 2011), providing further support to the proposal that, in order to undergo a productive entry into the membrane at low pH, these neurotoxins have to be bound to the membrane *via* two binding sites. The nature of the receptors apparently makes no difference, as we found that two polysialogangliosides or one polysialoganglioside plus a protein receptor support entry with the same pH dependence profile for the four neurotoxins tested here. These findings are at variance with those of Sun *et al*. (2011) who reported that one single polysialoganglioside binding site was sufficient to mediate the low pH induced translocation of BoNT/B into hippocampal neurons exposed in culture at low pH. However, there is only an apparent contradiction among the two studies, as these authors exposed their neurons to high potassium media and it is well known that membrane depolarization does induce fusion of synaptic vesicle with exposure on the lumen of the vesicle on the cell surface, including the BoNT/B binding domain of synaptotagmin. Therefore, they worked under conditions very similar to those that we used for BoNT/B in our study, and their findings provide further and independent support to our proposal of the "two feet on the ground" for the low pH-mediated entry of TeNT and BoNTs into the membrane.

As it is known that the reduction of the single interchain disulfide bridge of TeNT and BoNT/A (Schiavo *et al*., 1990; de Paiva *et al*., 1993) abolishes neurotoxicity, we tested here if reduction affects the low pH-induced entry of TeNT, BoNT/C and BoNT/D and have found that these three toxins after reduction lose their capability of entering into neurons. This result indicates that an intact SS interchain bridge is necessary at same stage of the process of low pH-nduced membrane insertion and translocation (Pirazzini *et al*., 2011).

The close similarity of the pH interval of membrane translocation for the four neurotoxins suggests that similar and conserved residues are protonated. Such residues have been identified by sequence comparison

and then their pKa values were estimated *via* the program PROPKA3.0 which considers the positions of the residue in the crystallographic structure; our analysis was based on the structure of BoNT/B because of its higher resolution (PDB: 2NP0) (Chai *et al*., 2006). All the carboxylate residues with pKa values close to the pH interval of *Figure 1* are on the same surface of the BoNT/B molecule that includes the interchain SS bond and the segment predicted by Eswaramoorthy *et al.* (2004) to have a high tendency to insert into membrane.

On this basis, we propose that this face of the BoNT/B and TeNT molecules becomes positively charged upon acidification and that it rotates on the two membrane receptors to lie flat on the negatively charged surface of the membrane. The first two segments that are proposed to insert into the lipid bilayer are the one mentioned above and the highly hydrophobic SS bond. This is followed by a concerted conformational change of both the L and H chains with creation of a chaperone-channel by the H chain, which conducts the partially unfolded L chain across the membrane. Our previous experimental evidences indicate that both the L and H chain expose part of their surface to lipids (Montecucco *et al*., 1985; Montecucco, 1986). Once the L chain is translocated, a H channel is open across the membrane and transports ions with a conductance determined in previous studies (Hoch *et al*., 1985; Donovan and Middlebrook 1986; Gambale and Montal, 1985; Koriazova and Montal, 2003; Fischer and Montal, 2007; Montal, 2010). In this view, the TeNT and BoNT channel characterized so far and reviewed recently (Montal, 2010) is a consequence of the membrane translocation of the L chain and not a pre-requisite for its translocation, as discussed more in depth previously (Montecucco and Schiavo, 1995).

Conclusion

The cellular assay of the membrane translocation of tetanus and botulinum neurotoxins will be very useful in studying the molecular aspects of this mysterious process also because it has generated a molecular model that is already under experimental test *via* generation and assay of the various activities of selected BoNT mutants.

Acknowledgements. *This work was supported by grants from the Ministero dell'Università e della Ricerca (Progetto PRIN) to O.R., from the Università di Padova, Progetto Strategico. to C.M., and from the National Institute of Health (NIHR) Centre for Health Protection Research at the Health Protection Agency to C.S..*

References

Binz T, Rummel A (2009) Cell entry strategy of clostridial neurotoxins. *J Neurochem* **109**: 1584-1595

Chai Q, Arndt JW, Dong M, Tepp WH, Johnson EA, Chapman ER, *et al*. (2006) Structural basis of cell surface receptor recognition by botulinum neurotoxin B. *Nature* **444**: 1096-1100

de Paiva A, Ashton AC, Foran P, Schiavo G, Montecucco C, Dolly JO (1993) Botulinum A like type B and tetanus toxins fulfils criteria for being a zinc-dependent protease. *J Neurochem* **61**:2338-2341

Donovan JJ, Middlebrook JL (1986) Ion-conducting channels produced by botulinum toxin in planar lipid membranes. *Biochemistry* **25**: 2872-2876

Eswaramoorthy S, Kumaran D, Keller J, Swaminathan S (2004) Role of metals in the biological activity of *Clostridium botulinum* neurotoxins. *Biochemistry* **43**: 2209-2216

Fischer A, Montal M (2007) Single molecule detection of intermediates during botulinum neurotoxin translocation across membranes. *Proc Natl Acad Sci USA* **104**: 10447-10452

Hoch DH, Romero-Mira M, Ehrlich BE, Finkelstein A, DasGupta BR, Simpson LL (1985) Channels formed by botulinum, tetanus, and diphtheria toxins in planar lipid bilayers: relevance to translocation of proteins across membranes. *Proc Natl Acad Sci USA* **82**: 1692-1696

Koriazova LK, Montal M (2003) Translocation of botulinum neurotoxin light chain protease through the heavy chain channel. *Nat Struct Biol* **10**: 13-18

Montal M (2010) Botulinum neurotoxin: a marvel of protein design. *Annu Rev Biochem* **79**: 591-617

Montecucco C (1986) How do tetanus and botulinum toxins bind to neuronal membranes? *Trends biochem sci* **11**: 314-317

Montecucco C, Schiavo G (1995) Structure and function of tetanus and botulinum neurotoxins. *Q Rev Biophys* **28**: 423-472

Montecucco C, Schiavo G, Tomasi M (1985) pH-dependence of the phospholipid interaction of diphtheria-toxin fragments. *Biochem J* **231**: 123-128

Pirazzini M, Rossetto O, Bolognese P, Shone CC, Montecucco C (2011) Double anchorage to the membrane and intact inter-chain disulfide bond are required for the low pH induced entry of tetanus and botulinum neurotoxins into neurons. *Cell Microbiol* **13**: 1731-1743

Rossetto O, Morbiato L, Caccin P, Rigoni M, Montecucco C (2006) Presynaptic enzymatic neurotoxins. *J Neurochem* **97**: 1534-1545

Rummel A, Bade S, Alves J, Bigalke H, Binz T (2003) Two carbohydrate binding sites in the H(Cc)-domain of tetanus neurotoxin are required for toxicity. *J Mol Biol* **326**: 835-847

Schiavo G, Papini E, Genna G, Montecucco C (1990) An intact interchain disulfide bond is required for the neurotoxicity of tetanus toxin. *Infect Immun* **58**: 4136-4141

Simpson LL, Coffield JA, Bakry N (1994) Inhibition of vacuolar adenosine triphosphatase antagonizes the effects of clostridial neurotoxins but not phospholipase A2 neurotoxins. *J Pharmacol Exp Ther* **269**: 256-262

Sun S, Suresh S, Liu H, Tepp WH, Johnson EA, Edwardson JM, Chapman ER (2011) Receptor binding enables botulinum neurotoxin B to sense low pH for translocation channel assembly. *Cell Host Microbe* **15**: 237-247

Williamson LC, Neale EA (1994) Bafilomycin A1 inhibits the action of tetanus toxin in spinal cord neurons in cell culture. *J Neurochem* **63**: 2342-2345

Rencontres en Toxinologie – Meeting on Toxinology, 2011
Editions de la SFET – SFET Editions
Accès libre en ligne sur le site – Free access on line on the site : http://www.sfet.asso.fr

Tethering peptide toxins for neurocircuitry, cell-based therapies and drug discovery

Ines IBAÑEZ-TALLON

Laboratory of Molecular Neurobiology, Max Delbruck Center for Molecular Medicine, Berlin 12135, Germany
Tel : +(49) 30 9406 3411 ; Fax : +(49) 30 9406 3411 ; E-mail : ibanezi@mdc-berlin.de

Abstract

Peptide neurotoxins isolated from animal venoms are widely employed in neuroscience research because of their ability to activate or inhibit specific ionic currents. However, because neurotoxins are soluble and dispersed into the media, their action cannot be restricted to a single cell population within a cell network. Here, we review a recombinant strategy based on genetically encoded membrane tethered toxins (t-toxins) for long-term inhibition of ion channels and receptors. Due to their membrane attachment, the activity of recombinant t-toxins is restricted to genetically targeted cells, without affecting identical channels on neighboring cells that do not express the t-toxin. This review describes the development and application of the t-toxin technology to the functional dissection of brain circuits and its potential translation to cell-based therapies and drug discovery

Des toxines peptidiques ancrées à la membrane pour l'étude des circuits neuronaux, thérapie cellulaire et découverte de médicament

Les neurotoxines peptidiques issues de venins d'animaux sont largement employées en neuroscience du fait de leur capacité à activer ou inhiber spécifiquement des courants ioniques. Cependant, les neurotoxines sont solubles et diluées dans le milieu et leur action ne peut être restreinte à une population cellulaire unique dans la cellule. Dans cette revue, nous présentons une stratégie recombinante basée sur l'expression de toxines ancrées à la membrane (t-toxines) afin d'inhiber de façon prolongée des récepteurs et canaux ioniques. Du fait de leur insertion dans la membrane, l'activité des t-toxines est restreinte aux cellules génétiquement ciblées, sans affecter les canaux ioniques identiques des cellules voisines n'exprimant pas ces t-toxines. Cette revue décrit le développement et les applications de cette technologie dans l'étude fonctionnelle des circuits neuronaux et dans son application potentielle en thérapie cellulaire ou dans la découverte de médicament.

Keywords : *Ion channel, tethered toxin, mouse genetic strategies, neurotransmission.*

Introduction

Historically, toxin-based methods for manipulating neuronal circuits have included microinjection of tetrodotoxin or other neurotoxic agents into target areas, and the local administration of anesthetics or other pharmacologic agents. Many of these manipulations, however, are not reversible and frequently disrupt more than one neuronal circuit. Powerful genetic approaches have provided new opportunities for manipulations of specific cell populations within neuronal circuits. For instance the identification of gene promoters [*i.e.* Bacterial Artificial Chromosomes (BACs)] that allow cell-type specific manipulations of functionally related neuronal populations (Gong *et al.*, 2002) can be used to trace neuronal connections, achieve cell-specific conditional mutagenesis or drive functional changes within circuits by *in vivo* microinjections with viral vectors (Hatten and Heintz, 2005; Luo *et al.*, 2008; Tolu *et al.*, 2010).

As research on venom toxins discovers new specific inhibitors and modulators of ion channels and receptors, the pharmacopeia of specific naturally occurring venom peptides continues to increase. Thus, single venom peptide toxins with characteristic cysteine backbones and selective affinities for voltage-gated sodium (Na_V), calcium (Ca_V), and potassium (K_V) ion channels, and ligand-gated receptors, such as nicotinic acetylcholine receptors (nAChRs), N-methyl-D-aspartate (NMDA) and G-protein coupled receptors (GPCRs) have been identified (for reviews see Terlau and Olivera, 2004; Twede *et al.*, 2009). Their high specificity makes them ideal tools for deciphering the contribution of ionic currents to neurophysiology, but their activity cannot be restricted to a single cell-population in brain slices or in a living organism and usually requires constant administration (*Figure 1A*). To bypass these limitations, we developed genetically encoded tethered toxins (t-toxins) that are bound to the cell surface by membrane tethers and act only on ion channels and receptors of the cell-population that expresses the t-toxin and not on identical receptors present in neighboring cells that do not express the t-toxin (Ibañez-Tallon *et al.*, 2004; *Figure 1B*).

In this review, we describe the combined use of genetically encoded membrane t-toxins with cell-specific genetic targeting strategies in mice as a novel approach to neurocircuitry that extends our ability to modify singular ionic currents in specific neurons *in vivo.*

Origin and design of membrane tethered toxins

The engineering of tethered toxins derived from the discovery of endogenous, cell-membrane bound prototoxins of the lynx1 family (Miwa *et al.*, 1999). Lynx1 belongs to the Ly-6/neurotoxin gene family and is an evolutionary precursor to snake venom toxins with structural homologies to the nicotinic acetylcholine receptor (nAChR) antagonists α- and κ-bungarotoxin. lynx1 is attached to the cell surface by a glycosylphosphatidylinositol (GPI) anchor and shows a complex disulfide fold (the tree finger fold), a characteristic feature of most peptide toxins (Miwa *et al.*, 1999). Functional analyses indicated that lynx1, and the closely related molecule lynx2, are not ligand or neurotransmitters, but directly assemble with nAChRs at the cell-membrane and modulate their functions in the presence of acetylcholine or nicotine (Miwa *et al.*, 1999; Ibanez-Tallon *et al.*, 2002; Miwa *et al.*, 2006; Tekinay *et al.*, 2009). The first recombinant membrane-bound toxins were designed by replacing lynx1 with the sequences encoding for bungarotoxins and α-conotoxins downstream of the secretory signal sequence, followed by a short linker and the GPI anchor signal sequence (Ibanez-Tallon *et al.*, 2004). This design directs the toxin peptide to the secretory pathway, where the signal sequence is cleaved and the GPI targeting sequence is substituted by a covalent bond to GPI, thereby anchoring the peptide to the extracellular side of the plasma membrane of the cell in which it is expressed (*Figure 1B*).

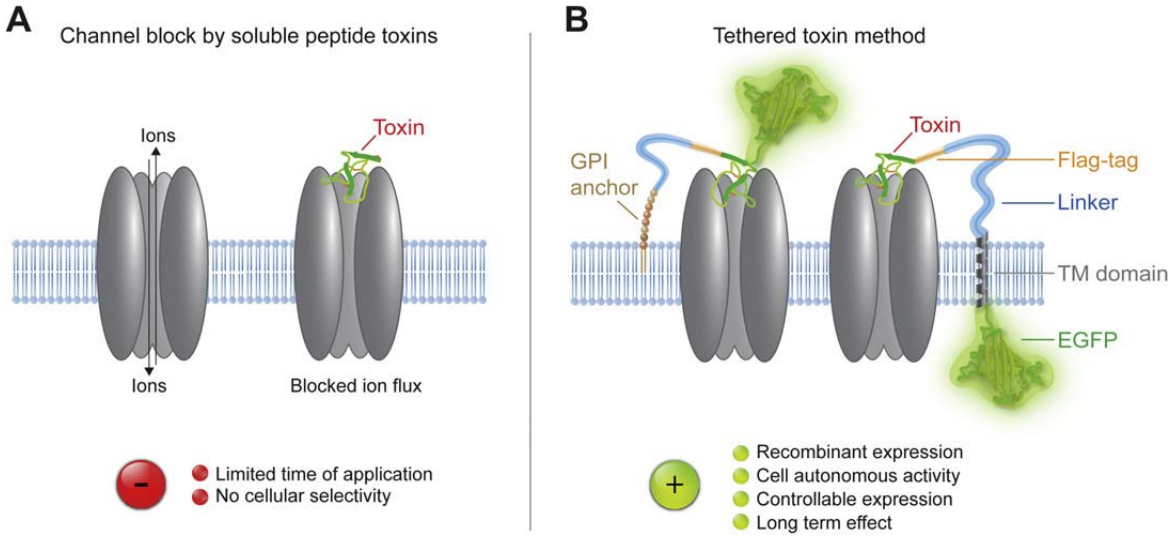

Figure 1. Illustration of ion channel inhibition by soluble peptide toxins or genetic expression of recombinant tethered-toxins. (**A**) Soluble peptide toxins cause instantaneous block of target ion channels, but their use *in vivo* is limited by the accessibility of the brain structure to be targeted, the necessity of constant re-administration and the lack of cellular selectivity within a circuit or cell network. (**B**) Genetically encoded toxins tethered to the membrane *via* a glycosylphosphatidylinositol (GPI) anchor or a transmembrane (TM) domain allow cell-autonomous block of ion channels and the integration of domains (*i.e.* Flag or other epitopes, EGFP or other markers) to monitor their long-term expression in targeted cells. From Auer and Ibañez-Tallon (2010).

Figure 1. Illustration de l'inhibition des canaux ioniques par des peptides solubles ou par des toxines ancrées à la membrane et exprimées de façon recombinante*. (**A**) Les toxines solubles provoquent un blocage immédiat du canal ionique ciblé mais leur utilisation* in vivo *est limitée par l'accessibilité des structures cérébrales à cibler, par la nécessité de les administrer en continu et par le manque de sélectivité cellulaire dans un réseau neuronal. (**B**) Les toxines recombinantes insérées dans la membrane grâce à une ancre de glycosylphosphatidulinositol (GPI) ou un domaine transmembranaire (TM) permettent un blocage des canaux ioniques indépendant de la cellule et l'insertion de marqueurs (Flag, épitropes, EGFP ou autres) afin de suivre leur expression prolongée dans la cellule ciblée. D'après Auer et Ibañez-Tallon (2010).*

The t-toxin design has been further optimized by introducing other membrane tethers, *i.e.* the transmembrane domain of the PDGF receptor (Auer *et al.*, 2010) as well as fluorescent markers (EGFP, mCherry and EBFP2) and immunotags (*i.e.* Flag-tag; *Figure 1B*). These modifications have greatly increased the ability to monitor the expression levels and subcellular localization of the recombinant molecules, which are important prerequisites for their use in neurocircuitry. So far, approximately 40 different t-toxins constructs have been cloned in our group, and their activity has been characterized on voltage- and ligand-gated ion channels (Ibanez-Tallon *et al.*, 2004; Holford *et al.*, 2009; Auer *et al.*, 2010; Sturzebecher *et al.*, 2010). Expression and functional assays of these recombinant tethered effectors have revealed that several elements are critical to achieve robust expression on the cell-surface and steric availability for functional binding of the t-toxin to the receptor or channel of interest. The affinity of the bioactive peptide for its cognate ion channel or receptor has to be taken into account. Other relevant features when designing t-toxin constructs is the choice of anchor and the length of the linker sequence bridging the toxin peptide to the GPI anchor or TM domain (*Figure 1B*). For more details on the design of t-toxins, please see Holford *et al.* (2009) and Auer and Ibanez-Tallon (2010).

Genetic approaches for t-toxin delivery to neuronal circuits

The fact that peptide toxins maintain their functionality when expressed exogenously in mammalian neurons opened up the possibility to implement an important number of genetic strategies for studies of neurocircuitry *in vivo* using genetically encoded recombinant t-toxins. Thus, studies *in vivo* have been possible using different genetic approaches to drive their cell-autonomous action. These include transgenesis in zebrafish (Ibanez-Tallon *et al.*, 2004), *Drosophila* (Wu *et al.*, 2008) and mouse (Sturzebecher *et al.*, 2010), as well as recombinant viral systems (Auer *et al.*, 2010; Hruska *et al.*, 2007). In particular, the possibility to encode t-toxins in viral vectors has further allowed the stable genetic delivery of t-toxins to a variety of mammalian cells, including neurons *in vitro* and *in vivo*. Furthermore, the use of viral vectors has provided the possibility to implement inducible and Cre recombinase-dependent approaches for regulated and cell-specific expression of t-toxins in mice that we will discuss later (Auer *et al.*, 2010). Here, we discuss some examples of the use of t-toxins with these genetic approaches to target specific neuronal populations in the mouse nervous system.

Selective manipulation of sodium voltage-gated currents in *Drosophila* and in mice with t-toxins

Given that initiation and propagation of electrical signals in excitable tissues depend on voltage-gated sodium channels (VGSC, Na_V), it is not surprising that many venom peptides target VGSC. Venom peptide toxins bind to different receptor sites on the channel protein. Few of them physically block the pore and prevent sodium conductance, while a great majority of toxins change channel gating by voltage-sensor trapping through binding to extracellular receptor sites (Caterall *et al.*, 2007). For example, μO-conotoxins partially block ionic influx by binding close to the pore of sodium channel types expressed in the heart ($Na_V1.5$), muscle ($Na_V1.4$) and peripheral nociceptive neurons ($Na_V1.8$; Leipold *et al.*, 2007), while δ-atracotoxins and β-scorpion toxins inhibit inactivation of activated channels inducing tetanus-like bursts of action potentials followed by plateau potentials resulting in neuronal transmission block and paralysis of the prey.

Circuit analyses have been done using tethered sodium toxins with these two opposed types of activities. For instance, δ-atracotoxin Hv1a has been used in its tethered form to alter the rhythmicity of circadian neurons in *Drosophila* with the GAL4-UAS transgenic system (Wu *et al.*, 2008), while our study employed the t-MrVIA μO-conotoxin and mouse BAC transgenesis to target nociceptive neurons and interfere with pain perception (Auer *et al.*, 2010; Sturzebecher *et al.*, 2010). In both cases, the tethered toxin specifically inhibited sodium voltage-gated currents within the genetically targeted neuronal population. Functional analyses of mouse nociceptive neurons expressing t-MrVIA revealed that the t-toxin acts at the membrane, as it can be released by enzymatic cleavage of the GPI anchor (Sturzebecher *et al.*, 2010). Importantly, the studies in transgenic mice indicated that t-MrVIA produced preferential inactivation of $Na_V1.8$ channels without compensation by $Na_V1.7$, as it occurs in $Na_V1.8$ knockout mice (Sturzebecher *et al.*, 2010). This is interesting since this channel is a target for the treatment of pain, and its relatively depolarized activation-voltage dependence may allow it to continue to function when nociceptive neurons are depolarized in the cold (*Figure 2*; Baker and Wen, 2010).

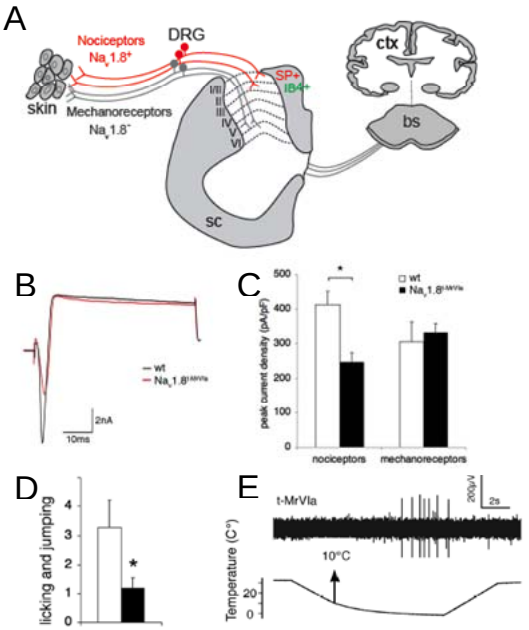

Figure 2. (**A**) **Schematic representation of the nociceptive cascade**; sensory neurons are indicated in *red*. (**B**, **C**) Electrophysiological recordings of dorsal root ganglia neurons from wt ant t-MrVIA transgenic mice demonstrate specific bloc of sodium currents in nociceptors but not in neighboring mechano-receptors. (**D**) $Na_V1.8$t-MrVIA mice showed negligible responses to noxious cold. Responses to noxious cold pain were measured by placing the mice on a 0^0C cooled plate, and scored as the number of paw licking and jumping. (**E**) Representative trace of a cutaneous C fiber of $Na_V1.8$t-MrVIA mouse showing start of firing at temperatures below 10°C.

Figure 2. *(**A**)* ***Représentation schématique du processus de nociception****; les neurones sensoriels sont indiqués en* rouge*. (**B**, **C**) Enregistrements électrophysiologiques des neurones de la corne dorsale ganglionaire de souris sauvages et transgéniques exprimant la t-MrVIA démontrant le blocage spécifique des courants sodiques nocicepteurs mais pas celui des mécano-récepteurs voisins. (**D**) Les souris $Na_V1.8$t-MrVIA montrent une réponse minime au froid. Les réponses à une douleur due au froid sont mesurées en plaçant la souris sur une plaque maintenue à 0°C et en comptant le nombre de léchage de pattes et de saut. (**E**) Tracé représentatif d'une fibre C cutanée de souris $Na_V1.8$t-MrVIA montrant le début de décharge à des températures inférieures à 10°C.*

Thus, these studies using t-toxins, taken together with previous studies on cold-sensitive neurons (Carr *et al.*, 2002; Zimmermann *et al.*, 2007), indicate that $Na_V1.8$ is the likely channel to encode for cold perception. As research on venom peptide toxins and synthetic peptide ligands progresses, it would be interesting to identify and test other antagonists and inactivation blockers of VGSC channels expressed in central neurons for neurocircuitry studies.

Silencing neurotransmission with calcium channel specific t-toxins

At presynaptic nerve terminals, the two voltage-gated calcium channels $Ca_V2.1$ and $Ca_V2.2$ play an essential and joint role in the electrochemical signal conversion by coupling the arriving presynaptic action potential to neurotransmitter release. The first step in this complex process is the opening of the voltage-gated $Ca_V2.1$ and $Ca_V2.2$ channels due to a rapid membrane depolarization that is caused by an arriving action potential. The resulting Ca^{2+} influx into the presynapse then enables the multimeric vesicle fusion machinery to fuse neurotransmitter (NT) filled vesicles with the synaptic membrane, thereby releasing NT to the synaptic cleft (Chua *et al.*, 2010; Caterall and Few, 2008). As the NT release is proportional to the third or fourth power of Ca^{2+} influx, a 2-fold change in presynaptic Ca^{2+} influx results in an 8 to 16-fold change in NT exocytosis (Zucker and Regehr, 2002). Thus, regulation of presynaptic calcium channels is an efficient way to control synaptic transmission. Besides deciphering distinct neuronal connections and their physiological functions, controlling the activity of these channels enables detailed studies of contributions of individual channels to neuronal circuits. With these aims in view, our group generated recombinant t-toxins that are able to block $Ca_V2.1$ and $Ca_V2.2$ channels by integration of the ω-agatoxins AgaIIIA and AgaIVA, as well as ω-conotoxins MVIIA and MVIIC. We found that these t-toxins were well expressed in cultured mammalian cells, primary cultures of hippocampal neurons and in neurons of mice injected with lentivirus encoding t-toxins (*Figure 3*). The capability to block one or both channels was then confirmed by electrophysiological recordings of HEK293-$Ca_V2.2$ cells and rat hippocampal neurons *in vitro* (Auer *et al.*, 2010). Overall, we found that AgaIVA and MVIIA provided the best blocking capabilities, and in fact that these two t-toxins were as effective as the soluble toxins in fully inhibiting their respective target channels in a cell (Auer *et al.*, 2010).

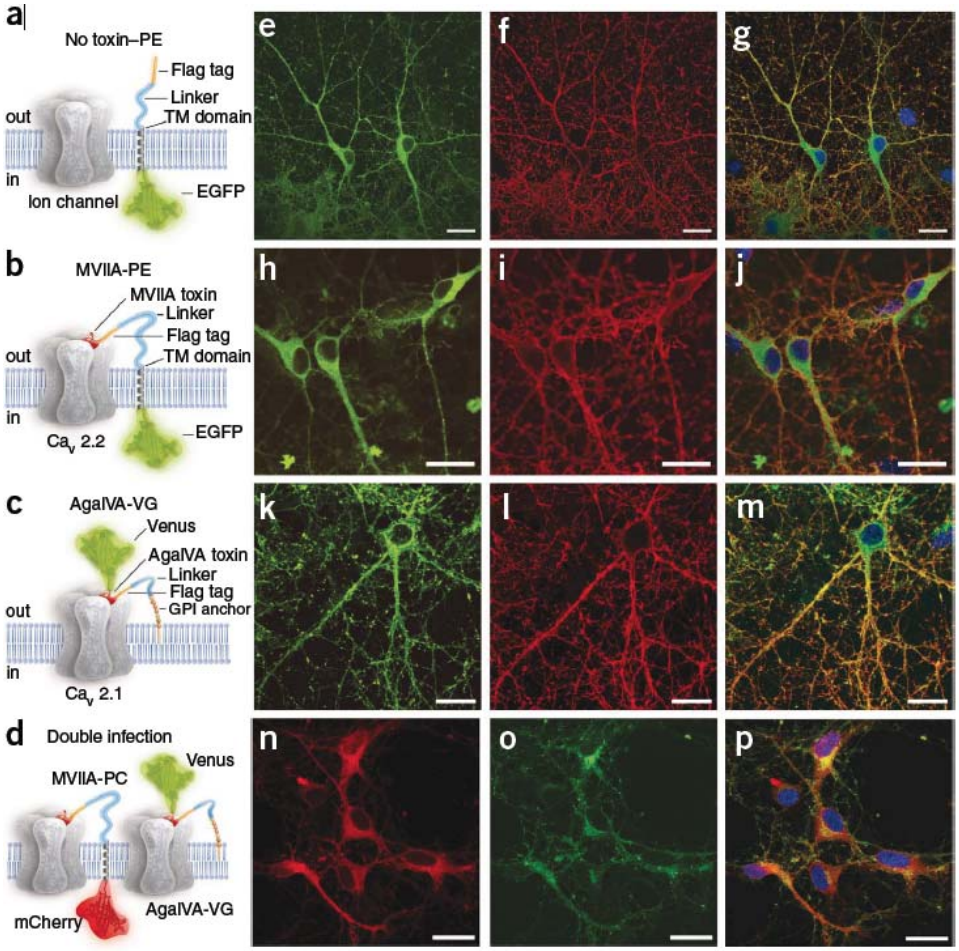

Figure 3. Expression of t-toxins in neurons. (**a**–**d**) Schematics of the membrane-tethered toxin variants: no toxin–PE negative control containing the PDGF receptor transmembrane (TM) domain and EGFP (**a**), MVIIA-PE (**b**), AgaIVA-VG containing extracellular Venus and a GPI anchor (**c**) and AgaIVA-VG and MVIIA-PC containing PDGF-R–TM domain and mCherry (**d**).(**e**–**p**) Fluorescence images of cells expressing constructs in **a**–**d** (**e**, **h**, **k**, **n**) Flag-epitope immunofluorescence images (**f**, **i**, **l**, **o**) and merged images in transduced rat hippocampal cultures (**g**, **j**, **m**, **p**). *Green*, EGFP and Venus; *red*, mCherry; *blue*, DAPI. Scale bars, 20 μm. From Auer *et al.* (2010).

Figure 3. Expressions de t-toxines dans les neurones. (**a**-**d**) *Schémas des variants de toxines ancrées à la membrane. Contrôle négatif avec le domaine TM du récepteur PGDF et l'EGFP mais sans toxine (***a***), MVIIA-PE (***b***), AgaIVA-VG contenant un domaine extracellulaire Venus et une ancre GPI (***c***) et AgaIVA-VG et MVIIA-PC contenant le domaine TM du récepteur PGDF et la mCherry (***d***). (**e**–**p**) Images de fluorescence des cellules exprimant les différentes constructions* **a**-**d** (**e**, **h**, **k**, **n**), *immunofluorescence de l'épitope Flag (***f***, ***i***, ***l***, ***o***) et images cumulées dans des cultures d'hippocampes de rat (***g***, ***j***, ***m***, ***p***).* Vert, *EGFP et Venus;* rouge, *mCherry;* bleu, *DAPI. Barres d'échelle, 20 μm. D'après Auer* et al. *(2010).*

We performed the first *in vivo* proof-of-function of Ca_V t-toxins in the nigro-striatal pathway of mice because of its unique behavioral phenotype after unilateral inhibition. The nigro-striatal pathway is part of the basal ganglia, which are associated with a variety of functions, including motor control and learning. They consist of two primary input structures [subthalamic nucleus (STN) and striatum], two primary output structures [substantia nigra pars reticulate (SNpr) and globus pallidus internal segment (GPi)], and two intrinsic nuclei [globus pallidus pars externa (GPe) and substantia nigra pars compacta (SNpc)] (Mink, 1996; Groenewegen, 2003). The SNpc consists of dopaminergic neurons, receives input from the striatum and sends most of its output back to the striatum *via* the medium forebrain bundle (mfb; *Figure 4*; Mink, 1996; Groenewegen, 2003). Basal ganglia disorders, like Parkinson's disease, which is caused by the death of dopaminergic (DA) neurons in SNpc, are typically characterized by an inability to correctly initiate and terminate voluntary movements, an inability to suppress involuntary movements, and an abnormal muscle tone (Takakusaki *et al.*, 2004). In the past, the neurotoxin 6-hydroxydopamine (6-OHDA) has been used extensively for the induction of unilateral lesion of DA neurons in the substantia nigra to induce circling behavior in rats. These studies played an essential role in the dissection of the nigro-striatal pathway and its role in motor coordination (Ungerstedt and Arbuthnott, 1970; Schwarting and Huston, 1996). In response to the resulting striatal DA depletion, a receptor-mediated supersensitivity, caused by increasing affinity and number of striatal D2-receptors in denervated postsynaptic neurons, develops (Schwarting and Huston, 1996). This supersensitivity on the side of the lesioned hemisphere usually causes the reversal of the rotational direction if DA agonists like apomorphine are administered (*Figure 4*; Ungerstedt and Arbuthnott, 1970; Schwarting and Huston, 1996).

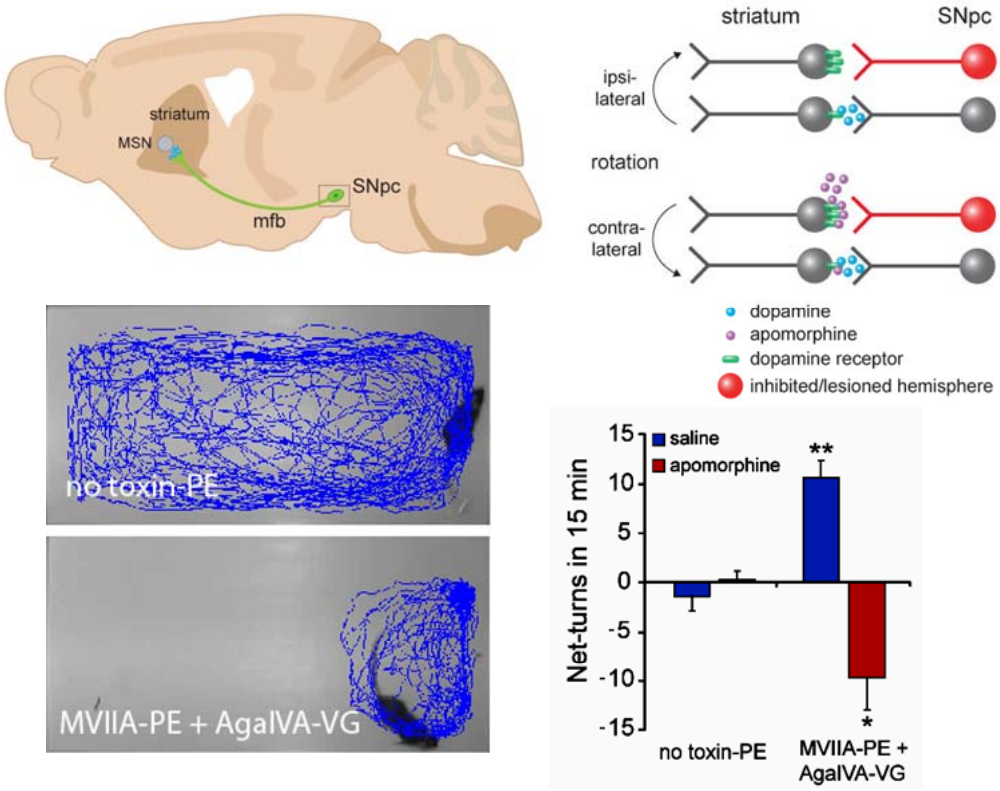

Figure 4. Representation of the nigro-striatal pathway and induced rotational behavior in mice stereotactically injected with t-toxins MVIIA-PE and AgaIVA-VG. Sagittal view of the basic nigro-striatal pathway. Dopaminergic neurons of the substantia nigra pars compacta (SNpc) project to the striatum *via* the medial forebrain bundle (mfb), and release dopamine to medium spiny neurons (MSN). This input is relayed *via* several circuits to the neocortex, finally regulating important physical conditions, including motor coordination. Lesion or inhibition of dopaminergic neurons from only one hemisphere leads to an imbalance in dopaminergic signaling. Higher activity on the intact side usually results in an ipsilateral rotational phenotype of the animal. If apomorphine, a dopamine receptor agonist, is administered, the imbalance is changed to the inhibited/lesioned side, due to increased receptor affinity and number of receptors, as a physiological reaction to the missing innervation. This results in a change of the rotational behavior to contralateral circling. From Auer *et al.* (2010).

Figure 4. Représentation de la voie nigrostriatale et du comportement de rotation induit chez la souris injectée avec les t-toxines MVIIA-PE and AgaIVA-VG. *Vue sagitale de la voie nigrostriatale. Les neurones dopaminergiques de la* pars compacta *de la substance noire (SNpc) projettent vers le striatum via le faisceau médian du cerveau antérieur (mfb) et relarguent la dopamine dans les* neurones épineux moyens *(MSN). Cette stimulation est relayée au travers de nombreux circuits du néocortex contrôlant d'importantes fonctions physiologiques comme la coordination motrice. La lésion ou l'inhibition des neurones dopaminergiques d'un seul hémisphère conduit à un déséquilibre de la signalisation dopaminergique. D'une activité renforcée du côté intact résulte un phénotype de rotation ipsilatérale de l'animal. Si l'apomorphine, un agoniste des récepteurs dopaminergiques, est administrée, le déséquilibre est transféré du côté inhibé ou lésé, du fait de l'affinité augmentée du récepteur et du nombre de récepteurs, réaction physiologique à l'innervation manquante. Cela résulte en un changement du comportement de rotation vers une rotation controlatérale. D'après Auer* et al. *(2010).*

Mice stereotactically injected in SNpc with lentiviruses encoding for both t-toxins (MVIIA-PE and AgaIVA-VG) displayed a robust rotational phenotype and reversal upon apomorphine administration. These findings strongly suggest an imbalance in the motor coordination of t-toxin injected mice, resulting from the inhibition of the dopaminergic nigro-striatal pathway by the action of both t-toxins (Auer *et al.*, 2010).

This first proof of function of the validity of using virally encoded t-toxins *in vivo* in the mouse demonstrates the general applicability of the t-toxin strategy as a straightforward method that can be used to block $Ca_V2.1$ and $Ca_V2.2$ calcium currents, resulting in cell-specific and cell-autonomous silencing of neurotransmission. These data also suggest that both t-toxins could be broadly applied for long-term inhibition of $Ca_V2.1$ and $Ca_V2.2$ channels individually or simultaneously, to allow the characterization of the channel contribution to physiological functions and circuit analyses in a wide variety of species.

Extension of the tethered toxin strategy to peptide ligands and further applications of t-toxins and t-peptides beyond neurocircuitry

The t-peptide strategy has been successfully extended to other bioactive peptides, such as ligand peptides for constitutive activation of GPCRs (Choi *et al.*, 2009; Fortin *et al.*, 2009), illustrating the general applicability of this approach for cell-surface modulation of receptors (*Figure 5*). Ion channels and receptors are involved in every physiological action from breathing to heart beating. Understanding the mechanics and functional activity of these macromolecular complexes is a grand challenge in science. The tethered-peptide method is one tool that has the potential to tackle certain aspects of this challenge, particularly in the area of cell-specific modulators. Genetically encoded cell-surface modulators can be adapted to a wide range of applications due to their small size, amenability to point mutagenesis, and relative ease to be combined with fluorescent markers. Inhibition or constitutive activation of ion channels and receptors can be attained in a cell-type specific manner depending on the selectivity of the neuroactive peptide or hormone.

Cell-based therapies

The tethered-peptide strategy represents a potential new avenue for the development of genetic therapies for chronic diseases caused by malfunction of ion channels and peptide ligand receptors. For instance, cases of severe chronic pain in humans, resistant to analgesics and opioids, are currently being treated with ω-conotoxin MVIIA (commercialized as Prialt; Zamponi *et al.*, 2009; Miljanich, 2004). However, the use of this toxin requires the implantation of intrathecal microinfusion pumps, which allow constant administration of the soluble drug to minimize the substantial side effects due to block of $Ca_V2.2$ channels present in the CNS. Genetic targeting of t-MVIIA to nociceptive neurons in transgenic mice has shown that these mice are protected from inflammatory and neuropathic pain (Auer *et al.*, 2010). Therefore the t-toxin could be a viable alternative therapy to avoid uncontrolled diffusion of the injected toxin and the necessity for repetitive treatments once safe viral methods for genetic intervention in humans will be implemented. Other disorders which have been traced to mutations in genes encoding ion channels or regulatory proteins, such as channelopathies (George, 2005), could also benefit from the use of specific toxins if these could be selectively targeted to the affected neuronal population. For instance t-toxins producing partial or total block of particular ion channel subtypes could be used in disorders caused by missense mutations that result in channel hyperactivity. Examples of hyperactive disorders include familial hemiplegic migraine type 1 (FHM-1) caused by gain-of-function mutations in P/Q-type ($Ca_V2.1$) calcium channels (Ophoff *et al.*, 1996), or different types of epilepsy such as autosomal dominant nocturnal frontal lobe epilepsy (ADNFLE) associated to mutations in nAChRs (Klaassen *et al.*, 2006). It could be interesting to use t-toxins to dissect the circuitry of the disease in these or other mouse mutant models of ion channel mutations. Conversely, activation of receptors with t-peptide ligands could be beneficial to control GPCRs in a cell-selective manner (*Figure 5*). For instance, isoforms of glucagon-like and calcitonin-gene-related peptides are presently being used to regulate insulin release and bone remodeling in diabetes and osteoporosis. Similarly, feeding regulation neuropeptides such as orexin or ghrelin could be targeted to circuits involved in appetite control, or tethered opioid peptides could be directed to nociceptive neurons.

With an ever-growing interest in identifying the potential of naturally occurring venom peptide toxins (Twede *et al.*, 2009), as well as novel ligands for orphan GPCRs encrypted in the human proteome (Jiang and Zhou, 2006), an increasing number of peptide based therapies could be possible. Furthermore, parallel development on the safety of viral methods for genetic intervention will increase the number of diseases to which the t-peptide strategy is applicable.

Drug discovery

Ion channels and GPCRs are some of the biggest molecular drug targets yet presently remain underexploited in drug discovery efforts. Peptide toxins, which are highly effective modulators of ion channels and GPCRs, offer an intriguing opportunity for increasing the drug development pipeline. Specific areas in which peptide toxins have demonstrated their potential include chronic pain (Miljanich, 2004) and myasthenic autoimmune response (Drachman, 1981). A major drawback to the universal usage of peptide toxins in the development of therapeutics has been the scarcity of obtaining the venom product. To circumvent this, most toxins are synthesized chemically, but this too has significant problems, one being obtaining the correct disulfide scaffold with in vitro folding. To combat these synthesis hurdles several structural strategies and characterization methods have been developed (Walewska *et al.*, 2009). However, even when the toxin is successfully synthesized, soluble toxins cannot be directed to single cell populations, are expensive, and have a limited time of application that makes their use in vivo problematic. The t-peptide strategy surmounts these limitations with the ability to recombinantly synthesize the toxins or peptide ligands in the cell itself, and co-express it with the

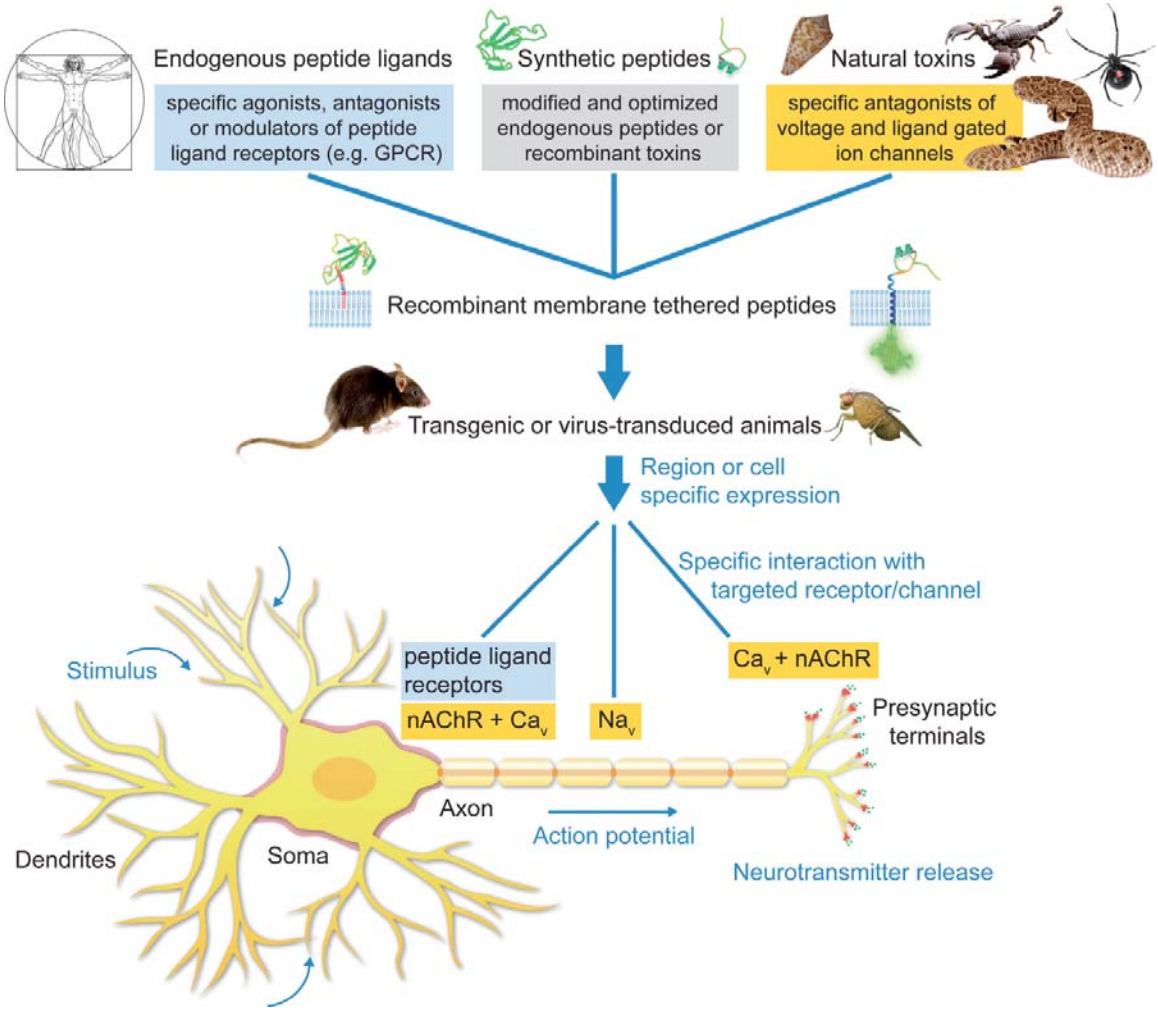

Figure 5. Applications of the tethered-peptide strategy. Endogenous peptide ligands, natural toxins, and synthetic, modified versions of ligands or toxins can be integrated into recombinant membrane-attached fusion constructs and applied *in vitro* in transfected or transduced cells in cell-culture, or *in vivo* in transgenic or virus-transduced animals. The t-peptide retains the specificity of the toxin/peptide ligand allowing controlled manipulation of distinct subtypes of ion channels and receptors in a given neuronal circuit without affecting other channels/receptors in the cell. From Holford *et al.* (2009).

Figure 5. Applications de la stratégie des toxines ancrées à la membrane. *Les ligands peptidiques endogènes et les toxines naturelles, synthétiques ou modifiées peuvent être intégrés dans les expressions recombinantes de peptides ancrés, fusionnés et utilisés* in vitro *dans des cellules transfectées ou transduites ou* in vivo *dans des animaux transgéniques ou génétiquement modifiés par des virus. Les t-peptides conservent la spécificité des toxines ou ligands peptidiques permettant la manipulation contrôlée de différents canaux ioniques et récepteurs dans un circuit neuronal particulier, sans affecter d'autres canaux et récepteurs de la cellule. D'après Holford* et al. *(2009).*

molecular target (receptor or channel) to be screened. Such a cell-surface peptide tethering strategy can readily introduce point mutations to interconvert tethered agonists into antagonists. Several recent reports use the t-peptide technology to characterize point mutants of peptide hormones against class B1 GPCRs (Ibañez-Tallon *et al.*, 2004; Fortin *et al.*, 2009). In a similar manner, the t-peptide technology could be applied to screen gene libraries of t-peptides against specific membrane proteins by co-expression in the same cell. T-peptides with activating or blocking capabilities could be monitored with functional assays, *i.e.* calcium influx. This type of screen could be beneficial to block channels that are hyperactive in certain diseases, for which no natural toxins have yet been identified. These features make the t-peptide genetic approach a promising strategy for drug discovery and development of targeted therapeutics.

Acknowledgements. *IIT is supported by grants from the DFG (SFB 665) and from the Helmholtz-Gemeinschaft. IIT is Group Leader at the Max Delbruck Center for Molecular Medicine.*

References

Auer S, Sturzebecher AS, Juttner R, Santos-Torres J, Hanack C, Frahm S, Liehl B, Ibanez-Tallon I (2010) Silencing neurotransmission with membrane-tethered toxins. *Nat Methods* **7**: 229-236

Auer S, Ibañez-Tallon I (2010) "The King is dead": Checkmating ion channels with tethered toxins. *Toxicon* **56**: 1293-1298

Baker MD, Wen H (2010) Tethered-toxin debut gets cold reception. *J Physiol* **588**: 1663

Carr RW, Pianova S, Brock JA (2002) The effects of polarizing current on nerve terminal impulses recorded from polymodal and cold receptors in the guinea-pig cornea. *J Gen Physiol* **120**: 395-405

Catterall WA, Cestele S, Yarov-Yarovoy V, Yu FH, Konoki K, Scheuer T (2007) Voltage-gated ion channels and gating modifier toxins. *Toxicon* **49**: 124-141

Catterall WA, Few AP (2008) Calcium channel regulation and presynaptic plasticity. *Neuron* **59**: 882-901

Choi C, Fortin J, McCarthy EV,Oksman L, Kopin AS., Nitabach MN (2009) Cellular dissection of circadian peptide signals using genetically encoded membrane-tethered ligands. *Curr Biol* **19**: 1167–1175

Chua JJ, Kindler S, Boyken J, Jahn R (2010) The architecture of an excitatory synapse. *J Cell Sci* **123**: 819-823

Drachman DB (1981) The biology of myasthenia gravis. *Annu Rev Neurosci* **4**: 195–225

Dutertre S, Lewis RJ (2010) Use of venom peptides to probe ion channel structure and function. *J Biol Chem* **285**: 13315-13320

Fortin J, Zhu Y, Choi C, Beinborn M, Nitabach MN, Kopin AS (2009) Membrane-tethered ligands are effective probes for exploring class B1 G protein-coupled receptor function. *Proc Natl Acad Sci USA* **106**: 8049–8054

George AL (2005) Inherited disorders of voltage-gated sodium channels. *J Clin Invest* **115**: 1990-1999

Gong S, Yang XW, Li C, Heintz N (2002) Highly efficient modification of bacterial artificial chromosomes (BACs) using novel shuttle vectors containing the R6Kgamma origin of replication. *Genome Res* **12**: 1992-1998

Groenewegen H J (2003) The basal ganglia and motor control. *Neural Plast* **10**: 107-120

Hatten ME, Heintz N (2005) Large-scale genomic approaches to brain development and circuitry. *Annu Rev Neurosci* **28**: 89-108

Holford M, Auer S, Laqua M, Ibañez-Tallon I (2009) Manipulating neuronal circuits with endogenous and recombinant cell-surface tethered modulators. *Front Mol Neurosci* **2**: 21

Hruska M, Ibanez-Tallon I, Nishi R (2007) Cell-autonomous inhibition of alpha 7-containing nicotinic acetylcholine receptors prevents death of parasympathetic neurons during development. *J Neurosci* **27**: 11501-11509

Ibañez-Tallon I, Miwa JM, Wang HL, Adams NC, Crabtree GW, Sine SM, Heintz N (2002) Novel modulation of neuronal nicotinic acetylcholine receptors by association with the endogenous prototoxin lynx1. *Neuron* **33**: 893-903

Ibañez-Tallon I, Wen H, Miwa JM, Xing J, Tekinay AB, Ono F, Brehm P, Heintz N (2004) Tethering naturally occurring peptide toxins for cell-autonomous modulation of ion channels and receptors *in vivo*. *Neuron* **43**: 305-311

Jiang Z, Zhou Y (2006) Using silico methods predicting ligands for orphan GPCRs. *Curr Protein Pept Sci* **7**: 459-464

Klaassen A, Glykys J, Maguire J, Labarca C, Mody I, Boulter J (2006) Seizures and enhanced cortical GABAergic inhibition in two mouse models of human autosomal dominant nocturnal frontal lobe epilepsy. *Proc Natl Acad Sci USA* **103**:19152-19157

Leipold E, DeBie H, Zorn S, Borges A, Olivera BM, Terlau H, Heinemann SH (2007) muO conotoxins inhibit Na_V channels by interfering with their voltage sensors in domain-2. *Channels (Austin)* **1**: 253-262

Luo L, Callaway EM, Svoboda K (2008) Genetic dissection of neural circuits. *Neuron* **57**: 634-660

Miljanich GP (2004) Ziconotide: neuronal calcium channel blocker for treating severe chronic pain. *Curr Med Chem* **11**: 3029-3040

Mink JW (1996) The Basal Ganglia: Focused selection and inhibition of competing motor programs. *Prog Neurobiol* **50**: 381-425

Miwa JM, Ibanez-Tallon I, Crabtree GW, Sánchez R, Sali A, Role LW, Heintz N (1999) lynx1, an endogenous toxin-like modulator of nicotinic acetylcholine receptors in the mammalian CNS. *Neuron* **23**: 105-114

Miwa JM, Stevens T, King S, Caldarone B, Ibaneztallon I, Xiao C, Fitzsimonds R, Pavlides C, Lester H, Picciotto M (2006) The prototoxin lynx1 acts on nicotinic acetylcholine receptors to balance neuronal activity and survival *in vivo*. *Neuron* **51**: 587-600

Ophoff RA, Terwindt GM, Vergouwe MN, van Eijk R, Oefner PJ, Hoffman SM, Lamerdin JE, Mohrenweiser HW, Bulman DE, Ferrari M, Haan J, Lindhout D, van Ommen GJ, Hofker MH, Ferrari MD, Frants RR (1996) Familial hemiplegic migraine and episodic ataxia type-2 are caused by mutations in the Ca^{2+} channel gene CACNL1A4. *Cell* **87**: 543–552

Phui Yee JS, Nanling G, Afifiyan F, Donghui M, Siew Lay P, Armugam A, Jeyaseelan K (2004) Snake postsynaptic neurotoxins: gene structure, phylogeny and applications in research and therapy. *Biochimie* **86**: 137-149

Schwarting RKW, Huston JP (1996) The unilateral 6-hydroxydopamine lesion model in behavioral brain research. Analysis of functional deficits, recovery and treatments. *Prog Neurobiol* **50**: 275-331

Stürzebecher AS, Hu J, Smith ES, Frahm S, Santos-Torres J, Kampfrath B, Auer S, Lewin G R, Ibanez-Tallon I (2010) An *in vivo* tethered toxin approach for the cell-autonomous inactivation of voltage-gated sodium channel currents in nociceptors. *J Physiol Lond* **588**: 1695-1707

Takakusaki K, Saitoh K, Harada H, Kashiwayanagi M (2004) Role of basal ganglia-brainstem pathways in the control of motor behaviors. *Neurosci Res* **50**: 137-151

Tekinay AB, Nong Y, Miwa JM, Lieberam I, Ibanez-Tallon I, Greengard P, Heintz N (2009) A role for LYNX2 in anxiety-related behavior. *Proc Natl Acad Sci USA* **106**: 4477-4482

Terlau H, Olivera BM (2004) *Conus* venoms: a rich source of novel ion channel-targetedp. *Physiol Rev* **84**: 41-68

Tolu S, Avale ME, Nakatani H, Pons S, Parnaudeau S, Tronche F, Vogt A, Monyer H, Vogel R, de Chaumont F, Olivo-Marin JC, Changeux JP, Maskos U (2010) A versatile system for the neuronal subtype specific expression of lentiviral vectors. *FASEB J* **24**: 723-730

Twede VD, Miljanich G, Olivera BM, Bulaj G (2009) Neuroprotective and cardioprotective conopeptides: an emerging class of drug leads. *Curr Opin Drug Di De* **12**: 231-239

Ungerstedt U, Arbuthnott GW (1970) Quantitative recording of rotational behavior in rats after 6-hydroxy-dopamine lesions of the nigrostriatal dopamine system. *Brain Res* **24**: 485-493

Walewska A, Zhang M, Skalicky, JJ, Yoshikami D, Olivera BM, Bulaj G (2009) Integrated oxidative folding of cysteine/ selenocysteine containing peptides: improving chemical synthesis of conotoxins. *Angew Chem Int Ed Engl* **48**: 2221-2224

Wu Y, Cao G, Pavlicek B, Luo X, Nitabach MN (2008) Phase coupling of a circadian neuropeptide with rest/activity rhythms detected using a membrane-tethered spider toxin. *PLoS Biol* **6**: e273

Zamponi GW, Lewis RJ, Todorovic SM, Arneric SP, Snutch TP (2009) Role of voltage-gated calcium channels in ascending pain pathways. *Brain Res Rev* **60**: 84-89

Zimmermann K, Leffler A, Babes A, Cendan CM, Carr RW, Kobayashi J, Nau C, Wood JN, Reeh PW (2007) Sensory neuron sodium channel $Na_V1.8$ is essential for pain at low temperatures. *Nature* **447**: 855-858

Zucker RS, Regehr WG (2002) Short-term synaptic plasticity. *Annu Rev Physiol* **64**: 355-405

Toxines et Transferts ioniques – Toxins and Ion transfers
Rencontres en Toxinologie – Meeting on Toxinology, 2011
Editions de la SFET – SFET Editions
Accès libre en ligne sur le site – Free access on line on the site : http://www.sfet.asso.fr

New aspects on membrane translocation of the pore-forming Clostridium botulinum *C2 toxin*

Eva KAISER, Katharina ERNST, Claudia KROLL, Natalie BÖHM, Holger BARTH*

Institut für Pharmakologie und Toxikologie, Universität Ulm, D-89081 Ulm, Germany

** Corresponding author ; Tel : +49 731 500 65503 ; E-mail : holger.barth@uni-ulm.de*

Abstract

C2 toxin from Clostridium botulinum *is a binary toxin which consists of two non-linked proteins, which are the transport component C2II and the enzyme component C2I. Activated C2II (C2IIa) mediates the transport of C2I into the cytosol of eukaryotic target cells, where C2I mono-ADP-ribosylates actin. This results in depolymerization of actin filaments, cell-rounding and delayed cell death. During cellular uptake, C2IIa is a ring-shaped heptamer with two different functions. First, C2IIa binds to its cell receptor and assembles with C2I what triggers receptor-mediated endocytosis of the C2IIa/C2I complex. Later, in acidified endosomes, C2IIa changes its conformation due to the low pH and inserts into the endosomal membrane, thereby forming a translocation pore for C2I. Subsequently, C2I translocates as an unfolded protein through the C2IIa pore across endosomal membranes into the cytosol. We discovered recently that C2I translocation is facilitated by host cell chaperones, such as heat shock protein Hsp90 and cyclophilin A, a peptidyl-prolyl cis/trans isomerase. The pharmacological inhibition of these factors prevents translocation of C2I into the cytosol and thus protects cells from intoxication with C2 toxin.*

Nouveaux aspects sur la translocation à travers les membranes de la toxine C2 de Clostridium botulinum *formant des pores*

La toxine C2 de Clostridium botulinum *est une toxine binaire consistant en deux protéines non reliées entre elles qui sont, d'une part, le composant de transport C2II et, d'autre part, le composant enzymatique C2I. Le composant de transport activé (C2Iia) est responsable du transport de C2I dans le cytosol des cellules eucaryotes cibles où il mono-ADPribosyle l'actine. Ceci conduit à la dépolymérisation des filaments d'actine, à l'arrondissement puis à la mort des cellules. Au cours de l'entrée dans la cellule, C2IIa forme un heptamère en anneau ayant deux fonctions différentes. Premièrement, C2IIa se lie à son récepteur cellulaire et s'assemble avec C2I, ce qui déclenche l'endocytose du complexe C2IIa/C2I. Ensuite, dans les endosomes acidifiés, C2IIa change de conformation à cause du bas pH et s'insère dans la membrane de l'endosome formant ainsi un pore de translocation pour C2I. Ainsi, C2I est transporté sous une forme dépliée à travers le pore constitué par C2IIa dans la membrane de l'endosome. Récemment, nous avons montré que la translocation de C2I est facilitée par des protéines chaperonnes de la cellule hôte, telles que la protéine du choc thermique (Hsp90) et la cyclophiline A qui est une peptide-prolyl-cis/trans isomérase. L'inhibition pharmacologique de ces facteurs empêche la translocation de C2I dans le cytosol et protège ainsi les cellules des effets toxiques de la toxine C2.*

Keywords : *C2 toxin, chaperone proteins,* Clostridium botulinum*, endocytose, pore-formation.*

Introduction

Bacterial AB-type exotoxins act as enzymes in eukaryotic cells and exploit vesicular traffic pathways of their host cells to deliver their enzyme moieties (A-subunits) into the cytosol (Sandvig and Olsnes, 1984; Montecucco *et al.*, 1994; Olsnes *et al.*, 2000; van der Goot and Gruenberg, 2006). This implies, however, that following internalization of the toxin, the A-subunits must translocate across an intracellular membrane to escape from endosomal vesicles into the cytosol. Several toxins translocate from acidified endosomal vesicles and it was found that the translocation domains of such toxins form pores into endosomal membranes which mediate the pH-dependent translocation of the A-subunits (Sandvig and Olsnes, 1980; Sandvig and Olsnes, 1981; Olsnes *et al.*, 1988).

Binary toxins are a special variation of AB-type toxins because their A- and B-subunits are located on two different proteins (for review see Barth *et al.*, 2004). The single A- and B-components are not toxic when applied to cells or animals but exhibit their cytotoxic effects when applied in combination. The A- and B-components assemble on the surface of target cells to form a biologically functional toxin complex which is then internalized *via* receptor-mediated endocytosis. In acidic endosomal vesicles, the B-components form pores and

the A-components translocate through these pores into the cytosol where they modify their substrate molecules. Besides the two toxins from *Bacillus anthracis*, lethal toxin and edema toxin, the clostridial actin-ADP-ribosylating toxins are binary toxins. The latter comprises *Clostridium botulinum* C2 toxin, on the one hand, and the iota like-toxins *C. perfringens* iota toxin, *C. difficile* toxin (CDT) and *C. spiroforme* toxin, on the other hand (for review see Barth *et al.*, 2004). Their A-components are mono-ADP-ribosyltransferases that covalently transfer ADP-ribose from NAD^+ onto arginine-177 of G-actin what induces depolymerization of actin filaments and results in the complete destruction of the actin cytoskeleton of eukaryotic target cells (Aktories *et al.*, 1986). Finally, intoxicated cells undergo delayed caspase-dependent apoptosis (Heine *et al.*, 2008).

C. botulinum type C and D strains produce the binary C2 toxin (Ohishi *et al.*, 1980), a potent enterotoxin that consists of C2I (enzyme component, ~49 kDa) and C2II (binding/translocation component, ~ 80 or 100 kDa depending on the strain). C2I selectively mono-ADP-ribosylates G-actin at arginine-177 (Aktories *et al.*, 1986). The uptake of C2 toxin into cells starts with binding of activated C2IIa to the receptor on target cells and the subsequent formation of the C2IIa/C2I complex on the cell surface. C2II requires proteolytic activation ("nicking") to form ring-shaped heptamers (Barth *et al.*, 2000) with an inner diameter of about 2-3 nm (Schleberger *et al.*, 2006). Importantly, only the activated C2IIa heptamers can bind to the receptor and assemble with C2I (Barth *et al.*, 2000; Stiles *et al.*, 2002).

Membrane translocation of C2 toxin requires host cell chaperones

Following receptor-mediated endocytosis, C2I translocates from early acidified endosomes into the cytosol. Acidification of the endosomal lumen triggers a conformational change of C2IIa heptamers, which then expose hydrophobic residues on their surface and insert into the endosomal membranes and form pores. We found that pore formation by C2IIa is an absolutely essential prerequisite for the translocation of C2I from the endosomal lumen into the cytosol (Blöcker *et al.*, 2003).

The narrow inner lumen of C2IIa pores implies that C2I must (at least partially) unfold to translocate through the pore. We used a dihydrofolate reductase (DHFR)-C2I fusion protein to demonstrate that C2I indeed unfolds during membrane translocation (Haug *et al.*, 2003b). How does C2I become refolded after membrane translocation? In 2003, we have found that the chaperone Hsp90 is crucial for translocation and/or refolding of C2I in mammalian cells (Haug *et al.*, 2003a). The specific pharmacological inhibition of Hsp90 activity by radicicol (Rad) or geldanamycin (GA) blocked the uptake of C2I into the cytosol and consequently, cells were protected from the cytoxic effects of C2 toxin. When we investigated the underlying mechanism in more detail, we found that the Hsp90 inhibitors prevented translocation of C2I (Haug *et al.*, 2003a), demonstrating that Hsp90 is involved in the membrane translocation of C2 toxin. Later, we obtained comparable results for the related binary Iota toxin from *Clostridium perfringens* (Haug *et al.*, 2004).

More recently, we could show that membrane translocation of C2I also depends on the activity of the protein-folding helper enzyme cyclophilin A (CyP-A), a peptiyl/prolyl *cis/trans* isomerase (PPIase; Kaiser *et al.*, 2009). Cyclosporin A (CsA), a specific pharmacological inhibitor of cyclophilins, prevented intoxication of mammalian cells including HeLa, Vero and CaCo-2 cell lines, with C2 toxin and inhibited the uptake of C2I into the cytosol (*Figure 1*). As the Hsp90 inhibitors, CsA had no effect on the early steps of toxin uptake or on the enzyme activity of C2I, but clearly inhibited membrane translocation of C2I from early acidified endosomes into

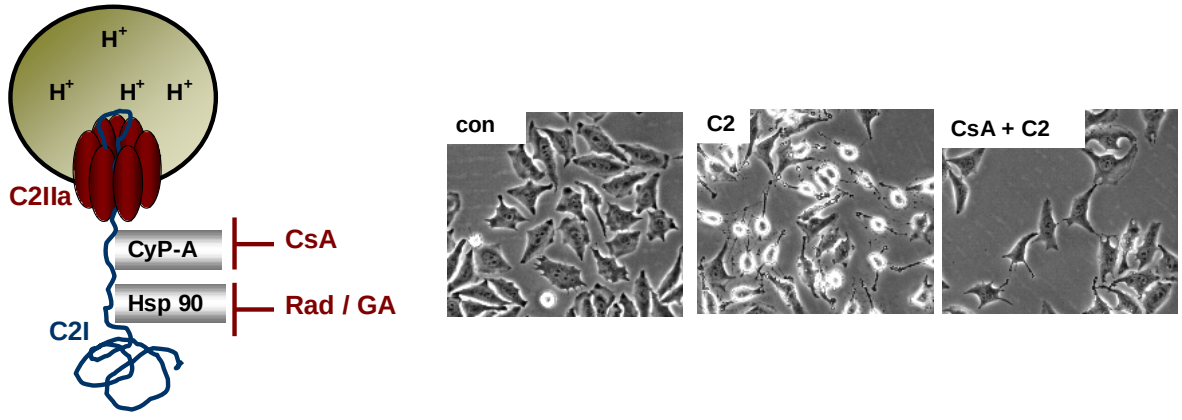

Figure 1. Current model of membrane translocation of the binary *C. botulinum* C2 toxin. Translocation of C2I requires the C2IIa pore in the endosomal membrane, as well as the activity of the chaperone Hsp90 and the prolyl isomerase cylophilin A (CyP-A; *left panel*). The specific pharmacological inhibitors cyclosporin A (CsA) and radicicol or geldanamycin inhibit translocation of C2I across endosomal membranes into the cytosol and protect cells from intoxication with C2 toxin (*right panels*; Kaiser *et al.*, 2009). Con: control.

***Figure 1. Modèle actuel de la translocation membranaire de la toxine binaire C2 de* C. botulinum.** *La translocation de C2I nécessite le pore C2IIa dans la membrane endosomale, ainsi que l'activité de la chaperonne Hsp90 et de la prolyl-isomérase cyclophiline A (CyP-A; panneau de gauche). Les inhibiteurs pharmacologiques spécifiques, cyclosporine A (CsA) et radicicol ou geldanamycine, inhibent la translocation de C2I à travers les membranes endosomales dans le cytosol et protègent les cellules contre l'intoxication par la toxine C2 (*panneaux de droite*; Kaiser* et al.*, 2009). Con: contrôle.*

the cytosol *in vitro* as well as in intact cultured cells. We used isolated early endosomes to study membrane translocation of C2I *in vitro*. C2 toxin-loaded early endosomes were incubated with fresh cytosol to trigger the release of C2I from these endosomes. The succesfull translocation of C2I into the cytosol was shown by C2I-catalyzed ADP-ribosylation of actin. When cytosol was pre-treated with CsA to inhibit cyclophilin prior to addition to C2 toxin-loaded endosomes, C2I did not translocate. By using a specific inhibitory antibody, we could demonstrate that CyP-A is the crucial cyclophilin which facilitates membrane translocation of C2 toxin. Translocation of C2I was also prevented when the cytosol was pre-incubated with antibody against CyP-A, indicating that CyP-A is necessary for membrane translocation of C2I (Kaiser *et al*., 2009).

Conclusion

Although the combined application of inhibitors suggested that cyclophilin and Hsp90 work synergistic during C2I translocation, the precise mechanism how these host cell factors facilitate membrane translocation of C2 toxin is not known so far and subject to our present research activities.

Acknowledgements. *The work was supported by the Deutsche Forschungsgemeinschaft (DFG) Priority Program SPP 1150 (BA 2087/1-3) and grant BA 2087/2-1.*

References

Aktories K, Bärmann M, Ohishi I, Tsuyama S, Jakobs KH, Habermann E (1986) Botulinum C2 toxin ADP-ribosylates actin. *Nature* **322**: 390-392

Barth H, Aktories K, Popoff MR, Stiles BG (2004) Binary bacterial toxins: biochemistry, biology, and applications of common *Clostridium* and *Bacillus* proteins. *Microbiol Mol Biol Rev* **68**: 373-402

Barth H, Blöcker D, Behlke J, Bergsma-Schutter W, Brisson A, Benz R, Aktories,K (2000) Cellular uptake of *Clostridium botulinum* C2 toxin requires oligomerization and acidification. *J Biol Chem* **275**: 18704-18711

Blöcker D, Pohlmann K, Haug G, Bachmeyer C, Benz R, Aktories K, Barth H (2003) *Clostridium botulinum* C2 toxin: Low pH-induced pore formation is required for translocation of the enzyme component C2I into the cytosol of host cells. *J Biol Chem* **278**: 37360-37367

Haug G, Aktories K, Barth H (2004) The host cell chaperone Hsp90 is necessary for cytotoxic action of the binary iota-like toxins. *Infect Immun* **72**: 3066-3068

Haug G, Leemhuis J, Tiemann D, Meyer DK, Aktories K, Barth H (2003a) The host cell chaperone Hsp90 is essential for translocation of the binary *Clostridium botulinum* C2 toxin into the cytosol. *J Biol Chem* **278**: 32266-32274

Haug G, Wilde C, Leemhuis J, Meyer DK, Aktories K, Barth H (2003b) Cellular uptake of *Clostridium botulinum* C2 toxin: Membrane translocation of a fusion toxin requires unfolding of its dihydrofolate reductase domain. *Biochemistry* **42**: 15284-15291

Heine K, Pust S, Enzenmuller S, Barth H (2008) ADP-ribosylation of actin by the *Clostridium botulinum* C2 toxin in mammalian cells results in delayed caspase-dependent apoptotic cell death. *Infect Immun* **76**: 4600-4608

Kaiser E, Pust S, Kroll C, Barth H (2009) Inhibition of peptidyl prolyl *cis/trans* isomerases (PPIases) by Cyclosporin A and Tacrolimus (FK506) protects mammalian cells from intoxication with *Clostridium botulinum* C2 toxin by preventing toxin translocation into the cytosol. *Cell Microbiol* **11**: 780-795

Montecucco C, Papini E, Schiavo G (1994) Bacterial protein toxins penetrate cells *via* a four-step mechanism. *FEBS Lett* **346**: 92-98

Ohishi I, Iwasaki M, Sakaguchi G (1980) Purification and characterization of two components of botulinum C2 toxin. *Infect Immun* **30**: 668-673

Olsnes S, Moskaug JO, Stenmark H, Sandvig K (1988) Diphteria toxin entry: protein translocation in the reverse direction. *Trends Biochem Sci* **13**: 348-351

Olsnes S, Wesche J, Falnes PO (2000) Uptake of protein toxins acting inside cells. In *Bacterial Protein Toxins*. Aktories K, Just I (eds) pp 1-19. Springer, Berlin

Sandvig K, Olsnes S (1980) Diphtheria toxin entry into cells is facilitated by low pH. *J Cell Biol* **87**: 828-832

Sandvig K, Olsnes S (1981) Rapid entry of nicked diphtheria toxin into cells at low pH. Characterization of the entry process and effects of low pH on the toxin molecule. *J Biol Chem* **256**: 9068-9076

Sandvig K, Olsnes S (1984) Receptor-mediated entry of protein toxins into cells. *Acta Histochem* **29**: 79-94

Schleberger C, Hochmann H, Barth H, Aktories K, Schulz GE (2006) Structure and action of the binary C2 toxin from *Clostridium botulinum*. *J Mol Biol* **364**: 705-715

Stiles BG, Blocker D, Hale ML, Guetthoff MA, Barth H (2002) *Clostridium botulinum* C2 toxin: binding studies with fluorescence-activated cytometry. *Toxicon* **40**: 1135-1140

Van der Goot FG, Gruenberg J (2006) Intra-endosomal membrane traffic. *Trends Cell Biol* **16**: 514-521

Toxines et Transferts ioniques – Toxins and Ion transfers
Rencontres en Toxinologie – Meeting on Toxinology, 2011
Editions de la SFET – SFET Editions
Accès libre en ligne sur le site – Free access on line on the site : http://www.sfet.asso.fr

Ion channel toxins for drug discovery and development

Richard LEWIS*, Ching-I Anderson WANG, Sébastien DUTERTRE, Irina VETTER

Institute for Molecular Bioscience, The University of Queensland, Brisbane 4072, Australia

** Corresponding author ; Tel : +33 617 3346 2984 ; Fax : +33 617 3346 2010 ;*
E-mail : r.lewis@imb.uq.edu.au

Abstract

Venoms from scorpions, spiders, sea anemones and cone snails comprise complex mixtures of peptides and mini-proteins, many of which have evolved to selectively target ion channels for prey capture and/or defence. Sodium channels including $Na_v1.7$ and 1.8 play key roles in pain pathways and selective inhibitors offer potential for the treatment of difficult to manage painful conditions. To accelerate ligand discovery at this target, we have developed a high throughput assay for $Na_v1.7$ and next generation transcriptomics to identify novel sequences. To guide the rational development of inhibitors, we have constructed a molecular model of sodium channels to generate docking simulations that can help identify interacting residues and opportunities for improving selectivity and/or potency.

Les toxines ciblant les canaux ioniques pour la découverte et le développement de médicaments

Les venins de scorpions, d'araignées, d'anémones de mer et de cônes comprennent des mélanges complexes de peptides et de mini-protéines, dont beaucoup ont évolué pour cibler sélectivement les canaux ioniques pour la capture des proies et/ou la défense. Les canaux sodium, dont $Na_v1.7$ et 1.8, jouent des rôles clés dans les voies de la douleur et les inhibiteurs sélectifs offrent un potentiel pour le traitement du mal à gérer les conditions douloureuses. Pour accélérer la découverte de ligands à cette cible, nous avons développé un test à haut débit pour $Na_v1.7$ et des transcriptomes de la prochaine génération pour identifier de nouvelles séquences. Afin de guider le développement rationnel d'inhibiteurs, nous avons construit un modèle moléculaire des canaux sodium pour générer des simulations d'amarrage qui peuvent aider à identifier les résidus impliqués dans les interactions et les possibilités d'améliorer la sélectivité et/ou l'efficacité.

Keywords : *Conotoxin, pain, sodium channel, venom peptide.*

Introduction

Venom peptides provide a rich source of peptides with highly diverse sequences and structures evolved for prey capture and/or defence (Lewis and Garcia, 2003; Fry *et al.*, 2009). Not surprisingly given their pivotal roles in essential physiological processes, many venom peptides have been found to target ion channels, including a number with clinical potential that target voltage-gated calcium and potassium channels, ligand-gated NMDA glutamate and nicotinic acetylcholine receptors (nAChR), and the sodium-dependent norepinephrine transporter (*Table 1*). Toxins have proved especially useful in dissecting the physiological roles of different Na_v channels, as well as helping to identify up to seven distinct, ligand-accessible binding sites on these large membrane proteins. Tetrodotoxin (TTX), the first sodium channel toxin identified, acts at site 1 in the P-loop region of the ion conducting pore of TTX-sensitive $Na_v1.1$-1.4, 1.6 and 1.7 at low nM concentrations, and at TTX-resistant $Na_v1.5$, 1.8 and 1.9 at µM concentrations. In contrast, alkaloid toxins from frogs and plants (batrachotoxin, veratridine) act at site 2, polyether toxins from dinoflagellates (brevetoxins and ciguatoxins) act at site 5, pyrethroids from plants act at site 7, while venom peptides act at or near sites 1, 3/6 and 4.

Venom peptides acting at Na_v subtypes include scorpion toxins acting at sites 3 and 4, spider toxins acting at or near sites 1 and 4 on mammalian targets or site 3 on insect targets, and cone snail toxins acting at or near sites 1, 4 and 3/6. Cone snail toxins acting at Na_v subtypes include the globular µ-conotoxins which possess an exposed arginine/lysine in loop 2 required for high affinity at $Na_v1.2/1.4$. The therapeutic potential of µ-conotoxins is presently limited, since they preferentially target $Na_v1.4$ and 1.2, and have only weak or no detectable affinity at the validated therapeutic targets $Na_v1.7$ or 1.8. However, models built from the recently described crystal structure of a bacterial voltage-gated sodium channel have opened up opportunities to rationally develop inhibitors of more therapeutically relevant subtypes. In this review, opportunities for the accelerated discovery of venom peptides targeting sodium channels are examined that have the potential to generate leads to new ion channel therapies to treat difficult to manage painful conditions.

Table 1. Potential ion channel and related therapeutics from venoms.
Tableau 1. *Canaux ioniques et thérapeutiques de venins potentiels.*

Name	AAs	S-S bonds	Source	Ion channel target	Site of injection	Indication	Stage
Prialt® (ω-MVIIA)	25	3	*Conus magus*	$Ca_V2.2$	Intrathecal	Chronic pain	Approved 2004
Xen2174 (χ-MrIA)	13	2	*Conus marmoreus*	Norepinephrine transporter	Intrathecal	Severe pain	Phase 2b
CNSB004 (ω-CVID)	27	3	*Conus catus*	$Ca_V2.2$	Subcutaneous	Neuropathic pain	Phase 2a
ShK-192	35	3	*Stichodactyla helianthus*	$K_V1.3$ channel	Parenteral	Autoimmune disease	Phase 1
CGX-1051 (κ-PVIIA)	27	3	*Conus purpurascins*	Shaker-type K_V channel	Parenteral (i.v. injection)	Myocardial infarction	Phase 1
ACV-1 (α-Vc1.1)	16	2	*Conus victoriae*	$GABA_B$ and nAChR	Parenteral (s.c. injection)	Neuropathic pain	Phase 2a
CGX-1007 (Conantokin-G)	17	0	*Conus geographus*	NMDA receptor	Intrathecal	Epilepsy	Phase 1

Venom peptide modulators of sodium channels

The μ-conotoxins are amongst the first venom peptides identified to inhibit Na^+ channels. These highly positively charged 16–25 amino acid (a.a.) peptides possess a globular structure stabilised by a network of three disulfide bonds. Nuclear magnetic resonance (NMR) solution structures of SIIIA, TIIIA, PIIIA, GIIIA, GIIIB, KIIIA and SmIIIA reveal all have a similar fold except SIIIA, which has a much shorter loop 1 and an helical motif between residues 11–16 (Schroeder *et al.*, 2008) not seen in the larger μ-conotoxins like TIIIA (Lewis *et al.*, 2007). All μ-conotoxins possess either an exposed arginine or lysine in loop 2 that is important for high affinity at $Na_v1.2$ and 1.4, although this role is less critical for SIIIA and KIIIA, where the pharmacophore has shifted into the helical region of the peptide (Schroeder *et al.*, 2008). The therapeutic potential of μ-conotoxins is presently limited, since they preferentially target $Na_v1.4$ and 1.2 and have weak or no detectable affinity at the validated therapeutic targets $Na_v1.7$ or 1.8. A docking model depicting how μ-conotoxin TIIIA might plug the selectivity filter of the muscle Na^+ channel ($Na_v1.4$) is shown in *Figure 3B*. This model highlights the critical role of Arg13 for the high affinity interaction with $Na_v1.4$. As our understanding of the overall architecture of the outer vestibule of the Na^+ channel develops, conotoxins able to block specific Na^+ channel subtypes may start to be rationally designed.

Cone snail venoms also contain two classes of hydrophobic Na^+ channel toxins, the μO-conotoxins MrVIA and MrVIB isolated from *Conus marmoreus* and the more diverse δ-conotoxins isolated from a range of mollusc and fish hunting cone snails. The μO-conotoxins are 31 a.a. peptides that preferentially block (~ 15-fold selective) $Na_v1.8$ and 1.4 over other Na_v subtypes by interfering with the domain II voltage sensor of the Na^+ channel (Leipold *et al.*, 2007). Unfortunately, structure-activity relationships for μO-conotoxins at different Na_v subtypes have been hampered by difficulties folding and purifying these hydrophobic peptides efficiently. The 27–31 residue δ-conotoxins have structures reminiscent of the μO-conotoxins; however, these activating peptides work by inhibiting Na^+ channel inactivation like the α scorpion toxins (Barbier *et al.*, 2004). The δ-conotoxins include TxVIA a selective activator of mollusc Na^+ channels, and EVIA which selectively activates mammalian neuronal Na^+ channels.

Finally, two conotoxins belonging to the ι-conotoxin class have been identified as Na_v activators that are without effects on Na_v inactivation. ι-RXIA is a large, 46 residue peptide from the I superfamily that forms an ICK motif, while LtIIIA is a small, 17 residue peptide belonging to the M superfamily of conotoxins.

Potential for peptide inhibitors of sodium channels to treat pain

Voltage-gated sodium (Na_v1-9) channels are 4-domain membrane proteins essential for electrical signalling in cells. Naturally occurring mutations to Na_v can lead to epilepsy, migraine and several pain-free and painful conditions. Knockout studies in mice have shown that $Na_v1.7$, 1.8 and 1.9 play key roles in pain pathways and suggest that inhibition of these subtypes might reduce pain without introducing significance adverse effects commonly associated with non-specific inhibitors like local anaesthetics, which are often efficacious only at or near toxic levels. Thus more selective venom peptides that target Na_v subtypes selectively expressed in nociceptive nerves (Na_v1. 7 and 1.8), or are upregulated in pain states ($Na_v1.3$) could significantly advance the treatment of chronic pain.

The recent finding that loss of function mutations at $Na_v1.7$ ablates human pain genetically validates $Na_v1.7$ as a new therapeutic target (Cox *et al.*, 2006). Presently spiders appear to be the best source of $Na_v1.7$ inhibitors. These appear to inhibit channel opening by binding to extracellular surface residues involved in channel gating (Schmalhofer *et al.*, 2008; Xiao *et al.*, 2010). Small neuronally active μ-conotoxins like μ-SIIIA and μ-SIIIB define a new pharmacophore for interactions at $Na_v1.2$ and $Na_v1.4$ (Lewis *et al.*, 2007; Schroeder *et al.*, 2008). Interestingly, SIIIB and the recently reported KIIIA (Zhang *et al.*, 2007) also have weak to moderate potency at $Na_v1.7$, opening the way to the development of μ-conotoxins with improved $Na_v1.7$ selectivity that can reverse chronic pain behaviours without dose-limiting side-effects. Confirming $Na_v1.8$ knockout studies, our discovery that μO-conotoxin inhibitors of $Na_v1.8$ sodium channel (Daly *et al.*, 2004)

reverse inflammatory and neuropathic pain states without motor deficits (Ekberg *et al.*, 2006) opens the way to the development of novel peptide inhibitors at this pivotal pain target.

Accelerated assays for sodium channel inhibitor

Traditional approaches to identify novel, subtype-selective modulators of Na_v suffer from drawbacks. While electrophysiological techniques can provide high quality data that offer mechanistic insights into the state-dependence of inhibition, despite the development of novel fully automated patch-clamp technology this approach can currently achieve medium throughput at best and requires highly skilled personnel. In contrast, fluorescence-based assays measuring changes in membrane potential or intracellular sodium concentration have the potential for assaying a large number of compounds but often require specialized excitation and emission filters and are prone to artefacts and sensitivity problems. Similarly, radioligand binding assays are particularly prone to high false negative rates due to the large number of putative allosteric sites on Na_v and in addition cannot provide functional information. Finally, an inherent problem with these approaches are difficulties encountered with cloning and heterologous expression of the large Na_v channel complexes, which further restrict the development of functional assays with sufficient capacity.

To overcome these problems, we have developed a novel high throughput assay based on fluorescent calcium signaling mediated through TTX-sensitive $Na_v1.2$ and $Na_v1.7$ endogenously expressed in the human neuroblastoma cell line SH-SY5Y. Activation of these endogenously expressed Na_v isoforms by the alkaloid veratridine results in influx of Na^+ ions and subsequent membrane depolarization. This membrane depolarization in turn generates a Ca^{2+} influx through endogenously expressed voltage-gated L- and N-type calcium channels that can be detected by fluorescent Ca^{2+} dyes such as Fluo-4 in high throughput format. Block of $Na_v1.2$ by the conotoxin TIIIA or stimulation in the presence of the scorpion toxin OD1 produces a $Na_v1.7$-specific assay, and conversely block of $Na_v1.7$ by low concentrations of ProTxII isolates Na_v responses mediated by $Na_v1.2$. The ability to detect changes in Na^+ channel activity using Ca^{2+} dyes such as Fluo-4 takes advantage of the extremely high sensitivity inherent to fluorescent Ca^{2+} imaging. In addition, this assay can detect both pore blockers and gating modifier toxins as Na^+ channels are expressed at physiological membrane potential in a native context, and provides a cheap, readily available alternative for the high-throughput identification of novel Na^+ channel inhibitors. A pipeline from venom to sequence is exemplified in *Figure 1*, showing result for the detection, isolation and sequencing of MrVIA from *Conus marmoreus*.

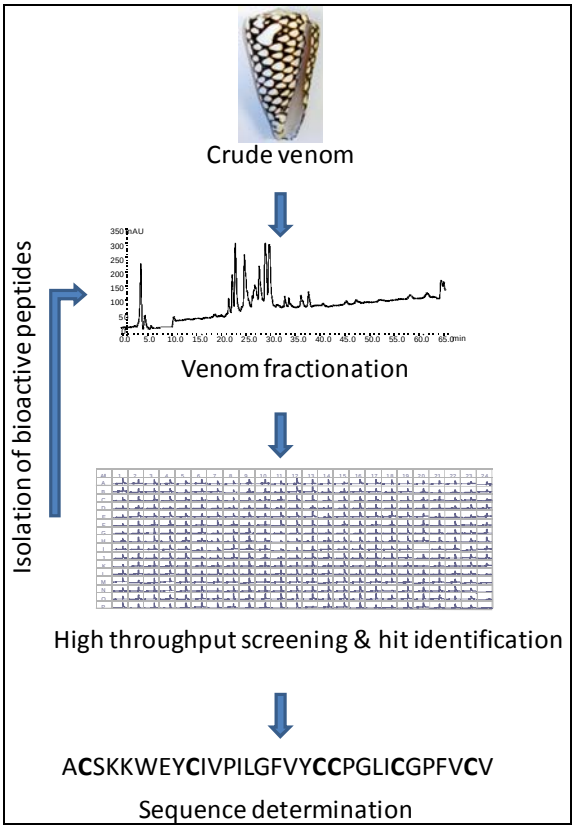

Figure 1. Application of a FLIPR-based high throughput assay for $Na_v1.7$ for the discovery of Na^+channel inhibitors. Illustrated is the identification and sequence obtained for MrVIB identified in the crude venom of *Conus marmoreus*.

***Figure 1**. Application d'une analyse à haut débit pour $Na_v1.7$, basée sur la méthode FLIPR, pour la découverte d'inhibiteurs de canaux Na^+. L'identification et la séquence obtenue pour MrVIB identifié dans le venin brut de* Conus marmoreus *sont illustrées ici.*

Transcriptomic / proteomic discovery

Thanks to large scale genomic projects, such as the Human Genome Project, technologies for high throughput DNA sequencing are now widely available for genome and transcriptome analysis of non-model organisms. Indeed, these "next-generation sequencing" technologies, as opposed to the traditional Sanger sequencing, have delivered on the promise of sequencing DNA and RNA at unprecedented speed and reduced cost, thereby enabling impressive scientific achievements and novel biological applications (Morozova *et al.*, 2009). Different platforms are available, each having their own pros and cons, and the choice made by the user will depend on the final application. For example, the 454-pyrosequencing technology from Roche provides the longest reads (300–350 bp on average), a clear advantage for the accurate assembly of contigs in the absence of a reference genome. Particularly relevant to venom-based discovery projects, transcriptome analysis of venom gland mRNA has the potential to reveal all toxin sequences in one single experiment (Hu *et al.*, 2011). This strategy will undoubtedly accelerate the discovery of novel isoforms and families of toxins, assuming that appropriate bioinformatic support is provided. Unfortunately, in the case of cone snails, the high prevalence of post-translational modifications preclude direct discovery process from transcriptomic data alone, and proteomic data integration are required to determine the correct form of the mature compound (*Figure 2*).

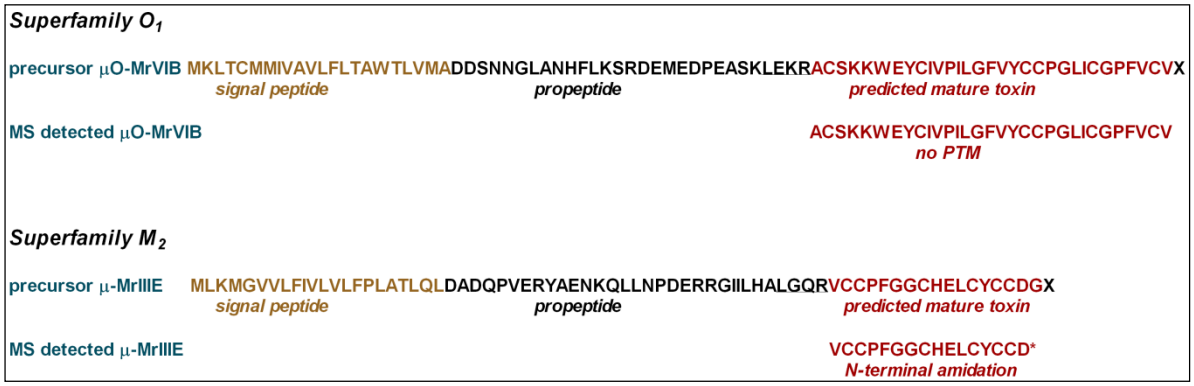

Figure 2. Integration of transcriptomic and proteomic data. Here, we illustrate the need of combined transcriptomic and mass spectrometry (MS) data for the correct identification of mature venom peptides. In the venom gland transcriptome of *Conus marmoreus*, we have found the precursors of Na^+ channel toxins, μO-MrVIB and μ-MrIIIE. In the case of MrVIB, the mature peptide detected by MS is identical to the predicted mature peptide. However, in the case of MrIIIE, MS detected peptide revealed the post-translational cleavage of the C-terminal glycine residue, creating an amidated mature peptide. Post-translational modifications (PTMs) can have dramatic effects on stability and biological activity of peptides, hence the need to clearly identify them.

Figure 2. *Intégration de données transcriptomiques et protéomiques. Dans cette figure, nous illustrons la nécessité de combiner les données de transcritpomiques et de protéomiques pour l'identification correcte des toxines matures. Dans le transcriptome de* Conus marmoreus*, nous avons identifié les précurseurs des toxines agissant sur les canaux sodium, μO-MrVIB et MrIIIE. Dans le cas de MrVIB, le peptide détecté par spectrométrie de masse (SM) se révèle identique à la séquence prédite à partir du précurseur. Cependant, dans le cas de MrIIIE, la SM révèle le clivage du résidu glycine en position N-terminale, laissant un peptide mature amide. Les modifications post-traductionnelles peuvent avoir des effets importants sur la stabilité et l'activité biologique des peptides, d'où la nécessité de les identifier clairement.*

Mass spectrometry (MS) has become a method of choice to study the complexity of venoms. Soft ionisation technologies (ESI and MALDI) are almost exclusively utilized to unravel the composition of these proteinaceous mixtures (Davis *et al.,* 2009; Escoubas *et al.,* 2008). While venoms can be studied as a whole sample (mass fingerprinting or profiling), a pre-fractionation step will usually provide a better resolution, diminution of the ion suppression effect and higher coverage. Recent improvements in sensitivity (dynamic range) and accuracy of mass spectrometers are allowing high throughput analysis from minute sample. For instance, using a combined Orbitrap-ETD with a targeted chemical derivatization strategy, de novo sequencing of 31 peptide toxins could be obtained from just 7% of the crude venom of a single *Conus textile* (Ueberheide *et al.,* 2009). Combining the sequence database deduced from transcriptomics with the masses extracted from crude venom MS analysis is emerging as a remarkably powerful approach. A major issue is the correct assignment of each detected mass to a sequence. Here, MS/MS will be essential to confirm the cleavage sites and the presence/nature of post-translational modifications (PTMs).

Rational development of peptidic sodium channel inhibitors

Voltage-gated ion channels (VGICs) share a common structural arrangement with four homologous subunits that form a central ion conducting pore. As is the case for most transmembrane proteins, structure determination is technically challenging, especially for mammalian VGICs which are multi-domain proteins comprised of over 2,000 amino acids. This structural complexity has hampered the rational drug design for channel-associated diseases. In the absence of a detailed 3D molecular view of VGICs, a wealth of information on functional domains of VGICs was only obtainable from structure-activity relationships (SARs) of small molecule or peptide inhibitors, including μ-conotoxins GIIIB (Li *et al.*, 2000) and TIIIA (Lewis *et al.*, 2007).

A breakthrough in revealing the ion selectivity and ion conduction pathway of VGICs at the molecular level came with the determination of high resolution crystal structures of mammalian K_v (Long *et al.*, 2005) and

more recently bacterial Na_vAb (Payandeh *et al.*, 2011). Given that VGICs share a conserved structural architecture, homology modeling, in combination with docking simulation, provides an alternative approach to study the molecular basis of ligand-Na_v interactions. Our preliminary data, derived from docking simulation of µ-conotoxin TIIIA to an homology model of human $Na_v1.4$ generated using crystal structure of Na_vAb (Payandeh *et al.*, 2011), have shown that the inhibition of µ-conotoxin TIIIA likely occurs *via* an extensive network of ionic interaction at the extracellular mouth of the ion conducting pathway (*Figure 3*). This docking pose is supported by SAR studies of µ-conotoxin GIIIB at $Na_v1.4$ (Li *et al.*, 2000) and our previous mutational studies on TIIIA (Lewis *et al.*, 2007). This demonstrates that by combining homology modeling and related computational studies, such as docking or molecular dynamic simulation, useful insights into SARs in VGICs can be obtained that might help in the rational design of subtype selective inhibitors.

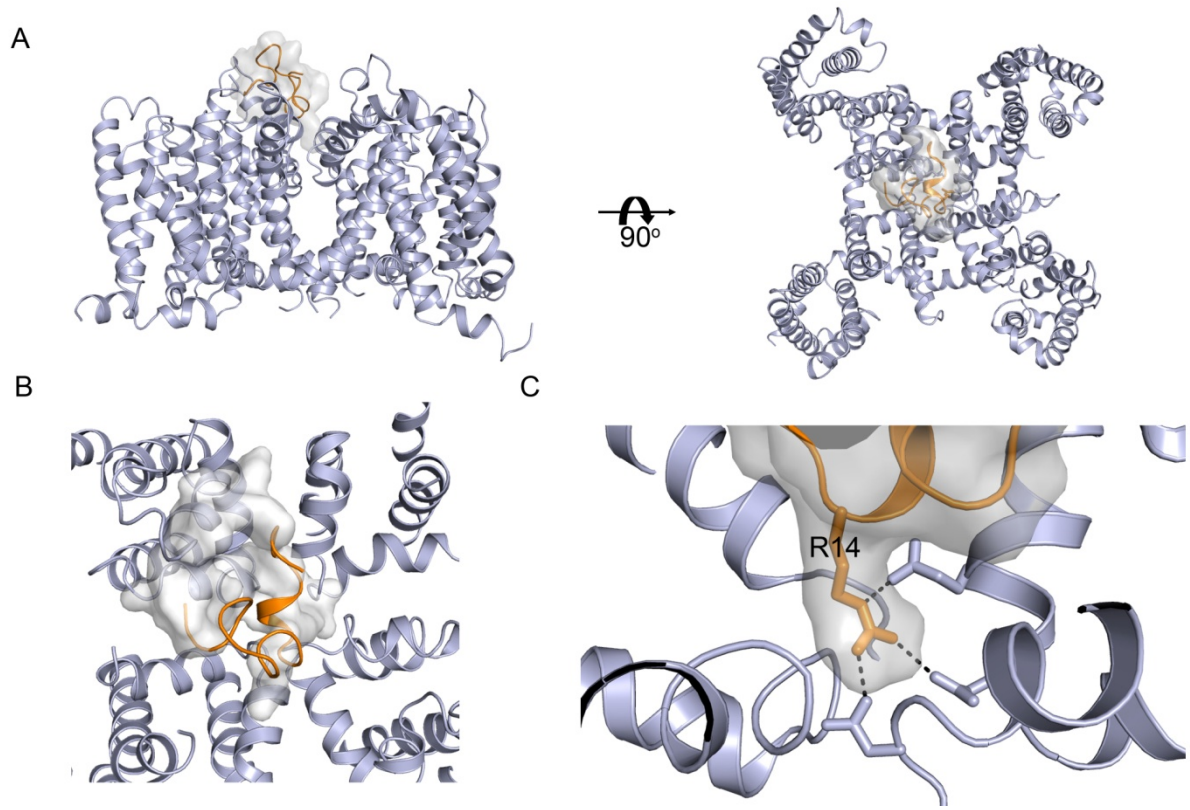

Figure 3. Docking simulation of µ-conotoxin TIIIA (*orange* with *grey transparent molecular surface*) to homology model of human $Na_v1.4$ (*slate*). The predicted unstructured extracellular loops between transmembrane helix 5 and extracellular P1 in subunits 1 and 3 were removed for clarity. (**A**) The docking simulation reveals that µ-conotoxin TIIIA binds at the extracellular entry of $Na_v1.4$, suggesting that it is a pore blocker. (**B**) Docking reveals a large contact area (represented in *white transparent molecular surface*) between µ-conotoxin TIIIA and $Na_v1.4$, in agreement with its high binding affinity (~ 0.1 nM; Lewis *et al.*, 2007). (**C**) A detailed analysis of this docking complex shows that R14 on µ-conotoxin TIIIA forms an extensive ionic interaction network (*black dash lines*) with two glutamate and one aspartate residues on $Na_v1.4$. This ionic network is also observed in the studies of µ-conotoxin GIIIB and skeletal muscle (µ1) Na^+ channel (Li *et al.*, 2000) and supports our previous mutational studies showing that R14A-TIIIA reduces µ-conotoxin TIIIA potency at $Na_v1.4$ by ~100 fold (Lewis *et al.*, 2007).

Figure 3. *Simulation d'amarrage de la µ-conotoxine TIIIA (*en orange *avec* la surface moléculaire transparente en gris*) au modèle homologue du canal $Na_v1.4$ humain (*en ardoise*). Les boucles extracellulaires non structurées prédites entre l'hélice transmembranaire 5 et le P1 extracellulaire dans les sous-unités 1 et 3 ont été retirées pour plus de clarté. (**A**) La simulation d'amarrage révèle que la µ-conotoxine TIIIA se lie à l'entrée extracellulaire de $Na_v1.4$, ce qui suggère que c'est un bloqueur du pore. (**B**) L'amarrage révèle une grande surface de contact (représentée par* la surface moléculaire transparente blanche*) entre la µ-conotoxine TIIIA et Nav1.4, en accord avec son affinité de liaison élevée (~ 0,1 nM; Lewis* et al.*, 2007). (**C**) Une analyse détaillée de ce complexe d'amarrage montre que R14 sur la µ-conotoxine TIIIA forme un vaste réseau d'interactions ioniques (*tirets noirs*) avec deux résidus glutamate et un résidu aspartate sur $Na_v1.4$. Ce réseau ionique est également observé dans les études de la µ-conotoxine GIIIB et le canal Na^+ du muscle squelettique (µ1; Li* et al.*, 2000) et soutient nos études mutationnelles précédentes montrant que R14A-TIIIA réduit par ~ 100 fois l'efficacité de la µ-conotoxine TIIIA vis-à-vis du canal $Na_v1.4$ (Lewis* et al.*, 2007).*

Conclusions

A combination of accelerated bioassay and transcriptomic/proteomic approaches has the potential to greatly accelerate new conotoxin discovery. Through the development of several new Na^+ assays, we are now well-placed to focus these new tools to the discovery of new sodium channel inhibitors with potential to selectively inhibit pain pathways. Using the recently determined crystal structure for a bacterial sodium channel, we are able to start to

rationally design modifications to new and existing Na^+ sodium channel inhibitors with potential to generate more selective inhibitors that could be lead to a new generation of peptide therapeutics to treat pain.

Acknowledgements. *This work is supported by an NHMRC Program Grant and an NHMRC Research Fellowship.*

References

Barbier J, Lamthanh H, Le Gall F, Favreau P, Benoit E, Chen H, Gilles N, Ilan N, Heinemann SH, Gordon D, Ménez A, Molgó J. (2004) A δ-conotoxin from *Conus ermineus* venom inhibits inactivation in vertebrate neuronal Na^+ channels but not in skeletal and cardiac muscles. *J Biol Chem* **279**: 4680-4685

Cox JJ, Reimann F, Nicholas AK, Thornton G, Roberts E, Springell K, Karbani G, Jafri H, Mannan J, Raashid Y, Al-Gazali L, Hamamy H, Valente EM, Gorman S, Williams R, McHale DP, Wood JN, Gribble FM, Woods CG (2006) An SCN9A channelopathy causes congenital inability to experience pain. *Nature* **444**: 894-898

Daly NL, Ekberg JA, Thomas L, Adams DJ, Lewis RJ, Craik DJ (2004) Structures of μO-conotoxins from *Conus marmoreus*. Inhibitors of tetrodotoxin (TTX)-sensitive and TTX-resistant sodium channels in mammalian sensory neurons. *J Biol Chem* **279**: 25774-25782

Davis J, Jones A, Lewis RJ (2009) Remarkable inter- and intra-species complexity of conotoxins revealed by LC/MS. *Peptides* **30**: 1222–1227

Ekberg J, Jayamanne A, Vaughan CW, Aslan S, Thomas L, Mould J, Drinkwater R, Baker MD, Abrahamsen B, Wood JN, Adams DJ, Christie MJ, Lewis RJ (2006) μO-conotoxin MrVIB selectively blocks $Na_v1.8$ sensory neuron specific sodium channels and chronic pain without motor deficits. *Proc Natl Acad Sci* **103**: 17030-17035

Escoubas P, Quinton L, Nicholson GM (2008) Venomics: unravelling the complexity of animal venoms with mass spectrometry. *J Mass Spectrom* **43**: 279-295

Fry BG, Roelants K, Champagne DE, Scheib H, Tyndall JD, King GF, Nevalainen TJ, Norman JA, Lewis RJ, Norton RS, Renjifo C, Rodríguez de la Vega RC (2009) The Toxicogenomic Multiverse: Convergent recruitment of proteins into animal venoms. *Annu Rev Genomics Hum Genet* **10**: 483-511

Hu H, Bandyopadhyay PK, Olivera BM, Yandell M (2011) Characterization of the *Conus bullatus* genome and its venom-duct transcriptome. *BMC Genomics* **25**: 12-60

Leipold E, DeBie H, Zorn S, Borges A, Olivera BM, Terlau H, Heinemann SH (2007) μO conotoxins inhibit Na_V channels by interfering with their voltage sensors in domain-2. *Channels (Austin)* **1**: 253-262

Lewis RJ, Garcia ML (2003) Therapeutic potential of venom peptides. *Nat Rev Drug Discov* **2**: 790-802

Lewis RJ, Schroeder CI, Ekberg J, Nielsen KJ, Loughnan M, Thomas L, Adams DA, Drinkwater R, Adams DJ, Alewood PF (2007) Isolation and structure-activity of μ-conotoxin TIIIA, a potent inhibitor of TTX-sensitive voltage-gated sodium channels. *Mol Pharmacol* **71**: 676-685

Li RA, Ennis IL, *et al.* (2000) Novel structural determinants of μ-conotoxin (GIIIB) block in rat skeletal muscle (μ1) Na^+ channels. *J Biol Chem* **275**: 27551-27558

Long SB, Campbell EB, *et al.* (2005) Crystal structure of a mammalian voltage-dependent Shaker family K^+ channel. *Science* **309**: 897-903

Payandeh J, Scheuer T, *et al.* (2011) The crystal structure of a voltage-gated sodium channel. *Nature* **475**: 353-358

Schmalhofer WA, Calhoun J, Burrows R, Bailey T, Kohler MG, Weinglass AB, Kaczorowski GJ, Garcia ML, Koltzenburg M, Priest BT (2008) ProTx-II, a selective inhibitor of $Na_V1.7$ sodium channels, blocks action potential propagation in nociceptors. *Mol Pharmacol* **74**: 1476-1484

Schroeder CI, Ekberg J, Nielsen KJ, Adams D, Loughnan M, Thomas L, Adams DJ, Alewood PF and Lewis RJ (2008) Neuronally selective μ-conotoxins from *Conus striatus* utlise an α-helical motif to target mammalian sodium channels. *J Biol Chem* **283**: 21621-21628

Ueberheide BM, Fenyö D, Alewood PF, Chait BT (2010) Rapid sensitive analysis of cysteine rich peptide venom components. *Proc Natl Acad Sci* USA **106**: 6910-6915

Xiao Y, Blumenthal K, Jackson JO 2nd, Liang S, Cummins TR (2010) The tarantula toxins ProTx-II and huwentoxin-IV differentially interact with human $Na_v1.7$ voltage sensors to inhibit channel activation and inactivation. *Mol Pharmacol* **78**: 1124-1134

Zhang MM, Green BR, Catlin P, Fiedler B, Azam L, Chadwick A, Terlau H, McArthur JR, French RJ, Gulyas J, Rivier JE, Smith BJ, Norton RS, Olivera BM, Yoshikami D, Bulaj G (2007) Structure/function characterization of micro-conotoxin KIIIA, an analgesic, nearly irreversible blocker of mammalian neuronal sodium channels. *J Biol Chem* **282**: 30699-30706

Toxines et Transferts ioniques – Toxins and Ion transfers
Rencontres en Toxinologie – Meeting on Toxinology, 2011
Editions de la SFET – SFET Editions
Accès libre en ligne sur le site – Free access on line on the site : http://www.sfet.asso.fr

G protein-coupled receptors, an unexploited family of animal toxins targets: exploration of green mamba venom for novel ligands on adrenoceptors

Arhamatoulaye MAÏGA[1], Gilles MOURIER[1], Loic QUINTON[2], Céline ROUGET[3], Philippe LLUEL[3], Stefano PALEA[3], Denis SERVENT[1], Nicolas GILLES[1*]

[1] CEA, iBiTec-S, Service d'Ingénierie Moléculaire des Protéines (SIMOPRO), F-91191 Gif sur Yvette, France ; [2] Laboratoire de spectrométrie de masse – Département de Chimie- GIGA-R– Université de Liège, Liège B-4000, Belgium ; [3] UROsphere S.A.S., Faculté des Sciences Pharmaceutiques, Université Paul Sabatier, F-31062 Toulouse, France

** Corresponding author ; E-mail : Nicolas.gilles@cea.fr*

Abstract

At a time when pharmaceutical companies are having trouble finding new low molecular weight drugs and when biologics are becoming more common, animal venoms constitute a valid but still underexploited source of novel drug candidates. Animal venoms are large combinatorial libraries of biologically active peptides that encompass a wide variety of structures and pharmacological activities. As such, they represent a resource of up to 40,000,000 novel molecules that can be developed as drug leads and diagnostics tools. Here, we describe how, in the Dendroaspis angusticeps *venoms, we succeed to discover and characterize novel toxins active on adrenoceptors.*

Les récepteurs couplés aux protéines G, une famille inexploitée de cibles des toxines animales : exploration du venin du mamba vert pour de nouveaux ligands adrénergiques

Alors que l'industrie pharmaceutique à de plus en plus de difficultés à trouver de nouveaux médicaments de faibles poids moléculaires et que les « biologics » sont de plus en vogues, les venins d'animaux constituent une source valide, mais toujours sous-exploitée, de nouveaux candidats thérapeutiques. Les venins d'animaux constituent une vaste librairie combinatoire de peptides, biologiquement actifs, recouvrant une large diversité de structures et d'activités pharmacologiques. Ainsi, ils représentent une ressource de plus de 40 millions de nouvelles molécules pouvant être développées comme candidats thérapeutiques et comme outils de diagnostic. Ici, nous décrivons comment, à partir du venin de Dendroaspis angusticeps*, nous avons réussi à découvrir et à caractériser de nouvelles toxines actives sur les récepteurs adrénergiques.*

Keywords : *Animal toxins, benign prostate hypertrophy, drug development, G-protein coupled receptor, hypotension,* in vivo *experiments, screening.*

Introduction

Pharmacological activities of animal toxins stems mostly from their effects on ion channels which play an important role in controlling the mobility of the prey of the venomous animal. Intriguingly, only a few tens of the 3,000 known toxins are active against G protein-coupled receptors (GPCRs). GPCRs are membrane proteins constituted by seven transmembrane segments that transduce external stimuli into the cell and control almost all physiological processes in humans (Jacoby *et al.*, 2006). GPCRs constitute the largest family of membrane proteins (between 1,500 and 2,000 encoded by the human genome) and are the targets of over 25% of the 1,065 approved drugs for which molecular targets could be identified (Jacoby *et al.*, 2006). Belong the 356 GPCRs activated by endogenous agonists (Vassilatis *et al.*, 2003), only about 60 GPCR subtypes are currently targeted by marketed drugs, with another 220 remaining unexploited, mostly due to a lack of specific ligands.

We looked for identifying novel animal toxins active against GPCRs, the most frequently exploited class of treatment targets, with the aim to develop novel research tools and drug candidates. Screening of green mamba (*Dendroaspis angusticeps*) venom against adrenoceptors identified two novel venom peptides. ρ-Da1a showed a sub-nanomolar affinity for the α1a-adrenoceptors (AR) while ρ-Da1b displayed nanomolar affinities for the three α2-ARs. These two venom peptides have sequences similar to those of muscarinic toxins and belong to the three-finger-fold protein family. α1a-AR is the primary target for the treatment of prostate hypertrophy, and α2-ARs are the prototype of GPCRs not currently used as treatment targets due to a lack of specific ligands.

Screening of green mamba venom on adrenoceptors

To identify novel animal toxins active on GPCRs, we screened the green mamba (*Dendroaspis angusticeps*) venom on the nine AR subtypes and discovered two original venom peptides. Their amino-acid sequences were determined by Edman degradation and mass fragmentation techniques, and they both belong to the three finger fold peptide family, with high sequence similarities with the muscarinic toxins. All the following results have been obtained with their synthetic homologues.

Binding experiments showed that ρ-Da1a is specific to the α1aAR subtype with an affinity of 0.36 nM (*Figure 1*) while ρ-Da1b displayed affinities between 14 and 73 nM for the three α2-ARs subtypes (*Figures 2;* Maiga *et al.*, 2011; Quinton *et al.*, 2010; Rouget *et al.*, 2010). None of these peptide displayed activity to more than 30 other GPCRs, including the muscarinic receptors.

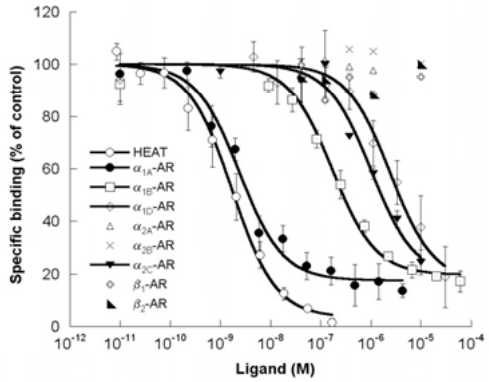

Figure 1. Pharmacological profile of ρ-Da1a on various adrenoceptor subtypes.

Inhibition of ^{3}H-prazosin on α1aAR with HEAT (○, 125iodo-2-[Beta-(4-hydroxyphenyl)-ethyl-aminomethyl] tetralone), and ρ-Da1a (●). Inhibition of ^{3}H-prazosin, ^{3}H-rauwolscine and ^{3}H-CGP-12177 on $h\alpha_{1B}$- (□), and α1dAR (◇), on α2aAR (Δ), α2bAR (x) and α2cAR (▼), on β1AR (+) and β2AR (►), respectively.

Figure 1. *Profil pharmacologique de la ρ-Da1a sur différents sous-types de récepteurs adrénergiques.*

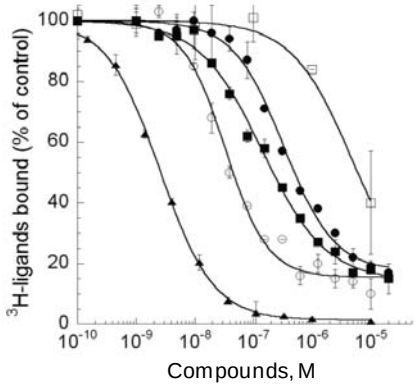

Figure 2. Pharmacological profile of ρ-Da1b on various adrenoceptor subtypes.

Inhibition of ^{3}H-rauwolscine on α2aAR with rauwolscine (▲) and ρ-Da1b (○), and α2bAR (■) or α2cAR (●) with ρ-Da1b. Inhibition of ^{3}H-prazosin by ρ-Da1b on α1aAR (□).

Figure 2. *Profil pharmacologique de la ρ-Da1b sur différents sous-types de récepteurs adrénergiques.*

Binding experiments were performed on membranes from eukaryotic cells expressing the different human receptors as previously described (Rouget *et al.*, 2010). *Les expériences de fixation on été réalisées sur des membranes de cellules eucaryotes exprimant les différents récepteurs humains, comme décrit précédemment (Rouget* et al*., 2010).*

Cell-based functional tests showed that both toxins displayed atypical pharmacological properties. Classical competitive antagonists, such as yohimbine, induce a parallel right-shift of agonist activation curves, which can be converted in a linear Schild plot representation with slope close to unit. ρ-Da1a antagonizes α1aAR in an insurmountable way by reducing agonist efficacy and preventing any Schild plot representation (*Figure 3*). ρ-Da1b antagonizes by a non-competitive manner α2aARs, since it induces a right shift of the activation curves, but with a Schild plot showing a slope significantly lower than unit (0.67) while the yohimbine one was closed to unit (0.97; *Figure 4*). The pA_2 values calculated were 5.93 for yohimbine and 5.32 for ρ-Da1b.

Both toxins display high selectivity for their respective targets and antagonize their receptor target in an atypical ways, at a time where clinicians are looking for modulators instead of pure competitors. α1aAR is the primary target for the treatment of lower urinary tract symptoms secondary to benign prostatic hyperplasia while α2ARs are implicated in uterine smooth muscle contraction, intestinal motility and orthosteric hypotension. Both toxins are under development as therapeutic candidates. The following presentation will focus on the interaction between ρ-Da1a and α1aAR.

ρ-Da1a as a drug candidate against lower urinary tract symptoms

Belonging to the lower urinary tract symptoms, benign prostatic hyperplasia is a very common disease affecting 90% of the 90 years old men. In order to reduce symptoms, like urinary obstruction, the first line of treatment consists on the blockage of the prostatic α1aAR to reduce prostatic tone. Tamsulosin, a classical competitive antagonist of α1aAR, represents 40% of the medical prescriptions against benign prostatic hyperplasia and will serve as a reference drug.

The insurmountable antagonist activity of ρ-Da1a described on α1aAR heterologously expressed in eukaryotic cells was also found on isolated prostate muscle from rabbit (*Figure 5*) as well as from human (*Figure 7*). On its own, tamsulosin on rabbit prostate muscle induce the classical parallel right-shift of phenylephrine activation curves (*Figure 6*). ρ-Da1a, unlike tamsulosin, is able to totally abolish muscular tone whatever the concentration of agonist used.

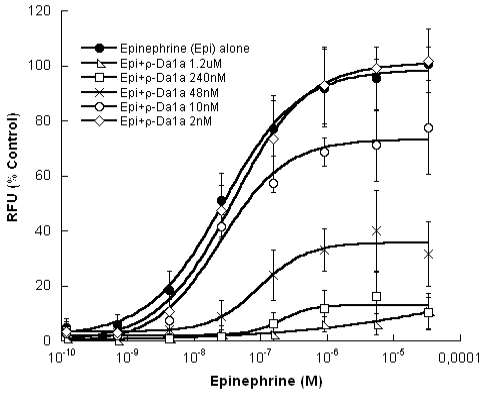

Figure 3. Functional characterization of ρ-Da1a on Chinese hamster ovary (CHO) cells expressing α1aAR.

Concentration-response curves for epinephrine activation in the presence of increasing concentrations of ρ-Da1a.

Figure 3. *Caractérisation fonctionnelle de la ρ-Da1a sur α1aAR exprimé dans des cellules CHO.*

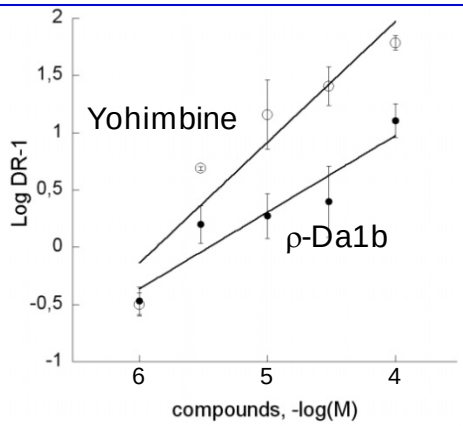

Figure 4. Functional characterization of ρ-Da1b and yohimbine on COS [CV-1 (simian) in Origin, and carrying the SV40 genetic material] cells co-expressing α2aAR and the chimeric G-protein GqTop.

Schild plot representation of concentration-response curves for epinephrine in the presence of antagonists.

Figure 4. *Caractérisation fonctionnelle de la ρ-Da1a et de la yohimbine sur α2aAR co-exprimé avec la protéine G chimérique GqTop dans des cellules COS*

Experiments were performed on a Flex Station II, following the cells calcium release induced by receptors' activation. *Les experiences ont été réalisées sur la station de travail "Flex Station II", après la liberation de calcium induite par l'activation des récepteurs.*

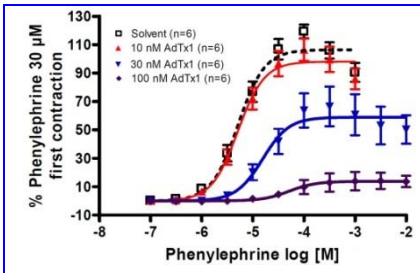

Figure 5. ρ-Da1a (AdTx1) on rabbit isolated prostate muscle.

Figure 5. *ρ-Da1a (AdTx1) sur le muscle prostatique isolé de lapin.*

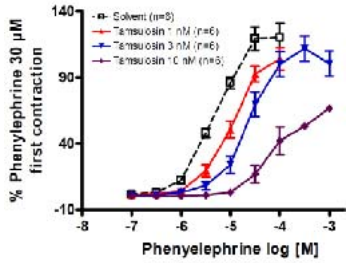

Figure 6. Tamsulosine on rabbit prostate muscle.

Figure 6. *Tamsulosine sur le muscle prostatique isolé de lapin.*

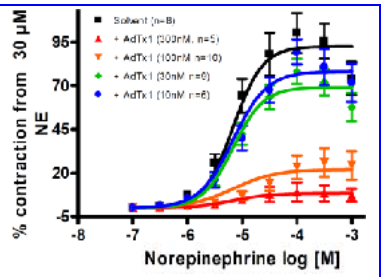

Figure 7. ρ-Da1a (AdTx1) on human isolated prostate muscle.

Figure 7. *ρ-Da1a (AdTx1) sur le muscle prostatique isolé humain.*

Cumulative concentration-response curves for α1aAR agonists were obtained in prostatic strips after 30 min incubation with solvent or antagonist. Contractile responses to agonists are presented as mean of the maximal tension. *Les courbes "concentration-réponse" pour les agonistes de α1aAR ont été obtenues sur des tranches prostatiques après 30 min d'incubation avec le solvant ou l'agoniste. Les réponses contractiles aux agonistes sont les moyennes de la tension maximale.*

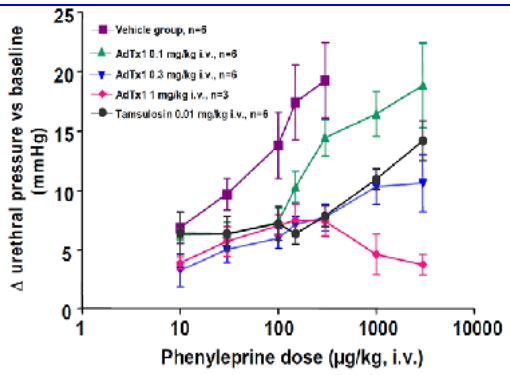

Figure 8. Effects of ρ-Da1a (AdTx1) and tamsulosin on intra urethral pressure.

Figure 8. *Effets de la ρ-Da1a* (AdTx1) *et de la tamsulosine sur la pression intra urétrale.*

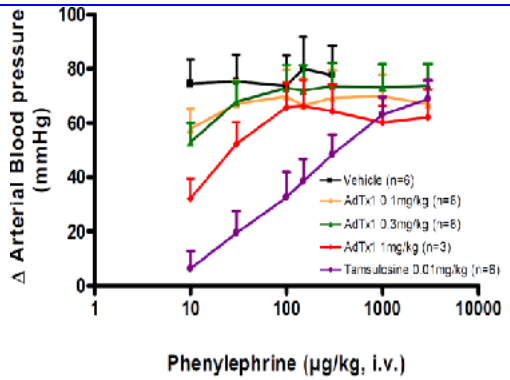

Figure 9. Effects of ρ-Da1a (AdTx1) and tamsulosin on arterial pressure.

Figure 9. *Effets de la ρ-Da1a* (AdTx1) *et de la tamsulosine sur la pression artérielle.*

Vehicle, ρ-Da1a and tamsulosin were injected intravenously (i.v.) 30 min before injections of increased concentrations of phenylephrine in anesthetized male rats. *Le vecteur, la ρ-Da1a et la tamsulosine ont été injectés (i.v.) 30 min avant les injections de concentrations croissantes de phényléphrine dans des rats mâles anesthésiés.*

We finally evaluated the *in vivo* ρ-Da1a efficacy to reduce urethral sphincter tone on anesthetized male rats. The urethral effect was used as a model for prostatic tone. In parallel, in order to quantify the major side effects of tamsulosin, *i.e.* the hypotension due to the blockage of the α1bAR subtype, arterial pressure was also monitored during experiments. *Figure 8* shows that, thanks to its insurmountable antagonist property, 0.3 mg of ρ-Da1a (corresponding to 40 nmoles, blue curve in *Figure 8*) displayed the same relaxant effect than 0.01 mg of tamsulosin (corresponding to 20 nmoles, black curve in *Figure 8*), despite the fact that tamsulosin has a ten fold higher affinity (0.035 nM) than ρ-Da1a (0.36 nM) on α1aAR. In addition, while 20 nmoles of tamsulosin induced a large fall in arterial pressure (violet curve in *Figure 9*), the corresponding amount of ρ-Da1a induced only a small decrease (green curve in *Figure 9*). The fact that ρ-Da1a induces much less side effects is directly connected to its better selectivity than tamsulosin, as the ρ-Da1a affinity for the α1bAR is 53 nM (*i.e.* 150 fold higher α1aAR selectivity *vs* α1bAR), while tamsulosin has an affinity of 0.7 nM (*i.e.* 20 fold higher α1aAR selectivity *vs* α1bAR).

As a conclusion, antagonistic potency of ρ-Da1a on α1aAR (pK_B = 8.2) is very close to tamsulosin potency (pK_B = 8.9) whereas, *in vivo*, ρ-Da1a demonstrated the same efficacy as tamsulosin to reduce prostatic tone but with much less hypotension. In addition, ρ-Da1a have shown no *per os* activity, as expected based on its peptidic nature.

Molecular interaction between ρ-Da1a and α1aAR

ρ-Da1a is the first peptide ligand specific to α1aAR and nothing is known about its interaction with its receptor. The mode of action of MT7, a three-finger-fold toxin sharing 55% sequence identity with ρ-Da1a, has been studied in details. MT7 significantly affects the dissociation kinetics of ^{3}H-N methyl scopolamine and ^{3}H-acetylcholine (Mourier *et al.*, 2003; Olianas *et al.*, 2000) and leaves a small residual binding on equilibrium binding experiments (Fruchart-Gaillard *et al.*, 2006). As a negative allosteric modulator, MT7 reduces carbamylcholine efficacy and potency on M1 muscarinic receptors expressed in CHO cells (Olianas *et al.*, 2000) and, in agreement with an allosteric mode of action, MT7 binding site is located on external loops 2 and 3 of the M1 muscarinic receptor (Kukkonen *et al.*, 2004).

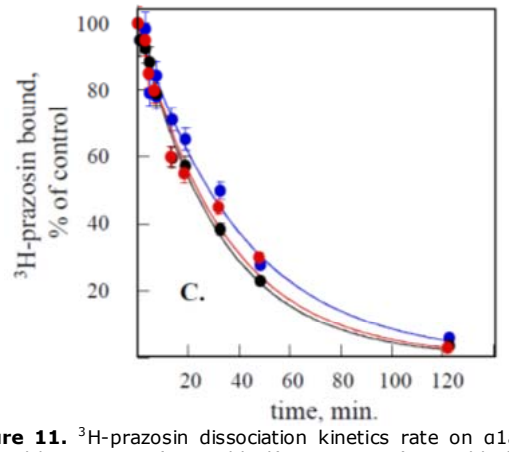

Figure 11. ^{3}H-prazosin dissociation kinetics rate on α1aAR induced by prazosin (1 µM, *black*) or ρ-Da1a (1 µM, *blue*) or both (*red*).

Figure 11. *Cinétique de dissociation de la ^{3}H -prazosine sur α1aAR induite par la prazosine (1 µM,* noir*) ou la ρ-Da1a (1µM,* bleue*) ou les deux (*rouge*).*

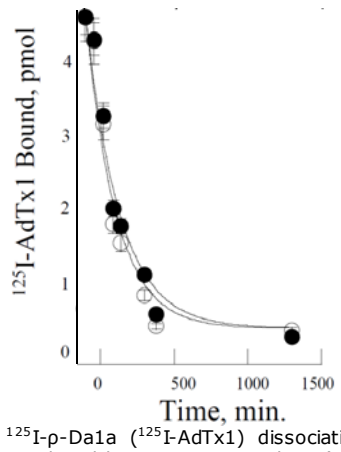

Figure 12. ^{125}I-ρ-Da1a (^{125}I-AdTx1) dissociation kinetics rate on α1aAR induced by 1 µM ρ-Da1a alone (*open circles*) or in addition with 1 µM prazosin (*close circles*).

Figure 12. *Cinétique de dissociation de la ^{125}I-ρ-Da1a (^{125}I-AdTx1) induite par 1 µM de ρ-Da1a seule (*cercles blancs*) ou en association avec 1 µM de prazosine (*cercles noirs*).*

Binding tests were realized on human α1aAR express in yeast (Quinton *et al.*, 2010). *Les tests de fixation ont été réalisés sur des α1aAR humains, exprimés dans la levure (Quinton* et al.*, 2010).*

ρ-Da1a share similarities with MT7, as it leaves also a residual binding (*Figure 1*) and reduces agonist efficacy (*Figure 3*). We thus wanted to characterize ρ-Da1a mode of action, by binding and mutagenesis studies. Most of the negative allosteric modulators change their radiotracer dissociation kinetics rates, as already shown with MT7. We looked on the influence of ρ-Da1a and prazosin on their own dissociation kinetics rates. ρ-Da1a had no influence on ^{3}H-prazosin kinetics rate (*Figure 11*), and prazosin had no influence of ^{125}I-ρ-Da1a kinetics rate (*Figure 12*). These results are in favor of a competitive mode of action between ρ-Da1a and prazosin on the α1aAR.

We aimed to confirm the competitive behavior of ρ-Da1a on α1aARs at the molecular level. Two regions of biogenic amine receptors, the external loop 2 and the orthosteric pocket, were previously identified as crucial for the binding of various ligands. Preliminary results seem to confirm that ρ-Da1a is a competitive ligand since it interacts with residues localized into the orthosteric pocket of the receptor. Complementary work should now be done to confirm this point and to understand how a large peptide like ρ-Da1a, which can be represented as a 35 Å isosceles triangle of around 10 Å thickness, is able to interact with residues located insight the buried orthosteric pocket of the receptor.

Conclusion

This work presents part of large screening tests done on collection of GPCRs and illustrate that this family of receptors is a valid target for venom toxins. Reticulated toxins, by their pharmacological and biochemical properties, deserve to be extensively developed as drug candidates, on a time where peptide drugs are positively considered by the pharmaceutical industry.

References

Fruchart-Gaillard C, Mourier G, Marquer C, Menez A, Servent D (2006) Identification of various allosteric interaction sites on M1 muscarinic receptor using 125I-Met35-oxidized muscarinic toxin 7. *Mol Pharmacol* **69**(5): 1641-1651

Jacoby E, Bouhelal R, Gerspacher M, Seuwen K (2006) The 7 TM G-protein-coupled receptor target family. *Chem Med Chem* **1**(8): 761-782

Kukkonen A, Perakyla M, Akerman KE, Nasman J (2004) Muscarinic toxin 7 selectivity is dictated by extracellular receptor loops. *J Biol Chem* **279**(49): 50923-50929

Maiga A, Mourier G, Quinton L, Rouget C, Gales C, Denis C, Lluel P, Senard JM, Palea S, Servent D, Gilles N (2011) G protein-coupled receptors, an unexploited animal toxin targets: Exploration of green mamba venom for novel drug candidates active against adrenoceptors. *Toxicon* (in press)

Mourier G, Dutertre S, Fruchart-Gaillard C, Menez A, Servent D (2003) Chemical synthesis of MT1 and MT7 muscarinic toxins: critical role of Arg-34 in their interaction with M1 muscarinic receptor. *Mol Pharmacol* **63**(1): 26-35

Olianas MC, Maullu C, Adem A, Mulugeta E, Karlsson E, Onali P (2000) Inhibition of acetylcholine muscarinic M(1) receptor function by the M(1)-selective ligand muscarinic toxin 7 (MT-7). *Br J Pharmacol* **131**(3): 447-452

Quinton L, Girard E, Maiga A, Rekik M, Lluel P, Masuyer G, Larregola M, Marquer C, Ciolek J, Magnin T, Wagner R, Molgo J, Thai R, Fruchart-Gaillard C, Mourier G, Chamot-Rooke J, Menez A, Palea S, Servent D, Gilles N (2010) Isolation and pharmacological characterization of AdTx1, a natural peptide displaying specific insurmountable antagonism of the alpha(1A)-adrenoceptor. *Br J Pharmacol* **159**(2): 316-325

Rouget C, Quinton L, Maiga A, Gales C, Masuyer G, Malosse C, Chamot-Rooke J, Thai R, Mourier G, De Pauw E, Gilles N, Servent D (2010) Identification of a novel snake peptide toxin displaying high affinity and antagonist behaviour for the alpha2-adrenoceptors. *Br J Pharmacol* **161**(6): 1361-1374

Vassilatis DK, Hohmann JG, Zeng H, Li F, Ranchalis JE, Mortrud MT, Brown A, Rodriguez SS, Weller JR, Wright AC, Bergmann JE, Gaitanaris GA (2003) The G protein-coupled receptor repertoires of human and mouse. *Proc Natl Acad Sci USA* **100**(8): 4903-4908

Toxines et Transferts ioniques - Toxins and Ion transfers
Rencontres en Toxinologie - Meeting on Toxinology, 2011
Editions de la SFET - SFET Editions
Accès libre en ligne sur le site - Free access on line on the site : http://www.sfet.asso.fr

Anti-tumor snake venoms peptides

Sameh SARRAY[1,2], Raoudha ZOUARI[1], Jed JEBALI[1], Ines LIMAM[1], Amine BAZAA[1], Maram MORJANE[1], Zeineb ABDELKAFI[1], Olfa ZIRI[1], Najet SRAIRI[1], Salma DAOUED[1], Jose LUIS[3,5], Mohamed EL AYEB[1*], Naziha MARRAKCHI[1,4]

[1] Laboratory of Venoms and Toxins, Pasteur Institute of Tunis, 1002 Tunis-Belvédère, Tunisia ; [2] Faculty of Science, El Manar Campus, Tunis, Tunisia ; [3] INSERM, UMR 911, 13385 Marseille, France ; [4] Faculty of Medecine of Tunis, Tunis, Tunisia ; [5] Aix-Marseille University, CRO2, 13385 Marseille, France

** Corresponding author ; Tel : (00216)-71-783-022 ; Fax : (00216)-71-791-833 ;*
E-mail : mohamed.elayeb@pasteur.rns.tn

Abstract

Snake venoms contain more than 100 different proteins and peptides and are an important source of biomolecules that selectively target several membrane receptors, such as cell adhesion molecules (integrins, cadherins …). International research and development in this area, based on multidisciplinary approaches including molecular screening, proteomics, genomics and pharmacological tests in vitro, ex vivo *and* in vivo *assays, allowed the identification and characterization of highly specific molecules. Since recently, several peptides and peptidomimetics are used as medicament, such as cilengitide based on RGD motif, which targets specifically glioblastoma and actually is in clinical trial III. For over twenty years, the Laboratory of Venoms and Toxins from Pasteur Institute of Tunis has characterized from* Macrovipera lebetina *and* Cerastes cerastes *venoms, several peptidic molecules with pharmacological* potency*. These molecules belong to different families (phospholipases, disintegrins, C-type lectins and metalloproteinases). We have demonstrated that these proteins present anti-tumor, anti-angiogenic and/or pro-apoptotic activities. Our results show that C-type lectin and phospholipases A2 interact with $\alpha 5\beta 1$ and αv integrins whereas lebestatin, a small disintegrin, targets $\alpha 1\beta 1$ integrin, a collagen receptor.*

Les peptides anti-tumoraux issus de venins de serpents

Les venins de serpents contiennent un mélange de protéines et de peptides différents qui représentent une importante source de biomolécules ciblant sélectivement les récepteurs membranaires tels que les molécules d'adhésion cellulaire (intégrines, cadhérines …). La recherche internationale et de développement dans ce domaine, basée sur une approche pluridisciplinaire incluant le dépistage moléculaire, protéomique et des tests pharmacologiques in vitro, ex vivo *et* in vivo*, a permis l'identification et la caractérisation de molécules très spécifiques. Récemment, plusieurs peptides et peptidomimétiques sont utilisés comme médicaments, tels que le cilengitide, un pentapeptide basé sur le motif RGD, qui cible spécifiquement le glioblastome. Ce peptide est actuellement en phase III d'essais cliniques. Depuis plus de vingt ans, le Laboratoire des Venins et Toxines de l'Institut Pasteur de Tunis a caractérisé, à partir des venins de* Macrovipera lebetina *et de* Cerastes cerastes*, plusieurs molécules peptidiques ayant un potentiel pharmacologique. Ces molécules appartiennent à différentes familles (phospholipases, désintégrines, lectines de type C et métalloprotéases). Nous avons démontré que ces protéines présentent des activités anti-tumorales, anti-angiogéniques et/ou pro-apoptotiques. L'étude des mécanismes d'action de ces molécules a montré que les lectines de type C et les phospholipases A2 interagissent avec les intégrines αv et $\alpha 5\beta 1$, alors que la lébestatine, une disintégrine courte, cible l'intégrine $\alpha 2\beta 1$, un récepteur du collagène.*

Keywords : *Cancer cells, integrin, snake venom.*

Introduction

Snake bite is still a serious threat in both developed and under-developed countries. The worldwide mortality caused by snake envenomation is estimated at 50,000 deaths annually (Deshimaru *et al.*, 1996).

Snake venom contains complex mixtures of pharmacologically active molecules, including organic and mineral components, small peptides and proteins (Markland, 1998; Fry, 1999). Venoms of Viperidae and Crotalidae snakes (vipers and rattlesnakes) contain a number of different proteins that interfere with the coagulation cascade, the normal hemostatic system and tissue repair. Consequently, the envenomation by these snakes generally results in persistent bleeding. These proteins can be grouped into a few major proteins

families including enzymes (serine proteinase, Zn^{2+}-dependent metalloproteinases and group II phospholipase A2 isoenzymes) and proteins with no enzymatic activity (C-type lectin-like proteins and disintegrins) (Menez, 2002; Juarez *et al.*, 2004). The biological effects of venoms are complex because different components have distinct actions and may, in addition, act in concert with other molecules. The synergetic action of venom proteins may enhance their activities or contribute to the spreading toxins.

Cerastes cerastes and *Macrovipera lebetina* represent the most important poisonous snakes in Tunisia. In the Laboratory of Venoms and Toxins at the Pasteur Institute of Tunis, these venoms have been subjected to ample research of new molecules with physiological effect. Thus, we have purified and characterized proteins belonging to the family of C-type lectin (lebecetin and lebectin), phospholipase A2 (MVL-PLA2, CC-PLA2-1 and CC-PLA2-2), short disintegrins (lebestatin) and disintegrin-like peptides (leberagin-C). All these molecules target specific integrins and present anti-tumor and anti-angiogenic activities.

C-type lectin proteins

C-type lectin proteins (CLPs) are a family of snake venom proteins that are structurally homologous to the carbohydrate recognition domain of animal C-type lectins. CLPs are 30 kDa proteins consisting of the association of two subunits. In spite of their highly conserved primary structure (40-70% similarity), CLPs are characterized by very distinct biological activities (Marcinkiewicz *et al.*, 2000; Wang *et al.*, 2001 and references therein). For example, several CLPs inhibit von Willebrand factor (vWF) binding to the GPIb/IX complex, thus impeding platelet agglutination, whereas alboaggregins activate the GPIb complex, causing platelet agglutination. Other CLPs exhibit anticoagulant activities by binding to vWF or to the coagulation factors IX and/or X, while convulxin induces platelet aggregation by activating the collagen receptor GPVI (for a review see Andrews and Berndt, 2000). Besides the action on platelet aggregation, it has been reported that snake venom CLPs can affect integrin function. EMS16, a CLP from *Echis multisquamatus* was the first example of a different class of venom proteins showing an antagonistic effect on integrins (Marcinkiewicz *et al.*, 2000). In addition, BJcuL, from the snake *Bothrops jararacussu* inhibits tumor and endothelial cell growth (de Carvalho *et al.*, 2001) and rhodocetin from *Calloselasma rhodostoma* antagonises tumor invasion (Eble *et al.*, 2002).

We recently reported that lebectin and lebecetin, two C-type lectins from *Macrovipera lebetina*, are potent inhibitors of cell adhesion, migration and invasion of tumor cells (Sarray *et al.*, 2004, 2007).

Previously, all snake venom CLPs were known to interfere with integrin activity by inhibiting the collagen receptor $\alpha2\beta1$. This is the case of EMS16 (Marcinkiewicz *et al.*, 2000), bilinexin (Du *et al.*, 2001), aggretin (Suzuki-Inoue *et al.*, 2001) and rhodocetin (Eble *et al.*, 2002). However, the $\alpha2\beta1$ integrin is likely not involved in the effect of CLPs used in our studies. Indeed, none of the two peptides inhibit attachment of fibrosarcoma cells (HT1080) to type I collagen, the ligand of $\alpha2\beta1$ integrin in these cells (Cardarelli *et al.*, 1992). Moreover, neither migration, nor invasion is affected by the peptides when using collagen as substrata.

Both venom lectins (lebectin and lebecetin) appear to exert their effect on cell adhesion, migration, invasion and proliferation by inhibiting $\alpha5\beta1$ and αv-containing integrins. Moreover, the inhibition of $\alpha5\beta1$ and αv integrins is likely due to the binding of venom peptides, as both lebectin and lebecetin co-immunoprecipitate with these integrins. Lebectin and lebecetin are thus the first examples of venom C-type lectins inhibiting an integrin other than the collagen receptor $\alpha2\beta1$ (Sarray *et al.*, 2007). Furthermore, lebectin acts as a very potent inhibitor (IC_{50} ~ 0.5 nM) of human brain microvascular endothelial cells (HBMEC) adhesion and migration on fibronectin by blocking the adhesive functions of both the $\alpha5\beta1$ and αv integrins. In addition, lebectin strongly inhibits both HBMEC *in vitro* tubulogenesis on Matrigel™ (IC_{50} ~ 0.4 nM) and proliferation. Finally, using both a chicken CAM assay and a Matrigel™ plug assay in nude mice (*Figure 1*), we showed that lebectin displays potent anti-angiogenic activity *in vivo*.

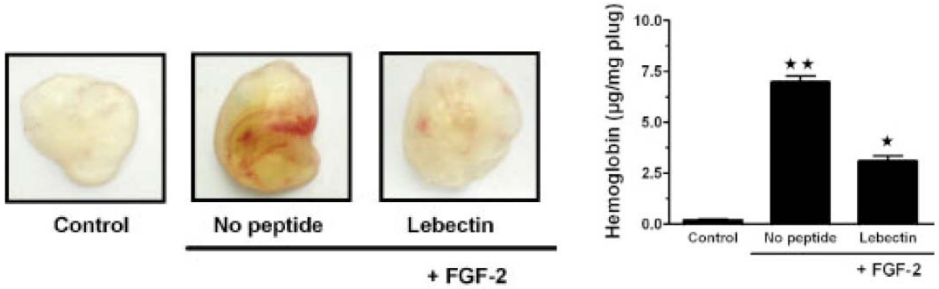

Figure 1. Lebectin blocks *in vivo* angiogenesis. Control: CD-1-nuBR mice were injected subcutaneously with 0.5 ml of Matrigel™ alone or with Matrigel™ containing FGF-2 (125 ng) with or without lebectin (5 µg). After 7 days, the mice were euthanized and the Matrigel™ plugs excised. Representative Matrigel™ plugs from each of the different conditions were photographed (*left panels*). Neovessel formation was quantified by measurement of hemoglobin in the Matrigel™ (*right*). Two mice were used per group and the experiment was repeated twice. Statistically significant differences, as compared to control FGF-2 conditions (as well as between the two control conditions), are indicated by* for $P < 0.05$ and ** for $P < 0.001$.

Figure 1. *La lebectine bloque l'angiogenèse* in vivo. *Contrôle: les souris (CD-1-nuBR) ont été injectées par voie sous cutanée avec 0,5 ml de Matrigel™ seul ou avec du Matrigel™ contenant le FGF-2 (125 ng) avec ou sans lebectine (5 µg). Après 7 jours, les souris sont euthanasiées et le Matrigel™ de chacune des différentes conditions a été photographié (*panneaux de gauche*). La formation de néovaisseaux a été quantifiée par mesure de l'hémoglobine (*droite*). Deux souris ont été utilisées par groupe et l'expérience a été répétée deux fois. Les différences statistiquement significatives, comparées aux conditions contrôle, sont indiquées par * pour $P < 0,05$ et ** pour $P < 0,001$.*

Lebectin thus represents a new C-type lectin with anti-angiogenic properties, having thus great potential for the treatment of angiogenesis-related diseases (Pilogret *et al.*, 2007). Recently, we demonstrated that lebectin induces a strengthening of intercellular adhesion by promoting N-cadherin/catenin complex reorganisation at cell-cell contact (Sarray *et al.*, 2009).

Phospholipases A2

Phospholipases A2 (PLA2s; EC 3.1.1.4) are among the best-characterized components of snake venom. Based on their source, amino acid sequences and disulfide bond patterns, snake venom PLA2s (svPLA2s) are classified into group I and group II PLA2 (Six and Dennis, 2000). They are interesting proteins, containing 120-130 amino acids that are cross-linked by seven disulfide bonds. In addition to their enzymatic activity for the cleavage of ester bonds at the sn-2 position of 1,2-diacyl-3-sn-phosphoglycerides, svPLA2s display several pharmacological effects, including pre- or post-synaptic neurotoxicity, cardiotoxicity, myotoxicity and platelet aggregation modulation (for a review see Kini, 2003).

We have isolated three PLA2 from Tunisian vipers venoms: MVL-PLA2 (*Macrovipera lebetina*; Bazaa *et al.*, 2009), CC-PLA2-1 and CC-PLA2-2 (*Cerastes cerastes*; Zouari-Kessentini *et al.*, 2009). They inhibited, in a dose-dependent manner, adhesion of IGR39 melanoma and HT1080 fibrosarcoma cells to fibrinogen and fibronectin. Furthermore, MVL-PLA2, CC-PLA2-1 and CC-PLA2-2 abolished HT1080 cell migration towards fibrinogen and fibronectin. Hence, we showed for the first time that svPLA2s inhibit adhesion and migration of tumor cells. We also demonstrated that these effects were not mediated by the phospholipase catalytic activity but through the inhibition of $\alpha 5\beta 1$ and αv integrins. Given the key role of $\alpha 5\beta 1$ and $\alpha v\beta 3$ in neo-angiogenesis, we decided to further evaluate the capacity of svPLA2s to exert an anti-angiogenic activity. Indeed, svPLA2s efficiently inhibited endothelial cell adhesion and migration to fibrinogen and fibronectin in a dose-dependent manner (Kessentini-Zouari *et al.*, 2010). We showed that this anti-adhesive effect was mediated by $\alpha 5\beta 1$ and αv-containing integrins. Using Matrigel™ and chick chorioallantoïc membrane (CAM) assays, we demonstrated that the three isolated svPLA2s, significantly inhibited angiogenesis both *in vitro* and *ex vivo* (*Figure 2*).

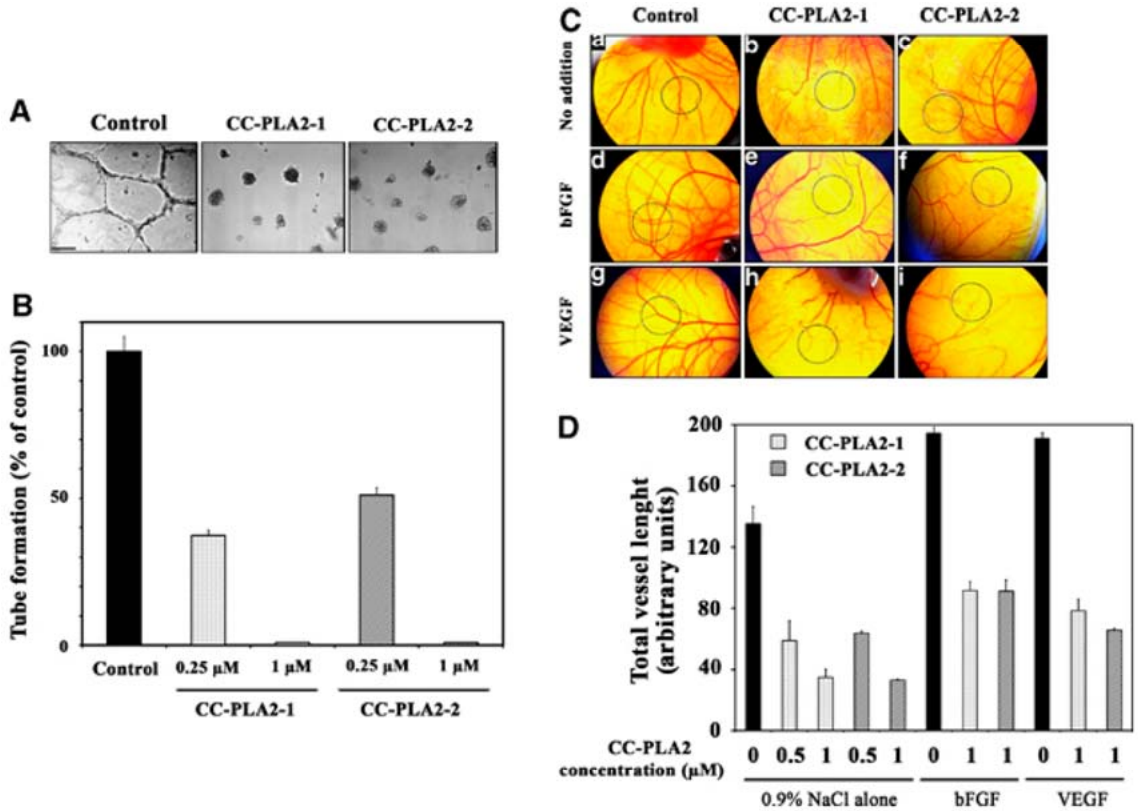

Figure 2. CC-PLA2s block *in vitro* and *in vivo* angiogenesis. (**A**) Representative tubulogenesis assay after pretreatment of HBMEC with 1 mM CC-PLA2-1 or CC-PLA2-2 for 30 min at room temperature. Cells ($2x10^4$) were then added to the Matrigel-coated wells in culture medium and allowed to form capillary like structures for 18 h at 37°C. Scale bar = 100 µm. (**B**) Quantification of the capillary-like structures formed in the gel after treatment with the indicated concentrations of CC-PLA2-1 or CC-PLA2-2. (**C**) The CAM models were prepared using 8-day-old chick embryos. Filter disks were soaked in (**a**) 0.9% NaCl alone, (**b**) 1 µM CC-PLA2-1, (**c**) 1 µM CC-PLA2-2, (**d**) 200 ng bFGF, (**e**) 200 ng bFGF and 1 µM CC-PLA2-1, (**f**) 200ng bFGF and 1 µM CC-PLA2-2, (**g**) 200 ng VEGF, (**h**) 200 ng VEGF and 1 µM CC-PLA2-1, (**i**) 200 ng VEGF and 1 µM CC-PLA2-2. After incubation for 72 h, CAMs were photographed with a digital camera. Each group contained four CAMs and the experiment was repeated three times. (**D**) The quantitative measurement of total vessel length was performed on 50% of the total CAM surface treated in the absence (*black columns*) or in the presence of CC-PLA2-1 (*white columns*) or CC-PLA2-2 (*grey columns*).

Figure 2. *CC-PLA2 bloque l'angiogenèse* in vitro *et* in vivo. *(**A**) Processus de tubulogenèse après prétraitement des cellules HBMEC avec 1 mM de CC-PLA2-1 ou CC-PLA2-2 pendant 30 min à température ambiante. Les cellules (2x10^4) ont ensuite été ajoutées dans des puits cotés avec du Matrigel et mises en culture pendant 18 h à 37°C pour former des structures en forme de capillaire. Barre d'échelle = 100 µm. (**B**) Quantification des structures capillaires formées dans le Matrigel après traitement avec les concentrations indiquées de CC-PLA2-1 ou CC-PLA2-2. (**C**) Les modèles CAM ont été préparés en utilisant des embryons de poulet de 8 jours. Les disques ont été trempés dans (**a**) 0,9% de NaCl, (**b**) 1 µM de CC-PLA2-1, (**c**) 1 µM de CC-PLA2-2, (**d**) 200 ng de bFGF, (**e**) 200 ng de bFGF et 1 µM de CC-PLA2-1, (**f**) 200 ng de bFGF et 1 µM CC-PLA2-2, (**g**) 200 ng de VEGF, (**h**) 200 ng de VEGF et 1 µM de CC-PLA2-1, (**i**) 200 ng de VEGF et 1 µM de CC-PLA2-2. Après une incubation de 72 h, les CAM ont été photographiées avec un appareil photo numérique. (**D**) La mesure quantitative de la longueur totale des vaisseaux a été réalisée sur 50% de la surface totale traitée en l'absence (*colonnes noires*) ou en présence de CC-PLA2-1 (*colonnes blanches*) ou CC-PLA2-2 (*colonnes grises*).*

We have also found that the actin cytoskeleton and the distribution of αvβ3 integrin, a critical regulator of angiogenesis and a major component of focal adhesions, were disturbed after MVL-PLA2 treatment. In order to further investigate the mechanism of action of this protein on endothelial cells, we analyzed the dynamic instability behavior of microtubules in living endothelial cells. Interestingly, we showed that MVL-PLA2 significantly increased microtubule dynamicity in endothelial cells by 40% (*Figure 3*). We propose that the enhancement of microtubule dynamics may explain the alterations in the formation of focal adhesions, leading to inhibition of cell adhesion and migration (Bazaa *et al.*, 2010).

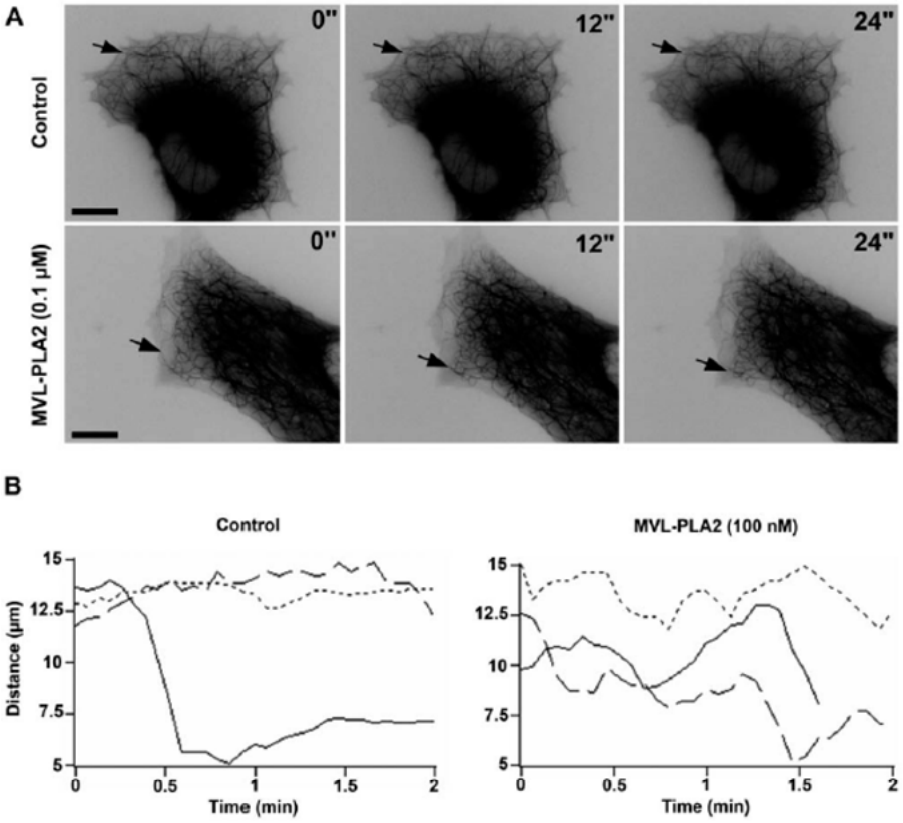

Figure 3. MVL-PLA2 increases microtubule (MT) dynamics in Human Microvascular Endothelial Cells (HMEC-1). (**A**) Time-lapse sequence of video frames of the plus ends of several MT in a control cell (*top panels*) or in a cell treated with 100 nM MVL-PLA2 (*bottom panels*). Arrowheads indicate one MT end for which the position did not change over a period of 24 s in the control cell and one MT that underwent a shortening event in the treated cell. Time is indicated in seconds. Scale bar: 10 µm. (**B**) Life history plots of the length changes of 3 representative MTs in living HMEC-1 cells treated or not (*control*) with 100 nM MVL-PLA2. In the presence of 100 nM MVL-PLA2, MTs are characterized by more extensive growth and shortening events compared to control cells.

Figure 3. *La MVL-PLA2 augmente la dynamique des microtubules (MT) dans les cellules endothéliales microvasculaires humaines (HMEC-1). (**A**) Séquence d'images vidéo des terminaisons (+) dans une cellule contrôle (*panneaux supérieurs*) ou dans une cellule traitée avec 100 nM de MVL-PLA2 (*panneaux inférieurs*). Les flèches indiquent une extrémité MT pour laquelle la position n'a pas changé sur une période de 24 s dans la cellule de contrôle et un MT qui a subi un raccourcissement dans la cellule traitée. Le temps est indiqué en secondes. Barre d'échelle: 10 µm. (**B**) Suivi des changements de longueur de 3 MT dans une cellule HMEC-1 traitée avec 100 nM de MVL-PLA2 ou non (contrôle). En présence de 100 nM de MVL-PLA2, les MT sont caractérisés par des phases de croissance plus importante et de raccourcissement plus nombreuses que dans la cellule contrôle.*

Disintegrins

Disintegrins are a family of low molecular weight proteins present in many Viperidae venoms. They are divided into five different subgroups according to their polypeptide length and number of disulfide bonds. The long

subgroup (83 amino acids) with seven disulfide bonds includes bitistatin. The medium subgroup (68-73 amino acids) with six disulfide bonds contains kistrin, flavoridin and barbourin. The third subgroup includes the short disintegrins, single polypeptide chains of 49-51 amino acids with four disulfide bonds. Echistatin and eristostatin belong to this group. The disintegrin domains of PIII snake-venom metalloproteinases, containing approximately hundred amino acids with 16 cysteine residues involved in the formation of eight disulfide bonds, constitute the fourth subgroup of the disintegrin family. Unlike short-, medium- and long-sized disintegrins, which are single-chain molecules, the fifth subgroup is composed of homo- and heterodimers (Calvete *et al.*, 2005). Snake disintegrins are potent and specific antagonists of several integrins.

Lebestatin, a new member of the lysine-threonine-serine (KTS)-disintegrin family, was purified to homogeneity from Tunisian snake (*Macrovipera lebetina*) venom. It is a single-chain polypeptide composed of 41 amino acids. The amino-acid sequence of lebestatin shows that it displays a pattern of cysteines similar to other short disintegrins, but contains the sequence KTS rather than RGD in its integrin-binding loop. Lebestatin presents a high homology with obtustatin and viperistatin. It interacts specifically with the $\alpha 1\beta 1$ integrin. It was thus able to inhibit both adhesion and migration of PC12 and $\alpha 1\beta 1$ integrin-expressing CHO cells (CHO-$\alpha 1$) to type I and IV collagens. This disintegrin also affected adhesion and migration of endothelial cells and exhibited an anti-angiogenic effect *in vivo* when using the 8-day-old embryo chick chorioallantoic membrane model (Kallech-Ziri *et al.*, 2005).

Leberagin-C, a new member of the disintegrin-like/cysteine-rich (D/C) family, was purified to homogeneity from the venom of Tunisian snake *Macrovipera lebetina*. It is a monomeric protein with a molecular mass of 25,787 Da. Its complete sequence of 205 amino acid residues was established by cDNA cloning. Leberagin-C shows many conserved sequences with other known D/C proteins, like the SECD binding sites and a pattern of 28 cysteines. It is the first purified protein from *Macrovipera lebetina* venom with only two disintegrin-like/cysteine-rich domains. It was able to inhibit the adhesion of melanoma tumor cells on fibrinogen and fibronectin, by interfering with the function of $\alpha v\beta 3$ and, to a lesser extent, with $\alpha v\beta 6$ and $\alpha 5\beta 1$ integrins. To our knowledge, leberagin-C is the sole described D/C protein that does not specifically interact with the $\alpha 2\beta 1$ integrin. Structure-activity relationship study of leberagin-C suggested that there are some important amino acid differences with jararhagin, the most studied PIII metalloproteinase from *Bothrops jararaca*, notably around the SECD motif in its disintegrin-like domain. Other regions implicated in leberagin-C specificity could not be excluded (Limam *et al.*, 2010).

Conclusion

Several proteins and peptides were purified from *Macrovipera lebetina* and *Cerastes cerastes* venoms. These proteins are characterized as efficient modulators of integrin functions. They exhibit *in vitro* and *ex vivo* anti-tumor and anti-angiogenic activity. Thus, it is conceivable that these proteins could be used as models for designing new compounds with therapeutic value and open new potent and selective drugs for the treatment of many types of cancer.

Acknowledgements. *We thank Prof. Louzir Hechmi (Pasteur Institute of Tunis) for his continuous interest in this study and for his support. Dr. Benlasfar Zakaria (Veterinary Laboratory) is acknowledged for providing viper venom. We also thank the INSERM, the ARCUS program, the PACA Cancéropôle and region for financial support.*

References

Andrews RK, Berndt MC (2000) Snake venom modulators of platelet adhesion receptors and their ligands. *Toxicon* **38**: 775-791

Bazaa A, Luis J, Srairi-Abid N, Kallech-Ziri O, Kessentini-Zouari R, Defilles C, Lissitzky J C, El Ayeb M, Marrakchi N (2009) MVL-PLA2, a phospholipase A2 from *Macrovipera lebetina transmediterranea* venom, inhibits tumor cells adhesion and migration. *Matrix Biol* **28**: 188-193

Bazaa A, Pasquier E, Defilles C, *et al.* (2010) MVL-PLA2, a snake venom phospholipase A2, inhibits angiogenesis through an increase in microtubule dynamics and disorganization of focal adhesions. *PLoS One* **5**: e10124

Calvete J J, Marcinkiewicz C, *et al.* (2005) Snake venom disintegrins: evolution of structure and function. *Toxicon* **45**: 1063-1074

Cardarelli PM, Yamagata S, Taguchi I, Gorcsan F, Chiang SL, Lobl T (1992) The collagen receptor alpha 2 beta 1, from MG-63 and HT1080 cells, interacts with a cyclic RGD peptide. *J Biol Chem* **267**: 23159-23164

de Carvalho DD, Schmitmeier S, Novello JC, Markland FS (2001) Effect of BJcuL (a lectin from the venom of the snake *Bothrops jararacussu*) on adhesion and growth of tumor and endothelial cells. *Toxicon* **39**: 1471-1476

Deshimaru M, ogawa T, Nose T, Nikandrov NN, *et al.* (1996) Accelerated evolution of crotalinae snake venom gland serine protease. *FEBS Lett* **397**: 83-88

Du XY, Navdaev A, Clemetson JM, Magnenat E, Wells TN, Clemetson KJ (2001) Bilinexin, a snake C-type lectin from *Agkistrodon bilineatus* venom agglutinates platelets *via* GPIb and $\alpha 2\beta 1$. *Thromb Haemost* **86**: 1277-1283

Eble JA, Niland S, Dennes A, Schmidt-Hederich A, Bruckner P, Brunner G (2002). Rhodocetin antagonizes stromal tumor invasion *in vitro* and other alpha2beta1 integrin-mediated cell functions. *Matrix Biol* **21**: 547-558

Eble JA, Niland S, Dennes A, Schmidt-Hederich A, Bruckner P, Brunner G (2002) Rhodocetin antagonizes stromal tumor invasion *in vitro* and other alpha2beta1 integrin-mediated cell functions. *Matrix Biol* **21**: 547-558

Fry BG (1999) Structure -function properties of venom components from Australian elapids. *Toxicon* **38**: 11-32

Juarez P, Sanz L, Calvete JJ (2004) Snake venomics: characterization of protein families in *Sistrurus barbouri* venom by cysteine mapping, N-terminal sequencing, and tandem mass spectrometry analysis *Proteomics* **4**: 327-338

Kessentini-Zouari R, Jebali J, Taboubi S, *et al.* (2010) CC-PLA2-1 and CC-PLA2-2, two *Cerastes cerastes* venom-derived phospholipases A2, inhibit angiogenesis both *in vitro* and *in vivo*. *Lab Invest* **90**: 510-519

Kini RM (2003) Excitement ahead: structure, function and mechanism of snake venom phospholipase A2 enzymes. *Toxicon* **42**: 827-840

Limam I, Bazaa A, Srairi-Abid N, *et al.* (2010) Leberagin-C, A disintegrin-like/cysteine-rich protein from *Macrovipera lebetina transmediterranea* venom, inhibits alphavbeta3 integrin-mediated cell adhesion. *Matrix Biol* **29**: 117-126

Marcinkiewicz C, Lobb RR, *et al.* (2000) Isolation and characterization of EMS16, a C-lectin type protein from *Echis multisquamatus* venom, a potent and selective inhibitor of the $\alpha 2\beta 1$ integrin. *Biochemistry* **39**: 9859-9867

Markland FS (1998) Snake venoms and the hemostatic system. *Toxicon* **36**: 1749-1800

Menez A (2002) Perspectives in molecular toxinology, *Wiley Chichester*

Olfa KZ, Jose L, Salma D, *et al.* (2005) Lebestatin, a disintegrin from *Macrovipera* venom, inhibits integrin-mediated cell adhesion, migration and angiogenesis. *Lab Invest* **85**: 1507-1516

Pilogret A, Conesa M, Sarray S, *et al.* (2007) Lebectin, a *Macrovipera lebetina* venom-derived C-type lectin, inhibits angiogenesis both *in vitro* and *in vivo*. *J Cell Physiol* **211**: 307-315

Sarray S, Berthet V, Calvete JJ, *et al.* (2004) Lebectin, a novel C-type lectin from *Macrovipera lebetina* venom, inhibits integrin-mediated adhesion, migration and invasion of human tumour cells. *Lab Invest* **84**: 573-581

Sarray S, Delamarre E, Marvaldi J, El Ayeb M, Marrakchi N., Luis J (2007) Lebectin and lebecetin, two C-type lectins from snake venom,inhibit $\alpha 5\beta 1$ and αv-containing integrins. *Matrix Biology* **26**: 306-313

Six DA, Dennis EA (2000) The expanding superfamily of phospholipase A(2) enzymes: classification and characterization. *Biochim Biophys Acta* **1488**: 1-19

Suzuki-Inoue K, Ozaki Y, Kainoh M, *et al.* (2001) Rhodocytin induces platelet aggregation by interacting with glycoprotein Ia/IIa (GPIa/IIa, Integrin α2β1). Involvement of GPIa/IIa-associated src and protein tyrosine phosphorylation. *J Biol Chem* **276**: 1643-1652

Wang R, Kong C, Kolatkar P, *et al.* (2001) A novel dimer of a C-type lectin-like heterodimer from the venom of *Calloselasma rhodostoma* (Malayan pit viper). *FEBS Lett* **508**: 447-453

Zouari-Kessentini R, Luis J, Karray A, *et al.* (2009) Two purified and characterized phospholipases A2 from *Cerastes cerastes* venom, that inhibit cancerous cell adhesion and migration. *Toxicon* **53**: 444-453

Toxines et Transferts ioniques – Toxins and Ion transfers
Rencontres en Toxinologie – Meeting on Toxinology, 2011
Editions de la SFET – SFET Editions
Accès libre en ligne sur le site – Free access on line on the site : http://www.sfet.asso.fr

Effect of Dinoponera quadriceps *venom on chemical-induced seizures models in mice*

Kamila LOPES[1*], Emiliano RIOS[2], Rodrigo DANTAS[2], Camila LIMA[2], Maria LINHARES[2], Alba TORRES[1], Ramon MENEZES[2], Yves QUINET[3], Alexandre HAVT[4], Marta FONTELES[2], Alice MARTINS[1]

[1] *Department of Clinical and Toxicological Analysis, Faculty of Pharmacy, Federal University of Ceará, Fortaleza, Ceará, Brazil ;* [2] *Laboratory of Neuropharmacology, Department of Physiology and Pharmacology, Federal University of Ceará, Fortaleza, Ceará, Brazil ;* [3] *Laboratory of Entomology, State University of Ceará, Fortaleza, Ceará, Brazil ;* [4] *Biomedicine Institute, Department of Physiology and Pharmacology, Federal University of Ceará, Fortaleza, Ceará, Brazil*

* *Corresponding author ; Tel : +55 (0) 85 3366-8269 ; Fax : +55 (0) 85 3366-8292 ;*
E-mail : kamila_farm@yahoo.com.br

Abstract

Natural toxins, derived from plants, animals or other organisms, have shown an important role in the development of pharmacological tools. Dinoponera *and* Paraponera*, two common ant genera in Brazil, are among the groups that show potential medical interest. In this work, we investigated the effect of* Dinoponera quadriceps *venom (*DQv*) on chemical-induced seizures models in mice.* DQv *presented effect only in models of seizures induced by pentylenetetrazole. Pretreatment with this venom increased significantly the time to first seizure and proved a tendency to delay the death time of mice. Analyzing thiobarbituric acid reactive substances revealed that DQv reduces the malondialdehyde amount only in prefrontal cortex. These results strongly suggest a possible neuroprotective effect of the venom.*

Effet du venin de Dinoponera quadriceps *sur des modèles de convulsion chimiquement induits chez la souris*

Des toxines naturelles, dérivées de plantes, d'animaux ou d'autres organismes, ont démontré leur rôle important dans le développement d'outils pharmacologiques. Dinoponera *et* Paraponera*, deux genres de fourmis communs au Brésil, figurent parmi les groupes d'intérêt médical potentiel. Nous avons étudié l'effet du venin de* Dinoponera quadriceps *(*DQv*) sur des modèles de convulsion chimiquement induits chez la souris.* DQv *présentait un effet uniquement sur des modèles de convulsion chimiquement induits par le pentylènetétrazole. Un prétraitement avec ce venin augmentait de façon significative le temps de la première convulsion et a démontré une tendance à retarder le temps de la mort des souris. L'analyse des substances réagissant avec l'acide thiobarbiturique a révélé que DQv réduit la quantité de malondialdéhyde seulement dans le cortex préfrontal. Ces résultats suggèrent fortement un effet neuroprotecteur possible du venin.*

Keywords : Dinoponera quadriceps *venom, pentylenetetrazole, pilocarpine, seizures, strychnine.*

Introduction

Natural toxins, derived from plants, animals or other organisms, have shown an important role in the development of therapeutic values with substances. Thus, Brazil has an extensive biological diversity and appears as a rich environment for studying natural products. Venoms of arthropods, such as scorpions, spiders and wasps, appear as potential sources of neuroactive substances, providing new tools for rational drug design.

Ants are among the most biologically diverse organisms on Earth (Hoffman, 2010). The subfamily *Ponerinae* includes ants with large size, which even measure up to 3.0 cm in diameter, and is represented by various genus such as *Dinoponera*, *Paraponera* and *Diacamma*. This subfamily is distributed mainly along the South America, and some species can be found in the Cerrado, Caatinga and Atlantic Forest (Schoeters and Billen, 1995; Siquieroli *et al*., 2007). Ants of medical interest belong to the genus *Dinoponera* and *Paraponera* (Haddad Junior *et al*., 2005). Previous studies demonstrated that the venom *Ponerinae* subfamily is composed of complex mixtures of proteins and neurotoxins (Lima and Brochetto-Braga, 2003).

Some animal models have been developed to analyze the pro- or anticonvulsant activity of various substances, such as models of seizures induced by pentylenetetrazole (PTZ), pilocarpine (PILO) and strychnine (STRC).

Materials and methods

Venom, chemicals and drugs

The ants were collected in Maranguape, Ceará, Brazil. The *Dinoponera quadriceps* venom (DQv) was extracted in the Laboratory of Entomology (State University of Ceará, UECE, Fortaleza, Brazil). PTZ, PILO and STRC were purchased from Sigma Chemical Co., USA.

Models of chemical-induced seizures and behavioral assessment

Male Swiss mice (28-33g) were pretreated with DQv (0.5 or 2.0 mg/kg, i.p., n=8). After 30 minutes, seizures were induced with PTZ (80 mg/kg, i.p.), PILO (400 mg/kg, i.p.) or STRC (3.0 mg/kg, i.p.) (Yilmaz *et al.*, 2007; Turski *et al.*, 1983; Aprison *et al.*, 1987). Then, the animals were placed in individual cages and observed over time. For the behavioral assessment, latency time to the first seizure and latency of death within the first 30 minutes were recorded. Control group of each model was treated only with the inductor agents.

Measurement of oxidative stress parameters by lipid peroxidation degree

Three brain areas of mice (prefrontal cortex, hippocampus and striatum) were dissected, after behavioral assessment, to determine the lipid peroxidation degree. According to Huong *et al.* (1998), lipid peroxide formation was analyzed by measuring the thiobarbituric acid reactive substances (TBARS), *i.e.* malondialdehyde (MDA) levels. The brain areas were homogenized in sodium phosphate buffer. The homogenates were mixed with 35% perchloric acid and centrifuged. Then, thiobarbituric acid (1.2%) was added to the supernatants which were heated in a boiling water bath for 30 min. Finally, the MDA levels were determined by absorbance at 535 nm.

Committee of Ethics

The protocols were accepted by the Ethics Committee on Animal Research of the Federal University of Ceará (protocol nº 43/2011).

Statistical analysis

Results are presented as the mean ± standard error of the mean (S.E.M.) of eight experiments for each group. Differences between groups were compared using analysis of variance (ANOVA) and Student-Newman-Keuls as *post hoc* test with significance set at 5%.

Results and Discussion

Effects of DQv on chemical-induced seizures models

Behavioral observation revealed that DQv (0.5 mg/kg), in PTZ-induced seizures mice, increased significantly the time to the first seizure (155.40 ± 27.70 sec *versus* 79.75 ± 3.90 sec for the control group; *Figure 1A*) and presented tendency to increase survival and the time to death (444.30 ± 82.47 sec, *i.e.* 12.5% survival, *versus* 307.40 ± 36.52 sec, *i.e.* 0% survival for the control group; *Figure 2A*). No significant alteration in both PILO- and STRC-induced models was observed (*Figures 1B, C and 2B, C*).

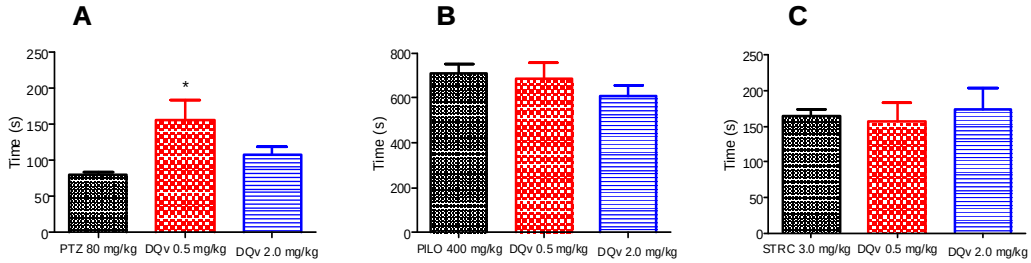

Figure 1. Effects of DQv on latency of the first seizure in the models of PTZ (**A**), PILO (**B**) and STRC (**C**). Results are expressed as means ± S.E.M (n=8). * P < 0.05 compared to the control group.

Figure 1. *Effets du DQv sur la latence de la première convulsion dans les modèles du PTZ (**A**), de la PILO (**B**) et de la STRC (**C**). Les résultats représentent les moyennes ± les erreurs standards de la moyenne (E.S.M.) de 8 expériences. * P < 0,05 comparé au groupe contrôle.*

PTZ, PILO and STRC have different mechanisms of action. The convulsant mechanism of action of PTZ is poorly understood but it was reported that PTZ is able to inhibit chloride channels associated with γ-aminobutyric acid type A (GABAA) receptors, reducing the inhibitory neurotransmission mediated by GABA (Silva *et al.*, 1998). Other studies showed that PILO induces the development of seizures, status epileptics and brain damage in rodents (Turski *et al.*, 1989; Marinho *et al.*, 1997) but the blockade of glutamatergic receptors prevents the propagation of seizures induced by PILO and brain damage (Jope *et al.*, 1986; Marinho *et al.*, 1997; Morrisett *et al.*, 1987). STRC, a competitive antagonist of glycine, exerts its inhibitory effects on the central nervous system, causing a severe seizure that usually leads the animals to death (Mazzambani, 2005). According this, our results demonstrate that DQv effects are probably not related to the cholinergic and glycinergic pathways but could be involved with the modulation of chloride channels.

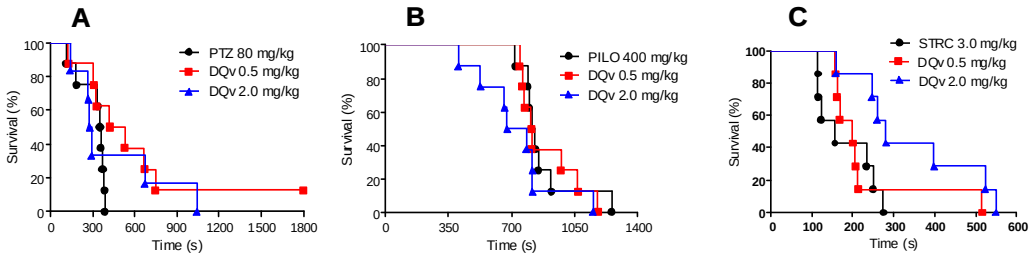

Figure 2. Effects of DQv on latency of death in models of PTZ (**A**), PILO (**B**) and STRC (**C**). Results are expressed as means ± S.E.M. (n=8).

Figure 2. *Effets du* DQv *sur la latence de la mort dans les modèles du PTZ (**A**), de la PILO (**B**) et de la STRC (**C**). Les résultats représentent les moyennes ± E.S.M. (n=8).*

Ants, as well as bees and wasps, belong to the order of Hymenoptera. It was reported recently that the venom of the ant *Dinoponera australis* contains more than 75 proteins and peptides, including modifiers of ion channels (Hoffman, 2010; Johnson *et al.*, 2010). Cunha *et al.* (2005) observed that the denatured venom of the wasp *Polybia ignobilis* presents anticonvulsant activity in some animal models. In addition, the neurotoxin AvTx7, isolated from *Agelaia vicina* wasp venom, has been reported to inhibit glutamate uptake in a dose-dependent and non-competitive manner (Pizzo *et al.*, 2004).

Effects of DQv on oxidative stress parameter

We observed that pretreatment with DQv (2.0 mg/kg) decreased MDA amount only in the cortex of PTZ model mice (38.86 ± 3.43 µg of MDA/g of tissue *versus* 58.74 ± 3.76 µg of MDA/g of tissue for the control group) (*Figure 3A*). Modifications of this parameter were not found within another cerebral area of PTZ model animals, as well as in PILO- and STRC-induced models whatever the cerebral area was studied.

Oxidative stress in the central nervous system has been shown in various models of experimental epilepsy, such as the PTZ model (Gupta *et al.*, 2003; Patsoukis *et al.*, 2004) and is characterized by an imbalance between oxidant and antioxidant substances. According to Patel (2004), epileptic seizures can result from free radical production and oxidative damage in cell structures such as lipids, protein and DNA. Bashkatova *et al.* (2003) demonstrated that TBARS formation is increased in the brain cortex of rats during PTZ-induced seizures. However, the rise of lipid peroxidation in brain tissues after convulsions is decreased by substances with antioxidant properties (Yamamoto and Tang, 1996; Gupta *et al.*, 2001). We observed that previous administration of DQv is able to cause a reduction of MDA levels in cortex. Thus, it is likely that this venom contains a component with antioxidant property that has affinity for some specific structure(s) present in the prefrontal cortex. This activity may be involved, at least in part, in a neuroprotective action since the increase in levels of free radicals and decrease of antioxidant defense mechanisms in seizure processes are well documented. Thus, a substance able to reduce the oxidative stress levels may ameliorate the damaging effects caused by convulsions.

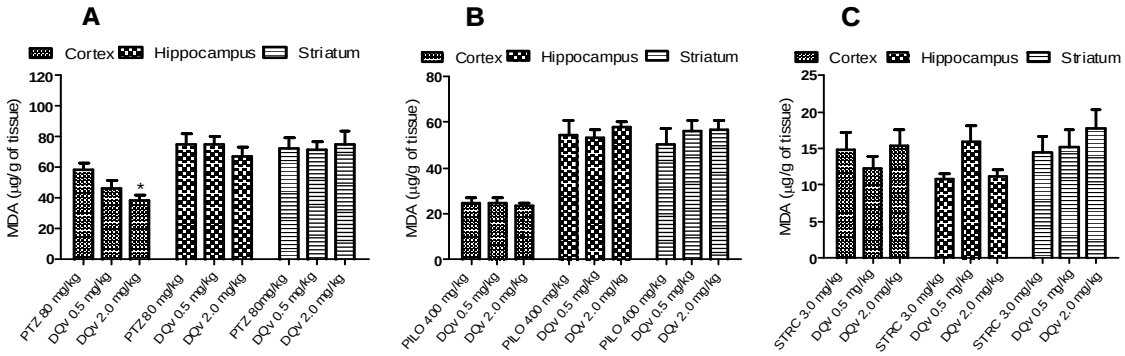

Figure 3. Effects of DQv in the lipid peroxidation degree, by measurement of MDA levels in three brain areas, in models of PTZ (**A**), PILO (**B**) and STRC (**C**). Results are expressed as means ± S.E.M (n=8). * P < 0.05 compared to the control group.

Figure 3. *Effets du DQv sur le degré de péroxydation des lipides, par la mesure des niveaux de MDA dans trois aires du cerveau, dans les modèles du PTZ (**A**), de la PILO (**B**) et de la STRC (**C**). Les résultats représentent les moyennes ± E.S.M. de 8 expériences. * P < 0,05 comparé au groupe contrôle.*

Conclusion

In the present work, we show that pretreatment with DQv is able to cause some neuroprotective effects on PTZ-induced seizures. In behavioral assessment, the venom increased the time to the first seizure and showed a tendency to enhance the time of death. We observed that DQv reduces MDA (as an oxidative parameter) levels in prefrontal cortex. Further investigations are needed to elucidate the involved molecular mechanisms of action, as well as to identify the venom component(s) responsible for DQv effects.

Acknowledgements. *We are grateful to the CAPES and CNPQ for financial support.*

References

Aprison MH, Lipkowitz KB, Simon JR (1987) Identification of a glycine-like fragment on the strychnine molecule. *J Neurosci Res* **17**:209-213

Bashkatova V, Narkevich V, Vitskova G, Vanin A (2003) The influence of anticonvulsant and antioxidant drugs on nitric oxide level and lipid peroxidation in the rat brain during pentylenetetrazole-induced epileptiform model seizures. *Prog Neuropsychopharmacol Biol Psychiatry* **27**: 487-492

Cunha AOS, Mortari MR, Oliveira L, Carolino ROG Coutinho-Netto J, Dos Santos WF (2005) Anticonvulsant effects of the wasp *Polybia ignobilis* venom on chemically induced seizures and action on GABA and glutamate receptors. *Comp Biochem Physiol* **41**: 50-57

Gupta YK, Chaudhary G, Sinha K, Srivastava AK (2001) Protective effect of resveratrol against intracortical FeCl3 inducedmodel of posttraumatic seizures in rats. *Methods Find Exp Clin Pharmacol* **23**: 241-244

Gupta YK, Veerendra Kumar MH, Srivastava AK (2003) Effect of *centella asiatica* on pentylenetetrazole-induced kindling, cognition and oxidative stress in rats. *Pharmacol Biochem Behav* **74**: 579-585

Haddad Junior V, Cardoso JLC, Moraes RHP (2005) Description of an injury in a human caused by a false tocantira (*Dinoponera gigantean*, Perty, 1833) with a revision of folkloric, pharmacological and clinical aspects of the giant ants of the genera *Paraponera* and *Dinoponera* (sub-family ponerinae). *Rev Inst Med trop S Paulo* **47**: 235-238

Hoffman DR (2010) Ant venoms. *Curr Opin Allergy Clin Immunol* **10**: 342-346

Huong NT, Matsumoto K, Kasai R, Yamasaki K, Watanabe H (1998) *In vitro* antioxidant activity of Vietnamese ginseng saponin and its components. *Biol Pharm Bull* **21**: 978-981

Johnson SR, Copello JA, Evans MS, Suarez AV (2010) A biochemical characterization of the major peptides from the venom of the giant neotropical hunting ant *Dinoponera australis*. *Toxicon* **55**: 702-710

Jope RS, Morisett RA, Snead OC (1986) Characterization of lithium potentiation of pilocarpine-induced status epilepticus in rats. *Exp Neurol* **91**: 471-480

Lima PRM, Brochetto-Braga MR (2003) Hymenoptera venom review focusing on *Apis mellifera*. *J Venom Anim Toxins incl Trop Dis* **9**: 149-162

Marinho MMF, Sousa FCF, Bruin VMS, Aguiar LMV, Pinho RSN, Viana GSB (1997) Inhibitory action of a calcium channel blocker (nimodipine) on seizures and brain damage induced by pilocarpine and lithium-pilocarpine in rats. *Neurosci Lett* **235**: 13-16

Mazzambani L (2005) Avaliação das propriedades farmacológicas dos compostos imídicos cíclicos selecionados e da agmatina no sistema nervoso central. Dissertação (Mestrado). Programa de Mestrado Acadêmico em Ciências Farmacêuticas. Universidade Vale do Itajaí. Itajaí – São Paulo

Morrisett RA, Jope RS, Snead OC (1987) Effects of drugs on the initiation and maintenance of status eplepticus induced by administration of pilocarpine to lithium-pretread rats. *Exp Neurol* **97**: 193-200

Patel M (2004) Mitochondrial dysfunction and oxidative stress: Cause and consequence of epileptic seizures. *Free Radic Biol Med* **37**: 1951-1962

Patsoukis N, Zervoudakis G, Panagopoulos NT, Georgiou CD, Angelatou F, Matsokis NA (2004) Thiol redox state (TRS) and oxidative stress in the mouse hippocampus after pentylenetetrazol induced epileptic seizure. *Neurosci Lett* **357**: 83-86.

Pizzo AB, Beleboni RO, Fontana ACK, Ribeiro AM, Miranda A, Coutinho-Netto J, Santos WF (2004) Characterization of the actions of AvTx7 isolated from *Agelaia vicina* (Hymenoptera: Vespidae) wasp venom on synaptosomal glutamate uptake and release. *J Biochem Mol Toxicol* **18**: 61-68

Schoeters E, Billen J (1995) Morphology and ultrastructure of the convoluted gland in the ant *Dinoponera australis* (Hymenoptera:Formicidae). *Int J Insect Morphol Embryol* **24**: 323-332

Silva LF, Pereira P, Elisabetsky E (1998) A neuropharmacological analysis of PTZ-induced kindling in mice. *Gen Pharmac* **31**: 47-50

Siquieroli ACS, Santana FA, Rodrigues RS, Vieira CU, Cardoso R, Goulart LR, Bonetti AM (2007) Phage display in venom gland in *Dinoponera australis* (HYMENOPTERA:FORMICIDAE). *J Venom Anim Toxins* **13**: 291

Turski L, Ikonomidou C, Turski WA, Bortolotto ZA, Cavalheiro EA (1989) Review: Cholinergic mechanisms and epileptogenesis. The seizures induced by pilocarpine: a novel experimental model of intractable epilepsy. *Synapse* **3**: 154-171

Turski WA, Cavalheiro EA, Schwartz M, Czuczwar SJ, Kleinrok Z, Turski L (1983) Limbic seizures produced by pilocarpine in rats: a behavioural, electroencephalographic and neuropathological study. *Behav Brain Res* **9**: 315-335

Yamamoto H, Tang H (1996) Melatonin attenuates L-cysteine-induced seizures and lipid peroxidation in the brain of mice. *J Pineal Res* **21**: 108-113

Yilmaz I, Sezer Z, Kayir H, Uzbay TI (2007) Mirtazapine does not affect pentylenetetrazole- and maximal electroconvulsive shock-induced seizures in mice. *Epilepsy Behav* **11**: 1-5

Toxines et Transferts ioniques – Toxins and Ion transfers
Rencontres en Toxinologie – Meeting on Toxinology, 2011
Editions de la SFET – SFET Editions
Accès libre en ligne sur le site – Free access on line on the site : http://www.sfet.asso.fr

Effect of L-amino acid oxidase isolated from Bothrops marajoensis *snake venom on the epimastigote forms of* Trypanosoma cruzi

Ticiana PEREIRA[1*], Rodrigo DANTAS[2], Alba TORRES[1], Clarissa MELLO[1], Danya LIMA[1], Marcus Felipe COSTA[1], Marcos TOYAMA[3], Maria de Fátima OLIVEIRA[1], Helena MONTEIRO[2], Alice MARTINS[1]

[1] *Department of Clinical and Toxicological Analysis, Pharmacy Faculty, Federal University of Ceará, Fortaleza, Ceará, Brazil ;* [2] *Department of Physiology and Pharmacology- Federal University of Ceará, Fortaleza, Ceará, Brazil ;* [3] *São Vicente Unity, Campus of Litoral Paulista, Paulista State University (UNESP), São Paulo, Brazil*

* *Corresponding author ; Tel : +55 (0) 85 3366-8269 ; E-mail : ticianapraciano@gmail.com*

Abstract

L-amino acid oxidases from snakes' venom have bactericidal, leishmanicidal and trypanocidal activity. Epimastigote forms of Trypanosoma cruzi *were treated with different doses (100-3.125 µg/mL) of L-amino acid oxidase isolated from* Bothrops marajoensis *venom (LAAOBM) in the absence or presence of catalase. We observed that LAAOBM demonstrated dose-dependent trypanocidal activity after 48 h and 72 h incubation. In the presence of catalase, this activity was completely abolished after 48 h incubation and was markedly reduced after 72 h incubation. These results show that L-amino acid oxidase from* B. marajoensis *venom exerts a trypanocidal activity and that the removal of hydrogen peroxide (H_2O_2) by addition of catalase is able to abolish or decrease the cell death induced by this oxidase.*

Effet de la L-amino-acide oxydase isolée du venin du serpent Bothrops marajoensis *sur les formes épimastigotes de* Trypanosoma cruzi

Les L-amino-acide oxydases isolées du venin de serpents ont une activité bactéricide, leishmanicide et trypanocide. Les formes épimastigotes de Trypanosoma cruzi *ont été traitées avec différentes doses (100–3,125 µg/mL) de L-amino-acide oxydase isolée du venin du serpent* Bothrops marajoensis *(LAAOBM) en l'absence ou la présence de catalase. Nous avons observé que la LAAOBM montrait une activité trypanocide, dépendante de la dose, après 48 h et 72 h d'incubation. En présence de catalase, cette activité était complètement supprimée après 48 h d'incubation et largement réduite après 72 h d'incubation. Ces résultats montrent que la L-amino-acide oxydase du venin de* B. marajoensis *a une activité trypanocide et que la suppression de péroxyde d'hydrogène (H_2O_2), par l'addition de catalase, est capable d'abolir ou de réduire la mort cellulaire produite par cette oxydase.*

Keywords : Bothrops marajoensis, *epimastigote forms, L-amino acid oxidase, snake venom,* Trypanosoma cruzi.

Introduction

Snake venoms comprise a complex mixture of proteins, peptides, lipids and other substances, such as phospholipases A_2, metalloproteases and L-amino acid oxidases, that vary in proportions and characteristics among the different species (Queiroz *et al.*, 2008; Alves *et al.*, 2008).

L-amino acid oxidases are a family of flavoenzymes that catalyze oxidative deamination of L-amino acids to produce the corresponding α-ketoacids, hydrogen peroxide (H_2O_2) and ammonia (Ehara *et al.*, 2002; Du and Clemetson, 2002). These flavoenzymes are largely studied due their biological effects including bactericidal, leishmanicidal and trypanocidal activity (Stábeli *et al.*, 2004; Izidoro *et al.*, 2006; Deolindo *et al.*, 2010; De Melo Alves Paiva *et al.*, 2011).

Chagas disease is a parasitosis caused by the protozoan *Trypanosoma cruzi* which continues to represent a health problem for an estimated 28 million people, living mostly in Latin America (Maya *et al.*, 2010). It is recognized by the World Health Organization (WHO) as one of the world's 13 most neglected tropical diseases (Hotez *et al.*, 2007). The drugs available to treat Chagas disease are nifurtimox and benznidazole (BZN). However, due to toxicity and prolonged therapy, these treatments are not effective. It is worth noting that side

effects are observed in up to 40% of patients. They include nausea, vomiting, abdominal pain and several neurological effects (Marin-Neto *et al.*, 2009).

Within this context, the toxins may represent a rich therapeutic potential and/or provide data for development of pharmacology tools. The present study demonstrates the cytotoxic effect of L-amino acid oxidase isolated from *Bothrops marajoensis* venom on epimastigote forms of *T. cruzi*.

Materials and methods

Venom and reagents

The L-amino acid oxidase isolated from *B. marajoensis* venom (LAAOBM) was kindly donated by Dr. Marcos H. Toyama (Paulista State University, UNESP, São Paulo, Brazil). Benzonidazole was donated by LAFEPE (Phamaceutical Laboratory of Pernambuco State), and catalase was purchased from Sigma.

Trypanocidal activity

Epimastigote forms of *T. cruzi* were grown at 28°C in Liver Infusion Tryptose (LIT) medium supplemented with 10% fetal bovine serum. The epimastigotes used for all experiments were those from the log-growth phase (6^{th} day). The experiments were performed in 96-well plates at a density of $1x10^6$ parasites/mL treated with different doses (100–3.125 µg/mL) of LAAOBM in the absence or presence of catalase (90 µg/mL). BZN was used as the reference drug. The plates were incubated for 48 or 72 h, and the cell viability was determined by quantification in a Neubauer Chamber. Cultures of the parasite without treatment were considered as 100% growth.

Statistical analyses

Results are presented as the mean ± standard error of the mean (S.E.M.) of three experiments in triplicate. The statistical significance of data was determined by ANOVA, Dunett, *post-test*.

Results and Discussion

The cellular viability of epimastigote forms of *T. cruzi* was investigated after treatment with LAAOBM. LAAOBM demonstrated a dose-dependent cytotoxic effect on epimastigote forms with 50% inhibition doses (ID_{50}) of 16.58 µg/mL and 13.52 µg/mL after 48 h and 72 h incubation, respectively (*Figure 1A* and *B*). Recent studies have reported trypanocidal activity for L-amino acid oxidases isolated from *B. atrox* (Alves Paiva, 2011), *B. jararaca* (Deolindo, 2010) and *B. marajoensis* (Torres, 2010).

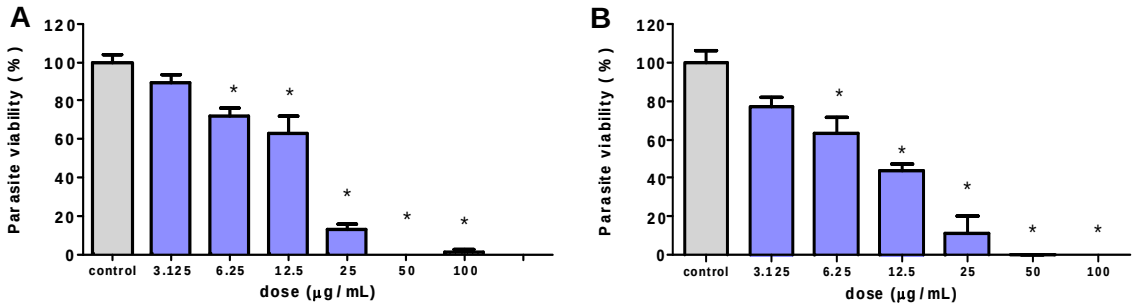

Figure 1. Effects of different doses of LAAOBM on epimastigote forms of *T. cruzi* treated for 48 h (**A**) and 72 h (**B**). The graph represents means ± S.E.M. of data (n=3). The statistical significance of data was determined by ANOVA, Dunett, *post-test*. * P < 0.05 compared to the corresponding control group.

Figure 1. *Effets de différentes doses de LAAOBM sur les formes épimastigotes de* T. Cruzi *traitées pendant 48 h (**A**) et 72 h (**B**). Les graphiques représentent les moyennes ± l'erreur standard de la moyenne (E.S.M.) des résultats (n=3). La signification statistique des résultats a été determinée par ANOVA, Dunett,* post-test. ** P < 0,05 comparé au groupe contrôle.*

The toxicity of L-amino acid oxidases is thought to be due to the production of H_2O_2 (Zhang *et al.*, 2004a). This production might be the underlying mechanism for trypanocidal activity (Du and Clemetson, 2002). In order to test this hypothesis, we studied the trypanocidal activity of various doses of LAAOBM in the presence of a given dose of catalase (*i.e.* 90 µg/mL), an enzyme known to suppress the production of H_2O_2. Our results show that in the group treated with both LAAOBM and catalase for 48 h, only an about 40% cell death was observed at the highest dose (100 µg/mL) of LAAOBM whereas at lower doses, no significant effect of LAAOBM occurred (*Figure 2A*). These results indicate that the inhibition of cytotoxic effect of LAAOBM by catalase is probably due to the breakdown of H_2O_2 production (Stabéli *et al.*, 2007; Deolindo *et al.*, 2010; Naumann *et al.*, 2011). However, in the group treated with both LAAOBM and catalase for 72h, an about 40-50% cell death reduction was observed whatever the LAAOBM doses were (*Figure 2B*). These results indicate that the cell death induced by 3.125-6.25 and 25-100 µg/mL LAAOBM for 72 h was increased and decreased, respectively by catalase. Indeed, it has been reported in the literature that the biological actions of ophidian L-amino acid oxidases are only partly dependent on H_2O_2, suggesting that there are specific receptors or targets on the cells (Li *et al.*, 2008; Zhang *et al.*, 2004b).

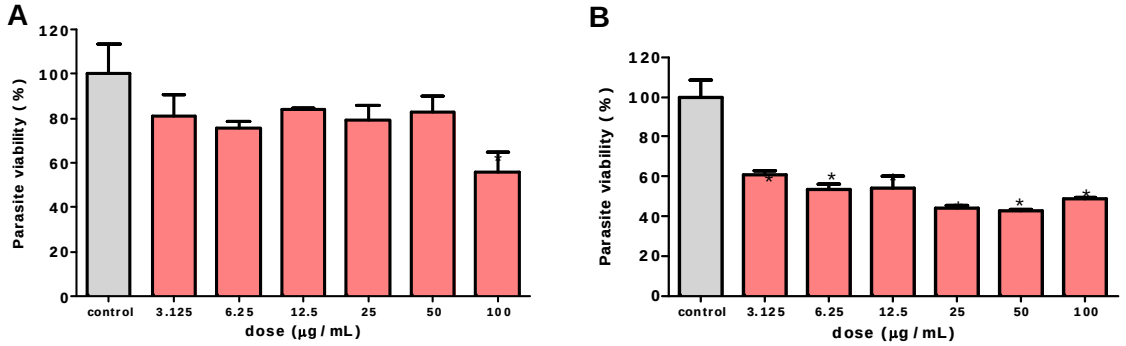

Figure 2. Effects of different doses of LAAOBM on epimastigote forms of *T. cruzi* treated for 48 h (**A**) and 72 h (**B**) in the presence of 90 µg/mL catalase. The graph represents means ± S.E.M. of data (n=3). The statistical significance of data was determined by ANOVA, Dunett, *post-test*. * P < 0.05 compared to the corresponding control group.

Figure 2. *Effets de différentes doses de LAAOBM sur les formes épimastigotes de* T. cruzi *traitées pendant 48 h (**A**) et 72 h (**B**) en présence de 90 µg/mL de catalase. Les graphiques représentent les moyennes ± E.S.M. des résultats (n=3). La signification statistique des résultatsa été determinée par ANOVA, Dunett,* post-test. ** P < 0,05 comparé au groupe contrôle.*

The *Figure 3* demonstrates the cytotoxic effect of BZN on epimastigote forms treated for 48 h and 72 h.

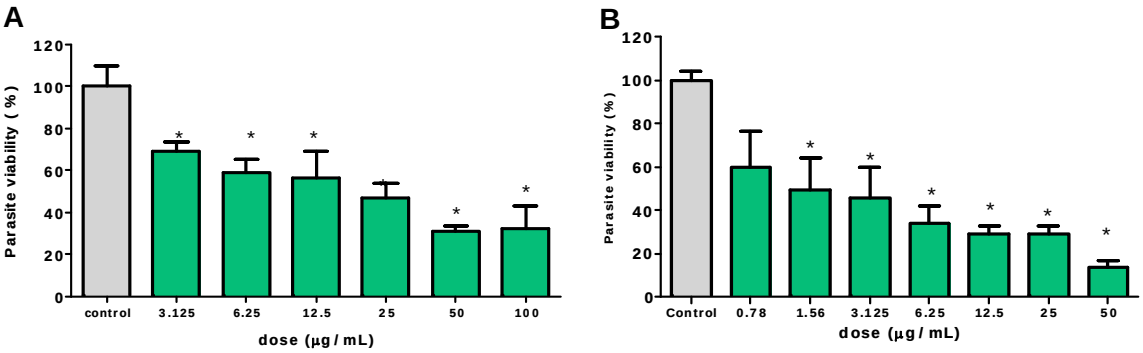

Figure 3. Effects of different doses of BZN on epimastigote forms of *T. cruzi* treated for 48 h (**A**) and 72 h (**B**). The graph represents means ± S.E.M. of data (n=3). The statistical significance of data was determined by ANOVA, Dunett, *post-test*. # P < 0.05 compared to the corresponding control group.

Figure 3. *Effets de différentes doses du benznidazole sur les formes épimastigotes de* T. cruzi *traitées pendant 48 h (**A**) et 72 h (**B**). Les graphiques représentent les moyennes ± E.S.M. (n=3). La signification statistique des résultats a été determinée par ANOVA, Dunett,* post-test. ** P < 0,05 comparé au groupe contrôle.*

Conclusion

L-amino acid oxidase, an enzyme widely distributed among different snake species, has been reported to have several biological effects. Our results show that L-amino acid oxidase from *B. marajoensis* venom exerts a trypanocidal activity on epimastigote forms of *T. cruzi* and that the removal of H_2O_2 by addition of catalase abolishes or markedly reduces the cell death induced by this oxidase.

Acknowledgements. *We are grateful to the CAPES, CNPQ and FUNCAP for financial support.*

References

Alves Paiva R, De Freitas, FR, Antonucci GA, Paiva HH, De Lourdes PBM, Rodrigues KC, Lucarini R, Caetano RC, Linhares RPRC, Gomes Martins CH, De Albuquerque S, Sampaio SV (2011) Cell cycle arrest evidence, parasiticidal and bactericidal properties induced by L-amino acid oxidase from *Bothrops atrox* snake venom. *Biochimie* **93**: 941-947

Alves RM, Antonucci GA, Paiva HH, Cintra AC, Franco JJ, Mendonça-Franqueiro EP, Dorta DJ, Giglio JR, Rosa JC, Fuly AL, Dias-Baruffi M, Soares AM, Sampaio SV (2008) Evidence of caspase-mediated apoptosis induced by l-amino acid oxidase isolated from *Bothrops atrox* snake venom. *Comp Biochem Physiol A Mol Integr Physiol* **151**: 542-550

Deolindo P, Teixeira-Ferreira AS, DaMatta RA, Alves EW (2010) L-amino acid oxidase activity present in fractions of *Bothrops jararaca* venom is responsible for the induction of programmed cell death in *Trypanosoma cruzi*. *Toxicon* **56**: 944-955

Du XY, Clemetson KJ (2002) Snake venom L-amino acid oxidases. *Toxicon* **40**: 659-665

Ehara T, Kitajima S, Kanzawa N, Tamiya T, Tschuchiya T (2002) Antimicrobial action of achacin is mediated by L-amino acid oxidase activity. *FEBS Lett* **531**: 509-598

Hotez PJ, Molyneux DH, Fenwick A, *et al.* (2007) Control of neglected tropical diseases. *N Engl J Med* **357:** 1018–1027

Izidoro LFM, Ribeiro MC, Souza GRL (2006). Biochemical and functional characterization of an L-amino acid oxidase isolated from *Bothrops pirajai* snake venom. *Bioorg Medic Chemi* **14**: 7034-7043

Li R, Zhu S, Wu J, Wang, W, Lu Q, Clemetson KJ (2008) L-amino acid oxidase from *Naja atra* activates and binds to human platelets. *Acta Biochm Biophys Sin* **40** :19-26

Marin-Neto JA, Rassi JrA, Avezum JrA, Mattos AC, Rassi A, Morillo CA, Sosa-Estani S, Yusuf S (2009).The benefit Trial: testing the hypothesis that trypanocidal therapy is beneficial for patients with chronic Chagas heart disease. *Mem Inst Oswaldo Cruz* **104**: 319-324

Maya JD, Orellana M, Ferreira J, Kemmerling U, López-Muñoz R (2010) Chagas disease: Present status of pathogenic mechanisms and chemotherapy. *Biol Rese* **43**: 323-331

Naumann GB, SILVA LF, Silva L, Faria G, Richardson M, Evangelista K, Kohlhff M, Gontijo CMF, Navdaev A, Rezende FF, Eble JA, Sanchez EF (2011). Cytotoxicity and inhibition of platelet aggregation caused by na l-amino acid oxidase from *Bothrops leucurus* venom. Biochimi Biophys Acta **1810** :683-694.

Queiroz GP, Pessoa LA, Portaro FC, Furtado Mde F, Tambourgi DV (2008) Interspecific variation in venom composition and toxicity of Brazilian snakes from *Bothrops genus*. *Toxicon* **52**: 842-851

Stábeli RS, Marcussi S, Carlos GB (2004) Platelet aggregation and antibacterial effects an L-amino acid oxidase purified from *Bothrops alternatus* snake venom. *Bioorg Medic Chemi* **12**: 2881-2886

Stábeli RG, Sant'ana, CD, Ribeiro PH, Costa TR, Ticli FK, Pires MG, Nomizo A, Albuquerque S, Malta-Neto N, Martins M, Sampaio SV, Soares AM (2007) Cytotoxic L-amino acid oxidase from *Bothrops moojeni*: Biochemical and functional characterization. *Biol Macrom* **41**: 132-140

Torres AF, Dantas RT, Toyama MH, Diz Filho E, Zara FJ, Queiroz MGR, Nogueira NAP, De Oliveira AR, Toyana DO, Monteiro HSZ, Martins AMC (2010) Antibacterial and antiparasitic effects of *Bothrops marajoensis* venom and its fractions: Phospholipase A2 and L-amino acid oxidase. *Toxicon* **55**: 795–804

Zhang H, Teng M, Niu L, Wang Y, Liu Q, Huang Q, Dong Y, Liu P (2004a) Purification, partial characterization, crystallization and structural determination of AHP-LAAO, a novel L-amino acid oxidase with cell apoptosis-inducing activity from *Agkistrodon halys pallas* venom. *Acta crysto* **60**: 974-977

Zhang H, Yang Q, Sun M, Teng M, Liu P (2004b) Hydrogen peroxide produced by two amino acid oxidases mediates antibacterial actions. *J Microbiol* **42**: 336-339

Toxines et Transferts ioniques – Toxins and Ion transfers
Rencontres en Toxinologie – Meeting on Toxinology, 2011
Editions de la SFET – SFET Editions
Accès libre en ligne sur le site – Free access on line on the site : http://www.sfet.asso.fr

Neurotoxicity of Staphylococcus aureus *leucotoxins : interaction with the store operated calcium entry complex in central and sensory neurons*

Emmanuel JOVER[1*], Benoît-Joseph LAVENTIE[2], Mira TAWK[2], Bernard POULAIN[1], Gilles PREVOST[2]

[1] *INCI – UPR-CNRS 3212, Neurotransmission et sécrétion neuroendocrine, 5 rue Blaise Pascal, F-67084 Strasbourg cedex, France ;* [2] *Université de Strasbourg, Physiopathologie et Médecine Translationnelle EA-4438, Institut de Bactériologie, 3 rue Koeberlé, F-67000 Strasbourg, France*

** Corresponding author ; Tel : +33 (0)3 8845 6647 ; Fax : +33 (0)3 8860 1664 ;*
E-mail : jover@inci-cnrs.unistra.fr

Abstract

Infectious diseases due to Staphylococcus aureus *include painful symptoms suggesting involvement of the nervous system. This led us to evaluate the potential neurotoxicity of bi-component leucotoxins released by this bacterium. In rat granular neuronal cells, low concentration of leucotoxins causes the release of significant amounts of glutamate due to an increase in $[Ca^{2+}]_i$. By monitoring the $[Ca^{2+}]_i$ changes with the fluorescent indicator Fura-2, we found that the $[Ca^{2+}]_i$ imbalance is due to the interaction of leucotoxins with the store operated Ca^{2+} entry complex. Indeed, drugs targeting the refilling of intracellular Ca^{2+} stores [Sarco-Endoplasmic Reticulum Ca^{2+}-ATPase (SERCA), H^+-ATPase] and antagonists of the store operated Ca^{2+} entry complex blunted, or reduced considerably, the leucotoxin induced $[Ca^{2+}]_i$ elevation. Simultaneously, signal transduction pathways that include the phosphatidylinositol 3-kinase and the ADPribosyl cyclase CD38 were activated. Moreover, confocal analysis of immunolabelled neurons shows that, shortly after binding, the leucotoxin was localised with the Ca^{2+} sensor stromal interacting molecule Stim1 in the same endosomal compartment. Furthermore, the mobilisation of free internal Ca^{2+} is antagonized by specific anti-Stim1 antibodies. Our results suggest that, following toxin internalisation, Ca^{2+} stored in the endosomal compartment leaks out, probably inducing the Stim1 aggregation to the membrane protein ORAI1, which leads to a subsequent increase in $[Ca^{2+}]_i$.*

Neurotoxicité des leucotoxines de Staphylococcus aureus *: interaction avec le complexe impliqué dans l'influx de calcium dépendant de la libération des réserves calciques intracellulaires dans des neurones centraux et sensoriels*

Les infections à Staphylococcus aureus *comportent souvent des syndromes douloureux qui peuvent suggérer une atteinte du système nerveux. Partant de cette idée, nous avons cherché à évaluer le potentiel neurotoxique des leucotoxines à deux composants libérées par la bactérie. Sous l'effet des leucotoxines, les neurones granulaires de rat en culture libèrent du glutamate suite à une augmentation de $[Ca^{2+}]_i$. Nous avons suivi les variations de $[Ca^{2+}]_i$ à l'aide de l'indicateur fluorescent Fura-2 et nous observons que les changements en $[Ca^{2+}]_i$ sont dus à l'interactions de leucotoxines avec le complexe impliqué dans l'influx de calcium dépendant de la libération des réserves calciques intracellulaires (SOCE pour « Store Operated Calcium Entry »). Les drogues qui bloquent le remplissage des réserves de Ca^{2+} intracellulaires [SERCA pour « Sarco-Endoplasmic Reticulum Ca^{2+}-ATPase », H^+-ATPase] et des antagonistes du complexe SOCE, bloquent, ou réduisent considérablement, les élévations de $[Ca^{2+}]_i$ provoquées par la leucotoxine. Aussi, le blocage des activités phosphatidylinositol 3-kinase et de l'ADPribosyl cyclase CD38 inhibe l'effet de la leucotoxine sur la $[Ca^{2+}]_i$. A l'aide d'un dérivé fluorescent de la sous-unité HlgB nous avons suivi la localisation de la toxine après fixation; les analyses en microscopie confocale situent la leucotoxine dans le même compartiment que la protéine senseur de Ca^{2+} Stim1 (pour « Stromal interacting molecule 1 »). La mobilisation du Ca^{2+} intracellulaire est aussi bloquée par des anticorps dirigés contre Stim1. Nos résultats suggèrent qu'après internalisation, la leucotoxine favorise la sortie du Ca^{2+} de l'endosome, ce qui pourrait faciliter l'agrégation de Stim1 à la protéine ORAI1 et entrainerait l'augmentation du $[Ca^{2+}]_i$.*

Keywords : *Neurotoxicity, staphylococcal leucotoxins, stromal interacting molecule 1, store operated calcium entry.*

Introduction

Staphylococcus aureus strains causing human pathologies produce several toxins, including a pore-forming protein family formed by the single-component α-hemolysin and the bicomponent leucotoxins. The last comprise two protein elements, S and F, which co-operatively form the active toxin. α-Hemolysin is always expressed by *S. aureus* strains, whereas bicomponent leucotoxins are more specifically involved in a few diseases. The pore-forming toxins (PFTs) are expressed as water soluble monomeric proteins that assemble on the membranes of the target cells to form bilayer-spanning pores (Menestrina *et al.*, 2003). Even before protein extension in the bilayer is completed, the formation of an oligomeric pre-pore can trigger Ca^{2+}-mediated activation of some white cells, initiating an inflammatory response. Major advances have been made over the last decade in the understanding of the structure and mechanism of pore formation by PFTs from *S. aureus* (Kaneko and Kamio 2004; Gonzalez *et al.*, 2008; Yamashita *et al.*, 2011). In contrast, much less is known about all the cell targets of *S. aureus* PFTs and the responses of cells confronted with the presence of leucotoxins.

Our work focused on neurons sensitivity to *S. aureus* PFTs. We used rat cerebellar granular to study intracellular $[Ca^{2+}]$ variations. The leucotoxin HlgC/HlgB evoked rises of free $[Ca^{2+}]_i$ that were blocked or strongly reduced by antagonists of the store operated Ca^{2+} entry (SOCE) system. Antagonists of phosphatidylinositol 3-kinase and ADPribosyl cyclase CD38 blocked the intracellular $[Ca^{2+}]$ variations activated by the leucotoxin. The toxin was internalised and was found in a compartment where it partially colocalized with the Stromal interacting molecule Stim-1.

Intracellular Ca^{2+} mobilization by *Staphylococcus aureus* leucotoxins

We used the Fura-2 calcium fluorescent indicator to observe intracellular $[Ca^{2+}]$ variations. As shown in *Figure 1*, the cerebellar granular neurons reacted to the presence of the leucotoxin HlgC/HlgB through a transient peak of $[Ca^{2+}]_i$ that was followed by the return to a new resting value of $[Ca^{2+}]_i$ higher than the initial (*Figure 1A*). The latency between toxin application and the rise of $[Ca^{2+}]_i$ was asynchronous between cells. Depending on the concentrations of leucotoxin, a second rise of $[Ca^{2+}]_i$ often followed with a variable delay. To be able to compare sets of cells incubated with different toxin concentrations and pharmacological drugs, three parameters were measured from individual cell responses: (i) the amplitude of $[Ca^{2+}]_i$ at the peak, (ii) the time latency to reach the peak of $[Ca^{2+}]_i$ and (iii) the proportion of cells displaying a second $[Ca^{2+}]_i$ rise. The point plots presented in *Figure 1B* (peak amplitude) and *1C* (latency of the response) report the responses variability at different toxin concentrations. However, the pooling of the data from a large number of independent experiments showed a significant concentration dependent effect on median and mean values of the peak amplitude and the time latency of the response (*Table 1*). Therefore, the peak $[Ca^{2+}]_i$ amplitude and the time latency will be presented in *Figures* as box plots with median and percentiles.

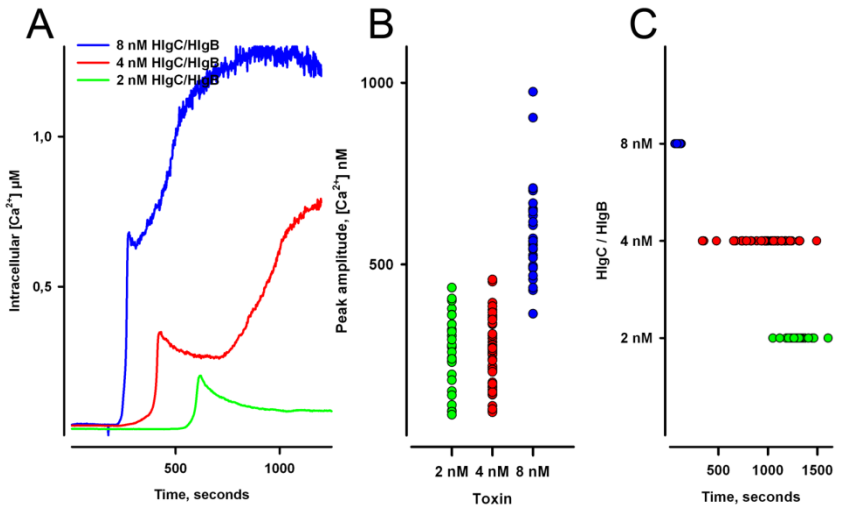

Figure 1. The leucotoxin HlgC/HlgB induced intracellular $[Ca^{2+}]$ variations in granular neurons in a concentration dependent manner. The results are from three independent records obtained at different leucotoxin concentrations. (**A**) Examples from individual cell at three concentrations, illustrating that increasing concentrations of toxin tend to reduce the latency of the response, to increase the amplitude of the peak and to produce an secondary $[Ca^{2+}]_i$ rise. However, as shown by the point plots in (**B**) for the peak amplitude or in (**C**) for the latency of the response, in a group of cells (same dish) the variability of the responses is high. Nevertheless, pooling a large numbers of independent experiments, confirms the concentration dependence of the effect. This is illustrated in *Table 1*.

Figure 1. *Les variations de $[Ca^{2+}]$ intracellulaire provoquées par la leucotoxine HlgC/HlgB dépendent de la concentration. Les résultats présentés ici ont été obtenus avec trois boites de cellules enregistrées à des concentrations différentes. (**A**) Exemples de trois cellules enregistrées à des concentrations de toxine différentes qui illustrent que lorsque la concentration augmente le temps de réponse diminue, l'amplitude du pic de Ca^{2+} augmente et il peut apparaitre une deuxième augmentation de $[Ca^{2+}]_i$. Mais, comme le montrent les nuages de points en (**B**) pour le pic de $[Ca^{2+}]$ et en (**C**) pour la latence, les réponses sont très variables d'une cellule à l'autre. Cependant, la réunion des valeurs issues d'un grand nombre d'expériences confirme la relation ente la concentration de toxine et l'amplitude moyenne des réponses. Ceci est illustré à l'aide du* Tableau 1.

Table 1. Values for the $[Ca^{2+}]_i$ peak amplitude (**A**) and the time latency (**B**) from a large number of experiments (three different concentrations) were pooled together in order to compare the mean, the median and the percentiles and to evaluate the statistical significance. The differences between the three groups are statistically significant ($P < 0.001$) according the one way ANOVA analysis of variance.

Tableau 1. *Les valeurs de l'amplitude de la $[Ca^{2+}]_i$ (**A**) et du délai de réponse (**B**) pour un nombre élevé d'enregistrements (trois concentrations de toxine) sont réunies afin de comparer les moyennes, les médianes et les percentiles et de vérifier si les trois groupes sont statistiquement différents. Le test ANOVA d'analyse de variances considère les différences significatives ($P < 0.001$).*

A Toxin concentration	Mean of Peak amplitude	Median of Peak amplitude	25 %	75 %	Cells (exp)
2 nM	178 ± 89 nM	159.2 nM	110.4 nM	227.8 nM	396 (14)
4 nM	355 ± 223 nM	297.8 nM	197.8 nM	469.7 nM	862 (24)
8 nM	416 ± 228 nM	389.9 nM	234.5 nM	542.6 nM	178 (6)

B Toxin concentration	Mean of time latency	Median of time latency	25 %	75 %	Cells (exp)
2 nM	687 ± 413 s	701 s	300 s	1026 s	396 (14)
4 nM	551 ± 445 s	423 s	144 s	868 s	862 (24)
8 nM	221 ± 237 s	125 s	88 s	232 s	178 (6)

The activity of different leucotoxins was then compared. Starting at 2 nM toxin, near 100% of granular neurons were sensitive to the leucotoxin HIgC/HIgB. However, under similar conditions, 20 nM leucotoxin HIgA/HIgB was necessary to activate 40% of granular neurons and 2 nM leucocidin LukS-PV/LukF-PV modified $[Ca^{2+}]_i$ in less than 20% of neurons.

Intracellular stores Ca^{2+} mobilization

To determine the contribution of intracellular Ca^{2+} stores to the leucotoxin HIgC/HIgB, neurons were incubated in the presence of 1 µM thapsigargin or 0.2 µM bafilomycin to prevent loading of reticular Ca^{2+} stores by SERCA or acidic Ca^{2+} stores by H-ATPase, respectively. In both cases, the activity of leucotoxin (4 nM) was strongly reduced (*Figure 2A*).

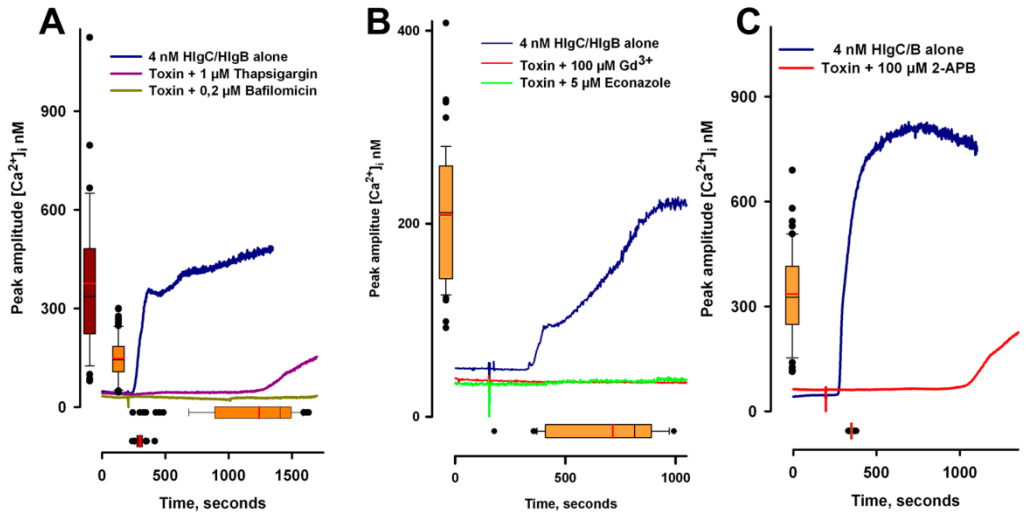

Figure 2. Contribution of intracellular Ca^{2+} stores to the leucotoxin HIgC/HIgB activity and antagonist effect of drugs active on the store operated calcium entry. (**A**) Incubation of neurons with 1 µM thapsigargin before addition of leucotoxin strongly inhibits the $[Ca^{2+}]_i$ changes. Results are presented by a single trace, mean of all records from a same dish, and as box plots that present the median, the percentile and the mean as a *red line*. The box plots gather results from three experiments. (**B**) Blocking effect of Gd^{3+} and econazole and (**C**) of 2-APB; all drugs known to antagonize store operated calcium entry (SOCE). The same representation as in *A* is shown, except for SOCE antagonists where no $[Ca^{2+}]_i$ changes were observed or they were extremely reduced.

Figure 2. *Contribution des réserves calciques intracellulaires à l'activité de la leucotoxine HIgC/HIgB et effet antagoniste des drogues qui agissent sur l'entrée de calcium activée à partir des réserves. (**A**) Les neurones pré-incubés avec 1 µM de thapsigargine donnent des réponses très réduites et dispersées à l'application de leucotoxine. Les résultats sont présentés sous la forme d'un seul tracé qui est la moyenne de ceux des toutes les cellules d'un même enregistrement. Les boites longeant les axes représentent les médianes, les percentiles et les moyennes* (trait rouge) *des valeurs de trois expériences. (**B**) Effet bloquant du Gd^{3+} et de l'éconazole et (**C**) du 2-APB; trois drogues connues pour leurs effets antagonistes de SOCE. Mêmes représentations qu'en* A, *à l'exception des antagonistes SOCE pour lesquels pas ou peu de changements de $[Ca^{2+}]_i$ étaient observés.*

In 7 independent experiments, 56% of the cells incubated with thapsigargin (154 out of 277 cells) showed a leucotoxin induced transient peak of low amplitude. Blockade of the vesicular H-ATPase by 0.2 µM bafilomycin strongly reduced the leucotoxin HlgC/HlgB induced $[Ca^{2+}]_i$ changes. Leucotoxin induced delayed transient increases of $[Ca^{2+}]_i$, that hardly ever reached twice the amplitude of the resting value, in 60% of treated cells. Interestingly, granular neurons are known to keep an active Ca^{2+} entry pathway, independent of VOCCs, which is antagonized by molecules known to operate in SOCE and TRP channels (Pinilla *et al*., 2005). We, therefore, tested whether the leucotoxin effect may be altered by drugs modifying SOCE activity (Bird *et al*., 2008). When 100 µM Gd^{3+} (*Figure 2B*) or 100 µM La^{3+} (not shown) were present in the bath a few minutes before the leucotoxin, its effect was totally blunted. The antagonist econazole (5 µM) completely prevented the toxin-induced rise in $[Ca^{2+}]_i$ (*Figure 2B*). Application before the toxin of 100 µM 2-APB, a cell permeable modulator of Inositol (1,4,5)-P3-induced Ca^{2+} release that targets SOCE, decreased by 40% the average of the peak amplitude (203 ± 56 nM *versus* 335 ± 126 nM) and increased more than 10 times the average of the time latency (1140 ± 159 s *versus* latency 99 ± 8 sec) (*Figure 2C*). Furthermore, cells incubated for 15 min in the presence of 90 µM dantrolene, which blocks ryanodine receptors at 10 µM and Ins(1,4,5)-P3 receptors at 50 µM, showed a reduced amplitude (144 ± 27 nM) and a delayed toxin response (latency 593 ± 176 s) compared to control cells.

When the contribution of extracellular Ca^{2+} to the leucotoxin effect was evaluated, a resting activity of the toxin (i.e. $[Ca^{2+}]_i$ rise) could still be observed in neurons incubated in 3 µM and in 30 µM $[Ca^{2+}]_e$ buffer. But cells bathing in a free Ca^{2+} buffer (0 mM Ca^{2+} - 5 mM EGTA) kept constant the resting $[Ca^{2+}]_i$ for the whole recording period in presence of the toxin. These results suggest that extracellular Ca^{2+} also contributes to the accumulation of cytosolic free Ca^{2+}, which reinforces the SORE hypothesis.

Leucotoxin internalization and interaction with Stim-1

The SOCE complex works through the interaction between the reticular Ca^{2+} sensor stromal interacting molecule (Stim) and the plasma membrane Ca^{2+} channel Orai (Parekh and Putney 2005; Varnai *et al*., 2009; Collins and Meyer 2011). We used specific antibodies targeting Stim-1 to disrupt the equilibrium of SOCE system before challenging the neurons with the leucotoxin. Both the average of the peak amplitude and the response latency were modified when antibodies were added 20 min before the toxin (*Figures 3A* and *B*). The goat polyclonal N-19 antibody was less effective than the mouse monoclonal A-8 antibody, which recognizes the C-terminal region of the molecule.

Simultaneously, we checked for the subcellular location of the leucotoxin HlgC/HlgB tagged with Alexa-488 in HlgB, and the Stim-1 protein using the same antibodies to immune-label the cells. *Figure 4* shows that the toxin localizes in an internal compartment which is also labeled by the anti-Stim antibodies. In this example, the co-localization ratio was of 85% (Pearson's correlation: 0.69). Internalization of the leucotoxin HlgC/HlgB was verified by the labeling of the external leaflet of the plasma membrane with the B subunit of the cholera toxin. An example is given in *Figure 5*, where the co-localization ratio between the two molecules was of 46% (Pearson's correlation: 0.4).

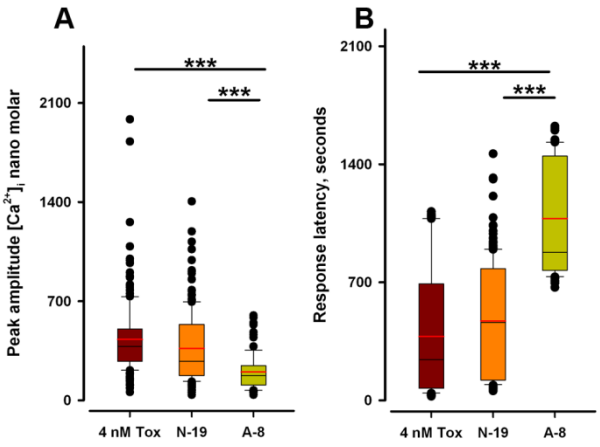

Figure 3. Effect of incubating granular neurons with specific antibodies against the Stim1 molecule prior to the $[Ca^{2+}]_i$ measurements. (**A**) Peak amplitude; (**B**) time latency. The plots, indicating the mean (*red line*), the median (*black line*) and the percentiles, present values from three independent experiments. Control, 190 cells; N-19 antibody, 188 cells; A-8 antibody, 85 cells. The results were statistically significant according to the Kruskal-Wallis test ($P < 0.001$).

Figure 3. *Effet de l'incubation des neurones avec des anticorps anti-Stim1 sur l'augmentation de $[Ca^{2+}]_i$. (**A**) Valeur maximale au pic, (**B**) délai de réponse. Sont représentées les moyennes (*ligne rouge*), les médianes (*ligne noire*) et les percentiles des trois expériences. Contrôle, 190 cellules; anticorps N-19, 188 cellules; anticorps A-8, 85 cellules. Le test de Kruskal-Wallis considère les résultats statistiquement différents ($P < 0.001$).*

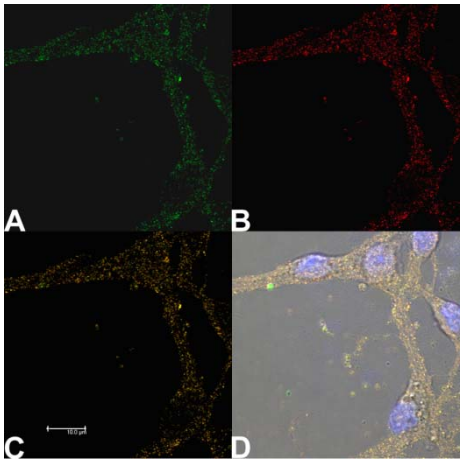

Figure 4. Neurons labelled with leucotoxin HlgC/HlgB-Alexa-488 (*green*) and the anti-Stim1 H-19 antibody (*red*). Images show a 0.3 µm optical section captured with a Leica SP5-II microscope equipped with quantitative co-localization software. Images correspond to pixels labelled with both markers; (**A**) toxin, (**B**) H-19 and (**C**) merge. (**D**) Superimposition of the fluorescence to the Nomarski view of the observed area (nuclei are labelled with Hoechst 33258).

Figure 4. *Neurones marqués avec la leucotoxine HlgC/HlgB-Alexa-488 (*vert*) et l'anticorps anti-Stim1 (*rouge*). Les images montrent une coupe optique de 0.3 µm obtenue à l'aide d'un microscope Leica SP5-II équipé d'un programme pour la quantification des colocalisations. (**A**) Pixels marqués par la toxine, (**B**) par H-19, (**C**) colocalisation. (**D**) Superpositions des vues de fluorescence et Nomarski (les noyaux sont marqués avec du Hoechst 33258).*

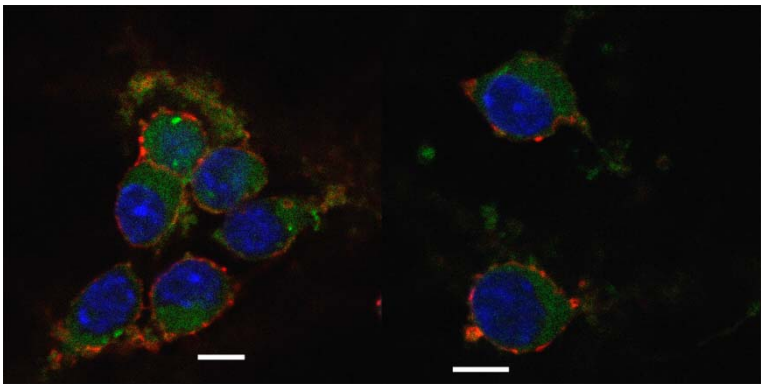

Figure 5. Neurons labelled with leucotoxin HlgC/HlgB-Alexa-488 (*green*), the cholera toxin B subunit-Alexa-594 (*red*) and Hoechst 33258 (*blue*). Images show the merge of the three markers signal acquired independently; an optical section of 0.3 µm is presented. Bars size = 5 µm.

Figure 5. *Neurones marqués avec la leucotoxine HlgC/HlgB-Alexa-488 (*vert*), la sous-unité B de la toxine cholérique couplée à l'Alexa-594 (*rouge*) et du Hoechst 33258 (*bleu*). Les images correspondent à la superposition du signal des trois marqueurs saisis indépendamment; section optique de 0.3 µm. Barres de calibration = 5 µm.*

Conclusion

The results presented here form a first step to evaluate the potential risk that a local or systemic infection of *S. aureus* can be for the nervous system. Leucotoxins mobilize $[Ca^{2+}]_i$ in cerebellar granular neurons while preserving the cellular integrity, independently of the toxin concentration. This Ca^{2+} mobilization was prevented by incubation with drugs targeting the refilling of intracellular Ca^{2+} stores. Moreover, known SOCE inhibitors as 2-APB or dantrolene were effective at high concentrations for blocking the leucotoxin effect. On the other hand, the use of antibodies directed against the proteins involved in SOCE, particularly against the endoplasmic reticulum sensor of Ca^{2+} levels Stim1 (Liou *et al.*, 2005; Roos *et al.*, 2005), inhibited leucotoxin-induced $[Ca^{2+}]_i$ variations and were found in the same internal compartment.

Overall, our results qualify leucotoxins as disruptive agents for the SOCE complex. However, the experimental data presented here are not sufficient to infer that the leucotoxin, after binding to the membrane, activates a signalling pathway that impinges in SOCE. Similarly, we cannot infer that the toxin binds to, or directly acts through Stim1 or ORAI1. A working hypothesis would be that the internalised leucotoxin, by its presence in endosomes carrying Stim1, starts a process which includes the Ca^{2+} release from the endosome and that may be followed by the formation of the Stim1/ORAI1 complex. More work is needed to determine the basis of the initial Ca^{2+} mobilisation.

References

Bird GS, DeHaven WI, *et al*. (2008) Methods for studying store-operated calcium entry. *Methods* **46**: 204-212

Collins SR, Meyer T (2011) Evolutionary origins of STIM1 and STIM2 within ancient Ca^{2+} signaling systems. *Trends Cell Biol* **21**: 202-211

Gonzalez M, Bischofberger M, *et al*. (2008) Bacterial pore-forming toxins: The (w)hole story? *Cell Mol Life Sci* **65**: 493-507

Kaneko J, Kamio Y (2004) Bacterial two-component and hetero-heptameric pore-forming cytolytic toxins: structures, pore-forming mechanism, and organization of the genes. *Biosci Biotechnol Biochem* **68**: 981-1003

Liou J, Kim ML, *et al*. (2005) STIM is a Ca^{2+} sensor essential for Ca^{2+}-store-depletion-triggered Ca^{2+} influx. *Curr Biol* **15**: 1235-1241

Menestrina G, Dalla Serra M, *et al*. (2003) Ion channels and bacterial infection: the case of β-barrel pore-forming protein toxins of *Staphylococcus aureus*. *FEBS Lett* **552**: 54-60

Parekh AB, Putney JW Jr. (2005) Store-operated calcium channels. *Physiol Rev* **85**: 757-810

Pinilla PJG, Hernández AT, *et al*. (2005) Non-stimulated Ca^{2+} leak pathway in cerebellar granule neurones. *Biochem Pharmacol* **70**: 786-793

Roos J, DiGregorio PJ, *et al*. (2005) STIM1, an essential and conserved component of store-operated Ca^{2+} channel function. *J Cell Biol* **169**: 435-445

Varnai P, Hunyady L, *et al*. (2009) STIM and Orai: the long-awaited constituents of store-operated calcium entry. *Trends Pharmacol Sci* **30**: 118-28

Yamashita K, Kawai Y, *et al*. (2011) Crystal structure of the octameric pore of staphylococcal γ-hemolysin reveals the β-barrel pore formation mechanism by two components. *Proc Natl Acad Sci USA* **108**: 17314-17319

Toxines et Transferts ioniques – Toxins and Ion transfers
Rencontres en Toxinologie – Meeting on Toxinology, 2011
Editions de la SFET – SFET Editions
Accès libre en ligne sur le site – Free access on line on the site : http://www.sfet.asso.fr

Atypical profile of paralytic shellfish poisoning toxins in clams from the Gulf of Gabes (Southern Tunisia)

Riadh MARROUCHI[1], Evelyne BENOIT[2], Jean Pierre LECAER[3], Jordi MOLGO[2], Riadh KHARRAT[1*]

[1] *Laboratoire des Toxines Alimentaires, Institut Pasteur de Tunis, 13 Place Pasteur, B.P. 74, 1002 Tunis-Belvédère, Tunisie ;* [2] *CNRS, Institut de Neurobiologie Alfred Fessard - FRC2118, Laboratoire de Neurobiologie et Développement – UPR3294, 1 avenue de la Terrasse, F-91198 Gif sur Yvette cedex, France ;* [3] *CNRS, Institut de Chimie des Substances Naturelles, 1 avenue de la Terrasse, F-91198 Gif sur Yvette cedex, France*

* *Corresponding author ; Tel : +21671842609 ; Fax : +21671842755 ; E-mail : riadh.kharrat@pasteur.rns.tn*

Abstract

*Currently, there are at least 28 known paralytic shellfish toxin derivatives classified into four groups based on their chemical structure. Since 2006, many samples collected from the Gulf of Gabes (Southern Tunisia) were tested positive using the mouse bioassay (MBA) despite the absence of gymnodimines, the only family of marine biotoxins detected in Tunisian shellfish. This paper reports the analyses of toxic clams (*Ruditapes decussatus*) collected along the Gulf of Gabes coasts (Southern Tunisia) during the period 2006-2009. Toxic compounds were detected by liquid chromatography-mass spectrometry (LC–MS) in all clams extracts known to be contaminated according to the MBA. Three molecular ions were identified ($M+H^+$): 431.14 m/z, 453.12 m/z and 469.10 m/z. Toxicity events coincided with the presence of the dinoflagellate* Gymnodinium catenatum*, species associated worldwide with the production of paralytic shellfish poisoning (PSP) toxins. The presence of toxic species,* i.e. G. catenatum*, and detection of PSP-like toxins in clams warn of potential PSP problems in the Gulf of Gabes.*

Détection d'une toxicité atypique chez les palourdes du golfe de Gabes

*La famille des toxines paralysantes renferme actuellement plus de 28 dérivés qui sont classés en quatre groupes en fonction de leur structure chimique. En 2006, plusieurs échantillons de palourdes (*Ruditapes decussatus*) collectées dans le golfe de Gabès ont été testés positifs par le test biologique sur souris, malgré l'absence de gymnodimines qui sont depuis longtemps connues pour être responsables de la contamination des palourdes du golfe de Gabès. L'analyse par chromatographie liquide–spectrométrie de masse (LC-MS) des fractions toxiques a permis d'identifier trois composés de masse moléculaire ($M+H^+$): 431.14 m/z, 453.12 m/z et 469.10 m/z. Les épisodes de toxicité coïncidaient avec la présence du dinoflagellé* Gymnodinium catenatum*, espèce connue pour produire des phycotoxines ayant un effet paralysant. En conclusion, la détection de composés toxiques (toxines ayant un effet paralysant) ayant des masses moléculaires non habituelles et l'apparition du dinoflagellé* G. catenatum *dans le milieu constituent des indices pour des problèmes potentiels de contamination des palourdes du golfe de Gabès par des phycotoxines paralysantes.*

Keywords : Gymnodinium catenatum*, liquid chromatography-mass spectrometry, mouse bioassay, paralytic shellfish toxins.*

Introduction

Toxins associated with Paralytic Shellfish Poisoning (PSP) are among the most acutely toxic substances known (Asp *et al.*, 2004). Currently, there are at least 28 known PSP toxin derivatives (Llewellyn, 2006). They can be classified into four groups based on their chemical structure as follows: saxitoxins (saxixotoxin: STX, decarbamoyl saxitoxin: dcSTX, neosaxitoxin: neoSTX, decarbamoyl neosaxitoxin: dcneoSTX, and nonsulfated STX), gonyautoxins (GTX1 to 6, dcGTX1 to 4, and single-sulfated GTX), C-toxins (C1 to 4, doubly sulfated C-toxins), and other variants identified in *Lyngbya wollei* (LWTX1 to 6) (Clemente *et al.*, 2010).

PSP toxins are synthesized by several *Alexandrium* species (Schantz *et al.*, 1966), *Gymnodinium catenatum* (Oshima *et al.*, 1987), *Pyrodinium bahamense* (Harada *et al.*, 1982) and freshwater cyanobacteria (Garcia *et al.*, 2010; Araoz *et al.*, 2010).

STX, a carbamate toxin, is generally considered the most potent. Other highly potent carbamate toxins include neoSTX and GTX1 to 4 while the N-sulphocarbamoyl (C) toxins are generally considered to be less potent (Turrell *et al.*, 2007). STX and derivatives are potent marine neurotoxins which block voltage-dependent

sodium channels in excitable cells (Long *et al.*, 1990). Consumption of shellfish contaminated by PSP toxins causes paresthesia, astenia, distonia, ataxia, dyspnea, hypotension, tachycardia, vomiting, skeletal muscle paralysis (Garcia *et al.*, 2010) and death, which can occur in severe cases when respiratory assistance is delayed or absent.

Officially, the traditional mouse bioassay (MBA; AOAC, 1990) has been the only method adapted for the detection of PSP toxins in bivalves. Recently, pre-column oxidation high-performance liquid chromatography (HPLC) technique was approved and has been validated for monitoring STX, neoSTX, GTX2 and GTX3 together, GTX1 and GTX4 together, dcSTX, GTX5, C1 and C2 together, and C3 and C4 together, in mussels, clams, oysters and scallops (Etheridge, 2010).

In 1994, clams collected from Boughrara lagoon (Gulf of Gabes, Southern Tunisia) were tested positive using the MBA. Further investigations revealed that gymnodimine-A was responsible for the toxicity of Tunisian clams (Biré *et al.*, 2002). The causative dinoflagellate was later identified as *Karenia cf. selliformis* (Drira *et al.*, 2008). Bivalve mollusks are monitored for PSP toxins regularly since 1998, covering the entire coast. Currently, the official regulatory method for monitoring PSP toxins in shellfish remains the AOAC International MBA (AOAC, 1990).

In 2006, many samples collected from the same area were tested positive despite the absence of gymnodimines. This paper reports on the analyses of toxic clams (*Ruditapes decussatus*) collected along the Gulf of Gabes coasts (Southern Tunisia) during the period 2006-2009 in which there was a bloom of *G. catenatum*.

Materials and methods

Materials

Samples of clams (*Ruditapes decussatus*) were collected weekly from the Gulf of Gabes between September 2006 and December 2009. Sampling was carried out and controlled by the "Commissariat Régional au Développement Agricole de Médnine" (CRDA, Southern Tunisia). Samples were kept at +4°C until analyzed. Acetonitrile, diethyl ether and dichloromethane (DCM) were purchased from Panreac Quimica SA (Spain), acetone from Carlo Erba reagents (France), trifluoroacetic acid (TFA) and Tween 60 from Sigma-Aldrich (Ireland).

Toxicity assays

Toxicity analyses were carried out using the MBA according to the AOAC method (1990) for PSP toxin monitoring. Briefly, 100 g of homogenized tissues were mixed with 100 ml of 0.1M HCl and the extract was boiled for 5 min. After cooling, the pH was adjusted to 2-3 by 5 M HCl or 0.1 M NaOH. Then, the mixture was transferred to a graduated cylinder, diluted to 200 ml by distilled water and centrifuged at 3000 g for 15 min. The supernatant (1 ml) was injected intraperitoneally (i.p.) into three 20 g male adult Swiss-Webster mice. The mice were observed for 24 h, and signs of illness and death times were recorded. The values are expressed in µg STX eq/100 g meat.

The MBA based on the protocol of Yasumoto *et al.* (1978) was used to detect Diarrhoeic Shellfish Poisoning (DSP) toxins. Briefly, 20 g of digestive glands were extracted three times with acetone. Each extract was evaporated to dryness, suspended in 4 ml of 1% Tween-60 saline and injected i.p. into male adult Swiss-Webster mice (20 g, three mice). The mice were observed for 24 h, and signs of illness and death times were recorded. Control mice were injected i.p. with only 4 ml of 1% Tween-60 saline (three mice receiving 1 ml/mice).

Samples extraction and solvent partition

Samples shown to be positive according to the MBA were further studied. Extraction was performed using methods previously published (Kharrat *et al.*, 2008; Marrouchi *et al.*, 2009). Briefly, 20 g of meat were minced and extracted three times, with 50 ml acetone each time, using a screw mixer. The combined acetone extract was filtered and evaporated in a rotary evaporator with a temperature-controlled bath. The residual aqueous layer was defatted with diethyl ether (1:1) and extracted with dichloromethane (1:1) three times. Aqueous, diethyl ether and dichloromethane layers were evaporated to dryness and suspended in 1 ml of MilliQ water to be used for toxicity assays and chromatographic analysis.

Chromatographic analysis

Following liquid/liquid extraction, the water-soluble extract, which possessed the entire toxic activity, was analyzed by a reversed-phase HPLC C18 symmetry column (4.6 x 250 mm, 5 µm, Waters). Elution was done with a mobile phase composed of a gradient of solvent A (aqueous phase: Milli-Q water + 0.1% TFA) and solvent B (organic phase: acetonitrile + 0.1% TFA), whose proportions were controlled by a programmable pump system. A linear gradient from 10-90% B was run between 2 and 35 min. Temperature was fixed to 25°C, and the run lasted for 35 min. Series of fractions were hand-collected, lyophilized, and tested for activity. The active fraction was further purified using analytical reversed-phase HPLC C18 symmetry column, under the same conditions as reported above. Individual fractions were collected, lyophilized, and stored at -20°C until use.

HPLC-ESI-LC analysis

The HPLC equipment was formed by a binary system U3000 Dionex. Samples were carried out with manual injector with a 25 µl sample loop .The column used was a Zorbax SB-C18 (1 mm, 15 mm, 3 µm). The products were eluted using a linear gradient between 5 and 50% of acetonitrile in 40 min, and then with an increase

gradient to 100% on 5 min. This system was coupled to a mass spectrometer (MS) LTQ-ORBITRAP instrument from THERMO Fisher (Bremen, Germany) equipped with an electrospray (ESI) source. The injection volume was 25 µl. The mobile phase for analysis was solvent A (water + 0.1% formic acid) and solvent B (acetonitrile + 0.09% formic acid).

Mass measurement was done in positive mode using the ORBITRAP set to a resolution of 6000 at m/z 400 Da. The automatic gain control was fixed to a target of 5.106. The scan was set between m/z 200 and 1700. Data were analyzed using the Xcalibur software from Thermo Instrument Systems Inc.

Results and Discussion

No mortality was recorded on mice injected with clams extracts using the AOAC (1990) MBA method. However, toxicity was observed in all the mice injected with extracts using MBA based on the protocol of Yasumoto *et al.* (1978). Mice injected with diethyl ether or dichloromethane layers, as well as those injected with only Tween-60 saline, showed neither mortality nor signs of toxicity up to 24 h, whereas an acute toxicity was observed in all mice injected (i.p. or intracerebroventricularly) with the crude water soluble extract for all samples tested positive for DSP toxins. Common mouse toxic symptoms included paralysis of hind legs followed by rapid death (*i.e.* within 5 min after injection of high amounts of water soluble toxic extract).

The bio-guided chromatographic fractionation of the water soluble toxic extract was used to identify the peak corresponding to the elution of toxic compounds. As shown in *Figure 1*, toxicity was concentrated exclusively in a peak eluated at 8.18 min. Toxic peaks were traced by MS (*Figure 2*), and three molecular ion were detected ($M+H^+$): 431.14 m/z, 453.12 m/z and 469.10 m/z. Toxic compounds were detected by LC–MS in all clams extracts shown to be contaminated using the MBA.

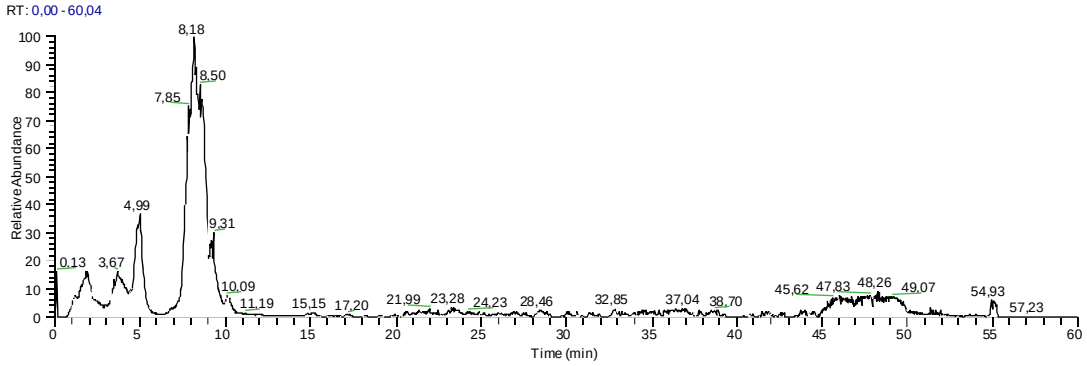

Figure 1. Chromatogram of toxic fraction eluated at 8.18 min and purified from water soluble toxic extract.

Figure 1. *Chromatogramme de la fraction toxique éluée à 8,18 min et purifiée à partir de l'extrait aqueux toxique.*

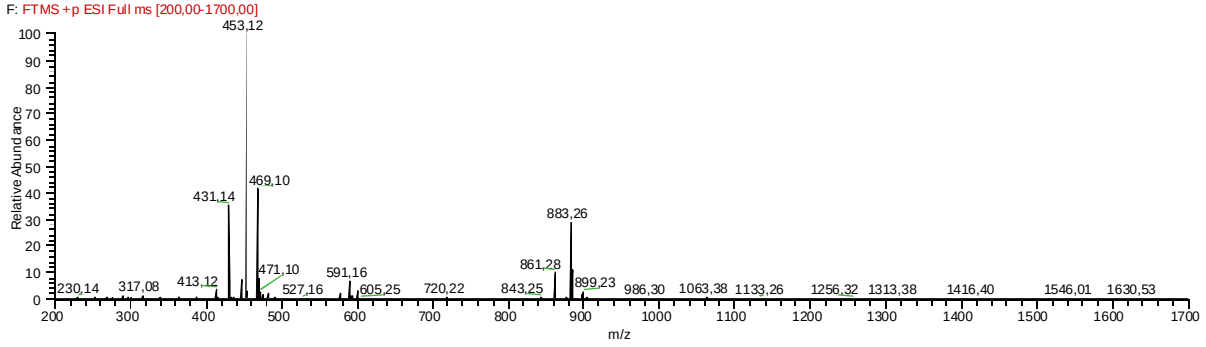

Figure 2. Base peak LC–MS chromatogram (m/z 200–1700) extracted from LC–MS analyses of the fraction eluated at 8.18 min.

Figure 2. *Chromatogramme LC-MS du pic de base (m/z 200–1700) extrait des analyses LC-MS de la fraction éluée à 8,18 min.*

It should be noted that episodes of toxicity coincided with the presence of *G. catenatum*, species associated worldwide with the production of PSP toxins (Oshima *et al.*, 1987; Vale, 2010) on Tunisian coasts of the Gulf of Gabes (Dammak-Zouari *et al.*, 2009). This species proliferates episodically in summer and autumn and resides in the central zone of the Gulf of Gabes (Dammak-Zouari *et al.*, 2009).

Recently, several hydrophobic hydroxybenzoate analogues have been found. Apparently, their production is related to *G. catenatum* (Negri *et al.*, 2003; Vale, 2008) although this species is known to produce hydrophilic analogues (Negri *et al.*, 2007).

In the Mediterranean coasts, episodes of contamination by PSP toxins were recorded in Morocco, and the toxicity in shellfish has been associated with *G. catenatum* (Taleb *et al.*, 2001). The same phenomenon was observed after blooms of *Alexandrium minitum* in Italy (Honsell *et al.*, 1996) and *A. catenella* in Spain (Vila *et al.*, 2001).

The presence of toxic species, *G. catenatum*, and detection of PSP-like toxins in clams warn of potential PSP problems in the Gulf of Gabes. We have to be vigilant of the population of the toxic species on the coasts and the levels of these toxins in shellfish. We must remember that clams harvesting [production reaches 500 tones during the last five years (FAO, 2011)] have considerable importance for the national economy since this sector generates 6000 jobs and provides considerable revenue currency (7 million Euros per year; Hamza, 2003).

Conclusion

In this paper, we report that clams collected in coastal water of the Gulf of Gabes contain some PSP toxins-like, although in very small amounts. To our knowledge, this is the first report of PSP toxins in shellfish from the Gulf of Gabes where DSP occurs more frequently. More investigations are needed to elucidate the structure of these new toxic compounds and to adapt appropriate tests for their monitoring.

Acknowledgements. *This work was performed in the context of cooperation between French CNRS and Tunisian Pasteur Institute.*

References

AOAC (1990) Paralytic shellfish poison, biological method, final action. In *Official Methods of Analysis*. AOAC (ed) 15th Ed, Method no 959.08. Arlington, VA

Aráoz R, Molgó J, Tandeau de Marsac N (2010) Neurotoxic cyanobacterial toxins. *Toxicon* **56**: 813-828

Asp TN, Larsen S, Aune T (2004) Analysis of PSP toxins in Norwegian mussels by a post-column derivatization HPLC method. *Toxicon* **43**: 319-327

Biré R, Krys S, Fremy JM, Dragacci S, Stirling D, Kharrat R (2002) First evidence on occurrence of gymnodimine in clams from Tunisia. *J Nat Toxins* **11**: 269-275

Clemente Z, Busato RH, Ribeiro CAO, Cestari MM, Ramsdorf WA, Magalhaes VF, Wosiack AC, Silva de Assis HC (2010) Analyses of paralytic shellfish toxins and biomarkers in a southern Brazilian reservoir. *Toxicon* **55**: 396-406

Dammak-Zouari H, Hamza A, Bouain A (2009) Gymnodiniales in the Gulf of Gabes (Tunisia). *Cah Biol Mar* **50**: 153-170

Drira Z, Hamza A, Belhassen M, Ayadi H, Bouaïn A, Aleya L (2008) Dynamics of dinoflagellates and environmental factors during the summer in the Gulf of Gabes (Tunisia, Eastern Mediterranean Sea). *Scientia Marina* **72**: 59-71

Etheridge SM (2010) Paralytic shellfish poisoning: sea food safety and human health perspectives. *Toxicon* **56**: 108-122

Garcia C, Barriga A, Diaz JC, Lagos M, Lagos N (2010) Route of metabolization and detoxication of paralytic shellfish toxins in humans. *Toxicon* **55**: 135-144

FAO (2011) http://www.fao.org/news/story/fr/item/73856/icode/

Hamza A (2003) Le statut du phytoplancton dans le Golfe de Gabes. Thèse de doctorat en Sciences Biologiques. Université de Sfax. 298 pp

Harada T, Oshima Y, Kamiya K, Yasumoto T (1982) Confirmation of paralytic shellfish toxins in the dinoflagellate *Pyrodinium bahamense var. compressa* and bivalves in Palau. *Bull Jpn Soc Sci Fish* **48**: 821-825

Honsell G, Poletti R, Pompei M, Sidari L, Milandri A, Casadei C, Viviani R (1996) *Alexandrium minutum Halim* and PSP contamination in the northern Adriatic Sea (Mediterranean Sea). In *Harmful and Toxic Algal Blooms*. Yasumoto T, Oshima Y, Fukuyo Y (eds) pp 77-80. Intergovernmental Oceanographic Commission, UNESCO

Llewellyn LE (2006) Saxitoxin, a toxic marine natural product that targets a multitude of receptors. *Nat Prod Rep* **23**: 200-222

Long RR, Sargent JC, Hammer K (1990) Paralytic shellfish poisoning: a case report and serial electrophysiologic observations. *Neurology* **40**: 1310-1311

Negri A, Stirling D, Quilliam M, Blackburn S, Bolch C, Burton I, Eaglesham G, Thomas K, Walter J, Willis R (2003) Three novel hydroxybenzoate saxitoxin analogues isolated from the dinoflagellate *Gymnodinium catenatum*. *Chem Res Toxicol* **16**: 1029-1033

Negri A.P, Bolch CJS, Geier S, Green DH, Park TG, Blackburn SI (2007) Widespread presence of hydrophobic paralytic shellfish toxins in *Gymnodinium catenatum*. *Harmful Algae* **6**: 774-780

Oshima Y, Hasegawa M, Yasumoto T, Hallegraeff G, Blackburn S (1987) Dinoflagellate *Gymnodinium catenatum* as the source of paralytic shellfish toxins in Tasmanian shellfish. *Toxicon* **25**: 1105-1111

Schantz EJ, Lynch JM, Vayada G, Masumoto K, Rapoport H (1966) The purification and characterization of the poison produced by Gonyaulax catenella in axenic culture. *Biochemistry* **5**: 1191-1195

Taleb H, Vale P, Jaime E, Blaghen M (2001) Study of paralytic shellfish poisoning toxin profile in shellfish from the Mediterranean shore of Morocco. *Toxicon* **39**: 1855-1861

Turrell EA, Lacaze JP, Stobo L (2007) Determination of paralytic shellfish poisoning (PSP) toxins in UK shellfish. *Harmful Algae* **6**: 438-448

Vale P (2008) Complex profile of hydrophobic paralytic shellfish poisoning compounds in *Gymnodinium catenatum* detected by liquid chromatography with fluorescence and mass spectrometry detection. *J Chromatogr A* **1195**: 85-93

Vale P (2010) Metabolites of saxitoxin analogues in bivalves contaminated by *Gymnodinium catenatum*. *Toxicon* **55**: 162-165

Vila M, Delgado M, Camp J (2001) First detection of widespread toxic events caused by *Alexandrium catenella* in the Mediterranean Sea. In *Harmful Algal Blooms 2000*, Proc 9th Int Conf Harmful Algal Blooms. Hallegraeff GM, Blackburn SI, Bolch CJ, Lewis RJ (eds). IOC, Paris

Yasumoto T, Oshima Y, Yamaguchi M (1978) Occurrence of a new type shellfish poisoning in the Tohoku district. *Bull Jap Soc Sci Fish* **44**:1249-1255

Toxines et Transferts ioniques – Toxins and Ion transfers
Rencontres en Toxinologie – Meeting on Toxinology, 2011
Editions de la SFET – SFET Editions
Accès libre en ligne sur le site – Free access on line on the site : http://www.sfet.asso.fr

Etude toxico-cinétique et biologique du venin de scorpion Androctonus mauretanicus *chez le lapin*

Fatima CHGOURY[1*], Naoual OUKKACHE[1], Nadia EL GNAOUI[2], Hakima BENOMAR[2], Rachid SAÏLE[3], Noreddine GHALIM[1]

[1] Laboratoire des Venins et Toxines, Institut Pasteur du Maroc, Casablanca, Maroc ; [2] Laboratoire Anatomi-pathologie, Institut Pasteur du Maroc, Casablanca, Maroc ; [3] Unité Associée au CNRST-URAC34- Université Hassan II, Faculté des Sciences Ben M´sik, Casablanca, Maroc

** Corresponding author ; Tel : (212) 06 62 47 27 95 ; Fax : (212) 05 22 26 09 57 ;*
E-mail : fchgoury@gmail.com

Résumé

Les toxines des venins de scorpions sont responsables de la quasi-totalité des symptômes et des désordres biologiques observées après envenimation scorpionique accidentelle ou expérimentale. L'immunothérapie reste la seule thérapie efficace contre ce fléau. Pour améliorer les conditions d'utilisation de l'anti-venin, une première envenimation expérimentale par le venin de scorpion Androctonus mauretanicus *(*Am*) a été réalisée chez des lapins pour évaluer les paramètres toxico-cinétiques de ce venin : volumes totaux de distribution (Vd_{ss} et Vd_{β}), clairance totale (Cl_T) et demi-vie terminale ($t_{1/2\beta}$). Une deuxième envenimation expérimentale par ce venin a été faite chez des lapins pour étudier les variations des marqueurs biochimiques : glucose, urée, créatinine, transaminases (AST et ALT), CPK et LDH au niveau sanguin. Après administration du venin (24 h), les animaux témoins et envenimés ont été sacrifiés et leurs organes ont été prélevés pour réaliser une étude histologique sur les parenchymes cardio-pulmonaires, hépatiques et rénaux. L'étude toxico-cinétique du venin* Am *a montré que ce dernier se distribue rapidement du compartiment vers les tissus. Les résultats de l'étude physiopathologique ont montré une augmentation significative des paramètres biochimiques étudiés. Cette augmentation s'explique par l'observation d'importantes lésions tissulaires (œdèmes, foyers hémorragiques, infiltration des cellules inflammatoires, …).*

Biological and toxicokinetics study of Androctonus mauretanicus *scorpion venom in rabbit*

The toxins of scorpion venom are responsible for the majority of the symptoms and biological disorders observed after accidental or experimental scorpion envenomation. Immunotherapy is the only specific and effective treatment against scorpion's stings. To improve the use of anti-venom, a first experimental study with Androctonus mauretanicus *(*Am*) scorpion venom was conducted in rabbits. We have evaluated the venom toxicokinetics parameters: total volume of distribution (Vd_{ss} and Vd_{β}), total clearance (Cl_T) and terminal half-life ($t_{1/2\beta}$). A second experimental envenomation with this venom was made in rabbits to study changes in biochemical markers: glucose, urea, transaminases (AST and ALT), CPK and LDH in blood. After administration of venom (24 hr), control and envenomed animals were sacrificed and their organs were taken to study the effect of* Am *venom on histological structures on heart, lungs, liver and kidneys. The results revealed that the venom was rapidly distributed from blood to tissues. Biochemical analysis showed a significant increase in all parameters translating a serious damage tissue. The histological study of organs showed disruption and tissue alterations caused by* Am *venom, expressed especially by foci hemorrhagic, edema, infiltration of inflammatory cells, ….*

Keywords : Androctonus mauretanicus *scorpion venom, pathophysiology, toxicokinetics.*

Introduction

Au Maroc, comme dans de nombreux pays tropicaux et sub-tropicaux, les envenimations par piqûres de scorpions constituent un réel problème de santé publique rencontré surtout durant la saison estivale. Le scorpion *Androctonus mauretanicus* est le plus incriminé dans de nombreux cas d'envenimations graves et souvent mortelles surtout chez les enfants (Ghalim et *al*., 2000, El Hafny et Ghalim, 2002). Selon les données épidémiologiques, les envenimations scorpioniques représentent 30 à 50% de l'ensemble des intoxications reçues dans les structures sanitaires avec un taux d'incidence pouvant atteindre 8,2 ‰ de la population à risque (Soulaymani-Bencheikh et *al*., 2004). Les venins de scorpions sont riches en toxines létales douées d'actions physiopathologiques importantes induisant des dysfonctionnements multifactoriels touchant la quasi-

totalité des systèmes vitaux chez l'homme dont le pronostic vital peut être engagé (Adi-bessalem et *al*., 2008, Oukkache et *al*, 2009). La sévérité de l'envenimation scorpionique nécessite des traitements spécifiques et symptomatiques associés et précoces (Ismail., 1995). L'amélioration de la prise en charge des patients envenimés nécessite une meilleure connaissance du mécanisme d'action du venin sur les différentes fonctions vitales pour pouvoir établir un schéma thérapeutique plus spécifique et plus efficace.

Première étude : Etude toxico-cinétique du venin de scorpion *Am*

Deux groupes de lapins albinos (2,8 - 3 kg) ont été utilisés dans cette étude. Le premier groupe constitué de quatre lapins, a reçu une dose sub-létale du venin (100 µg/kg) par voie sous cutanée (s.c.). Le deuxième groupe, constitué aussi de quatre lapins, a reçu une dose sub-létale du venin (100 µg/kg) par voie intraveineuse (i.v.). Des prélèvements sanguins sur les huit lapins ont été effectués sur tubes secs avant envenimation et 5, 15, 30, 60, 120, 180, 240, 300, 360 min après administration du venin. Les concentrations sériques du venin circulant ont été déterminées par ELISA. Les paramètres toxico-cinétiques [volumes totaux de distribution (Vd_{ss} et Vd_{β}), clairance totale (Cl_T) et demi-vie terminale ($t_{1/2\beta}$)] ont été évalués en utilisant le logiciel Kinetica (InnaPhase, France).

Deuxième étude : Etude biochimique et histologique après envenimation par le venin *Am*

Deux autres lots de lapins albinos (2,8 - 3 kg) ont été soumis à une envenimation expérimentale par une une autre dose sub-létale (617,5 µg/kg) d'un autre lot de venin de scorpion *Am*. Les prélèvements sanguins ont été réalisés entre 0 min et 1440 min. Le dosage sérique des paramètres biochimiques (glycémie, urée, créatinine, transaminases, LDH et CPK) a été effectué selon les recommandations de l'automate KODAK VITROS Chemistry (Ortho Clinical Diagnostics, USA). Après envenimation (24 h), les organes des animaux (témoins et envenimés) ont été prélevés pour la réalisation des coupes histologiques (7 µm), colorés à l'hématéine-éosine pour l'examen microscopique.

Expression des résultats

Les résultats des paramètres biochimiques ont été traités statistiquement par le test ANOVA, ils sont présentés sous la forme de moyenne de 4 essais ± écart-type. Les valeurs de *p* inférieures à 0,05 sont considérées significatives.

L'étude toxico-cinétique a montré que le venin de scorpion *Am* se distribue rapidement du compartiment sanguin vers les tissus (*Figures 1 et 2*). La concentration maximale du venin a été détectée 5 min après injection du venin par voie s.c. (T_{max} = 0,5 h). La demi-vie terminale est de 2,8 h, valeur proche de celle obtenue après injection i.v. (3,2 h). Les volumes de distribution sont compris entre 317 et 380 ml/kg. La clairance corporelle est de l'ordre de 82 ml/kg/h (*Tableau 1*).

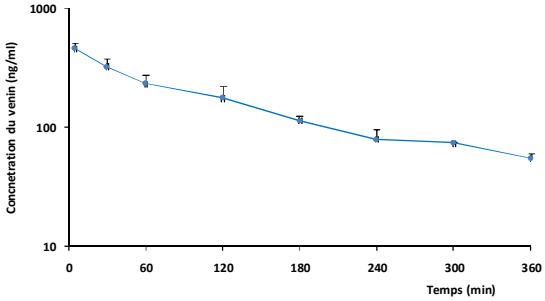

Figure 1. Cinétique du venin de scorpion *Androctonus mauretanicus* par voie intraveineuse (au temps zéro) chez le lapin. Concentration du venin exprimée en ng/ml, échelle semi-logarithme.

Figure 1. *Kinetics of* Androctonus mauretanicus *venom intravenously (at time zero) in rabbit. Concentration of venom expressed in ng/ml, semi-logarithmic scale.*

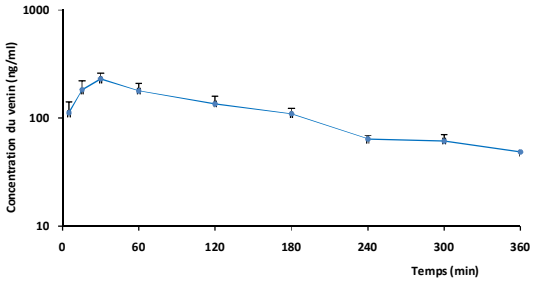

Figure 2. Cinétique du venin de scorpion *Androctonus mauretanicus* par voie sous cutanée (au temps zéro) chez le lapin. Concentration du venin exprimée en ng/ml, échelle semi-logarithme.

Figure 2. *Kinetics of* Androctonus mauretanicus *venom subcutaneously (at time zero) in rabbit. Concentration of venom expressed in ng/ml, semi-logarithmic scale*.

Tableau 1. Paramètres toxico-cinétiques du venin de scorpion *Androctonus mauretanicus*.

Table 1. *Toxico-kinetics parameters of* Androctonus mauretanicus *scorpion venom.*

Voie d'administration	C_{max} (µg/ml)	Tmax (h)	$t_{1/2\beta}$ (h)	Vd_{β} (ml/kg)	Vd_{ss} (ml/kg)	Cl_T (ml/kg/h)
Intraveineuse	-	-	3,2 ± 0,2	379,88 ± 32,87	316,77 ± 39,79	82,32 ± 1,54
Sous-cutanée	0,240 ± 0,037	0,5 ± 0,0	2,8 ± 1,1	562,74 ± 162,97	688,20 ± 98,58	143,42 ± 16,50

Les résultats de l'analyse biochimique ont montré une augmentation significative des marqueurs biochimiques étudiés (glucose, urée, créatinine, transaminases, LDH et CPK). Nous avons noté le taux maximal de glucose sanguin 90 min après injection du venin (*Figure 3*). Les concentrations sanguines maximales de

l'urée et de la créatinine sanguines ont été observées 15 min après envenimation (*Figures 4 et 5*). Les concentrations sériques optimales en transaminases AST et ALT ont été enregistrées respectivement en 90 min et 120 min (*Figure 6*). Les concentrations sanguines maximales en LDH et CPK ont été détectées 90 min après l'administration du venin *Am* (*Figure 7*).

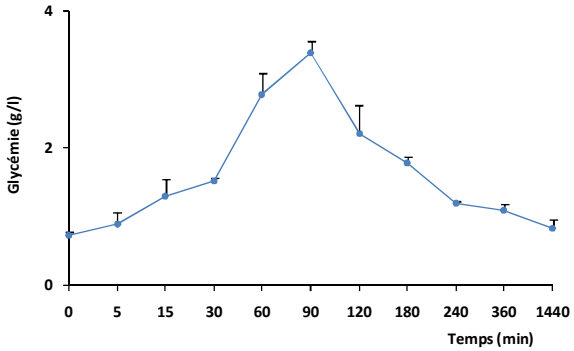

Figure 3. Variation de la glycémie après envenimation expérimentale (au temps zéro) chez le lapin.

Figure 3. *Variation in glycemia after experimental scorpion envenomation (at time zero) in rabbit.*

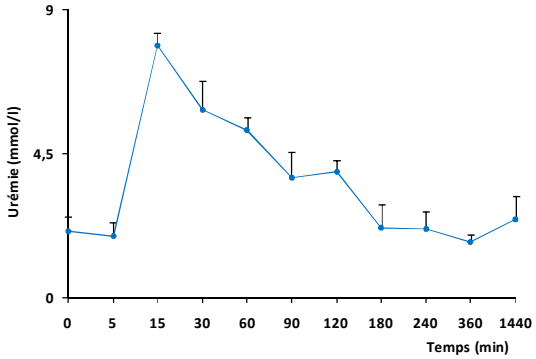

Figure 4. Variation de l'urée après envenimation expérimentale (au temps zéro) chez le lapin.

Figure 4. *Variation in uremia after experimental scorpion envenomation (at time zero) in rabbit.*

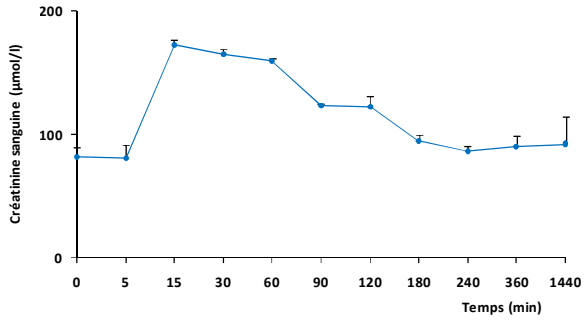

Figure 5. Variation de la créatinine sanguine après envenimation scorpionique expérimentale (au temps zéro) chez le lapin.

Figure 5. *Variation in serum creatinine after experimental* scorpion envenomation *(at time zero) in rabbit.*

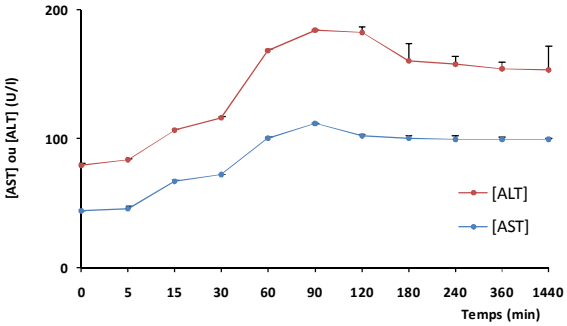

Figure 6. Variation des AST et ALT sériques après envenimation scorpionique expérimentale (au temps zéro) chez le lapin.

Figure 6. *Variation in serum AST and ALT after* experimental *scorpion envenomation (at time zero) in rabbit.*

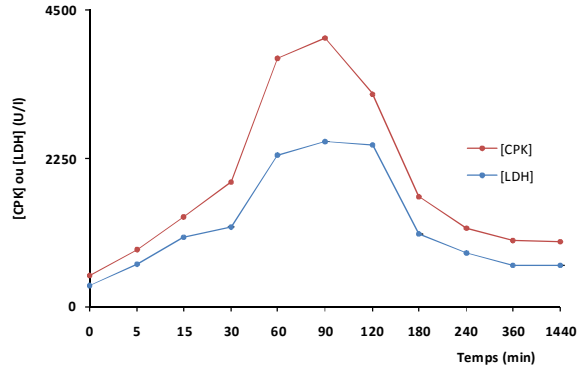

Figure 7. Variation des LDH et CPK sériques après envenimation scorpionique expérimentale (au temps zéro) chez le lapin.

Figure 7. *Variation in serum LDH and CPK after experimental scorpion envenomation (at time zero) in rabbit.*

Des altérations sévères au niveau de la structure du parenchyme des différents tissus examinés 24 heures après envenimation des lapins par le venin d'*Am* ont été observées sur des coupes histologiques (*Tableau 2*). Au niveau du myocarde, le venin a provoqué des dégénérescences des myofibrilles, des hémorragies avec une infiltration des cellules inflammatoires. Au niveau du parenchyme pulmonaire, on a noté une rupture des cloisons inter-alvéolaires, un élargissement des parois alvéolaires, une importante infiltration de cellules inflammatoires et la présence d'œdème avec des foyers de congestion et de suffusion hémorragiques. Au niveau hépatique, des hémorragies interstitielles, des dilatations des sinusoïdes et une infiltration des cellules inflammatoires ont été observées. Les lésions élémentaires des hépatocytes sont prédominantes avec turgescence et nécrose hépatocytaire. Les noyaux de certaines cellules sont pycnotiques, d'autres sont en état

de caryolyse ou nécrose. Au niveau rénal, les effets du venin *Am* ont provoqué des hémorragies, une dégénérescence ou lésion de l'épithélium tubulaire au niveau de la médullaire. An niveau de la zone corticale, une dilatation de la lumière des tubules et une désorganisation de glomérules avec destruction de la capsule de Bowman.

Tableau 2. Lésions tissulaires engendrées 24 h après envenimation scorpionique expérimentale chez le lapin (grossissement x40).
Table 2. *Tissue damage 24 hr after experimental scorpion envenomation in rabbit (magnification x40).*

	Cœur (Heart)	**Poumon (Lung)**	**Foie (Liver)**	**Rein (Kidney)**
Témoin (Control)	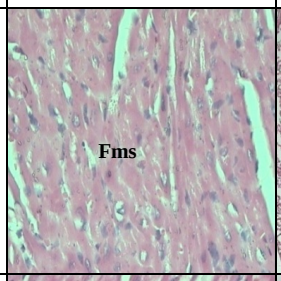	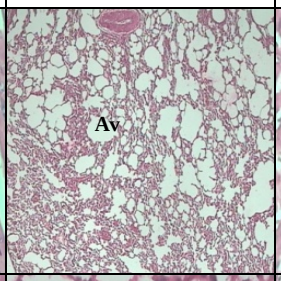	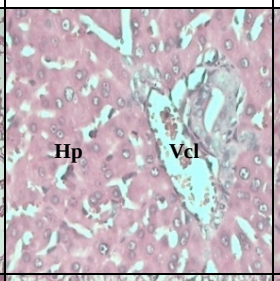	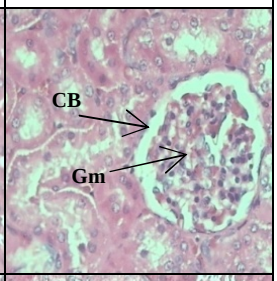
Envenimé (Envenomed)	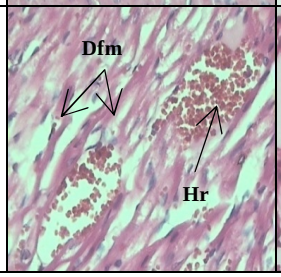	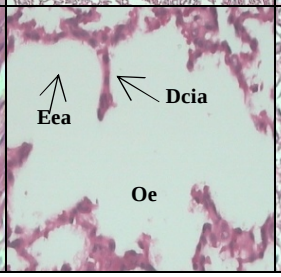	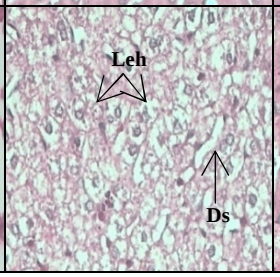	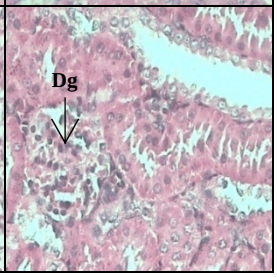

Fms : Fibres musculaires striées (*Striated muscle fibers*), Dfm : Dégénérescence des myofibrilles (*Degeneration of myofibrils*), Hr : Hémorragie (*Hemorrhage*). Av : Alvéole (*Alveolus*), Dcia : Dilatation des cloisons interalvéolaires (*Expansion of interalveolar walls*), Eea : Elargissement des espaces alvéolaires (*Extension of alveolar spaces*), Oe : Œdème (*Edema*). Hp : Hépatocyte (*Hepatocyte*), Vcl : Veine centrolobulaire (*Central vein*), Leh : Lésion élémentaire hépatocytaire (*Elementary lesion hepatocyte*), Ds : Dilatation des sinusoides (*Dilatation of sinusoids*). Gm : Glomérule (*Glomerulus*), CB : Capsule de Bowman (*Bowman's capsule*), Dg : destruction glomérulaire (*Glomerular destruction*).

Conclusion

Le venin de scorpion *Am* est caractérisé par une diffusion rapide dans l'organisme. Il est doué d'un pouvoir toxique élevé qui est responsable de nombreuses perturbations métaboliques accompagnées d'importantes désorganisations tissulaires.

Références

Adi-bessalem S, Hammoudi-triki D, Laraba-djebari F (2008) Pathophysiological effects of *Androctonus australis hector* scorpion venom tissue damages and inflammatory response. *Exp Toxicol Pathol* **60**: 373-380

El Hafny B, Ghalim N (2002) Evolution clinique et taux circulant du venin dans les envenimations scorpioniques au Maroc. *Bull Soc Pathol Exot* **3**: 200-204

Ghalim N, El Hafny B, Sebti F, Jaafar H, Lazar N, Moustanir R, Benslimane H. Scorpion envenomation and serotherapy in Morocco (2000). *Am J Trop Med Hyg* **62**: 277-283

Ismail M (1995) The scorpion envenoming syndrome. *Toxicon* **33**: 825-858

Oukkache N, Malih I, Chgoury F, El Gnaoui N, Saïle R, Benomar H, Hassar M, Ghalim N (2009) Modifications histopathologiques après envenimation scorpionique expérimentale chez la souris. La revue médicopharmaceutique N°53 **5**: 48-52

Soulaymani-Bencheikh R, Semlali I, Ghani A, Badri M, Soulaymani A (2004) Implantation et analyse d'un registre des piqûres de scorpion au Maroc. *Santé publique* **43**: 487-498

Toxines et Transferts ioniques – Toxins and Ion transfers
Rencontres en Toxinologie – Meeting on Toxinology, 2011
Editions de la SFET – SFET Editions
Accès libre en ligne sur le site – Free access on line on the site : http://www.sfet.asso.fr

Ion imbalance, tissue damage and inflammatory response induced by kaliotoxin

Amina LADJEL-MENDIL[1,2], Nesrine SIFI[1,2], Marie-France MARTIN-EAUCLAIRE[3], Fatima LARABA-DJEBARI[1,2*]

[1] *Laboratoire de Biologie Cellulaire et Moléculaire, Faculté des Sciences Biologiques, Université des Sciences et de la Technologie « Houari Boumédienne » (USTHB), El Alia BP 32, 16111 Bab Ezzouar, Alger, Algérie ;* [2] *Laboratoire de Recherche et de Développement sur les Venins, Institut Pasteur d'Algérie, Alger, Algérie;* [3] *CNRS UMR6231, CRN2M, IFR11 Institut Jean Roche, Université de la Méditerranée, Faculté de Médecine secteur Nord, CS80011, Bd Pierre Dramard, F-13344 Marseille cedex 15, France*

** Corresponding author ; Fax : +213 21336077 ; E-mail : flaraba@hotmail.com*

Abstract

The aim of this study is to investigate the ion balance importance in the regulation of various biological processes by using kaliotoxin (specific inhibitor of potassium channels) injected to mice by intracerebroventricular route. Obtained results indicate that the electrolyte dysfunction induced by kaliotoxin is the principal cause of toxic effects. It is responsible for massive neurotransmitter release which could be, in turn, involved in the induced pathologic effects. These effects are characterized by an inflammatory response associated to leukocyte infiltration and an increase of two biomarkers' enzymatic activities (EPO and MPO). Tissue damage correlated with metabolic changes was also observed.

Déséquilibre ionique, altérations tissulaires et réponse inflammatoire induits par la kaliotoxine

L'objectif de cette étude est de montrer l'importance de l'équilibre ionique dans la régulation de différents processus physiologiques en utilisant la kaliotoxine (bloquant spécifique des canaux potassium) injectée à des souris par voie intracérébroventriculaire. Les résultats obtenus montrent que le déséquilibre ionique provoqué par la kaliotoxine est la principale cause des effets toxiques. Il est responsable de la libération massive des neurotransmetteurs qui, a leur tour, sont impliqués dans les effets pathologiques induits. Ces derniers se traduisent par une réponse inflammatoire associée à une infiltration leucocytaire et à une augmentation des activités enzymatiques de deux biomarqueurs (EPO et MPO). Des altérations tissulaires corrélées avec des déséquilibres métaboliques sont également observées.

Keywords : *Kaliotoxin, ionic balance, inflammation.*

Introduction

Excitable cells express voltage-gated potassium (K_V) channels. Due to their high ion selectivity and distribution in many tissues, K_V channels play an important role in a variety of physiological processes including the regulation of neuronal and cardiac electrical pattern, muscle contractility, neurotransmitter release, hormone secretion, regulation of cell secretion and activation of lymphocytes. This diversity of function is reflected in their sensitivities to various blockers (Mourre *et al.*, 1999). Potent tools are used to identify and characterize these membrane proteins. Among these tools, kaliotoxin, a neurotoxin purified from *Androctonus australis hector* venom and exhibiting a high affinity for K_V channels (K_V1.1) of the mammalian nervous system, has been used to study the functional role of K_V channels (Laraba-Djebari *et al.*, 1994). Binding of kaliotoxin to their targets induces an ion transfer dysfunction which could be responsible for the induced specific pharmacological properties.

Ionic imbalance induced by kaliotoxin

Injection of kaliotoxin to mice induced an electrolyte dysfunction accompanied by modification of seric levels of Ca^{++}, Na^{+} and K^{+} (*Figure 1*). These electrolyte changes (hypercalcemia, hyponatremia and hypokalimia, respectively) may be associated with kaliotoxin binding to its targets. This could be responsible for the hyperexcitability-induced massive release of cathecholomines and acetylcholine which are the cause of the toxin-induced pathophysiological effects (Ismail, 1995; Possani *et al.*, 1999).

Tissue damage and biochemical modification induced by kaliotoxin

Inoculation of the purified kaliotoxin by intracerebroventricular route induced severe disturbance of nervous

and cardiopulmonary functions. This tissue damage was observed in the cerebral cortex (oedema, hemorrhage, necrosis and neuronal darkness), myocardium (interstitial oedema, hemorrhage and hypertrophy) and pulmonary parenchyma (interstitial oedema and thickening of interalveolar septa). It was also accompanied by an important increase in some biomarker levels of the vital organes [creatine phosphokinase (CPK) and lactate dehydrogenase (LDH)].

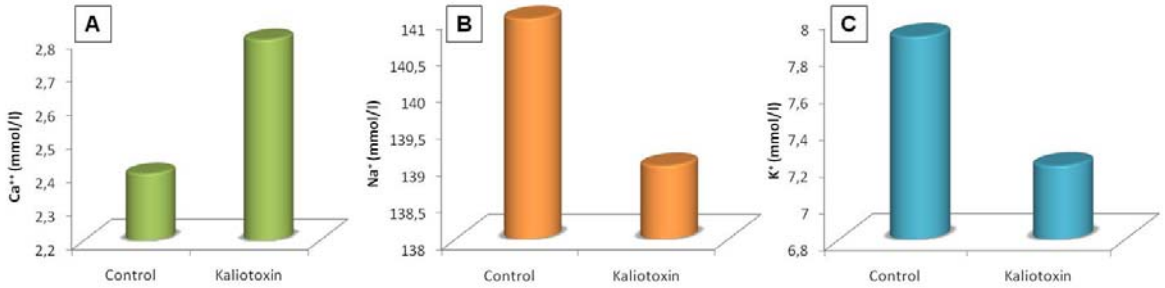

Figure 1. Seric levels of Ca^{++} (**A**), Na^{+} (**B**) and K^{+} (**C**) of intoxined mice with kaliotoxin (electrolyte disturbance).

Figure 1. *Taux des électrolytes Ca^{++} (**A**), Na^{+} (**B**) et K^{+} (**C**) au niveau du sérum des souris intoxinées avec la kaliotoxine (déséquilibre électrolytique).*

Tissue alterations of organs can be explained by the release of cholinergic and adrenergic neuromediators from sympathetic and parasympathetic nerve terminals induced by the binding of scorpion toxins to their targets (Ismail, 1995; De Davila *et al.*, 2002). The presence of metabolic enzymes in the blood serum is usually used as a marker for the *in vivo* diagnosis of tissue injuries. High seric levels of the enzymes CPK and LDH are most likely a consequence of cerebral, myocardial and pulmonary damage. Hence, after extensive tissue destruction, these enzymes are known to be released into the serum (Daisley *et al.*, 1999; Adi-Bessalem *et al.*, 2008).

Inflammatory response

The inflammatory response was analyzed by evaluation of the recruitment of cell population in the vascular compartment and cell infiltration in tissue. The obtained results showed that kaliotoxin injection induced an inflammatory response marked by the presence of neutrophils followed by lymphocytes, monocytes, eosinophiles and basophiles in sera. A significant increase in eosinophil peroxidase activity (EPO) and myloperoxydase (MPO) was observed in the brain and lungs, indicating an infiltration of eosinophiles and neutrophiles in these organs.

Leukocyte recruitment at the site of injury is involved in the host defense against offending agent and is a key mediator in the inflammatory response. Neutrophiles are usually the cell type that reaches the site of injury and predominates in an immediate inflammatory reaction (Smith, 1994).

Conclusion

The present results show that the fixation of kaliotoxin to its targets induces an ion transfer's dysfunction which could be responsible for the induced complex pathophysiological effects such as tissue damage, metabolic alterations and inflammatory response. These results strongly suggest the involvement of ionic balance in various regulations (nervous and cardio-respiratory systems, inflammatory reaction).

References

Adi-Bessalem S, Hammoudi-Triki D, Laraba-Djebari F (2008) Pathophysiological effects of *Androctonus australis hector* scorpion venom: Tissue damages and inflammatory response. *Exp Toxicol Pathol* **60**: 373-380

Laraba-Djebari F, Legros C, Crest M, Ceard B, Romi R, Mansuelle P, Jacquet PG, van Rietschoten J, Gola M, Rochat H, Bougis P, Martin-Eauclaire M-F (1994) The kaliotoxin family enlarged: purification, characterization, and precursor nucleotide sequence of KTX from *Androctonus australis* venom. *J Biol Chem* **269**: 32835-32843

Smith GA (1994) Neutrophils, host defense, and inflammation. A double-edged sword. *J Leukoc Biol* **56**: 672-686

Ismail M (1995) The scorpion envenoming syndrome. *Toxicon* **33**: 825–858

Daisley H, Alexander D, Miller P (1999) Acute myocarditis following *Tityus trinitatis* envenoming: morphological and pathophysiological characteristics. *Toxicon* **37**: 159–165

Possani LD, Becerril B, Delpierre M, Tytgat J (1999) Scorpion toxins specific for sodium channels. *Eur J Biochem* **264**: 287–300

Mourre C, Marina NC, Martin-Eauclaire M-F, Bessone R, Jacquet G, Gola M, Seth LA, Crest M (1999) Distribution in rat brain of binding sites of kaliotoxin, a blocker of Kv1.1 and Kv1.3 α-subunits. *J Pharmacol Exp Ther* **291**: 943–952

De Davila CAM, Davila DF, Donis JH, De Bellarbarba GA, Villarred V, Barbosa JS (2002) Sympathetic nervous system activation, antivenin administration and cardiovascular manifestation of scorpion envenomation. *Toxicon* **40**: 1339-1346

Toxines et Transferts ioniques – Toxins and Ion transfers
Rencontres en Toxinologie – Meeting on Toxinology, 2011
Editions de la SFET – SFET Editions
Accès libre en ligne sur le site – Free access on line on the site : http://www.sfet.asso.fr

Cytotoxic and antioxidant activities of scorpion venom on cell lines

Djelila HAMMOUDI-TRIKI, Fatima LARABA-DJEBARI*

Laboratoire de Biologie Cellulaire et Moléculaire, Faculté des Sciences Biologiques, Université des Sciences et de la Technologie « Houari Boumédienne » (USTHB), El Alia, BP 32, 16111 Bab Ezzouar, Alger, Algérie ; Laboratoire de Recherche et de Développement sur les Venins, Institut Pasteur d'Algérie, Alger, Algérie

** Corresponding author ; Fax : +213 21336077 ; E-mail : flaraba@hotmail.com*

Abstract

Scorpion venom components act as a toxic agent that influence immune response including leukocyte, cytokine and reactive oxygen species release. Tissue damage and acute lung injury following envenomation by Androctonus australis hector *(*Aah*) is in part due to the activation of this response. However, the cellular and molecular mechanisms remain unclear. The present study was undertaken to analyze the toxic effects of* Aah *venom on cell lines. Biochemical analyses were also conducted to evaluate oxidative/antioxidative balance disorders induced after cellular stimulation. The results showed that* Aah *venom induced cytotoxic effects on splenocytes isolated from BALB/c mice and Vero cells in a time- and dose-dependent manner. Hydrogen peroxide production increase was observed at 24 h in the supernatant of cell culture compared to the control. In addition, lipid peroxidation was also induced in the same manner, as measured by malonaldehyde (MDA) production, with mobilization of glutathione. Lactate deshydrogenase (LDH) release into extracellular medium and in the supernatants of spleen cultures indicated a decrease of cell viability, probably due to cell membrane damage. This release in supernatants and the fragmentation of cellular DNA could be the consequence of oxidative stress responsible for cell membrane alterations leading to the inhibition of some enzymatic activities.*

Cytotoxicité et activités antioxydantes du venin de scorpion sur des lignées cellulaires

Les venins de scorpions agissent comme des agents toxiques sur la réaction immunitaire induisant l'activation des leucocytes, des cytokines et des espèces réactives d'oxygène. Des altérations tissulaires et la formation d'un œdème aigu, suite à l'envenimation par le scorpion Androctonus australis hector *(*Aah*) sont la conséquence de cette activation. Cependant, les mécanismes cellulaires et moléculaires induits par le venin d'*Aah *demeurent méconnus. Cette étude a été entreprise pour analyser les effets toxiques du venin sur des lignées cellulaires. Une analyse biochimique a été également menée afin d'évaluer les perturbations au niveau de la balance oxydative/antioxydative induites après stimulation cellulaire. Les résultats obtenus montrent que le venin présente des effets cytotoxiques, qui dépendent de la dose et du temps, sur les splénocytes isolés à partir de souris BALB/c et des cellules Vero. L'augmentation de la production d'H_2O_2 a été observée après 24 h dans les surnageants de culture cellulaire comparés au témoin. Par ailleurs, le venin induit une peroxydation lipidique évaluée par une production du malonaldéhyde (MDA) et une mobilisation de glutathion. La libération de lactate déshydrogénase (LDH) dans le milieu extracellulaire et dans les surnageants de culture cellulaires serait due aux altérations de la membrane cellulaire. La fragmentation de l'ADN cellulaire pourrait être également la conséquence d'un stress oxydatif responsable des changements cellulaires et de l'inhibition de quelques activités enzymatiques.*

Keywords : *Cell lines, cytotoxicity, oxidative stress, venom.*

Introduction

The pathogenesis caused by scorpion envenomation could be a model to understand the complex immune response. In this model, inflammatory response is essential for structural and functional repair of injured tissue observed in scorpion pathology (Adi-Bessalem *et al.*, 2008; Petricevich, 2010).

Tissues damage during inflammation by two separate oxidative pathways involves the synthesis of superoxide anion and the production of various cytokines, active substances and enzyme activities. Spleen cells refer to cells that line hollow organs and glands and those that make up the outer surface of the body and constitute another inevitable target. Kidney tissues also constitute an inevitable target for action of different components. Therefore, these cell lines are an appropriate *in vitro* model system to evaluate the toxicity and

the events involved in the cell death caused by *Androctonus australis hector* (*Aah*) venom. The aim of this study was to assess the direct action of venom on cultured cells. Cytotoxicity of *Aah* venom was determined on splenocytes and renal cell lines.

Effects of *Aah* scorpion venom on cell viability

Cytotoxicity was studied for the two types of cells. The studies were performed under similar conditions to enable a direct comparison of the results in order to evaluate the effects of *Aah* venom on viability of monkey (Vero) and mice spleen cell lines. Growing cultures of cells were exposed to venom at doses ranging from 0 to 100 µg/ml for 24, 48 and 72 h. As shown in *Figure 1*, a dose-dependent decrease of cell viability was clearly observed with increasing venom doses. Interestingly, when exposed to various venom doses, spleen cells were more strongly affected than the Vero cell lines (*Figure 1*). The *Aah* venom doses producing 50% of cytotoxicity (ID_{50}) were 17 µg/ml for spleen cells and 85 µg/ml for Vero cells. It is well known from the literature that crude or purified components of venom are likely to contain bioactive compounds which may be responsible for, or contribute to, the observed toxicity since cells exposed to these several components showed decreased cell viability. Hence, morphological defects inhibit functional activities, the metabolism of cells, or lead to a particular activation stage of these cells that exhibits oxidative stress (Kumar *et al.*, 2003).

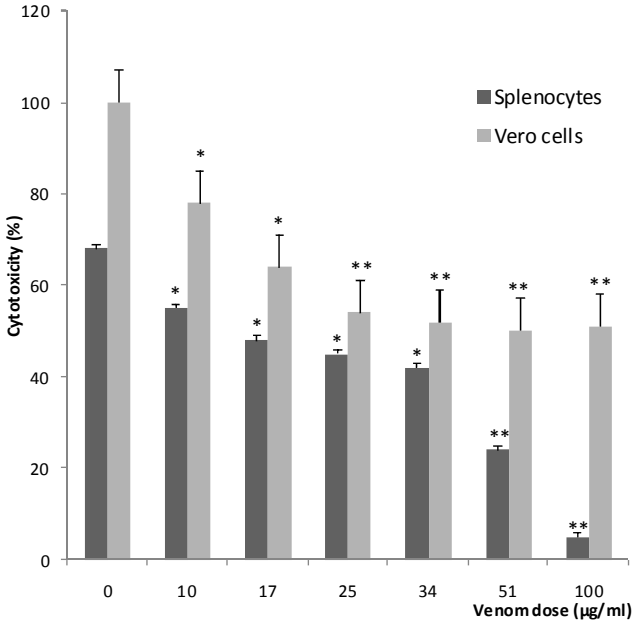

Figure 1. Effect of *Aah* venom dose on spleen and Vero cells. Cells were incubated for 48 h in RMPI-1640 medium containing various doses of *Aah* venom. Cells were isolated from BALB/c mice (1×10^6 cells/ml), and cultured in 96-well flat-bottomed microtiter. Each value represents the mean ± standard deviation (n = 3). * $P \leq 0.05$ and ** $P \leq 0.001$, *versus* control.

Figure 1. *Effet de la dose de venin* Aah *sur les splénocytes et les cellules Vero. Les cellules ont été incubées pendant 48 h dans un milieu RMPI-1640 contenant des doses croissantes de venin* Aah*. Les cellules ont été isolées à partir de souris BALB/c (1×10^6 cellules/ml) et mises en culture dans des microplaques de 96 puits à fond plat. Chaque valeur représente la moyenne ± la déviation standard (n = 3). * $P \leq 0,05$ et ** $P \leq 0,001$,* versus *contrôle.*

Assessment of antioxidant activity

Malonaldehyde (MDA) level, an index of lipid peroxidation, and glutathione were analyzed spectrophotometrically. The rate of MDA and glutathione increased according to the venom doses (10, 17, 34, 51, 68 and 85 µg/ml), 48 h after cell culture. However, the increase in the MDA rate was significantly more important for Vero lines (*Table 1*). The onset of lipid peroxidation persisted for several hours, suggesting an important role from oxidative stress in the cell cytotoxicity induced by *Aah* venom. *Aah* venom induced also an increase in superoxide anion (H_2O_2) in spleen cells. The production of superoxide anion might be due to receptor competition, superoxide dismutase and/or catalase activities. Cell death was investigated by measuring the release of lactate dehydrogenase (LDH) in the culture medium. The intracellular LDH was found to be released when cell membrane damage occurred and/or when the cells were visibly dead. Cell membrane integrity can be assessed by monitoring the passage to the outside of substances that are normally sequestered into cells. LDH has been identified and allowed to measure relative numbers of live and dead cells within the same cell population (Decker *et al.*, 1988).

Lipid peroxidation and H_2O_2 products are known to be highly reactive or even toxic compounds associated with oxidative stress induction. These substances, when produced in high amounts, may cause disturbances in cell functions and subsequent pathophysiological action.

Table 1. Effects of *Aah* venom (10 µg/ml) on oxidative/antioxidative balance, 48 h after cell stimulation.

Tableau 1. *Les effets du venin d'*Aah *(10 µg/ml) sur la balance oxydative/antioxydative, 48 h après stimulation cellulaire.*

Samples	H_2O_2 (µmoles)	MDA (nM)	Glutathione (nmole / min)	LDH (U / l)
Control	25.00±1.03	90.00± 5.56	2.25±1.30	100.0±8.8
Spleen cells	125.0±11.5	150.0±10.7*	3.25±1.40	190.0±11.9
Vero cells	ND	225.0±10.7**	3.5±1.5	ND

Each value represents the mean ± standard deviation (n = 3). * P ≤ 0.05 and ** P ≤ 0.001, *versus* control.

*Chaque valeur représente la moyenne ± la déviation standard (n = 3). * P ≤ 0,05 et ** P ≤ 0,001,* versus *contrôle.*

Conclusion

The present results, regarding the *Aah* venom cell toxicity, could be the way through which oxidative stress is mediated. This may help to determine whether oxidative stress or proteases are involved in the cardiopulmonary damages caused by the venom. However, understanding the molecular cell cytotoxicity mechanisms following envenomation, as well as characterization of the venom compounds responsible for the observed effects, have yet to be determined.

References

Adi-Bessalem S, Hammoudi-Triki D, Laraba-Djebari F (2008) Pathophysiological effects of *Androctonus australis hector* venom. *Exp Toxicol Pathol* **60**: 373-380

Decker T, Lohmann-Matthes ML (1988) A quick and simple method for the quantitation of lactate deshydrogenase release in measurements of cellular cytotoxicity and tumor necrosis factor (TNF) activity. *J Immunol Methods* **115**: 61–69

Dousset E, Carrega L, Steinberg JG (2005) Evidence that free radical generation occurs during scorpion envenomation. *Comp Biochem Physiol* **140**: 221–226

Kumar O, Sugendran K, Vijayaraghavan R (2003) Oxidative stress associated hepatic and renal toxicity induced by ricin in mice. *Toxicon* **41**: 333-338

Petricevich VL (2010) Scorpion venom and the inflammatory response. *Mediators of Inflammation* **2010**: 1-16

Toxines et Transferts ioniques – Toxins and Ion transfers
Rencontres en Toxinologie – Meeting on Toxinology, 2011
Editions de la SFET – SFET Editions
Accès libre en ligne sur le site – Free access on line on the site : http://www.sfet.asso.fr

Zn^{2+} : a required ion for biological and enzymatic activities of procoagulant metalloproteinase (CCSV-MPase) isolated from Cerastes cerastes *venom*

Fatah CHERIFI[1,2], Jean-Claude ROUSSELLE[3], Abdelkader NAMANE[3], Fatima LARABA-DJEBARI[1,2*]

[1] *Laboratoire de Biologie Cellulaire et Moléculaire, Faculté des Sciences Biologiques, Université des Sciences et de la Technologie « Houari Boumédienne » (USTHB), El Alia, BP 32, 16111 Bab Ezzouar, Alger, Algérie ;*
[2] *Laboratoire de Recherche et de Développement sur les Venins, Institut Pasteur d'Algérie, Alger, Algérie ;*
[3] *Institut Pasteur, Plate-Forme de Protéomique, CNRS URA 2185, 75724 Paris cedex15, France*

* *Corresponding author ; Fax : (+) 213 21 60 33 77 ; E-mail : flaraba@hotmail.com*

Abstract

Cerastes cerastes *snake venom contains diverse proteins with a variety of biological and physiological activities. Most of them are proteases which are the largest group of proteins in Viperidae venoms. In this study, we describe the requirement of zinc in the metalloproteinase activity of CCSV-MPase. CCSV-MPase hydrolyzes natural substrates such as casein, haemoglobin and fibrinogen. It also hydrolyzes benzoyl-L-arginine-ethyl-ester (BAEE) as a synthetic substrate. The proteolytic and esterasic activities of CCSV-MPase were inhibited by ethylene diamine tetraacetic acid (EDTA) and 1.10 O-phenantroline, chelators of bivalent cation metals and Zn^{2+}, respectively. CCSV-MPase is therefore a zinc-metalloproteinase with fibrinogenase activity. Hence, CCSV-MPase hydrolyzes the Bβ chain of human fibrinogen* in vitro*, releasing fibrinopeptide B only. This fibrinolytic activity was also found to be inhibited by 1.10 O-phenantroline. Proteomic analysis of CCSV-MPase, using LCMS/MS, revealed some sequence similarities between CCSV-MPase and five Zn^{2+}-metalloproteinases from other venoms.*

Zn^{2+} : un ion nécessaire aux activités biologiques et enzymatiques de la métalloprotéinase procoagulante (CCSV-MPase) isolée à partir du venin de Cerastes cerastes

Le venin du serpent Cerastes cerastes *contient une variété de protéines ayant des activités biologiques et physiologiques diverses. La plupart d'entre elles sont des protéinases constituant le plus grand groupe de protéines dans les venins de Viperidae. Dans cette étude, nous décrivons la nécessité de l'ion zinc pour les activités enzymatiques et biologiques d'une métalloprotéinase appelée CCSV-MPase. CCSV-MPase hydrolyse des substrats naturels tels que la caséine, l'hémoglobine et le fibrinogène, ainsi que le benzoyl-L-arginine-éthyl-ester (BAEE) comme substrat synthétique. Les activités protéolytiques et estérasiques de la CCSV-MPase sont inhibées par l'acide éthylène diamine tétraacétique (EDTA) et le 1,10 O-phénantroline. CCSV-MPase est donc une Zn^{2+}-métalloprotéinase ayant une activité enzymatique sur le fibrinogène. Ainsi, CCSV-MPase hydrolyse la chaîne Bβ du fibrinogène humain* in vitro*, libérant seulement le fibrinopeptide B. Cette activité fibrinolytique est aussi inhibée par le 1,10 O-phénantroline. L'analyse protéomique de CCSV-MPase par LCMS/MS a révélé quelques similitudes de séquence entre CCSV-MPase et cinq autres Zn^{2+}-métalloprotéinases isolées à partir d'autres venins.*

Keywords : *1.10 O-Phenantroline, β-fibrinogenase, proteomic analysis, zinc-metalloproteinase.*

Introduction

Viperidae and Crotalidae venoms are rich sources of hydrolytic enzymes which produce a complex pattern of clinical and toxic effects such as haemorrhage and blood-clotting disorders because they act at various steps of blood coagulation (Rivière and Bon, 1999; Braud *et al*., 2000; Castro *et al.*, 2004; Castro and Rodriguez, 2006; Kornalik, 1990; Liu *et al*., 2006). These components have antagonist functions, while some of them act synergistically (Laraba-Djebari *et al*., 1995). Among these components, metalloproteinases are widely found in Viperidae venoms. They may cause local haemorrhage following accidental or experimental envenoming (Kamiguti, 2005; Chérifi *et al.,* 2010). Some of these metalloproteinases are known to display fibrino(gen)lytic activity.

Cerastes cerastes venom is a mixture of bioactive molecules. Some molecules isolated from this venom act on blood coagulation, *i.e.* three phospholipases A_2 (Laraba-Djebari and Martin-Eauclaire, 1990; Zouari-Kessentini *et*

al., 2009) and thrombin-like enzymes, coagulant fraction V (El-Asmar *et al*., 1986), proteinase RP34 (Laraba-Djebari *et al*., 1992), afaâcytin (Laraba-Djebari *et al*., 1995), cerastotin (Marrakchi *et al*., 1997a), cerastocytin (Marrakchi *et al*., 1997b), anticoagulant protease fraction (Chérifi and Laraba-Djebari, 2007), and aggregant serine protease (Chérifi and Laraba-Djebari, 2008). Only two metalloproteinases have been recently purified from *Cerastes cerastes* venom: haemorrhagic metalloproteinase CcH1 (Boukhalfa-Abib *et al.,* 2009) and non-haemorrhagic metalloproteinase CCSV-MPase (Chérifi *et al.,* 2010). Proteomic analysis of *Cerastes cerastes* venom has shown the presence of at least 37 Zn^{2+}-metalloproteinases (Bazaa *et al*., 2005). CCSV-MPase was identified by proteomic study (Chérifi *et al.,* 2010). Here, we report requirement of Zn^{2+} for its activities.

MALDI MS/MS analysis and identification of CCSV-MPase

For mass spectrometry (MS) analysis of CCSV-MPase, 4800 MALDI TOF/TOF Analyzer was operated in positive reflector ionization mode (m/z range: 800 to 4000). 3000 laser shots/spot were used to ensure S/N quality for precursor selection. Internal calibration of the MS spectra using the Glu-1 fibrino peptide B ($[M+H]^+$ = 1570.670) was performed automatically. For the MS/MS experiment, 2 kV positive CID ON methods were chosen. Non-redundant ions with a S/N> 30 were selected as precursors and submitted to CID fragmentation (4000 laser shots/precursor, up to 15 precursors/spot). MS/MS queries were carried out using a local copy of MASCOT search engine 2.1 embedded into GPS-Explorer Software 3.5 on the NCBInr database. MASCOT files of the identified proteins were re-tested with Scaffold software which used two independent search engines (MASCOT and X! Tandem) and a workflow including PeptideProphet (peptide filtering) and ProteinProphet (protein identification filtering). The results obtained with two search engines were then automatically combined, and only proteins with a minimum of two distinct peptides (peptide confidence index ≥ 95) and a protein confidence index ≥ 95% were taken into consideration.

Proteomic analysis led to 312 collected fractions after off-line nano liquid chromatography of digested CCSV-MPase. Overall; 1207 MS/MS spectra were acquired. Analysis LC/MS/MS of tryptic fragments of CCSV-MPase showed some sequence similarity with other metalloproteinases isolated from other venoms (*Table 1*).

Table 1. Some identified proteins by LC-MALDI-MS/MS with sequence similarities to CCSV-MPase.

Tableau 1. *Quelques protéines identifiées par LC-MALDI-MS/MS ayant une homologie de séquence avec la* CCSV-MPase.

Protein	*Accession number*	*Species*	*Molecular mass (kDa)*	*Peptide number*	*Scaffold protein confidence index*
Group III snake venom metalloproteinase	gi| 83523642	*Echis oecllatus*	69714	3	100
Zinc metalloproteinase-brevilysin-H6	gi|190358877	*Gloydius blomhoffi brevicaudus*	68199	2	998
Zinc metalloproteinase berythractivase	gi| 82216043	*Bothops erythmelas*	68513	3	100
Disintegrin CV-11beta	gi|123913579	*Cerastes vipera*	7000	3	100

Effect of inhibitors on the enzymatic activities of purified CCSV-MPase

Various inhibitors were used to determine the metal ion effect on the CCSV-MPase activities. Enzymes were pre-incubated with 5 mM ethylene diamine tetraacetic acid (EDTA), ethylene glycol tetraacetic acid (EGTA), phenylmethylsulfonyl fluoride (PMSF), heparin, 1.10 phenanthroline, antithrombin III and aprotinin (*Figures 1* and *2*). Activities were measured using casein and benzoyl-L-arginine-ethyl-ester (BAEE) as natural and synthetic substrates, respectively.

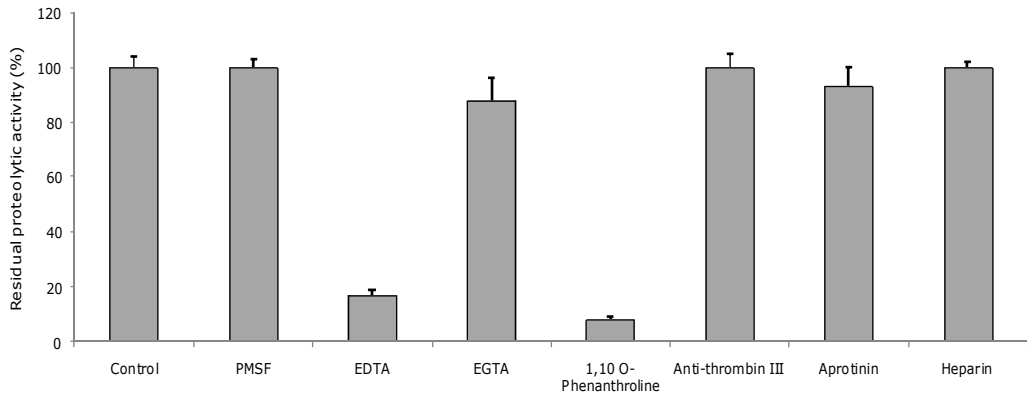

Figure 1. Inhibitor effect of CCSV-MPase proteolytic activity.

Figure 1. *Effet des inhibiteurs sur l'activité protéolytique de CCSV-MPase.*

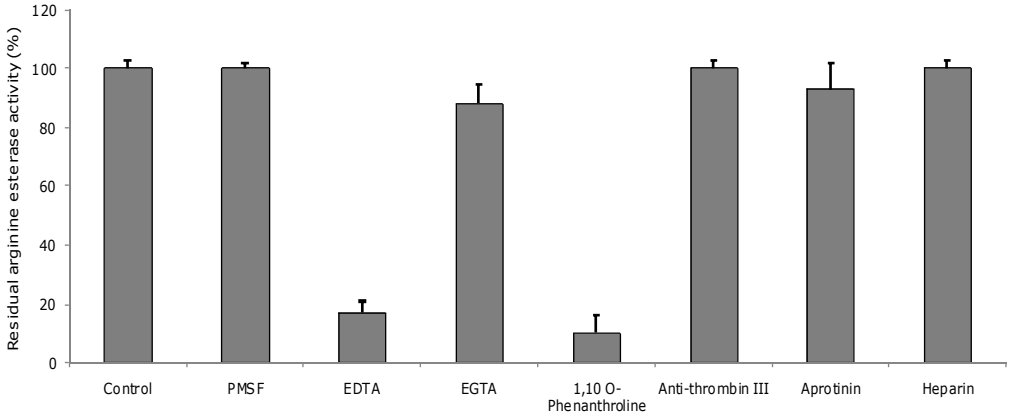

Figure 2. Inhibitor effect on arginine ester hydrolase activity of CCSV-MPase.

***Figure 2.** Effet des inhibiteurs sur l'activité arginine ester hydrolase de CCSV-MPase.*

The use of inhibitors indicated that only EDTA and 1,10 phenanthroline inhibit completely the proteolytic activity of CCSV-MPase while PMSF, heparin, aprotinin and EGTA have no significant effect on this activity. These results strongly suggest that CCSV-MPase could be a zinc-dependant metalloproteinase with no requirement of Ca^{2+} for its catalytic activity.

Conclusion

CCSV-MPase is a metalloproteinase displaying a proteolytic activity on natural and synthetic substrates. This proteolytic activity is sensitive to EDTA as a chelator of all bivalent ions as well as to 1.10 O-phenantroline, a unique specific chelator of zinc. However, both enzymatic and biological activities of CCSV-MPase are non-affected by the presence of EGTA, a specific chelator of calcium. Regarding the chelator action and the sequence analogies between CCSV-MPase and other previously isolated Zn^{2+}-metalloproteinases, it seems that Zn^{2+} is required for biological and enzymatic activities of CCSV-MPase.

The partial amino acid sequence of CCSV-MPase was identified by MALDI-TOF MS/MS analysis. CCSV-MPase has 15 amino acids in common with group III snake venom metalloproteinase isolated from *Echis ocellus* and 39 amino acids with zinc-metalloproteinase-disintegrin berythractivase purified from *Bothrops erythromelas*. Proteomic approach of CCSV-MPase leads to classify this metalloproteinase into the P-III class of snake venom metalloproteinases containing a proteinase domain and two other domains: disintegrin-like metalloproteinase and cystein-rich domain.

References

Bazaa A, Marrakchi N, El-Ayeb M, Sanz L, Calvete JJ (2005) Snake venomics: Comparative analysis of the venom proteomes of the Tunisian snakes *Cerastes cerastes*, *Cerastes vipera* and *Macrovipera lebetina*. *Proteomics* **5**: 4223-4235

Boukhalfa-Abib H, Meksem A, Laraba-Djebari F (2009) Purification and biochemical characterization of a novel hemorrhagic metalloproteinase from horned viper (*Cerastes cerastes*) venom. *Comp Bioch Physiol Part C* **150**: 285-290

Braud S, Bon C, Wisner H (2000) Snake venom proteins acting on haemostasis. *Biochimie* **82**: 851-859

Castro H.C, Zingali RB, Albuquerque MG, Pujol-Luz M, Rodrigues (2004) CR Snake venom thrombin-like enzymes: from reptilase to now. *Cell Mol Life Sci* **61**: 843-856

Castro HC, Rodriguez C (2006) Current status of snake venom thrombin-like enzymes. *Toxin Rev* **25**: 291-238

Chérifi F, Laraba-Djebari F (2007) Purification et caractérisation d'une fraction anticoagulante et protéolytique du venin de *Cerastes cerastes*. In *Toxines émergentes: nouveaux* risques. Collection Rencontres en Toxinologie, Goudey-Perrière F, Benoit E, Marchot P, Popoff MR (eds) pp 372-373. Paris: Lavoisier

Chérifi F, Laraba-Djebari F (2008) Mise en évidence et caractérisation d'une fraction coagulante et agrégante du venin de *Cerastes cerastes.* In *Toxines et fonctions cholinergiques neuronales et non neuronales*. Benoit E, Goudey-Perrière F, Marchot P et Servent D (eds) pp 153-154. Publications de la SFET, Châtenay-Malabry, France, Epub on http://www.sfet.asso.fr (ISSN 1760-6004)

Chérifi F, Rousselle JC, Namane A, Laraba-Djebari F (2010) CCSV-MPase, a novel procoagulant metalloproteinase from *Cerastes cerastes* venom : Purification, biochemical characterization and protein identification. *Protein J* **29**: 466-474

El-Asmar MF, Shaban E, Hagag M, Tu A (1986) Coagulant component in *Cerastes cerastes* (Egyptian Sand Viper) venom. *Toxicon* **24**: 1037-1044

Kamiguti AS (2005) Platelets as target of snake venom metalloproteinases. *Toxicon* **45**: 1041-1049

Kornalik F (1990) Toxins affecting blood coagulation and fibrinolysis. In *Handbook of Toxicology*. Shier WT, Mebs D (eds) pp 697-709. Marcel Dekker, New York

Laraba-Djebari F, Martin-Eauclaire MF (1990) Purification and characterization of a phospholipase A_2 from *Cerastes cerastes* (Horn viper) snake venom. *Toxicon* **28**: 637-646

Laraba-Djebari F, Martin-Eauclaire MF, Marchot P (1992) A fibrinogen-clotting serine proteinase from *Cerastes cerastes* (Horned viper) with arginine–esterase and amidase activities. Purification, characterization and kinetic parameter determination. *Toxicon* **30**: 1399-1410

Laraba-Djebari F, Martin-Eauclaire MF, Mauco G, Marchot P (1995) Afaâcytine and α,β-fibrinogenase from *Cerastes cerastes* (Horned viper) venom, activates purified Factor X and induces serotonin release from human blood platelet. *Eur J Biochem* **233**: 756-765

Liu S, Sun M-Z, Greenway FT (2006) A noval plasminogen activator from *Agkistrodon blomhoffi ussurensis* venom (ABUSV-PA): purification and characterization. *Bioch Biophys Res Commun* **384**: 1279-1287

Marrakchi N, Barbouche R, Guermazi S, Karoui H, Bon C, El-Ayeb M (1997a) Cerastotin, a serine protease from *Cerastes cerastes* venom, with platelet-aggregating and agglutinating properties. *Eur J Biochem* **247**: 121-128

Marrakchi N, Barbouche R, Guermazi S, Bon C, El-Ayeb M (1997b) Procoagulant and platelet-aggregating properties of Cerastocytin from *Cerastes cerastes* venom. *Toxicon* **35**: 261-272

Rivière G, Bon C (1999) Immunothérapie antivenimeuse des envenomations ophidiennes: vers une approche rationnelle d'un traitement empirique. *Ann Inst Pasteur (Paris)* **10**: 173-182

Zouari-Kessentini R, Luis-José L, Karry A, Kallech-Ziri O, Srairi-Abid N, Bazaa A, Loret E, Bezzine S, El-Ayeb M, Marrakchi N (2009) Two purified and characterized phospholipases A2 from *Cerastes cerastes* venom, those inhibit cancerous cell adhesion and migration. *Toxicon* **53**: 444-453

Toxines et Transferts ioniques – Toxins and Ion transfers
Rencontres en Toxinologie – Meeting on Toxinology, 2011
Editions de la SFET – SFET Editions
Accès libre en ligne sur le site – Free access on line on the site : http://www.sfet.asso.fr

Preliminary characterization of the most dangerous snake venoms of Morocco

Naoual OUKKACHE[1*], Balkiss BOUHAOUALA-ZAHAR[2], Noreddine GHALIM[1]

[1] *Venoms & Toxins Laboratory, Pasteur Institute of Morocco, 1 Place Louis Pasteur, 20360 Casablanca, Morocco ;*
[2] *Laboratoire des Venins et Toxines, Institut Pasteur de Tunis, 13 Place Pasteur, BP74, 1002 Tunis, Tunisie*

* *Corresponding author ; Fax : +212 (5)22260957 ; E-mail : oukkache.naoual@gmail.com*

Abstract

Ophidian envenomation is a serious public health problem in many countries in the world. Over 5 million of the accident cases occur each year causing more than 100,000 deaths. In Africa, more than 20,000 deaths per year are registered and 400,000 victims of envenomation keep severe and permanent functional sequels. In Morocco, the snake bites are frequent and of greater severity in children. They occur mostly in rural areas. The incidence of these bites remains poorly understood and largely underestimated. The epidemiological data are not well known due to the absence of a national registry, as well as non-medical intensive care of a significant proportion of envenomed that use only traditional treating methods. Better characterization of the biological activities of Morocco snake venoms is of great importance, not only to elucidate the molecular mechanisms of the venom action, but also to seek new approaches for the patient treatment. In this study, we report a preliminary venom characterization of Cerastes cerastes *(Cc) and* Vipera lebetina *(Vl) and the cross-reactivity that may exist between their venoms and* Bitis arietans *(Ba). These venoms are known to be very toxic and contain several proteins that differ by molecular weights. Interestingly, both Cc and Vl venoms are characterized by a high hemorrhagic and phospholipase A2 activities and their ability to degrade the α and γ chains of fibrinogen. They display a very low proteolytic activity with the casein test. After injection in mice, Cc and Vl venoms induce myonecrosis in skeletal and cardiac muscles that is most likely the consequence of a direct action of myotoxins and an indirect action of hemorrhagic molecules present in the venoms. In mice, this myonecrosis produces a decrease of creatine phosphokinase concentration in the muscle and its increase in the serum. As expected, Cc venom is a good immunogen and induces high protective antivenom against Vl and Ba venom antigens, higher than that of the antivenom produced against the Vl venom.*

Caractérisation préliminaire des venins des serpents les plus dangereux du Maroc

Les envenimations ophidiennes constituent un sérieux problème de santé publique dans de nombreux pays du monde. A l'échelle mondiale, plus de 5 millions de cas d'envenimations surviennent chaque année provoquant plus de 100 000 décès. En Afrique, plus de 20 000 décès sont enregistrés et 400 000 victimes d'envenimation gardent des séquelles fonctionnelles graves et permanentes. Au Maroc, les morsures de serpents, principalement des vipères, restent fréquentes et de gravité plus importante chez l'enfant. Elles se produisent surtout en milieu rural. L'incidence réelle de ces morsures et leur gravité restent mal connues et largement sous-estimées. Les données épidémiologiques restent mal connues du fait de l'absence d'un registre national et de la non-médicalisation d'une proportion importante des patients victimes d'envenimation et recourant à des procédés traditionnels. Ainsi, une meilleure caractérisation de l'activité biologique des venins de serpents est très importante, non seulement pour élucider certains mécanismes moléculaires, mais aussi afin de rechercher de nouvelles approches pour le traitement des patients. Ce travail porte sur une caractérisation préliminaire des venins de Cerastes cerastes *(Cc) et de* Vipera lebetina *(Vl) et l'étude des immunoréactivités croisées entre les venins de ces deux vipères et celui d'une autre vipère* Bitis arietans *(Ba). Nous avons montré que les venins Cc et Vl sont très toxiques et contiennent plusieurs protéines qui diffèrent par leur poids moléculaire. Ces deux venins possèdent une faible activité protéolytique sur les tests standards et une très forte activité hémorragique et phospholipasique. Ils ont aussi la capacité de dégrader les sous-unités α et γ du fibrinogène. Suite à une injection, les venins Cc et Vl induisent une nécrose des muscles squelettique et cardiaque qui serait la conséquence d'une action directe des myotoxines et indirecte des hémorragines des venins. Cette myonécrose produit une diminution de la concentration en créatine phosphokinase au niveau musculaire et son augmentation au niveau sérique. Soulignons que le venin Cc est un très bon immunogène capable d'induire la production d'un antivenin possédant un pouvoir protecteur contre les antigènes des venins Vl et Ba. Cette capacité protectrice est plus élevée que celle engendrée par l'antivenin produit spécifiquement contre le venin Vl.*

Keywords : *Biological activities, cross reaction, snake venom.*

Introduction

In North Africa, there are many species of front fanged snakes but only a few are known to be dangerous. The foremost medically important species belong to Viperidae [*i.e. Cerastes Cerastes*, Cc (horned viper); *Bitis arietans*, Ba; *Vipera mauritanica* (*Vipera lebetina*, Vl] which were reported as dramatically responsible for hemorrhagic effects (Chippaux and Goyffon, 1998) and Elapidae family of snakes (*i.e. Naja haje*, Nh) mostly incriminate in neurotoxic effects (Chippaux and Goyffon, 2006). The majority of bites (53% of venomous animal bites and 5.6% of registered lethality) occur in rural areas during the summer season. They are inflicted on the feet or ankles, most of the time during the evening when people tread on snake, sometimes at night while sleeping or moving. In Morocco, most snake bite envenomings are inflicted by snakes belonging to Viperidae and Elapidae families (Chani *et al*., 2008).

Venom glands are very specialized tissues that possess a high capacity of protein secretion, and are a rich source of active proteins. Snake venoms are known to contain a complex mixture of pharmacologically active molecules, including organic and mineral components, small peptides and proteins. According to their major toxic effect, snake venoms may be conveniently classified as neurotoxic (Elapidae) or hemorrhagic (Viperidae). For instance, envenomings by *Vipera lebetina* and *Cerastes cerastes* are characterized by hemorrhage and abnormalities in the blood coagulation system, while the venom of the cobra *Naja haje* is mainly neurotoxic and affects the nervous system (Chippaux *et al*., 1999).

Viperidae snake venoms contain a number of different proteins (*i.e.* proteases, fibrinolytic enzymes) that induce alterations in the blood coagulation cascade and interfere with the normal haemostatic system and tissue repair, resulting usually in an observed persistent bleeding. Studies on patients envenomed by some species of the Viperidæ family revealed a fascinating variation in clinical manifestations, ranging from neurological perturbations to increased capillary permeability and edema. These pathological outcomes may be due to the additive or synergistic effects of various enzymes and toxins present in the venom (Teixeira *et al*., 2005).

Fighting measurement against envenoming and concomitantly to the symptomatic handling, specific treatment consisting of immunotherapy, using polyvalent antivenom, is still of great importance. When administered at due time, antivenom is considered as the only efficient treatment of snake envenomed patients. Experimental data and clinical observations confirmed the rapid venom neutralizing effect of potent antivenom (Chippaux and Goyffon, 1998; Quesada *et al*., 2006). However, to produce effective and safe antivenom, more precise biological and biochemical characterizations of the venom composition and analysis of the neutralization capacity of antivenom are essential. This prompted us to look for the venom biochemical contains and to investigate the enzymatic and biological properties of the most endemic snake venoms in Morocco: *Cerastes cerastes* and *Vipera lebetina*. In this paper, we studied the immune cross reactivity between Cc and Vl venoms and compared to Ba venom (one of the most dangerous viper in Morocco) with the main objective to identify the best candidates (venom or a mixture of venoms) to address the best way to produce the most efficient and protecting antivenom.

Material and methods

Venoms

Cc, Vl, Ba and Nh venoms were extracted by manual stimulation, centrifuged, lyophilized and kept at -20°C at the experimental Center of Pasteur Institute of Morocco.

Protein content

The protein content of venoms samples was determined by the colorimetric method of Markewell *et al*. (1978). Bovine serum albumin (BSA, Sigma) was used for standard assay.

SDS-polyacrylamide gel electrophoresis

Sodium dodecyl sulfate - polyacrylamide gel electrophoresis (SDS-PAGE) was carried out as previously described (Laemmli, 1970). Samples were pretreated under reducing conditions (using β-mercaptoethanol).

Determination of median lethal dose

Swiss strain male mice of 2 months aged, weighing 18-20 g, were used. All the procedures involving animals were in accordance with the ethical principles in animal research adopted by the World Health Organization (WHO, 1981).

Lethal potency of venom (in µg per mice) was assessed by intravenously routes as recommended by the World Health Organization (WHO, 1981). Increasing amounts were injected into mice (groups of five mice) in final volumes of 500 µl. Percent of mortality was recorded 24 h after injections. The median lethal dose (LD_{50}) was determined according to the method described by the Software package (Prism 4 5GraphPad, Inc.).

Proteolytic activity

Proteolytic activity was estimated using casein as substrate, according to previously described method (Lomonte and Gutiérrez, 1983). Venoms were used at 50, 100 and 200 µg doses. Blank was made without venom sample. The caseinolytic activity was expressed in U/mg, *i.e.* as following: $A_{U/mg}$ = (ΔA280/mg of venom) × 100.

Procoagulant activity

Coagulant activity was determined in human plasma (Theakston and Reid, 1983). Citrated blood samples

(1 volume of 129 mM trisodium citrate and 9 parts of blood) were centrifuged at 1,700 g for 15 min at 4°C and plasma was recovered. The coagulation activity was estimated after addition of venom serial dilutions. The minimum coagulant dose (MCD) was defined as the least amount of venom resulting in clot formation of human plasma through 60 s at 37°C.

Phospholipase A2 activity

The phospholipase A2 activity was determined as described by Holzer and Mackessy (1996). Specific activity was expressed as following: produced substrate nM/min/mg of venom.

Hemorrhagic activity

Hemorrhagic activity was assessed as described by Kondo *et al*. (1960) and modified by Theakston and Reid (1983). Increasing venom doses (15 to 31 µg in 50 µl of saline solution) were injected by intradermal route (i.d.) in mice. Hemorrhagic measurements were recorded after 2 h, according to the kinetics assay (after this time interval, the hemorrhagic areas are reabsorbed; Furtado *et al.,* 1991). Diameters were measured and the minimum hemorrhagic dose (MHD) was defined as the venom dose that induced a lesion of 10 mm diameter. All procedures involving the use of animals were approved by the Ethical Committee for the Use of Animals (WHO, 1981).

Histological study

To analyze the histopathological effects of venom, two groups of six mice were used. Each mouse received a sublethal dose of venom by intraperitoneal route (i.p.). The animal was sacrificed 60 min after venom injection, and organ tissues of 5 µm thickness were investigated through microscopic examination.

Assay of creatine phosphokinase in the blood

Assay of creatine phosphokinase (CPK) concentration in blood were performed after 3 h of venom injection. Serum was recovered from blood by centrifugation. CPK measurement was performed according to the recommendations of the sheets of the Chemistry Kodak VITROS System (USA).

Fibrinogenolytic activity

Proteolytic activity upon fibrinogen was measured as described by Rodrigues *et al*., (2000) with some modifications. Fibrinogen solution (2mg/ml) in 20 µl phosphate buffered saline (PBS) was incubated with venom dilution at 37°C for 2 h. Fibrinogenic activity was stopped using 20 µl of a solution containing 10% (v/v) glycerol, 10% (v/v) β-mercaptoethanol, 2% (v/v) SDS and 0.05% (w/v) bromophenol blue. Fibrinogen hydrolysis was demonstrated using SDS-PAGE.

Antivenom production

Monospecific antivenom was produced as follows. Horses were hyper-immunized subcutaneously with increasing doses of Cc or Vl venom, at multiple sites near the lymphatic system. Complete Freund Adjuvant (CFA) was used for primary immunization and incomplete Freund Adjuvant (IFA) for secondary immunization. Boosts were made using a saline solution (0.85% NaCl). Hyper-immunization program was assessed by injection of same dose, at two weeks intervals, until the antibody titer reaches a high level. At the end of the immunization program, horses were bled, plasma proteins fractionated by precipitation with ammonium sulfate and immunoglobulins enzymatically digested to produce $F(ab')_2$ fragments. The fractions containing $F(ab')_2$ fragments were extensively dialyzed against saline solution (Raw, 1991).

Double immunodiffusion for the control of the specificity of the antivenom

Double immunodiffusion assay was performed using slides containing 5 ml of 1% Agarose (Sigma) in PBS (pH 7.4). Wells were punched and filled with 20 µl of 20 mg/ml venom proteins or with 100 µl of antivenom solution. After 48 h incubation at 37°C, the slides were washed with 0.15 M NaCl for 72 h, the solution being changed each 12 h, before dried at 37°C and stained with Coomasie Brilliant Blue R (Bio-Rad).

Determination of effective doses (ED_{50})

A fixed amount (3 LD_{50}) of venom was incubated with increasing (0 to 300 µl) volumes of antivenom, for 30 min at 37°C. Each mixture (0.5 ml) was injected by i.p. and intravenous (i.v.) routes into five mice. Death was recorded up to 48 h. As control, mice received 3 LD_{50} of venom without antiserum treatment. Data were analyzed using the method of the Software package (Prism 4 5GraphPad, Inc.), and effective neutralization was expressed as effective dose 50% (ED_{50}). ED_{50} was defined as the volume (µl) needed to prevent death in 50% of the injected mice with 3 LD_{50} venom dose.

Results

Protein content and lethal dose 50% (LD_{50}) of snake venoms

Mice were used throughout to evaluate the toxicity of tested venoms. First, we estimated the protein concentrations, using BSA as standard. Our results showed that 1 mg of lyophilized venom contains 1,000 µg of Vl proteins and about 987 µg of Cc proteins. Thus, we considered 1 mg of venom has an average of 1 mg of proteins. Herein, protein is corresponding to the total dry weight venom used to study biological effects. Toxicity was assessed by i.v. injection of increasing amount of venom. The toxicity assessment was repeated three times. The Cc venom is the most toxic with an LD_{50} of 5.75 µg/mouse; Vl venom displays an LD_{50} that average 5.97 µg/mouse. However, Ba venom is approximately 10 fold less toxic (LD_{50} of 52.54 µg/mouse).

Biochemical characterization of *Cerastes cerastes* and *Vipera lebetina* venoms

The SDS-PAGE protein profiles were analyzed following coomassie blue staining. *Figure 1* shows that all venoms differ in composition, number and intensity of peptide bands. According to the molecular weight makers, both Cc and Vl venoms contain three major classes of proteins with relative molecular weights (MW) of approximately 14, 30 and 67 kDa. However, Nh venom profile reveals protein bands of lower molecular weights with ranging values from 21 kDa to less than 10 kDa. Interestingly, Cc venom presents richer number of protein bands.

In comparison, a number of protein bands showing singular molecular masses and present in Cc venom were absent in Vl venom profiles. Moreover, intensity of the protein bands is variable suggesting disparity in quality and quantity of the venoms' protein composition.

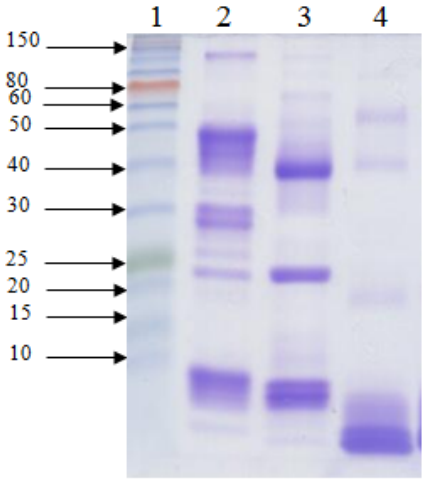

Figure 1. SDS-PAGE profiles of venoms. Electrophoretic separation of venom was performed on a vertical slab of 15% acrylamide under reducing condition. *Lane 1*: molecular mass markers (kDa); *Lane 2*: Cc venom sample; *Lane 3*: Vl venom sample; *Lane 4*: Nh venom sample. The markers indicated in the left are expressed as kDa. Gel was stained using Coomassie blue.

Figure 1. *Profil de SDS-PAGE des venins. La séparation électrophorétique des venins a été réalisée sur une un gel vertical de 15% d'acrylamide dans des conditions réductrices.* Piste 1*: marqueur de poids moléculaire (kDa);* Piste 2*: venin de Cc;* Piste 3*: venin de Vl;* Piste 4*: venin de Nh.*

Proteolytic, coagulant and phospholipase A2 activities

Casein substrate was used to determine the proteolytic activity displayed by snake venoms. According to the results, proteolytic activity is estimated of 31 ± 1.5 U/mg and 20.2 ± 6.0 U/mg for of Vl and Cc venoms, respectively.

A procoagulant activity in human plasma was detected for both Cc and Vl venoms. Compared to value recorded for the positive control (8.00 ± 2.67 nM/min/mg, *Crotalus durissus terrificus venom),* Cc venom showed higher phospholipase activity (25.0 ± 3.0 nM/min/mg) when compared to Vl (7.0 ± 5.0 nM/min/mg) and Nh (6,7 ± 4.0 nM/min/mg) venom activities. Among all recorded phospholipase activity, we conclude that Cc venom present the most intensive one.

Hemorrhagic activity

Intradermal injection was used to estimate hemorrhagic potency of the venoms. Our results show that Cc and Vl venoms are endowed with a hemorrhagic feature. This activity is dose dependent and proportional to the injected dose (*Figure 2*).

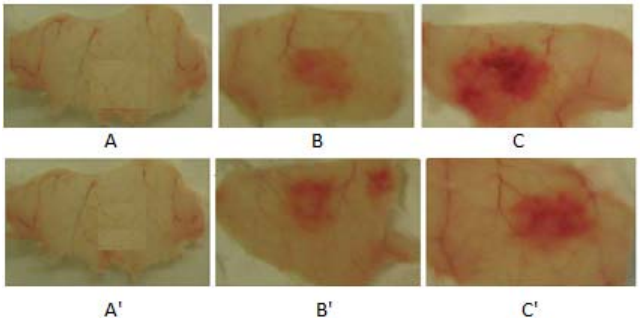

Figure 2. Recording of hemorrhagic activity of Cc (**A**, **B**, **C**, **D**) and Vl venoms (**A'**, **B'**, **C'**, **D'**) of the "Skin-Test". This activity is dose dependent. **A**: control, **B**: 5 µg, **C**: 10 µg, **D**: 20 µg of injected venom.

Figure 2. *Détermination de l'activité hémorragique du venin de Cc* (**A**, **B**, **C**, **D**) et *Vl* (**A'**, **B'**, **C'**, **D'**) *par le "Skin-Test". L'activité est dépendante de la dose.* **A**: contrôle, **B**: 5 µg, **C**: 10 µg, **D**: 20 µg de venin injecté.

The minimal hemorrhagic dose (MHD) was used to evaluate the hemorrhagic power. Our results demonstrated that an i.d. inoculation induces a strong hemorrhage with MHD of 0.128 and 0.630 µg/mouse for

Cc and Vl venoms, respectively. Nh venom has no hemorrhagic effect, even if we clearly observed the presence of edema and myotoxicity symptoms (*Figure 3*).

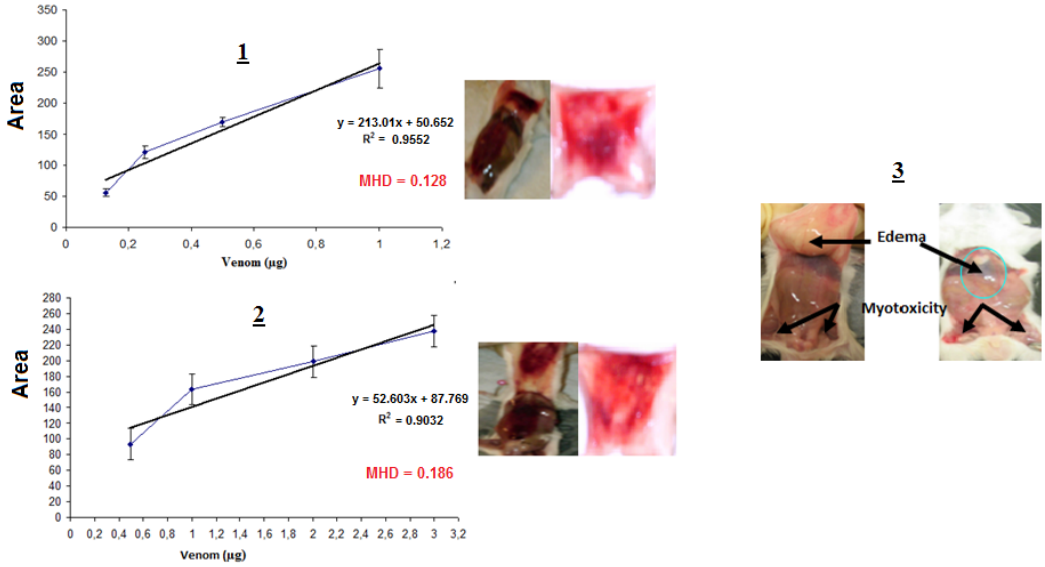

Figure 3. Minimum hemorrhagic dose (MHD) of Vl (**1**), Cc (**2**) and Nh (**3**) venoms.

Figure 3. *Détermination de la dose minimale d'hémorragie des venins de Vl (**1**); Cc (**2**) et Nh (**3**).*

Effects of the venoms on muscle metabolism

Evaluation of enzyme activity of creatine phosphokinase (CPK) in blood is the method used for estimating pathological effects such as myonecrosis. The serum CPK concentration was recorded 3 h after induced envenomation. For both Cc and Vl venoms, we observed a 3 fold increase of CPK serum concentration and this variation was depending on the dose of venoms.

Change in muscle tissue of mice

The intramuscular injection of the venom causes tissue changes such as intense hemorrhages, edema, myonecrosis and inflammatory infiltrates. The alterations are more severe in the case of Cc venom effect analysis (*Figure 4*).

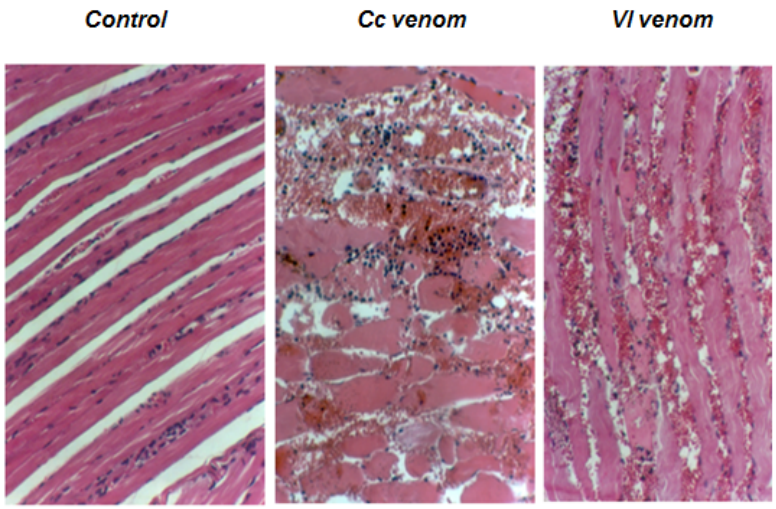

Figure 4. Effect of sublethal dose of Cc and Vl (7 µg/20g mice) venoms on the intestinal tissue.

Figure 4. *Effet de la dose sublétale (7 µg/20g souris) des venins de Cc et Vl sur les tissus intestinaux.*

Fibrinogenolytic activity

Vl and Cc venoms have a fibrinolysis activity on two subunits of fibrinogen (α and γ). This activity is not detected for Nh venom.

Indeed, the ability of Vl and Cc venoms to degrade α and γ chains of fibrinogen is evident. However, degradation of β chain was not detectable (*Figure 5*).

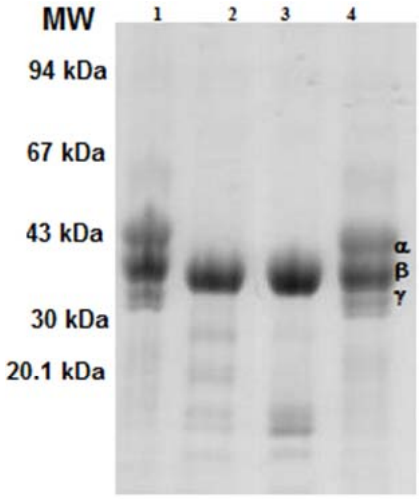

Figure 5. Fibrinogen degradation profile. *Lane 1*: Nh; *Lane 2*: Cc; *Lane 3*: Vl venoms; *Lane 4*: fibrinogen.

Figure 5. *Profil de dégradation du fibrinogène.* Piste 1*: venin de Nh;* Piste 2*: venin de Cc;* Piste 3*: venin de Vl et* Piste 5*: fibrinogène.*

Purity of the plasma fraction containing F(ab')$_2$

Purity of plasma and serum fractions containing F(ab')$_2$ fragments was checked by electrophoresis assay. According to our results, the absence of contaminating bands shows the purity of the purified F(ab')$_2$ fragments. The concentration of the protein of the antivenom solution was determined and estimated ranging about 70 mg/ml (*Figure 6*).

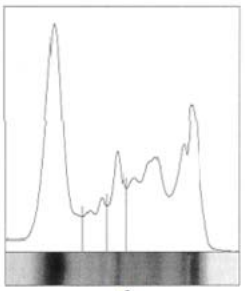

A

Fractions	%	g/dl
Albumins	38.1	3.44
Alpha	7.2	0.65
Beta	9.2	0.65
Gama	45.5	4.11

Total Proteins = 9,03 g / dl

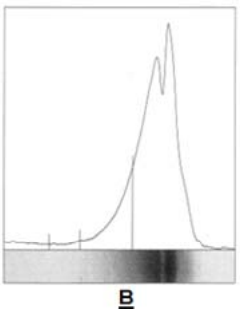

B

Fractions	%	g/dl
Albumins	3.2	0.22
Alpha	2.0	0.14
Beta	16.2	1.4
Gama	78.6	5.51

Total Proteins = 7.01 g / dl

Figure 6. Electrophoresis profile of serum (**A**) and purified plasma containing F(ab')$_2$ (**B**). Analysis of results was made by Software (SDS CELM 60 - Software for densitometry scanner).

Figure 6. *Profil d'électrophorèse du sérum (**A**) et du plasma purifié contenant F(ab')$_2$ (**B**).*

Control of the specificity of the antivenom

Qualitative immunodiffusion assay was used to check antivenom specificity against particular venom. Strong specific immunoprecipitation was observed among Cc venom and monospecific Cc antivenom. Similar result was obtained with Vl venom and its antivenom (*Figure 7*). For both monospecific antivenoms, the immunoprecipitation bands demonstrate the existence of specific antibodies against different venom proteins.

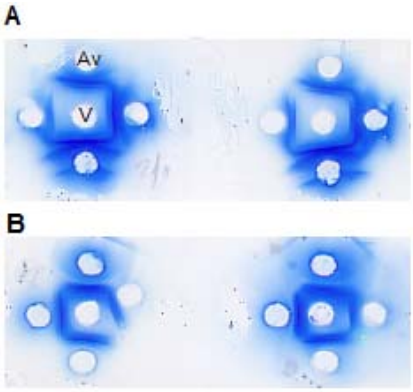

Figure 7. Double immunodiffusion of the Cc venom (*V*) against Cc antivenom (*Av*) with different dilutions (1, 1/2, 1/4 and 1/8) (**A**) and purified Vl venom against Vl antivenom with different dilutions (1, 1/2, 1/4 and 1/8) (**B**).

Figure 7. *Contrôle de la spécificité des antivenins produits par la technique de double immunodiffusion des venins (*V*) Cc (**A**) et Vl (**B**) et de leurs antivenins (*Av*) respectifs.*

Determination of effective doses (ED_{50})

In order to analyze the ability of monovalent Cc and Vl antivenoms in neutralizing the lethal effect of Cc, Vl and Ba venoms, *in vivo* experiments were performed. *Table 1* show that both monovalent antivenoms (*i.e.* Cc and Vl antivenoms) were able to neutralize the toxicity of venom molecules responsible for the lethality. Indeed, Cc antivenom was more effective in neutralizing Ba venom, with an ED_{50} of 84.3 µl/mouse, when compared to Vl antivenom capacity (ED_{50} of 117.3 µl/mouse).

Table.1. Determination of neutralizing effective doses (ED_{50}) in mouse.

Tableau 1. *Détermination de la dose effective de neutralisation, chez la souris.*

	ED_{50} in µl/ mouse (95% c.i.)	
Venom	Cc antivenom	Vl antivenom
***Cerastes cerastes* (Cc)**	**18.7**	78.0
***Vipera libetina* (Vl)**	62.4	**48.3**
***Bitis arietans* (Ba)**	84.3	117.3

Cc antivenom was more effective in neutralizing Vl venom with an ED_{50} of 62.4 ul/animal than Ba venom (ED_{50} of 84.3 µl/mouse). In the same way, Vl antivenom neutralizing capacity was higher against Cc venom than Ba venom (ED_{50} of 78.0 and 117.3 µl/mouse, respectively). However, the best protective effect is obtained with a given antivenom and venom used in the program of immunization (*i.e.* 18.7 and 48.3 µl/mouse for Cc and Vl, respectively).

Discussion and Conclusion

The snake bites are common causes of injury and death in several regions of the world where they are considered as an important public health problem. Their epidemiology is known only in a fragmentary way and is under estimated to 5 million cases of poisoning per year with a mortality rate of 2.5%.

In Morocco, the vipers are responsible for large number of accidents which may reflect the general abundance of this species and the increased level of marked contact. The accidents occurring by these snakes are mainly characterized by hemorrhage damage (Chani *et al*., 2008).

The aim of the present study was to evaluate the biochemical characteristics, as well as the enzymatic and biological properties, of venoms from Cc and Vl, two vipers endemic in Morocco. To study the cross-reactivity that may exist between the venoms, horse specific antivenoms were produced with the aim to identify the best candidate or mixture for producing highly protecting antivenom to fight snake envenomation in North Africa.

First, dried venoms were biochemical investigated. Gel electrophoresis analysis demonstrated several protein bands certainly responsible for most of the observed biological effects (Teixeira *et al.,* 2006; Warrel, 2010). Proteolytic activity following casein test was low compared to other venom reported in the literature (*i.e. Philodryas* venom). Interestingly, we noticed a total absence of coagulant activity, on the contrary to Colubridae family venoms. Phospholipase A2 activity was an important characteristic observed with Cc and Vl venoms. We estimated this activity four times higher in Cc venom than in Vl venom, when compared to the positive control. Our results are in accordance with recently reported studies (Teixeira *et al*., 2006; Warrel, 2010; Hamza *et al*., 2010). It is worth noting that phospholipase A2 from Cc venom was well studied, sequenced and characterized by Laraba-Djebari *et al.* (1990).

Cc and Vl venoms were characterized by their ability to degrade fibrinogen subunits (*i.e.* α and γ chains). However, Nh (belonging to Elapidae family) venom did not display any detectable hemorrhagic activity. Nevertheless, we highlighted the presence of edema with symptoms of myotoxicity, very lower proteolytic and phospholipase activities, and an absence of fibrinogenolytic activity with this venom.

Hemorrhage is one of the most significant pathophysiological effects induced by viper snakes. In this study, we have shown that Cc and Vl venom injections induce myonecrosis in skeletal and heart muscles, which likely resulted from myotoxin direct action and hemorragin indirect action. The myonecrosis produced a reduction of CPK concentration in muscle and its increase in serum (Boukhalfa *et al*., 2009).

Cc and Vl venoms were immunogenic and able to induce high level of specific antibody titers when inoculated in horses. Indeed, monovalent Cc and Vl antivenoms cross-recognized several protein bands within Cc and Vl venoms, and were able to cross-reactively recognize Ba venom. The data obtained from *in vivo* neutralization clearly indicate that both monovalent Cc and Vl antivenoms contain a high ratio of specific antibodies capable to recognize, and without doubt neutralize, Cc, Vl and Ba venom components. The best cross-reactivity was observed with Cc antivenom.

In conclusion, our results are in accordance with recently published data (André *et al*., 2010; Furtado, 2005). Moreover, our investigation clearly demonstrate that viper venoms of Morrocco contain homologous proteins displaying hemorrhagic (39, 67 and 100 kDa), caseinolytic (72 to 74 kDa), phospholipasis (13 kDa), anticoagulant, myonecrotic (75 and 100 kDa) and edematous (29 to 39 kDa) activities. Our results point out the high immunogenicity of Cc venom, leading to induce a horse antivenom able to highly protect against Cc, Vl and Ba whole venoms. Indeed, this protecting capacity is high when compared to the Vl specific antivenom product.

References

André Z, Marisa MTR, Maria FDF (2010) Preliminary biochemical characterization of the venoms of five Colubridae species from Brazil. *Toxicon* **55**: 666-669

Boukhalfa AH, Meksem A, Laraba-Djebari F (2009) Purification and biochemical characterization of a novel hemorrhagic metalloproteinase from *Cerastes cerastes* (horned viper) venom. *Comp Biochem Physiol, Part C* 1**50**: 285-290

Chani M, L'Kassimi H, Abouzahir A, Nazi M, Mion G (2008) A propos de trois observations d'envenimations vipérines graves au Maroc. *Ann Fr Anesth Réanim* **17**: 330-334

Chippaux JP, Goyffon M (1998) Venoms, antivenoms and immunotherapy. *Toxicon* **36**: 823-846

Chippaux JP, Lang J, Amadi Eddine S (1999) Treatment of snake envenomations by a new polyvalent antivenom composed of highly purified $F(ab')_2$: results of a clinical trial in northern Cameroon. *Am J Trop Med Hyg* **61**: 1017-1018

Chipaux JP, Goyffon M (2006) Envenimations et intoxications par les animaux venimeux ou vénéneux. I. Généralités. *Med Trop* **66**: 215-220

Furtado MFD, Colletto GMMD, Dias da Silva W (1991) Controle de qualidade dos venenos animais e dos correspondentes antivenenos. I- Padronizacao dos métodos de ensaio das atividades bioquímicas e farmacológicas dos venenos de algumas espécies do gênero Bothrops e crotalus usando amostras secas a temperatura ambiente ou liofilizadas. *Memórias Instituto Butantan*. **53**: 149-159

Furtado MFD (2005) Biological and immunological properties of the venom of *Bothrops alcatraz*, an endemic species of pitviper from Brazil. *Comp Biochem Physiol, Toxicol Pharmacol* **141**: 117-123

Gutiérrez JM, Gene JA, Rojas G, Cerdas L (1985) Neutralization of proteolytic and hemorrhagic activities of Costa Rica snake venoms by a polyvalent antivenom. *Toxicon* **23**: 887-893

Hamza L, Gargioli C, Castelli S, Rufini S, Djebari FL (2010) Purification and characterization of a fibrinogenolytic and hemorrhagic metalloproteinase isolated from *Vipera lebetina* venom. *Biochimie* **92**: 797-805

Holzer M, Mackessy SP (1996) An aqueous endpoint assay of snake venom phospholipase A_2. *Toxicon* **34**: 1149-1155

Kondo H, Kondo S, Ikesawa I, Murata R, Ohsaka A (1960) Studies of the quantitative method for determination of hemorrhagic activity of Habu snake venom. *Jpn J med Sci Biol* **13**: 43-51

Laemmli UK (1970) Cleavage of structural proteins during the assembly of the head of bacteriophage T4. *Nature* **227**: 680–685

Laraba-Djebari F, Martin-Eauclaire MF (1990) Purification and characterization of PLA2 from *Cerastes cerastes* (horn viper) snake venom. *Toxicon* **28**: 637-647

Lomonte B, Gutiérrez JM (1983) La actividad proteolítica de los venenos de serpientes de Costa Rica sobre caseína. *Rev Biol Trop* **31**: 37-40

Markewell M, Hass SM, Bieber LL, Tolbert NE (1978) A modification of the Lowry procedures to simplify protein determination in membrabe and lipoprotein samples. *Anal Biochem* **87**: 206-210

Quesada L, Sevcik C, Lomonte B, Rojas E, Gutiérrez JM (2006) Pharmacokinetics of whole IgG equine antivenom: comparison between normal and envenomed rabbits. *Toxicon* **48**: 255-263

Raw R, Guidolin H, Higashi, Kelen EMA (1991) Antivenoms in Brazil: preparation. In *Handbook of Natural Toxins*. Tu AT (ed) Vol 5, pp 557-581. Marcel Dekker, New York

Teixeira RMM, Paixao-Cavalcante D, Tambourgi DV, Furtado MF (2006) Duvernoy's gland secretion of *Philodryas olfersii* and *Philodryas patagoniensis* (Colubridae): neutralization of local and systemic effects by commercial bithropic antivenom (*Bothrops genus*). *Toxicon* **47**: 95-103

Theakston RDG, Reid HA (1983) Development of simple standard assay procedures for the characterization of snake venoms. *Bull WHO* **61**: 949-956

Warrel DA (2010) WHO Library Cataloguing-in-Publication data Guidelines for the management of snake-bites. *WHO Regional Office for South-East Asia*

Toxines et Transferts ioniques – Toxins and Ion transfers
Rencontres en Toxinologie – Meeting on Toxinology, 2011
Editions de la SFET – SFET Editions
Accès libre en ligne sur le site – Free access on line on the site : http://www.sfet.asso.fr

A monitoring study of repetitive surgical oocyte harvest in Xenopus laevis

Patricia VILLENEUVE, Geoffroy ESNAULT, Evelyne BENOIT, Jordi MOLGÓ, Rómulo ARÁOZ*

*CNRS, Centre de Recherche de Gif-sur-Yvette - FRC3115, Institut de Neurobiologie Alfred Fessard - FRC*2118*, Laboratoire de Neurobiologie et Développement - UPR3294, 91198 Gif-sur-Yvette, France*

** Corresponding author ; Tel : +33 (0) 1 6982 4170 ; Fax : +33 (0) 1 6982 3447 ;*
E-mail : araoz@inaf.cnrs-gif.fr

Abstract

Xenopus laevis *oocytes provide a successful electrophysiological model for heterologous* de-novo *expression of channels and receptors as well as for the incorporation of exogenous membrane preparations rich in receptors/channels for pharmaco-toxinological studies. The method of choice for oocyte harvesting is repetitive surgical laparotomy of female adult* Xenopus*. The lack of policies regulating oocyte surgery in France prompted us to design a follow-up study to assess the effect of repetitive laparotomy on* Xenopus*. To this end, we used a batch of 24 female* Xenopus *which were tagged with an electronic chip. The amphibians were housed by colonies of eight in 20-L plastic containers. Groups of six amphibians were operated every two, three, four and six months. The weight of each female amphibian was recorded before and after the operation. The recovery from anesthesia, the incision healing, the* Xenopus *behavior and the skin health were also monitored. The impact of repetitive surgery on the oocytes survival following nanoinjection with cDNA, mRNA or* Torpedo *membranes was systematically assessed. Here, we show that repetitive surgery every two months does affect animal weight. In addition, a four-months-recovery period should be allowed between each laparotomy. However, repetitive surgery does reduce the number of* Xenopus *used for electrophysiological/pharmaco-toxinological characterization of receptors and channels.*

Suivie des effets de l'extraction chirurgicale répétitive d'ovocytes chez Xenopus laevis

Les ovocytes de Xenopus laevis *constituent un modèle d'électrophysiologie réussi pour l'expression* de-novo *des canaux et récepteurs, l'incorporation de membranes exogènes riches en récepteurs et canaux et leur caractérisation pharmaco-toxinologique. La méthode acceptée pour l'extraction d'ovocytes est la laparotomie répétitive de xénopes adultes. L'absence de régulations concernant l'extraction d'ovocytes de xénopes femelles en France nous a incités à suivre et à évaluer l'effet de laparotomies répétitives sur les xénopes. Dans ce but, nous avons utilisé un lot de 24 xénopes femelles, marquées avec une puce électronique. Les amphibiens ont été placés par colonies de huit dans des bacs en plastique de 20 litres. Des groupes de six xénopes ont été opérés tous les deux, trois, quatre et six mois. Le poids de chaque xénope a été déterminé avant et après l'intervention. Leur récupération de l'anesthésie, leur guérison de l'incision pratiquée, leur comportement ainsi que l'état de leur peau ont également été surveillés. L'impact des laparotomies répétitives sur la survie des ovocytes après nano-injection avec de l'ADN, l'ARN ou des préparations de membranes de torpille a été systématiquement évalué. Nous montrons ici que la chirurgie répétée tous les deux mois affecte le poids de l'animal. De plus, une période de récupération de quatre mois est nécessaire entre chaque laparotomie. Cependant, la chirurgie répétitive réduit effectivement le nombre de xénopes utilisées pour la caractérisation électrophysiologique/pharmaco-toxinologique des récepteurs et des canaux.*

Keywords : *Heterologous expression, voltage-clamp electrophysiology,* Xenopus laevis*.*

Introduction

The African Clawed Frog *Xenopus laevis* is an amphibian of the order Anura and the family Pipidae. *X. laevis* is an aerobic amphibian but behaves as an entirely aquatic animal. It needs to breath air but it does not need land-based existence. *X. laevis* is very susceptible to desiccation, and can die from being out of the water for a few hours (Goldin, 1992).

Gurdon *et al.* (1971) originally demonstrated that *Xenopus* oocytes can be used to express exogenous messenger RNA (mRNA) when microinjected into the cytoplasm. The contribution of *Xenopus* oocyte microinjection methods to the rapid progress seen in molecular and cellular biology since their introduction as

an heterologous expression model is remarkable (Soreq and Seidman, 1992; Brown, 2005). The nicotinic acetylcholine receptor (nAChR) was the first functional receptor to be expressed in *Xenopus* oocytes following microinjection of exogenous messenger RNA coding for *Torpedo* nAChRs subunits that allowed the electrophysiological and molecular characterization of the cholinergic receptor (Barnard *et al.*, 1982; Sakmann *et al.*, 1982). Rapidly, *Xenopus* oocytes became one of the most widely used systems for heterologous expression and functional characterization of ion channels, receptors and transport proteins after microinjection of mRNA or cDNA (for reviews, see Lester, 1988; Soreq and Seidman, 1992). *Xenopus* oocytes were also shown to be able to incorporate purified *Torpedo* electroplaque membranes into their plasma membrane (Marsal *et al.*, 1995). Later, human functional receptors issued from surgically resected and from *post-mortem* brain tissues were microtransplanted into the plasma membrane of *Xenopus* oocytes (Miledi *et al.*, 2002; Bernareggi *et al.*, 2007). The advantage of the transplantation of biological membranes into *Xenopus* oocytes is that native receptors/channels can be reconstituted together with their associated lipids and proteins.

Female *Xenopus* produce thousands of oocytes over their lifetime period. The oocytes were morphologically classified into six stages according to their development (Dumont, 1972). Stage V-VI oocytes are used for electrophysiological studies. These oocytes of ~1.2 mm diameter show a clearly defined vegetative pole and an animal pole where the nucleus is located. Repetitive surgery on a single female *Xenopus* is a commonly worldwide accepted practice for oocyte extraction since it reduces the number of laboratory amphibians to be used. However, there is no consensus on the number and frequency of laparotomies that could be performed on one female *Xenopus*. As example, the Guidelines for egg and oocyte harvesting in *Xenopus laevis* limit the number of surgical oocyte harvesting procedures to six (the sixth being a terminal surgery), and fix a recovery time of at least 4 weeks for the female *Xenopus* between each surgery (ARAC, 2005). The Boston University, which is committed to observe Federal Guidelines and AAALAC International Guidelines for humane care and use of animals, recommend 4 repetitive surgeries per female *Xenopus* (the fourth being terminal) and a minimum of one month recovery period between surgical oocyte extractions (Boston University, 2009). In contrast, in Switzerland, only one terminal operation is consented (Bertrand *et al.*, 2008). The lack of guidelines regulating *X. laevis* surgery for oocyte extraction in France prompted us to undertake a monitoring study to assess the effect of repetitive surgery on *X. laevis* tagged with an electronic chip.

Materials and methods

Xenopus laevis culturing

Xenopus laevis tagged with an electronic chip were purchased from the *Xenopus* Biological Resources Center (University of Rennes 1, France; *Figure 1A*). The cylindrical chip FDX B of 12 mm long and 2.12 mm diameter made of transparent bio-glass (Real Trace, Villebon sur Yvette, France) was inserted subcutaneously in the ventral side of the left leg of the amphibians using an injector (Real Trace; *Figure 1B* and *C*). The *Xenopus* were housed at the animal facilities conditioned at 21°C with a light/dark cycle of 12 h and fed with trout pellets twice a week and with living bloodworms (Aquarélite, France) once a week. The water was dechlorinated by passage through a charcoal activated filter (Cuno, 3M Purification Inc., St. Paul, MN, USA) and was thermo-regulated to a temperature of 20°C. Water quality was controlled twice a week using a potassium iodide starch paper indicator to avoid any chlorine traces that can harm the skin of the amphibians. At the beginning of this study, the *Xenopus* were disposed in groups of 12 amphibians in 20 liters plastic containers (*Figure 1A*). We have observed that the number of female *Xenopus* per tank could affect oocyte quality and therefore, in the third year of this follow-up study, the number of *Xenopus* per tank was reduced to 8.

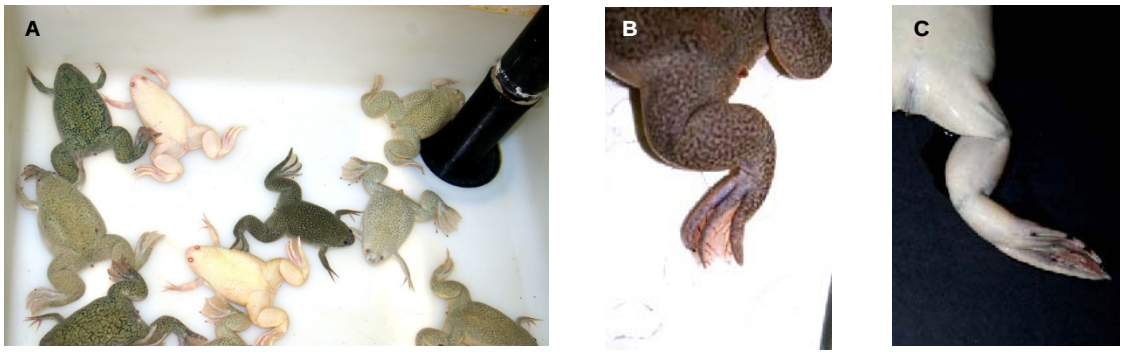

Figure 1. *Xenopus laevis* tagged with an electronic chip were purchased from the *Xenopus* Biological Resource Center (University of Rennes 1, France). (**A**) Female *Xenopus* were housed in colonies of 12 amphibians at the beginning of this trial. (**B**) Dorsal view of a "chip"-tagged left leg of a female *Xenopus*. (**C**) Ventral view of the left leg of a female *Xenopus* tagged with an electronic chip. The FDX B chip of 12 mm long and 2.12 mm diameter is clearly seen. The electronic chips were fully tolerated, without secondary effects, through the whole study (3 years for the first batch of 12 animals).

Figure 1. *Les* Xenopus laevis *marquées avec une puce électronique ont été achetées au Centre de Ressources Biologiques de Xénopes (Université de Rennes 1, France). (**A**) Les* Xenopus *femelles ont été logées par colonies de 12 amphibiens au début de cet essai. (**B**) Vue dorsale d'une* Xenopus *femelle marquée à la patte gauche avec une "puce". (**C**) Vue ventrale de la patte gauche d'une* Xenopus *femelle marquée avec une puce électronique. La puce FDX B de 12 mm de long et 2,12 mm de diamètre est clairement visible. Les puces électroniques ont été parfaitement tolérées, sans effets secondaires, au cours de l'ensemble de l'étude (3 ans pour le premier lot de 12 animaux).*

Oocyte defollicularization

The ovarian lobes were pulled apart into small pieces using a pair of forceps and placed in a 10-mL OR2 solution (88 mM NaCl, 1 mM $MgCl_2$, 5 mM HEPES; pH 7.6) containing 1 mg/mL collagenase type I (Sigma). The whole was incubated for 10 min under gentle shaking. The small pieces of partially digested ovarian lobes were washed three times with 50 mL OR2 solution and once with 50 mL Barth's solution (88 mM NaCl, 1 mM KCl, 0.41 mM $CaCl_2$, 0.82 mM $MgSO_4$, 2.5 mM $NaHCO_3$, 0.33 mM $CaNO_3$, 7.5 mM Hepes; pH 7.6). Finally, the treated ovarian lobes were transferred into a plastic Petri dish (56 mm diameter) containing 10 mL Barth's solution supplied with 2 mg/mL kanamycin (Sigma). The connective tissue and the follicular cell layer of stage V-VI oocytes, were removed under a stereoscopic microscope using a pair of forceps. The defolliculated oocytes were transferred into a 56 mm Petri dish containing 10 mL Barth's solution. The quality of the oocytes was controlled and groups of 50 oocytes were dropped into 35 mm plastic Petri dishes containing 5 mL Barth's solution supplied with 2 mg/mL kanamycin. The oocytes treated in this manner stick to the clean surface of plastic Petri dishes facilitating the microinjection.

Surgical extraction of ovarian lobes from *X. laevis*

The amphibian to be operated was identified by positioning the petSCAN RT 100V5 scanner (Real Trace) 5 - 10 cm over the tagged leg. The amphibian was isolated in a 3-L plastic container for 1 h to reduce handling stress. The *Xenopus* was anaesthetized by immersion for 20 min in a water bath containing 1 g/L ethyl-3-amino benzoate methanesulfonate salt (Sigma, St. Louis, MO, U.S.A.). The laparotomy was performed using autoclaved material. An incision of 1 cm through the skin and muscle was performed in the inferior ventral side of the *Xenopus*. Several ovarian lobes were extracted with sterile forceps and immediately immersed in 10 mL OR2 solution. The muscle plane was sutured using undyed braided absorbable suture (Ethicon, Johnson & Johnson, New Brunswick, NJ, U.S.A.), and the epidermal layer was sutured using a blue non-absorbable suture (Ethicon). Afterwards, the *Xenopus* was placed in a water bath taking care not cover the dorsal side of the amphibian to allow respiration through the skin. Once the *Xenopus* was recovered from anesthesia, the recipient was filled with water and the amphibian was observed for 1 day before being replaced into the main tank.

Microinjection of purified membranes, cDNA and mRNA into *Xenopus* oocytes

Torpedo electrocyte membranes, rich in muscle type ($\alpha 1_2\beta\gamma\delta$) nicotinic acetylcholine receptors (nAChRs), were purified as previously described (Krieger, 2007). Aliquots of 20 µL of *Torpedo* membranes (2.7 mg/mL total proteins) in 5 mM glycine were conserved at -80°C until use. For microtransplantation, a volume of 50 nL of *Torpedo* electrocyte membrane solution was injected into the vegetative pole of *Xenopus* oocytes using a micro-syringe pump controller, Micro4™ (World Precision Instruments, Sarasota, FL, U.S.A.), mounted on a stereoscopic microscope. Glass micropipets for microinjection (3.5 nL, World Precision Instruments) were prepared using the micropipet puller PP-830 (Narishige Scientific Instruments, Tokio, Japan). Following microinjection, *Xenopus* oocytes were incubated at 18°C. Incorporation of *Torpedo* electrocyte membranes into the plasma membrane of the oocyte took place 1 day after microinjection.

To express $\alpha 4\beta 2$ nAChR, 50 nL of an aqueous mixture of pRcCMV cDNA vectors encoding for human $\alpha 4$ and $\beta 2$ nAChR subunits (kindly provided by Dr P. J. Corringer, Pasteur Institute, Paris, France), were injected into the animal pole of *Xenopus* oocytes. A 12 ng amount of each plasmid was injected. Plasmids were purified using an endotoxin-free plasmid maxiprep kit (GenElute™, Sigma). The injected oocytes were incubated for 3 days at 18°C *prior* to electrophysiological experiments.

The expression of human $\alpha 7$ nAChR was obtained following injection of 50 nL aqueous mRNA (5 ng) in the vegetative pole of *Xenopus* oocytes. Messenger RNA was prepared using a mMESSAGE mMACHINE® SP6 kit from Ambion (Austin, TX, U.S.A.) and, as template, pcDNA3.1 cDNA vector encoding human $\alpha 7$ nAChR subunit (kindly provided by Prof. I. Bermudez, Oxford Brookes University, Oxford, U.K.). Translation of mRNA into functional $\alpha 7$ nAChRs took place after 48 h incubation at 18°C.

Experimental design

A group of 12 female *Xenopus* was divided into four groups: Group 1, amphibians operated every two months; Group 2, amphibians operated every three months; Group 3, amphibians operated every four months; and Group 4, amphibians operated every six months. The number of repetitive interventions *prior* to euthanasia was five with the exception of Group 1. The parameters measured for each individual were: *(i)* the weight *prior* and following chirurgical intervention, in a weekly basis, *(ii)* the recovery from anesthesia, *(iii)* the behavior of female *Xenope* following laparotomy, *(iv)* the incision healing and the skin health of the amphibians and *(v)*, the quality of *Xenopus* oocytes for the expression and incorporation of nAChRs into their membranes.

Results and Discussion

Xenopus eggs and oocytes continue to play a central role in many biological disciplines including developmental studies, structural biology, cell biology, physiology, pharmacology, toxinology, biochemistry to mention some of them (Brown, 2004). For the purpose of electrophysiological characterization of excitable membrane proteins, *Xenopus* oocytes not only efficiently translate exogenous mRNA or cDNA but, in addition, they are able to process post-translational modifications necessary for the correct folding and positioning of a synthesized protein at the plasma membrane of the oocyte (Barnard and Miledi, 1982; Soreq and Seidman, 1992). Finally, the microtransplantation into *Xenopus* oocytes of human brain membranes from frozen tissues containing

functional receptors and channels opens new avenues for pharmacology of receptor-associated brain disorders (Miledi *et al.*, 2002).

Xenopus could be easily stressed. When this happens, they can lose their skin and regurgitate their food. The protocol we apply for surgical extraction of *Xenopus* oocytes is in accordance to the existing international guidelines (ARAC, 2005; Boston University, 2009; IACUC Guidelines, 2001, 2007) to minimize animal distress (*Figure 2*). Following laparotomy, the amphibians were placed in a separate room at 20°C for observation. Their initial behavior when they were replaced into their colonies was to slide down the other amphibians and to stay quiet for a prolonged period back the black siphon corner of their tank (see *Figure 1A*). The members of the colony have never shown signs of aggression towards the operated amphibians. There is no need for us to take out the skin sutures since they disappear in a week, and there was no *Xenopus* mortality associated with the laparotomy.

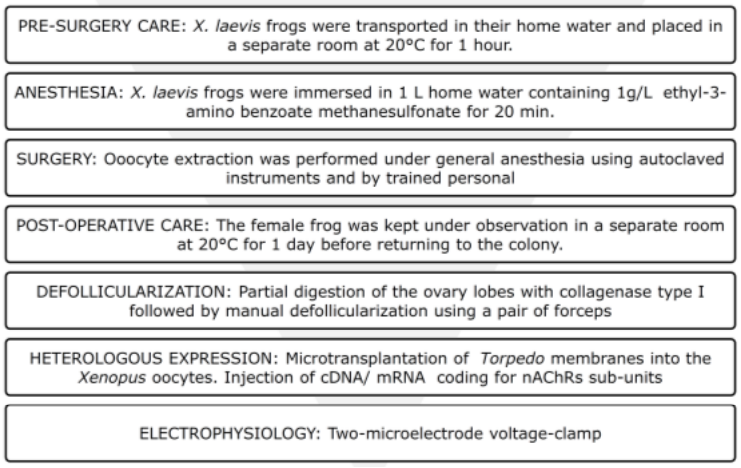

Figure 2. Summarized protocol for surgical extraction of *Xenopus* oocytes for electrophysiological/pharmaco-toxinological studies.

Figure 2. *Résumé du protocole pour l'extraction chirurgicale d'ovocytes de xénopes pour les études électrophysiologiques/pharmaco-toxinologiques.*

To assess the effect of multiple surgeries of oocyte extraction on female *Xenopus*, we have surveyed the weight of the amphibians in a weekly-basis, before and after laparotomy. The survey of female *Xenopus* from Group 1 that were operated every 2 months showed that their weight was stable although they had a tendency to decrease with negative slopes varying from -0.025 to -0.006 (*Figure 3A*). Then, the female *Xenopus* of Group 1 have lost 5.6 ± 2.6 g (n = 3) in a period of 200 days. In addition, the scar under the incision zone was hypertrophied, which rendered oocyte extraction difficult. These observations led us to stop performing the surgery every two months for the female *Xenopus* of Group 1.

Figure 3B shows the evolution of the weight of Group 2, *i.e.* female *Xenopus* that were operated every 3 months for five times. The weight of these females was stable although a tendency to increase with positive slopes varying from 0.005 to 0.018 was observed. *Xenopus* of Group 2 have gained 4.1 ± 2.3 g (n = 3) in the whole period of the study.

Figure 3C illustrates the evolution of the weight of female *Xenopus* of Group 3 that were operated every 4 months. There was a clear increase tendency of their weight, with a positive slope ranging from 0.005 to 0.25. Group 4, *i.e.* amphibians that were operated every 6 months for oocyte extraction, showed a weight profile similar to that of Group 3 (data not shown).

These results indicate that laparotomy performed every two months affects the weight of the amphibians (~10% after three operations). In several cases, the scars under the skin of female *Xenopus* of Group 1 were hypertrophied and difficulties for suturing the muscle and epidermal layers were experienced. It was the raison why this group was operated only three times. However, repetitive laparotomies did not seriously affect the weight of the amphibians whenever an adequate recovery time is allowed to female *Xenopus* subject to surgery for oocyte harvest. A recovery time of three months for female *Xenopus* subject to laparotomy for oocytes harvest is thus here proposed.

Figure 3D illustrates a batch of twelve amphibians operated every ~3 months. It is worth noting that the operated female *Xenopus* lost in average 4.53 ± 1.14 g after each laparotomy (n = 12; 45 laparotomies). Yet, the amphibians recovered back to their average weight in two weeks. Repetitive surgery for oocyte extraction is an accepted procedure that promotes the reduction of the total number of amphibians used over long term.

The quality of the oocytes also reflects the amphibian health. Therefore, we have also surveyed the quality of the oocytes for heterologous expression of nAChRs and electrophysiological studies. Repetitive laparotomies did not affect the size of stage V – VI oocytes. Oocyte survival after nanoinjection was also not affected by repetitive laparotomies. Finally, repetitive laparotomies neither affect heterologous expression of receptor proteins nor *Torpedo* membrane incorporation into the plasma membrane of *Xenopus* oocytes for electrophysiological/pharmaco-toxinological studies.

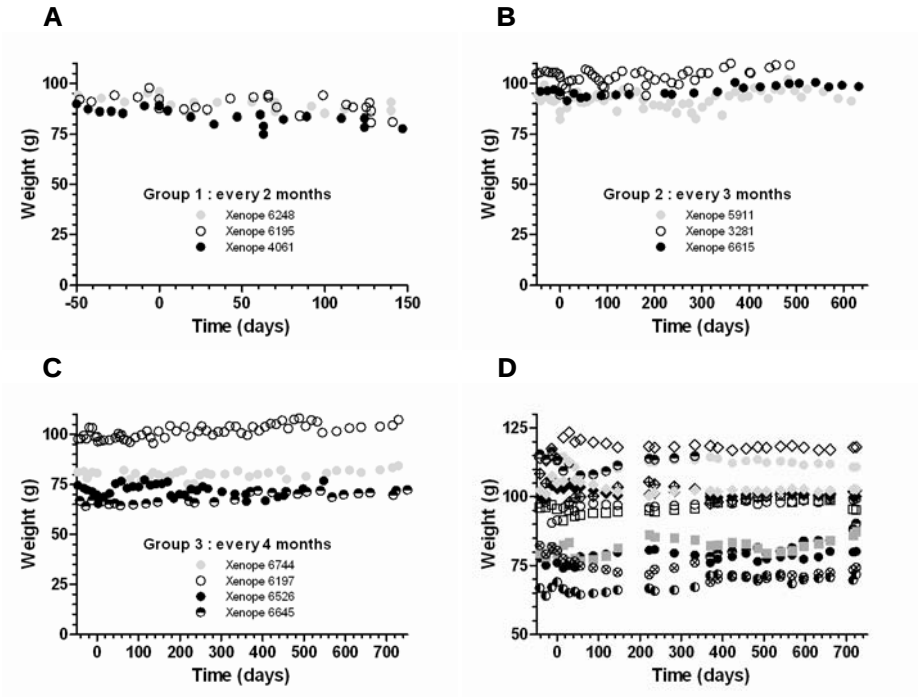

Figure 3. Evolution of the weight of female *Xenopus* subject to repetitive laparotomy. A. Group 1: female *Xenopus* operated every 2 months. B. Group 2: female *Xenopus* operated every 3 months. C. Group 3: female *Xenopus* operated every 4 months. D. Batch of female *Xenopus* of year 2009 which were operated every 3 months: 6094 (•), 6456 (○), 5338 (►), 4685 (▲), 6588 (♦), 6645 (△), 6836 (▷), 1998 (□), 5334 (■), 6953 (♦), 4273 (▼) and 6156 (•). The "zero" in the abscise axe indicate the first operation practiced to the female *Xenopus*.

Figure 3. *Evolution du poids de xénopes femelles sujettes aux laparotomies répétitives. (**A**) Groupe 1: xénopes femelles opérées tous les 2 mois. (**B**) Groupe 2: xénopes femelles opérées tous les 3 mois. (**C**) Groupe 3: xénopes femelles opérées tous les 4 mois. (**D**) Lot de xénopes femelles de l'année 2009 qui ont été opérées tous les 3 mois: 6094 (•), 6456 (○), 5338 (►), 4685 (▲), 6588 (♦), 6645 (△), 6836 (▷), 1998 (□), 5334 (■), 6953 (♦), 4273 (▼) and 6156 (•). Le "zéro" dans l'axe des abscisses indique la première opération pratiquée à la xénope femelle.*

Conclusion

Repetitive surgery for oocyte extraction is a usual practice worldwide accepted which may be justified considering the *REDUCTION* in the total number of animals used over a long term period, without affecting the quality of the obtained results. The aim of this paper was to assess the effects of multiple surgeries on female *Xenopus* by using chip-tagged amphibians to individualize each animal. An electronic chip is a *REFINEMENT* alternative to minimize pain, as well as to distress and enhance *Xenopus* well-being, as it is promoted by the 3 R's in animal research (*REDUCTION*, *REFINEMENT*, and *REPLACEMENT*; Russell and Burch, 1959).

Electronic chips are low-cost devices representing ~1% of the cost of a living female *Xenopus*, and its use should be encouraged to individualize the amphibians for surveying the weight of the animal, which is a measurable indicator of *Xenopus* health.

In conclusion, a minimum of three months recovery between each laparotomy should be allowed to female *Xenopus* subject to repetitive laparotomies for oocyte extraction.

Acknowledgements. *This work was supported in part by research grants from the "Agence Nationale de la Recherche" (ANR CES 2008-ARISTOCYA), STC-CP2008-1-555612 (ATLANTOX) and 2009-1/117 PHARMATLANTIC (to J.M.). The technical assistance of Valérie Lavallée and Morgane Roulot is acknowledged.*

References

ARAC (2005) Guidelines for egg and oocyte harvesting in *Xenopus laevis*. NIH (http://oacu.od.nih.gov/ARAC/oocyte.pdf)

Boston University (2009) *Xenopus* surgical oocyte harvest, Police and Guidelines. Institutional Animal Care and Use Committee (http://www.bu.edu/orccommittees/iacuc/policies-and-guidelines/xenopus-surgical-oocyte-harvest/)

Barnard EA, Miledi R, Sumikawa K (1982) Translation of exogenous messenger RNA coding for nicotinic acetylcholine receptors produces functional receptors in *Xenopus* oocytes. *Proc R Soc Lond B Biol Sci* **215**: 241-246

Bernareggi A, Dueñas Z, Reyes-Ruiz JM, Ruzzier F, Miledi R (2007) Properties of glutamate receptors of Alzheimer's disease brain transplanted to frog oocytes. *Proc Natl Acad Sci USA* **104**: 2956-2960

Bertrand D, Bertrand S, Cassar S, Gubbins E, Li J, Gopalakrishnan M (2008) Positive allosteric modulation of the alpha7 nicotinic acetylcholine receptor: ligand interactions with distinct binding sites and evidence for a prominent role of the M2-M3 segment. *Mol Pharmacol* **74**:1407-1416

Brown D (2004) A tribute to the *Xenopus laevis* oocyte and egg. *J Biol Chem* **279**: 45291-45299

Dumont JN (1972) Oogenesis in *Xenopus laevis* (Daudin). I. Stages of oocyte development in laboratory maintained animals. *J Morphol* **136**: 153-180

Goldin AL (1992) Maintenance of *Xenopus laevis* and oocyte injection. *Meth Enzymol* **207**: 266-279

IACUC Guidelines (2001) Guidelines for harvesting frog oocytes. Johns Hopkins University, USA (http://web.jhu.edu/animalcare/policies/frog-oocytes.html)

IACUC Guidelines (2007) Collection of *Xenopus* oocytes. University of California, San Francisco, USA (http://www.iacuc.ucsf.edu/Policies/awSPxenopus.asp)

Lester HA (1988) Heterologous expression of excitability proteins: route to more specific drugs? *Science* **241**: 1057-1063

Marsal J, Tigyi G, Miledi R (1995) Incorporation of acetylcholine receptors and Cl^- channels in *Xenopus* oocytes injected with *Torpedo* electroplaque membranes. *Proc Natl Acad Sci USA* **92**: 5224-5228

Miledi R, Eusebi F, Martínez-Torres A, Palma E, Trettel F (2002) Expression of functional neurotransmitter receptors in *Xenopus* oocytes after injection of human brain membranes. *Proc Natl Acad Sci USA* **99**: 13238-13242

Palma E, Spinelli G, Torchia G, Martinez-Torres A, Ragozzino D, Miledi R, Eusebi F (2005) Abnormal GABAA receptors from the human epileptic hippocampal subiculum microtransplanted to *Xenopus* oocytes. *Proc Natl Acad Sci USA* **102**: 2514-2518

Sakmann B, Methfessel C, Mishina M, Takahashi T, Takai T, Kurasaki M, Fukuda K, Numa S (1985) Role of acetylcholine receptor subunits in gating of the channel. *Nature* **318**: 538-543

Soreq H, Seidman S (1992) *Xenopus* oocyte microinjection: From gene to protein. *Meth Enzymol* **207**: 225-265

Russell WMS, Burch RL (1959) The principles of humane experimental technique (Methuen& Co., London, 1959; reprinted by Universities Federation for Animal Welfare, Potters Bar, UK, 1992)

Toxines et Transferts ioniques

Ce livre électronique est le quatrième volume de la nouvelle série de livres électroniques directement édités par la SFET, après sept ouvrages imprimés et distribués par Elsevier puis la Librairie Lavoisier depuis 2001. Il rassemble 30 articles organisés en quatre chapitres : Toxines et canaux ioniques, Toxines formant des pores, Toxines en tant qu'outils d'études ou agents thérapeutiques et Toxines diverses. La majorité de ces articles illustre parfaitement le thème « Toxines et Transfert ioniques » retenu cette année par le Conseil Scientifique de la SFET pour les 19èmes Rencontres en Toxinologie (RT19, 2011). Qu'ils soient écrits par des chercheurs de renommée internationale ou par de plus jeunes chercheurs, ces articles mettent en évidence le dynamisme de la communauté toxinologiste dans l'identification et la compréhension du mode de fonctionnement de ces toxines d'origines animales et bactériennes qui perturbent, par leur impact sur les flux ioniques, des processus physiologiques vitaux. De plus, l'exploitation des ces toxines en tant qu'outils d'études de leur récepteurs et canaux cibles ainsi que de leur potentialité thérapeutique est mise en évidence dans différents articles. Enfin, un certain nombre d'articles illustre des résultats récents et originaux, en dehors du thème central des RT19, démontrant la diversité des recherches actuellement mises en œuvre en toxinologie. Ces 19èmes Rencontres en Toxinologie réuniront dans le centre de conférence de l'Institut Pasteur de Paris plus d'une centaine de participants, français comme étrangers, témoignant de la volonté de notre Société de continuer à développer et promouvoir la recherche en Toxinologie.

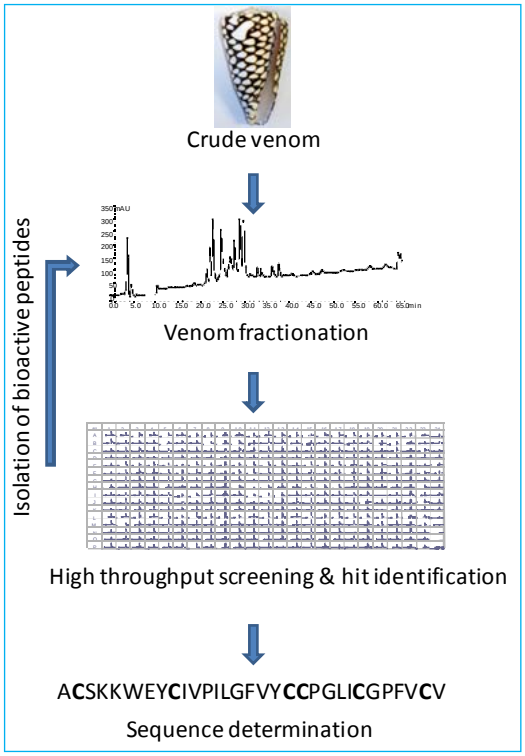

Toxins and Ion transfers

This ebook is the fourth issue of the new series of e-books directly edited by the SFET, after seven books printed and distributed by Elsevier and then Librairie Lavoisier publishers since 2001. It gathers 30 articles organized in four sections: Toxins and ion channels, Pore-forming toxins, Toxins as tools and therapeutics and Miscellanous. The major part of these articles closely reflects the theme retained by the Scientific Board of the SFET for the 19th Meeting on Toxinology (RT19, 2011): "Toxins and Ion transfers". Written either by well-known or young researchers, these articles highlight the dynamism of the toxinologist community in the identification and study of the mode of action of these animal and bacterial toxins affecting ion transfers and finally vital physiological processes. Furthermore, the use of these toxins as tools for studies of their receptors and ion channels targets and their therapeutic potential is highlighted in various articles. Finally, a number of articles illustrates recent and original results, outside the central theme of the RT19, showing the diversity of research currently being implemented in toxinology. This 19th Meeting in Toxinology will be held in the Conference Center of the Pasteur Institute in Paris and meet over a hundred French and foreign participants, reflecting the willingness of our Society to keep developing and promoting research in Toxinology.

Denis Servent,
President of the SFET

ISSN : 1760-6004